TUM School of Computation,
Information and Technology

TECHNISCHE UNIVERSITÄT MÜNCHEN

Quantum Spin Glass Models

CHOKRI MANAI

Vollständiger Abdruck der von der TUM School of Computation, Information and Technology der Technischen Universität München zur Erlangung des akademischen Grades eines

Doktors der Naturwissenschaften (Dr. rer. nat.)

genehmigten Dissertation.

Vorsitz: Prof. Dr. Robert König

Prüfer*innen der Dissertation:

1. Prof. Dr. Simone Warzel
2. Prof. Dr. Dr. h.c. mult. Herbert Spohn
3. Prof. Dr. László Erdős

Die Dissertation wurde am 25.01.2023 bei der Technischen Universität München eingereicht und durch die TUM School of Computation, Information and Technology am 26.04.2023 angenommen.

Acknowledgments

First and foremost, I want to take the chance to express my deepest gratitude to my doctoral supervisor Simone Warzel, who introduced me to the field of disordered models, a topic which perfectly met my mathematical interest. In the past four years, Simone has not only guided me through my doctoral journey, but she also shared her extensive scientific and personal knowledge with me. I have always enjoyed our mathematical discussions and little chats, and I am very blessed to have had a supervisor who has always had an open ear for me, has sincerely been interested in my ideas and in me as person. Thank you very much Simone for this unique opportunity!

I also want to thank Robert König for taking the role of the commission's head, Herbert Spohn and László Erdős for being part of the examining committee, and Christian Brennecke for reading and evaluating this thesis. I am pleased to have had the chance to collaborate with Juan P. Garrahan, Hajo Leschke and Rainer Ruder, and lately with my friend and colleague Vjosa Blakaj. I am very thankful that the secretaries Miriam Manlik, Mariola Nicpon-Stasch and Silvia Schulz have taken care of almost all administrative business. Special thanks go to our TopMath coordinator Katja Kröss who has been very supportive and has put a lot of effort to make of TopMath an excellent program. Moreover, I want to say thank you to Eva-Maria "Evi" Rott and Patrick Wittig for proofreading parts of this thesis and to Alexander Kliesch who helped me with some formalities.

Two years of my PhD time were overshadowed by the Corona pandemic and the resulting restrictions. I am very happy that Simone Warzel kept closely in touch with me in those challenging times. I am glad to have met my colleagues and friends Alexander Kliesch and Markus Hasenöhrl, which softened the isolation experienced by most of us in this period. I also appreciate the friendships with Patrick Wittig and Simon Töpfer, with whom I studied before at TU Braunschweig, and with my TopMath colleagues Eva-Maria Rott, Yifan Jia and Thiago Carvalho Corso with whom I took many master courses.

During my PhD time, I have met numerous bright, interesting and pleasant people. I cannot list them all here, but I still try my best. Thank you, Amanda Young, Frederik Ravn Klausen, Ngọc Phuong "Phini" Trần, Vera Pazukhina, Daniel Matthes, Charlotte Dietze, Nicco Mietzsch, Leonard Wetzel, Kevin Kögler, Bonifaz Baumann, David Schönwerth, Michael Wolf, Shin Ho Choe, Cambyse Rouzé, Zahra Baghali Khanian, Farzin Salek Shishavan, Tim Möbus, Emilio Onorati, Libor Caha, Quirin Vogel, Beatriz Cardoso Dias, Pablo Costa Rico, Haojian Li, Hjalmar Rall and Paul Gondolf.

I would have not come so far without the tremendous support, encouragement and love by my family. I love you Tarak, Hayet, Hind and Moiz Manai!!! And I love you Pauli for being the cutest cat in the world!

“ *Le temps est la meilleur des critiques; et la patience le meilleur des professeurs.* **”**

——— FRÉDÉRIC CHOPIN

Zusammenfassung

Spingläser sind ungeordnete magnetische Spinsysteme mit einem hohen Grad an Frustration. Daraus resultiert eine komplexe Energielandschaft. Jene Modelle finden Anwendung in vielen Disziplinen, wie zum Beispiel der Wahrscheinlichkeitstheorie, der mathematischen Biologie und der statistischen Physik. Daher gab es in den letzten Jahrzehnten aus physikalischer und mathematischer Seite viele Bemühungen Spingläser besser zu verstehen. Von besonderer Bedeutung ist Giorgio Parisis Beitrag, welcher 2021 mit dem Physiknobelpreis gewürdigt wurde. Parisi entwickelte nicht nur die Replica-Methode, um den Grenzwert der freien Energie im Sherrington-Kirkpatrick (SK) Modell zu berechnen, sondern erkannte die Bedeutung der Replica-Überlappung als funktionalen Ordnungsparameter. Die Parisi-Formel, welche eine immanente hierarchische Struktur des Gibbsmaßes auf dem Produktraum multipler Replicas sichtbar macht, und ihr rigoroser Beweis durch Arbeiten von Guerra und Talagrand können als Meilensteine der klassischen Theorie der Spin-Gläser angesehen werden.

Diese Dissertation widmet sich der Untersuchung von Quanten-Spingläsern, welche der Quantennatur von Materie Rechnung tragen. Konkret betrachten wir Hamilton-Operatoren der Bauform $H = U + \Gamma T$ auf dem Hypercubus. Dabei steht U stellvertretend für ein Potential eines klassischen Spinglasmodells, wie zum Beispiel des SK-Modells oder des Random Energy Model (REM) und der Term ΓT entspricht einem transversalen Magnetfeld mit Magnetfeldstärke Γ. Dabei wollen wir analysieren wie das transversale Feld die thermodynamischen Eigenschaften klassischer Spingläser beeinflusst. Das Studium von Quanten-Spingläsern trägt nicht nur zum Verständnis frustrierter Systeme bei, sondern ist auch von Bedeutung bei der Bewertung adiabatischer Quantenalgorithmen, die ein vielversprechender Ansatz zur Lösung von Optimierungsproblemen auf Quantencomputern darstellen. In den 1990er begannen Physiker sich systematisch mit Quanten-Spingläsern zu beschäftigen. Dabei werden analytisch die nicht rigorose Replica-Methode und die statische Approximation angewandt. Diese Methoden erlaubten es Goldschmidt den korrekten Grenzwert für das Quantum Random Energy Model (QREM) - dem REM mit transversalem Feld - zu bestimmen. Jedoch beruhen viele Arbeiten auch auf numerische Methoden und die meisten Quanten-Spinglas-Modelle, wie das Quantum Sherrington-Kirkpatrick Modell (QSK), sind noch in vielen Zügen unverstanden.

Trotz der Bedeutung von Quanten-Spingläsern liegen nur sehr wenige rigorose Resultate derzeit vor. Die Publikationen auf denen diese Dissertation beruht gehören zu den ersten Anstrengungen, einem mathematisches Verständnis von Quanten-Spingläsern näher zu kommen. Insbesondere entwickelten wir Methoden, um Goldschmidts Formel für die freie Energie im QREM zu beweisen und verfeinerten unsere Techniken, um darüber hinaus eine detaillierte spektrale Analysis des QREM-Hamiltonian zu bewerkstelligen. Dies ermöglichte uns die energetisch tiefen Eigenzustände zu charakterisieren und die nächste Ordnung (bezüglich der Systemgröße) der Grundzustandsenergie und freien Energie zu berechnen. Des

weiteren haben wir hierarchische Quanten-Spingläser, Verallgemeinerungen des QREM, untersucht was zur vollständigen Charakterisierung verschiedener Phasendiagramme führte, welche noch nicht in der Physikliteratur beschrieben wurden. Schließlich haben wir uns mit dem QSK-Modell auseinandergesetzt, wo es uns gelang für tiefe Temperaturen und ein hinreichend schwaches transversales Feld eine Spinglasordnung nachzuweisen.

Abstract

Spin glasses form a class of highly disordered frustrated spin systems, which attained major attention from mathematicians and physicists in the last decades. The importance of spin glass models results from their applications to a variety of fields, e.g., probability theory, mathematical biology, and statistical mechanics; to name a few. The physical relevance of spin glasses has lately become manifest by the award of the Nobel Prize in Physics 2021 to Giorgio Parisi, who was the first to realize that spin glass behavior is reflected in a functional order parameter and computed successfully the limit of the free energy of the Sherrington-Kirkpatrick (SK) model based on a replica calculation. Parisi's formula which encodes a hidden hierarchical structure of the limiting Gibbs measure of multiple replicas and its rigorous mathematical proof by Guerra and Talagrand can be considered as major milestones in the classical spin glass theory.

This thesis is devoted to the study of quantum spin glasses, that is, spin glasses which incorporate quantum effects. To be more precise, our aim is to study transverse field models with a Hamiltonian $H = U + \Gamma T$, where U represents the potential of a classical disordered system such as the SK model or the Random Energy Model (REM), and the term ΓT describes a transversal magnetic field of strength Γ. Here, we want to understand how the transversal field affects the thermodynamical properties of the underlying model. Results on quantum spin glasses not only enhance our understanding of frustrated spin systems, but also are of importance for the evaluation of quantum adiabatic algorithms, which form a promising algorithm scheme which might be implemented on quantum computers. In the 90's physicists started to investigate these types of models analytically via the replica trick and a static approximation for the path-integral representation and to a large extent also numerically. For instance, Goldschmidt predicted the (correct) formula for the free energy of the REM with transversal field, the Quantum Random Energy Model (QREM). However, most quantum spin glass models such as the Quantum Sherrington-Kirkpatrick model (QSK) are yet not fully understood.

Despite the importance of quantum spin glasses, rigorous results are still rare and the publications, on which this thesis is based, are among the first systematic attempts towards a mathematical understanding of quantum spin glasses. In particular, we have managed to prove Goldschmidt's formula for the QREM and used this as starting point to provide a detailed spectral analysis of the QREM Hamiltonian, that is, we give a precise description of the low energy states and compute the finite size corrections of the ground state energy and free energy. Moreover, we discuss hierarchical quantum spin glasses - generalizations of the QREM - where we give complete phase diagrams which were even unknown in the physics literature. Last but not least, we contribute to the study of the QSK, where we establish a spin glass phase for low temperatures and a weak magnetic field.

List of contributed articles

Core articles as principal author

I) Chokri Manai and Simone Warzel.
Phase diagram of the quantum random energy model.
Journal of Statistical Physics 180: 654–664 (2020).
https://doi.org/10.1007/s10955-020-02492-5.
(see also article [128] in the bibliography)

II) Chokri Manai and Simone Warzel
Generalized random energy models in a transversal magnetic field: free energy and phase diagrams.
Probability and Mathematical Physics 3: 215–245 (2022).
https://doi.org/10.2140/pmp.2022.3.215.
(see also article [130] in the bibliography)

III) Chokri Manai and Simone Warzel
The de Almeida-Thouless Line in Hierarchical Quantum Spin Glasses.
Journal of Statistical Physics 186: 14 (2022).
https://doi.org/10.1007/s10955-021-02860-9.
(see also article [131] in the bibliography)

Further articles as principal author

IV) Chokri Manai and Simone Warzel
Spectral Analysis of the Quantum Random Energy Model.
Commun. Math. Phys. (2023).
https://doi.org/10.1007/s00220-023-04743-4
Extended version: https://arxiv.org/abs/2202.00334.
(see also article [132] in the bibliography)

V) Chokri Manai and Simone Warzel.
The quantum random energy model as a limit of p-spin interactions.
Reviews in Mathematical Physics 33: 2060013 (2020).
https://doi.org/10.1142/S0129055X20600132.
(see also article [129] in the bibliography)

Articles as co-author

VI) Hajo Leschke, Chokri Manai, Rainer Ruder and Simone Warzel.
Existence of replica-symmetry breaking in quantum glasses.
Physical Review Letters 127: 207204 (2021).
https://link.aps.org/doi/10.1103/PhysRevLett.127.207204.
(see also article [125] in the bibliography)

VII) Juan P. Garrahan, Chokri Manai and Simone Warzel.
Trajectory phase transitions in non-interacting systems: all-to-all dynamics and the random energy model.
Philosophical Transactions of the Royal Society A 381: 20210415 (2022).
https://doi.org/10.1098/rsta.2021.0415.
(see also article [88] in the bibliography)

I, Chokri Manai, am the principal author of the Core Articles I, II and III, and of the Articles IV and V. I am coauthor of the articles VI and VII. Core Articles I, II and III and Articles VI and VII are printed in the appendix as they have been published. The published version of Article IV was required to be shortened in the revision process. Thus, I have decided to include the more comprehensive preprint version of Article IV in the appendix. Moreover, due to copyright issues the appendix contains the preprint version of Article V.

Contents

Chapter 1

Introduction

Spin glass models were originally introduced to describe experimentally observed magnetic alloys, such as iron (Fe) weakly diluted in gold (Au), which exhibit peculiar dynamical properties at low temperatures: for instance slow relaxation to equilibrium after turning out an external field, a phenomenon which is referred to as aging [52]. These experimental findings highly contrast what one expects for ferromagnetic or paramagnetic solids. While the spins in ferromagnets tend to point in the same direction, spin glasses are governed by random interactions between the spins. That is, some pairs of spins prefer to be parallel, while other pairs want to be anti-parallel. Hence, there is no configuration satisfying most preferences; one speaks of a high degree of frustration. Highly frustrated systems are characterized by a complex energy landscape, for which it is even hard to find the minimal energy configuration. Thus, understanding spin glass models is a very challenging task which has been faced by condensed matter physicists, mathematical physicists and probabilists for about five decades [6,42,70,99,135,155,166]. Complex structures, of course, do not only emerge in statistical physics, but in a variety of scientific disciplines. Consequently, the study of spin glasses has a huge impact on very different fields such as combinatorial optimization, theoretical computer science, machine learning and mathematical biology [20, 21, 24, 59, 136].

In particular, mean-field spin glass models, where all particles interact with each other, have attained considerable attention as they are more feasible than short-range models, yet equipped with a rich physical structure. This structure was discovered by Parisi in his revolutionizing work on the Sherrington-Kirkpatrick (SK) model. He found an exact solution for the free energy of the SK model, which is based on the ingenious idea of replica-symmetry breaking [135, 155]. The so-called replica overlap remains a random quantity in the infinite-particle limit, but the overlap's limiting distribution, the so-called Parisi measure, governs the system and takes the role of the order parameter. Giorgio Parisi was awarded the Nobel Prize in Physics 2021 among other scientific contributions for his breakthrough on understanding spin glasses via the replica-symmetry breaking scheme and the underlying hierarchical organization of multi-overlaps, which is commonly believed to be universal for mean-field spin glass models. Parisi's work did not only inspire physicists to extend his methods to other disordered models, but also motivated mathematicians to understand Parisi's solution from a rigorous point view. While for a long time only partial results, mainly focusing on the high temperature phase, had been established, Guerra's and Talagrand's efforts cumulated in a proof of the Parisi formula for the free energy [99, 179, 181]. Together with Panchenko's result on the ultrametricity of the Gibbs measure [151], these works can be seen as milestones of the classical spin glass theory. Despite all the sketched progress, there are still many open

questions. For example, a description of the Parisi measure for low temperatures in the SK model [16] and an examination of the spin glass models' dynamical properties, which characterize spin glasses in the laboratory, are still lacking.

Classical spin glass models such as the SK model consider Hamiltonians which are random functions of the N-particle spin configuration. Although such models are able to depict important aspects of spin glass physics, they can only form a caricature of real metal alloys as they ignore the quantum nature of matter. Quantum spin glass models implement the law of quantum physics by considering Hamiltonians which are random operators with the spin-$\frac{1}{2}$ operators as building blocks. Quantum spin glass models have been studied in the physics literature for a long time and have recently gained more attention [23, 24, 29, 44, 68, 78, 95, 96, 111, 121, 138, 158, 175]. One research strand focuses on the question where a glass phase is found and to which degree Parisi's replica symmetry breaking scheme governs the physics of mean-field quantum spin glasses [78, 138, 188, 193]. Due to the quantum nature however, further interesting directions of research open up. An important example is the study of quantum phase transitions at zero temperature, which often reflect a disruptive change of the ground state's properties [68, 106]. Moreover, the possibility of quantum tunneling through energy barriers leads to new ergodic-nonergodic transitions, which are also closely related to the degree of the eigenstates' localization [29, 111, 124].

Certainly, the resulting non commutative situation makes the analysis more challenging and, thus, our understanding of quantum spin glasses is rather limited in contrast to classical spin glasses. We will mainly consider in this thesis the simplest class of quantum spin glasses, where a classical spin glass is enriched by an additional transverse magnetic field. The most prominent example is the Quantum Sherrington-Kirkpatrick (QSK) model, for which most physical predictions are based on numerics or not reliable approximations such as the static approximation. This calls for a rigorous analysis, which clarifies our picture of quantum spin glasses. Unfortunately, there is a lack of mathematical work on quantum spin glass models. There are few results on the QSK, which have been developed independently from this thesis [3, 53, 126], but the literature on simpler models such as the Quantum Random Energy Model (QREM) is almost vacant. The main aim of this thesis is to make a first attempt to systematically study quantum spin glasses and to encourage further research on this interesting multi-disciplinary topic, which lies at the intersection of quantum physics, statistical mechanics, probability theory and operator theory with various applications in condensed matter physics, mathematical biology and quantum computing.

In the following parts of the introduction, we will introduce the basic concepts of statistical mechanics and quantum physics, and we will introduce the (quantum) spin glass models, which will be considered in the main body of the thesis. Concurrently, we try to give some context to and intuition behind the models.

1.1 Statistical Mechanics and Classical Spin Glasses

We start our journey by introducing classical spin glass models which we will be encountered in the rest of this thesis. To this end, we will need to recall some concepts and notation from statistical mechanics.

1.1.1 Some Preliminaries on Statistical Mechanics

Let us first describe the general setting. Our configuration space for N particles will always be the Hamming cube $\mathcal{Q}_N := \{-1, 1\}^N$, and its elements are denoted by $\boldsymbol{\sigma} = (\sigma_1, \dots, \sigma_N)$. We think of the N

particles to have only one degree of freedom, namely its internal spin which can only take the values ± 1. In the literature one can also find models where the internal spin is more generally a vector which may take infinitely many values [55, 154], but we will only consider spin glass models on the Hamming cube. Each model comes with its family of random Hamiltonians $H_N : \mathcal{Q}_N \to \mathbb{R}$, which is a random process on the Hamming cube. As usual, $H_N(\boldsymbol{\sigma})$ models the energy of a specific configuration $\boldsymbol{\sigma}$. Of course, formally the family $(H_N)_{N\in\mathbb{N}}$ is a sequence of random variables on some probability space $(\Omega, \mathscr{A}, \mathbb{P})$, however we will take the point of view which focuses on the random variables themselves and the underlying probability space is rarely explicitly mentioned. The existence of the presented models will be typically clear and the discussed assertions and events will not depend on the exact form of the probability space and, thus, with a slight abuse of notation $\mathbb{P}$ will always denote the probability with respect to the model's disorder and, similarly, $\mathbb{E}$ denotes the expectation with respect to the disorder. In this thesis, we assume a basic familiarity with common notions and results in probability theory as they can be found in [112], but somewhat more advanced concepts will at least be recalled.

If a Hamiltonian H_N is given, as usual we associate with H_N the *partition function*

$$Z_N(\beta) = \sum_{\boldsymbol{\sigma}\in\mathcal{Q}_N} e^{-\beta H_N(\boldsymbol{\sigma})}, \tag{1.1}$$

and the *pressure*

$$\Phi_N(\beta) = \ln Z_N(\beta), \tag{1.2}$$

where $\beta \geq 0$ denotes the *inverse temperature*, i.e., $\beta = 1/T$ with the ordinary temperature T. From the point of view of statistical mechanics, we consider the canonical ensemble with fixed particle number N at a certain inverse temperature β. The thermodynamics in the canonical ensemble is governed by the free energy $F_N(\beta) = -\frac{1}{\beta}\ln Z_N(\beta)$, which in particular encodes the internal energy and entropy. Up to a multiple factor Φ_N and F_N agree with each other, and for convenience we mainly consider the pressure, which is always convex and for most spin glass models positive [52, 181]. The notions pressure and free energy are sometimes used interchangeably.

In physical systems, the pressure is typically an extensive quantity, i.e., it scales (almost) linearly in the particle number N if N is large enough [83, 167]. We are mostly interested in the so-called *thermodynamic limit* $N \to \infty$, where one expects that the specific pressure $\frac{1}{N}\Phi_N(\beta)$ converges, and we will denote its limit (if it exists) by $p(\beta)$. We stress that for disordered models the partition function and pressure are random variables. However, it will turn out for all models we study that the specific pressure $\frac{1}{N}\Phi_N(\beta)$ is *self-averaging*, i.e., $\frac{1}{N}\Phi_N(\beta)$ sharply concentrates around its mean $\frac{1}{N}\mathbb{E}[\Phi_N(\beta)]$. In particular, the limit $p(\beta)$ will usually be deterministic and, as we are used to in statistical mechanics, phase transitions can be read off from a non-analytic behavior of p. We remark that $\mathbb{E}[\Phi_N(\beta)]$ is often referred to as the *quenched* average in contrast to the physically less interesting *annealed* average $\ln \mathbb{E}[Z_N(\beta)]$, where the expectation is pulled into the logarithm. However, the annealed pressure is often easier to compute and for high temperatures it may give some physical insight.

Let us finally introduce the Gibbs measure μ_β on $\mathcal{Q}_N$ which is defined via its weights on a configuration $\boldsymbol{\sigma}$,

$$\mu_\beta(\boldsymbol{\sigma}) = \frac{e^{-\beta H_N(\boldsymbol{\sigma}))}}{Z_N(\beta)}. \tag{1.3}$$

The Gibbs measure controls the thermal fluctuations. The average of a function $f : \mathcal{Q}_N \to \mathbb{R}$ with respect to μ_β will be denoted by $\langle f \rangle_\beta$. Of course, the Gibbs measure is itself random and one needs to face two layers of randomness in spin glasses: the disorder of the Hamiltonian H_N and the fluctuations due to the Gibbs measure. A crucial idea in spin glass theory is to consider *replicas*, that is, one studies a duplicated system. For any $k \in \mathbb{N}$ we copy the configuration space k-times and we equip $\mathcal{Q}_N^{\otimes k}$ with the product Gibbs measure $\mu_\beta^{\otimes k}$. The picture is that we draw k-replicas $\boldsymbol{\sigma}^1, \dots, \boldsymbol{\sigma}^k$ of spin configurations independently from each other with the probability law given by μ_β. The average with respect to $\mu_\beta^{\otimes k}$ will be denoted by $\langle \cdot \rangle_\beta^{\otimes k}$. The analysis of the static thermodynamics boils down to the study of the pressure and the Gibbs measure for large particle numbers N. More details on the thermodynamical formalism can be found in standard textbooks such as [36, 83, 161, 167].

1.1.2 Classical Spin Glass Models

Having introduced the mathematical objects of interest, we continue with a description of spin glass model Hamiltonians H_N. In classical spin glasses, the Hamiltonian H_N consists of two terms

$$H_N(\boldsymbol{\sigma}) = U(\boldsymbol{\sigma}) + \sum_{i=1}^{N} h_i \sigma_i,$$

where the second terms corresponds to an external magnetic field in vertical direction with (in general random) weights h_i. The spin glass properties are encoded in the potential U consisting of random interactions which leads to frustration and unexpected magnetic properties. Thus, a spin glass model is characterized by the choice of U.

The theory of spin glasses had its starting point in the seminal work by Edwards and Anderson in 1975 [70]. The so called Edwards-Anderson (EA) model is a random Ising-type model on the lattice $\mathbb{Z}^d$ for some $d \in \mathbb{N}$. That is, we take a finite box $\Lambda_L = [-L, L]^d \cap \mathbb{Z}^d$, $N = (2L+1)^d$ and we label the spin components σ_v with the vertices $v \in \Lambda_L$. Moreover, we associate with the box Λ_L the canonical undirected subgraph of $\mathbb{Z}^d$ with edges $E = \{\{x, y\} | x, y \in \Lambda_L, \quad \|x - y\|_1 = 1\}$ with the 1-norm $\|\cdot\|_1$. The corresponding potential is then given by

$$U_{\mathrm{EA}}(\boldsymbol{\sigma}) = \sum_{\{x,y\} \in E} g_{x,y} \sigma_x \sigma_y \tag{1.4}$$

with a collection of independent identically distributed (i.i.d.) random variables $(g_{x,y})_{\{x,y\} \in E}$ with the law of a standard normal variable. A standard Gaussian or, respectively, a standard normal variable is as always a real random variable with probability density

$$\rho(x) := \frac{1}{\sqrt{2\pi}} e^{-\frac{1}{2}x^2}.$$

We recall that $g_{x,y} \equiv -1$ corresponds to the famous d-dimensional Ising model, the paradigmatic example for a ferromagnet on the lattice. Based on the intuition that spin glass behavior is a result of competing ferromagnetic ($g_{x,y} < 0$) and antiferromagnetic ($g_{x,y} > 0$) interactions, the Edwards-Anderson model is a natural choice. However, it quickly turned out that understanding the thermodynamics of next-neighbor random models by analytic means appears to be not feasible. For instance, until today it is not completely

clear if the replica-symmetry breaking picture describes the EA model since there are competing concepts such as the droplet picture [81] and the metastate prescription [142, 143]. Some basic rigorous results on the EA model can be found in [52].

The complexity of the EA model motivated Sherrington and Kirkpatrick to introduce a mean-field version of the potential U in (1.4) [166]. The Sherrington-Kirkpatrick (SK) model's potential for N particles is given by

$$U_{\mathrm{SK}}(\boldsymbol{\sigma}) = \frac{1}{\sqrt{N}} \sum_{1 \le i < j \le N} g_{i,j} \sigma_i \sigma_j \tag{1.5}$$

with i.i.d. standard Gaussians $(g_{i,j})_{1 \le i < j \le N}$. Here, the term *mean-field* reflects the fact that all particles interact with each other in the SK model and not only neighboring spins. As a result, the underlying lattice geometry disappears, which typically simplifies the physics drastically. A prime example for this approach is the Curie-Weiß model,

$$U_{\mathrm{CW}}(\boldsymbol{\sigma}) = -\frac{1}{N} \sum_{i,j} \sigma_i \sigma_j =: -N m(\boldsymbol{\sigma})^2, \tag{1.6}$$

the mean-field version of the canonical Ising model on the lattice. While there are no explicit formulas for the free energy in the Ising models for dimensions $d \ge 3$, the Curie-Weiß is a solvable model and its physics, in particular present phase transitions, is encrypted in a single real number – the average magnetization $\langle m \rangle_\beta = \langle \frac{1}{N} \sum_{i=1}^N \sigma_i \rangle_\beta$. One says that the magnetization takes the role of the order parameter [36, 83]. The SK model can also be regarded as disordered Curie-Weiß model and, thus, one may hope that there exists a similarly simple order parameter. Already Sherrington and Kirkpatrick realized in their pioneering work that the so-called replica overlap,

$$R_N(\boldsymbol{\sigma}, \boldsymbol{\sigma}') := \frac{1}{N} \sum_{i=1}^N \sigma_i \sigma_i' \in [-1, 1]$$

for $\boldsymbol{\sigma}, \boldsymbol{\sigma}' \in \mathcal{Q}_N$, is of central importance. Namely, the covariance of the Gaussian process U_{SK} may be written in terms of R_N,

$$\mathbb{E}[U_{\mathrm{SK}}(\boldsymbol{\sigma}) U_{\mathrm{SK}}(\boldsymbol{\sigma}')] = \frac{N}{2} R_N(\boldsymbol{\sigma}, \boldsymbol{\sigma}')^2 - \frac{1}{2}.$$

Let us pause for a moment and note that the covariance grows linearly with N. As a rule of thumb, if the potential is not too correlated, the minimal energy $\min U$ is then of order N as well. Thus, ground state energy and pressure are then extensive as they should be in physical systems. This explains the prefactor $N^{-1/2}$ in (1.5) which is different from the deterministic situation in the Curie-Weiß model (1.6).

Sherrington and Kirkpatrick considered the thermal average of the replica overlap $\langle R_N \rangle_\beta^{\otimes 2}$, which measures the closeness of two spin configurations that are randomly picked following the law of the Gibbs distribution. They assumed that in presence of an external field the replica overlap concentrates around its average $\mathbb{E}[\langle R_N \rangle_\beta^{\otimes 2}]$ just as the magnetization in the Curie-Weiß model does. The resulting replica-symmetric solution which can be found in Section 4.3, however, turned out to be wrong. It was Parisi's insight that the situation in the SK model is much more complicated: the replica overlap remains a random quantity even in the infinite particle limit and its distribution takes the role of the order parameter. One speaks of a functional order parameter since the system is governed by a whole distribution function, not a mere real number. Furthermore, the situation, where the replica overlap becomes not self-averaging

for low temperatures, is referred to as *replica-symmetry breaking*. Together with the assumption that the multi-overlap organize in an ultrametric manner, the replica-symmetry breaking scheme leads to the famous Parisi formula. Parisi's original derivation is not rigorous as it invokes the *replica trick*. The idea is to make use of the following elementary representation of the natural logarithm

$$\lim_{n\to 0} \frac{x^n - 1}{n} = \ln x.$$

But instead of computing $\mathbb{E}[Z_N^n]$ for small numbers n, only the moments of the partition function for integers $n \in \mathbb{N}$ are considered. The limit $n \to 0$ is derived via an extrapolation. The replica trick has not found a rigorous justification hitherto, and the proof of the Parisi formula follows another route which will be presented in Section 5.1. The SK model stems from statistical mechanics, but nevertheless it has found application in other field. For instance, the Max-Cut problem on an Erdős-Rényi graph can be rephrased in terms of an SK spin glass with Bernoulli weights $g_{i,j}$ [59,137]. Here comes *universality* into play: while the SK model is defined in terms of Gaussian couplings, the limit of the specific pressure $p_{\mathrm{SK}}(\beta)$ does not depend on the distribution as long as $g_{i,j}$ are i.i.d. random variables with $\mathbb{E}[g_{i,j}] = 0, \mathbb{E}[g_{i,j}^2] = 1$ and $\mathbb{E}[|g_{i,j}|^3] < \infty$ [48]. This allows one to find asymptotic expression for the Max-Cut size on Erdős-Rényi graphs in terms of the SK minimal energy and, recently, an efficient algorithm for finding an approximate maximal cut has been found [137].

The SK model can be generalized to the situation where not only two but $p \in \mathbb{N}$ spins interact with each other,

$$U_p(\boldsymbol{\sigma}) = \frac{1}{N^{(p-1)/2}} \sum_{i_1,\dots,i_p=1}^{N} g_{i_1,\dots,i_p} \sigma_{i_1} \cdots \sigma_{i_p}, \tag{1.7}$$

where the $(g_{i_1,\dots,i_p})_{1\le i_1,\dots,i_p\le N}$ are again i.i.d. standard normal variables. U_p gives rise to the p-spin model and if the potential U is a linear combination of different U_p one arrives at the mixed p-spin models. Note that in contrast to the SK model, we include self-interactions in (1.7) because it leads to a convenient formula for the covariance process,

$$\mathbb{E}[U_p(\boldsymbol{\sigma})U_p(\boldsymbol{\sigma}')] = N R_N(\boldsymbol{\sigma},\boldsymbol{\sigma}')^p$$

for $\boldsymbol{\sigma},\boldsymbol{\sigma}' \in \mathcal{Q}_N$. We will see in Chapter 5 that Parisi's solution can be extended to all mixed p-spin models. From a physical point of view, there is the broad picture that the models get less involved as p increases. This is reflected in the Gardener transition for $p \ge 3$. While its predicted that the replica overlap in the SK model changes from being zero to a a continuous random variable (*continuous replica symmetry breaking*) at $\beta = 1$, one expects that the p-spin models undergo a 1-step replica symmetric breaking at the critical temperature, i.e., the replica overlap's distribution has only mass at two values. Only for even lower temperatures continuous replica symmetry breaking should occur.

Following this intuition, Derrida considered the formal $p \to \infty$ limit, leading to a Gaussian process with covariance $\mathbb{E}[U_\infty(\boldsymbol{\sigma})U_\infty(\boldsymbol{\sigma}')] = N\delta_{\boldsymbol{\sigma},\boldsymbol{\sigma}'}$ with the Kronecker delta $\delta_{\boldsymbol{\sigma},\boldsymbol{\sigma}'}$, which is only 1 if $\boldsymbol{\sigma} = \boldsymbol{\sigma}'$ and otherwise vanishes [61,62]. Derrida's Random Energy Model (REM) can alternatively be written as

$$U_{\mathrm{REM}}(\boldsymbol{\sigma}) = \sqrt{N} g_{\boldsymbol{\sigma}} \tag{1.8}$$

with 2^N i.i.d standard Gaussians $(g_{\boldsymbol{\sigma}})_{\boldsymbol{\sigma}\in\mathcal{Q}_N}$. The REM was introduced to the mathematical literature by Ruelle [164]. Due to the lack of correlations, the REM is of course only a toy model for spin glasses. Despite its simplicity, the REM shows a glass transition and captures some features of more complicated glass models. Due to the independence of the REM potential, it permits a precise analysis and, thus, the REM allows a first understanding of glass behavior. That was very important when the Parisi solution had not been established yet. We will give an overview of the equilibrium properties of the REM in Section 2.1.

Shortly after having put forward the REM, Derrida introduced a family of hierarchical spin glasses which are built upon the REM and are dubbed Generalized Random Energy Models (GREM). The simplest variant is the 2-level GREM for which one needs to divide the total spin vector $\boldsymbol{\sigma} = \boldsymbol{\sigma}_1\boldsymbol{\sigma}_2$ into two blocks $\boldsymbol{\sigma}_1 = (\sigma_1, \dots, \sigma_{\lceil xN\rceil})$ and $\boldsymbol{\sigma}_2 = (\sigma_{\lceil xN\rceil+1}, \dots, \sigma_N)$ for some $x \in (0,1)$. The GREM potential is then given by

$$U_{\mathrm{GREM}}(\boldsymbol{\sigma}) = \sqrt{Na_1}\, g_{\boldsymbol{\sigma}_1} + \sqrt{Na_2}\, g_{\boldsymbol{\sigma}_1\boldsymbol{\sigma}_2} \tag{1.9}$$

with some $a_1, a_2 > 0$ satisfying $a_1 + a_2 = 1$ and two mutually independent Gaussian processes $(g_{\boldsymbol{\sigma}_1})_{\boldsymbol{\sigma}_1\in\mathcal{Q}_{\lceil xN\rceil}}$ and $(g_{\boldsymbol{\sigma}_1\boldsymbol{\sigma}_2})_{\boldsymbol{\sigma}\in\mathcal{Q}_N}$. In that way, (1.9) gives rise to a correlated Gaussian process but the correlation structure is ultrametric facilitating the analysis of the GREM. In Chapter 4 we will consider more generally GREM potentials with any number of levels $n \in \mathbb{N}$ and even its continuous version, the CREM. The study of the Gibbs measure in the GREM leads to Ruelle cascades which govern also the overlap distribution in mixed p-spin models. In that sense, the GREM captures important features of the more involved SK model.

The interest in the REM and GREM goes far beyond its caricature of a spin glass. For instance, the GREM is closely related to the study of Branching Brownian Motions (BBM). One can think of a BBM as follows. One starts with a single Brownian motion B_t, and after an exponential time T the path splits into two independent Brownian motions starting at B_T. This process is continued for both paths independently from each other and so on. It turns out that the extremal process of a BBM is closely related to the low energy statistics of the CREM (see [37] and the references therein). A second example is the analysis of the REM in the context of aging and metastability. The idea is to consider a particular Markov jump process on $\mathcal{Q}_N$, the Glauber dynamics. The continuous Markov time process X_t on $\mathcal{Q}_N$ is defined via the transition rates

$$r(\boldsymbol{\sigma}, \boldsymbol{\sigma}') = \begin{cases} \frac{1}{N} e^{\beta U(\boldsymbol{\sigma})} & \text{if } \sum_{i=1}^N \mathbb{1}_{\sigma_i \neq \sigma_i'} = 1, \\ 0 & \text{else,} \end{cases}$$

for $\boldsymbol{\sigma} \neq \boldsymbol{\sigma}'$, some $\beta > 0$ and a potential U on $\mathcal{Q}_N$. If U is chosen to be the REM potential, one can show that the process stays at particular low energy configurations for a long time [25, 26, 49, 89, 91]. This phenomenon has become known as aging and the REM is an important model for which that can be rigorously established. The last application we want to discuss lies in the field of mathematical biology. Here, U_{REM} models a rugged fitness landscape of species, i.e., the value $U_{\mathrm{REM}}(\boldsymbol{\sigma})$ encodes the competitiveness of the species $\boldsymbol{\sigma}$ [20, 21, 71, 104]. If employed with a dynamics which incorporates the biological evolution, one may analyze which species survive for large times. In this context the REM is also called the "House of Cards" model. The analysis of the evolution is also intimately related to the Quantum Random Energy, which will be introduced in the next section.

The SK model, the mixed p-spin model, the REM and its generalizations the GREM and CREM form the classical backbone for the quantum models we will study in the main body of this thesis. There are plenty of other spin glass models of which some are discussed in [135] from a physical point of view and, rigorously, in [181]. A discussion of all these models is beyond the scope of this thesis. Nevertheless, we would like to close this section by presenting a further spin glass model, the Hopfield model, which in contrast to the models discussed so far did not originate in statistical mechanics. John Hopfield was interested in modeling neural networks [105]. For simplicity, one assumes that a single neuron σ_i can only take two states -1 ("passive") and $+1$ ("active"). Thus, the configuration space of N neurons is again the Hamming cube $\mathcal{Q}_N$. Each neuron may change its state depending on an input signal r_i, which in turn depends on the total configuration $\boldsymbol{\sigma}$. One again considers the simplest choice, where r_i depends linearly on all other neuron states, i.e.,

$$r_i = \sum_{j=1}^{N} g_{i,j}\sigma_j\sigma_i.$$

The additional factor σ_i is present to favor the current states. So far, the situation looks similar to the SK model. The difference comes with the choice of the couplings $g_{i,j}$ which are chosen according to Hebb's rule [102]. The idea is that the network functions as an autoassociative memory and tries to pull the current state to one of M states $\boldsymbol{\tau}^1, \dots \boldsymbol{\tau}^M \in \mathcal{Q}_N$, which have been saved so far. The saved states are typically assumed to be drawn from the uniform distribution on $\mathcal{Q}_N$, independently from each other. The interactions are consequently given by

$$g_{i,j} = \sum_{k=1}^{M} \tau_i^k \tau_j^k.$$

The network's dynamics is a continuous-time Markov chain where each neuron $\sigma_i(t)$ changes to a new value ± 1 with rates proportional to $\exp(\pm\beta r_i)$ for some $\beta > 0$. From the machine learning perspective, one is mainly interested in the case where $M = \alpha N$ and the question of the network's *capacity* arises. The capacity α_c is defined as the maximal value α for which the network remembers its saved patterns, i.e., if one starts close to a configuration $\boldsymbol{\tau}^k$ the Markov chain should be attracted by this particular state $\boldsymbol{\tau}^k$. Numerical experiments suggest that $\alpha_c \approx 0.14$ [105]. Spin glass physics can enhance our understanding on this result, as the steady state of the update rule is given by the Gibbs measure at inverse temperature β of the corresponding Hopfield Hamiltonian

$$U_{\mathrm{HF}}(\boldsymbol{\sigma}) = -\sum_{k=1}^{M} \sum_{1\le i,j\le N} \tau_i^k \tau_j^k \sigma_i \sigma_j.$$

Note that the special case $M = 1$ and $\boldsymbol{\tau}^1 = (1, \dots, 1)$ correspond to the Curie-Weiß model. To put it in other words, one can think of the Hopfield model as sum of translated Curie-Weiß potentials. Rigorous results on the Hopfield model for small α can be found in [181]. A complete picture for higher values of α is still lacking.

1.2 Quantum Statistical Physics and Quantum Spin Glasses

1.2.1 Some Concepts from Quantum Mechanics and Quantum Statistics

Before specifying the quantum models of interest, let us first introduce the general notions from quantum statistical physics which will be used throughout this thesis. We can only give a brief overview here and for a comprehensive discussion of quantum mechanics and quantum statistical physics from a mathematical point of view, we refer to standard textbooks [159, 163, 167, 183].

In contrast to classical statistical mechanics, the systems state is not simply a point in the configuration space, but rather a vector ψ in a Hilbert space $\mathcal{H}$. We will often call such an $\psi \in \mathcal{H}$ a *wavefunction*. In our situation, the N-particle Hilbert space $\mathcal{H}_N$ will coincide with the 2^N-dimensional vector space

$$\mathcal{H}_N = \ell^2(\mathcal{Q}_N) := \{\psi : \mathcal{Q}_N \to \mathbb{C}\}, \tag{1.10}$$

the vector space of complex valued functions on $\mathcal{Q}_N$ endowed with the scalar product

$$\langle \psi, \varphi \rangle := \sum_{\boldsymbol{\sigma}} \bar{\psi}(\boldsymbol{\sigma})\varphi(\boldsymbol{\sigma}) \tag{1.11}$$

for $\psi, \varphi \in \ell^2(\mathcal{Q}_N)$ and the canonical norm $\|\psi\| := \langle \psi, \psi \rangle^{1/2}$. As one can read off from (1.10) and (1.11), we use the physics convention that the scalar product is antilinear in the first component and linear in the second one. An orthonormal basis of $\ell^2(\mathcal{Q}_N)$ – a collection of orthogonal, norm one vectors spanning the Hilbert space $\ell^2(\mathcal{Q}_N)$ – is given by the canonical basis $|\boldsymbol{\sigma}\rangle$ (sometimes also denoted by $\delta_{\boldsymbol{\sigma}}$),

$$|\boldsymbol{\sigma}\rangle(\boldsymbol{\sigma}') = \delta_{\boldsymbol{\sigma},\boldsymbol{\sigma}'}.$$

The notation already suggests that one may think of $|\boldsymbol{\sigma}\rangle$ as the quantum state corresponding to the classical spin configuration $\boldsymbol{\sigma}$.

The *observables*, the physical quantities that can be measured in a laboratory, are now given by self-adjoint linear operators on $\mathcal{H}$. A self-adjoint operator $A : \mathcal{H} \to \mathcal{H}$ is a densely defined, closed linear operator with $A = A^*$, where we denote by A^* the adjoint operator. In the finite-dimensional setup we mainly consider, one can think of a linear operator A as a Hermitian square matrix with matrix elements $A_{i,j} = \langle e_i, Ae_j \rangle$ with respect to a certain orthonormal basis $(e_i)_{1 \le i \le d}$.

At this point, we want to recall Dirac's bra-ket notation which we will frequently use in the following. One denotes for some $\psi \in \mathcal{H}$ by $|\psi\rangle$ the vector ψ itself and $\langle\psi|$ is a short-hand notation for the linear functional $l_\psi \in \mathcal{H}^\star$,

$$l_\psi(\varphi) := \langle \psi, \varphi \rangle.$$

The bra-ket notation foots on the fact that the dual space $\mathcal{H}^\star$, the complex vector space of all linear maps from $\mathcal{H}$ to $\mathbb{C}$, is anti-unitarily equivalent to the original Hilbert space $\mathcal{H}$ by Riesz' representation theorem [159]. Then, one may write

$$\langle \varphi | A | \psi \rangle = \langle \varphi, A\psi \rangle$$

for the $\varphi - \psi$ matrix elements of the observable A. The bra-ket notation is particularly convenient to denote the orthogonal projection $|\psi\rangle\langle\psi|$ to a (normalized) wavefunction $\psi \in \mathcal{H}$. More precisely, $|\psi\rangle\langle\psi|$ is the self-adjoint rank-one operator

$$|\psi\rangle\langle\psi|(\varphi) = \langle\psi, \varphi\rangle\psi,$$

for $\varphi \in \mathcal{H}$.

As commonly known, a self-adjoint operator on a d-dimensional space can be unitarily diagonalized by the spectral theorem. In other words, each self-adjoint operator $A = A^*$ acting on a d-dimensional space $\mathcal{H}$ possesses an orthonormal basis $(\psi_j)_{j=1,\dots,d}$ of eigenvectors, i.e., $A\psi_j = \lambda_j\psi_j$ with the real eigenvalues $(\lambda_j)_{j=1,\dots,d}$ of A. Using the bra-ket notation, the spectral decomposition can be compactly written as

$$A = \sum_{j=1}^{d} \lambda_j |\psi_j\rangle\langle\psi_j|.$$

The spectral theorem gives rise to the functional calculus, i.e., for any complex-valued function $f : \mathbb{R} \to \mathbb{C}$ we may define the operator $f(A)$ via

$$f(A) = \sum_{j=1}^{d} f(\lambda_j) |\psi_j\rangle\langle\psi_j|.$$

If our system is found in the state $\varphi \in \mathcal{H}$, the probability that the observable takes the simple eigenvalue λ_j is given by $|\langle\psi_j, \varphi\rangle|^2$, equipping the spectral decomposition with a physical meaning. This correspondence has become known under the name *Born's rule* and reflects the intrinsic probabilistic nature of quantum physics. In contrast, if a classical system is found at a specific point in the configuration space, all observables take a deterministic value. In the case that the configuration space is $\mathcal{Q}_N$ and the corresponding Hilbert space $\ell^2(\mathcal{Q}_N)$, we assign to a classical observable $V : \mathcal{Q}_N \to \mathbb{R}$ a quantum observable,

$$V := \sum_{\boldsymbol{\sigma}} V(\boldsymbol{\sigma})\, |\boldsymbol{\sigma}\rangle\langle\boldsymbol{\sigma}|, \tag{1.12}$$

which with a slight abuse of notation is denoted again by V. The correspondence (1.12) will be mostly used to associate to a classical spin glass potentials U a corresponding random diagonal operator.

As in classical statistical mechanics, the physics is governed by a Hamiltonian H describing the system's energy. As observable, the Hamiltonian is a self-adjoint operator on $\mathcal{H}$ and the time evolution of a wavefunction ψ is described by the Schrödinger equation (in natural units)

$$\partial_t \psi_t = -iH\psi_t, \tag{1.13}$$

where $\psi_t : \mathbb{R} \to \mathcal{H}$ describes the state of the system at times $t \in \mathbb{R}$. If H is time-independent, the unique solution of (1.13) is given by $\psi_t = U_t\psi_0$ with

$$U_t := e^{-itH}.$$

The family $(U_t)_{t\in\mathbb{R}}$ forms a strongly continuous group of unitaries and is reminiscent of Stone's theorem [159]. The eigenvectors of a Hamiltonian will often be called *eigenfunctions*, *eigenstates* or just *states* and the eigenvalues are often titled as *state energies* or just *energies*. Of particular importance is the state with the lowest energy, the *ground state*.

We will mostly consider random Hamiltonians H_N on $\ell^2(\mathcal{Q}_N)$, which shall model a quantum spin glass. One can think of H_N as random matrix and as in the classical situation, we will mostly forget about the underlying probability space. The time evolution of spin glasses is an interesting and challenging feat, but the main aim of this thesis is to gain insight into the equilibrium thermodynamics of quantum spin glasses. To this end, we need to adapt the notions for classical canonical ensembles to the quantum world. For a Hamiltonian H_N on $\ell^2(\mathcal{Q}_N)$, we define the partition function as

$$Z_N(\beta) := \operatorname{Tr} e^{-\beta H_N} = \sum_{\boldsymbol{\sigma}} \langle \boldsymbol{\sigma} | e^{-\beta H_N} | \boldsymbol{\sigma} \rangle, \tag{1.14}$$

where Tr denotes the trace of a matrix and, accordingly, we set the quantum pressure

$$\Phi_N(\beta) = \ln Z_N(\beta). \tag{1.15}$$

(1.14) and (1.15) coincide with the corresponding classical definitions (1.1) and (1.2) if the Hamiltonian H_N is classical, i.e., diagonal in the configuration basis $|\boldsymbol{\sigma}\rangle$. The pressure is again a random variable for disordered models; and it is convex and typically positive. The limit of the specific pressure will be again denoted by $p(\beta)$. If the Hamiltonian H_N depends on other parameters, say $\boldsymbol{\alpha}$, we often write $Z_N(\beta, \boldsymbol{\alpha})$ to make the dependence on the additional parameters present.

The thermodynamics of a model is encoded in the pressure Φ_N and, thus, one of our main goals will be to understand how Φ_N behaves for large N. We recall that the evaluation of the trace does not depend on the chosen basis and, hence, if $(E_j)_{j=1,\dots 2^N}$ denote the energies of H_N (including multiplicities), one has

$$Z_N(\beta) = \sum_j e^{-\beta E_j}.$$

Consequently, pressure and partition function only depend on the spectrum of H_N, which makes the importance of a spectral analysis apparent. However, if one wants to understand the system's state and thermal averages of other observables, the eigenfunctions of H_N also play a major role. The quantum analog of the classical Gibbs measure μ_β is the Gibbs state ρ_β, which is a *density matrix* on $\ell^2(\mathcal{Q}_N)$. We recall that a density matrix ρ on a Hilbert space $\mathcal{H}$ is a self-adjoint, positive semi-definite operator with trace one. The Gibbs state is defined as

$$\rho_\beta := \frac{e^{-\beta H_N}}{Z_N(\beta)},$$

generalizing (1.3). The thermal average of an observable A is denoted by $\langle A \rangle_\beta$ and defined as

$$\langle A \rangle_\beta := \operatorname{Tr}(\rho_\beta A).$$

We stress that for disordered systems the Gibbs state is a random density matrix. As for classical spin glasses, replicas form an important concept. The product space becomes the k-fold tensor product $\ell^2(\mathcal{Q}_N) \otimes \cdot \otimes \ell^2(\mathcal{Q}_N)$ equipped with the density matrix $\rho_\beta^{\otimes k} := \rho_\beta \otimes \cdots \otimes \rho_\beta$.

1.2.2 Quantum Spin Glass Models

After these preliminaries on quantum mechanics and quantum statistical physics, we turn to the description of quantum spin glass models. The Hamiltonians H_N of interest are constructed in terms of spin-$\frac{1}{2}$ operators. At this point, it is instructive to note that

$$\ell^2(\mathcal{Q}_N) \simeq \mathbb{C}^2 \otimes \cdots \otimes \mathbb{C}^2, \tag{1.16}$$

that is, the Hilbert space $\ell^2(\mathcal{Q}_N)$ is isomorphic to the N-fold tensor product of $\mathbb{C}^2$. To put it in other words, we can think of the N-particle Hilbert space as consisting of N qubits, similarly as in the classical world where we considered N classical bits. On $\mathbb{C}^2$, the *Pauli matrices* or *spin-$\frac{1}{2}$ operators* are

$$S^x := \begin{pmatrix} 0 & 1 \\ 1 & 0 \end{pmatrix}, \qquad S^y := \begin{pmatrix} 0 & -i \\ i & 0 \end{pmatrix}, \qquad S^z := \begin{pmatrix} 1 & 0 \\ 0 & -1 \end{pmatrix}, \tag{1.17}$$

which are all Hermitian matrices with -1 and 1 as eigenvalues. Moreover, they satisfy the canonical commutator relations

$$[S^v, S^w] = 2i \sum_{u=x,y,z} \varepsilon_{v,w,u} S^u$$

for $v, w \in \{x, y, z\}$. Here, $[A, B] := AB - BA$ denotes the commutator of two linear operators and $\varepsilon_{v,w,u}$ is the Levi-Civita symbol, which vanishes if v, w, u is not a permutation of x, y, z and otherwise agrees with the sign of the permutation mapping x, y, z to v, w, u in this order. In physics, the spin-$\frac{1}{2}$ operators are defined as $\frac{1}{2}$-multiple of the Pauli matrices from (1.17), but we defer from this convention here. We now make use of (1.16) to define for $v \in \{x, y, z\}$ and $j = 1, \dots N$ the corresponding spin operator S_j^v acting on the j-th qubit,

$$S_j^v = \mathbb{1}^{\otimes(j-1)} \otimes S^v \otimes \mathbb{1}^{\otimes(N-j)}$$

with the identity operator $\mathbb{1}$.

Let us now eventually consider some concrete examples for quantum spin glass models. As we have already discussed in the classical setting, short-range spin glasses are not feasible. Consequently, we will only consider mean-field quantum spin glasses. To motivate the first model, we first note that the configuration bases $|\boldsymbol{\sigma}\rangle$ diagonalizes all spin-z operators S_j^z, namely $S_j^z|\boldsymbol{\sigma}\rangle = \sigma_j|\boldsymbol{\sigma}\rangle$. This allows us to write the classical SK potential from (1.5) (interpreted as diagonal operator) as

$$U_{\mathrm{SK}} = \frac{1}{\sqrt{N}} \sum_{1 \le i < j \le N} g_{i,j} S_i^z S_j^z.$$

A very natural instinct is now to replace the commuting interaction terms $S_i^z S_j^z$ by Heisenberg-type interactions

$$H_{\mathrm{HSK},N} := \frac{1}{\sqrt{N}} \sum_{1 \le i < j \le N} g_{i,j} \vec{S}_i \cdot \vec{S}_j = \frac{1}{\sqrt{N}} \sum_{1 \le i < j \le N} g_{i,j} \sum_{v=x,y,z} S_i^v S_j^v. \tag{1.18}$$

The Hamiltonian in (1.18) gives rise to the Heisenberg-Sherrington-Kirkpatrick (HSK) model. Unfortunately, a rigorous analysis of the HSK model appears to be not achievable with the currently available methods. So far, there exists not even an argument which shows the existence of the limiting specific pressure. A main obstacle is that the interpolation technique, which was employed by Guerra and Toninelli

to establish the limit in the SK model [100], loses its power if applied to models with quantum interactions. Another challenge – which will be also present in the transversal field models to be discussed next – one has to face is the sparsity of the random matrix $H_{\mathrm{HSK},N}$. Indeed, the HSK Hamiltonian is vastly different from prominent ensembles, such as the Gaussian Unitary Ensemble (GUE), intensely studied in random matrix theory. As a result, the canonical methods of random matrix theory, for example the moment method, only reveal the properties of the *bulk*, consisting of eigenvalues which grow like $\sqrt{N}$ [72]. However, spin glass features can only be understood if one has got some information about the extensive eigenvalues growing linearly in N. Even from the physical side, the HSK is not well understood and its analysis is based on numerical computations or not reliable approximations [92, 93, 162]. The study of quantum spin glasses which contain "real" quantum interactions might be a rewarding research area in the future.

Our main focus are transversal field models with Hamiltonians of the form

$$H_N = U + \Gamma T \tag{1.19}$$

with a classical spin glass potential U, e.g. the REM potential U_{REM}, a nonnegative constant $\Gamma \geq 0$, which can be interpreted as the strength of the transversal magnetic field, and the operator

$$T := -\sum_{j=1}^{N} S_j^x, \tag{1.20}$$

being the negative sum of the spin-x operators. The operator T from (1.20) agrees up to a sign with the adjacency matrix of the Hamming cube endowed with the Hamming distance $d(\boldsymbol{\sigma}, \boldsymbol{\sigma}') := \frac{1}{2}\sum_{i=1}^{N} |\boldsymbol{\sigma}_i - \boldsymbol{\sigma}_i'|$ as graph distance and its action on a wavefunction $\psi \in \ell^2(\mathcal{Q}_N)$ can be alternatively written as

$$(T\psi)(\boldsymbol{\sigma}) = -\sum_{\boldsymbol{\sigma}' \,:\, d(\boldsymbol{\sigma},\boldsymbol{\sigma}')=1} \psi(\boldsymbol{\sigma}').$$

In Section 2.2, we discuss the spectral properties of T and we will see that T gives rise to a probabilistic representation of the quantum pressure in terms of Poissonian paths. The path-integral representation is one reason why transversal field models are more approachable than quantum spin glasses with quantum interactions. Another reason is that the randomness is restricted to the diagonal of the operator, such that one can separate the glass behavior from the paramagnetic perturbation T to some degree by means of matrix analytic methods. Moreover, some classical strategies such as Gaussian interpolation can be adapted to transversal field models.

In spite of being simpler than the HSK model, transversal field models (1.19) display a rich physics which is only partly understood. One not only expects a glass transition even for $\beta = 0$, but also ergodic behavior for high temperatures and strong enough transversal fields. It is anticipated that ergodicity is carried by quantum tunneling. On the other hand, quantum spin glasses in there glass phase might serve as important models for many-body localization [175]. Let us take as an example the arguably physically most influential quantum spin glass, the Quantum Sherrington-Kirkpatrick (QSK) model. The QSK Hamiltonian is the random matrix H_N from (1.19) with $U = U_{\mathrm{SK}}$. While for the classical SK models one knows that the glass transition occurs at $\beta = 1$, and also in presence of a vertical field there is an analytic prediction for the transition in form of the de Almeida-Thouless line [57], such a closed expression for the phase

separation line in the QSK model has not been found yet [175]. Indeed, most prediction on the QSK are based on numerics, which can only be performed for small particle numbers N since the dimension of the Hilbert space grows exponentially. Also, analytic work is typically based on approximations, which may not be valid as has been shown in [126]. Thus, one has to be careful with the interpretation of the results in the physics literature (in particular concerning more subtle properties such as ergodicity), and a mathematical study of the QSK is very much required. What we know so far about the QSK is rather limited and will be presented in Chapter 5.
In the case of the Quantum Hopfield model, one knows even less. Some physical predictions are collected in [175]. On the rigorous side, the only result we know about concerns the $\alpha \to 0$-limit [165]. It has been shown that the pressure satisfies for small $\alpha > 0$,

$$\Phi_N(\beta, \Gamma, M = \alpha N) - \Phi_N(\beta, \Gamma, M = 1) = \mathcal{O}(\alpha^3),$$

where here and in the rest of this thesis $\mathcal{O}, o$ stand for Landau's O-notation, see e.g. [144, Chapter 3.2.1]. That is, the Quantum Hopfield model resembles for small pattern number M the Curie-Weiß model in a transverse field.
The situation improves if one considers simpler quantum spin glasses such as the Quantum Random Energy Model (QREM) with $U = U_{\text{REM}}$ or, more generally, hierarchical quantum spin glasses with a GREM (or CREM) Gaussian process. The QREM has been studied actively since the 1990s [23, 95, 110, 111, 124] and many precise prediction on the thermodynamics have been figured out. We will discuss the literature on the QREM in more detail in Section 3.5. However, there is barely any rigorous work and one aim of this thesis is to fill this gap. In Chapter 2 and 3 – based on our articles [128, 129, 132] – we confirm Goldschmidt's formula for the specific pressure [95] and give a precise description of the low energy spectrum. Since the QREM is probably the simplest quantum spin glass, ergodic properties are most likely to be formally established in the QREM. We hope to stimulate further research in this direction. Surprisingly, more general hierarchical quantum spin glasses have not been considered yet in the physics literature despite the popularity of Derrida's models in the classical setting. In that sense, the phase diagrams, that we have derived in [130, 131] and which will be presented in Chapter 4, contribute to the physics literature. Our results show multiple phase transition and clarify the different behavior of a transversal and a longitudinal field. We hope that these work shed some light on the nature of quantum spin glasses.

1.2.3 Applications of Quantum Spin Glasses

We want to close this section by providing two motivating applications of quantum spin glasses. The first example lies in the field of quantum computing and our second application is motivated by mathematical biology, and has been already announced in the discussion of the REM.

The Quantum Adiabatic Algorithm and Spin Glasses

Quantum computers are built of qubits, i.e. spin-$\frac{1}{2}$ particles, instead of classical $0-1$-bits and the classical Boolean gates are replaced by unitary gates. By exploiting the fundamental quantum principles such as superposition and entanglement, quantum computers may outperform classical devices by far. The probably most famous quantum algorithms, which speed up their classical counterparts, are Grover's

and Shor's algorithm (see [144] and the references therein). The Grover search algorithm only needs $\mathcal{O}\left(\sqrt{N}\right)$ operations to find a specific element in an unstructured array of length N. Shor's algorithm challenges classical cryptography as it allows to find the prime factors of an integer in polynomial time. These exciting results made quantum computing a very active and fast developing area of research. Even leading tech companies invest in quantum computing research since they hope that quantum devices will turn to a profitable technology in the 21st century. However, there has not been found an efficient quantum algorithm for NP-complete problems; and future will show if a realization of quantum computers with a large number of qubit will eventually succeed.

We are here interested in the Quantum Adiabatic Algorithm (QAA), which might be implemented on quantum computers in the future [24]. Suppose, we are given a complicated Hamiltonian H_0 on a finite-dimensional Hilbert space $\mathcal{H}$ and we are interested in the ground state ψ and ground state energy E_{GS} of H_0. The basic idea of QAA is to consider first another simpler Hamiltonian H_1 whose ground state φ is easy to prepare. We now slowly interpolate between H_0 and H_1, that is, we consider the time-dependent Hamiltonian

$$H(t) = \left(1 - \frac{t}{T}\right) H_1 + \frac{t}{T} H_0$$

for $t \in [0, T]$ which agrees with H_1 at the beginning and ends up at H_0. The corresponding Schrödinger evolution is given by

$$\frac{d}{dt}\varphi_t = -iH(t)\varphi_t. \tag{1.21}$$

Starting with the initial condition $\varphi_0 = \varphi$ one might hope that, if the final time T is chosen large enough or, equivalently, the Hamiltonian $H(t)$ changes slowly enough, the final state φ_T under the propagation of (1.21) resembles the sought after ground state ψ of H_0. This intuition is made precise by the Quantum Adiabatic Theorem of which several versions exist. Let us present one of them.

Theorem 1.1 (Theorem 3 and Theorem 4 in [109])
Let $T > 0$ and H_0 and H_1 be as above with unique ground states ψ and φ. Let us further denote by $\Delta(t)$ the spectral gap of $H(t)$, that is, the difference between ground state energy and first excited energy of $H(t)$ and we set

$$\Delta = \inf_{t\in[0,T]} \Delta(t),$$

which in fact does not depend on T. Then,

$$|\langle \varphi_T, \psi\rangle|^2 \geq 1 - \frac{c(\|H_0\| + \|H_1\|)}{T\Delta^2}, \tag{1.22}$$

with the operator norm $\|\cdot\|$ and some constant $c > 0$.

An important application of QAA are classical NP-hard combinatorial optimization problems such as the Travelling Salesman problem or the Max-Cut problem on a graph. These problems can be encoded in a potential U on $\mathcal{Q}_N$ by relating each configuration $\boldsymbol{\sigma}$ to a possible path or, respectively, cut of the graph. $U(\boldsymbol{\sigma})$ agrees then with the classical objective function of the optimization problem and the goal is to find the minimum of U. The simpler Hamiltonian H_1 is typically chosen to be the transversal field T as it ground state is equally delocalized over the Hamming cube. Thus, studying the performance of QAA at solving combinatorial optimization problems coincides with the analysis of transversal field models from (1.19). We note that in this case the ground state is unique for $t \neq T$ due to the Perron-Frobenius theorem.

Furthermore, if one wants to understand how well QAA works in general, spin glasses form a well-suited benchmark as finding the ground state of spin glasses is a generically hard task [24].
The estimate (1.22) tells us that level-crossing is avoided if one chooses $T \gg \Delta^{-2}$. Unfortunately, it is expected that Δ is exponentially small in N for most spin glass models and this has been proven for the QREM [9, 132]. Nevertheless, if one does not ask for an approximation of the ground state itself, but only for a relative approximation of the ground state energy, a polynomial time T might be sufficient. To clarify this point, one needs a good understanding of quantum spin glasses' behavior under time evolution [24, 110, 111, 139].

Mutation-Selection Models and Spin Glasses

We now turn to an application of quantum spin glasses in the context of mutation-selection models in theoretical population genetics. We follow the exposition [104]. We consider an infinite population whose individuals are described by their genotype taking a value in $\{1, \dots, M\}$. Let $p_i(t)$ denote the relative fraction of the genotype i in the total population at time t. Of course, $\sum_i p_i(t) \equiv 1$. The evolution of $(p_i(t))_{i=1,\dots,M}$ is governed by a system of ordinary differential equations (ODE)

$$\frac{d}{dt}p_i(t) = [R_i - \bar{R}(t)]p_i(t) + \sum_j [m_{i,j}p_j(t) - m_{j,i}p_i(t)]. \tag{1.23}$$

R_i is the *Malthusian fitness* of type i and can be understood as difference between birth and death rate. The evolution (1.23) favors species of higher fitness reflecting a Darwinistic understanding of genetic evolution. $\bar{R}(t) = \sum_i R_i p_i(t)$ is the mean fitness at time t and $m_{i,j}$ is the mutation rate from j to i. The ODE (1.23) can be seen as Master equation for a jump process, which is in general not Markovian due to the time-dependent factor $\bar{R}(t)$.
The most prominent genotype space is the Hamming cube $\mathcal{Q}_N$ with $M = 2^N$ and the values of σ_i can be interpreted as two different alleles of a biallelic multilocus model. It is then natural to assume that only one allele mutates at the same time, that is, $m_{\boldsymbol{\sigma},\boldsymbol{\sigma}'} \neq 0$ only if $d(\boldsymbol{\sigma}, \boldsymbol{\sigma}') \leq 1$. For simplicity we will assume that the transition rates are all equal to some $\Gamma > 0$ and, in particular, symmetric. However, asymmetric models which favor a mutation towards $+1$ are considered in the literature as well. Note that then $m_{\boldsymbol{\sigma},\boldsymbol{\sigma}} = -\Gamma N$ for all $\boldsymbol{\sigma} \in \mathcal{Q}_N$. Introducing the probability vector $\boldsymbol{p}(t)$ with components $p_{\boldsymbol{\sigma}}(t)$ for $\boldsymbol{\sigma} \in \mathcal{Q}_N$, the ODE (1.23) becomes

$$\frac{d}{dt}\boldsymbol{p}(t) = -(H_N + \bar{R}(t))\boldsymbol{p}(t) \tag{1.24}$$

with the Hamiltonian $H_N = -R + \Gamma T + \Gamma \mathbb{1}$, where R is the diagonal operator with diagonal elements $R(\boldsymbol{\sigma})$. Up to the factor $\bar{R}(t)$, the dynamics is governed by a transversal field Hamiltonian. This correspondence was first noted in [20] and opens the door to an analysis of gene mutation models with methods from statistical physics. Moreover, there is biological evidence that the fitness landscape $R(\boldsymbol{\sigma})$ should be rugged, that is, it should contain several local minima. As spin glass models are characterized by rugged energy landscapes, they form a popular and instructive model for R. Up to any identity shift, we end up with the study of quantum spin glasses. In fact, the relation between the quantum model corresponding to H_N and the gene mutation-selection process (1.24) is even closer since physical properties of H_N are reflected in characteristics of the evolution. Let us demonstrate that idea for the normalized ground state

ψ of H_N. We first note that the Perron-Frobenius theorem implies that the normalized ground state ψ is unique (up to a phase), and ψ can be chosen to be positive. Moreover, we can explicitly solve (1.23) in terms of the semigroup $T(t) = e^{-tH_N}$ and the start distribution $\boldsymbol{p}_0$ at time $t = 0$,

$$\boldsymbol{p}(t) = \frac{T(t)\boldsymbol{p}_0}{\sum_{\boldsymbol{\sigma},\boldsymbol{\sigma}'} T_{\boldsymbol{\sigma},\boldsymbol{\sigma}'}(t) p_{\boldsymbol{\sigma}'}}$$

with the matrix elements $T_{\boldsymbol{\sigma},\boldsymbol{\sigma}'}$ of T. For large t the exponential matrix $T(t)$ is governed by the ground state of H_N and, thus, for any start distribution

$$\lim_{t\to\infty} \boldsymbol{p}(t) = \frac{1}{\|\psi\|_{\ell^1}}\psi$$

with the ℓ^1-norm $\|\psi\|_{\ell^1} := \sum_{\boldsymbol{\sigma}} |\psi(\boldsymbol{\sigma})|$. The normalization with respect to the ℓ^1-norm (instead of the physically more common ℓ^2-norm) amounts to the fact that we consider probability distributions. $\frac{1}{\|\psi\|_{\ell^1}}\psi$ can be interpreted as equilibrium distribution as it forms a stationary solution of (1.24). We remark that the ℓ^2-normalized physical ground state ψ, or more precisely its squared components $\psi(\boldsymbol{\sigma})^2$, gives rise to the *ancestral distribution*. This biological interpretation of ψ relies on the ODE (1.23) underlying probabilistic description in terms of branching processes. The ancestral distribution can be found by studying the branching process backwards in time [104].

1.3 Outline and Main Results of the Thesis

We close the introduction by giving an overview of the forthcoming chapters and the results discussed therein.

1. Chapter 2 starts with the systematic study of the QREM. In a first preliminary Section 2.1, we review the thermodynamics of the REM. This allows us to get more familiar with basic concepts such as the pressure, self-averaging and the replica overlap in this simple setting. Section 2.2 continues with preparatory considerations on the transversal field T. For the reader's convenience we collect some simple facts on the eigenstates of T and take the chance to introduce the path-integral framework, which will be used in forthcoming sections several times. In Section 2.3, the QREM Hamiltonian is considered. We present the surprisingly simple Goldschmidt formula for the specific pressure, which tells us that the QREM behaves either as the classical REM or as pure quantum paramagnet. We sketch our proof from Core Article I [128] and present next our result from Article V [129], which draws a connection between the QREM and the quantum p-spin models. The final Section 2.4 deals with our Article VII [88], where we consider the large deviations of path observables in the REM. After giving an overview on trajectory thermodynamics, it becomes apparent that the path integral representation implies that dynamical properties of spin glasses are in fact closely related to the static thermodynamics of quantum spin glasses. We then focus on the REM under the all-to-all dynamics. In this situation, we have managed to determine the rate function of the potential integrated along paths.

2. Chapter 3 continues the study of the QREM. Here, we mainly discuss the results of Article IV [132], where we have provided a detailed analysis of the low energy states in the glass phase $\Gamma < \beta_c$ and

in the paramagnetic phase $\Gamma > \beta_c$. In Section 3.1 we begin with some heuristics. Based on second order perturbation theory, we obtain a first idea on the $\mathcal{O}(1)$ ground state energy shift in both phases. In the following Sections 3.2 and 3.3 we not only confirm these predictions on the ground state energy, but we will also see that the whole low energy spectrum is governed by a deterministic shift of the eigenvalues of U or, respectively, ΓT. Moreover, the corresponding eigenfunctions are sharply localized in the glass phase and completely delocalized in the paramagnetic phase. This establishes a localization-delocalization transition at the edge of the spectrum in high contrast to the Anderson model on a finite-dimensional lattice. In Section 3.4 we determine the pressure up to order $o(1)$. As the corresponding proofs a rather long, we are not able to present them in their entirety, but we still describe some key steps, so that reader gets an idea on how a variety of methods come into play in the spectral analysis of the QREM. The final Section 3.5 puts our results into the context of the mathematics and physics literature and discusses further reaching conjectures on ergodicity and many-body localization in the QREM.

3. Chapter 4 is devoted to the study of hierarchical quantum spin glasses. In Section 4.1, we recall the thermodynamics of the GREM and its continuous cousin, the CREM. In particular, the known results on the pressure, the extremal statistics and the distribution of the replica overlap are summarized. The following Section 4.2 presents our theorems from Core Article II [130] on their quantum version. We give an explicit expression for the pressure in the thermodynamic limit, whose rich structure is reflected in the corresponding phase diagrams. The main tools for the proof, the peeling principle and the by now standard Gaussian interpolation, are discussed. We are further interested in the de Almeida-Thouless (AT) line in quantum models for which we have to consider an additional longitudinal field. In Section 4.3, we give an overview on replica-symmetry and the AT transition in the classical SK model. Then, we are prepared to study the quantum AT line in the QCREM in Section 4.4. We summarize our results from Core Article III [131] and in particular focus on the difference between implementing the vertical field by means of standard z-spin operators and making use of a hierarchical field. We will see that the first choice causes an increasing glass phase as the vertical field becomes stronger, whereas the later choice is more physical since a hierarchical field destabilizes the glass phase.

4. Chapter 5 focuses on the Quantum Sherrington-Kirkpatrick model. The classical SK model is the prime example for a mean-field spin glass and the underlying structure is believed to be universal. In Section 5.1 we describe the Parisi formula for mixed p-spin potentials. Thereafter, we show the central ideas which lead to a rigorous proof of the Parisi formula, namely the Aizenman-Sims-Starr scheme, Guerra's interpolation bound and Panchenko's ulltrametricity theorem based on the Ghirlanda-Guerra identities. After having familiarized ourselves with the emergent hierarchical replica structure in the SK model, we move on to the quantum SK model. We concentrate on recently established rigorous results for the QSK: an infinite-dimensional Parisi type formula for the specific pressure introduced in [3], and an analysis of the high-temperature phase and the annealed pressure carried out in [126]. The later work shows the absence of glass order for $\beta < 1$. The complementary result that there is a glass phase for $\beta > 1$ and a weak transversal field has been established in our Article VI [125]. In Section 5.3, we present the methods which have enabled us to prove the persistence of the glass phase.

Chapter 2

The Quantum Random Energy Model: Phase Diagram

In this chapter, we begin with a review of our results on the QREM and trajectory dynamics in the REM by presenting the main ideas and novel theorems of Core Article I [128], Article V [129] and Article VII [88]. We will first recall the classical Random Energy Model and present the limit theorems for its pressure and replica overlap. We close this first section with a discussion of the REM partition function's fluctuations. Our second section then focuses on the transversal field T. We collect some common knowledge on its spectral properties and we further present how the partition function of transversal field models can be reformulated in terms of path integrals. While we will not make use of the Feynman-Kac representation in the analysis of the QREM, it is an important method widely used in the physics literature, and it will reappear in the discussion of trajectory dynamics. The third section is largely a summary of the main theorem in Core Article I. We discuss Goldschmidt's formula for the QREM pressure and the resulting phase diagram. We also give an overview of our proof method. Moreover, we incorporate the main result of Article V, which shows that the QREM can be considered as limit of quantum p-spin models - generalizing the well-known fact that the REM is the limit of classical p-spin interactions. The final section introduces the concept of trajectory thermodynamics, that is, the study of trajectory observables along a Markov dynamics. We deal with the REM potential integrated along paths and mainly study its large deviations. We will see that analyzing trajectories of classical spin glasses is closely related to the study of quantum spin glasses. For instance, the QREM resembles the trajectory thermodynamics of the REM under a next neighbor random walk. The main findings in Article VII, however, focus on the all-to-all dynamics where the paths may jump from a configuration to any different configuration with the same probability. In this situation, we have found an explicit expression for the rate function of the corresponding large deviation principle.

2.1 The Random Energy Model

As we have mentioned in the introduction, the REM has become important in a variety of fields. However, we will only discuss the aspects of the REM in context of spin glass theory as we will only make use of its thermodynamical properties in the forthcoming sections and chapters. Our presentation is largely based on Chapter 9 in [36]. The independence of the potential $U_{\mathrm{REM}}(1.8)$ – which we will simply denote

by U in this chapter – simplifies the analysis of the REM compared to other spin glass models drastically; yet the REM phase diagram is nontrivial as it exhibits a glass phase with a nonvanishing order parameter. We start our review on the REM by discussing its extremal properties. In fact, the extremal properties of independent processes are well known: after an appropriate rescaling the minimum converges in distribution to either a Gumbel, Fréchet or Weibull random variable [122]. The Gaussian distribution falls into the Gumbel class and the needed rescaling s_N follows from a direct computation,

$$s_N(x) := -\beta_c N + \frac{\ln(N \ln 2) + \ln(4\pi)}{2\beta_c} - \frac{x}{\beta_c}.$$

The numerical constant $\beta_c := \sqrt{2 \ln 2}$ will appear frequently in the discussion of the REM and QREM as $-\beta_c$ coincides with the specific ground state energy of the REM in the thermodynamic limit. A precise characterization of the REM minimum is given by the following proposition.

Proposition 2.1 (Lemma 9.1.1 in [36])
Let U be the REM potential on $\mathcal{Q}_N$. Then,

$$\mathbb{P}\left[\min_{\boldsymbol{\sigma} \in \mathcal{Q}_N} U(\boldsymbol{\sigma}) \geq s_N(x)\right] = (1 - 2^{-N} e^{-x + o(1)}) \to e^{-e^{-x}},$$

where the $o(1)$ estimate is uniform on any bounded interval. In particular, we have almost surely and in mean

$$\lim_{N \to \infty} \min_{\boldsymbol{\sigma} \in \mathcal{Q}_N} \frac{1}{N} U(\boldsymbol{\sigma}) = -\beta_c = -\sqrt{2 \ln 2}.$$

Typically, the analysis of spin glasses becomes more difficult for lower temperatures since replica symmetric breaking leads to a more involved distribution of the replica overlap with respect to the Gibbs measure. In particular, understanding the ground state is a very challenging problem in spin glass models. Since standard extreme value theory leads to a precise description of the REM minimum, it is not surprising that the limit of the REM pressure can be computed for all temperatures. To motivate this classical result on the REM, we recall that the partition function $Z_N(\beta) = \sum_{\boldsymbol{\sigma} \in \mathcal{Q}_N} e^{-\beta U(\boldsymbol{\sigma})}$ is just the sum of 2^N independent random variables. Hence, it is natural to guess that Z_N concentrates around its mean due to the law of large numbers, i.e.,

$$Z_N(\beta) \approx \mathbb{E}[Z_N(\beta)] = 2^N e^{\frac{1}{2}\beta^2 N}.$$

One would conclude that the annealed and quenched specific pressure agree asymptotically:

$$\frac{1}{N}\mathbb{E}[\Phi_N(\beta)] \approx \frac{1}{N} \ln\left(\mathbb{E}[Z_N(\beta)]\right) = \frac{1}{2}\beta^2 + \ln 2.$$

However, one quickly realizes that this calculation cannot be true for all inverse temperatures, as it would imply an unbounded ground state energy. More precisely, the derivative of the pressure coincides up to a sign with the internal energy,

$$\frac{d}{d\beta}\frac{1}{N}\mathbb{E}[\Phi_N(\beta)] = -\frac{1}{N}\langle U \rangle_\beta = -\frac{1}{N}\frac{\mathbb{E}[\sum_{\boldsymbol{\sigma} \in \mathcal{Q}_N} U(\boldsymbol{\sigma}) e^{-\beta U(\boldsymbol{\sigma})}]}{Z_N(\beta)} \leq -\frac{1}{N} \min_{\boldsymbol{\sigma} \in \mathcal{Q}_N} U(\boldsymbol{\sigma}) = \beta_c + o(1).$$

So, the maximal slope of the specific pressure is β_c in the thermodynamic limit, which tells us that annealed and quenched pressure cannot agree for $\beta > \beta_c$. The simplicity of the REM is reflected in the fact that these simple heuristics correctly predict the limit of the specific pressure: annealed and quenched pressure agree for $\beta \leq \beta_c$; and for $\beta > \beta_c$ the pressure grows linearly with slope β_c:

Theorem 2.2 ([62, 148], Theorem 9.1.2 in [36])
The specific pressure in the REM converges in mean,

$$\lim_{N\to\infty} \frac{1}{N}\mathbb{E}[\Phi_N(\beta)] = p_{REM}(\beta) := \begin{cases} \frac{1}{2}\beta^2 + \ln 2, & \text{if } \beta \leq \beta_c \\ \beta_c\beta & \text{if } \beta > \beta_c. \end{cases} \tag{2.1}$$

The main challenge in the proof of Theorem 2.2 is the high temperature regime, where one has to verify that annealed and quenched pressure asymptotically agree. To that end, one may use the second moment method - a widely used technique in spin glass theory [6, 181] to bound the variance of the (truncated) partition function. The low temperature regime follows by employing convexity and the characterization of the minimum in Proposition 2.1 [36]. From the limit (2.1), we can read off a second-order phase transition at the critical inverse temperature β_c, where quenched and annealed pressure start to differ. We recall that the *entropy* S of a probability measure μ on a discrete space Ω is defined as $S(\mu) := \sum_{\omega\in\Omega} -\mu(\omega)\ln(\mu(\omega)) \geq 0$ and

$$\Phi_N(\beta) = -\beta\langle U\rangle_\beta + S(\mu_\beta),$$

with the Gibbs measure $\mu_\beta(\boldsymbol{\sigma}) := e^{-\beta U(\boldsymbol{\sigma})}/Z_N(\beta)$ [167]. Consequently, the specific entropy of the REM vanishes for $\beta \geq \beta_c$, that is, the REM undergoes a transition to a completely frozen phase where only the minimum and a non-extensive number of excited configurations dominate the thermodynamics. That drastic freezing of the system is very specific to the REM.

Next, we want to embed the REM in the context of spin glass theory. To do so, we note that the order parameter of the REM transition is in fact Parisi's functional order parameter, which is omnipresent in the study of classical spin glasses [155, 181]. Let μ_N^P the measure on $[-1, 1]$ characterizing the mean replica overlap distribution, that is,

$$\mu_N^P([-1, q]) := \mathbb{E}\left[\langle \mathbb{1}_{R_N\leq q}\rangle_\beta^{\otimes^2}\right] = \mathbb{E}\left[\frac{\sum_{\boldsymbol{\sigma},\boldsymbol{\sigma}'} \mathbb{1}_{R_N\leq q}(\boldsymbol{\sigma},\boldsymbol{\sigma}')e^{-\beta(U(\boldsymbol{\sigma})+U(\boldsymbol{\sigma}'))}}{Z_N(\beta)^2}\right]. \tag{2.2}$$

The limit of μ_N^P can be computed explicitly in the REM:

Proposition 2.3 (Theorem 9.4.1 and Lemma 9.5.1 in [36])
The measure μ_N^P converges weakly,

$$\mu_N^P \xrightarrow{w} \mu^P = \begin{cases} \delta_0 & \text{if } \beta \leq \beta_c \\ \frac{\beta_c}{\beta}\delta_0 + \left(1 - \frac{\beta_c}{\beta}\right)\delta_1 & \text{if } \beta > \beta_c \end{cases}$$

with δ_x being the point measure at x.

We see that the Parisi measure undergoes a transition from a pure point measure to a sum of two point measures at the critical inverse temperature β_c, reflecting the glass nature of the REM. One speaks of an *1-step replica symmetric breaking*, since the Parisi measure's support changes from one point to two points at β_c. In case of the REM, one can even determine the limit of the random distribution of the replica overlap, that is, without taking the sample mean in (2.2). The overlap distribution then converges weakly to a random measure $\chi\delta_1 + (1-\chi)\delta_0$, where the random variable χ can be described in terms of a Ruelle process [36, 152]. We will discuss this point more generally for the GREM in Section 4.1.
We want to close this section by discussing the fluctuations of the pressure. Theorem 2.2 is formulated as the convergence of the quenched expectation and it is natural to wonder if the specific pressure converges almost surely, too. That is indeed true and it is strongly related to the fact that the fluctuations of the specific pressure $\frac{1}{N}\Phi_N$ are much smaller than its expectation and vanish in the limit - which is sometimes stated as the pressure being *self-averaging*. The mathematical tool to control fluctuations in Gaussian spin glass models is the Gaussian concentration inequality:

Theorem 2.4 (Theorem 1.3.4 in [181])
Let $F : \mathbb{R}^M \to \mathbb{R}$ be a Lipschitz function with Lipschitz constant L, and $g_1, \dots, g_M$ be independent standard Gaussian variables. Then

$$\mathbb{P}(|F(g_1, \dots, g_M) - \mathbb{E}F(g_1, \dots, g_M)| \geq Lt) \leq 2\exp\left(-\frac{t^2}{4}\right)$$

To obtain the explicit constants in the above formulation of the Gaussian concentration inequality, one employs the Gaussian interpolation method for a proof. An elegant approach, which is only based on the orthogonal invariance of standard Gaussian variables but yields a slightly weaker estimate, can be found in [133, 157]. A simple application of Theorem 2.4 shows that specific pressure in the REM converges to p_{REM} almost surely and in r-th mean for all $r \in [1, \infty)$. The Gaussian concentration inequality is a very general results, and can be used to derive useful concentration bounds even in situations where evaluating the expectation $\mathbb{E}F(g_1, \dots, g_M)$ is not feasible.
The drawback is that Theorem 2.4 does not reveal the exact order of the fluctuations. However, in order to obtain a full understanding of a model, a precise description of the degree of randomness is crucial. In the case of the REM the systematic study of its fluctuations originated in [85] and found its completion in [41]. To describe the results in the low temperature phase, we need to recall the definition of a *Poisson point process*. A *point process* on a measurable space $(\mathbb{X}, \mathcal{X})$ is a measurable map from some probability space to the space $(\mathbf{N}(\mathbb{X}), \mathcal{N}(\mathbb{X}))$ of all measures taking only values in $\mathbb{N}_0 \cup \{+\infty\}$. The sigma-algebra $\mathcal{N}(\mathbb{X})$ is defined to be the smallest sigma-algebra such that the map $\nu \mapsto \nu(B)$ is measurable for all $B \in \mathcal{X}$. A (σ-finite) Poisson process with intensity measure λ on $(\mathbb{X}, \mathcal{X})$ is a point process η on $(\mathbb{X}, \mathcal{X})$ such that [120, Definition 3.1]

1. λ is σ-finite and for every $B \in \mathcal{X}$ the random variable $\eta(B)$ is Poisson distributed with parameter $\lambda(B)$
2. For every $n \in \mathbb{N}$ and pairwise disjoint sets $B_1, \dots B_n \in \mathcal{X}$ the random variables $\eta(B_1), \dots \eta(B_n)$ are independent.

For each σ-finite measure λ there exists a Poisson point process with intensity measure λ and, moreover, the distribution of the Poisson point process is uniquely determined by λ. For a proof of this well-known

theorem and more details on Poisson processes we refer the reader to [120]. We will denote by $\mathcal{P}_\lambda$ a Poisson point process on $\mathbb{R}$ with intensity measure λ. We are ready to formulate the results on the fluctuations in the REM.

Theorem 2.5 ([41], Theorem 9.2.1 in [36])
The partition function of the REM has the following fluctuations:

1. *If $\beta < \beta_c/2$, then*
$$e^{\frac{N}{2}(\ln 2-\beta^2)} \ln \frac{Z_N(\beta)}{\mathbb{E}Z_N(\beta)} \quad \underrightarrow{w} \quad \mathcal{N}(0,1).$$
We denote by $\mathcal{N}(m,v)$ the distribution of a Gaussian with mean m and variance v.

2. *If $\beta = \beta_c/2$, then*
$$e^{\frac{N}{2}(\ln 2-\beta^2)} \ln \frac{Z_N(\beta)}{\mathbb{E}Z_N(\beta)} \quad \underrightarrow{w} \quad \mathcal{N}(0,1/2).$$

3. *If $\beta_c/2 < \beta < \beta_c$, then with the short-hand notation $\alpha := \beta/\beta_c$*
$$e^{\frac{N}{2}(\beta_c-\beta)^2+\frac{\alpha}{2}[\ln(N\ln 2)+\ln(4\pi)]} \ln \frac{Z_N(\beta)}{\mathbb{E}Z_N(\beta)} \quad \underrightarrow{w} \quad \int_{-\infty}^{\infty} e^{\alpha z}(\mathcal{P}_{e^{-x}dx}(dz) - e^{-z}dz).$$
Here, dx corresponds to the canonical Lebesgue measure on $\mathbb{R}$.

4. *If $\beta = \beta_c$, then*
$$e^{\frac{1}{2}[\ln(N\ln 2)+\ln(4\pi)]} \left(\frac{Z_N(\beta)}{\mathbb{E}Z_N(\beta)} - \frac{1}{2} + \frac{\ln(N\ln 2)+\ln(4\pi)}{4\sqrt{\pi \ln(2) N}} \right)$$
$$\underrightarrow{w} \int_{-\infty}^{0} e^{\alpha z}(\mathcal{P}_{e^{-x}dx}(dz) - e^{-z}dz) + \int_0^{\infty} e^{\alpha z}\mathcal{P}_{e^{-x}dx}(dz).$$

5. *If $\beta > \beta_c$, then*
$$e^{-N[\beta\beta_c]+\frac{\alpha}{2}[\ln(N\ln 2)+\ln(4\pi)]} Z_N(\beta) \quad \underrightarrow{w} \quad \int_{-\infty}^{\infty} e^{\alpha z}\mathcal{P}_{e^{-x}dx}(dz),$$
and
$$\Phi_N(\beta) - \mathbb{E}[\Phi_N(\beta)] \quad \underrightarrow{w} \quad \ln \int_{-\infty}^{\infty} e^{\alpha z}\mathcal{P}_{e^{-x}dx}(dz) - \mathbb{E}\ln\left[\int_{-\infty}^{\infty} e^{\alpha z}\mathcal{P}_{e^{-x}dx}(dz)\right].$$

Let us briefly discuss the fluctuation results of Theorem 2.5. The appearance of an exponential Poisson point process for low temperatures $\beta > \beta_c$ may be anticipated. By Theorem 2.2 we already know that energies close to the minimum govern the partition function for $\beta > \beta_c$, and it is a well known fact that under mild conditions the order statistics of an independent process is Poissonian. In case of the REM this reads as
$$\sum_{\boldsymbol{\sigma}\in\mathcal{Q}_N} \delta_{s_N^{-1}(U(\boldsymbol{\sigma}))} \to \mathcal{P}_{e^{-x}\,dx}. \tag{2.3}$$

That we have a central limit theorem (CLT) for small β, is not very surprising either, since the partition function is the sum of 2^N independent copies of the random variable $e^{\beta\sqrt{N}g}$, where g denotes a standard Gaussian. Indeed, in the regime $\beta < \beta_c/2$ the Lindeberg condition is satisfied. However, a natural first guess would be to expect a CLT to hold in the full non-glassy phase $\beta < \beta_c$. Instead, we see an additional transition at $\beta_c/2$, which is not present in the REM phase diagram. This new transition can be understood as follows. The fluctuations are essentially ruled by the second moment of $Z_N(\beta)$. However, $\mathbb{E}[Z_N^2(\beta)]$ contains a term which essentially corresponds to the partition function at inverse temperature 2β. Hence, the extremal process becomes already visible at $\beta = \beta_c/2$. While the fluctuations in both phases $\beta_c/2 < \beta < \beta_c$ and $\beta > \beta_c$ are of Poisson nature, there is still a key difference between the two regimes. For $\beta_c/2 < \beta < \beta_c$ the partition function's fluctuations are exponentially small compared to its mean $\mathbb{E}Z_N(\beta)$, whereas for $\beta > \beta_c$ the fluctuations are of the same order as $Z_N(\beta)$ itself.

2.2 Transversal Field and Path Integral Formalism

We start this section by collecting some generally known spectral properties of T as operator on $\ell^2(\mathcal{Q}_N)$. To this end, we recall from (1.20) that we may express T as the negative sum of Pauli-x-matrices,

$$T = -\sum_{i=1}^{N} S_i^x = -\sum_{i=1}^{N} \mathbb{1} \otimes \cdots \otimes \mathbb{1} \otimes S^x \otimes \mathbb{1} \otimes \cdots \otimes \mathbb{1},$$

where S_i^x acts on the i-th spin. This representation directly implies that an orthogonal basis consisting of eigenstates of T is given by product states formed by the eigenvectors $|+\rangle := 1/\sqrt{2}(e_1 + e_{-1})$ and $|-\rangle := 1/\sqrt{2}(e_1 - e_{-1})$ of S^x at each site. Here, e_1 and e_{-1} form the natural z-eigenstates for one spin. These product states coincide with the natural orthonormal basis for the Hadamard transformation, which diagonalizes T, and may be indexed by subsets $A \subset \{1, \dots, N\}$,

$$\Psi_A(\boldsymbol{\sigma}) := \frac{1}{\sqrt{2^N}} \prod_{j \in A} \sigma_j.$$

Note that all eigenvectors Ψ_A are maximally uniformly delocalized over the Hamming cube; in drastic contrast to the eigenstates of U which sit on one site. The eigenvalue corresponding to Ψ_A is $2|A| - N$ with the cardinality $|A|$ of the set A. Consequently, the spectrum of T consists of $N + 1$ eigenvalues,

$$\operatorname{spec} T = \{2n - N \mid n \in \mathbb{N}_0,\ n \leq N\},$$

with degeneracy given by the binomials $\binom{N}{n}$. In particular, the unique ground-state of T is $\Psi_\emptyset$ with energy $-N$. We stress that the norm of T and U are of the same order, in contrast to previous work concerning the Anderson model on the Hamming cube with a normalized Laplacian [19]. Last but not least, the specific pressure $p_{\mathrm{PAR}}(\beta)$ of the operator T does not depend on N and is given by

$$p_{\mathrm{PAR}}(\beta) := \frac{1}{N} \ln \operatorname{Tr} e^{-\beta T} = \frac{1}{N} \ln \left[\left(\operatorname{Tr} e^{-\beta S^x} \right)^N \right] = \ln 2 \cosh(\beta).$$

In particular the magnetization in x-direction,

$$m_x := -\frac{1}{N}\frac{\operatorname{Tr} T e^{-\beta T}}{\operatorname{Tr} e^{-\beta T}} = \frac{d}{d\beta} p_{\mathrm{PAR}}(\beta) = \tanh \beta, \tag{2.4}$$

grows from 0 to 1 as β increases.

In the second part of this section, we want to introduce the path integral representation for the partition function of general transversal field Hamiltonians $H = V + \Gamma T$, where V denotes an arbitrary potential on the Hamming cube. While we will not make direct use of the path integral formalism in the analysis of the QREM, it is the most common approach for quantum spin glasses in the physics literature [175] and some rigorous work on the QSK relies on path integrals [3, 126]. We will encounter the Feynman-Kac formula again in Section 2.4, when we study the trajectory dynamics. The key observation is that all matrix elements of $-T$ are nonnegative and, thus,

$$\langle \boldsymbol{\sigma} | e^{-\lambda T} | \boldsymbol{\sigma}' \rangle \geq 0$$

for all $\lambda \geq 0$ and $\boldsymbol{\sigma}, \boldsymbol{\sigma}' \in \mathcal{Q}_N$. We now invoke the Lie-Trotter formula [159, Theorem VIII.29],

$$e^{-\beta H} = \lim_{m\to\infty} [e^{-\beta V/m} e^{-\beta \Gamma T/m}]^m.$$

We can then rewrite the partition functions m-th Trotter approximation,

$$\sum_{\boldsymbol{\sigma}\in\mathcal{Q}_N} \langle \boldsymbol{\sigma} | [e^{-\beta V/m} e^{-\beta\Gamma T/m}]^m | \boldsymbol{\sigma} \rangle = \sum_{\boldsymbol{\sigma}_0, \boldsymbol{\sigma}_1, \dots \boldsymbol{\sigma}_{m-1} \in \mathcal{Q}_N} e^{-\frac{\beta}{m}\sum_{j=0}^{m-1} V(\boldsymbol{\sigma}_j)} \prod_{j=0}^{m-1} \langle \boldsymbol{\sigma}_j | e^{-\beta\Gamma T/m} | \boldsymbol{\sigma}_{j+1} \rangle$$

with $\boldsymbol{\sigma}_m = \boldsymbol{\sigma}_0$. After a normalization, we can interpret the factors $\langle \boldsymbol{\sigma}_j | e^{-\beta\Gamma T/m} | \boldsymbol{\sigma}_{j+1} \rangle$ as transition probabilities of a Markov chain along which the potential V is summed. In the $m \to \infty$ limit the first term should become a proper integral, the transition probabilities turn to transition rates which agree with the off-diagonal matrix elements of T, and the Markov chain should turn into a continuous time Markov jump process. Such a jump process can be interpreted as path on the Hamming cube. This is indeed true and the resulting identity can be seen as a Feynman-Kac type formula. The original Feynman-Kac formula deals with Schrödinger operators $-\Delta + V$ on $\mathbb{R}^d$ and the paths are distributed according to the Wiener measure [168]. In our case the path measure is based on independent Poisson processes.

To formulate the Feynman-Kac representation rigorously, we need to introduce some notation. We follow the construction in [3]. Let Ξ denote the space of càdlàg-paths from $[-1, 1]$. We work with the Borel σ-algebra on Ξ which is defined with respect to the Skorohod topology [112]. Moreover, let η_i be N independent Poisson point processes on $[0, 1]$ with intensity $\Gamma\beta dx$. These point processes allow us to define the random spin paths ξ_i,

$$[0, 1] \ni t \mapsto \xi_i(t) = (-1)^{\eta_i([0,t])} \in \Xi.$$

By construction, the functions $\xi_i(t)$ are càdlàg paths with almost surely finitely many jumps at the times t_j which form the support of the Poisson point process η_i. Consequently, the number of jumps in any

subinterval of length L follows a Poisson distribution with parameter $\beta\Gamma L$. We further denote by ν the distribution of ξ_i on Ξ and introduce the measure

$$\nu_0(A) := \frac{\nu(A\mathbb{1}_{\xi_i(1)=\xi_i(0)})}{\nu(\mathbb{1}_{\xi_i(1)=\xi_i(0)})}$$

which conditions on closed paths. Finally, we write $\xi = (\xi_1, \dots, \xi_N)$ and for any initial configuration $\boldsymbol{\sigma}$ we consider $\boldsymbol{\sigma} \cdot \xi(t) := (\sigma_1\xi_1(t), \dots, \sigma_N\xi_N(t))$ the corresponding process starting at $\boldsymbol{\sigma}$. The path integral representation is then given by the following theorem:

Theorem 2.6 (Corollary B.3 in [126])
For any potential V on $\mathcal{Q}_N$ and positive parameters $\beta, \Gamma > 0$ the partition function of the Hamiltonian $H = V + \Gamma T$ can be reformulated in terms of the path measure ν_0,

$$\operatorname{Tr} e^{-\beta H} = \sum_{\boldsymbol{\sigma}} \langle \boldsymbol{\sigma} | e^{-\beta H} | \boldsymbol{\sigma} \rangle = (\cosh \beta\Gamma)^N \sum_{\boldsymbol{\sigma} \in \mathcal{Q}_N} \int_{\Xi^N} d\nu_0^N \, e^{-\beta \int_0^1 V(\boldsymbol{\sigma} \cdot \xi(t))\, dt}, \tag{2.5}$$

where the path measure ν_0 is constructed as above and depends on $\beta\Gamma$.

In fact, one can use the path integral formalism to compute all matrix elements $\langle \boldsymbol{\sigma} | e^{-\beta H} | \boldsymbol{\sigma}' \rangle$ by considering Poisson jump processes starting at $\boldsymbol{\sigma}$ and terminating at $\boldsymbol{\sigma}'$. In [126], the path integral formula is even stated as an operator identity.

The main advantage of the Feynman-Kac representation is that the quantum partition function becomes a classical object. Indeed, if one interprets the term $\int_0^1 V(\boldsymbol{\sigma} \cdot \xi(t))\, dt$ as energy function of a path, we see that the path integral can be seen as the partition function of this energy functional. In particular, one deals with commutative expressions and one can apply methods of probability theory to analyze the path integrals. In contrast, a direct approach to $e^{-\beta H}$ typically requires matrix analysis techniques as one deals with the noncommuting operators V and T. However, the càdlàg path space Ξ takes over the role of the configuration space - an infinite dimensional set compared to the much simpler Hamming cube $\mathcal{Q}_N$. Furthermore, if V is itself random as in the case of spin glasses, one has to deal with two probability measures, one describing the disorder and the second one the path distribution. Perhaps, the most severe challenge one has to face if one applies the path integral formula to quantum spin glasses, is the fact that the partition function will typically be dominated by rare paths. That is, one has to understand the large deviation properties of Poisson jump processes, which is a highly nontrivial task and leads to infinite dimensional variational problems [126].

2.3 Goldschmidt's formula and the Phase Diagram

In this section, we start our analysis of the QREM. We recall that the model Hamiltonian $H_N = U + \Gamma T$ acts on the 2^N dimensional Hilbert space $\ell^2(\mathcal{Q}_N)$ and that the REM potential $U = U_{\text{REM}}$ is understood as diagonal operator with respect to the z-basis $|\boldsymbol{\sigma}\rangle_{\boldsymbol{\sigma} \in \mathcal{Q}_N}$, that is, $U|\boldsymbol{\sigma}\rangle = U(\boldsymbol{\sigma})|\boldsymbol{\sigma}\rangle$. We will focus here on the thermodynamical limit of the pressure

$$\Phi_N(\beta, \Gamma) := \ln Z_N(\beta, \Gamma) = \ln \operatorname{Tr} e^{-\beta H},$$

and defer a more precise analysis of the QREM to the next chapter. Our main result in this section is Goldschmidt's formula for the limit of the specific pressure in the QREM:

Theorem 2.7 (Theorem 1 in [128])
For any $\Gamma, \beta \geq 0$, *we have the almost sure convergence as* $N \to \infty$*:*

$$\lim_{N\to\infty} \frac{1}{N}\Phi_N(\beta,\Gamma) = p_{\mathrm{QREM}}(\beta,\Gamma) := \max\{p_{\mathrm{REM}}(\beta), p_{\mathrm{PAR}}(\beta\Gamma)\}. \tag{2.6}$$

As in the REM, the QREM pressure is self-averaging. This is a direct consequence of the Gaussian concentration inequality (Theorem 2.4). The computation is presented in [128] as first remark after Theorem 1. Therefore, the specific pressure $\frac{1}{N}\Phi_N(\beta,\Gamma)$ converges also in mean to $p_{\mathrm{QREM}}(\beta,\Gamma)$.
Goldschmidt derived the formula (2.6) using the path integral formalism, we introduced in the last section [95]. He combined the so-called replica trick with a static approximation of the path-overlap.
As it has already been explained in the introduction, the replica trick is a common non-rigorous method in spin glass theory. One computes the fractional moments $\mathbb{E}[Z^n]$ for $n \to 0$ by extrapolating results on the integer moments. While the replica trick gives rise to correct predictions on spin glasses, a mathematical justification is yet to be found even in the classical setting - despite numerous efforts.
The static approximation concerns the dominant paths in the path-integral formula. One assumes that the main contribution to the partition function is due to paths $\boldsymbol{\sigma}(t) \in \Xi^N$ whose overlap $R_N(\boldsymbol{\sigma}(t), \boldsymbol{\sigma}(t'))$ is in fact a time-independent constant c. Then, one maximizes the resulting expression with regard to c.
While Goldschmidt's approach ultimately leads to the correct formula for the QREM pressure, it is known that the static approximation is not valid for more involved models such as the QSK [126]. Thus, it is very important to develop new tools to gain insight to the physics of quantum spin glasses. Our proof of Goldschmidt's formula can be seen as first step in this direction, as we make no use of the path integral representation, but instead we study the QREM Hamiltonian directly via operator theoretic methods. We will give an overview of our proof strategy and the underlying intuition in the following subsection below.
Let us discuss here the physical consequences of Theorem 2.7. The resulting QREM phase diagram is presented in Figure 2.3. There are three different phases: a qunatum paramagnetic phase, a classical non-glass phase and a classical glass-phase. The phase separation line between the classical phases and the paramagnetic phase is given by the curve $p_{\mathrm{REM}}(\beta) = p_{\mathrm{PAR}}(\beta\Gamma)$ in the $\beta - \Gamma$ plane. For fixed β, one may alternatively characterize the transition point by a critical field strength $\Gamma_c(\beta)$,

$$\Gamma_c(\beta) := \frac{1}{\beta}\operatorname{arcosh}(\exp(p_{\mathrm{REM}}(\beta))).$$

The critical field strength $\Gamma_c(\beta)$ is a monotone increasing function with $\Gamma_c(0) = 1, \Gamma_c(\beta_c) = \beta_c^{-1}\operatorname{arcosh}(2)$ and $\lim_{\beta\to\infty}\Gamma_c(\beta) = \beta_c$. The latter reveals a quantum phase transition at $\Gamma = \beta_c$. Recalling that the specific ground state energy of the REM is given by $-\beta_c$, the ground state transition occurs at the field strength Γ where the specific ground state energies of U and ΓT agree.
For fixed β, the QREM is in the quantum paramagnetic phase if $\Gamma > \Gamma_c(\beta)$ and in one of REM phases if $\Gamma < \Gamma_c(\beta)$. As for $\Gamma > \Gamma_c(\beta)$ the QREM pressure coincides with the paramagnetic one, we observe a magnetization $m_x = \tanh(\beta\Gamma) > 0$ (see also (2.4)). Whereas, for $\Gamma < \Gamma_c(\beta)$ the pressure does not depend on Γ and, thus, $m_x = 0$. In particular the magnetization m_x is discontinuous at Γ_c which reflects a first-order magnetic phase transition. For $\Gamma < \Gamma_c(\beta)$, the QREM pressure $p_{\mathrm{QREM}}(\beta,\Gamma)$ agrees with $p_{\mathrm{REM}}(\beta)$,

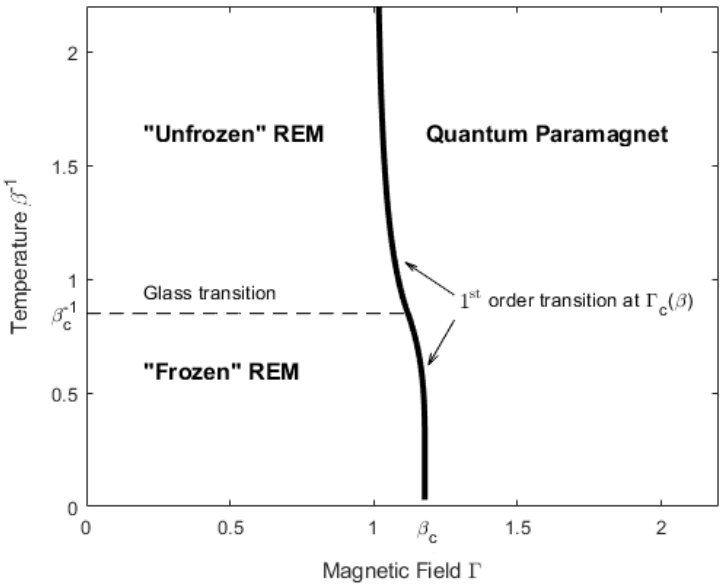

Figure 2.1: Phase diagram of the QREM as a function of the transversal magnetic field Γ and the temperature β^{-1} [95, 128]. The first-order transition occurs for fixed β at $\Gamma_c(\beta)$. The freezing transition is found at the temperature β_c^{-1}, which is unchanged in the presence of a magnetic field with strength $\Gamma < \Gamma_c(\beta)$.

which implies that we still find the glass transition at $\beta = \beta_c$. The glass phase is again characterized by a vanishing specific entropy.

To sum up the discussion, the QREM behaves as if the Hamiltonian was either just the REM potential U or a pure paramagnet ΓT. Indeed, the thermal averages $N^{-1}\langle T\rangle_{\beta,\Gamma}$ and $N^{-1}\langle U\rangle_{\beta,\Gamma}$ tend to zero in the classical phase and, respectively, in the paramagnetic phase. That U and T appear to avoid each other, forms our main intuition for the proof of Theorem 2.7.

2.3.1 A Glimpse of the Proof

We have seen that Goldschmidt's formula suggests a picture of the QREM where T and U do not interact with each other, almost as if $H = T \oplus U$. Of course, that cannot be quite true. However, this can still be seen as guiding idea for our proof. The underlying mathematical foundation for decomposing the QREM Hamiltonian into an almost direct sum, is the fact that the REM deep holes are typically separated from each other. If $\boldsymbol{\sigma}$ is a configuration with energy $U(\boldsymbol{\sigma}) = -\alpha N$, then the configurations $\boldsymbol{\sigma}'$ close to $\boldsymbol{\sigma}$ will typically have an energy $U(\boldsymbol{\sigma}) = \mathcal{O}(\sqrt{N})$. As we have seen, the eigenstates of T are completely delocalized and, thus, the low energy eigenfunctions, which form an exponentially small fraction of the set of eigenstates, cannot localize enough to detect the very isolated deep holes of the REM.

After these heuristics, we want to be more precise. We prove Theorem 2.7 by providing an asymptotically sharp lower and upper bound. The lower bound is based on Gibbs' variational principle, which we state here for completeness:

Proposition 2.8 (Theorem 2.13 in [47])
Let H be a symmetric matrix on $\mathbb{C}^n$. Then,

$$\ln \operatorname{Tr} e^H = \sup_{\rho \in \mathcal{D}_n} [\operatorname{Tr}(\rho H) - \operatorname{Tr} \rho \ln(\rho)],$$

where $\mathcal{D}_n := \{\rho \in \mathbb{C}^{n\times n} \mid \rho \geq 0, \operatorname{Tr} \rho = 1\}$ denotes the set of all density matrices on $\mathbb{C}^n$. The unique maximizer is the Gibbs state $\rho = e^H / \operatorname{Tr} e^H$.

Based on the broad picture that T and U do not interlace, it is natural to apply Gibbs' variational principle with the unperturbed trial states $\rho_U = e^{-\beta U}/\operatorname{Tr} e^{-\beta U}$ and $\rho_T = e^{-\beta\Gamma T}/\operatorname{Tr} e^{-\beta\Gamma T}$. Indeed, this is enough to establish

$$\liminf_{N\to\infty} \frac{1}{N}\Phi_N(\beta,\Gamma) \geq p_{\mathrm{QREM}}(\beta,\Gamma)$$

almost surely (see Lemma 1 in [128]). Establishing the upper bound, is the more difficult part of the proof. To this end, we introduce for any $\varepsilon > 0$ the large deviation set

$$\mathcal{L}_\varepsilon := \{\boldsymbol{\sigma} \in \mathcal{Q}_N \mid U(\boldsymbol{\sigma}) \leq -\varepsilon N\},$$

and we want to show that $\mathcal{L}_\varepsilon$ does not percolate. It is convenient to introduce the notion of *gap-connectedness*. We say that $\boldsymbol{\sigma}, \boldsymbol{\sigma}'$ are *gap-connected* if $d(\boldsymbol{\sigma}, \boldsymbol{\sigma}') \leq 2$, where d denotes the Hamming distance

$$d(\boldsymbol{\sigma}, \boldsymbol{\sigma}') := \frac{1}{2}\sum_{i=1}^{N} |\sigma_i - \sigma_i'|.$$

Then, we may decompose $\mathcal{L}_\varepsilon$ into maximal gap-connected components C_ε, that is, $\mathcal{L}_\varepsilon = \dot{\bigcup}_{C_\varepsilon \in \mathcal{C}_\varepsilon} C_\varepsilon$, where $\mathcal{C}_\varepsilon$ is the collection of the maximal gap-connected sets.

We stress that $\mathcal{L}_\varepsilon$ is a random set and, hence, $\mathcal{C}_\varepsilon$ depends on the disorder. Making use of the independence of U and some simple combinatorics, we show that there exist some $K = K(\varepsilon)$ such that

$$\mathbb{P}\left(\max_{C_\varepsilon \in \mathcal{C}_\varepsilon} |C_\varepsilon| > K\right) \leq e^{-cN}$$

for some $c = c(\varepsilon)$ and all N large enough [128, Lemma 2]. Therefore, if we denote by $\Omega_{\varepsilon,N}$ the event where $\max_{C_\varepsilon \in \mathcal{C}_\varepsilon} |C_\varepsilon| \leq K$ holds true, we may restrict our analysis to this family of sets. The almost sure convergence is guaranteed by the Borel-Cantelli lemma [112, Theorem 4.18].

The next step consists in separating the large deviation set $\mathcal{L}_\varepsilon$ from the rest of the Hamming cube. To this end, we introduce the operator A_ε, which describes the hopping of configurations $\boldsymbol{\sigma} \in \mathcal{L}_\varepsilon$ and can be seen as the restriction of T to $\mathcal{L}_\varepsilon$ with Neumann boundary conditions. More precisely, $\langle \boldsymbol{\sigma} | A_\varepsilon | \boldsymbol{\sigma}' \rangle = \langle \boldsymbol{\sigma} | T | \boldsymbol{\sigma}' \rangle$ if $\boldsymbol{\sigma} \in \mathcal{L}_\varepsilon$ or $\boldsymbol{\sigma}' \in \mathcal{L}_\varepsilon$, and all other matrix elements are set to zero. The definition of gap-connectedness was designed in such a way that A_ε is a direct sum of operators A_{C_ε} which correspond to the maximal components C_ε. Combined with a Frobenius norm estimate, we arrive at

$$\|A_\varepsilon\| \leq \max_{C_\varepsilon \in \mathcal{C}_\varepsilon} \sqrt{2N|C_\varepsilon|} \leq \sqrt{2KN},$$

that is an $O(\sqrt{N})$ upper bound for the operator norm of A_ε [128, Lemma 3]. This suggests that we can "delete" A_ε without changing the pressure in leading order. This can be made rigorous by invoking the Golden-Thompson inequality, which we recall next.

Proposition 2.9 (Corollary IX.3.6 in [28])
For any Hermitian matrices A, B on $\mathbb{C}^n$, we have

$$\operatorname{Tr} e^{A+B} \leq \operatorname{Tr} e^A e^B.$$

We are now ready to put the pieces together. If we denote by $U_{\mathcal{L}_\varepsilon}$ and $U_{\mathcal{L}_\varepsilon^c}$ the restriction of U to $\mathcal{L}_\varepsilon$ and its complement, the Golden-Thompson inequality yields

$$\begin{aligned} Z(\beta,\Gamma) &\leq \operatorname{Tr} e^{-\beta U_{\mathcal{L}_\varepsilon} \oplus (U_{\mathcal{L}_\varepsilon^c} + \Gamma(T - A_\varepsilon))} e^{-\beta\Gamma A_\varepsilon} \\ &\leq e^{\beta\Gamma\|A_\varepsilon\|} \left(\operatorname{Tr}_{\ell^2(\mathcal{L}_\varepsilon)} e^{-\beta U_{\mathcal{L}_\varepsilon}} + e^{\beta\varepsilon N} \operatorname{Tr}_{\ell^2(\mathcal{L}_\varepsilon^c)} e^{-\beta\Gamma(T-A_\varepsilon)} \right) \\ &\leq e^{\beta\Gamma\sqrt{2KN}} \left(e^{\Phi_N(\beta,0)} + e^{\beta\varepsilon N} e^{N p_{\mathrm{REM}}(\beta\Gamma)} \right) \end{aligned}$$

For the first line we note that indeed after subtracting A_ε the operator $U_{\mathcal{L}_\varepsilon^c} + \Gamma(T - A_\varepsilon)$ only acts nontrivially on the subspace $\ell^2(\mathcal{L}_\varepsilon^c)$ – which explains the direct sum. The next step consists of the simple inequality $\operatorname{Tr} BD \leq \|D\| \operatorname{Tr} B$ for positive matrices B, D and we use the lower bound $U_{\mathcal{L}_\varepsilon^c} \geq -\varepsilon N$ to estimate the second term. The last line makes use of the trivial bound $\operatorname{Tr}_{\ell^2(\mathcal{L}_\varepsilon)} e^{-\beta U_{\mathcal{L}_\varepsilon}} \leq e^{\Phi_N(\beta,0)}$ and of the fact that all matrix elements of $-\beta T$ are positive and thus the subtraction by A_ε decreases the trace. In total, if we take the $N \to \infty$ limit and recall that $\varepsilon > 0$ was arbitrary, we obtain the matching upper bound

$$\limsup_{N\to\infty} \frac{1}{N} \Phi_N(\beta,\Gamma) \leq p_{\mathrm{QREM}}(\beta,\Gamma).$$

More details can be found in [128].

2.3.2 The QREM as p-spin limit

Derrida' s original motivation to introduce the REM stems from the following observation. The p-spin potential U_p (see also (1.7)),

$$U_p(\boldsymbol{\sigma}) := \frac{1}{\sqrt{N^{p-1}}} \sum_{i_1,i_2,\dots i_p} g_{i_1,i_2,\dots i_p} \sigma_{i_1}\sigma_{i_2}\cdots\sigma_{i_p}$$

with i.i.d standard normal variables $g_{i_1,i_2,\dots i_p}$ forms a centered Gaussian process on the Hamming cube with covariance matrix $\mathbb{E}[U_p(\boldsymbol{\sigma})U_p(\boldsymbol{\sigma}')] = N R_N(\boldsymbol{\sigma},\boldsymbol{\sigma}')^p$. In the $p \to \infty$ limit, the covariance formally converges to $N\delta_{\boldsymbol{\sigma},\boldsymbol{\sigma}'}$, if we ignore the little subtlety at the pairs $\boldsymbol{\sigma}' = -\boldsymbol{\sigma}$. That is of course the REM potential since centered Gaussians are uniquely characterized by their covariance function.

While these heuristic considerations draw a connection between the REM and p-spin models, their relation is in fact closer. Namely, in case of the pressure one can exchange the thermodynamic limit $N \to \infty$ and the $p \to \infty$ limit. Indeed, if we introduce the limiting pressure f_p,

$$f_p(\beta) := \lim_{N\to\infty} N^{-1}\mathbb{E}\left[\ln \sum_{\boldsymbol{\sigma}\in\mathcal{Q}_N} e^{-\beta U_p(\boldsymbol{\sigma})}\right]$$

- which indeed exists due to Panchenko's version of the Parisi formula for mixed p-spin models [153] - we have $\lim_{p\to\infty} f_p(\beta) = p_{\mathrm{REM}}$. This result is well-known in the spin glass literature [36, 181], however its proof is typically omitted.

For this reason, we present the short argument here. We first invoke a maximal inequality [35, Theorem 2.5], which shows that for all Gaussian processes with bounded variance N on $\mathcal{Q}_N$, we have $\mathbb{E}\min_{\boldsymbol{\sigma}\in\mathcal{Q}_N} U(\boldsymbol{\sigma}) \geq -\beta_c N$. In particular we conclude that the right derivative $\delta_+ f_p(\beta) \leq \beta_c$ is uniformly bounded by β_c. The second ingredient is that an application of the second moment method yields that annealed and quenched pressure agree in an enlarging interval if p increases. Indeed,

$$f_p(\beta) = \frac{1}{2}\beta^2 \quad \text{for } \beta \leq \beta_c(1-c_p),$$

where c_p is a sequence converging to zero as $p \to \infty$ [36, Theorem 11.2.7]. A standard convexity argument then implies $\lim_{p\to\infty} f_p(\beta) = p_{\mathrm{REM}}$.

We would like to extend this result to quantum p-spin models and the QREM. Here, we face three major obstacles. First, the quantum analog of f_p,

$$f_p(\beta,\Gamma) := \lim_{N\to\infty} N^{-1}\mathbb{E}\left[\ln \mathrm{Tr}\, e^{-\beta(U_p+\Gamma T)}\right]$$

is unfortunately not known to exist for $p \geq 3$. However, we expect that the methods presented in [3] for the QSK can be extended to general mixed p-spin models. This would immediately imply the existence of $f_p(\beta,\Gamma)$. Secondly, even though annealed and quenched pressure agree for low temperatures in the quantum setting [126], the corresponding expression for the annealed pressure is involved and its limit will depend on p. Eventually, and perhaps most importantly, Gaussian comparison fails in the quantum setting. While for classical spin glasses, Slepian's lemma [179, Proposition 1.3.3] shows that the pressure is a monotone decreasing function of the potential's correlation (if its variance remains fixed), there is no analogous result for quantum spin glasses.

In [129], we avoided tackling these obstacles by considering a closely related problem. Instead of exchanging the $p \to \infty$ and $N \to \infty$ limits, we deal with a coupled limit, where $p = p(N)$ grows as function of N.

Theorem 2.10 (Theorem 2.2 in [129])
Let $p(N)$ be a sequence of natural numbers which satisfies a superlogarithmic growth condition, i.e.,

$$\lim_{N\to\infty} \frac{p(N)}{\ln(N)} = \infty.$$

For any $\beta, \Gamma \geq 0$, we have the almost sure convergence

$$\lim_{N\to\infty} \frac{1}{N} \Phi_{N,p(N)}(\beta,\Gamma) = \lim_{N\to\infty} \frac{1}{N} \ln\left(\operatorname{Tr} e^{-\beta(U_{p(N)}+\Gamma T)}\right) = p_{QREM}(\beta,\Gamma).$$

While our theorem does not justify the exchange of the $p \to \infty$ and $N \to \infty$ limits in the quantum case, it still yields a profound justification to consider the QREM as limit of quantum p-spin models. Note that the growth assumption on $p(N)$ is comparatively mild. The superlogarithmic condition is a consequence of our proof technique which is essentially an adaption of the proof of Theorem 2.7. The main new challenge is of probabilistic nature: we need to control the diameter of the large deviation set's components. In the QREM it was fairly easy to show that the connected components are of size $\mathcal{O}(1)$. Under the superlogarithmic growth condition, we show that the size is bounded by $o(N)$ - which is good enough to derive Theorem 2.10. Establishing the $o(N)$ estimate for the components' diameter requires some geometrical and combinatorial considerations and some estimates on correlated Gaussians. The details are executed in the proofs of Proposition 3.1 and Lemma 3.2 in [129].

2.4 Trajectory Phase Transitions in the REM

If one seeks for an understanding of a model's thermodynamical properties, one usually considers the partition function or, respectively, the pressure. The pressure encodes several thermodynamical quantities such as the internal energy, entropy and magnetization; and a study of the pressure reveals the nature of the Gibbs measure. While an analysis of the pressure allows one to determine the static equilibrium characteristics of a model, the pressure does not depict the dynamical thermodynamics of trajectories. Dynamical phase transitions, however, are of relevance in the study of spin glasses as they reflect changes in the activity of the glass and, hence, allow a dynamical characterization of glass phases [87, 134]. In [88], we consider the trajectory dynamics of the REM. We will see shortly that studying trajectories in classical spin glasses is closely related to the static equilibrium analysis of spin glasses in a transversal field, providing another promising application of quantum spin glass models.

As the thermodynamics of trajectories is not as commonly studied as the static equilibrium thermodynamics, we will briefly introduce the main concepts. We consider a continuous-time Markov chain on the Hamming cube $\mathcal{Q}_N$ with trajectories $\boldsymbol{\xi} : [0,\infty) \to \mathcal{Q}_N$. Such a Markov process is uniquely characterized by its generator on $\ell^2(\mathcal{Q}_N)$ [112],

$$W := \sum_{\boldsymbol{\sigma},\boldsymbol{\tau}\in\mathcal{Q}_N,\boldsymbol{\sigma}\neq\boldsymbol{\tau}} w_{\boldsymbol{\sigma}\to\boldsymbol{\tau}} |\boldsymbol{\tau}\rangle\langle\boldsymbol{\sigma}| - \sum_{\boldsymbol{\sigma}\in\mathcal{Q}_N} r_{\boldsymbol{\sigma}} |\boldsymbol{\sigma}\rangle\langle\boldsymbol{\sigma}|,$$

with escape rates $r_{\boldsymbol{\sigma}} = \sum_{\boldsymbol{\tau}\neq\boldsymbol{\sigma}} w_{\boldsymbol{\sigma}\to\tau}$ and transition rates $w_{\boldsymbol{\sigma}\to\boldsymbol{\tau}} \geq 0$. If the trajectory $\boldsymbol{\xi}$ is located at some $\boldsymbol{\sigma}$, the waiting time for the next time jump follows an exponential distribution with parameter $r_{\boldsymbol{\sigma}}$, that is the waiting time is a random variable with probability distribution $r_{\boldsymbol{\sigma}} e^{-r_{\boldsymbol{\sigma}} x}$ on $[0,\infty)$. When the waiting time has passed, $\boldsymbol{\xi}$ jumps from $\boldsymbol{\sigma}$ to $\boldsymbol{\tau}$ with probability $w_{\boldsymbol{\sigma}\to\boldsymbol{\tau}}/r_{\boldsymbol{\sigma}}$. This interpretation of the jump process is fully contained in the master equation

$$\partial_t |p_t\rangle = W |p_t\rangle,$$

where W is understood as an operator on $\ell^1(\mathcal{Q}_N)$ and $|p_t\rangle$ describes the probability distribution of $\boldsymbol{\xi}$ at time t, i.e., $p_t(\boldsymbol{\sigma}) = \langle \boldsymbol{\sigma}|p_t\rangle \geq 0$ and $\sum_{\boldsymbol{\sigma}\in\mathcal{Q}_N} p_t(\boldsymbol{\sigma}) = 1$.

We will only consider the situation where $w_{\boldsymbol{\sigma}\to\boldsymbol{\tau}} = w_{\boldsymbol{\tau}\to\boldsymbol{\sigma}}$ such that W is a symmetric matrix. The rates $r_{\boldsymbol{\sigma}}$ are typically chosen to be extensive in the particle number N. The most relevant examples for us are the generator of the simple random walk, i.e., $w_{\boldsymbol{\sigma}\to\boldsymbol{\tau}} = 1$ if $\boldsymbol{\sigma}$ and $\boldsymbol{\tau}$ are neighbors,

$$W_{\mathrm{RW}} = \sum_{\boldsymbol{\sigma},\boldsymbol{\tau}\in\mathcal{Q}_N, d(\boldsymbol{\sigma},\boldsymbol{\tau})=1} |\boldsymbol{\tau}\rangle\langle\boldsymbol{\sigma}| - N \sum_{\boldsymbol{\sigma}\in\mathcal{Q}_N} |\boldsymbol{\sigma}\rangle\langle\boldsymbol{\sigma}| = -T - N\mathbb{1},$$

and the all-to-all dynamics, where the path jumps to any other configuration with equal probability,

$$W_{\mathrm{all}} = \frac{N}{2^N} \sum_{\boldsymbol{\sigma},\boldsymbol{\tau}\in\mathcal{Q}_N, \boldsymbol{\sigma}\neq\boldsymbol{\tau}} |\boldsymbol{\tau}\rangle\langle\boldsymbol{\sigma}| - \frac{N(2^N-1)}{2^N} \sum_{\boldsymbol{\sigma}\in\mathcal{Q}_N} |\boldsymbol{\sigma}\rangle\langle\boldsymbol{\sigma}| = N(|\Psi_\emptyset\rangle\langle\Psi_\emptyset| - \mathbb{1}).$$

Our main aim is then to study trajectory observables, which are typically quantities integrated along the path $\boldsymbol{\xi}$. In our case, we consider the energy integrated along the curve,

$$U_t[\boldsymbol{\xi}] := \int_0^t U(\boldsymbol{\xi}(s))\, ds,$$

for $t > 0$ and we want to gain insight into the distribution of $U_t[\boldsymbol{\xi}]$ with respect to the trajectory probability $\hat{\mathbb{P}}_t$. Here, the probability $\hat{\mathbb{P}}_t$ takes only the randomness of the Markov process into account, not the disorder arising from U. Hence, $\hat{\mathbb{P}}_t$ is a random measure if U is random. We will always assume that the trajectories start with the uniform distribution at $t = 0$. In [88], we have focused on the situation where U is the REM potential.

Of course, by the central limit theorem the typical value of $U_t[\boldsymbol{\xi}]$ is close to zero. So, our main purpose is to get good estimates for the probability of rare events of the form $\hat{\mathbb{P}}_t(U_t[\boldsymbol{\xi}] \approx \alpha N)$. That is, we study the large deviations of trajectory observables under an unbiased dynamics - W does not depend on U! At first sight these trajectory dynamics appear to be related to the analysis of Glauber dynamics in the context of aging and metastability [25,26,49,91]. However, we stress that the Glauber process is a biased dynamics as it depends on U and one considers under this biased Markov chain the typical events, not the rare ones.

Coming back to the analysis of $\hat{\mathbb{P}}_t$, we introduce the moment generating function

$$\mathbf{M}(t,\lambda) := \int e^{-\lambda U_t[\boldsymbol{\xi}]} \hat{\mathbb{P}}_t(d\boldsymbol{\xi}),$$

which is typically denoted by Z in the physics literature, but we have chosen here a different notation to avoid confusion. $\mathbf{M}(t,\lambda)$ takes the role of the partition function for trajectory ensembles and, similarly, the specific pressure is substituted by the scaled cumulant generating function (SCGF),

$$\theta_N(t,\lambda) := \frac{1}{Nt} \ln \mathbf{M}(t,\lambda).$$

In order to approach the moment generating function via operator methods, we reexpress $\mathbf{M}(t,\lambda)$ as matrix element. Note that W generates a positive semigroup and, thus, a similar approach as presented in Section 2.2 yields a path-integral formula also in this case. The result is

$$\mathbf{M}(t,\lambda) = 2^{-N} \sum_{\boldsymbol{\sigma},\boldsymbol{\tau}\in\mathcal{Q}_N} \langle \boldsymbol{\sigma}|e^{t(W-\lambda U)}|\boldsymbol{\tau}\rangle = \langle \Psi_\emptyset|e^{tW_\lambda}|\Psi_\emptyset\rangle,$$

with the tilted generator $W_\lambda = W - \lambda U$. We note that in the case of $W = W_{\mathrm{RW}}$ the tilted generator is up to a identity shift a rescaled QREM Hamiltonian. We see that trajectory dynamics are intimately related to the study of quantum spin glasses. In contrast to the partition function Z however, the moment generating function $\mathbf{M}(t,\lambda)$ does not only depend on the spectrum of W_λ, but also on the overlap of its eigenfunctions with the flat state $\Psi_\emptyset$. This difference makes the analysis of $\mathbf{M}(t,\lambda)$ comparatively more difficult, and this is the reason why we have focused on the simpler all-to-all dynamics in [88]. In that case, we compute the limit of $\theta_N(t,\lambda)$ and the limit of the specific (negative) free energy $f_N(T,\lambda) := \frac{T}{N}\ln 2^{-N}\mathrm{Tr}\, e^{(W-\lambda U)/T}$:

Theorem 2.11 (Theorem 1 in [88])
Let U be the REM potential and $W = W_{all}$ the generator of the all-to-all dynamics. Then, for any $t > 0$ and $\lambda > 0$ the SCGF converges almost surely,

$$\lim_{N\to\infty} \theta_N(t,\lambda) = \theta(t,\lambda) := \max\{0, t^{-1}(p_{REM}(t\lambda) - \ln 2) - 1\},$$

and extends by symmetry to negative values, that is, $\theta(t,-\lambda) = \theta(t,\lambda)$. The free energy f_N also converges almost surely,

$$\lim_{N\to\infty} f_N(t,\lambda) = f(t,\lambda) := \max\{-T\ln 2, T(p_{REM}(\lambda/T) - \ln 2) - 1\}.$$

The dynamical and static phase diagrams resulting from Theorem 2.11 are presented in Figure 2.4. In both cases one observes three phases, similarly as in the QREM, but the exact form of the separation lines is different. In that sense these findings confirm again that the trajectory thermodynamics cannot simply be derived from the static phase diagram. We now want to have a closer look at the three emergent dynamical phases.

Our classification is based on the *dynamical activity* in the phases. The dynamical activity is the average number of jumps $\langle J\rangle$ of trajectories under the tilted generator W_λ [87, 90]. To compute the activity, we define the doubly tilted partition sum $\mathbf{M}(t,\lambda,s) := \langle \Psi_\emptyset|e^{tW_{\lambda,s}}|\Psi_\emptyset\rangle$ with the additionally tilted generator

$$W_{\lambda,s} = Ne^{-s}|\Psi_\emptyset\rangle\langle\Psi_\emptyset| - N(1-2^{-N}(1-e^{-s}))\mathbb{1} - \lambda U,$$

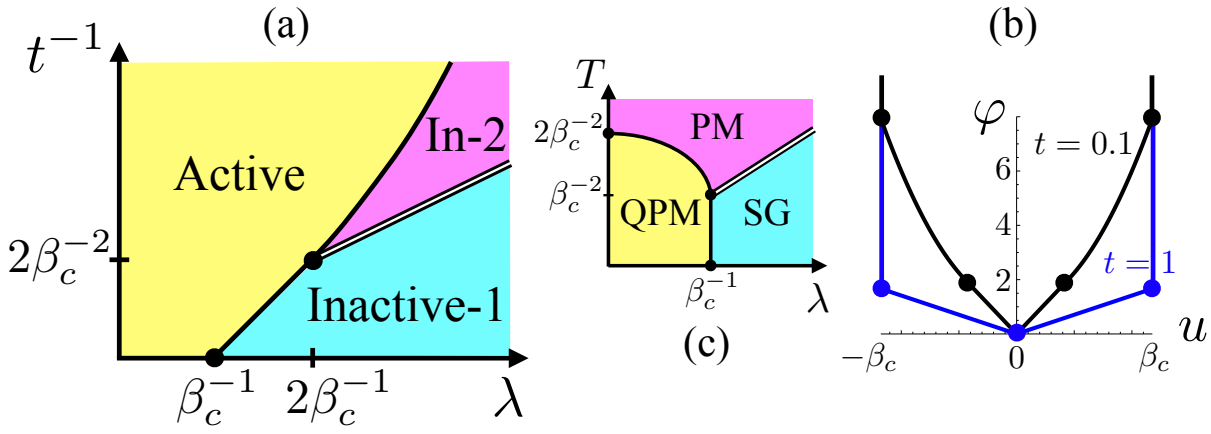

Figure 2.2: Static and dynamical phase diagram of the all-to-all QREM [88, Figure 1]. (a) Dynamical phase diagram of the REM with the all-to-all dynamics in the thermodynamic limit $N \to \infty$. The x-axis corresponds to the coupling parameter λ conjugated to the time-integrated REM energy and the y-axis corresponds to the inverse of the time t. The full lines indicate first-order transitions between the active and first and second inactive trajectory phases, whereas the double line shows the 1-step replica symmetry breaking transition between the two inactive phases. (b) Rate function $\varphi(t,u)$ for two different values of t. For $t^{-1} = 1 < 2\beta_c^{-2}$ (blue line) consists of a linear portion corresponding to the active phase (with $-\beta_c < u < \beta_c$) and an infinitely high jump at $\pm\beta_c$ which marks the transition to the first inactive phase. For $t^{-1} = 10 > 2\beta_c^{-2}$ the rate function describes the coexistence between the three phases (black). The linear portion between 0 and $\sqrt{2t}$ describes again the active phase. In the second inactive phase, $|u|$ can take values with decreasing probability between $\sqrt{2t}$ and β_c. The rate function is infinite for any $|u|$ beyond β_c indicating that this event has zero probability (under a "typical" sample of disorder). (c) Thermal phase diagram of the all-to-all QREM, which consists of three phases, too. However, the location of the phase transitions differs compared to the trajectory phase diagram.

where only the off-diagonal terms are deformed in order to detect the number of jumps. Indeed, if we introduce the the off-diagonal part W^{off} and the diagonal part W^{dia} of the generator, we may write using the Lie-Trotter formula

$$\begin{aligned}
\mathbf{M}(t,\lambda,s) &= \lim_{M\to\infty} \sum_{\boldsymbol{\sigma}_0,\boldsymbol{\sigma}_1,\ldots,\boldsymbol{\sigma}_M} e^{\frac{t}{M}\sum_{i=0}^{M-1} W^{\mathrm{dia}}(\lambda,s)(\boldsymbol{\sigma}_i)} \prod_{i=0}^{M-1} \langle \boldsymbol{\sigma}_i | \mathbb{1} + \frac{t}{M} W^{\mathrm{off}}(\lambda,s) | \boldsymbol{\sigma}_{i+1} \rangle \\
&= \lim_{M\to\infty} \sum_{\boldsymbol{\sigma}_0,\boldsymbol{\sigma}_1,\ldots,\boldsymbol{\sigma}_M} e^{-sJ(\boldsymbol{\sigma}_0,\boldsymbol{\sigma}_1,\ldots,\boldsymbol{\sigma}_M)} e^{\frac{t}{M}\sum_{i=0}^{M-1} W^{\mathrm{dia}}(\lambda,0)(\boldsymbol{\sigma}_i)} \prod_{i=0}^{M-1} \langle \boldsymbol{\sigma}_i | \mathbb{1} + \frac{t}{M} W^{\mathrm{off}}(\lambda,0) | \boldsymbol{\sigma}_{i+1} \rangle, \\
&= \int e^{-\lambda U_t[\boldsymbol{\xi}]} e^{-sJ(\boldsymbol{\xi})} \mathbb{P}_t(d\boldsymbol{\xi})
\end{aligned}$$

where $J(\boldsymbol{\sigma}_0,\boldsymbol{\sigma}_1,\ldots,\boldsymbol{\sigma}_M)$ and $J(\boldsymbol{\xi})$ denote the number of jumps of the discrete path $\boldsymbol{\sigma}_0,\boldsymbol{\sigma}_1,\ldots,\boldsymbol{\sigma}_M$ and, respectively, of the continuous-time jump process $\boldsymbol{\xi}$. These considerations immediately imply

$$-\partial_s \ln \mathbf{M}(t,\lambda,s)|_{s=0} = \frac{\int e^{-\lambda U_t[\boldsymbol{\xi}]} J(\boldsymbol{\xi}) \mathbb{P}_t(d\boldsymbol{\xi})}{\int e^{-\lambda U_t[\boldsymbol{\xi}]} \mathbb{P}_t(d\boldsymbol{\xi})} = \langle J \rangle.$$

The dynamical phase is characterized by $\theta(t,\lambda) = 0$ and a specific activity $(Nt)^{-1}\langle J \rangle$ approaching one in the thermodynamic limit. This active phase consists of the region $|\lambda| < \beta_c(2t)^{-1} + \beta_c^{-1}$ in case $t^{-1} < 2\beta_c^{-2}$,

and of $|\lambda| < \sqrt{2t^{-1}}$ in case $t^{-1} \geq 2\beta_c^{-2}$. The active phase is related to the QREM paramagnetic phase and is separated by a first order transition. The other phases are inactive as the specific activity $(Nt)^{-1}\langle J \rangle$ converges there to zero. The first inactive phase is found for $t^{-1} < 2|\lambda|\beta_c^{-1} - 2\beta_c^{-2}$. The trajectories localizes at the REM's extreme values and, hence, this regime resembles the REM glass phase. A second-order transition occurs between the first and second inactive phase. The second inactive phase is only found at times $t^{-1} > 2/\beta_c^2$ and can be seen as dynamical counterpart of the paramagnetic REM phase. In the long-time limit, $t \to \infty$, the value $\lambda = \beta_c^{-1}$ separates the active and first inactive phase, reflecting the transition in the largest eigenvalue of the tilted generator $W_\lambda = W - \lambda U$.
Let us come back to the original quest for a description of the large deviation properties of the trajectory observable $U_t[\boldsymbol{\xi}]$. We recall that a sequence of real random variables X_n is said to satisfy a *large deviation principle* with *rate function* S (and *speed* n) if

$$-\inf_{u \in I^\circ} S(u) \leq \liminf_{n\to\infty} \frac{1}{n} \ln \mathbb{P}\left(X_n \in I\right) \leq \limsup_{n\to\infty} \frac{1}{n} \ln \mathbb{P}\left(X_n \in I\right) = -\inf_{u \in \bar{I}} S(u)$$

holds true for any Borel set $I \subset \mathbb{R}$ [60]. Via the Gärtner-Ellis theorem [60, Thm 2.3.6], the rate function $S_t(u)$ of the large deviation principle obeyed by U_t is given by $t\varphi(t,u)$, where $\varphi(t,u)$ denotes the Legendre-Fenchel transform

$$\varphi(t,u) := \sup_\lambda \left(u\lambda - \theta(t,\lambda)\right) = \begin{cases} |u|\sqrt{\frac{2}{t}}, & |u| \leq \min\left\{\sqrt{2t}, \beta_c\right\}, \\ 1 + \frac{u^2}{2t}, & \text{else}, \\ \infty, & |u| > \beta_c. \end{cases}$$

The additional multiplication by t is necessary since we normalized by t in the definition of $\theta(t,\lambda)$. The dynamical phase diagram is also reflected in the behavior of $\varphi(t,u)$. For fixed t, one encounters one or two phase transitions depending on whether $t > \ln 2$ or not. If $t > \ln 2$, one only sees linear fluctuations and a totally frozen phase, whereas for $t < \ln 2$ one additionally encounters a phase with Gaussian fluctuations.

The proof of Theorem 2.11 is based on the observation that the tilted generator for the all-to-all dynamics is a rank-one perturbation of the diagonal REM potential. Therefore, any eigenvalue E is a solution of the fractional equation

$$\frac{1}{N} = \langle \Psi_\emptyset | (E + N + \lambda U)^{-1} | \Psi_\emptyset \rangle = \frac{1}{2^N} \sum_{\boldsymbol{\sigma}} \frac{1}{E + N + \lambda U(\boldsymbol{\sigma})}. \tag{2.7}$$

The corresponding eigenvectors ψ_E satisfy for all $\boldsymbol{\sigma}, \boldsymbol{\tau} \in \mathcal{Q}_N$:

$$\frac{\langle \boldsymbol{\sigma} | \psi_E \rangle}{\langle \boldsymbol{\tau} | \psi_E \rangle} = \frac{E + N + \lambda U(\boldsymbol{\tau})}{E + N + \lambda U(\boldsymbol{\sigma})}.$$

These results simplify the analysis of the all-to-all dynamics. For instance, (2.7) implies that all eigenvalues of W_λ except the largest one are up to a shift by $-N$ interlaced in between the REM's energies (cf. e.g. [9] and refs. therein for interlacing and finite-rank perturbation theory). In fact, the spectral analysis of W_λ has been already pursued in [7], where a comprehensive study of the spectrum and eigenfunctions is presented. Our findings can be deduced from the main results in [7].

Considering the next neighbor random walk is more subtle, as the tilted generator agrees up to a shift and scaling factor with the QREM Hamiltonian, which is not a simple rank-one perturbation. However, we will see in the next chapter that we are also able to derive precise spectral characteristics of the QREM. If one consults our proof for the all-to-all dynamics, one realizes that there is only one technical ingredient that has not been established for the QREM, yet. One would still need to show that

$$\lim_{N\to\infty} N^{-1} \ln\left(\frac{\langle\Psi_\emptyset|1_{(E-\delta,E+\delta N)}(H_{\mathrm{QREM}})|\Psi_\emptyset\rangle}{|\{\boldsymbol{\sigma}\in\mathcal{Q}_N|\,U(\boldsymbol{\sigma})\in(E-\delta,E+\delta N)\}|}\right) = -\ln 2 \tag{2.8}$$

holds true for all $\delta > 0$ sufficiently small and $-\beta_c N < E < -\Gamma N$. To prove that, one also needs to consider eigenfunctions clearly above the ground state energy in the localization regime. Despite this technical difficulty, we believe that (2.8) is true. Then, we could easily extend the results from this section to the next neighbor random walk.

Chapter 3

Spectral Analysis of the Quantum Random Energy Model

In this chapter, we continue our study of the QREM. We will present precise results on the low energy states and the pressure which have been published in [132]. Our first section is an informal discussion of the QREM, which will provide some intuition behind our spectral analysis of the QREM Hamiltonian. The next two sections consist of a discussion about the QREM low energy spectrum in the paramagnetic regime $\Gamma > \beta_c$ and in the glass phase $\Gamma < \beta_c$. We will see that the ground state wavefunction resembles the ground state of T and, respectively, U in either phase. We will also determine the next-to-leading order corrections of the ground state energy. Then, we turn to the analysis of the pressure, where we present the finite size corrections, too. In all three sections, we will mainly discuss the results and we can only highlight certain aspects of the proofs. The final section puts our theorems into the context of the extensively studied Anderson model. We will then comment on several interesting physical predictions, in particular, how our results contribute to these problems and the main mathematical challenges one has to face in a possible future rigorous verification of the physical claims. The presentation here follows in large parts the introduction of Article IV [132].

3.1 Some Heuristics

To give a first impression of our ideas, we start by providing some intuition and heuristics. Let us denote by $E_{\mathrm{GS}} := \inf \operatorname{spec} H_N$ the ground state energy of the QREM. We first note that Goldschmidt's formula (2.6) also entails an assertion on the limit of the specific ground state energy,

$$\lim_{N\to\infty} \frac{1}{N} E_{\mathrm{GS}} = -\lim_{\beta\to\infty} \frac{1}{\beta} p_{\mathrm{QREM}}(\beta,\Gamma) = \begin{cases} -\beta_c & \text{if } \Gamma < \beta_c, \\ -\Gamma & \text{if } \Gamma > \beta_c, \end{cases}$$

where we made use of the simple bound $-\beta E_{\mathrm{GS}} \leq \Phi_N(\beta,\Gamma) \leq \ln 2 - \beta E_{\mathrm{GS}}$. At least in the thermodynamic limit, the specific ground state energy agrees either with the REM minimum or the paramagnetic ground state energy. This suggests that in the glass phase $\Gamma < \beta_c$ the magnetic field ΓT can be treated as "small" perturbation and, similarly, for $\Gamma > \beta_c$ the REM potential U should be considered as perturbation. In order to obtain a first guess on the the ground state energy's next-leading order corrections, one may

invoke *second-order perturbation theory*, which we briefly recall here. Suppose we have a Hamiltonian $H = H_0 + \lambda H'$ on a finite-dimensional Hilbert space, where we think of λ as small coupling and of H' as perturbation of the reference Hamiltonian H_0. If we further assume that the ground state of H_0 is non-degenerate, then the ground state energy $E_{\mathrm{GS}}(\lambda)$ is analytic in a sufficiently small neighborhood of $\lambda = 0$ [113]. Hence, we have a power series expansion

$$E_{\mathrm{GS}}(\lambda) = E_{\mathrm{GS}}(0) + \sum_{k=1}^{\infty} a_k \lambda^k$$

for $|\lambda|$ small enough and some coefficients $a_1, a_2, \ldots$. The idea of second-order perturbation theory is to consider only the the power series up to second order without justifying that for the considered values of λ the higher-order terms are in fact negligible and that the power series expansion is applicable at all. Thus, second-order perturbation theory is clearly a non-rigorous approach, although it is successfully used in physics to deduce properties of complex systems. We finally recall that the coefficients a_1 and a_2 can be computed explicitly: if μ_k and ψ_k denote the ordered eigenvalues and eigenvectors of the unperturbed Hamiltonian H_0, we have

$$a_1 = \langle \psi_0 | H' | \psi_0 \rangle, \qquad a_2 = \sum_{k>0} \frac{|\langle \psi_k | H' | \psi_0 \rangle|^2}{\mu_0 - \mu_k}.$$

We see that the expression of a_2 makes use of the ground state's non-degeneracy. We now apply this method to the QREM Hamiltonian:

1. For $\Gamma < \beta_c$, second-order perturbation theory with $H_0 = U$ and $H' = T$ starting from the almost sure unique ground state $|\boldsymbol{\sigma}_{\min}\rangle$ with $\boldsymbol{\sigma}_{\min} := \arg\min U$, reads:

$$E_{\mathrm{GS}} \approx \min U + \Gamma \langle \boldsymbol{\sigma}_{\min} | T | \boldsymbol{\sigma}_{\min} \rangle + \Gamma^2 \sum_{\boldsymbol{\sigma} \neq \boldsymbol{\sigma}_{\min}} \frac{\left| \langle \boldsymbol{\sigma}_{\min} | \, T | \boldsymbol{\sigma}_{\min} \rangle \right|^2}{U(\boldsymbol{\sigma}_{\min}) - U(\boldsymbol{\sigma})} \approx \min U - \frac{\Gamma^2}{\beta_c}.$$

   The first-order term vanishes since the diagonal elements of T are zero. The sum in the second-order term is restricted to the neighbors of the minimum, whose potential term typically is only of the order $\mathcal{O}(\sqrt{N})$ and, thus, can be neglected. Using $U(\boldsymbol{\sigma}) \approx -\beta_c N$ one ends up with the final expression.

2. For $\Gamma > \beta_c$, we start second-order perturbation from the ground state $\Psi_\emptyset$ of T. This yields

$$\begin{aligned} E_{\mathrm{GS}} &\approx -N\Gamma + \langle \Psi_\emptyset | U | \Psi_\emptyset \rangle - \sum_{A \neq \emptyset} \frac{\left| \langle \Psi_\emptyset | \, U | \Psi_A \rangle \right|^2}{2|A|\,\Gamma} \\ &\approx -N\Gamma - \sum_{A \neq \emptyset} \frac{N 2^{-N}}{2|A|\,\Gamma} \approx -N\Gamma - \sum_{A \neq \emptyset} \frac{N 2^{-N}}{N\Gamma} \approx -N\Gamma - \frac{1}{\Gamma}. \end{aligned} \tag{3.1}$$

   The first correction $\langle \Psi_\emptyset | U | \Psi_\emptyset \rangle = 2^{-N} \sum_{\boldsymbol{\sigma} \in \mathcal{Q}_N} U(\boldsymbol{\sigma})$ is a normal variable with exponentially small variance and, thus, can be neglected. For the second term, we first recall the eigenvalues and eigenvectors of T. Then, we note that the random variables $\langle \Psi_\emptyset | \, U | \Psi_A \rangle$ form a collection of independent Gaussians with variance $N 2^{-N}$, so it appears reasonable to substitute the numerator

by its expectation. Finally, we use the approximation that most of the states of T are found near $|A| \approx N/2$, so that we may replace the denominator by its typical value $N\Gamma$ and we recall that the number of sets $A \neq \emptyset$ equals $2^N - 1$.

These computations go back to [110], where the finite-size corrections in the QREM have first been considered. In the following two sections we will not only see that the predictions concerning the ground state energy can be established rigorously, but we also give a precise description of the ground state wavefunction. For $\Gamma < \beta_c$ the ground state is sharply localized near the lowest-energy configuration of the REM and we will give quantitative bounds on the decay away from the minimal configuration. On the other hand, for $\Gamma > \beta_c$ the ground state is very much delocalized over the whole Hamming cube, resembling the ground state $\Psi_\emptyset$ of T. The localization-delocalization transition at extreme energies presented here relies on the delocalization properties of T on the Hamming cube, which fundamentally differ from the finite-dimensional Laplacian on the lattice. Consequently, our situation differs from the extensively studied Anderson model on $\mathbb{Z}^d$ as we will explain in more detail in Section 3.5. In both cases, the ground state is non degenerate and energetically separated by a gap of order $\mathcal{O}(1)$ from the rest of the spectrum. The ground-state gap only closes exponentially near $\Gamma = \beta_c$, which was predicted first in [110]. While the methods in Article IV [132] can be used to estimate the minimal spectral gap, this has already been proven in [2] by use of the adiabatic theorem and, thus, we will not cover its re-derivation by our techniques in this chapter.

3.2 The Delocalization Regime

The heuristics from the last section show that for $\Gamma > \beta_c$ one should expect a deterministic shift of the ground state energy by $-\frac{1}{\Gamma}$. The first main theorem does not only confirms this prediction, but also covers the whole low energy spectrum below $-\beta_c N$:

Theorem 3.1 (Theorem 1.3 in [132])
For $\Gamma > \beta_c$, any $\tau \in (0,1)$ and $\eta > 0$ and for sufficiently large N - except for an event of exponentially small probability - all eigenvalues of $H_N = \Gamma T + U$ below $-(\beta_c + 2\eta)N$ are found in the union of intervals of radius $\mathcal{O}(N^{\frac{\tau-1}{2}})$ centered at

$$(2n - N)\Gamma + \frac{N}{(2n-N)\Gamma} \tag{3.2}$$

with $n \in \{m \in \mathbb{N}_0 \,|(2m-N)\Gamma < -(\beta_c+2\eta)N\}$. Moreover, the ball centered at (3.2) contains exactly $\binom{N}{n}$ eigenvalues of H_N .

In order to simplify the presentation, here and in the following we refrain from specifying the exception sets with exponentially small probability and how the constants hidden in the $\mathcal{O}$-notation depend on different parameters. In [132] we give a precise description of these technicalities.
Note that Theorem 3.1 implies in particular that for $\beta_c < \Gamma$ the ground state energy is given by

$$E_{\mathrm{GS}} = -\Gamma N - \frac{1}{\Gamma} + o(1)$$

with overwhelming probability. Since the energy shift with respect to the ground state of ΓT coincides with the prediction based on naive second-order perturbation theory (3.1), one expects that the corresponding first-order perturbation theory for eigenvectors is accurate as well. Hence, one may guess that the ground state in the paramagnetic phase is close to the fully paramagnetic state $\Psi_\emptyset$. This hypothesis is confirmed by the next main theorem of this section:

Theorem 3.2 (Theorem 1.4 in [132])
In the situation of Theorem 3.1 with $0 < \eta < (\Gamma - \beta_c)/4$, the ℓ^2-normalized ground state ψ of $H_N = \Gamma T + U$ satisfies except for an event of exponentially small probability:

1. *The ℓ^2-distance of ψ and $\Psi_\emptyset$ is $\|\psi - \Psi_\emptyset\| = \mathcal{O}(N^{\frac{\tau-1}{2}})$.*
2. *The ground state ψ is exponentially delocalized in the maximum norm, i.e.,*

$$\|\psi\|_\infty^2 \leq 2^{-N} e^{N\gamma((\beta_c+\eta)/(2\Gamma))+o(N)}, \tag{3.3}$$

where $\gamma : [0,1] \to \mathbb{R}$ denotes the binary entropy

$$\gamma(x) := -x \ln x - (1-x)\ln(1-x). \tag{3.4}$$

Our bound on the ℓ^2-distance of the ground-state wavefunction $\Psi_\emptyset$ is not optimal, and we presume that an upper bound of order $N^{-\frac{1}{2}}$ holds true. Moreover, the delocalization estimate (3.3) is presumably not sharp either. In fact, in the proof of Theorem 3.8 in [132] we introduce a method, which improves the estimate (3.3) if $\Gamma - \beta_c$ is small. We expect that a more elaborate version of this argument yields the sharp exponential decay $\|\psi\|_\infty^2 \leq 2^{-N+o(N)}$, which would stress even more the similarities between ψ and $\Psi_\emptyset$. The estimate (3.4) is based on a simple path integral bound, which can be employed for all eigenstates with energy below $-\beta_c N$ [132, Proposition 3.5]. Also, the first assertion in 3.2 is a rather immediate consequence of Theorem 3.1. On the other hand, the proof of Theorem 3.1 involves several methods from which we will present the most important ones in the following. The complete proof is carried out in [132, Section 3].

We have already mentioned in Chapter 2 that in the our understanding of the paramagnetic regime stems from the intuition that the completely delocalized low energy states of T find it hard to detect the REM potential's isolated large deviations. To prove Theorem 3.1, we need to convert this picture into quantitative bounds. To this end, we define the spectral projections for $\varepsilon \in (0,1)$,

$$Q_\varepsilon := \mathbb{1}_{(-\varepsilon N, \varepsilon N)}(T), \qquad P_\varepsilon := \mathbb{1} - Q_\varepsilon,$$

where Q_ε consists of the spectral bulk, whereas P_ε is formed by the spectral edges. If ε is chosen not too small, most eigenstates are found in the range of Q_ε. Thus, guided by our picture on the REM energy landscape, the operator $P_\varepsilon U P_\varepsilon$ should be small in norm. A convenient method to prove this claim is the so-called *Matrix Bernstein Inequality*.

Theorem 3.3 (Theorem 1.6.2 in [187])
Let $A_1, \ldots, A_M$ be independent, centered random matrices of dimension $N \times N$. Further suppose

that $\|A_k\| \leq L$ holds true almost surely for $k = 1, \dots, M$ with a uniform bound L. Moreover, we introduce the sum of the matrices A_k,

$$S := \sum_{k=1}^{M} A_k,$$

and the matrix variance statistics

$$v(S) := \|\mathbb{E}[SS^*]\| = \left\| \sum_{k=1}^{M} \mathbb{E}[A_k A_k^*] \right\|.$$

Then, we have an upper bound on $\mathbb{E}[\|S\|]$,

$$\mathbb{E}[\|S\|] \leq \sqrt{2\ln(2M)v(Z)} + \frac{L}{3}\ln(2M),$$

and a tail estimate

$$\mathbb{P}(\|S\| \geq t) \leq 2N \cdot \exp\left(-\frac{t^2/2}{v(S) + Lt/3}\right)$$

for all $t \geq 0$.

To apply this theorem to the term $P_\varepsilon U P_\varepsilon$, one rewrites the operator as sum of independent matrices $P_\varepsilon U P_\varepsilon = \sum_{\boldsymbol{\sigma}} U(\boldsymbol{\sigma}) P_\varepsilon |\boldsymbol{\sigma}\rangle\langle\boldsymbol{\sigma}| P_\varepsilon$. The Matrix Bernstein inequality then implies

$$\mathbb{E}\left[\|P_\varepsilon U P_\varepsilon\|\right] \;\leq\; C\sqrt{N}\sqrt{\frac{\dim P_\varepsilon}{2^N}}, \tag{3.5}$$

and $\|P_\varepsilon U P_\varepsilon\|$ is concentrated around its mean. In fact, similar bounds hold true for not necessarily Gaussian potentials such as the higher moments of U^p of U [132, Proposition 3.1 and Corollary 3.2]. We note that a simple Chernoff bound yields

$$\dim P_\varepsilon = \sum_{\left|k - \frac{N}{2}\right| > \frac{\varepsilon N}{2}} \binom{N}{k} \;\leq\; 2^{N+1} e^{-\varepsilon^2 N/2}.$$

Consequently, the estimate (3.5) remains exponentially small if we choose $\varepsilon = N^{(\tau-1)/2}$ with $\tau \in (0,1)$. At this point, we see the cause for the parameter τ in the assertions of Theorem 3.1. If we fix τ, then with overwhelming probability we have the situation that $P_\varepsilon H_N P_\varepsilon \approx \Gamma T P_\varepsilon$ as the contribution of U is exponentially small and

$$Q_\varepsilon H_N Q_\varepsilon \geq Q_\varepsilon(\min U - \Gamma\varepsilon N)Q_\varepsilon,$$

that is, the Q-block does not contain the lower energy states $E < -(\beta_c + \eta)N$, in which we are interested. These are promising premises to employ the so-called Feshbach-Schur-Krein complement formula.

Theorem 3.4 (Theorem 5.10 in [9])
Let H be a self-adjoint matrix on a finite dimensional Hilbert space $\mathcal{H}$, P an orthogonal projection and $Q := \mathbb{1} - P$ the complementary projector. Then, for any $z \in \mathbb{C} \setminus \mathbb{R}$

$$P(H - z)^{-1}P = \left[PHP - z - PH(QHQ - z)^{-1}HP\right]_P^{-1},$$

where the subscript P indicates that the inverse is understood on the Hilbert space $P\mathcal{H}$.

The Feshbach-Schur-Krein identity can be translated into an eigenvalue equation for the QREM Hamiltonian. Indeed, all eigenvalues E of H strictly below $-\|U\|_\infty - \Gamma\varepsilon N$ are given by the solutions to the implicit equation

$$0 \in \operatorname{spec}\big(T_\varepsilon(E)\big) \quad \text{with} \quad \begin{aligned} T_\varepsilon(E) &:= P_\varepsilon\Big(\Gamma T + \frac{N}{E}\Big) - E + Y_\varepsilon(E), \\ Y_\varepsilon(E) &:= P_\varepsilon U P_\varepsilon - \Big(P_\varepsilon \frac{N}{E} + P_\varepsilon U R_\varepsilon(E) U P_\varepsilon\Big), \\ R_\varepsilon(E) &:= (Q_\varepsilon H_N Q_\varepsilon - E Q_\varepsilon)^{-1}. \end{aligned}$$

If we neglect the operator $Y_\varepsilon(E)$ for the moment, one obtains a fractional equation in E. Plugging in the eigenvalues of T, one obtains the assertions of Theorem 3.1. The idea is to show that $\|Y_\varepsilon(E)\| = \mathcal{O}(N^{\frac{\tau-1}{2}})$ is uniformly bounded for the considered energies E. Theorem 3.1 then follows by standard perturbation theory. We already know that the first term of $Y_\varepsilon(E)$ is small. For the second term, one recalls that we consider energies $E < -(\beta_c + \eta)N$ which are separated by a distance of order $\mathcal{O}(N)$ from the spectrum of $Q_\varepsilon H_N Q_\varepsilon$. Therefore, one makes the ansatz

$$R_\varepsilon(E) = -\frac{1}{E} Q_\varepsilon + \Big(R_\varepsilon(E) + \frac{1}{E} Q_\varepsilon\Big) = -\frac{1}{E} Q_\varepsilon - \frac{1}{E} R_\varepsilon(E) Q_\varepsilon H_N Q_\varepsilon,$$

where we used the second resolvent with the zero operator for the final identity. Using the Matrix Bernstein inequality for $U^2 - N$, one sees that $P_\varepsilon \frac{N}{E} - \frac{1}{E} P_\varepsilon U^2 P_\varepsilon$ is exponentially small. The last term $\frac{1}{E} P_\varepsilon U R_\varepsilon(E) Q_\varepsilon H_N Q_\varepsilon U P_\varepsilon$ can be estimated by using the Matrix Bernstein inequality for higher moments of U, combined with standard resolvent bounds. For the details, we refer to Section 3.2 in [132], in particular to the proofs of Lemma 3.3 and Theorem 3.4.

3.3 The Localized Regime

The computations in Section 3.1 suggest that in the spin glass phase $\Gamma < \beta_c$ the ground state energy is shifted by a deterministic $\mathcal{O}(1)$-correction. As in the last section, we will not only confirm this prediction for the ground state, but rather consider an extensive fraction of the QREM low energy spectrum. We recall the large deviation set $\mathcal{L}_\varepsilon = \{\boldsymbol{\sigma} \,|\, U(\boldsymbol{\sigma}) \leq -\varepsilon N\}$ with $\varepsilon \in (0, \beta_c)$, which already occurred in the proof of Goldschmidt's formula. Our goal is to relate the large deviations for $\varepsilon > 0$ large enough with the corresponding low energy states of the QREM.

To characterize localization properties of the eigenvectors in the canonical z-basis, we introduce

$$B_R(\boldsymbol{\sigma}) := \{\boldsymbol{\sigma}' \,|\, d(\boldsymbol{\sigma}, \boldsymbol{\sigma}') \leq R\}, \qquad S_R(\boldsymbol{\sigma}) := \{\boldsymbol{\sigma}' \,|\, d(\boldsymbol{\sigma}, \boldsymbol{\sigma}') = R\},$$

which stand for the Hamming ball and sphere of radius R, which are defined in terms of the Hamming distance $d(\boldsymbol{\sigma}, \boldsymbol{\sigma}') := \frac{1}{2}\sum_{i=1}^N |\sigma_i - \sigma_i'|$.

Theorem 3.5 (Theorem 1.5 in [132])
For $\Gamma < \beta_c$ and $\delta > 0$ small enough, the following applies for sufficiently large N with overwhelming probability:

1. *The eigenvalues E of $H_N = \Gamma T + U$ below $-(\beta_c - \delta)N$ and the low-energy configurations $U(\boldsymbol{\sigma})$ are in a one-to-one correspondence such that*

$$E = U(\boldsymbol{\sigma}) + \frac{\Gamma^2 N}{U(\boldsymbol{\sigma})} + \mathcal{O}(N^{-1/4}). \tag{3.6}$$

   In particular, the estimate $\mathcal{O}(N^{-1/4})$ is independent of $\boldsymbol{\sigma} \in \mathcal{L}_{\beta_c - \delta}$.

2. *The ℓ^2-normalized eigenvector ψ corresponding to E and $\boldsymbol{\sigma}$ concentrates near this configuration in the sense that:*

   (a) Close to extremum: *For any $K \in \mathbb{N}$ and for all $\boldsymbol{\sigma}' \in S_K(\boldsymbol{\sigma})$:*

$$|\psi(\boldsymbol{\sigma}')| = \mathcal{O}(N^{-K}), \quad \text{and} \quad \sum_{\boldsymbol{\sigma}' \notin B_K(\boldsymbol{\sigma})} |\psi(\boldsymbol{\sigma})|^2 = \mathcal{O}(N^{-(K+1)}).$$

   (b) Far from extremum: *For any $0 < \alpha < 1$, there is some $c_\alpha \in (0, \infty)$ such that*

$$\sum_{\boldsymbol{\sigma}' \notin B_{\alpha N}(\boldsymbol{\sigma})} |\psi(\boldsymbol{\sigma}')|^2 \leq e^{-c_\alpha N}.$$

We observe an extreme localization regime in which the eigenvectors are strongly localized – each in its own large deviation $\boldsymbol{\sigma}$ of the REM. In essence, our localization results show that there is no tunneling between the large deviation sites for low enough energies. Theorem 3.5 in particular covers the ground-state of the QREM and thus extends the result [19, Lemma 2.1] on the leading asymptotics of the ground-state energy in the parameter regime $\Gamma = \kappa/N$ with $\kappa > 0$. A further discussion of the localization results in context of the Anderson model will be given in the last section of this chapter. The estimates on the decay rate of the eigenvectors close to the extremum are optimal; and far from the extremum they are optimal up to determining the decay rate c_α. From the proof of Theorem 3.5 in [132], one can read off a (non-optimal) threshold for the value of δ and also more precise error terms for the eigenvalues.
We recall that the minimum of the REM and its extremal statistics are well known, see Proposition 2.1 and (2.3). Since Theorem 3.5 discusses the whole low energy spectrum, a similar result for the QREM is an immediate consequence.

Corollary 3.6 (Corollary 1.5 in [132])
Let $\Gamma < \beta_c$ and let

$$s_N(x;\Gamma) := -\beta_c N + \frac{\ln(N \ln 2) + \ln(4\pi)}{2\beta_c} - \frac{\Gamma^2}{\beta_c} - \frac{x}{\beta_c}. \tag{3.7}$$

Then, the rescaled eigenvalue process spec H_N *of the QREM Hamiltonian $H_N = \Gamma T + U$ converges weakly,*

$$\sum_{E \in \operatorname{spec} H_N} \delta_{s_N^{-1}(E;\Gamma)} \to \mathcal{P}_{e^{-x}\,dx}.$$

In particular, the ground state energy converges weakly

$$E_{GS} - \left(-\beta_c N + \frac{\ln(N \ln 2) + \ln(4\pi)}{2\beta_c} - \frac{\Gamma^2}{\beta_c}\right) \to -\frac{X}{\beta_c},$$

where X is a random variable distributed according to the law of the maximum of the Poisson point process $\mathcal{P}_{e^{-x}\,dx}$ with intensity $e^{-x}\,dx$ on the real line .

We will now present some further results on the ground state wavefunction. In fact, the proof of Theorem 3.5 already shows that the ground state can be approximated very well by the first order correction arising from perturbation theory. More interestingly, we can even determine the ℓ^1-norm of the ground state, which converges to an explicit constant. This reflects again the sharp localization in the glass phase.

Theorem 3.7 (Theorem 1.7 in [132])
For $\Gamma < \beta_c$ and all N large enough, there is an $\delta > 0$ and $\boldsymbol{\sigma}_0 \in \mathcal{L}_{\beta_c-\delta}$ such that the positive ℓ^2-normalized ground state ψ of the QREM Hamiltonian is concentrated near $\boldsymbol{\sigma}_0$ with overwhelming probability in the sense that:

1. *the ℓ^2-distance of ψ and $\delta_{\boldsymbol{\sigma}_0}$ is $\|\psi - \delta_{\boldsymbol{\sigma}_0}\|^2 = \mathcal{O}\left(\frac{1}{N}\right)$, and its first order correction*

$$\xi := \sqrt{1 - \frac{\Gamma^2}{\beta_c^2 N}}\delta_{\boldsymbol{\sigma}_0} + \frac{\Gamma}{\beta_c N}\sum_{\boldsymbol{\sigma}\in S_1}\delta_{\boldsymbol{\sigma}}$$

   has the same energy as ψ up to order one, and $\|\psi - \xi\|^2 = \mathcal{O}\left(\frac{1}{N^2}\right)$.

2. *the ℓ^1-norm of ψ converges to a bounded constant:*

$$\|\psi\|_1 = \sum_{\boldsymbol{\sigma}} \psi(\boldsymbol{\sigma}) = \frac{\beta_c}{\beta_c - \Gamma} + o(1),$$

   and, for any $1 < p < \infty$: $\quad \|\psi\|_p^p = \sum_{\boldsymbol{\sigma}} |\psi(\boldsymbol{\sigma})|^p = 1 + o(1).$

Let us now comment on Theorem 3.7. First, the configuration $\boldsymbol{\sigma}_0$ on which the ground-state is asymptotically localized and the classical minimal configuration $\boldsymbol{\sigma}_{\min} := \arg\min U$ do not need to agree, but the probability $\mathbb{P}(\boldsymbol{\sigma}_0 \neq \boldsymbol{\sigma}_{\min}) \leq \frac{c}{N}$ vanishes for $N \to \infty$. Secondly, the methods on which the proofs of Theorem 3.5 and 3.7 are based on allow an expansion for the ground state energy up to N^{-K} for any fixed integer K. The correction corresponding to the order N^{-K} is determined by potential fluctuations on the sphere of radius $K + 1$. A similar expansion for the ground state eigenvector holds true as well. Thirdly, the ℓ^1-norm limit we provide here is of special interest if one treats the QREM as gen mutation model. As we have seen in Section 1.2.3 the ℓ^1-normalized state coincides with the equilibrium distribution of a corresponding mutation-selection model with the REM potential U as fitness landscape.

In the following, we will give an idea of the proof of Theorem 3.5. As we have seen in the proof of Goldschmidt's formula, the REM low energies do not percolate. As a first step, we want to obtain stronger results on the geometry of the large deviations sets. For our analysis it is important to guarantee that the low energy states are not just isolated, but in fact very far from each other. Some straightforward combinatorial and probabilistic estimates lead to the following conclusion [131, Lemma 4.2]: for every $\varepsilon > 0$ we find some $\alpha, \delta > 0$ such that with overwhelming probability

$$|U(\boldsymbol{\sigma}')| \leq \varepsilon N \quad \text{for all} \quad \boldsymbol{\sigma}' \in B_{2\alpha N}(\boldsymbol{\sigma}) \setminus \{\boldsymbol{\sigma}\} \text{ and } \boldsymbol{\sigma} \in \mathcal{L}_{\beta_c-\delta}.$$

In particular, the balls $B_{\alpha N}(\boldsymbol{\sigma}) \cap B_{\alpha N}(\boldsymbol{\tau})$ are disjoint for two different large deviations $\boldsymbol{\sigma} \neq \boldsymbol{\tau} \in \mathcal{L}_{\beta_c-\delta}$, which confirms that the low energies are far from each other with high probability. These considerations suggest the following proof strategy: one first determines the ground states $\psi_{\boldsymbol{\sigma}}$ of the QREM Hamiltonian restricted to Hamming balls $B_{\alpha N}(\boldsymbol{\sigma})$ with $\boldsymbol{\sigma} \in \mathcal{L}_{\beta_c-\delta}$. In a second step, one "glues" these balls Hamiltonians together with the rest operator, and verifies that the characteristics of the ball ground states survive this recomposition procedure.

After establishing Theorem 3.5 locally for the ball states, putting the pieces together is a rather routine argument: one shows that the spectrum of the "remainder" operator, collecting the terms outside the balls, is energetically separated from the regime of interest. Together with the exponential decay of the ball ground states $\psi_{\boldsymbol{\sigma}}$, the Feshbach-Schur-Krein method, we have introduced in the last section, guarantees that the low energy spectrum of H_N agrees up to an exponentially small error with the collection of ball ground state energies $E_{\boldsymbol{\sigma}}$. The only subtle part is to show that the low energy eigenvectors of H_N are each normwise close to a specific ball state $\psi_{\boldsymbol{\sigma}}$. To put it in other words, one needs to ensure that ball states $\psi_{\boldsymbol{\sigma}}$ do not mix, i.e., there is no tunneling between different balls. To this end, we invoke the so-called *spectral averaging principle* – a common technique in the field of random Schrödinger operators [9] – to establish a lower bound on the energetic separation between the ball ground state energies [132, Lemma 4.4]. This bound is exponentially small, yet for small $\delta > 0$ strong enough to prohibit mixing of the ball states. This is carried out in the Sections 4.4 and 4.5 in [132].

Here, we focus on the local analysis on the Hamming balls $B_{\alpha N}(\boldsymbol{\sigma})$, which forms the heart of the argument. Let us fix some $\boldsymbol{\sigma}_0 \in \mathcal{L}_{\beta_c-\delta}$ and $\alpha > 0$. We consider the restricted Hamiltonian $H_{\alpha N}(\boldsymbol{\sigma}_0)$ on the subspace $\ell^2(B_{\alpha N}(\boldsymbol{\sigma}_0))$, i.e., $H_{\alpha N}(\boldsymbol{\sigma}) = U + \Gamma T_{\alpha N}$ with the Dirichlet restriction $T_{\alpha N}$ to a Hamming ball which is defined via its matrix elements

$$\langle \boldsymbol{\tau} | T_{\alpha N} | \boldsymbol{\tau}' \rangle = \langle \boldsymbol{\tau} | T | \boldsymbol{\tau}' \rangle$$

for $\tau, \tau' \in B_{\alpha N}(\boldsymbol{\sigma}_0)$. Since the potential is dominated by a single deep-hole at $\boldsymbol{\sigma}$, our ansatz is to treat $H_{\alpha N}(\boldsymbol{\sigma})$ as an effective rank-one perturbation of $\Gamma T_{\alpha N}$ and we verify in a next step that neglecting the fluctuations of U around $\boldsymbol{\sigma}$ is in fact justified.

In order to invoke rank-one perturbation theory, one needs to control the Green function of $T_{\alpha N}$, that is,

$$G_{\alpha N}(\boldsymbol{\sigma}, \boldsymbol{\sigma}_0; E) := \left\langle \boldsymbol{\sigma} \right| (-T_{\alpha N} - E)^{-1} \left| \boldsymbol{\sigma}_0 \right\rangle .$$

Interestingly, despite being of relevance in the field of discrete mathematics, the spectral properties of $T_{\alpha N}$ are not well understood. So far, the main result in the literature concerns the minimal eigenvalue $E_N(\alpha)$,

$$E_N(\alpha) := \inf \operatorname{spec} T_{\alpha N} = -2\sqrt{(1-\alpha)\alpha} N + o(N),$$

which was proven first in [84, Proposition 8.5], and a better error bound has been given in [32]. We give a short proof for the lower bound $E_N(\alpha) \geq -2\sqrt{(1-\alpha)\alpha} N$ in [132, Lemma 2.1]. Due to the lack of spectral results on $T_{\alpha N}$, we had to derive estimates on $G_{\alpha N}(\boldsymbol{\sigma}, \boldsymbol{\sigma}_0; E)$ from scratch. Our bounds on the Green's function might be of independent interest:

Proposition 3.8 (Proposition 2.5 in [132])
Let $0 < \alpha < 1/2$, and $\varepsilon > 0$. Then, for $E \leq E_N(\alpha) - \varepsilon N$, all $\boldsymbol{\sigma} \in B_{\alpha N}(\boldsymbol{\sigma}_0)$ and all N large enough:

$$G_{\alpha N}(\boldsymbol{\sigma}, \boldsymbol{\sigma}_0; E) \leq \frac{1}{\varepsilon N} \binom{N}{d(\boldsymbol{\sigma}_0, \boldsymbol{\sigma})}^{-1/2} 2^{-\min\{d(\boldsymbol{\sigma}_0, \boldsymbol{\sigma}), \alpha_0(\alpha) N\}},$$

where $0 < \alpha_0(\alpha) < \alpha$ is the unique solution to the equation $2\sqrt{\alpha(1-\alpha)} = 3\sqrt{\alpha_0(1-\alpha_0)}$. Moreover, for any fixed $K \in \mathbb{N}$ there is some $C_K < \infty$ such that for all N large enough:

1. *for all $\boldsymbol{\sigma} \in S_K(\boldsymbol{\sigma}_0)$:* $G_{\alpha N}(\boldsymbol{\sigma}, \boldsymbol{\sigma}_0; E) \leq \frac{1}{\varepsilon N} \frac{C_K}{\sqrt{N^K}} \binom{N}{d(\boldsymbol{\sigma}_0, \boldsymbol{\sigma})}^{-1/2}$.

2. $\sum_{\boldsymbol{\sigma} \notin B_K(\boldsymbol{\sigma}_0)} G_{\alpha N}(\boldsymbol{\sigma}, \boldsymbol{\sigma}_0; E)^2 \leq \frac{C_K}{\varepsilon^2 N^{K+2}}$.

The proof of Proposition 3.8 exploits the radial symmetry of $G_{\alpha N}(\boldsymbol{\sigma}, \boldsymbol{\sigma}_0; E)$, that is, the Green function does only depend on $d(\boldsymbol{\sigma}, \boldsymbol{\sigma}_0)$. This observation translates into Ricatti type recursive relations which enable us to proceed by an inductive argument. The whole proof can be found in [132, Section 2].

Most importantly, the estimates on the Green function in Proposition 3.8 reflect the decay bounds on the eigenstates we propose in Theorem 3.5. This can be easily verified for the ground state $\psi_{\boldsymbol{\sigma}_0}$ of the ball Hamilton $H_{\alpha N}(\boldsymbol{\sigma}_0)$. Let $E_{\boldsymbol{\sigma}_0}$ be the ground state energy of the ball Hamiltonian. If we choose $\delta, \varepsilon, \alpha$ such that $\beta_c - \delta > 2\Gamma\sqrt{\alpha(1-\alpha)} + \varepsilon$, then by standard rank-one perturbation theory $E_{\boldsymbol{\sigma}_0}$ is the only eigenvalue below $-(\Gamma\sqrt{\alpha(1-\alpha)} + \varepsilon)N$. A simple Rayleigh-Ritz bound $E_{\boldsymbol{\sigma}_0} \leq \langle \boldsymbol{\sigma}_0 | H_{\alpha N}(\boldsymbol{\sigma}_0) | \boldsymbol{\sigma}_0 \rangle = U(\boldsymbol{\sigma}_0) \leq -(\beta_c - \delta)N$ provides a first, crude estimate on this eigenvalue. Employing again rank-one perturbation theory with the operator $H'_{\alpha N}(\boldsymbol{\sigma}_0) = H_{\alpha N}(\boldsymbol{\sigma}_0) - U(\boldsymbol{\sigma}_0)|\boldsymbol{\sigma}_0\rangle\langle\boldsymbol{\sigma}_0|$, we conclude that the ℓ^2-normalized eigenvector $\psi_{\boldsymbol{\sigma}_0}$ satisfies for all $\boldsymbol{\sigma} \in B_{\alpha N}(\boldsymbol{\sigma}_0)$:

$$\begin{aligned}\psi_{\boldsymbol{\sigma}_0}(\boldsymbol{\sigma}) &= -U(\boldsymbol{\sigma}_0)\, \psi_{\boldsymbol{\sigma}}(\boldsymbol{\sigma}) \langle \boldsymbol{\sigma} | \left(H'_{\alpha N}(\boldsymbol{\sigma}_0) - E_{\boldsymbol{\sigma}_0} \right)^{-1} | \boldsymbol{\sigma}_0 \rangle \leq -U(\boldsymbol{\sigma}_0) \langle \boldsymbol{\sigma} | \left(\Gamma T_{\alpha N} - (E_{\boldsymbol{\sigma}_0} + \varepsilon N) \right)^{-1} | \boldsymbol{\sigma}_0 \rangle \\ &\leq -U(\boldsymbol{\sigma}_0)\, \Gamma^{-1} \langle \boldsymbol{\sigma} | \left(T_{\alpha N} - (U(\boldsymbol{\sigma}_0) + \varepsilon N)\Gamma^{-1} \right)^{-1} | \boldsymbol{\sigma}_0 \rangle.\end{aligned}$$

Here, we used that $U \geq -\varepsilon N$ on $B_{\alpha N}(\boldsymbol{\sigma}_0) \setminus \{\boldsymbol{\sigma}_0\}$, our a priori bound on $E_{\boldsymbol{\sigma}_0}$. Moreover, we recall that T generates a positive semigroup, which implies that the matrix elements are $\langle \boldsymbol{\sigma} | \left(H'_{\alpha N}(\boldsymbol{\sigma}_0) - E_{\boldsymbol{\sigma}_0} \right)^{-1} | \boldsymbol{\sigma}_0 \rangle$ monotone with respect to the potential values of U. Proposition 3.8 readily implies the claimed decay estimates in Theorem 3.5. It remains to derive the ball energy $E_{\boldsymbol{\sigma}_0}$. Here, we combine the eigenvalue equation with the already established decay estimates. Namely, the eigenvalue equation at any $\boldsymbol{\sigma} \in S_1(\boldsymbol{\sigma}_0)$: yields

$$\begin{aligned}E_{\boldsymbol{\sigma}_0} \psi_{\boldsymbol{\sigma}}(\boldsymbol{\sigma}') &= U(\boldsymbol{\sigma}) \psi_{\boldsymbol{\sigma}_0}(\boldsymbol{\sigma}) - \Gamma \psi_{\boldsymbol{\sigma}_0}(\boldsymbol{\sigma}_0) - \Gamma \sum_{\boldsymbol{\sigma}' \in S_1(\boldsymbol{\sigma}) \setminus \{\boldsymbol{\sigma}\}} \psi_{\boldsymbol{\sigma}_0}(\boldsymbol{\sigma}') \\ &= U(\boldsymbol{\sigma}) \psi_{\boldsymbol{\sigma}_0}(\boldsymbol{\sigma}) - \Gamma \psi_{\boldsymbol{\sigma}_0}(\boldsymbol{\sigma}_0) + \mathcal{O}(N^{-1}).\end{aligned}$$

The $\mathcal{O}(N^{-1})$ estimate follows from the priorly derived concentration close to the deep hole. The eigenvalue equation can be rewritten as $\psi_{\boldsymbol{\sigma}_0}(\boldsymbol{\sigma}) = -\frac{\Gamma}{E_{\boldsymbol{\sigma}_0}-U(\boldsymbol{\sigma})}\left(\psi_{\boldsymbol{\sigma}_0}(\boldsymbol{\sigma}_0)+\mathcal{O}(N^{-1})\right)$, which we insert into the eigenvalue equation at the deep hole $\boldsymbol{\sigma}_0$:

$$\begin{aligned} E_{\boldsymbol{\sigma}_0}\psi_{\boldsymbol{\sigma}_0}(\boldsymbol{\sigma}_0) &= U(\boldsymbol{\sigma})\psi_{\boldsymbol{\sigma}_0}(\boldsymbol{\sigma}_0) - \Gamma \sum_{\boldsymbol{\sigma}\in S_1(\boldsymbol{\sigma}_0)} \psi_{\boldsymbol{\sigma}_0}(\boldsymbol{\sigma}) \\ &= U(\boldsymbol{\sigma}_0)\psi_{\boldsymbol{\sigma}_0}(\boldsymbol{\sigma}_0) + \frac{\Gamma^2}{E_{\boldsymbol{\sigma}_0}}\left(\sum_{\boldsymbol{\sigma}\in S_1(\boldsymbol{\sigma}_0)} \frac{\psi_{\boldsymbol{\sigma}_0}(\boldsymbol{\sigma}_0)+\mathcal{O}(N^{-1})}{1-U(\boldsymbol{\sigma})/E_{\boldsymbol{\sigma}_0}}\right) \\ &= \left[U(\boldsymbol{\sigma}_0) + \frac{\Gamma^2 N}{E_{\boldsymbol{\sigma}_0}} + \frac{\Gamma^2}{E_{\boldsymbol{\sigma}_0}}\left(\sum_{\boldsymbol{\sigma}\in S_1(\boldsymbol{\sigma}_0)} \frac{U(\boldsymbol{\sigma})}{E_{\boldsymbol{\sigma}_0}}\right)\right]\psi_{\boldsymbol{\sigma}_0}(\boldsymbol{\sigma}_0). \end{aligned}$$

The last line is a consequence of a Taylor expansion and some algebra. Note that typically $\left(\sum_{\boldsymbol{\sigma}\in S_1(\boldsymbol{\sigma}_0)} \frac{U(\boldsymbol{\sigma})}{E_{\boldsymbol{\sigma}_0}}\right) = \mathcal{O}(1)$ and one can show that there is a uniform bound on all Hamming balls by $\mathcal{O}(N^{3/4})$. That results in the expansion $E_{\boldsymbol{\sigma}_0} = U(\boldsymbol{\sigma}_0) + \frac{\Gamma^2 N}{U(\boldsymbol{\sigma}_0)} + \mathcal{O}(N^{-1/4})$, completing the local analysis.

3.4 The Pressure

The methods we introduced in the last two sections allow to pin down the pressure Φ_N up to order one in N in all three phases of the QREM: the glass phase ($\beta > \beta_c$ and $\Gamma < \Gamma(\beta)$), the classical 'unfrozen' REM phase ($\beta < \beta_c$ and $\Gamma < \Gamma(\beta)$) and the quantum paramagnetic phase ($\Gamma > \Gamma(\beta)$).

Theorem 3.9 (Theorem 1.10 in [132]) *1. If $\Gamma > \Gamma_c(\beta)$ the pressure $\Phi_N(\beta,\Gamma)$ is up to order one deterministic and one has the almost sure convergence*

$$\Phi_N(\beta,\Gamma) - (\ln 2\cosh(\beta\Gamma))N \to \frac{\beta}{\Gamma\tanh(\beta\Gamma)}.$$

2. If $\Gamma < \Gamma_c(\beta)$ and $\beta \leq \beta_c$, the pressure $\Phi_N(\beta,\Gamma)$ differs from the REM's pressure $\Phi_N(\beta,0)$ by a deterministic β-independent shift of order one, i.e., one has the almost sure convergence

$$\Phi_N(\beta,\Gamma) - \Phi_N(\beta,0) \to \Gamma^2.$$

3. If $\Gamma < \Gamma_c(\beta)$ and $\beta > \beta_c$, the pressure $\Phi_N(\beta,\Gamma)$ differs from the REM's pressure by a deterministic β-dependent shift of order one, i.e., one has the almost sure convergence

$$\Phi_N(\beta,\Gamma) - \Phi_N(\beta,0) \to \frac{\Gamma^2\beta}{\beta_c}.$$

As in the analysis of the low energy spectrum, we observe a deterministic order $\mathcal{O}(1)$-shift in either phase. Determining these shifts of the pressure heuristically, is not very difficult. For example, in the paramagnetic regime we have seen that the low eigenvalues of E are shifted to $E + \frac{N}{E} + o(1)$. Moreover, we know that the (unperturbed) paramagnetic pressure is governed by the eigenvalues close to $\langle \Gamma T\rangle_{\beta,\Gamma} = -\Gamma\tanh(\beta\Gamma)N$, which results formally in a shift of the internal energy by $\frac{1}{\Gamma\tanh(\beta\Gamma)}$. A similar approach yields a correct prediction for the shifts in the classical regime $\Gamma < \Gamma_c(\beta)$ as well. This idea can be made

easily rigorous in the glass phase, but for higher temperatures the dominant eigenvalues close to $\langle \Gamma T \rangle_{\beta,\Gamma}$ or, respectively, $\langle U \rangle_\beta$ will in general be located in the middle of the spectrum. However, Theorem 3.1 and Theorem 3.5 only cover the bottom of the spectrum. That we have to consider the shift of higher energies, is the main challenge in the proof of Theorem 3.9. We face this obstacle in the classical and paramagnetic phase differently.

If $\Gamma < \Gamma_c(\beta)$, we observe that $\frac{1}{N}\langle U \rangle_\beta = -\min\{\beta, \beta_c\} + o(1) < -\Gamma$ for N large enough. Hence, the pressure is dominated by energies which are below the paramagnetic ground state and, thus, can be labeled to REM energies $U(\boldsymbol{\sigma})$. However, in contrast to the scenario of Theorem 3.5 such a configuration $\boldsymbol{\sigma}$ does not need to be isolated, i.e., we cannot guarantee that there is no deep hole in the proximity of all energetically relevant configurations. The second important observation is that for any energy interval $[E - \delta N, E + \delta N]$ the fraction of non-isolated configurations $\boldsymbol{\sigma}$ with $U(\boldsymbol{\sigma}) \in [E - \delta N, E + \delta N]$ is exponentially small. Consequently, the contribution of non-isolated configurations to the pressure is of order $o(1)$, and for isolated configurations we are able to reproduce the energy formula (3.6).

The paramagnetic regime $\Gamma > \Gamma_c(\beta)$ is the more subtle phase. Namely, we have to consider parts of the QREM spectrum where the eigenvalues originate from both, ΓT and U. Understanding the eigenstates at energies where the spectra of U and ΓT interlace, is a difficult and largely open problem. In some sense, our main idea is to avoid an analysis of the interlaced spectrum by means of some technical tricks which are powerful enough to establish the $\mathcal{O}(1)$-corrections of the spectrum. We truncate the REM potential U such that its ground state lies higher than $\langle T \rangle_{\beta,\Gamma}$. For the Hamiltonian with the truncated potential one can use a version of Theorem 3.1 to derive the pressure up to order $o(1)$. A rather involved convexity argument allows us to extend these findings to the complete QREM Hamiltonian. The argument is carried out in [132, Section 5].

As a consequence of Theorem 3.9, we can extend the results of Theorem 2.5 to the QREM glass regime:

Corollary 3.10 (Corollary 1.11 in [132])
If $\Gamma < \Gamma_c(\beta)$ and $\beta > \beta_c$, we have the weak convergence:

$$e^{-N[\beta\beta_c]+\frac{\beta}{2\beta_c}[\ln(N\ln 2)+\ln 4\pi]-\frac{\beta\Gamma^2}{\beta_c}} Z_N(\beta,\Gamma) \to \int_{-\infty}^{\infty} e^{z\beta/\beta_c}\, \mathrm{PPP}_{e^{-x}\,dx}(dz).$$

The fluctuations of the QREM's partition function outside the spin glass phase are expected to be much smaller – for $\Gamma < \Gamma_c(\beta)$ and $\beta < \beta_c$ most likely on a similar scale as in the REM and for the paramagnetic regime presumably even smaller. Unfortunately, we have not managed yet to design methods which enable us to control fluctuations on an exponentially small scale.

3.5 The QREM in the Literature

We close this chapter by presenting related work in the mathematics and physics literature. We have already seen that the QREM emerges in several contexts such as mathematical biology and the study of aging and metastability. While the literature on these fields is large, as far as we know an analysis of the QREM has not been pursued and the methodology is rather different. The closest mathematical works concern the so-called Anderson model and in the first subsection we take the chance to sketch similarities and differences between prior works on the Anderson model and our study of the QREM. The situation

is different for the physics literature, where the QREM is a well-established model of which many facets have been studied. We want to give an overview of the physical studies on the QREM. We relate our results to the physical findings and discuss which physical predictions may be addressed in the future.

3.5.1 The QREM and the Anderson Model

In 1958, Anderson suggested in a seminal paper that impurities in a metal can drastically change its conducting properties [12]. Anderson introduced random Schrödinger operators on the lattice $\mathbb{Z}^d$ as an effective one-body model for electrons in a metal with defects. He predicted that if the disorder is strong enough, the electrons become localized such that there is no diffusion anymore. This phenomenon is referred to as *Anderson localization*. The Anderson Hamiltonian H_{A} can be defined on any (undirected) graph $G = (V, E)$ with vertices V and edges E. To this end, let $(W_v)_{v\in V}$ be a collection of i.i.d. real random variables and Δ_G denotes the graph Laplacian on $\ell^2(V)$,

$$(\Delta_G\varphi)(v) := \sum_{u:u\sim v} [\varphi(u) - \varphi(v)],$$

where $\varphi \in \ell^2(V)$ and $u \sim v$ is a short-hand notation for connected vertices. As usual, the potential $(W_v)_{v\in V}$ gives rise to a diagonal operator and the random Schrödinger operator is defined as

$$H_{\mathrm{A}} = \lambda W - \Delta_G$$

with $\lambda \geq 0$ measuring the degree of disorder. For finite graphs, H_{A} is simply a random matrix whereas for infinite graphs one may have an unbounded self-adjoint operator only defined on a suitable domain. On $\mathbb{Z}^d$, Anderson localization corresponds to the pure point spectrum while the absolutely continuous spectrum is interpreted as being formed by conducting states [9].

If G is the Hamming cube equipped with the Hamming distance, the graph Laplacian reads $\Delta_{\mathcal{Q}_N} = -T - N\mathbb{1}$. Thus up to an identity shift, the QREM Hamiltonian can be seen as a specific Anderson-type random Schrödinger on the Hamming cube. This mathematical equivalence can be used to invoke localization techniques originally developed for the Anderson model on the lattice. One example is the spectral averaging principle we have used in the glass regime. In [19], a QREM-like model on the Hamming cube with Δ_G replaced by $\frac{1}{N}\Delta_G$ has been analyzed by means of the heat equation corresponding to the Anderson Hamiltonian. One sometimes speak of the *parabolic Anderson model* when the semigroup perspective is put in the foreground. While ground state energy and some localization properties are examined in [19], the results therein are much weaker than what we have presented in Section 3.3. Most importantly, since $\frac{1}{N}\Delta_G$ is of lower order then U, their is no competition between localization and delocalization, which is a characterizing feature of the QREM.

The most canonical Anderson model is the random Schrödinger operator on a finite degree infinite graph. Despite the fact that the QREM can be formulated as Anderson Hamiltonian, we want to convince the reader that the viewpoint has to be considered with a grain of salt. In particular, the QREM is not just another derivative of the Anderson model on $\mathbb{Z}^d$. First, since the degree of $\mathcal{Q}_N$ increases with N, the low energy eigenstates of T are much more delocalized than the corresponding eigenstates of the Laplacian on a finite box in $\mathbb{Z}^d$. Secondly, there are many works such as [30] concerning the localization of the eigenstates in the bottom of the spectrum. However, the resulting localization is weaker than in the

QREM although the transversal field is normwise "stronger" than the Laplacian on $\mathbb{Z}^d$. Perhaps most importantly, in the finite-dimensional situation the ground state can never be delocalized in high contrast to the paramagnetic regime of the QREM. After all, we should recall that the Anderson model is an effective one-body model whereas the QREM is a many-body model. Hence, physical differences should not come as surprise.

3.5.2 Physical Predictions on the QREM

The physical treatment of the QREM originated in Goldschmidt's work [95]. We have already confirmed his formula on the specific pressure in Chapter 2. However, it would be still of interest to give an alternative proof based on the path integral approach. While deriving the annealed pressure via the Feynman-Kac formula is not too hard, a proof of Theorem 2.7 in this framework appears to be surprisingly difficult. On the other hand, it should be feasible to verify that the Parisi measure in the QREM glass phase agrees with the classical findings of Proposition 2.3 (see also Section 4.2.2). An important motivation for the study of quantum spin glasses, and more generally transverse field models, is the appearance of quantum phase transitions (QPT) at zero temperature. These ground state transitions may be of first order or may show a continuous change of the relevant order parameters [68]. QPT are unique to quantum models as they are driven by quantum fluctuations. Hence, transverse field models allow us to enhance our understanding of quantum physics. In the case of the QREM, Goldschmidt's formula reveals a QPT at $\Gamma = \beta_c$. For a full understanding of a QPT, one needs to examine how the transition is reflected in a change of the ground state wavefunction's properties. Our result on the localization in the glass phase and the delocalization in the paramagnetic phase show that the QPT in the QREM is accompanied by a drastic change of the system's behavior.

More recently, the QREM has gained considerable interest in the physics community as simple testing ground for more involved phenomena. A prominent example is the performance of the Quantum Adiabatic Algorithm (QAA) applied to hard optimization tasks (see also our discussion in 1.2.3). While QAA can be successfully used for many problems, it is known that there exists some Hamiltonians where QAA does not do better than Grover search [76]. However, the counter examples considered in [76] were specifically designed to make the QAA fail, and, hence, it remains open how the QAA performs "in general". In [24], it is argued that the generic performance of QAA can be evaluated by applying QAA to quantum spin glasses. Of course, the QREM, the arguably simplest quantum spin glass, is a natural starting point. In view of the quantum adiabatic theorem (see Theorem 1.1), one is tempted to determine the minimal gap of the QREM Hamiltonian. In [110], the authors start from second order perturbation theory to determine the ground start energy up to order $o(1)$. In the past few sections we confirmed these findings. That the QREM ground state almost resembles the REM minimal energy configuration $|\boldsymbol{\sigma}_{\min}\rangle$ or, respectively, the paramagnetic flat state $\Psi_\emptyset$, motivated the authors in [110] to think of the situation as an avoided level crossing. In simple terms, the picture is that both ground states always exist and live independently from each other their own lives. They are effectively only coupled by an interaction in form of the matrix overlap $\langle \Psi_\emptyset | \boldsymbol{\sigma}_{\min} \rangle$. From here, they predict an exponentially small gap $\Delta \approx 2^{-N/2}$. An exponentially small gap has been rigorously confirmed in [2], where it has been shown that $\Delta \leq CN^{3/2}2^{-N/6}$ holds true with overwhelmingly high probability. This suggests, that the QAA will only find the REM minimum after an exponentially long time, and thus, it barely outperforms Grover search. Unfortunately, an exponentially small gap is predicted to be generic for quantum spin glasses [24].

For instance, in [111] the random 3-XORSAT in a transverse field is considered. The random c-regular 3-XORSAT potential $U_{3-\mathrm{XORSAT}}(\boldsymbol{\sigma}) = \sum_{a=1}^{M}(1 - J_a\sigma_{i_1^a}\sigma_{i_2^a}\sigma_{i_3^a})$ consists of $M = cN/3$ patterns with i.i.d. Bernoulli weights J_a (i.e., $\mathbb{P}(J_a = \pm 1) = \frac{1}{2}$), and the indices i_k^a are picked uniformly among those choices which yield a c-regular graph. The cavity method and numerical computations provide evidence for an exponentially small gap in the quantum random 3-XORSAT model [111]. Proving an exponentially small gap for quantum spin glass models which are more involved than the QREM, appears to be challenging and arguably in most cases more difficult than establishing a quantum phase transition as it requires a detailed understanding of the ground states properties.

At first glance, the expected exponentially small gap for quantum spin glasses raises doubts on the applicability of QAA to hard optimization tasks. Of course, an exponentially long procedure time would not yield a crucial speed up compared to classical algorithms. On second thought however, one realizes that one is not necessarily interested in the exact minimal energy configuration, but rather in a "good" approximation. Here, a good approximation might be a spin configuration which is close to the minimum with respect to the Hamming distance or a site with energy close to the ground state energy. Under these less ambitious goals, a polynomial time T might be enough for a satisfactory result. In the QREM it is not expected, that a polynomial time is enough even for an energetic approximation [22]. The main reason is that the REM potential is completely unstructured and in that sense the worst-case scenario for any search algorithm. However, for a variety of models a single spin flip will not change the energy that much. Consequently, the low energy configurations form clusters in the Hamming cube. It is argued in [22] that the performance of QAA then depends on the tunneling rate between these clusters. A significantly shorter time may be needed to exclude tunneling, and, thus to find a configuration in the proximity of the minimal energy site. A rigorous justification of this intuition would require a good understanding of the energy landscape and a direct analysis of the adiabatic time evolution. Consequently, one needs to develop new techniques in order to treat the dynamics of quantum spin glass models, an interesting research direction for the future.

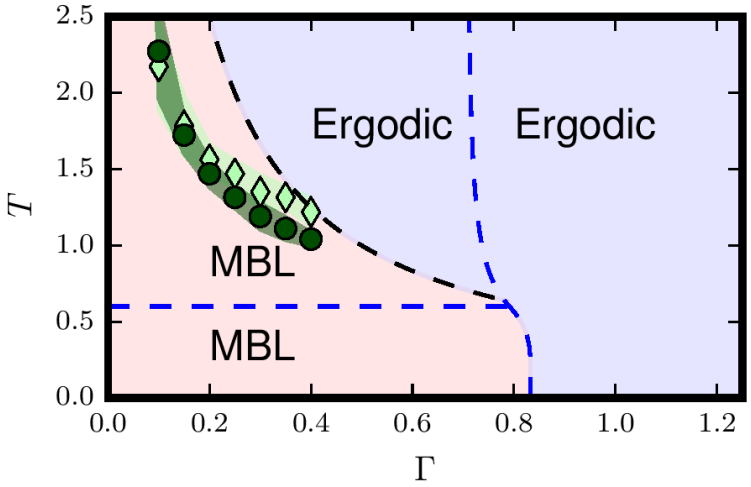

Figure 3.1: Many-body localization and ergodicity in the QREM. [23, Figure 1]. The blue-dashed line correspond to the static phase transitions of the QREMnin the $\Gamma - T$ plane (see also Figure 2.3). The dark-dashed line is the MBL-ergodicity transition predicted by a forward scattering analysis, the dark green dots refer to numerical computations and the light green diamonds to exact diagonalization.

Let us now turn to further physical phenomena which might be better understood in the realm of the QREM: *many-body localization* (MBL) and *ergodicity*. We cannot give an exhaustive discussion of MBL and ergodicity since the literature is vast and there are various definitions of both phenomena which are used interchangeably, but are not identical. We refer to the reviews [1, 140] and the references therein for more details. MBL and ergodicity are dynamical properties at heart and, hence, cannot be discussed in the context of static equilibrium physics. The general setting is as follows. We consider an N-body Hamiltonian H_N and we pick a "physical" state ψ we shall be typical for the system at some inverse temperature β. We are here on purpose vague because there is no general procedure on how to pick ψ, and the choice has to be justified for the concrete model. We think of $\psi = \psi_0$ being the initial state of our system and $\psi_t = e^{-itH_N}$ to be the state at some time t. Consider now for some large time T the time-averaged state $\hat{\rho}_T := \frac{1}{T}\int_0^T |\psi_t\rangle\langle\psi_t|$. The central question is: how well does the time averaged state $\hat{\rho}_T$ resemble the Gibbs state ρ_β? The states $\hat{\rho}_T$ and ρ_β will typically be not close to each other normwise, but one often observes thermalization, i.e., for any observable A acting on only few particles one has

$$\operatorname{Tr} A\hat{\rho}_T \approx \operatorname{Tr} A\rho_\beta \tag{3.8}$$

for large enough times T. If (3.8) is fulfilled, one speaks of ergodic behavior. Ergodicity follows in particular from the eigenstate thermalization hypothesis (ETH). ETH refers to the situation where (most) eigenstates ψ with energy $E \approx \langle H_N\rangle_\beta$ satisfy (3.8). In contrast, MBL is characterized by eigenstates ψ which are sharply localized on the Hamming cube (or more generally on the Fock space) and those ψ strongly violate the thermalization property (3.8). One expects that a "generic" physical system is ergodic and MBL only occurs in exotic systems such as strongly disordered metals. Moreover, quantum spin glasses should give rise to an ergodic phase and an MBL phase depending on the field strength Γ and inverse temperature β and, thus, quantum spin glasses may shed some light on the microscopic mechanisms which give rise to either phase [23, 121, 138, 139].

Numerical computation and analytic techniques such as perturbation theory and a forward scattering analysis have been employed, to gain insight into the localization-ergodicity transition in the QREM. While there is no concensus on the quantitative prescription of the dynamical phase transition, the qualitative picture appears to be as follows (see also Figure 3.1). The glass phase should be governed by many-body localization and the quantum paramagnetic phase is expected to be ergodic. Most interestingly, the classical paramagnetic phase is divided into an MBL part and ergodic fraction. Our localization Theorem 3.5 and 3.7 confirm MBL in the complete glass phase and in a fraction of the non-glassy phase REM regime. Our delocalization results in the quantum paramagnetic phase suggest ergodicity to hold true. However, a rigorous prove of the ETH seems to require considerable effort. Nevertheless, it would be of general interest as there no many tools at hand to prove ETH. Presumably, the most challenging part would be to show the localization-delocalization transition in the REM regime. One would need to understand when the REM low energy configurations start to tunnel, such that the REM deep holes away from the spectral edges mix and spread over the Hamming cube. We hope that this problem will be addressed in the future.

Chapter 4

Hierarchical Quantum Spin Glass Models

In this chapter, we study hierarchical quantum spin glasses, where the Generalized Random Energy Model (GREM) or Continuous Random Energy Model (CREM) takes the role of the random potential U and in comparison to the last two chapters we implement a more general random transversal field B. In the first Section 4.1, we review the classical GREM and CREM. We focus on the pressure, the extremal statistics and a description of the Gibbs measure via Ruelle cascades. The second Section 4.2 concentrates on the quantum versions QGREM and QCREM. We present the main results of Core Article II [130], which contains formulas for the specific pressure and a characterization of the phase diagrams showing a much richer structure than the QREM phase diagram. We will then give a hint on the proof ideas and comment on open problems regarding the QGREM and QCREM. In Section 4.3, we make a little excursion to the classical Sherrington-Kirkpatrick model to motivate the question of the de Almeida-Thouless (AT) line. Here, we familiarize ourselves with the replica symmetric solution and the interpolation method, before studying the much more sophisticated Parisi formula in Chapter 5. We close this chapter with Section 4.4 on the quantum AT line in the QCREM, where we analyze the influence of a random longitudinal field and a hierarchical vertical field on the phase diagram. This last section provides a summary of the results in [131].

4.1 Classical Hierarchical Spin Glasses

4.1.1 The n-level Generalized Random Energy Model

In this section, we want to review the classical GREM and the next subsection deals with its continuous analog, the CREM. We will largely follow the presentation in [36, Chapter 10].

Let us give a concrete construction of the n-level Generalized Random Energy Model. First, we need to pick a sequence of real numbers $0 = x_0 < x_1 < \cdots < x_n = 1$, which define a partition of spin configurations $\boldsymbol{\sigma} \in Q_N$ into n blocks $\boldsymbol{\sigma} = \boldsymbol{\sigma}_1 \dots \boldsymbol{\sigma}_n$. Each type σ_k consists of a fraction $x_k - x_{k-1}$ of spins. More precisely, we can write

$$\boldsymbol{\sigma}_k \in Q_N^{(k)} := \{-1, 1\}^{\lceil x_k N \rceil - \lceil x_{k-1} N \rceil}, \quad k \in \{1, \dots, n\}.$$

We further introduce a collection of independent standard Gaussian variables $X_{\boldsymbol{\sigma}_1}, X_{\boldsymbol{\sigma}_1\boldsymbol{\sigma}_2}, \dots, X_{\boldsymbol{\sigma}_1\boldsymbol{\sigma}_2\cdots\boldsymbol{\sigma}_n}$ and positive numbers $a_1, a_2, \dots a_n > 0$. For convenience, we assume that $\sum_{k=1}^n a_k = 1$, however all

results can be simply modified to the non-normalized case. The n-level GREM potential is then defined as

$$U(\boldsymbol{\sigma}) := \sqrt{N}\left(\sqrt{a_1}X_{\boldsymbol{\sigma}_1} + \sqrt{a_2}X_{\boldsymbol{\sigma}_1\boldsymbol{\sigma}_2} + \cdots + \sqrt{a_n}X_{\boldsymbol{\sigma}_1\boldsymbol{\sigma}_2\cdots\boldsymbol{\sigma}_n}\right).$$

The GREM is in contrast to the REM a correlated model, but with a built-in hierarchy which is reflected in its correlation structure. To compute $\mathbb{E}[U(\boldsymbol{\sigma})U(\boldsymbol{\sigma}')]$ for two configurations $\boldsymbol{\sigma}, \boldsymbol{\sigma}'$ one first considers the first blocks $\boldsymbol{\sigma}_1, \boldsymbol{\sigma}'_1$. If they disagree, we have a vanishing correlation $\mathbb{E}[U(\boldsymbol{\sigma})U(\boldsymbol{\sigma}')] = 0$, otherwise one considers the second blocks. If $\boldsymbol{\sigma}_2 \neq \boldsymbol{\sigma}'_2$, we conclude that $\mathbb{E}[U(\boldsymbol{\sigma})U(\boldsymbol{\sigma}')] = a_1 N$, otherwise we continue with the next block and so on. In that sense, the blocks $\boldsymbol{\sigma}_k$ define a hierarchy. More formally, U induces a distance function $d_U(\boldsymbol{\sigma}, \boldsymbol{\sigma}') := \mathbb{E}[|U(\boldsymbol{\sigma}) - U(\boldsymbol{\sigma}')|^2]^{1/2}$ on the Hamming cube which is an ultrametric, i.e., $d_U(\boldsymbol{\sigma}, \boldsymbol{\sigma}') \leq \max\{d_U(\boldsymbol{\sigma}, \boldsymbol{\sigma}''), d_U(\boldsymbol{\sigma}'', \boldsymbol{\sigma}')\}$ for any $\boldsymbol{\sigma}, \boldsymbol{\sigma}', \boldsymbol{\sigma}'' \in \mathcal{Q}_N$. It is instructive to rewrite the correlation function as follows:

$$\begin{aligned}\mathbb{E}[U(\boldsymbol{\sigma})U(\boldsymbol{\sigma}')] &= N(a_1\delta_{\boldsymbol{\sigma}_1,\boldsymbol{\sigma}'_1} + a_2\delta_{\boldsymbol{\sigma}_1\boldsymbol{\sigma}_2,\boldsymbol{\sigma}'_1\boldsymbol{\sigma}'_2} + \cdots + a_n\delta_{\boldsymbol{\sigma}_1\boldsymbol{\sigma}_2\cdots\boldsymbol{\sigma}_n,\boldsymbol{\sigma}'_1\boldsymbol{\sigma}'_2\cdots\boldsymbol{\sigma}'_n}) \\ &= A(q_N(\boldsymbol{\sigma}, \boldsymbol{\sigma}')).\end{aligned}$$

Here, we have introduced the lexicographic overlap

$$q_N(\boldsymbol{\sigma}, \boldsymbol{\sigma}') := \begin{cases} 1 & \text{if } \boldsymbol{\sigma} = \boldsymbol{\sigma}', \\ \frac{1}{N}(\min\{1 \leq i \leq N; \sigma_i \neq \sigma'_i\} - 1) & \text{else,} \end{cases} \tag{4.1}$$

and the distribution function $A\colon [0,1] \to [0,1]$ with jumps of height a_k at x_k for $k = 1, \ldots, n$. The term distribution function refers to an increasing function on $[0,1]$ with $A(0) = 0$ and $A(1) = 1$. Consequently, there is a one-to-one correspondence between n-level GREM potentials and distribution functions on $[0,1]$, which are step functions with exactly n jumps.

It turns out that the thermodynamics of the GREM is not governed by A itself, but rather by its concave hull $\bar{A}\colon [0,1] \to [0,1]$,

$$\bar{A} := \inf\{G\colon [0,1] \to [0,1] |\, G \text{ is concave, and } A(x) \leq G(x) \text{ for all } x \in [0,1]\}.$$

Note that $\bar{A}$ is well-defined since the set on the right-hand side is nonempty (it contains for the example $G \equiv 1$), and $\bar{A}$ is bounded from below by 0. Moreover, $\bar{A}$ is concave as infimum of concave functions and it is not hard to see that it is again a distribution function on $[0,1]$. In fact, in the case of a step function A, the concave hull $\bar{A}$ is a piecewise affine-linear function, which agrees at a (typically proper) subset $\{y_0, y_1, \ldots, y_m\} \subset \{x_0, x_1, \ldots, x_n\}$ with A and interpolates between y_i and y_{i+1} linearly. That is, there exist some indices $J_1 < J_2 < \ldots < J_m = n$ such that $y_l = x_{J_l}$ and $A(y_l) = \bar{A}(x_{J_l})$. At each interval $[y_{l-1}, y_l]$ of length $L_l := y_l - y_{l-1}$ the concave hull increases by the increment $\bar{a}_l := A(y_l) - A(y_{l-1})$. The slope is denoted by $\gamma_l := \bar{a}_l / L_l$. Finally, we set the partial pressures $\varphi^{(l)}(\beta)$,

$$\varphi^{(l)}(\beta) := \begin{cases} \frac{1}{2}\beta^2\bar{a}_l + L_l \ln 2 & \text{if } \beta \leq \sqrt{(2\ln 2)\gamma_l^{-1}} =: \beta_l, \\ \beta\sqrt{(2\ln 2)\bar{a}_l L_l} & \text{if } \beta > \sqrt{(2\ln 2)\gamma_l^{-1}}, \end{cases} \tag{4.2}$$

of which one can think as rescaled versions of the REM pressure p_{REM}. The specific GREM pressure $\frac{1}{N}\Phi_N(\beta)$ converges to the sum of the partial pressures $\varphi^{(l)}(\beta)$:

Theorem 4.1 ([46], Theorem 10.1.10 in [36])
The GREM specific pressure $\frac{1}{N}\Phi_N(\beta)$ converges almost surely and with the notation from above we have

$$\lim_{N\to\infty}\frac{1}{N}\Phi_N(\beta) = p_{GREM}(\beta) := \sum_{l=1}^{m}\varphi^{(l)}(\beta)$$

We see that if the concave hull $\bar{A}$ is supported by $m+1$ points $\{y_0, y_1, \dots, y_m\}$, then the GREM undergoes m transitions at the inverse temperatures

$$\beta_l := \sqrt{(2\ln 2)\gamma_l^{-1}},$$

where the l-th partial pressure switches from a quadratic growth to a linear function. If we decompose $\boldsymbol{\sigma} = \hat{\boldsymbol{\sigma}}_1\hat{\boldsymbol{\sigma}}_2\cdots\hat{\boldsymbol{\sigma}}_m$ according to the sequence $(y_l)_{l=1,\dots,m}$, this allows the following interpretation. At the inverse temperature β_1, the first block $\hat{\boldsymbol{\sigma}}_1$ freezes. That is, if we write $\hat{\boldsymbol{\sigma}}_1 = \boldsymbol{\sigma}_1\cdots\boldsymbol{\sigma}_{J_1}$, then first part of U is given by $U^{(1)}(\hat{\boldsymbol{\sigma}}_1) := \sqrt{a_1 N}X_{\boldsymbol{\sigma}_1} + \cdots + \sqrt{a_{l_1}N}X_{\boldsymbol{\sigma}_1\cdots\boldsymbol{\sigma}_{J_1}}$, and for $\beta > \beta_1$ the pressure is governed by those $\hat{\boldsymbol{\sigma}}_1$ with $U^{(1)}(\hat{\boldsymbol{\sigma}}_1) \approx \min U^{(1)}$. Similarly, at β_2 the second block $\hat{\boldsymbol{\sigma}}_2 := \boldsymbol{\sigma}_{J_1}\cdots\boldsymbol{\sigma}_{J_2}$ freezes at the minimal energy configurations of $U^{(2)}_{\hat{\boldsymbol{\sigma}}_1}(\hat{\boldsymbol{\sigma}}_2)$. This blockwise freezing continues until the inverse temperature β_m, where the total spin $\boldsymbol{\sigma}$ is found at the ground state of the complete GREM potential U. In summary, the thermodynamics of the GREM can be understood as hierarchical realization of m (not n) nested REM models.

As in the REM, we are also able to determine the extremal statistics of the GREM. In fact, Theorem 4.1 can be seen as consequence of the results concerning the low energy statistics of the GREM. The minimal values of the GREM are most conveniently described in terms of m-dimensional *Poisson cascades*, which we introduce next. Let $Y_{\hat{\boldsymbol{\sigma}}_1}, Y_{\hat{\boldsymbol{\sigma}}_1\hat{\boldsymbol{\sigma}}_2}, \dots Y_{\hat{\boldsymbol{\sigma}}_1\hat{\boldsymbol{\sigma}}_2\cdots\hat{\boldsymbol{\sigma}}_m}$ be a collection of i.i.d random variables, and $v_{N,1}, \dots v_{N,m}$ some real functions on $\mathbb{R}$ such that the following point processes

$$\begin{aligned}
\sum_{\hat{\boldsymbol{\sigma}}_1}\delta_{v_{N,1}(Y_{\hat{\boldsymbol{\sigma}}_1})} &\underrightarrow{w}\mathcal{P}_{e^{-x}dx}\\
\sum_{\hat{\boldsymbol{\sigma}}_2}\delta_{v_{N,1}(Y_{\hat{\boldsymbol{\sigma}}_1\hat{\boldsymbol{\sigma}}_2})} &\underrightarrow{w}\mathcal{P}_{e^{-x}dx} \qquad \text{for all } \hat{\boldsymbol{\sigma}}_1\\
&\vdots\\
\sum_{\hat{\boldsymbol{\sigma}}_m}\delta_{v_{N,1}(Y_{\hat{\boldsymbol{\sigma}}_1\hat{\boldsymbol{\sigma}}_2\cdots\hat{\boldsymbol{\sigma}}_m})} &\underrightarrow{w}\mathcal{P}_{e^{-x}dx} \qquad \text{for all } \hat{\boldsymbol{\sigma}}_1\hat{\boldsymbol{\sigma}}_2\cdots\hat{\boldsymbol{\sigma}}_m
\end{aligned}$$

converge weakly to Poisson point processes $\mathcal{P}_{e^{-x}dx}$ with intensity $e^{-x}dx$. Then, the m-dimensional point processes

$$\sum_{\hat{\boldsymbol{\sigma}}_1}\delta_{v_{N,1}(Y_{\hat{\boldsymbol{\sigma}}_1})}\sum_{\hat{\boldsymbol{\sigma}}_2}\delta_{v_{N,1}(Y_{\hat{\boldsymbol{\sigma}}_1\hat{\boldsymbol{\sigma}}_2})}\cdots\sum_{\hat{\boldsymbol{\sigma}}_m}\delta_{v_{N,1}(Y_{\hat{\boldsymbol{\sigma}}_1\hat{\boldsymbol{\sigma}}_2\cdots\hat{\boldsymbol{\sigma}}_m})}\underrightarrow{w}\mathcal{P}^{(m)}_{\mathrm{cas}}$$

converges to the m-dimensional *Poisson cascade* [36, Theorem 10.1.4]. In particular, it follows from the above description that $\mathcal{P}^{(m)}_{\mathrm{cas}}$ can be constructed iteratively: for $m = 1$, $\mathcal{P}^{(m)}_{\mathrm{cas}} \equiv \mathcal{P}_{e^{-x}dx}$ and for $m > 1$ one starts with a one-dimensional Poisson point process $\mathcal{P}_{e^{-x}dx}$ on $\mathbb{R}$ and to each point x of this process

one independently assigns a Poisson cascade $\mathcal{P}_{\text{cas}}^{(m-1)}$ with a set of support points $Q_x \subset \mathbb{R}^{m-1}$. The m-dimensional cascade is then given by $\sum_{x\in\mathcal{P}_{e^{-x}dx}, y_x\in Q_x} \sum \delta_{(x,y_x)}$ which defines a point process on $\mathbb{R}^m$.
As one might expect, in the case of the GREM the scaling functions $v_{N,l}$ from the above definition are related to the function $s_N(x)$ (3.7), which emerged in the discussion of the REM. This is a consequence of the GREM being blockwise equivalent to a rescaled REM:

Theorem 4.2 (Theorem 10.1.5 in [36])
Let the GREM potential be non-degenerate, that is, we have the strict inequalities $\gamma_1 > \gamma_2 > \cdots > \gamma_m$ between the slopes. Then with the notation from above

$$\sum_{\hat{\boldsymbol{\sigma}}_1} \delta_{s^{(-1)}_{L_1 N}\left(\frac{1}{\sqrt{\bar{a}_1}} U^{(1)}(\hat{\boldsymbol{\sigma}}_1)\right)} \sum_{\hat{\boldsymbol{\sigma}}_2} \delta_{s^{(-1)}_{L_2 N}\left(\frac{1}{\sqrt{\bar{a}_2}} U^{(2)}_{\hat{\boldsymbol{\sigma}}_1}(\hat{\boldsymbol{\sigma}}_2)\right)} \cdots \sum_{\hat{\boldsymbol{\sigma}}_m} \delta_{s^{(-1)}_{L_m N}\left(\frac{1}{\sqrt{\bar{a}_m}} U^{(m)}_{\hat{\boldsymbol{\sigma}}_1 \cdots \hat{\boldsymbol{\sigma}}_{m-1}}(\hat{\boldsymbol{\sigma}}_m)\right)} \xrightarrow{w} \mathcal{P}^{(m)}_{cas}.$$

Furthermore, if we introduce

$$S_{J,N}(x) = \sum_{l=1}^{m} \left(N\sqrt{2\ln 2 \bar{a}_l L_l} - \frac{1}{2}\sqrt{\frac{\gamma_l}{2\ln 2}} (\ln(2L_l \ln 2N) + \ln 4\pi) \right) + x,$$

then the minimal statistics – rescaled with $S^{-1}_{J,N}$ – converges weakly,

$$\sum_{\boldsymbol{\sigma}\in\mathcal{Q}_N} \delta_{S^{-1}_{J,N}(U(\boldsymbol{\sigma})} \xrightarrow{w} \int_{\mathbb{R}^m} \mathcal{P}^{(m)}_{cas}(dx_1, \ldots, dx_m) \delta_{\sum_{l=1}^m \sqrt{\bar{a}_l} x_l}$$

In particular, Theorem 4.2 tells us that the minimum of the GREM potential is found at

$$\min U = \sum_{l=1}^{m} \left(N\sqrt{2\ln 2 \bar{a}_l L_l} - \frac{1}{2}\sqrt{\frac{\gamma_l}{2\ln 2}} (\ln(2L_l \ln 2N) + \ln 4\pi) \right) + \mathcal{O}(1).$$

The final point we want to review about the GREM is its Parisi measure $\mu_N^P([-1,q]) = \mathbb{E}[\mu^P_{\text{dis},N}([-1,q])] = \mathbb{E}\left[\langle \mathbb{1}_{R_N \le q}\rangle_\beta^{\otimes^2}\right]$. In the REM, the Parisi measure converges weakly to either δ_0 in the high temperature phase or to a combination of δ_0 and δ_1 in the glass phase, mirroring a 1-step replica symmetry breaking. In the GREM, we have in total m-transitions which are reflected in its Parisi measure as well.

Proposition 4.3 (Theorem 10.2.7 in [36])
The Parisi measure μ_N^P converges weakly to a point measure μ^P which is only supported at the points $y_0, y_1, \ldots y_m$. Moreover, the limit μ^P is characterized by

$$\mu^P([y_l, 1]) = \begin{cases} 0 & \text{if } \beta \le \beta_l, \\ 1 - \frac{\beta_l}{\beta} & \text{if } \beta > \beta_l \end{cases}$$

for $l = 1, \ldots, m$.

That is, at each critical inverse temperature β_l the support of the Parisi measure μ^P increases by an additional point located at y_l. In total, we observe an m-level replica symmetry breaking in the GREM. So far, we have considered the distribution of the replica overlap after taking the mean over the sampling

disorder. In fact, one can also characterize the convergence of the random measure $\mu^P_{\mathrm{dis},N}$. The replica distribution is not self-averaging and, thus, its limit μ^P_{dis} will still be a nontrivial random measure. To present the distribution of μ^P_{dis}, we need to introduce the *Ruelle cascades* $\mathcal{W}^{(m)}_{\beta,\boldsymbol{\alpha}}$, which are also of relevance in the study of the SK model. $\mathcal{W}^{(m)}_{\beta,\alpha}$ is a point process on $(0,1]^m$ with parameters $\beta > 0$ and $\boldsymbol{\alpha} \in \mathbb{R}^m_+$. Its atoms $w(i) = (w_1(i), \dots w_m(i))$ can be described in terms of the atoms $x(i) = (x_1(i), \dots, x_m(i))$ of the m-dimensional Poisson cascade $\mathcal{P}^{(m)}_{\mathrm{cas}}$,

$$(w_1(i), \dots w_m(i)) = \left(\frac{\int \mathcal{P}^{(m)}_{\mathrm{cas}}(dy)\delta(y_1 - x_1(i))e^{\beta\langle\boldsymbol{\alpha},y\rangle}}{\int \mathcal{P}^{(m)}_{\mathrm{cas}}(dy)e^{\beta\langle\boldsymbol{\alpha},y\rangle}}, \dots, \frac{\int \mathcal{P}^{(m)}_{\mathrm{cas}}(dy)\delta(y_1 - x_1(i)) \cdots \delta(y_m - x_m(i))e^{\beta\langle\boldsymbol{\alpha},y\rangle}}{\int \mathcal{P}^{(m)}_{\mathrm{cas}}(dy)e^{\beta\langle\boldsymbol{\alpha},y\rangle}} \right).$$

The Ruelle cascades satisfy the important relation

$$\mathcal{W}^{(m)}_{\beta,\boldsymbol{\alpha}}(dw_1, \dots, dw_m) \overset{D}{=} \int_0^1 \mathcal{W}^{(m+1)}_{\beta,(\boldsymbol{\alpha},\alpha_{m+1})}(dw_1, \dots, dw_m, dw_{m+1}) \frac{w_{m+1}}{w_m}$$

in distribution. To formulate the convergence of the replica distribution, it is convenient to introduce the integer valued function $l(\beta) := \max\{l | \beta > \beta_l\}$ where $\beta_0 := 0$.

Theorem 4.4 (Theorem 10.1.14 and Theorem 10.1.15 in [36])
The disordered Parisi measure $\mu^P_{dis,N}$ converges in distribution and in mean to a random measure μ^P_{dis}. If $l(\beta) = 0$, we have $\mu^P_{dis} = \delta_0$ and otherwise μ^P_{dis} is a point measure with support $\{0, y_1, \dots, y_{l(\beta)}\}$ and random distribution function

$$1 - \mu^P_{dis}([-1, y_i]) = \int \mathcal{W}^{(l(\beta))}_{\beta, \frac{1}{\sqrt{2\ln 2}}\sqrt{\boldsymbol{\gamma}}}(dw_1, \dots, dw_{l(\beta)}) w_{l(\beta)}(1 - w_{i+1}),$$

for $i = 0, \dots, l(\beta) - 1$ and $\mu^P_{dis}([-1, y_{l(\beta)}]) = 1$. Here, $\sqrt{\boldsymbol{\gamma}} = (\sqrt{\gamma_1}, \dots, \sqrt{\gamma_{l(\beta)}})$ denotes the collection of the slope's square roots.

4.1.2 The Continuous Random Energy Model

To define the Continuous Random Energy Model (CREM), our starting point is the representation of the GREM covariance function in terms of the distribution function A, i.e., $\mathbb{E}[U(\boldsymbol{\sigma})U(\boldsymbol{\sigma}')] = A(q(\boldsymbol{\sigma}, \boldsymbol{\sigma}'))$. While the GREM requires A to be a step function, in the CREM we allow A to be any distribution function, in particular A can be continuous. Obviously, the CREM includes the GREM as special case, but we choose to call the finite-level case a GREM and the term CREM is reserved to describe more involved potentials. Let us remark that the CREM is well defined, that is, for any distribution function A there exists a unique centered Gaussian process on $\mathcal{Q}_N$ such that

$$\mathbb{E}[U(\boldsymbol{\sigma}), U(\boldsymbol{\sigma}')] = A(q(\boldsymbol{\sigma}, \boldsymbol{\sigma}')) \quad \text{for all } \boldsymbol{\sigma}, \boldsymbol{\sigma}' \in \mathcal{Q}_N.$$

Uniqueness is clear, as a centered Gaussian vector is characterized by its covariance matrix. For the existence, one notes that the lexicographic overlap q only takes the $N+1$ different values $0, \frac{1}{N}, \frac{2}{N}, \dots, 1$. That means for fixed N the CREM potential agrees with a N-level GREM whose distribution function A_N is chosen to be a step function which agrees with A at $q = 0, \frac{1}{N}, \frac{2}{N}, \dots, 1$. We see that the CREM can be understood as a GREM with an increasing number of levels as N grows.

The thermodynamics depends again on the concave hull $\bar{A}$ of A. The slopes γ_l and increments $\bar{a}_l$ are replaced by the right derivative $\bar{a}(x)$ of $\bar{A}(x)$. Here, we recall that the right derivative exists everywhere and is a decreasing function since $\bar{A}$ is concave [169]. Let us further introduce the function $x(\beta)$,

$$x(\beta) := \begin{cases} \sup\{x \in [0,1] | \bar{a}(x) > (2\ln 2)/\beta^2\} & \text{if } \{x \in [0,1] | \bar{a}(x) > (2\ln 2)/\beta^2\} \neq \emptyset \\ 0 & \text{else.} \end{cases} \tag{4.3}$$

The function $x(\beta)$ replaces the integer-valued function $l(\beta)$ from the discussion of the GREM and, as we will see shortly, can be recognized as the fraction of the spin block which is frozen. Indeed, we have the following result for the CREM pressure:

Theorem 4.5 (Theorem 10.2.4 in [36])
Let U be a CREM potential with distribution function A. Then, the specific pressure $\frac{1}{N}\Phi_N(\beta)$ converges almost surely

$$\lim_{N\to\infty} \frac{1}{N}\Phi_N(\beta) = p_{CREM}(\beta) := \sqrt{2\ln 2}\,\beta \int_0^{x(\beta)} \sqrt{\bar{a}(x)}\,dx + \frac{\beta^2}{2}(1 - \bar{A}(x(\beta))) + (1 - x(\beta))\ln 2.$$

The first $x(\beta)$-fraction of the Hamming cube contributes linearly to the specific pressure, i.e., this spin block is concentrated on the minimal configurations of the corresponding part of the CREM potential. The remaining fraction shows a quadratic contribution which agrees with the annealed specific pressure of the remaining potential. The glass transition occurs at the minimal inverse temperature β_c for which $x(\beta) > 0$ if $\beta > \beta_c$. An explicit expression is given by

$$\beta_c = \sqrt{(2\ln 2)/\lim_{x\downarrow 0} \bar{a}(x)},$$

which implies that $\beta_c = 0$ occurs if $\bar{A}$ has an infinite slope close to zero. In that case, we have a glass phase for all positive temperatures. On the other hand, a complete freezing, that is a vanishing specific entropy, occurs for those β where $x(\beta) = 0$. In contrast to the REM and GREM, it is possible that the CREM never freezes completely, namely if $\lim_{x\uparrow 1} \bar{a}(x) = 0$. On the other hand, if $\lim_{x\uparrow 1} \bar{a}(x) > 0$, for low enough temperatures the Gibbs measure is concentrated at those configurations $\boldsymbol{\sigma}$ with $U(\boldsymbol{\sigma})/N$ being close to the specific ground state energy $-\sqrt{2\ln 2}\int_0^1 \sqrt{\bar{a}(x)}\,dx$. Describing the extremal process of the CREM, is much more difficult than in the GREM and as far we as know has not been completely achieved. The common approach for describing the CREM minimum is to map it to the running maximum of a branching Brownian motion. This leads after a careful analysis to the subleading corrections of the minimal CREM energy [74].
These observations already suggest that the CREM has a substantially richer structure than the GREM. This is also mirrored in its Parisi measure

Proposition 4.6 (Theorem 10.2.7 in [36])
In the CREM, the averaged replica overlap distribution μ_N^P converges for any β to a measure μ^P supported on $[0,1]$. *Its distribution function is given by*

$$\mu^P([0,q]) = \begin{cases} \frac{\sqrt{2\ln 2}}{\beta\sqrt{\bar{a}(x)}} & \text{if } q < x(\beta), \\ 1 & \text{else.} \end{cases}$$

In particular, for a strictly increasing concave hull $\bar{A}$ the Parisi measure μ^P will contain an open interval in its support. One speaks of *continuous replica symmetry breaking* to distinguish this case from the finite-level replica symmetry appearing in the GREM.
Describing the limit of the random measure $\mu_{\mathrm{dis},N}^P$, is more involved compared to the GREM. Since the limit does not contain only finitely many atoms, a direct approach via cascades and related processes is not feasible. To understand the Gibbs measure, one derives Ghirlanda-Guerra identities, that is, one considers the Gibbs measure of n replicas $\boldsymbol{\sigma}^{(1)}, \dots, \boldsymbol{\sigma}^{(n)}$ for which one characterizing identities in mean. That is, instead of considering the disordered distribution of $R_N(\boldsymbol{\sigma}, \boldsymbol{\sigma}')$ one rather considers the *mean* distribution of n replicas for general n. It turns out, that the Ghirlanda-Guerra in the CREM uniquely characterize the distribution of μ_{dis}^P whose marginals at finitely many points are again described by Ruelle cascades [36, Chapter 10.2.2]. We will discuss the Ghirlanda-Guerra identities for mixed p-spin models in Chapter 5.

4.2 Phase Diagrams of the QGREM and QCREM

We want to discuss the quantum versions of the GREM and CREM, the QGREM and QCREM. That is, we consider a Hamiltonian of the form

$$H_N = U - B,$$

where U is an GREM or, more generally, a CREM potential and B models the transverse field, whose strength we allow to depend on the site i – in contrast to the uniform magnetic field ΓT in the last chapters. B is now the sum of the x-Pauli matrices $\boldsymbol{s}_j$ with (possibly random) weights $b_j \in \mathbb{R}$,

$$(B\psi)(\boldsymbol{\sigma}) := \sum_{j=1}^{N} b_j \left(\boldsymbol{s}_j\psi\right)(\boldsymbol{\sigma}), \qquad \left(\boldsymbol{s}_j\psi\right)(\boldsymbol{\sigma}) := \psi(\sigma_1, \dots, -\sigma_j, \dots, \sigma_N), \tag{4.4}$$

To avoid confusion with truncated operators which will occur later, we write $\boldsymbol{s}_j$ instead of S_j^x in this chapter. A simple computation exploiting the exponential series shows that the diagonal matrix-elements $\langle\boldsymbol{\sigma}|e^{-\beta(U-B)}|\boldsymbol{\sigma}\rangle$ and, consequently, the quantum partition function $\operatorname{Tr} e^{-\beta(U-B)}$, only depends on the absolute values $(|b_j|)_{j=1,\dots,N}$ [130, Lemma 1.1]. This observation is helpful if one wants to make use of the fact that H_N generates a positive semigroup,

$$\langle\boldsymbol{\sigma}|e^{-tH_N}|\boldsymbol{\sigma}'\rangle \geq 0,$$

if all the weights b_j are non-negative. This can be assumed without loss of generality as it has no impact on the partition function

We will only consider the case where the weights b_j are independent copies of an absolutely integrable random variable $\mathfrak{b}$ and we require them to be independent of the Gaussian potential U. In this chapter, we write for the partition function

$$Z_N(\beta, \mathfrak{b}) := \mathrm{Tr}\,\left[e^{-\beta H_N}\right],$$

and the pressure is denoted by

$$\Phi_N(\beta, \mathfrak{b}) := \ln Z_N(\beta, \mathfrak{b}).$$

If $\mathfrak{b} = -\Gamma$ is almost surely constant, we write as in the last chapters $B = -\Gamma T$ and $\Phi_N(\beta, \Gamma)$ for the pressure.

Our first main result concerns the pressure of the QGREM. We show that the specific pressure converges almost surely to a deterministic limit, which can be expressed in terms of the classical partial free energies (4.2) and the paramagnetic free energy. We stick to the notation from the previous section.

Theorem 4.7 (Theorem 1.2 in [130])
Let U be an n-level GREM with distribution function A, $\beta \geq 0$ and $\mathfrak{b}$ an absolutely integrable random variable. Then, the QGREM specific pressure converges almost surely,

$$\lim_{N\to\infty} \frac{1}{N}\Phi_N(\beta, \mathfrak{b}) = p_{QGREM}(\beta, \mathfrak{b}) := \max_{0\leq k\leq m} \left[\sum_{l=1}^{k} \varphi^{(l)}(\beta) + (1 - y_k)\mathbb{E}[\ln(2\cosh(\beta\mathfrak{b}))]\right]. \tag{4.5}$$

The maximum is taken over all points $\{y_0, y_1, \ldots, y_m\}$ supporting the convex hull $\bar{A}$ of A.

As in the classical case, the concave hull $\bar{A}$, rather than A, remains the determining function for the limit. The second term in (4.5) is the pressure of the random quantum paramagnet given by

$$p_{\mathrm{PAR}}(\beta\mathfrak{b}) := \frac{1}{N}\mathbb{E}\left[\ln \mathrm{Tr}\,\left[e^{\beta B}\right]\right] = \mathbb{E}[\ln(2\cosh(\beta\mathfrak{b}))],$$

which can be derived in the same way as has been shown for the constant field ΓT in Section 2.2. If $\mathfrak{b} \equiv -\Gamma$ is almost surely constant, the structure of the limit in (4.5) becomes more transparent if we introduce the critical field strengths

$$\Gamma_c^{(l)} := \frac{1}{\beta}\operatorname{arcosh}\left(\frac{1}{2}\exp\left(\frac{\varphi^{(l)}(\beta)}{L_l}\right)\right), \quad l \in \{1, \ldots, m\}.$$

In this situation, we may rephrase (4.5) as follows:

Corollary 4.8 (Corollary 1.3 in [130])
In the situation of Theorem 4.7 with $\mathfrak{b} = -\Gamma$ for some constant $\Gamma > 0$:

$$p_{QGREM}(\beta, \Gamma) = \sum_{l=1}^{m} \left(\varphi^{(l)}(\beta)\ \mathbb{1}_{\Gamma<\Gamma_c^{(l)}} + L_l \ln(2\cosh(\beta\Gamma))\ \mathbb{1}_{\Gamma\geq\Gamma_c^{(l)}}\right). \tag{4.6}$$

Just like the GREM being equivalent to m nested REM model, the QGREM pressure coincides with the sum of m weighted and rescaled QREM terms. In particular, there are as many magnetic first-order transitions as second-order glass transitions. The glass transitions continue to occur at the (classical)

critical inverse temperatures β_l as long as $\Gamma < \Gamma_c^{(l)}(\beta_l)$ and disappear for field strengths $\Gamma > \Gamma_c^{(l)}(\beta_l)$; see Figure 4.1. The specific magnetization in x-direction

$$m_x(\beta, \Gamma) := \frac{1}{\beta} \frac{\partial}{\partial \Gamma} \Phi(\beta, \Gamma)$$

changes discontinuously at $\Gamma = \Gamma_c^{(l)}$. At zero temperature, we find quantum phase transitions at the field strengths $\Gamma_{\mathrm{GS}}^l = \lim_{\beta \to \infty} \Gamma_c^{(l)}(\beta) = \sqrt{(2 \ln 2) \gamma^{(l)}}$. The physics described by (4.6) is that if we write $\boldsymbol{\sigma} = \hat{\boldsymbol{\sigma}}_1 \cdots \hat{\boldsymbol{\sigma}}_m$, each of the blocks $\hat{\boldsymbol{\sigma}}_l$ either shows a completely classical behavior or is of paramagnetic nature. For $\Gamma = 0$, all blocks are classical and as Γ increases and meets the critical field strength $\Gamma_c^{(l)}$ the block $\hat{\boldsymbol{\sigma}}_l$ switches to a paramagnetic behavior. Since $\Gamma^{(1)}(\beta) > \cdots > \Gamma^{(m)}(\beta)$, the transitions follow the reversed order of the blocks, i.e., $\hat{\boldsymbol{\sigma}}_m$ decides first to become paramagnetic, then $\hat{\boldsymbol{\sigma}}_{m-1}$ and so on. For $\Gamma > \Gamma^{(1)}$, all blocks are paramagnetic and the QGREM pressure then agrees with $p_{\mathrm{PAR}}(\beta\Gamma)$.

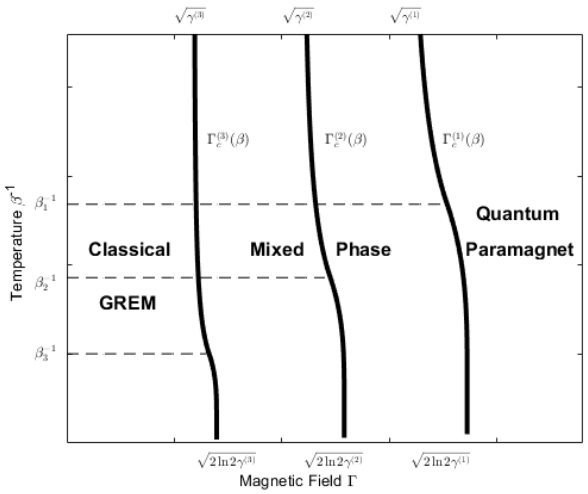

Figure 4.1: Phase diagram of the Quantum GREM as a function of the transversal constant magnetic field Γ and the temperature β^{-1} [130, Figure 1]. The figure shows an example with three second-order glass transitions (dotted lines) and three first-order magnetic transitions (bold lines). If $\Gamma < \Gamma_c^{(3)}(\beta_l)$ the free energy coincides with the classical one ($\Gamma = 0$), whereas for $\Gamma > \Gamma_c^{(l)}(\beta_l)$ the system becomes a pure quantum paramagnet. In between mixed quantum-classical phases appear.

Moving on to the more general CREM potentials, it is convenient to introduce truncated versions of the CREM pressure. For any $z \in [0, 1]$, we define

$$p_{\mathrm{CREM}}(\beta, z) := \sqrt{2 \ln 2} \beta \int_0^{\min\{x(\beta), z\}} \sqrt{\bar{a}(x)}\, dx + \mathbb{1}_{z > x(\beta)} \left(\frac{\beta^2}{2} (\bar{A}(z) - \bar{A}(x(\beta))) + (z - x(\beta)) \ln 2 \right). \tag{4.7}$$

For $z = 1$, that agrees with the limiting CREM pressure from Theorem 4.5. If $A = \bar{A}$, then the truncated pressure for $0 < z < 1$ can be understood as the limiting specific pressure of the CREM on the subgraph consisting of the first zN spins and ignoring the contribution of the remaining spins. As in the quantum GREM, the free energy of the quantum CREM converges almost surely and the limit may be expressed as a variational formula involving $p_{\mathrm{CREM}}(\beta, z)$:

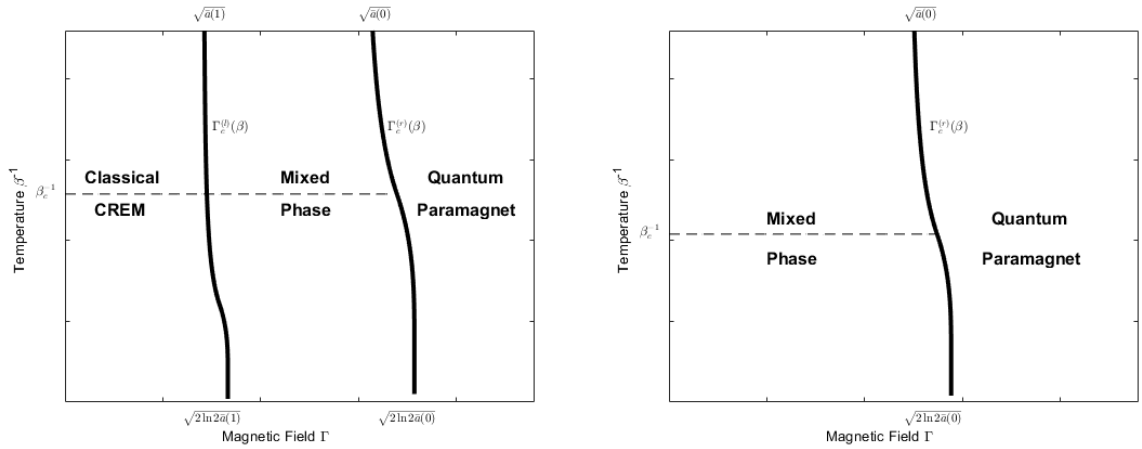

Figure 4.2: Both figures illustrate examples for the phase diagram of a Quantum CREM as a function of the transversal magnetic field Γ and the temperature β^{-1} [130, Figure 2]. The first plot contains two magnetic phase transitions (bold lines) into transversal magnetic order. The second plot shows the case of one magnetic phase transition. The dotted line corresponds to the glass transition at $\beta_c = \sqrt{(2\ln 2)/\bar{a}(0)}$. If $\bar{A}$ is continuously differentiable, the magnetic transitions are of second order.

Theorem 4.9 (Theorem 1.4 in [130])
Let U be a CREM potential described in terms of its distribution function A with concave hull $\bar{A}$ and $p_{CREM}(\beta, z)$ as in (4.7)*. Then, for any absolute integrable random variable $\mathfrak{b}$ the specific quantum pressure $\frac{1}{N}\Phi_N(\beta, \mathfrak{b})$ converges almost surely,*

$$\lim_{N\to\infty} \frac{1}{N}\Phi_N(\beta, \mathfrak{b}) = p_{QCREM}(\beta, \mathfrak{b}) := \sup_{0\le z\le 1} \left[p_{CREM}(\beta, z) + (1-z)\mathbb{E}\left[\ln 2\cosh(\beta\mathfrak{b})\right]\right]. \tag{4.8}$$

As we have now stated the main convergence results of this chapter, we remind the reader that the specific pressure in the QGREM and QCREM does not only converge almost surely, but also in mean. This is again a consequence of Gaussian concentration inequality (Theorem 2.4). Due to the additional randomness of the transversal field B, convergence in higher mean depends on the integrability of $\mathfrak{b}$. If $\mathfrak{b}$ is an L^r-random variable for some $r > 1$, the pressure even converges in r-th mean.
Theorem 4.9 is the natural generalization of Theorem 4.7 to the QCREM: the finite maximization is replaced by a continuous variational formula. This is a consequence of having infinitely many types of spins so that the fraction z of spins which behave classically is not restricted anymore to the finite number of support points y_l, but can be any number in $[0, 1]$. Accordingly, the partial pressures need to be replaced by a continuous truncation which is given in form of $p_{\mathrm{CREM}}(\beta, z)$. In order to characterize the magnetic phase transitions like in the QGREM , we replace the variational formula (4.8) by a more explicit expression in the constant field case $\mathfrak{b} = -\Gamma$.

To simplify the analysis, we assume from now that the concave hull $\bar{A}$ is a continuously differentiable function with a strictly increasing slope $\bar{a}(x)$. We note that $x(\beta)$ is either 0 or 1, or by definition of $x(\beta)$

(4.3) and the continuity of $\bar{a}(x)$ we have $\bar{a}(x(\beta)) = \frac{2\ln 2}{\beta^2}$. In either case, $p_{\mathrm{CREM}}(\beta, z)$ is differentiable with respect to z with derivative

$$\frac{\partial p_{\mathrm{CREM}}(\beta, z)}{\partial z} = \sqrt{(2\ln 2)\bar{a}(z)}\,\beta\,\mathbb{1}_{z<x(\beta)} + \left(\ln 2 + \frac{\beta^2}{2}\bar{a}(z)\right)\mathbb{1}_{z\geq x(\beta)}.$$

The monotonicity of $\bar{a}$ clearly implies that the partial derivative $\frac{\partial p_{\mathrm{CREM}}(\beta,\cdot)}{\partial z} : [0,1] \to [s(\beta), t(\beta)]$ is for any β a nondecreasing continuous function in z, whose range is a closed interval specified by its boundary values

$$s(\beta) := \frac{\partial p_{\mathrm{CREM}}(\beta, z)}{\partial z}\Big|_{z=1} \quad \text{and} \quad t(\beta) := \frac{\partial p_{\mathrm{CREM}}(\beta, z)}{\partial z}\Big|_{z=0}.$$

We are ready to give an explicit formula for the QCREM pressure:

Corollary 4.10 (Corollary 1.5 in [130])
In the situation of Theorem 4.9, let $\bar{A}$ be continuously differentiable with strictly increasing slope and $\mathfrak{b} \equiv -\Gamma$ almost surely. We set $g(\beta,\cdot) : [s(\beta), t(\beta)] \to [0,1]$ to be the inverse of the derivative $\frac{\partial p_{CREM}(\beta,z)}{\partial z}$ as a function of z. Then,

$$p_{QCREM}(\beta,\Gamma) = \begin{cases} p_{CREM}(\beta,1) & p_{PAR}(\beta\Gamma) \leq s(\beta), \\ p_{CREM}(\beta, g_\beta(p_{PAR}(\beta\Gamma))) + (1 - g_\beta(p_{PAR}(\beta\Gamma)))p_{PAR}(\beta\Gamma) & s(\beta) < p_{PAR}(\beta\Gamma) < t(\beta), \\ p_{PAR}(\beta\Gamma) & t(\beta) \leq p_{PAR}(\beta\Gamma). \end{cases}$$

We recall that $p_{PAR}(\beta\Gamma) = \ln 2\cosh(\beta\Gamma)$.

Corollary 4.10 implies that there are either one or two magnetic phase transitions, depending on $s(\beta)$. If $s(\beta) = \ln 2$ or, equivalently, $\bar{a}(1) = 0$, we find a single magnetic phase transition at the critical magnetization

$$\Gamma_c^{(r)}(\beta) = \frac{1}{\beta}\operatorname{arcosh}\left(\frac{1}{2}e^{t(\beta)}\right).$$

Otherwise, there is a second phase transition at

$$\Gamma_c^{(l)}(\beta) = \frac{1}{\beta}\operatorname{arcosh}\left(\frac{1}{2}e^{s(\beta)}\right).$$

We are able to compute the specific magnetization in transversal direction

$$m_x(\beta,\Gamma) = \frac{1}{\beta}\frac{\partial}{\partial\Gamma}p_{\mathrm{QCREM}}(\beta,\Gamma) = \begin{cases} 0 & p_{\mathrm{PAR}}(\beta\Gamma) \leq s(\beta), \\ (1 - g_\beta(p_{\mathrm{PAR}}(\beta\Gamma)))\tanh(\beta\Gamma) & s(\beta) < p_{\mathrm{PAR}}(\beta\Gamma) < t(\beta), \\ \tanh(\beta\Gamma) & t(\beta) \leq p_{\mathrm{PAR}}(\beta\Gamma), \end{cases}$$

which follows by taking the Γ-derivative of the explicit expression in Corollary 4.10. If $s(\beta) < p_{\mathrm{PAR}}(\beta\Gamma) < t(\beta)$, one recalls that $\frac{\partial p_{\mathrm{CREM}}(\beta,z)}{\partial z}\Big|_{z=g_\beta(p_{\mathrm{PAR}})} = p_{\mathrm{PAR}}$. Note that the magnetization is as result continuous. This transversal magnetic order does not vanish over the line $\Gamma_c^{(r)}(\beta)$, but rather only at $\Gamma_c^{(l)}(\beta)$ (which is absent in the case $\bar{a}(1) = 0$). If the derivative of $\bar{a}(x)$ exists at $x = 0$ or $x = 1$, the second derivative of

$p_{\mathrm{QCREM}}(\beta, \Gamma)$ has a jump at the respective critical magnetic fields and we have a second-order magnetic transition, in contrast to the observed first-order transitions in the QGREM (see also Figure 4.2).
In our work [130], we also discuss the non-hierarchical GREM, which was introduced in [33]. As it turns out that the quantum version of the non-hierarchical GREM has got the same phase diagram as a specific QGREM, we have not included its discussion here. It is still remarkable that for this simple model, we also discover a hierarchical reorganization of the system. Ultrametricty is a characteristic feature of classical spin glasses, and it is not clearly to what extent it governs quantum spin glasses. In the following subsection, we want to present some ideas on which the proof of the Theorem 4.7 and Theorem 4.9 are based. In another subsection we discuss what we expect for the extremal statistics and the Parisi measure in the QGREM and QCREM.

4.2.1 Peeling Principle and the Interpolation Argument

We have seen in the discussion of the QREM that if the deep holes of a energy landscape are isolated from each other, then the specific pressure simply coincides either with the classical one or the fully paramagnetic one in the thermodynamic limit. The idea of the peeling principle is to derive this result in much greater generality. The general setting is as follows. We pick a parameter $0 < x \leq 1$ and accordingly decompose the hypercube $\mathcal{Q}_N$ into two reduced hypercubes of spin arrays of length $\lceil xN \rceil$ and $N - \lceil xN \rceil$. We write

$$\boldsymbol{\sigma} = (\boldsymbol{\sigma}_1, \boldsymbol{\sigma}_2) \in \mathcal{Q}_N, \quad \text{where } \boldsymbol{\sigma}_1 \in \mathcal{Q}_N^{(1)} := \mathcal{Q}_{\lceil xN \rceil} \text{ and } \boldsymbol{\sigma}_2 \in \mathcal{Q}_N^{(2)} := \mathcal{Q}_{N - \lceil xN \rceil}.$$

We consider Hamiltonians $H = U - B$, where U is a random potential on $\mathcal{Q}_N$ and B is a random transversal field. Both, U and B, need to meet several assumptions. Let us start with the potential U.

Assumptions 4.11 (Assumption 2.1 in [130])
The random potential U on $\mathcal{Q}_N$ takes the form

$$U(\boldsymbol{\sigma}) = V_N(\boldsymbol{\sigma}) + X_{\boldsymbol{\sigma}_1}$$

with some random potential V_N which is independent of the random process $X_{\boldsymbol{\sigma}_1}$. The random variables $X_{\boldsymbol{\sigma}_1}$ with $\boldsymbol{\sigma}_1 \in \mathcal{Q}_N^{(1)}$ are absolutely integrable, centered, and satisfy:

1. *$X_{\boldsymbol{\sigma}_1}$ are independent and identically distributed for each fixed $N \in \mathbb{N}$.*
2. *The pushforward measures μ_N of the negative parts $X_{\boldsymbol{\sigma}_1}^- / N$ satisfy a large deviation principle (LDP) with a lower semi-continuous rate function $I : \mathbb{R} \to [0, \infty]$, i.e., for any Borel set $\mathcal{A} \subset \mathbb{R}$,*

$$-\inf_{x \in \mathrm{int}(\mathcal{A})} I(x) \leq \liminf_{N \to \infty} \frac{1}{N} \ln \mu_N(\mathcal{A}) \leq \limsup_{N \to \infty} \frac{1}{N} \ln \mu_N(\mathcal{A}) \leq -\inf_{x \in \mathrm{clos}(\mathcal{A})} I(x). \tag{4.9}$$

Moreover, we assume

$$\inf_{x \in (-\infty, -\varepsilon]} I(x) > 0 \tag{4.10}$$

for any $\varepsilon > 0$.

3. For any random weights $w_{\boldsymbol{\sigma}_1}$ which are independent from $X_{\boldsymbol{\sigma}_1}$ and further fulfill almost surely

$$w_{\boldsymbol{\sigma}_1} \geq 0, \quad \sum_{\boldsymbol{\sigma}_1 \in \mathcal{Q}_N^{(1)}} w_{\boldsymbol{\sigma}_1} = 1,$$

a generalized strong law holds true almost surely,

$$\lim_{N\to\infty} \frac{1}{N} \sum_{\boldsymbol{\sigma}_1 \in \mathcal{Q}_N^{(1)}} w_{\boldsymbol{\sigma}_1} X_{\boldsymbol{\sigma}_1} = 0. \tag{4.11}$$

The assumptions that U takes the form $U(\boldsymbol{\sigma}) = V_N(\boldsymbol{\sigma}) + X_{\boldsymbol{\sigma}_1}$ is chosen with the GREM in mind because it allows us to split the GREM potential iteratively in a independent process $X_{\boldsymbol{\sigma}_1}$ and some correlated rest $V_N(\boldsymbol{\sigma})$. But V_N can also cover longitudinal fields and this will be of importance in the discussion of de Almeida-Thouless line.

The LDP (4.9) together with (4.10) ensures that probabilities of the type $\mathbb{P}(X_{\boldsymbol{\sigma}_1} < -\varepsilon N)$ decay exponentially in N for any $\varepsilon > 0$. Assumption (4.11) is a rather technical condition which is convenient for the proof. Random variables $X_{\boldsymbol{\sigma}_1}$ which meet Assumption 4.11 are e.g. $X_{\boldsymbol{\sigma}_1} = \sqrt{Na}Y_{\boldsymbol{\sigma}_1}$ with independent standard Gaussians $Y_{\boldsymbol{\sigma}_1}$ and some $a > 0$, or $X_{\boldsymbol{\sigma}_1} = -NZ_{\boldsymbol{\sigma}_1}$, where $Z_{\boldsymbol{\sigma}_1}$ are independent and follow an exponential distribution with parameter N. In these examples, the rate function is given by the negative part of $I(x) = \frac{a}{2}x^2 \mathbb{1}_{x<0}$ or, respectively, $I(x) = |x|\mathbb{1}_{x<0}$.

Let us turn to the magnetic operator $\boldsymbol{B}$. The transversal magnetic field $\boldsymbol{B} = \sum_{j=1}^N b_j \boldsymbol{s}_j$ as in (4.4) consists of random variables (b_j) which we even allow to be not independent from each other. The transversal field $\boldsymbol{B}$ splits into two parts $\boldsymbol{B}^{1,x}$ and $\boldsymbol{B}^{2,x}$, which act exclusively on the respective part of the array,

$$\boldsymbol{B}^{1,x} := \sum_{i=1}^{\lceil xN \rceil} b_i \boldsymbol{s}_i, \quad \boldsymbol{B}^{2,x} := \sum_{i=\lceil xN \rceil + 1}^{N} b_i \boldsymbol{s}_i.$$

If $x = 1$, we simply set $\boldsymbol{B}^{2,1} = 0$. Subsequently, we assume the following on the transversal field $\boldsymbol{B}$:

Assumptions 4.12 (Assumption 2.2 in [130])
The random weights (b_j) are independent of the potential U and satisfy almost surely

$$\limsup_{N\to\infty} N^{-1} \sqrt{\sum_{j=1}^N |b_j|^2} = 0.$$

If the weights $(b_j)_{j=1,\dots,N}$ are independent copies of an absolute integrable random variable $\mathfrak{b}$, then Assumption 4.12 is satisfied [130, Lemma A.2]. If Assumption 4.11 and 4.12 hold true, our main results states that the pressure

$$\Phi_N(\beta) := \ln \mathrm{Tr}\, \left[e^{-\beta(U-B)}\right]$$

asymptotically agrees in leading order with the maximum of the pressures of partially quantum or classical type

$$\Phi_N^{(\mathrm{qm})}(\beta) := \ln \mathrm{Tr}\, \left[e^{-\beta(V_N-B)}\right] \quad \text{and} \quad \Phi_N^{(\mathrm{cl})}(\beta) := \ln \mathrm{Tr}\, \left[e^{-\beta(U-B^{2,x})}\right].$$

The formal statement is as follows:

Proposition 4.13 (Theorem 2.3 in [130])
Under Assumption 4.11 and 4.12, for any $x \in (0,1]$ we have the almost sure convergence

$$\limsup_{N\to\infty} \frac{1}{N} |\Phi_N(\beta) - \max\{\Phi_N^{(\mathrm{qm})}(\beta), \Phi_N^{(\mathrm{cl})}(\beta)\}| = 0.$$

Roughly speaking, the independent variables $(X_{\boldsymbol{\sigma}_1})$ and the accordingly restricted magnetic operator $B^{1,x}$ only contribute separately from each other to the pressure. This peeling principle can be seen as generalization of Goldschmidt's formula (2.6).

The limit formula for the QGREM pressure (4.5) is obtained via iterative use of Proposition 4.13. Let us make the idea transparent in the case of a 2-level GREM $U = \sqrt{N}\left(\sqrt{a_1}Y_{\boldsymbol{\sigma}_1} + \sqrt{a_2}Y_{\boldsymbol{\sigma}_1\boldsymbol{\sigma}_2}\right)$ with $|\boldsymbol{\sigma}_1| = xN$. We first use the peeling principle with $X = \sqrt{Na_2}Y_{\boldsymbol{\sigma}_1\boldsymbol{\sigma}_2}$ and $V = \sqrt{Na_1}Y_{\boldsymbol{\sigma}_1}$. This yields

$$\lim_{N\to\infty} \frac{1}{N} \left| \Phi_N(\beta) - \max\{\ln \mathrm{Tr}\, e^{-\beta U}, \ln \mathrm{Tr}\, e^{-\beta\sqrt{Na_1}Y_{\boldsymbol{\sigma}_1} - B}\} \right| = 0.$$

The second term is further simplified by invoking the peeling principle again with $X = \sqrt{Na_1}Y_{\boldsymbol{\sigma}_1}$, i.e.,

$$\lim_{N\to\infty} \frac{1}{N} \left| \Phi_N(\beta) - \max\{\ln \mathrm{Tr}\, e^{-\beta U}, \ln \mathrm{Tr}\, e^{-\beta\sqrt{Na_1}Y_{\boldsymbol{\sigma}_1} - B^{(2,x)}}, \ln \mathrm{Tr}\, e^{-\beta\sqrt{Na_1}Y_{\boldsymbol{\sigma}_1} - B^{(2,x)}}\} \right| = 0.$$

The first term in the maximization is the pure GREM, the last term the paramagnet and the middle term a truncated GREM in the first block and a paramagnet in the second block. For the general n-level GREM this leads to a formula much like in Theorem 4.7, however, the maximization seemingly needs to be carried out with respect to all $n+1$ points x_i. Some technical considerations show that in fact the maximum is attained at some y_l. The details can be found in [130, Section 2 and 3].

Let us discuss the main concept used to extend the QGREM results to the QCREM. As in the proof of the classical Theorem 4.5 [40], we make use of the Gaussian interpolation formula, which we state here for the seek of completeness:

Proposition 4.14 (Lemma 1.3.1 in [181])
Let $F : \mathbb{R}^M \to \mathbb{R}$ be a two times continuously differentiable function whose second partial derivatives grow at most exponentially, that is, for all $i,j = 1,\dots,M$ there exists some $c_{i,j} > 0$ such that

$$\left| \frac{\partial^2 F}{\partial x_i \partial x_j}(x) \right| \leq e^{c_{i,j}\|x\|}.$$

Moreover, let U and V be two $\mathbb{R}^M$-valued Gaussian vectors and we assume that U is independent from V. We introduce the interpolated Gaussian vector $U(t) = \sqrt{1-t}U + \sqrt{t}V$ and the function Θ,

$$\Theta(t) := \mathbb{E}[F(U(t))]$$

for $0 \leq t \leq 1$. Then, for $0 < t < 1$ we have

$$\Theta'(t) = \frac{1}{2}\sum_{i,j}\left(\mathbb{E}[V_iV_j - U_iU_j]\,\mathbb{E}\left[\frac{\partial^2 F}{\partial x_i \partial x_j}\right]\right).$$

To prove Theorem 4.9, we use Proposition 4.14 on the 2^N-dimensional Hamming cube $\mathcal{Q}_N$ with $F(U) = \operatorname{Tr} e^{-\beta(U+B)}$ and U, V being at first two arbitrary centered Gaussian processes,

$$\mathbb{E}_{U,V}\left[\Theta(1) - \Theta(0)\right] = \frac{1}{2}\sum_{\boldsymbol{\sigma},\boldsymbol{\sigma}'}\int_0^1 \left(\mathbb{E}[V(\boldsymbol{\sigma})V(\boldsymbol{\sigma}')] - \mathbb{E}[U(\boldsymbol{\sigma})U(\boldsymbol{\sigma}')]\right)\mathbb{E}_{U,V}\left[\frac{\partial^2\Theta(t)}{\partial U_{\boldsymbol{\sigma}}\partial U_{\boldsymbol{\sigma}'}} + \frac{\partial^2\Theta(t)}{\partial V_{\boldsymbol{\sigma}}\partial V_{\boldsymbol{\sigma}'}}\right]dt,$$

where $\mathbb{E}_{U,V}$ denotes the expectation with respect to U and V, that is, we do not take the average with respect to B. In contrast to the classical setting, the second partial derivatives of $\Theta(t)$ are more involved, but still can be computed via Duhamel's formula:

$$\frac{\partial^2\Theta(t)}{\partial U_{\boldsymbol{\sigma}}\partial U_{\boldsymbol{\sigma}'}} + \frac{\partial^2\Theta(t)}{\partial V_{\boldsymbol{\sigma}}\partial V_{\boldsymbol{\sigma}'}} = -\beta^2\frac{\langle\boldsymbol{\sigma}|e^{H_t}|\boldsymbol{\sigma}\rangle\langle\boldsymbol{\sigma}'|e^{H_t}|\boldsymbol{\sigma}'\rangle}{(\operatorname{Tr} e^{H_t})^2} + \beta^2\int_0^1 \frac{\langle\boldsymbol{\sigma}|e^{sH_t}|\boldsymbol{\sigma}'\rangle\langle\boldsymbol{\sigma}'|e^{(1-s)H_t}|\boldsymbol{\sigma}\rangle}{\operatorname{Tr} e^{H_t}}ds$$

with the abbreviation $H_t := -\beta(\sqrt{1-t}U + \sqrt{t}V - B)$. Now, we make use of the observation from the beginning of this section. Namely, we may assume without loss of generality that $b_j \geq 0$ such that the matrix elements $\langle\boldsymbol{\sigma}|e^{H_t}|\boldsymbol{\sigma}'\rangle$ are nonnegative for any $\boldsymbol{\sigma}, \boldsymbol{\sigma}'$. Moreover, we observe that

$$\sum_{\boldsymbol{\sigma},\boldsymbol{\sigma}'}\frac{\langle\boldsymbol{\sigma}|e^{H_t}|\boldsymbol{\sigma}\rangle\langle\boldsymbol{\sigma}'|e^{H_t}|\boldsymbol{\sigma}'\rangle}{(\operatorname{Tr} e^{H_t})^2} = 1 = \sum_{\boldsymbol{\sigma},\boldsymbol{\sigma}'}\int_0^1 \frac{\langle\boldsymbol{\sigma}|e^{sH_t}|\boldsymbol{\sigma}'\rangle\langle\boldsymbol{\sigma}'|e^{(1-s)H_t}|\boldsymbol{\sigma}\rangle}{\operatorname{Tr} e^{H_t}}ds,$$

where the first equality follows by definition of the trace and for the second identity we recall that $\sum_{\boldsymbol{\sigma}'}|\boldsymbol{\sigma}'\rangle\langle\boldsymbol{\sigma}'| = \mathbb{1}$. Consequently, we arrive at the bound

$$\left|\mathbb{E}_{U,V}\left[\Theta(1) - \Theta(0)\right]\right| \leq \beta^2\max_{\boldsymbol{\sigma},\boldsymbol{\sigma}'}\left|\mathbb{E}[U(\boldsymbol{\sigma})U(\boldsymbol{\sigma}')] - \mathbb{E}[V(\boldsymbol{\sigma})V(\boldsymbol{\sigma}')]\right|.$$

In the case where U and V are CREM processes with distribution functions A_U and A_V, this leads to the bound

$$\left|\mathbb{E}_{U,V}\left[\Theta(1) - \Theta(0)\right]\right| \leq \beta^2 N\|A_U - A_V\|_\infty.$$

From here, the idea is to approximate the CREM process by GREM processes and to show that Theorem 4.7 in the continuous limit indeed yields Theorem 4.9.

4.2.2 Open Problems: Extremal Statistics and the Parisi Measure

Our main results Theorem 4.7 and Theorem 4.9 provide a complete characterization of the phase diagram in the QGREM and, respectively, the QCREM. Thus, we have managed to extend the classical results on the specific pressure in the GREM (Theorem 4.1) and CREM (Theorem 4.5) to the quantum setting. On the other hand, we have presented in Section 4.1 more detailed results on the extremal statistics of the GREM and and a precise description of the Parisi measure in both models, the GREM and CREM. Rigorous results on that line have not been established for the QGREM and QCREM so far. In this section, we want to discuss what we expect to hold true for hierarchical quantum spin glasses and which methods might be used in (hopefully) forthcoming proofs.

As we have seen in Theorem 4.2, the extremal process of the GREM is governed by Poisson cascades which can be constructed iteratively following the block structure of the GREM. These findings generalize the elementary Poisson convergence in the REM. We recall that for the QREM, we have a given a precise

description of the low energy states and energies from which the extremal statistics in either phase follows, see Theorem 3.1 and Theorem 3.5. It is hence natural to expect that it is feasible to provide a similar precise analysis of the low energy spectrum in the QGREM. Of course, in the QGREM one needs to take care about several blocks $\hat{\boldsymbol{\sigma}}_l$ which all can be either paramagnetic or localized. However, one can still start from a naive second order perturbation theory with the reference state $\psi = |\hat{\boldsymbol{\sigma}}_1^0 \cdots \hat{\boldsymbol{\sigma}}_{l(\beta)}^0\rangle \otimes \Psi_{\emptyset}^{>l(\beta)}$. Here $\hat{\boldsymbol{\sigma}}_1^0 \cdots \hat{\boldsymbol{\sigma}}_{l(\beta)}^0$ denotes the minimal configuration of the truncated GREM potential at $l(\beta)$, which corresponds to the "frozen" part of the Hamming cube; and similarly $\Psi_{\emptyset}^{>l(\beta)}$ denotes the ground state of T restricted to the remaining Hamming cube. The predicted energy shift is in any phase a linear combination of energy corrections, which have already appeared in the discussion of the QREM. One can convince oneself that the predicted shifts depend on the whole distribution function A and not just $\bar{A}$. One should compare that to the classical subleading corrections in Theorem 4.2 for non-degenerate GREM processes (in the case of degenerated GREM processes one observes differences [39]). We think that our methods from Chapter 3 are strong enough to confirm these energy predictions for the QGREM. As in the proof of Theorem 4.7, one would need to consider the Hamiltonian blockwise and presumably an iterative argument would eventually lead to a description of the low energy states and eigenvalues. However, this procedure would require considerable additional effort. If those presumptions are correct, the extremal process would be a combination of the Poisson cascades describing the contribution of first $l(\beta)$ blocks and a deterministic gapped process related to the eigenvalues of T in the remaining part of the Hamming cube.

In the continuous case, we can say much less. We remind the reader that already the minimal statistics of the CREM is not well understood. We do not expect that the methods we have derived will provide further insight into the QCREM. Understanding the low energy properties of the QCREM beyond the leading order, appears to be a very challenging problem.

Let us turn to the Parisi measure in the QGREM, which we similarly define as $\mu_N^P(A) = \mathbb{E}[\langle \mathbb{1}_A(R_N(\boldsymbol{\sigma},\boldsymbol{\sigma'})\rangle_{\beta,\Gamma}^{\otimes 2}]$, for any Borel set $A \subset [-1,1]$ and the thermal average is understood to be with respect to the Gibbs state on the duplicated system $\rho_{\beta,\Gamma} \otimes \rho_{\beta,\Gamma}$. We conjecture that the natural extension of Proposition 4.3 holds true for the QGREM:

Conjecture 4.15
For any $\beta, \Gamma > 0$ the Parisi measure μ_N^P converges weakly to a measure $\mu_{\beta,\Gamma}^P$ supported on the points $\{y_0, \dots, y_m\}$. Let μ_β^P be the classical limit and let $\hat{l}$ where the maximum i attained in (4.5)*, i.e., the blocks $1, \dots, \hat{l}$ behave classically and the remaining ones are of paramagnetic nature. Then, except for the critical magnetizations $\Gamma_c^{(l)}$ the Parisi measure is characterized by*

$$\mu_{\beta,\Gamma}^P([q,1]) = \begin{cases} \mu_P^\beta([q,1]) & \text{if } q \le y_{\hat{l}} \\ 0 & \text{if } q > y_{\hat{l}} \end{cases}$$

Conjecture 4.15 is very natural in view of Theorem 4.7. If we write for the replica overlap

$$R_N(\boldsymbol{\sigma},\boldsymbol{\sigma'}) = R_N^{<=y_{\hat{l}}N}(\boldsymbol{\sigma},\boldsymbol{\sigma'}) + R_N^{>y_{\hat{l}}}(\boldsymbol{\sigma},\boldsymbol{\sigma'})$$

with $R_N^{<=y_{\hat{l}}}(\boldsymbol{\sigma},\boldsymbol{\sigma'}) = \frac{1}{N}\sum_{i<=y_{\hat{l}}N} \sigma_i\sigma_i'$ and $R_N^{>y_{\hat{l}}}(\boldsymbol{\sigma},\boldsymbol{\sigma'}) = \frac{1}{N}\sum_{i>y_{\hat{l}}N} \sigma_i\sigma_i'$. Since the blocks $\hat{\boldsymbol{\sigma}}_l$ with $l > \hat{l}$ show a paramagnetic order, it is natural to assume that we have $R_N^{>y_{\hat{l}}}(\boldsymbol{\sigma},\boldsymbol{\sigma'}) \approx 0$ as it is true for the pure

paramagnet which dominates the Hamiltonian for the later spin configurations. On the other hand, the distribution of the first part of the replica overlap $R_N^{<=y_{\hat{l}}}(\boldsymbol{\sigma},\boldsymbol{\sigma}') = \frac{1}{N}\sum_{i<=y_{\hat{l}}N}\sigma_i\sigma_i'$ should agree with the classical distribution as the thermodynamics coincide with the GREM for the first $y_{\hat{l}}N$ spins.

To prove Conjecture 4.15 one might try to adapt the classical technique which is used to derive Proposition 4.3: one takes the derivative of the GREM pressure with respect to the jump heights a_k of the GREM distribution function A and realizes that the obtained relations already characterize the averaged distribution of the lexicographic q. In a second step, one shows that lexicographic overlap and the replica overlap asymptotically agree [39, 40]. If one invokes these ideas in the QGREM, one observes that $\partial_{a_k}\Phi_N(\beta,\Gamma)$ is not that easy to compute anymore as one needs to apply Duhamel's formula and the main challenge is to cope with the Duhamel correlators. We have developed methods to analyze these correlators, but unfortunately these are only available in form of private notes and have not been published yet due to lack of time.

At first glance, it appears to be much more difficult to extend Theorem 4.4 on the disordered overlap distribution to the quantum setting. However, one might use the same trick which was used to derive the disordered distribution in the CREM. That is, one needs to extend the Ghirlanda-Guerra relations on multi-overlaps to the QGREM, which appears to be of comparable difficulty as a proof of Conjecture 4.15. This would eventually show that the distribution of R_N with respect to the GIbbs state is still describable in terms of Poisson-Dirichlet processes. We also expect that the Parisi measure in the continuous case satisfies the quantum analog of Proposition 4.6. It is hard to judge, if it is much more difficult to prove results for the QCREM then for the finite-level QGREM. The technique on the classical side is essentially the same but the analysis of the Duhamel correlator appears to be more involved than in the QGREM situation, where one only needs to consider finitely many blocks.

4.3 A Look at the de Almeida-Thouless Line in the SK Model

One central question about spin glasses in external magnetic fields is whether the fields destabilize the low-temperature glass phase or not. For the SK-model in a constant longitudinal field, de Almeida and Thouless [57] determined an equation for the critical temperature $T_c(h)$, which turns out to be decreasing in the field strength h and is known under the name de Almeida-Thouless (AT) line. More precisely, the AT line in the SK model separates the replica symmetric phase from the region, where replica symmetry breaking occurs. In the following, we want to provide some insight into the classical problem of the AT line in the SK model before discussing later the AT line in the context of hierarchical spin glasses. This section is largely based on the presentation in [181, Chapter 1.3-1.8, 13.2-13.3].

We consider the classical SK-Hamiltonian

$$H_N(\boldsymbol{\sigma}) = U(\boldsymbol{\sigma}) + h(\boldsymbol{\sigma}) := \frac{1}{\sqrt{N}}\sum_{i<j} g_{i,j}\sigma_i\sigma_j + h\sum_i \sigma_i,$$

where the first term corresponds to the SK potential and $h(\boldsymbol{\sigma}) := h\sum_i \sigma_i$ is the standard implementation of a vertical field of strength $h \geq 0$. A general paradigm for classical spin glasses is that the system is replica symmetric for high enough temperatures, i.e., the replica overlap $R_N(\boldsymbol{\sigma},\boldsymbol{\sigma}') \approx q$ concentrates around a specific value $q \in [0,1]$ with respect to the Gibbs measure. In the REM, this holds true with $q = 0$ for $\beta < \beta_c$, see Proposition 2.3. Let us assume for the moment that replica symmetry holds true for

some $\beta, h > 0$. What can we say about the pressure and the value of q? The idea is if $R_N(\boldsymbol{\sigma}, \boldsymbol{\sigma}') \approx q$, then the SK Hamiltonian is comparable to a Gaussian random field $\sqrt{q}\sum_{i=1}^N z_i\sigma_i$ whose covariance process agrees up to a constant shift with the SK covariance for $R_N(\boldsymbol{\sigma}, \boldsymbol{\sigma}') \approx q$. It was Guerra who realized how to use Gaussian interpolation (Proposition 4.14) to convert this sketched comparison into a rigorous upper bound for the pressure [98]. Let us present Guerra's beautiful idea: we introduce the interpolated Hamiltonian

$$H_t(\boldsymbol{\sigma}) = \sqrt{1-t}\sqrt{q}\sum_{i=1}^N z_i\sigma_i + \frac{\sqrt{t}}{\sqrt{N}}\sum_{i<j} g_{i,j}\sigma_i\sigma_j + h\sum_i \sigma_i$$

and the corresponding specific pressure $\Theta(t) := \frac{1}{N}\mathbb{E}[\ln \operatorname{Tr} e^{\beta H}]$ for some $\beta > 0$. Now, we apply Proposition 4.14; the resulting derivative can be compactly written as

$$\Theta(t)' = \frac{\beta^2}{2N}\mathbb{E}\left[\langle \Delta(\boldsymbol{\sigma}, \boldsymbol{\sigma})\rangle_t - \langle \Delta(\boldsymbol{\sigma}, \boldsymbol{\sigma}')\rangle_t\right],$$

where $\Delta(\boldsymbol{\sigma}, \boldsymbol{\tau}) := \mathbb{E}[U(\boldsymbol{\sigma})U(\boldsymbol{\tau}) - U'(\boldsymbol{\sigma})U'(\boldsymbol{\tau})]$ denotes the difference between the covariance processes. In our situation, we have

$$\Delta(\boldsymbol{\sigma}, \boldsymbol{\sigma}') = \frac{1}{2}(N R_N(\boldsymbol{\sigma}, \boldsymbol{\sigma}') - 1) - NqR_N(\boldsymbol{\sigma}, \boldsymbol{\sigma}').$$

This results in the remarkable expression

$$\Theta'(t) = \frac{\beta^2}{4}(1-q)^2 - \frac{\beta^2}{4}\mathbb{E}[\langle (R_N(\boldsymbol{\sigma}, \boldsymbol{\sigma}') - q)^2\rangle_t] + \mathcal{O}(1/N),$$

where the difficult term has a definite sign. Since $\Theta(0) = \mathbb{E}[\ln 2\cosh(\beta\sqrt{q}z + \beta h)]$ with a standard Gaussian z, we obtain Guerra's replica-symmetric bound

$$\lim_{N\to\infty}\frac{\Phi_N(\beta, h)}{N} \le p_{\mathrm{RS}}(q, \beta, h) := \mathbb{E}[\ln 2\cosh(\beta\sqrt{q}z + \beta h)] + \frac{\beta^2}{4}(1-q)^2.$$

Optimizing, with respect to q yields the determining equation $q = \mathbb{E}[\tanh^2(\beta\sqrt{q}z + \beta h)]$, which has always a unique solution q_{RS} for $h > 0$ [181, Proposition 1.3.8]. If the external field vanishes $h = 0$, there is only the solution $q = 0$ for high temperatures $\beta < 1$, and $p_{\mathrm{RS}}(0, \beta, 0)$ agrees with the annealed pressure. A second solution $q > 0$ emerges for low temperatures $\beta > 1$.

Let us remark that q_{RS} is a self-consistent choice, i.e., the Gibbs measure of the comparison Hamiltonian concentrates at $R_N(\boldsymbol{\sigma}, \boldsymbol{\sigma}') \approx q_{\mathrm{RS}}$. For high enough temperatures, a more subtle interpolation argument shows that $\langle (R_N(\boldsymbol{\sigma}, \boldsymbol{\sigma}') - q_{\mathrm{RS}})^2\rangle_t = \mathcal{O}(1/N)$ for any $t \in [0, 1]$ [181, Theorem 1.4.1], which by the above is enough to prove

$$\lim_{N\to\infty}\frac{1}{N}\Phi_N(\beta, h) = p_{\mathrm{RS}}(q_{\mathrm{RS}}, \beta, h).$$

Sherrington and Kirkpatrick originally claimed that the replica symmetric solution should hold for any temperature [166], but by now it is well known that this prediction must be wrong as it would lead to a

negative entropy for low temperatures [135]. The numerical calculations performed by de Almeida and Thouless suggest that the replica symmetric solution is valid if and only if

$$\mathbb{E}\left[\frac{\beta^2}{\cosh^4(\beta z\sqrt{q_{\mathrm{RS}}}+\beta h)}\right] \leq 1, \tag{4.12}$$

and the curve in the (β, h)-plane where equality holds, is the conjectured AT line which marks the transition between a high temperature phase and a glassy phase in the SK model. Since q_{RS} is monotone in h, the AT line is in accordance with the widely assumed hypothesis that magnetic fields destabilize the glass phase [135]. To obtain some intuition why the AT line is determined by (4.12), it is instructive to compute the variance of the replica overlap in the high temperature phase ($\beta < \frac{1}{2}$) [181, Corollary 1.8.6],

$$\mathbb{E}[\langle (R_N(\boldsymbol{\sigma}, \boldsymbol{\sigma}') - q)^2 \rangle] = \frac{\mathcal{O}(1)}{N(1-\beta^2(1-2q_{\mathrm{RS}}+\hat{q}))}$$

with $\hat{q} := \mathbb{E}[\tanh^4(\beta z\sqrt{q_{\mathrm{RS}}}+h)]$. The elementary identity $1-2q_{\mathrm{RS}}+\hat{q} = \mathbb{E}\left[\frac{1}{\cosh^4(\beta z\sqrt{q_{\mathrm{RS}}}+\beta h)}\right]$ then indicates that a transition might occur exactly at the AT line. An important step towards a proof was taken by Toninelli, who showed that if $\mathbb{E}\left[\frac{\beta^2}{\cosh^4(\beta z\sqrt{q_{\mathrm{RS}}}+\beta h)}\right] > 1$, then the replica symmetric solution is false [185]. Actually, Toninelli showed more: p_{RS} agrees with the limiting specific pressure if and only if

$$p_{\mathrm{RS}}(q_{\mathrm{RS}}, \beta, h) = \inf_{q,q',m} p_{\text{1-RSB}}(q, q', m, \beta, h)$$

with the so-called 1-step replica symmetry broken pressure

$$p_{\text{1-RSB}}(q, q', m, \beta, h) := \ln 2 + \frac{\beta^2}{4}(1-q')^2 - \frac{\beta^2}{4}m(q'^2 - q^2) + \frac{1}{m}\mathbb{E}[\ln \mathbb{E}_{z'}[(\cosh \beta Y' + \beta h)^m]],$$

where $0 \leq q \leq q' \leq 1$ and $0 < m \leq 1$ and $Y' = \sqrt{q}z + \sqrt{q'-q}z'$ with z, z' being two independent standard Gaussians. Conceptually, the 1-RSB corresponds to the assumption that the overlap R_N concentrates around the two values q, q' and m corresponds to the mass of the Parisi measure at q'. Considering arbitrarily high level of replica symmetry breaking, ultimately leads to the celebrated Parisi formula, which we discuss in the next Chapter 5.

In some sense, establishing the replica symmetry below the AT line is a calculus problem due to Toninelli's result. But the rather complicated 1-RSB formula makes the analysis challenging and, unfortunately, replica symmetry has not been established yet in the complete region above the predicted AT line. Nevertheless, there has been some progress in the last years. In [43], replica symmetry is shown in the region $\mathbb{E}\left[\frac{\beta^2}{\cosh^2(\beta z\sqrt{q_{\mathrm{RS}}}+\beta h)}\right] \leq 1$, which forms a rather big fraction of the predicted RS phase. Their approach is based on the TAP method, which analyzes local magnetizations (see also [4]). On the other hand, in [51] a brute force ansatz analyzing the Parisi functional is presented, which results in a complete confirmation of the AT line in the case where the magnetic field h is not constant but each of its weights are independent Gaussian variables.

4.4 The Quantum de Almeida-Thouless Line in the QCREM

We have seen that a rigorous verification of the conjectured AT line in the SK model has not been achieved so far. An analytic characterization of the AT line in the quantum SK model appears illusive at the moment and physical predictions are based on numerical simulations [193].

Just as the GREM and CREM were introduced by Derrida [63, 64] to qualitatively capture the thermodynamics of more complicated glasses, we aim to shed some light on the quantum AT line by studying the QCREM. To this end, we need to extend the QCREM Hamiltonian by an additional diagonal operator h representing the longitudinal field,

$$H_N = U + h - B,$$

where U is now a CREM potential and B denotes the (random) transversal field. The presumably most natural choice for h is the standard implantation of a longitudinal field from the last section,

$$h(\boldsymbol{\sigma}) = \sum_{j=1}^{N} h_j \sigma_j, \tag{4.13}$$

where we allow the weights h_i to be random fields. Already in the classical setting $B = 0$ it turns out, that a longitudinal field as in (4.13) causes the frozen phase of the CREM models to expand [14, 15, 38]. We will show in Section 4.4.1 that this unphysical behavior still emerges in the quantum setting.

On the other hand, Derrida and Gardner [65] suggested a hierarchical implementation of the longitudinal magnetic field, which then leads again to a destabilization of the frozen phase. This choice can be physically justified: one should recall that the GREM was designed as a hierarchical approximation of the more involved SK-model. Here, the idea is to choose the CREM distribution function A such that the entropy of likewise pair-correlated energies asymptotically coincides with the SK correlation $\frac{N}{2} R_N(\boldsymbol{\sigma}, \boldsymbol{\sigma}')$, i.e.,

$$\lim_{N\to\infty} \frac{1}{N} \ln\left(\frac{\left|\{\boldsymbol{\sigma} \,:\, R_N(\boldsymbol{\sigma}, \boldsymbol{\sigma}^0)^2 > 2a\}\right|}{\left|\{\boldsymbol{\sigma} \,:\, A(q_N(\boldsymbol{\sigma}, \boldsymbol{\sigma}^0)) > a\}\right|} \right) = 1$$

for all $a \in (0, 1)$ and a fixed, but arbitrary, reference state $\boldsymbol{\sigma}^0$. This determines the (non-normalized) SK approximation $A(x) = \frac{1}{2}\gamma(x)^2$ (see [131, Section 1.3] for a more detailed derivation). γ is the inverse function of

$$\gamma^{-1} : [0, 1] \to [0, 1], \quad \gamma^{-1}(x) := \frac{1-x}{2\ln 2} \ln(1-x) + \frac{1+x}{2\ln 2} \ln(1+x). \tag{4.14}$$

Following this line of thought, to understand the quantum AT line one should consider the hierarchical reorganization of the magnetic field as well. We define general hierarchical fields on $\mathcal{Q}_N$ as follows:

Definition 4.16 (Definition in [131])
We call a function $h : \mathcal{Q}_N \to \mathbb{R}$ a hierarchical field with reference state $\boldsymbol{\sigma}^0 \in \mathcal{Q}_N$ if there exists a function $\eta : [0, 1] \to \mathbb{R}$ such that

$$h(\boldsymbol{\sigma}) = N\eta(q_N(\boldsymbol{\sigma}, \boldsymbol{\sigma}^0)),$$

where q_N is the lexicographic overlap (4.1)*. Furthermore, h is said to be a regular hierarchical field, if η is a regular function on* $[0, 1]$*, i.e., η is a uniform limit of step functions.*

In Section 4.4.2, we will see present a formula for the specific pressure of the QCREM with a general regular hierarchical field. For the discussion of the quantum AT line, the case, where the choice of $\boldsymbol{\sigma}^0$ and η corresponds to a constant external magnetic field, is of particular relevance. We note that the constant longitudinal magnetic field of strength h can be written as $h\sum_{i=1}^N \sigma_i = hNR_N(\boldsymbol{\sigma},\boldsymbol{\sigma}^0)$ with the ferromagnetic state $\boldsymbol{\sigma}^0 = (+1,\dots,+1)$ which takes the role of the reference state in Definition 4.16. However, the pressure does not depend on the choice of the reference state.
To determine the appropriate overlap function η, we demand that the entropy agrees with the one of the ordinary magnetic field, i.e., the number of (positive) energy states agree on an exponential scale:

$$\lim_{N\to\infty}\frac{1}{N}\ln\left(\frac{\left|\{\boldsymbol{\sigma} : hR_N(\boldsymbol{\sigma},\boldsymbol{\sigma}^0) > a\}\right|}{\left|\{\boldsymbol{\sigma} : v(q_N(\boldsymbol{\sigma},\boldsymbol{\sigma}^0)) > a\}\right|}\right) = 1$$

for any $0 < a < h$. Comparing the asymptotics, leads to the choice

$$\eta(a) := h\gamma(a),$$

where γ is again the inverse function of (4.14). We refer to this choice as the hierarchical magnetic field of strength h. We will discuss the resulting quantum AT line in Section 4.4.2.

4.4.1 The QCREM with a random longitudinal field

Throughout this section we assume that the longitudinal field is of the form $h(\boldsymbol{\sigma}) = \sum_{j=1}^N h_j\sigma_j$ with random weights h_i which are independent copies of a real valued absolutely integrable random variable $\mathfrak{h}$. Moreover, the weights $(h_i)_i$, $(b_i)_i$ and the CREM process U shall be mutually independent from each other.
The de Almeida-Thouless line is encoded in the pressure $\Phi_N(\beta,\mathfrak{h},\mathfrak{b}) := \ln \operatorname{Tr} e^{-\beta H_N}$. The specific pressure converges almost surely:

Theorem 4.17 (Theorem 1 in [131])
Let $U(\boldsymbol{\sigma})$ be a CREM process with distribution function A and suppose that the longitudinal random field is implemented as in (4.13)*. For any $\beta \geq 0$ and any absolutely integrable random variables $\mathfrak{h},\mathfrak{b}$, the specific pressure converges almost surely,*

$$\lim_{N\to\infty}\frac{1}{N}\Phi_N(\beta,\mathfrak{h},\mathfrak{b}) = \sup_{0\leq z\leq 1}\left(\int_0^z \varphi(\beta,\mathfrak{h},x)\,dx + (1-z)\mathbb{E}[\ln 2\cosh(\beta\sqrt{\mathfrak{b}^2+\mathfrak{h}^2})]\right).$$

The density $\varphi(\beta,\mathfrak{h},x)$ is given by

$$\varphi(\beta,\mathfrak{h},x) := \begin{cases} \ln 2 + \bar{a}(x)\frac{\beta^2}{2} + \mathbb{E}[\ln\cosh\beta\mathfrak{h}] & if \quad \beta \leq \beta_c(x), \\ \beta(\bar{a}(x)\beta_c(x) + \mathbb{E}[\mathfrak{h}\tanh\beta_c(x)\mathfrak{h}]) & if \quad \beta > \beta_c(x), \end{cases}$$

where $\beta_c(x) = \beta_c(x,\mathfrak{h})$ is the unique positive solution of the self-consistency equation

$$\frac{\bar{a}(x)}{2}\beta_c(x)^2 = \ln 2 + \mathbb{E}[\ln\cosh\beta_c(x)\mathfrak{h}] - \beta_c(x)\mathbb{E}[\mathfrak{h}\tanh\beta_c(x)\mathfrak{h}].$$

Moreover, $\varphi(\beta, \mathfrak{h}, x)$ is a decreasing function of x and strictly increasing and convex in β, while $\beta_c(x)$ is increasing in x.

In the classical case without transversal magnetic field ($\mathfrak{b} = 0$), Theorem 4.17 generalizes the results of [38], who deal with the case that $\mathfrak{h}$ is constant, and the results of [14, 15], who consider the special case of a REM or two-level GREM in a random magnetic field. The proof does not require new methods but is rather technical as one has to analyze a constrained optimization problem [131, Section 3].
We briefly discuss the resulting quantum AT line. It turns out that the AT line of the general CREM has qualitatively the same shape as the one of the REM [131]. Hence, we restrict ourselves to the REM with constant fields $\mathfrak{h} = h$ and $\mathfrak{b} = \Gamma$ for some positive constants $h, \Gamma \geq 0$. In this situation, the limit of the specific pressure is given by (see [131, Corollary])

$$p_{\mathrm{QREM}}(\beta, h, \Gamma) = \max\{p_{\mathrm{REM}}(\beta, h), \ln 2\cosh(\beta\sqrt{h^2 + \Gamma^2})\},$$

$$p_{\mathrm{REM}}(\beta, h) = \begin{cases} \ln 2 + \frac{\beta^2}{2} + \ln\cosh\beta h & if \quad \beta \leq \beta_c(h) \\ \beta(\beta_c(h) + h\tanh(\beta_c(h)h)) & if \quad \beta > \beta_c(h) \end{cases}$$

where $\beta_c(h)$ is the unique positive solution of $\beta_c(h)^2 = 2r(\tanh(\beta_c(h)h))$ with the modified binary entropy $r(x) := -\left(\frac{1-x}{2}\ln\frac{1-x}{2} + \frac{1+x}{2}\ln\frac{1+x}{2}\right)$ defined on $[-1, 1]$.

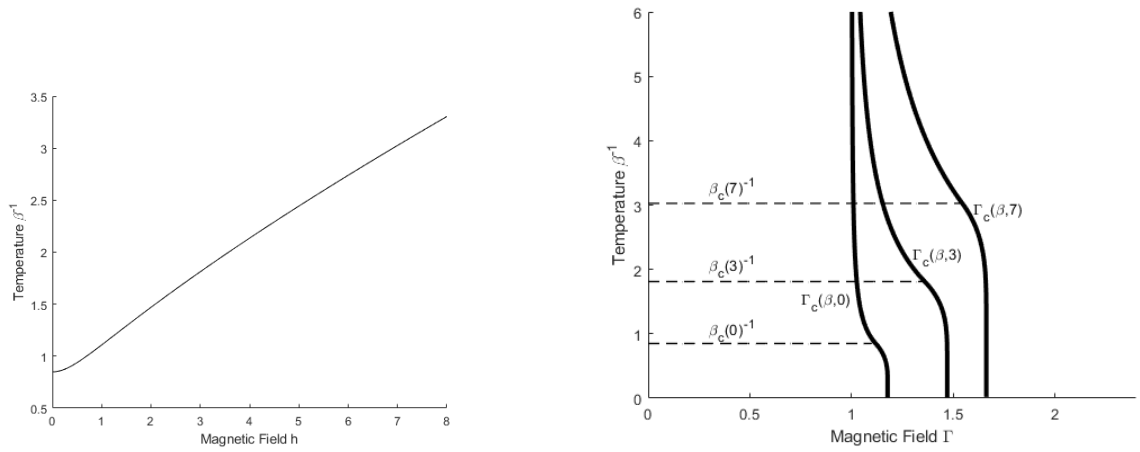

Figure 4.3: The left figures illustrates the freezing temperature $T_c(h) = \beta_c^{-1}(h)$ as a function of the longitudinal field h [131, Figure 1]. On the right is the $T - \Gamma$ phase diagram with the critical magnetic field $\Gamma_c(\beta, \Gamma)$ as well as the critical temperature evaluated at $h = 0, 3, 7$.

For fixed $h > 0$, the phase diagram, which is plotted in Figure 2.3, is very similar to the QREM without vertical field. The magnetic transition occurs at

$$\Gamma_c(\beta, h) := \sqrt{\beta^{-2}\,\mathrm{arcosh}\left(\frac{1}{2}\exp(p_{\mathrm{REM}}(\beta, h))\right)^2 - h^2}.$$

For fixed $h > 0$, glass order is find in the region $\beta > \beta_c(h)$ and $\Gamma < \Gamma_c(\beta, h)$. As one already observes in Figure 4.3, $\beta_c(h)$ is a decreasing and $\Gamma_c(\beta, h)$ is an increasing function of h, i.e., the glass phase expands as

the longitudinal field becomes stronger. These findings can be put on an analytic ground [131, Proposition 1]. An expanding glass phase is in high contrast to numerical calculations which suggest that in the QSK the longitudinal and transversal field destabilize the glass phase (cf. [147, 193] and [175]). In the next section we will see that we can overcome this problem with a hierarchical implementation of the longitudinal field.

4.4.2 The QCREM with a hierarchical longitudinal field

In this section, we assume that the longitudinal field h is a regular hierarchical field as in Definition 4.16 and we discuss the limit of the corresponding specific pressure $\frac{1}{N}\Phi_N(\beta, \mathfrak{b}, h)$.
To formulate our main result, we introduce the doubly-cut distribution function $A^{(y,z)} : [0, z-y] \to [0,1]$, $A^{(y,z)}(x) := A(x+y) - A(y)$. with corresponding concave hull $\bar{A}^{(y,z)}$ and the hull's right derivative $\bar{a}^{(y,z)}$. We further set $\varphi^{(y,z)} : \mathbb{R} \times [0, z-y] \to \mathbb{R}$,

$$\varphi^{(y,z)}(\beta, x) := \beta\sqrt{(2\ln 2)\,\bar{a}^{(y,z)}(x)}\mathbb{1}_{x<x^{(y,z)}(\beta)} + \left(\frac{\beta^2}{2}\bar{a}^{(y,z)}(x) + \ln 2\right)\mathbb{1}_{x\geq x^{(y,z)}(\beta)}$$

with

$$x^{(y,z)}(\beta) := \sup\left\{x \mid \bar{a}^{(y,z)}(x) > 2\ln 2/\beta^2\right\}.$$

In presence of any regular hierarchical field h, we have the following generalization of Theorem 4.9:

Theorem 4.18
Let $U(\boldsymbol{\sigma})$ be a CREM process, B a random transversal field with i.i.d weights (b_j) with the same distribution as $\mathfrak{b}$ and $h(\boldsymbol{\sigma}) = N\eta(q(\boldsymbol{\sigma}, \boldsymbol{\sigma}^0))$ a regular hierarchical field. Then, almost surely:

$$\begin{aligned} p(\beta, \mathfrak{b}, h) &:= \lim_{N\to\infty} \frac{1}{N}\Phi_N(\beta, \mathfrak{b}, h) \\ &= \sup_{0\leq y\leq z\leq 1}\left[\beta\eta(y) + \int_0^{z-y}\varphi^{(y,1)}(\beta, x)\,dx + (1-z)\mathbb{E}[\ln 2\cosh(\beta\mathfrak{b})]\right]. \end{aligned} \tag{4.15}$$

The proof of Theorem 4.18 is based on the peeling principle and can be found in [131, Section 2]. Most interestingly, the transversal field B and the hierarchical field h both destabilize the glass phase, albeit quite differently. While the hierarchical field tends to shrink the glass region in its most correlated sector first (it acts through the choice of y from the 'left'), the transversal field begins by changing the unfrozen region and the less correlated sector (it acts through the choice of z from the 'right').
If $A = \bar{A}$, i.e., A is a concave function we can simplify the variational formula (4.15). Then, $\varphi^{(y,1)}$ is a just a translation of $\varphi^{(0,1)} =: \varphi$ and we arrive at the simpler expression

$$p(\beta, \mathfrak{b}, h) = \sup_{0\leq y\leq z\leq 1}\left[\beta\eta(y) + \int_y^z \varphi(\beta, x)\,dx + (1-z)\mathbb{E}[\ln 2\cosh(\beta\mathfrak{b})]\right], \tag{4.16}$$

with

$$\varphi(\beta, x) = \beta\sqrt{(2\ln 2)\,\bar{a}(x)}\mathbb{1}_{x<x(\beta)} + \left(\frac{\beta^2}{2}\bar{a}(x) + \ln 2\right)\mathbb{1}_{x\geq x(\beta)},$$
$$x(\beta) := \sup\left\{x \mid \bar{a}(x) > (2\ln 2)/\beta^2\right\}.$$

On the other hand, if A is not concave (which is always the case if A is a step function) the behavior of $\varphi^{(y,1)}$ is more subtle as one has to take into account that the slope of the concave hull's linear segments will change as y increases. In particular, (4.16) does not necessarily hold true. In contrast to a transversal field, a hierarchical field might lead to a change of the determining concave hull. As discussed in [65], this happens for the hierarchical caricatures p-spin glasses with $p > 2$.

We will now briefly discuss the quantum de Almeida-Thouless (AT) line in the situation where $A = \bar{A}$ is continuously differentiable with derivative $\bar{a}$, and we consider a hierarchical magnetic field $\eta = h\gamma$ of strength $h \geq 0$ and a constant transversal field of strength Γ. We have particularly in mind the SK caricature $A(x) = \frac{1}{2}\gamma(x)^2$. A much more detailed discussion is presented in [131, Section 1.4].

We start with the limiting case $\Gamma = 0$. The supremum in (4.16) is attained at $z = 1$ and $y = y(\beta, h) \in (0, 1)$, which for fixed $\beta > 0$ and $h > 0$ is the unique solution of the equation

$$y = k\left(\frac{\varphi(\beta, y)}{\beta h}\right), \tag{4.17}$$

where $k : [0, \infty) \to (0, 1]$ is the inverse function of the derivative $\gamma' : (0, 1] \to [0, \infty)$ of γ. The glass phase is here characterized by $y(\beta, h) < x(\beta)$, which leads for fixed h to the critical inverse temperature

$$\beta_c(h) := \inf\{\beta \ : \ x(\beta) > k(2\ln 2/(\beta h))\,.\} \tag{4.18}$$

For $h = 0$, this reduces to $\beta_c := \sqrt{\frac{2\ln 2}{\bar{a}(0)}}$. The function $h \mapsto \beta_c(h)$ is the classical AT line of the CREM. $\beta_c(h)$ is an increasing function and

$$\lim_{h\to\infty} \beta_c(h) = \begin{cases} \infty & \text{if } \bar{a}(1) = 0, \\ \frac{2\ln 2}{\bar{a}(1)} & \text{if } \bar{a}(1) > 0. \end{cases}$$

For $h = 0$, the choice $A(x) = \frac{1}{2}\gamma(x)^2$ leads to a correct prediction of the point of the SK glass transition, but the critical exponent for $h \sim 0$ does not coincide with the observed exponent.

Next, we consider a vanishing vertical field $h = 0$, which is basically the scenario of Theorem 4.9. We recall that the maximum is then attained at

$$z(\beta, \Gamma) := \begin{cases} 1 & p(\beta\Gamma) \leq s(\beta) := \varphi(\beta, 1) \\ g_\beta(p(\beta\Gamma)) & s(\beta) < p(\beta\Gamma) < t(\beta) := \varphi(\beta, 0) \\ 0 & t(\beta) \geq p(\beta\Gamma) \end{cases} \tag{4.19}$$

with the notation of Corollary 4.10. For the SK approximation, we obtain a prediction of the quantum phase transition, $\lim_{\beta\to\infty} \Gamma_c(\beta, 0) = \sqrt{(2\ln 2)\bar{a}(0)} = 2\ln 2 \approx 1.38\ldots$, which does not agree with the perturbative or numerical prediction of approximately 1.51 in [192,193]. Nor does the behavior of $\Gamma_c(T^{-1}, 0)$ near $T = 0$ agree with the T^2-scaling predicted in [106]. Presumably, this is a defect of the hierarchical implementation of the glass' correlations.

To determine the pressure $p(\beta, \Gamma, h)$ in the general case of a constant transversal and longitudinal field $\Gamma, h > 0$, we also need to discuss the behavior of the variational expression (4.16) at the diagonal $y = z$, which corresponds to the situation without a CREM potential. In this case, the supremum is attained at

$$\sigma(\beta, \Gamma, h) := k\left(\frac{p(\beta\Gamma)}{\beta h}\right). \tag{4.20}$$

This enables us, to give a more explicit solution of (4.15):

Corollary 4.19 (Corollary 2 in [131])
Suppose that $A = \bar{A}$ is continuously differentiable. For a constant transversal field of strength $\Gamma > 0$ and the hierarchical magnetic field $h(\boldsymbol{\sigma}) = N h\gamma(q(\boldsymbol{\sigma}, \boldsymbol{\sigma}^0))$ of strength $h > 0$ the limiting pressure is given by

$$p(\beta, \Gamma, h) = \begin{cases} \beta h\gamma\left(y(\beta, h)\right) + \displaystyle\int_{y(\beta,h)}^{z(\beta,\Gamma)} \varphi(\beta, x)dx + (1 - z(\beta, \Gamma))\, p_{PAR}(\beta\Gamma), \\ \qquad\qquad\qquad\qquad\qquad\qquad\qquad\qquad p_{PAR}(\beta\Gamma) < \varphi(\beta, y(\beta, h)), \\ \beta h\gamma\left(\sigma(\beta, \Gamma, h)\right) + (1 - \sigma(\beta, \Gamma, h))\, p_{PAR}(\beta\Gamma), \\ \qquad\qquad\qquad\qquad\qquad\qquad\qquad\qquad p_{PAR}(\beta\Gamma) \geq \varphi(\beta, y(\beta, h)), \end{cases}$$

where $y(\beta, h)$, $z(\beta, \Gamma)$ and $\sigma(\beta, \Gamma, h)$ are specified in (4.17), (4.19) *and* (4.20) *respectively.*

For fixed $h > 0$ the contribution of the CREM process vanishes for $\Gamma > \Gamma_c(\beta, h)$ with

$$\Gamma_c(\beta, h) := \frac{1}{\beta} \operatorname{arcosh}\left(\tfrac{1}{2} e^{\varphi(\beta, y(\beta,h))}\right).$$

The critical field strength $\Gamma_c(\beta, h)$ marks a second order transition, where the derivative of the transversal magnetization m_x has a jump. The zero temperature limit $\beta \to \infty$ leads to the ground state Quantum AT line which is plotted in Figure 4.4.

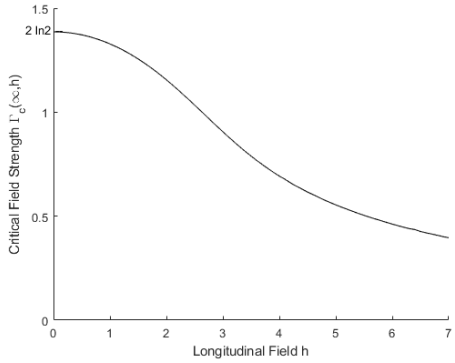

Figure 4.4: Plot of the Quantum AT line, i.e. the dependence of the critical transversal field $\Gamma_c(\beta, h)$ on the longitudinal field h for zero temperature, $\beta = \infty$ [131, Figure 2].

A low-temperature glass phase occurs if and only if

$$y(\beta, h) < \min\{x(\beta), z(\beta, \Gamma)\}.$$

Clearly, this is only possible if two conditions are satisfied simultaneously:

1. $z(\beta, \Gamma) > y(\beta, h)$, i.e. for transversal fields $\Gamma < \Gamma_c(\beta, h)$. From the monotonicity of $h \mapsto \varphi(\beta, y(\beta, h))$, we conclude, $\Gamma_c(\beta, h) \leq \Gamma_c(\beta, 0)$ for any $\beta, h > 0$.

2. $x(\beta) > y(\beta, h)$, i.e. for $\beta > \beta_c(h)$ given by (4.18), which we already identified as a monotone increasing function of h.

We thus conclude, that the presence of the transversal field $h > 0$ shrinks the spin glass' low-temperature phase. Qualitatively, this behavior is in accordance with the numerical findings in case of the Quantum SK-model [193]. However, more precise quantitative properties such as the critical exponents differ. Figure 4.5 plots the temperature-transversal field phase diagram for different values of h in case that $A = \bar{A}$ and $\bar{a}(1) = 0$.

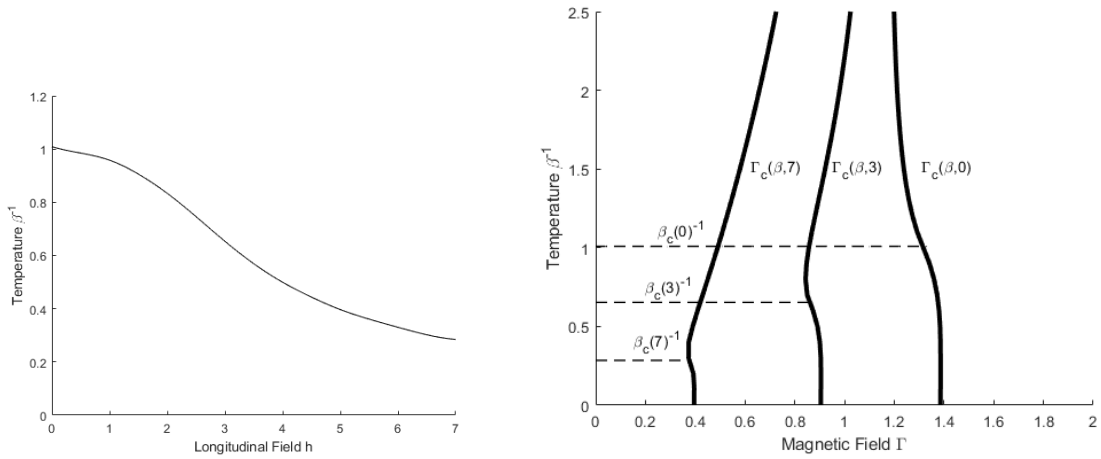

Figure 4.5: On the left is a plot of the critical temperature $\beta_c(h)$ as a function of the longitudinal field. On the right figure is the $T - \Gamma$ phase diagram with the critical magnetic field $\Gamma_c(\beta, \Gamma)$ as well as the critical temperature $\beta_c(h)^{-1}$ evaluated at $h = 0, 3, 7$ [131, Figure 3].

Chapter 5

The Quantum Sherrington-Kirkpatrick Model

This final chapter is devoted to the much more involved Sherrington-Kirkpatrick (SK) model. Section 5.1 introduces Parisi's sophisticated solution for the pressure in the more general setting of classical mixed p-spin Hamiltonians. We will try to transport some intuition behind the Parisi formula by presenting the main foundations of its proof: the cavity method and the Aizenman-Sims-Starr scheme [8], Guerra's interpolation method in the realm of Ruelle cascades [99, 153], and Ghirlanda-Guerra identities and the resulting ultrametricity of the Gibbs measure [94, 151]. After having familiarized ourselves with the classical SK model, in Section 5.2 we turn to the Quantum Sherrington-Kirkpatrick (QSK) model where we focus on the few rigorously established results, in particular the infinite-dimensional Parisi formula introduced in [3], and the study of the high temperature phase $\beta < 1$ in [126]. The final Section 5.3 discusses the main result from our Article VI [125], which shows that the QSK model exhibits glass order in the low temperature phase $\beta > 1$ in presence of a weak transversal field. We compare our findings with the predictions in the physics literature and describe our proof which is based on the Falk-Bruch inequality [73] and arguments which have been developed for the classical SK model [6, 42].

5.1 The Sherrington-Kirkpatrick Model: The Parisi Formula

We consider a mixed p-spin potential U with an external longitudinal field of strength $h \geq 0$, i.e., the classical Hamiltonian is given by

$$H_N(\boldsymbol{\sigma}) := U(\boldsymbol{\sigma}) + h \sum_{i=1}^{N} \boldsymbol{\sigma}_i = \sum_{p \geq 2} \beta_p U_p(\boldsymbol{\sigma}) + h \sum_{i=1}^{N} \boldsymbol{\sigma}_i, \tag{5.1}$$

where $\beta_p \geq 0$ are some nonnegative parameters which satisfy $\sum_{p \geq 2} \beta_p 2^p < \infty$ and U_p denotes the pure p-spin potential

$$U_p(\boldsymbol{\sigma}) = \frac{1}{N^{(p-1)/2}} \sum_{i_1, \ldots, i_p = 1}^{N} g_{i_1, \ldots, i_p} \sigma_{i_1} \cdots \sigma_{i_p}. \tag{5.2}$$

U is then a centered Gaussian process with covariance

$$\mathbb{E}[U(\boldsymbol{\sigma})U(\boldsymbol{\sigma}')] = N\xi(R_N(\boldsymbol{\sigma},\boldsymbol{\sigma}')) \qquad (5.3)$$
$$\xi(x) := \sum_{p\geq 2} \beta_p^2 x^p.$$

The classical SK model at temperature β corresponds to the case where $\beta_2 = \frac{\beta}{\sqrt{2}}$ and all other β_p vanish. The additional division by $\sqrt{2}$ is due to the summation over all (i,j) tuples in (5.2). For mixed p-spin potentials we think of the sequence $(\beta_p)_p$ to absorb the inverse temperature.
Without further ado, let us present Parisi's formula for the limit of the specific pressure. We follow the exposition in [152], but we have replaced the Gaussian field with a constant external field. The Parisi formula takes into account an arbitrarily high level of replica-symmetry breaking and, thus, generalizes the RS and 1-RSB formulas from Section 4.3. To describe an arbitrary point measure on $[0,1]$ with finite support, let $r \geq 1$ and we introduce the two sequences

$$0 = \zeta_{-1} < \zeta_0 < \cdots < \zeta_{r-1} < \zeta_r = 1,$$

and,

$$0 = q_0 < q_1 < \cdots < q_{r-1} < q_r = 1.$$

One should think of the both sequences defining a distribution function ζ of a point measure on $[0,1]$ with $\zeta(q_m) = \zeta_m - \zeta_{m-1}$. We will see shortly that ζ determines the pressure and is thus referred to as *functional order parameter* or *Parisi's order parameter*. Let $(z_m)_{1\leq m\leq r}$ be i.i.d standard Gaussians. We define recursively the random variables

$$X_r = \ln 2\cosh\left(\sum_{1\leq m\leq r} z_m(\xi'(q_m) - \xi'(q_{m-1}))^{1/2} + h\right),$$
$$X_l = \frac{1}{\zeta_l}\ln \mathbb{E}_{l+1}[\exp(\zeta_l X_{l+1})] \qquad \text{for } l = 0,\dots,r-1.$$

Here $\mathbb{E}_l$ denotes the expectation with respect to z_l and ξ is the function from (5.3). In particular X_0 is just a real number in the sense that it is not random, but of course X_0 is still a rather involved function of ζ, ξ and h. We are ready to define the *Parisi functional*

$$\mathscr{P}_{\xi,h}(\zeta) := X_0 - \frac{1}{2}\sum_{0\leq m\leq r-1} \zeta_m(\theta(q_{m+1}) - \theta(q_m)) \qquad (5.4)$$

with the abbreviation $\theta(x) := x\xi'(x) - \xi(x) = \sum_{p\geq 2}(p-1)\beta_p^2 x^p$. Probably, the deepest result in the field of spin glass theory is the following theorem which relates the Parisi functional (5.4) to the limit of the specific pressure of mixed p-spin Hamiltonians (5.1):

Theorem 5.1 ([153, 155, 179, 181] Theorem 3.1 in [152])
Let H_N be the mixed p-spin Hamiltonian from (5.1)*. Then, the pressure converges almost surely and with the notation from above the limit is given by*

$$\lim_{N\to\infty} \frac{1}{N}\Phi_N((\beta_p)_{p\geq 2}, h) = p_{Parisi}((\beta_p)_{p\geq 2}, h) := \inf_{\zeta} \mathscr{P}_{\xi,h}(\zeta), \tag{5.5}$$

where the infimum is taken over all distribution functions ζ corresponding to a probability measure on $[0, 1]$ *with finitely many atoms.*

A few comments are in order:

1. After Sherrington and Kirpatrick had introduced their model and the replica-symmetric solution, it was Parisi who had the ingenious insight that the thermodynamics is not governed by a few real parameters, but by a distribution function describing the nontrivial distribution of the replica overlap [155]. To arrive at the formula (5.5), Parisi used the so-called replica trick and he assumed anticipately that the limiting Gibbs measure exhibits a hierarchical nature. That is, the Gibbs measure resembles the structure we have seen in the GREM and CREM, see e.g. Theorem 4.4. It is widely believed, that the structure underlying the Parisi formula should be generic for classical mean field spin glasses. Although there exist similar variational formulas for related models such as the Crisanti-Sommer formula for the spherical p-spin model [55] (rigorously established in [180]), for a huge class of spin glass models such as the Hopfield model or the diluted SK model a similar expression describing the thermodynamics for all temperatures is lacking [181].

2. From the mathematical side, the Parisi formula had remained mysterious for a long time. There was no hope that the replica trick can be made rigorous, so new techniques needed to be invented. But also heuristically, Parisi's formula challenged our mathematical understanding of correlated systems. In particular, in view of Gibbs' variational principle (see Proposition 2.8) it is not very intuitive that the pressure is governed by a minimization instead of a maximization. For a long time, mathematicians only managed to establish partial results, concentrating on the high-temperature phase and qualitative assertions, see e.g. [6]. It was Guerra's work which opened the door towards an understanding of Parisi's formula via interpolating to simpler models. Together with Toninelli, he proved the existence of the limit for convex ξ [100, 101], which had been an open problem till then. Later, he further showed that the Parisi functional $\mathscr{P}_{\xi,h}(\zeta)$ forms a rigorous upper bound [99]. Based on these discoveries, Talagrand managed to prove the Parisi formula for even p by estimating the remainder term in Guerra's interpolating scheme [179]. Meanwhile, Aizenman, Sims and Starr introduced the so-called random overlap structures which translates Guerra interpolation method into the framework of the cavity method [8]. From this perspective, the main ingredient missing to prove Parisi's formula is to show that the limiting Gibbs measure is indeed of hierarchical nature. This was referred to as Parisi ultrametricity conjecture and was solved by Panchenko [151] who used ultrametricity to prove the Parisi formula in the generality of Theorem 5.1 [153].

3. We have presented in (5.4) the most explicit representation of the Parisi functional $\mathscr{P}_{\xi,h}(\zeta)$ for distribution functions ζ consisting of finitely many jumps. As has already been noted by Guerra

[99], the Parisi functional $\mathscr{P}_{\xi,h}(\zeta)$ is Lipschitz-continuous with respect to ζ. More precisely we have

$$|\mathscr{P}_{\xi,h}(\zeta_1) - \mathscr{P}_{\xi,h}(\zeta_2)| \leq \xi''(1) \int_0^1 |\zeta_1(t) - \zeta_2(t)|\, dt.$$

This allows us to extend the Parisi functional to arbitrary ζ, which is important if one wants to address the question of existence and uniqueness of the minimizer in (5.5). However, this line of thought does not reveal an explicit representation of $\mathscr{P}_{\xi,h}(\zeta)$ for continuous distribution functions ζ. Fortunately, there exists an alternative description of the Parisi functional in terms of the so-called Parisi PDE. Namely, the Parisi functional $\mathscr{P}_{\xi,h}(\zeta) = \Upsilon(0,h)$ agrees with the solution $\Upsilon(0,h)$ of the hyperbolic PDE

$$\partial_t \Upsilon = -\frac{\xi''(t)}{2}(\partial_x^2 \Upsilon + \zeta(t)(\partial_x \Upsilon)^2),$$

with boundary condition $\Upsilon(1,x) = \ln\cosh x$. The Parisi PDE has got a unique solution for any distribution function ζ; and one can show via the Cole-Hopf transformation that the solution agrees with (5.4) for a step-function ζ [152].

4. Yet another expression for the Parisi functional was discovered in [16]. Its description requires some knowledge of stochastic analysis, for which we refer to [112]. Let B_t be a Brownian motion, $\mathscr{F}_t$ its canonical filtration and $\mathscr{D} := \{(u_t)_{0\leq t\leq 1} |\, u_t \text{ adapted to } \mathscr{F}_t,\ |u_t| \leq 1\}$ be the set of adapted processes uniformly bounded by 1. The solution of the Parisi PDE is then given by

$$\Upsilon(0,x) = \max_{u\in\mathscr{D}} \left\{ \mathbb{E}\left[\ln\cosh\left(x + \int_0^1 \xi''(s)\zeta(s)u_s\, ds + \int_0^1 \sqrt{\xi''(s)}\, dB_s \right)\right] - \frac{1}{2}\int_0^1 \xi''(s)\zeta(s)\mathbb{E}[u_s^2]\, ds \right\}.$$

This solution enables one to prove that the Parisi functional is strictly convex in ζ and, thus, has a unique maximizer ζ^* [16]. The corresponding measure is the so-called Parisi measure μ^P.

One expects that the Parisi measure μ^P describes the limiting Gibbs distribution such as in Proposition 4.6. That holds true for *generic* mixed p-spin models. Here, we call a model generic if $D = \text{span}\{x^p |\, \beta_p \neq 0\}$, the linear space of all monomials x^p corresponding to a non-vanishing contribution of the p-spin potentials, is dense in the space $C[-1,1]$ of all continuous function with respect to the uniform norm $\|\cdot\|_\infty$.

Theorem 5.2 (Theorem 3.7 and Corollary 3.4 in [152])
Let H_N be a generic mixed p-spin Hamiltonian. Then, the mean Gibbs distribution $\mu^P_{N,\xi,h}(A) := \mathbb{E}[\langle \mathbb{1}_A(R_N(\boldsymbol{\sigma},\boldsymbol{\sigma}'))\rangle_{\xi,h}]$ converges weakly to the Parisi measure $\mu^P_{\xi,h}$, the unique minimizer of the Parisi functional. Moreover, the pressure is differentiable with respect to β_p and the partial derivatives characterize the moments of $\mu^P_{\xi,h}$, i.e.,

$$\frac{\partial p_{Parisi}((\beta_p)_{p\geq 2}, h)}{\partial \beta_p} = \beta_p \left(1 - \int_0^1 q^p\, d\mu^P_{\xi,h}\right).$$

A similar result for non-generic mixed p-spin models is still missing. One should note that $\mu^P_{N,\xi,h} \to \mu^P_{\xi,h}$ cannot hold true for the standard SK model, as the overlap distribution will also have support on $[-1,0)$ by symmetry. At least one has to consider a slightly perturbed model to avoid this problem. It seems to

be very hard to further characterize the Parisi measure $\mu^P_{\xi,h}$ at low temperatures. Most importantly, physicists believe that the Parisi measure should have continuous support at low temperatures, i.e., continuous replica-symmetry breaking should occur just like in the CREM [135]. This conjecture is of practical relevance since Montanari's efficient algorithm for finding approximate ground states in the SK model relies on this expected property of the Parisi measure. However, the best we know in this direction right now is that for low enough temperatures the number of the Parisi measures' support points will exceed any finite number K [18].

After having presented and discussed the Parisi formula, our main goal in the rest of this section is to illustrate the underlying mathematics which ultimately has lead to the proof of Theorem 5.1.

5.1.1 The Aizenman-Sims-Starr Scheme

A very influential idea in the realm of spin glass theory is the so-called *cavity method* [135, 181]. Here, one compares the N-particle system with the Hamiltonian consisting of $N + M$ spins, where we think of N being large and M a comparatively small number. The ansatz is that on one hand adding a few spins should not effect the Gibbs measure too much. On the other hand, by comparing the pressures $\Phi_{N+M} - \Phi_N \simeq Mp$, we still gain information about the limit of the specific pressure p. Let us now discuss this idea in the context of mixed p-spin models. We denote by $\boldsymbol{\sigma} = (\boldsymbol{\alpha}, \hat{\boldsymbol{\sigma}})$ the $N + M$ spin configuration and we consider the pure p-spin potential for different particle numbers

$$\begin{aligned} U_{p,N+M}(\boldsymbol{\sigma}) &= \frac{1}{(N+M)^{(p-1)/2}} \sum_{i_1,\dots,i_p=1}^{N+M} g_{i_1,\dots,i_p}\sigma_{i_1}\cdots\sigma_{i_p} \\ &= \Big(\frac{N}{N+M}\Big)^{(p-1)/2} U_{p,N}(\boldsymbol{\alpha}) + \sum_{j=1}^{M} \eta_{p,j,\boldsymbol{\alpha}}\hat{\sigma}_j + R_p(\hat{\boldsymbol{\sigma}},\boldsymbol{\alpha}). \end{aligned}$$

The first term consists of all contributions which are purely due to the first block $\boldsymbol{\alpha}$, which gives rise to the pure p-potential of N particles rescaled by $\left(\frac{N}{N+M}\right)^{(p-1)/2}$. In the "random field" term $\eta_{p,j,\boldsymbol{\alpha}}$ we collect all terms which contain $\hat{\sigma}_j$ and otherwise just $\boldsymbol{\alpha}$-terms. The remaining contributions with at least two $\hat{\sigma}_i, \hat{\sigma}_j$ are put together in $R_p(\hat{\boldsymbol{\sigma}}, \boldsymbol{\alpha})$. A direct calculation shows that $\mathbb{E}[R_p(\hat{\boldsymbol{\sigma}},\boldsymbol{\alpha})^2] = \mathcal{O}(M^2/N)$ and, thus, for $M \ll N$ the contribution of this term is $o(1)$ by standard interpolation, see Proposition 4.14. In a further step, we note that the covariance process of $U_{p,N}(\boldsymbol{\alpha})$ dominates that of $\left(\frac{N}{N+M}\right)^{(p-1)/2} U_{p,N}(\boldsymbol{\alpha})$ and with some additional independent Gaussian process $k_{p,\boldsymbol{\alpha}}$ we may write

$$U_{p,N}(\boldsymbol{\alpha}) = \Big(\frac{N}{N+M}\Big)^{(p-1)/2} U_{p,N}(\boldsymbol{\alpha}) + \sqrt{M}k_{p,\boldsymbol{\alpha}},$$

the factor $\sqrt{M}$ is chosen such that the process $k_{p,\alpha}$ does (almost) not depend on M. Indeed, $\eta_{p,j,\boldsymbol{\alpha}}$ and $k_{p,\boldsymbol{\alpha}}$ form independent Gaussian processes with covariances

$$\mathbb{E}[\eta_{p,j,\boldsymbol{\alpha}}\eta_{p,j',\boldsymbol{\alpha}'}] \approx \delta_{j,j'} p R_N(\boldsymbol{\alpha},\boldsymbol{\alpha}')^{p-1}, \tag{5.6}$$

$$\mathbb{E}[\kappa_{p,\boldsymbol{\alpha}}\kappa_{p,\boldsymbol{\alpha}'}] \approx (p-1)R_N(\boldsymbol{\alpha},\boldsymbol{\alpha}')^p. \tag{5.7}$$

Both relations follow from a straighforward Taylor expansion. With these preparatory considerations let us now compare the pressure Φ_{N+M} with Φ_N for a general mixed p-spin model. One computes

$$\mathbb{E}[\Phi_{N+M} - \Phi_N] = \mathbb{E}\left[\ln \frac{Z_{N+M}}{Z_N}\right] \approx \mathbb{E}\left[\ln\left(\frac{\sum_{\boldsymbol{\alpha},\hat{\boldsymbol{\sigma}}} e^{H'_N(\boldsymbol{\alpha})} e^{\sum_p \beta_p \sum_{j=1}^M (\eta_{p,j,\boldsymbol{\alpha}}+h)\hat{\sigma}_j}}{\sum_{\boldsymbol{\alpha}} e^{H'_N(\boldsymbol{\alpha})} e^{\sqrt{M}\sum_p \beta_p \kappa_{\boldsymbol{\alpha},p}}}\right)\right]$$
$$= \mathbb{E}\left[\left(\frac{\sum_{\boldsymbol{\alpha},\hat{\boldsymbol{\sigma}}} \omega_{\boldsymbol{\alpha}} e^{\sum_{j=1}^M (\eta_{j,\boldsymbol{\alpha}}+h)\hat{\sigma}_j}}{\sum_{\boldsymbol{\alpha}} \omega_{\boldsymbol{\alpha}} e^{\sqrt{M}\kappa_{\boldsymbol{\alpha}}}}\right)\right] =: A_M. \tag{5.8}$$

$H'_N(\boldsymbol{\alpha})$ contains the common terms of H_N and H_{N+M}, i.e., the external field on $\boldsymbol{\alpha}$ and the rescaled p-potential $\sum_p \beta_p \left(\frac{N}{N+M}\right)^{(p-1)/2} U_{p,N}(\boldsymbol{\alpha})$. The resulting contribution can clearly be expressed in form of random weights $\omega_{\boldsymbol{\alpha}}$ with $\sum_{\boldsymbol{\alpha}} \omega_{\boldsymbol{\alpha}} = 1$. Moreover, we have set $\eta_{j,\boldsymbol{\alpha}} = \sum_p \beta_p \eta_{p,j,\boldsymbol{\alpha}}$ and $\kappa_{\boldsymbol{\alpha}} = \sum_p \beta_p \kappa_{p,\boldsymbol{\alpha}}$. The relations (5.6) and (5.7) yield

$$\mathbb{E}[\eta_{j,\boldsymbol{\alpha}}\eta_{j',\boldsymbol{\alpha}'}] \approx \delta_{j,j'}\xi'(R_N(\boldsymbol{\alpha},\boldsymbol{\alpha}')), \tag{5.9}$$
$$\mathbb{E}[\kappa_{p,\boldsymbol{\alpha}}\kappa_{p,\boldsymbol{\alpha}'}] \approx \theta(R_N(\boldsymbol{\alpha},\boldsymbol{\alpha}')), \tag{5.10}$$

giving a first hint towards the Parisi formula. These cavity computations motivate the following definition:

Definition 5.3 (Definition 1 in [8])
A random overlap structure (ROSt) consists of a collection of random weights $\omega_{\boldsymbol{\alpha}}$ and a random kernel $R_{\boldsymbol{\alpha},\boldsymbol{\alpha}'}$ such that almost surely

1. $\sum_{\boldsymbol{\alpha}} \omega_{\boldsymbol{\alpha}} = 1$,
2. $R_{\boldsymbol{\alpha},\boldsymbol{\alpha}'}$ *defines a positive quadratic form with* $R_{\boldsymbol{\alpha},\boldsymbol{\alpha}} = 1$ *for all* $\boldsymbol{\alpha}$.

We accordingly define for any realization of $R_{\boldsymbol{\alpha},\boldsymbol{\alpha}'}$ independent Gaussian processes $\eta_{j,\boldsymbol{\alpha}}$ and $\kappa_{\boldsymbol{\alpha}}$ which satisfy (5.9) *and* (5.10) *as (strict) identities with R_N replaced by $R_{\boldsymbol{\alpha},\boldsymbol{\alpha}'}$. Moreover, we set A_M as in* (5.8).

The main observation is that the specific pressure can be characterized in terms of ROSts:

Theorem 5.4 (Theorem 1 in [8])
Suppose ξ is a convex function on $[-1,1]$ and $h \geq 0$ We demote by $p(\xi,h)$ the limit of specific pressure of the corresponding mixed p-spin Hamiltonian. Then, we have

$$p(\xi,h) = \lim_{M\to\infty} \frac{1}{M} \inf_{\omega_{\boldsymbol{\alpha}}, R_{\boldsymbol{\alpha},\boldsymbol{\alpha}'} ROSt} A_M(\xi,h,\omega_{\boldsymbol{\alpha}}, R_{\boldsymbol{\alpha},\boldsymbol{\alpha}'}). \tag{5.11}$$

The so-called Aizenman-Sims-Starr scheme provides a variational characterization of the pressure. By the motivational computations from above, the bound

$$p(\xi,h) \geq \limsup_{M\to\infty} \inf_{\omega_{\boldsymbol{\alpha}}, R_{\boldsymbol{\alpha},\boldsymbol{\alpha}'} ROSt} A_M(\xi,h,\omega_{\boldsymbol{\alpha}}, R_{\boldsymbol{\alpha},\boldsymbol{\alpha}'})$$

follows quite easily by choosing the ROSt as in 5.8 which gives a sharp approximation of the actual difference $\mathbb{E}[\Phi_{N+M} - \Phi_N]$. The corresponding upper bound is reminiscent of Guerra's broken replica

symmetry bound [99], but its proof is much more transparent in the ROSt picture. The idea is again a smart interpolation: consider a ROSt $\omega_{\boldsymbol{\alpha}}, R_{\boldsymbol{\alpha},\boldsymbol{\alpha}}$, the family of Hamiltonians

$$H_M(\boldsymbol{\alpha}, \hat{\boldsymbol{\sigma}}, t) := \sqrt{1-t}(U_M(\hat{\boldsymbol{\sigma}}) + \sqrt{M}\kappa_{\boldsymbol{\alpha}}) + \sqrt{t}\sum_{j=1}^{M} \eta_{j,\boldsymbol{\alpha}}\hat{\boldsymbol{\sigma}}_j$$

and a parameterized version of A_M,

$$A_M(t) = \mathbb{E}\left[\ln\left(\frac{\sum_{\boldsymbol{\alpha},\hat{\boldsymbol{\sigma}}} \omega_{\boldsymbol{\alpha}} e^{H_M(\boldsymbol{\alpha},\hat{\boldsymbol{\sigma}},t)}}{\sum_{\boldsymbol{\alpha}} \omega_{\boldsymbol{\alpha}} e^{\sqrt{M}\kappa_{\boldsymbol{\alpha}}}}\right)\right]$$

where we have $A_M(0) = \Phi_M$ and $A_M(1) = A_M$. Using Gaussian interpolation in form of Proposition 4.14 and the convexity of ξ it follows that $\frac{d}{dt}A_M \geq 0$ from which the other bound follows.

5.1.2 Parisi's Formula via Ruelle Cascades

In view of the Aizenman-Sims-Starr scheme, we need to crystallize the ROSt which leads to the Parisi functional (5.4). It turns out that the Ruelle cascades, we encountered in the context of the GREM (see Theorem 4.4), do the job. However, a slightly different description of those processes is more convenient in the context of the SK model – instead of an exponential density we require the underlying Poisson processes to have a fractional density. These "fractional" Ruelle cascades result from the "exponential" Ruelle cascades by a change of density. However, for the reader's convenience and to set the notation, let us briefly describe the construction from scratch.

For a parameter $\xi \in (0,1)$ we denote by Π_ζ the Poisson point process on $(0,\infty)$ with intensity $\zeta x^{-(1+\zeta)}dx$. Let $(u_n)_{n\in\mathbb{N}}$ be the decreasing enumeration of points in Π_ζ and we set the normalized weights

$$\omega_n := \frac{u_n}{\sum_k u_k}.$$

One readily checks that despite having an infinite expectation value, $\sum_k u_k$ is almost surely finite and the process $(\omega_n)_{n\geq 1}$ is well defined and called the *Poisson-Dirichlet process* $PD(\zeta)$. The Poisson-Dirichlet process occurs naturally in the context of random partitions and the description of large prime factors [67, 116]. The processes $(u_n)_{n\geq 1}, (\omega_n)_{n\geq 1}$ enjoy numerous beautiful properties. In the context of Parisi's formula, the identity

$$\mathbb{E}\left[\ln\sum_n u_n X_n\right] = \mathbb{E}\left[\ln\sum_n u_n\right] + \frac{1}{\zeta}\ln\mathbb{E}[X^\zeta] \tag{5.12}$$

is of particular relevance. $(X_n)_{n\in\mathbb{N}}$ consists of i.i.d. copies of a positive random variable X with $\mathbb{E}[X^\zeta] < \infty$ and $(X_n)_{n\in\mathbb{N}}$ shall be independent from the appearing Poisson process.

We now turn to the construction of the r-level Ruelle cascades for some integer $r \geq 1$. The process is indexed by $\mathbb{N}^r$. Ruelle cascades are inherently hierarchic and it is very useful to think of $\mathscr{A} = \mathbb{N}^0 \cup \mathbb{N} \cup \cdots \cup \mathbb{N}^r$ as rooted tree with root $\{\emptyset\}$ and leaves consisting of the sequences of interest in $\mathbb{N}^r$. Very much like in the construction of the Parisi functional, we consider sequences $0 < \zeta_0 < \zeta_1 < \cdots \zeta_{r-1} < \zeta_r = 1$ and $0 = q_0 < q_1 < \cdots < q_r = 1$. For each interior vertex $\boldsymbol{\alpha} \in \mathscr{A} \setminus \mathbb{N}^r$ we set a Poisson process $\Pi_{\boldsymbol{\alpha}} = \Pi_{\zeta_{|\boldsymbol{\alpha}|}}$, where $|\boldsymbol{\alpha}|$ denotes the number of entries of $\boldsymbol{\alpha}$. All processes shall be mutually independent and consist of

points $u_{\boldsymbol{\alpha}1} > u_{\boldsymbol{\alpha}2} > \cdots$. Note that the indices $\boldsymbol{\alpha}k$ can again be interpreted as vertices of $\mathscr{A}$. For each leave $\boldsymbol{\alpha} \in \mathbb{N}^r$ we introduce the process $v_{\boldsymbol{\alpha}}$ and the normalized weights $\omega_{\boldsymbol{\alpha}}$,

$$v_{\boldsymbol{\alpha}} = u_{\alpha_1} u_{\alpha_1\alpha_2} \cdots u_{\alpha_1\ldots\alpha_n}, \qquad \omega_{\boldsymbol{\alpha}} = \frac{v_{\boldsymbol{\alpha}}}{\sum_{\boldsymbol{\alpha}\in\mathbb{N}^r} v_{\boldsymbol{\alpha}}}. \tag{5.13}$$

As the notation suggests, $\omega_{\boldsymbol{\alpha}}$ are the weights we want to use in the desired ROSt. It remains to prescribe the overlap kernel $R_{\boldsymbol{\alpha},\boldsymbol{\alpha}'}$. An instructive observation is that defining $R_{\boldsymbol{\alpha},\boldsymbol{\alpha}'} = \langle h_{\boldsymbol{\alpha}}, h_{\boldsymbol{\alpha}'}\rangle$ with the help of some vectors $h_{\boldsymbol{\alpha}}$ guarantees positivity of the overlap matrix. To this end, let $\mathcal{H}$ be an infinite dimensional Hilbert space and $(e_{\boldsymbol{\alpha}})_{\boldsymbol{\alpha}\in\mathscr{A}}$ a collection of orthonormal vectors in $\mathcal{H}$. We set

$$h_{\boldsymbol{\alpha}} = \sum_{k=1}^{r} e_{\alpha_1\ldots\alpha_k}(q_k - q_{k-1})^{1/2}, \tag{5.14}$$

and $R_{\boldsymbol{\alpha},\boldsymbol{\alpha}'} = \langle h_{\boldsymbol{\alpha}}, h_{\boldsymbol{\alpha}'}\rangle$. The overlap structure is ultrametric as the overlap only depends on the shared vertices in the paths from the root to $\boldsymbol{\alpha}$ and $\boldsymbol{\alpha}'$. We have completed the construction of the needed ROSt. An iterative use of (5.12) now implies the following representation of the Parisi functional:

Proposition 5.5 (Lemma 3.1 in [152])
Let ζ be a distribution function of a measure with finite support and $\omega_{\boldsymbol{\alpha}}, R_{\boldsymbol{\alpha},\boldsymbol{\alpha}'}$ the corresponding ROSt from above. Then, the Parisi functional can be written as

$$\mathscr{P}_{\xi,h}(\zeta) = \mathbb{E}\left[\ln\left(2\sum_{\boldsymbol{\alpha}\in\mathbb{N}^r}\omega_{\boldsymbol{\alpha}}\cosh\eta_{\boldsymbol{\alpha}}\right)\right] - \mathbb{E}\left[\ln\left(\sum_{\boldsymbol{\alpha}\in\mathbb{N}^r}\omega_{\boldsymbol{\alpha}}\exp\kappa_{\boldsymbol{\alpha}}\right)\right]. \tag{5.15}$$

Comparing the right-hand side of (5.15) with (5.8), shows that $\mathscr{P}_{\xi,h}(\zeta) = A_1(\xi, h, \omega_{\boldsymbol{\alpha}}, R_{\boldsymbol{\alpha},\boldsymbol{\alpha}'})$ with the notation from the last section. The seemingly obscure iterative construction of $\mathscr{P}_{\xi,h}(\zeta)$ becomes natural within the cavity method, using Ruelle cascades as ansatz for the limiting Gibbs measure. Let us remark that by copying the Ruelle cascades M times, we can relate $\mathscr{P}_{\xi,h}(\zeta)$ to A_M, and in particular from Theorem 5.4 it follows that $p(\xi, h) \leq \mathscr{P}_{\xi,h}(\zeta)$. This establishes the easier half of the Parisi formula.

5.1.3 Ghirlanda-Guerra Identities and Ultrametricity

We have already seen how the Parisi functional arises as an upper bound for the pressure. In this section, we close the discussion of the Parisi formula by explaining what ideas are used to show that $\inf_\zeta \mathscr{P}_{\xi,h}(\zeta)$ agrees with the specific pressure in the thermodynamic limit. To this end, we recall that in our discussion of the Aizenman-Starr-Sims scheme, it turned out that the ROSt saturating (5.11) corresponds to the Gibbs measure of the p-spin Hamiltonian for high particle number N. To put it in other words, one needs to show that the limiting Gibbs distribution of $R_N(\boldsymbol{\sigma}, \boldsymbol{\sigma}')$ can be well approximated by Ruelle cascades because exactly those ROSt give rise to the Parisi functional. As we will see, the originally by Parisi proclaimed hierarchical reorganization of the replicas plays major role.

The foundation of the following argument lies in Ghirlanda-Guerra relations, which were originally discovered in the SK model [94] and relate expression of $n + 1$ multioverlaps to the distribution of just n replicas. Let us consider the Ghirlanda-Guerra relations in a general framework:

Definition 5.6 ([94], [152])
Let G be a random measure on a separable Hilbert space $\mathcal{H}$ and $(h_l)_l$ an i.i.d. sample of vectors distributed according to G. Let us denote by $\langle\cdot\rangle$ the average with respect to the infinite product measure $G^{\otimes\infty}$ and by $Q_{l,l'} = \langle h_l, h_{l'}\rangle$ the overlaps. We say that G satisfies the Ghirlanda-Guerra identities if for any $n \geq 1$ and any bounded measurable functions $f = f((Q_{l,l'})_{l\neq l'\leq n})$ and $g : \mathbb{R} \to \mathbb{R}$, we have

$$\mathbb{E}[\langle f g(Q_{1,n+1})\rangle] = \frac{1}{n}\mathbb{E}[\langle f\rangle]\mathbb{E}[\langle g(Q_{1,2})\rangle] + \frac{1}{n}\sum_{l=2}^{n}\mathbb{E}[\langle f g(Q_{1,l})\rangle]. \tag{5.16}$$

As mentioned before, the power of Ghirlanda-Guerra identities lies in relating a function of $n+1$ overlaps to just n overlaps. This restrictive property (5.16) will be only satisfied by very few random measures. The prime example are the Ruelle cascades from the section before: with the weights $\omega_{\boldsymbol{\alpha}}$ from (5.13) and the vectors $h_{\boldsymbol{\alpha}}$ from (5.14) we set $G(\{h_{\boldsymbol{\alpha}}\}) = \omega_{\boldsymbol{\alpha}}$. A rather long computation, making use of the underlying Poissonian structure, shows that measure G satisfies the Ghirlanda-Guerra identities [152, Theorem 2.10]. An important consequence is that we obtain all moments of the overlaps in this setting,

$$\mathbb{E}[\langle Q_{1,2}^n\rangle] = \sum_{m=1}^{r} q_m^n(\zeta_m - \zeta_{m-1}),$$

which justifies to think of ζ as the distribution of the overlap.
Obviously, the Ghirlanda-Guerra identities are stable under weak convergence. In particular, if we take a sequence of discrete distribution functions such that $\zeta_n \to \zeta$ converges weakly, then the distribution of the multioverlaps $(Q_{l,l'})$ converges weakly, too, and the limiting distribution can be generated by random measure G on a Hilbert space. This follows from the Dovbysh-Sudakov representation theorem [152, Theorem 1.10]. One can think of this measure as a continuous Ruelle cascade, where the single overlap $Q_{1,2}$ follows the distribution determined by ζ. We remark that after embedding the CREM replica overlap into a Hilbert space, the resulting limiting Gibbs measure is exactly of this type.
Surprisingly, we have already presented all random measures which satisfy Ghirlanda-Guerra identities:

Theorem 5.7 ([151], Theorem 2.13 in [152])
If a measure G satisfies the Ghirlanda-Guerra identities, the distribution of the whole overlap array $(Q_{l,L'})_{l,l'\geq 1}$ is uniquely determined by the distribution of $Q_{1,2}$ under $\mathbb{E}G^{\otimes 2}$. Moreover, the overlap $Q_{1,2}$ takes almost surely no negative values.

We stress that Theorem 5.7 says that the averaged (!) distribution of two replicas already determines the complete disordered distribution of arbitrarily many overlaps. This is a very far reaching result as it tells us that the continuous Ruelle cascades are the only random measures which possibly can satisfy Ghirlanda-Guerra identities. That the overlap $Q_{1,2}$ only takes positive value under Ghirlanda-Guerra relations, is known as Talagrand's positivity principle. Note that if we establish Ghirlanda-Guerra identities, the positivity allows us to relax the convexity condition on ξ from the previous discussion (e.g. in Theorem 5.4) to only hold on $[0, \infty)$, which covers the odd p-powers as well.
The proof of Theorem 5.7 relies on a very deep fact, namely that the Ghirlanda-Guerra identities imply an ultrametric overlap structure. This was known as Parisi's ultrametricity conjecture and its proof by Panchenko confirmed Parisi's intuition on the hierarchical reorganization of the overlaps.

Theorem 5.8 ([151], Theorem 2.14 in [152])
Suppose that the random measure G satisfies the Ghirlanda-Guerra identities. Then, the overlap array $(Q_{l,l'})_{l,l'\geq 1}$ is ultrametric, i.e.,

$$\mathbb{E}[\langle \mathbb{1}_{Q_{1,2}\geq \min\{Q_{1,3},Q_{2,3}\}}\rangle] = 1.$$

Ultrametricity is a very restrictive property and combining it again with the Ghirlanda-Guerra identities, it allows one to determine iteratively the whole distribution of the overlap array $Q_{l,l'}$. Panchenko's proof of Theorem 5.8 relies on an involved argument making use of invariance properties resulting from the Ghirlanda-Guerra identities.

Let us comment on how the Ghirlanda-Guerra identities appear in the context of mixed p-spin Hamiltonians. One can show that for generic models the Ghirlanda-Guerra identities hold true in the thermodynamic limit [152, Corollary 3.2]. Unfortunately, this is not always true and the SK model forms a counterexample: the $\boldsymbol{\sigma} \to -\boldsymbol{\sigma}$ symmetry is in conflict with the positivity of the overlap following from the Ghirlanda-Guerra identities. The idea is to perturb the original Hamiltonian by an independent generic one to enforce the validity of the Ghirlanda-Guerra identities. The perturbation should be weak enough such that the specific pressure is not effected in the thermodynamic limit. So, let H_N be the mixed p-spin Hamiltonian of interest and let us consider for $x_p \in [0,3]$ and $s_N \geq 0$ the perturbed Hamiltonian

$$H'_{N,(x_p)_p,s_N}(\boldsymbol{\sigma}) := H_N(\boldsymbol{\sigma}) + s_N \sum_{p\geq 2} 2^{-p} x_p U_p(\boldsymbol{\sigma}).$$

Let $(\boldsymbol{\sigma}^l)_{l\geq 1}$ be i.i.d. replicas sampled with respect to the Gibbs measure of H'_N and $R_{l,l'} := R_N(\boldsymbol{\sigma}^l, \boldsymbol{\sigma}^{l'})$ be the corresponding replica overlaps. Let us further introduce, for $n, m \geq 1$ and a function f of the replica overlaps $(R_{l,l'})_{l,l'\leq n}$, the function $\Delta(f,n,m)$,

$$\Delta(f,n,m) := \left| \mathbb{E}[\langle f\, R^m_{1,n+1}\rangle] - \frac{1}{n}\mathbb{E}[\langle f\rangle]\mathbb{E}[\langle R^m_{1,2}\rangle] - \frac{1}{n}\sum_{l=2}^{n} \mathbb{E}[\langle f\, R^m_{1,l}\rangle] \right|,$$

measuring the validity of the Ghirlanda-Guerra identities. The mixed p-spin Hamiltonian satisfies the Ghirlanda-Guerra identities at least in average:

Theorem 5.9 ([94],Theorem 3.2 in [152])
Let $s_N = N^\gamma$ with $-1/4 < \gamma < 0$. Then, the limit of the specific pressure agrees for H_N and H'_N and we have for any natural numbers n, m and any measurable overlap function $f : (R_{l,l'})_{l,l'\leq n} \to \mathbb{R}$

$$\lim_{N\to\infty} \mathbb{E}_x[\Delta(f,n,m)] = 0,$$

where the expectation $\mathbb{E}_x$ is understood with respect to the uniform choice $x_p \in [0,3]$.

This weaker form of the Ghirlanda-Guerra identities is enough to establish the Parisi formula. After having demonstrated the main concepts in the realm of the classical SK model, we now turn to the Quantum SK (QSK) model.

5.2 The Quantum Sherrington-Kirkpatrick Model

Just like the SK model has been a prime example for mean-field spin glasses, one expects that the analysis of the QSK model reveals the universal structure underlying transversal field spin glass models. We recall that the QSK Hamiltonian is given by

$$H_N = U + \Gamma T$$

with the SK potential U from (1.5). Not surprisingly, the QSK model has received much attention in the physics literature. Its investigation started in the 1980s using numerical methods and non-rigorous replica computations [78, 96, 139, 189, 192, 193] and is still ongoing due to its importance in the context of quantum adiabatic algorithms [10, 22, 24, 45, 68, 77, 117] and in the study of ergodicity in disordered quantum models [23, 121, 138, 158, 172]. Despite numerous efforts, the physics of the QSK is not well understood and in fact there exist contradicting predictions in the literature, in particular when it comes to numerical values of transition points. The numerics is very challenging and exact diagonalization can only be applied up to $N \approx 20$. Analytic methods on the other hand start typically from oversimplifying assumptions such as the static approximation in the path integral framework, which by now is known to be wrong even in the high-temperature region [126]. Therefore, one has to be careful with the interpretation of the physical results. Nevertheless, it appears to be consensus that there exists a glass phase for $\beta > 1$ and Γ small enough and glass order vanishes for stronger magnetic fields or higher temperatures (see also Figure 5.1). In particular, a quantum phase transition for the ground state $\beta = \infty$ is expected. However, an understanding of the model which is comparable to Parisi's picture in the classical SK model is currently not available, even on a heuristic level. Subsequent question which are caused by the quantum nature such as localization properties of eigenstates seem to be inaccessible with the existing methods.

The discussed limitations of the physical treatment call for a rigorous mathematical study which reveals the underlying structure of the QSK and eventually leads to clear picture of quantum spin glasses. Unfortunately, the QSK is a challenging model and so far only very few results have been established from the mathematical side. Quantum spin glasses have been approached via random matrix methods, e.g. in [72]. This bulk analysis reveals interesting phase transitions for the density of states. However, one should recall that most eigenvalues are of order $\mathcal{O}(\sqrt{N})$ and, thus, those methods do not allow any conclusion on the states of extensive energies governing the thermodynamics. As far as we know, the first study of the QSK pressure goes back to Crawford [53]. Here, in the first part the problem of universality is addressed. It is shown, by extending the argument of Carmona and Hu for the classical SK model [48], that the pressure Φ_N is on leading order not affected if the Gaussians couplings $g_{i,j}$ defining the SK potential are replaced by i.i.d. random variables $z_{i,j}$ with $\mathbb{E}[z_{i,j}] = 0, \mathbb{E}[z_{i,j}^2] = 1$ and $\mathbb{E}[|z_{i,j}|^3] < \infty$. In the second part, Crawford claims to prove the existence of the limit $\lim_{N\to\infty} \frac{1}{N}\Phi_N$ by modifying the classical argument of Guerra and Toninelli [100, 101], however the proof contains an error which is apparently not easy to fix.

More recently, there have been two works which make an important step towards a better understanding of the QSK [3, 126]. We will present their main results in the following two subsections. Then, Section 5.3 deals with our article [125] which establishes the existence of a glass phase in the QSK.

5.2.1 An Infinite-Dimensional Parisi Formula

Adhikari and Brennecke prove a Parisi-type formula for the specific pressure in the QSK model [3], building up on Panchenko's general result on vector spin glasses [154]. We will see similarities with the classical Parisi formula for mixed p-spin formulas but the resulting variational expression is even more involved. To present the result, we need to introduce some notation. We first recall the path integral representation from (2.5),

$$Z_N(\beta,\Gamma) = \operatorname{Tr} e^{-\beta H} = (\cosh \beta\Gamma)^N \sum_{\boldsymbol{\sigma}\in\mathcal{Q}_N} \int_{\Xi^N} d\nu_0^N e^{-\beta \int_0^1 U(\boldsymbol{\sigma}\cdot\xi(t))\,dt}$$

with the notation from Theorem 2.6 and the SK potential U. We embed the the space of càdlàg paths Ξ into $L^2([0,1])$ and ν_0 has only support on the paths ξ with $\|\xi\|_2 = 1$ (ξ denotes here paths and should not be confused with the function ξ from Section 5.1). To lighten notation, we write $\boldsymbol{\sigma}(t) := \boldsymbol{\sigma}\cdot\xi(t)$ in the following. The role of the replica overlap is now taken by the path overlap

$$Q(\boldsymbol{\sigma},\boldsymbol{\sigma}')(t,t') := \frac{1}{N}\sum_{i=1}^N \sigma_i(t)\sigma_i'(t'), \tag{5.17}$$

which measures the replica overlap of two path configurations at times t and t'. Writing $\sum_{i=1}^N \sigma_i(t)\sigma_i'(t') = \sum_{i=1}^N |\sigma_i\rangle\langle\sigma_i'|(t,t')$, the path overlap (5.17) can be understood as kernel of an operator-valued map from $L^2([0,1]^N\times[0,1]^N)$ to the set of trace-class operators $\mathcal{J}_1$ on $L^2([0,1])$. We note that the covariance process of the path-integrated potential

$$\mathbb{E}\left[\int_0^1 U(\boldsymbol{\sigma}(t))\,dt \int_0^1 U(\boldsymbol{\sigma}'(t'))\,dt'\right] = N\|Q(\boldsymbol{\sigma},\boldsymbol{\sigma}')\|_{\mathrm{HS}}^2 \tag{5.18}$$

is governed by the Hilbert-Schmidt-norm of Q and, thus, the path overlap is indeed the analog of the replica overlap in the classical SK model. In contrast to the classical setting where $R_N(\boldsymbol{\sigma},\boldsymbol{\sigma}) \equiv 1$, the so-called self-overlap

$$R(\boldsymbol{\sigma})(t,t') := Q(\boldsymbol{\sigma},\boldsymbol{\sigma})(t,t')$$

is not fixed, which is a major difference which already arises in the study of finite-dimensional spin glasses. $R(\boldsymbol{\sigma})(t,t')$ gives similarly rise to an operator-valued map whose range is contained in the set

$$\Gamma = \{\rho\in\mathcal{J}_1 | 0\le\rho\le\mathbb{1}\}$$

with the standard partial order for self-adjoint operators. The main idea behind Panchenko's result on vector spin glasses is that one should first fix the self-overlap and then the constrained pressure is again given by a Parisi-type functional. In the setting of paths, we fix a self overlap ρ and consider the set of discrete monotone paths $\zeta\in\Pi_\rho$ with $\zeta(0)=0$ and $\zeta(1)=\rho$. That is, there exist times $0=m_0<m_1<\cdots<m_{r-1}<m_r=1$ and operators $0=\zeta_0<\zeta_1<\cdots<\zeta_r=\rho$ such that $\zeta(t)=\zeta_k$ for $m_{k-1}<t\le m_k$ and $k=1,\dots,r$. Such a discrete path is equipped with independent centered Gaussian

processes $X_k = (X_k(t))_{0\le t\le 1}$ with covariance $\mathbb{E}[X_k(t)X_k(t')] = (\zeta_k - \zeta_{k-1})(t,t')$ for $k = 1,\dots,r$. Let further $\lambda \in \mathcal{L}_s$ be a bounded self-adjoint operator and we define the random variables Y_k inductively via

$$\begin{aligned} Y_r &= \ln \int_\Xi d\nu_0 \exp\left(\sum_{j=1}^r \int_0^1 \beta\xi(t)X_j(t) + \operatorname{Tr}\lambda|\xi\rangle\langle\xi|\right) \\ Y_k &= \frac{1}{m_k}\ln \mathbb{E}_{k+1}[\exp(m_k Y_{k+1})] \end{aligned}$$

where $\mathbb{E}_{k+1}$ is the expectation with respect to the randomness of X_{k+1}. Here λ can be understood as Lagrange parameter, which fixes the self-overlap to be ρ. The Parisi functional is then given by

$$\mathscr{P}(\rho,\zeta,\lambda,\beta,\Gamma) := Y_0 + \frac{\beta^2}{4}\left(\int_0^1 \|\zeta(t)\|_{\mathrm{HS}}^2\, dt - \|\rho\|_{\mathrm{HS}}^2\right) - \operatorname{Tr}\lambda\rho.$$

A straight-forward interpolation argument shows that the Parisi functional $\mathscr{P}(\rho,\zeta,\lambda,\beta,\Gamma)$ is Lipschitz-continuous in ζ and, thus, can be extended to continuous paths ζ [3, Lemma A.1]. We note the dependence on Γ which is hidden in the path measure ν_0. To make use of the Parisi formula for vector spin glasses, one considers the d-dimensional subspace $\mathcal{V}_d$ of $L^2([0,1])$ generated by the first d elements of the Fourier basis e_k with $e_1 \equiv 1$, $e_{2k} = \sqrt{2}\sin(2\pi kt)$ and $e_{2k+1}(t) = \sqrt{2}\cos(2\pi kt)$. With the orthogonal projector P_d onto $\mathcal{V}_d$, one sets

$$\Gamma^d := P_d\Gamma P_d \qquad \mathcal{L}_s^d := P_d\mathcal{L}_s P_d,$$

and the action of P_d is understood element wise. We are now ready to state the Parisi formula

Theorem 5.10 (Theorem 2.1 in [3])
For any $\beta,\Gamma \ge 0$, we have the Parisi-type formula for the quenched pressure $\Phi_N(\beta,\Gamma)$

$$\lim_{N\to\infty}\frac{1}{N}\mathbb{E}[\Phi_N(\beta,\Gamma)] = \ln(2\cosh(\beta\Gamma)) + \lim_{d\to\infty}\sup_{\rho\in\Gamma^d}\left[\inf_{\zeta\in\Pi_\rho,\lambda\in\mathcal{L}_s^d}\mathscr{P}(\rho,\zeta,\lambda,\beta,\Gamma)\right]. \tag{5.19}$$

The proof in [3] implicitly shows the existence of the limit on the right-hand side of (5.19) and, thus, in particular the existence of the limit of the specific pressure in the QSK model. Of course, by Gaussian concentration, see Proposition 2.4, the specific pressure converges also almost surely. Most likely, the right-hand side of (5.19) can be replaced by $\sup_{\rho\in\Gamma}\left[\inf_{\zeta\in\Pi_\rho,\lambda\in\mathcal{L}_s}\mathscr{P}(\rho,\zeta,\lambda,\Gamma)\right]$. The appearance of the $d\to\infty$ limit is due to the proof technique which heavily relies on Panchenko's result for finite dimensional vector spin glasses [154]. The main new insight is that since the Poisson process typically does not jump too many times, it can be approximated very well by a few Fourier basis elements. To make this idea precise, the interpolation machinery is used, which requires considerable work. Evidently, the formula (5.19) is very involved. Future will tell if one can deduce physical properties of the QSK from Theorem 5.10.

5.2.2 The High Temperature Phase: Annealed Pressure and Absence of Glass Order

The paper [126] mainly studies the QSK model in the high-temperature phase $\beta < 1$. We recall that in the classical setting ($\Gamma = 0$) the high temperature phase of the SK model is characterized by an asymptotic equality of the specific quenched pressure $\mathbb{E}\frac{1}{N}\ln Z_N(\beta)$ and annealed pressure $\frac{1}{N}\ln \mathbb{E}Z_N(\beta)$. This moti-

vates the analysis of the annealed pressure in the QSK. In contrast to the SK model, where the annealed pressure is simply given by $\frac{\beta^2}{4}$, in the QSK there is no such elementary expression. Nevertheless, one may give a variational formula for the annealed pressure. Using again the path-integral framework, we note that

$$\mathbb{E}[Z_N(\beta,\Gamma)] = (2\cosh(\beta\Gamma))^N \int_{\Xi^N} d\nu_0^N \exp\left(\frac{\beta^2}{4}\left(N\int_0^1\int_0^1 Q^2(\xi,\xi)(t,t')dt\,dt' - 1\right)\right), \tag{5.20}$$

where we used that every initial spin $\boldsymbol{\sigma} \in \mathcal{Q}_N$ contributes the same in expectation and the term in the exponential follows by the known exponential moment of a Gaussian random variable and the covariance (5.18). To further analyze (5.20), one needs to understand the probability distribution of the path overlap $Q(\xi,\xi)(t,t')$ under the Poissonian path measure ν_0^N. To this end, large deviation theory is a convenient tool. For $\beta,\Gamma \geq 0$ and $\psi \in L^2([0,1]^2)$ we introduce the cumulant generating function

$$\Lambda_{\beta,\Gamma}(\psi) := \ln\left(\int_\Xi d\nu_0 \exp\left(\int_0^1\int_0^1 \psi(t,t')\xi(t)\xi(t')dt\,dt'\right)\right) \tag{5.21}$$

Note that ξ in (5.21) consists only of one component. The function $\Lambda_{\beta,\Gamma}(\psi)$ probes the probability of the overlap Q being close to ψ. The functional Λ enjoys numerous useful properties: it is a 1-Lipschitz function and convex in ψ and its functional derivative $\Lambda'(\psi)$ is also 1-Lipschitz and given by

$$\Lambda'_{\beta,\Gamma}(\psi)(s,s') = e^{-\Lambda_{\beta,\Gamma}(\psi)}\int_\Xi d\nu_0\ \xi(s)\xi(s')\exp\left(\int_0^1\int_0^1 \psi(t,t')\xi(t)\xi(t')dt\,dt'\right),$$

i.e., $\frac{d}{da}\Lambda_{\beta,\Gamma}(\psi + a\varphi)|_{a=0} = \langle \Lambda'_{\beta,\Gamma}(\psi), \varphi\rangle$ [126, Lemma 4.1]. The rate function of the path overlap is then governed by the Legendre transform $\Lambda^* : L^2([0,1]^2) \to \mathbb{R}\cup\{\infty\}$,

$$\Lambda^*_{\beta,\Gamma}(\varphi) := \sup_{\psi\in L^2([0,1]^2)} (\langle\psi,\varphi\rangle - \Lambda(\psi)).$$

One observes that if $\Lambda^*_{\beta,\Gamma}(\varphi) < \infty$, then $|\varphi| \leq 1$ and $\langle 1,\varphi\rangle > 0$. An infinite-dimensional version of the well-known Varadhan lemma yields [60]:

Theorem 5.11 (Theorem 3.1 and Theorem 4.3 in [126])
For any $\beta,\Gamma \geq 0$, the specific annealed pressure converges and we have the formula

$$\lim_{N\to\infty}\frac{1}{N}\ln(\mathbb{E}[Z_N(\beta,\Gamma)]) = \ln(2\cosh(\beta\Gamma)) + \sup_{\psi\in L^2([0,1]^2)}(\Lambda_{\beta,\Gamma}(\psi) - \beta^{-2}\langle\psi,\psi\rangle) \tag{5.22}$$

$$= \ln(2\cosh(\beta\Gamma)) + \sup_{\varphi\in L^2([0,1]^2)}\left(\frac{\beta^2}{4}\langle\varphi,\varphi\rangle - \Lambda^*_{\beta,\Gamma}(\varphi)\right). \tag{5.23}$$

Both suprema in (5.22) *are attained at some ψ and φ and a maximizing ψ satisfies the Euler-Lagrange equation $\psi = \frac{\beta^2}{2}\Lambda'_{\beta,\Gamma}(\psi)$.*

Unfortunately, the maximizer in (5.22) is not known. However, in the weak disorder limit, i.e., if $\beta\Gamma$ is kept constant and $\beta \to 0$, the maximizer ψ resembles the function $\frac{\beta^2}{2}\mu(t,t')$ with

$$\mu(t,t') := \frac{\cosh(\beta\Gamma(1-2|t-t'|))}{\cosh(\beta\Gamma)},$$

which is simply the path overlap one obtains for the pure paramagnetic Hamiltonian $\beta\Gamma$. This allows one to compute the second-order Taylor expansion in β for weak disorder [126, Theorem 5.3]. Most interestingly, one concludes from these computations that the among physicists popular static approximation [177, 189, 192], where on assumes that the maximizer $\psi \equiv c$ agrees with a constant c, is wrong even in the high temperature phase.

Let us briefly mention how Theorem 5.11 is related to the Parisi-type result (5.19). The following derivation is not intended to be a formal argument, but a rigorous proof should not be too difficult either. To this end, we consider the Parisi functional $\mathscr{P}(\rho,\zeta,\lambda,\beta,\Gamma)$ for the path $\zeta_{\mathrm{RS}}(t) = \rho\mathbb{1}_{\{1\}}(t)$. This path may be interpreted as "replica-symmetric" situation since the path-overlap takes with probability 1 the value of the self-overlap ρ. We obtain with a Hilbert-Schmidt Lagrange multiplier λ the simpler expression

$$\mathscr{P}(\rho,\zeta_{\mathrm{RS}},\lambda,\beta,\Gamma) = \ln\left(\int_\Xi d\nu_0 \exp\left(\frac{\beta^2}{2}\int_0^1\int_0^1 \rho(t,t')\xi(t)\xi(t')dt\,dt' + \int_0^1\int_0^1 \lambda(t,t')\xi(t)\xi(t')dt\,dt'\right)\right)$$

$$\begin{aligned}&- \frac{\beta^2}{4}\|\rho\|_{\mathrm{HS}}^2 - \int_0^1\int_0^1 \lambda(t,t')\rho(t,t')dt\,dt' \\ &= \Lambda(\beta^2\rho/2+\lambda) - \langle\rho,\lambda\rangle - \frac{\beta^2}{4}\langle\rho,\rho\rangle.\end{aligned}$$

We have used that Y_0 is up to the translation by λ simply the exponential moment of the Gaussian X_1 with covariance ρ. Now, we note that if we take the infimum with respect to $\lambda(t,t') \in L^2$ we obtain

$$\inf_{\lambda\in L^2} \mathscr{P}(\rho,\zeta_{\mathrm{RS}},\lambda,\beta,\Gamma) = -\Lambda^*_{\beta,\Gamma}(\rho) + \frac{\beta^2}{4}\langle\rho,\rho\rangle.$$

Taking the supremum with respect to ρ, we end up with the variational expression (5.23). This should answer the question risen in [126] on how these both formulae relate to each other. In some sense, the annealed pressure optimizes solely the self-overlap and is not affected by replica symmetry breaking. This resembles the classical situation. Conceptually, if annealed and quenched pressure agree, we should have no replica symmetry breaking. On the other hand, the optimizer in (5.19) can be of replica-symmetric nature, while quenched and annealed pressure do not coincide. The reason for that is that the optimal self-overlap from Theorem 5.11 might lead to a broken solution in (5.19) while the whole system chooses another self-overlap whose minimizing Parisi (overlap) measure is trivial. This explains why in [126, Theorem 2.4] a difference between annealed and quenched pressure is observed for low temperatures and strong magnetic fields although for these parameters no spin glass order is expected.

The second main result in [126] is that annealed and quenched pressure agree for $\beta < 1$, just like in the classical SK model.

Theorem 5.12 (Theorem 6.3 in [126])
For $\beta < 1$ and any $\Gamma \geq 0$, annealed and quenched pressure agree, i.e.,

$$\lim_{N\to\infty} \frac{1}{N} \ln \mathbb{E}[Z_N(\beta,\Gamma)] = \lim_{N\to\infty} \frac{1}{N} \mathbb{E}[\ln Z_N(\beta,\Gamma)].$$

Theorem 5.12 is derived by adapting the corresponding proof for the classical model [6]. The main idea is to apply the so-called second moment method. Suppose one has shown that $\mathbb{E}[Z_N^2] \leq c\mathbb{E}[Z_N]^2$ for some absolute constant $c > 0$. The idea is then to invoke the Payley-Zygmund inequality [112]

$$\mathbb{P}(Z_N \geq x\mathbb{E}[Z_N]) \geq (1-x)^2 \frac{\mathbb{E}[Z_N]^2}{\mathbb{E}[Z_N^2]} \geq \frac{(1-x)^2}{c}$$

for $0 < x < 1$, which guarantees that Z_N is of the same order as $\mathbb{E}[Z_N]$ with a nonvanishing probability. Recalling that by Gaussian concentration $\frac{1}{N} \ln Z_N$ concentrates around its mean, by the above $\frac{1}{N}\mathbb{E}[\ln Z_N] \approx \frac{1}{N} \ln \mathbb{E}[Z_N]$. That is, to prove Theorem 5.12 it is enough to show $\mathbb{E}[Z_N^2] \leq c\mathbb{E}[Z_N]^2$. To arrive at such a bound, one notes that Z_N^2 coincides with the partition function of a a duplicated system. Making use of the path-integral framework and Gaussian linearization the claim follows after a little computation [126, Lemma 6.1].

In the classical SK model there is no glass order for $\beta < 1$, i.e., the distribution of the replica overlap R_N under the Gibbs measure concentrates around 0. To establish the absence of glass order in the quantum setting, one similarly needs to show that distribution of under the (duplicated) Gibbs density matrix $\rho_{\beta,\Gamma}^{\otimes 2}$ with $\rho_{\beta,\Gamma} := e^{\beta H}/Z_N(\beta,\Gamma)$ is trivial. Theorem 5.12 – or to be more precise the computation leading to the second moment estimate $\mathbb{E}[Z_N^2] \leq c\mathbb{E}[Z_N]^2$ – has the following important consequence:

Corollary 5.13 (Corollary 6.3 in [126])
For $\beta < 1$ and any $\Gamma \geq 0$, we have

$$\lim_{N\to\infty} \mathbb{E}\left[\mathrm{Tr}\,\left(\rho_{\beta,\Gamma}^{\otimes 2} R_N^2(\boldsymbol{\sigma},\boldsymbol{\sigma}')\right)\right] = 0. \tag{5.24}$$

Of course, (5.24) implies that the replica overlap concentrates around 0 in the thermodynamical limit. The complementary problem, namely establishing glass order for lower temperatures, is the main topic of the next section.

5.3 Existence of the Glass Phase

In order to be consistent with the work [125], in this section we write for the QSK Hamiltonian acting on $\ell^2(\mathcal{Q}_N)$

$$H_N := J\,U + bT$$

with parameters $J > 0, b \geq 0$ and $U = U_{\mathrm{SK}}$ is the SK potential. Of course, the additional parameter J does not reveal any new physics as its always equivalent to a model with $J = 1$ and a different temperature and field strength. As usual, the thermal average of some observable A with respect to H_N at some temperature $\beta > 0$ will be denoted by $\langle A\rangle_{\beta J,\beta b} := \mathrm{Tr}\, Ae^{-\beta H}/\mathrm{Tr}\, e^{-\beta H}$. If A acts on two replicas, $\langle\cdot\rangle_{\beta J,\beta b}^{\otimes 2}$

is understood as average with respect to independently drawn copies of the original system. We will measure spin-glass order with the help of the Edwards-Anderson parameter q_{EA},

$$q_{\mathrm{EA}} := \frac{2}{N(N-1)} \sum_{1\leq j<k\leq N} \langle S_j^z S_k^z \rangle_{\beta J,\beta b}^2 = \frac{N}{N-1} \langle R_N^2 \rangle_{\beta J,\beta b}^{\otimes 2} - \frac{1}{N-1}, \tag{5.25}$$

where the second identity is immediate from the operator identity $R_N := N^{-1} \sum_{j=1}^N S_j^z \otimes S_j^z$. We already know that for $\beta J < 1$ the Edward-Anderson parameter $q_{\mathrm{EA}} \to 0$ vanishes almost surely for any $b \geq 0$ as $N \to \infty$. We have show in [125] that $\liminf_{N\to\infty} \mathbb{E}[q_{\mathrm{EA}}] > 0$ for $\beta J > 1$ and $b > 0$ small enough, confirming a glass transition also in presence of a transversal field. We stress that the results in [125] form the first prove of glass order in the field of quantum spin glasses.

The main strategy is to establish a lower bound on $\mathbb{E}[q_{\mathrm{EA}}]$ and to conclude from the lower bound the positivity of the Edwards-Anderson parameter in a second step. To formulate the lower bound, we need to introduce the function $\Lambda : [0,\infty] \to [0,1]$, implicitly defined via

$$\Lambda(r \tanh(r)) = r^{-1} \tanh(r) \tag{5.26}$$

Λ is monotone-decreasing, convex, satisfies $\Lambda(0) = 1$, and it can be estimated from below according to $\Lambda(t) \geq t^{-1}(1 - e^{-t}) \geq \max\{0, 1 - t/2\}$ [69]. Then, we have the following estimate:

Theorem 5.14 (Theorem 1 in [125])
The mean of the spin-glass order parameter (5.25) *has a lower bound according to*

$$\mathbb{E}[q_{\mathrm{EA}}] \geq \Lambda\Big(2\beta b\, \mathbb{E}\big[\langle S_1^x \rangle_{\beta J,\beta b}\big]\Big) + \frac{2}{\beta J} \frac{1}{N-1} \mathbb{E}\big[\big\langle U \big\rangle_{\beta J,\beta b}\big]\,. \tag{5.27}$$

It is valid for any $\beta > 0$, $J > 0$, $b \geq 0$, and all $N \geq 2$.

We will comment later on the proof of Theorem 5.14. Instead, let us first discuss how we use (5.27) to show that $\mathbb{E}[q_{\mathrm{EA}}]$ does not vanish for $\beta J > 1$ and b small enough. To this end, we estimate the right-hand side of (5.27). To estimate $\langle S_1^x \rangle_{\beta J,\beta b}$, one may use the trivial bound $\langle S_1^x \rangle_{\beta J,\beta b} \leq 1$. In [125], we show that a differential inequality results in the slightly better bound $\langle S_1^x \rangle_{\beta J,\beta b} \leq \tanh(\beta b)$. To bound $\mathbb{E}[\langle U \rangle_{\beta J,\beta b}]$, one may make use of the limiting specific ground state energy $\kappa := -\lim_{N\to\infty} \frac{1}{N} \min U$. Its existence is guaranteed by Parisi's formula and numerical computations suggest $\kappa \approx 0.763$ [54]. We arrive at the explicit lower bound

$$\overline{q}(\beta J, \beta b) := \liminf_{N\to\infty} \mathbb{E}[q_{\mathrm{EA}}] \geq \Lambda\big(2\beta b \tanh(\beta b)\big) - \frac{2\kappa}{\beta J}. \tag{5.28}$$

The maximal magnetic field strength b for which the right-hand side of (5.28) is positive grows with β and in particular it allows to prove a glass phase in the zero temperature limit $\beta \to \infty$ up to a magnetic field strength $b = J/(4\kappa) \approx 0.328\, J$. However, a main drawback of the simple ground state bound is that even for $b = 0$ it only shows glassiness for $\beta J > 2\kappa$, which does not agree with the known classical transition point $\beta J = 1$. To establish the persistence of spin-glass order in the regime $1 < \beta J < 2\kappa$ for a sufficiently small field strength b, our main idea is that $\mathbb{E}[\langle U \rangle_{\beta J,\beta b}]$ should be close to its classical value ($b = 0$) if b is small enough. This intuition can be made precise by invoking the convexity of the

pressure. While this argument works in the whole parameter region $\beta J > 1$, it only proves glass order for very small $b > 0$.

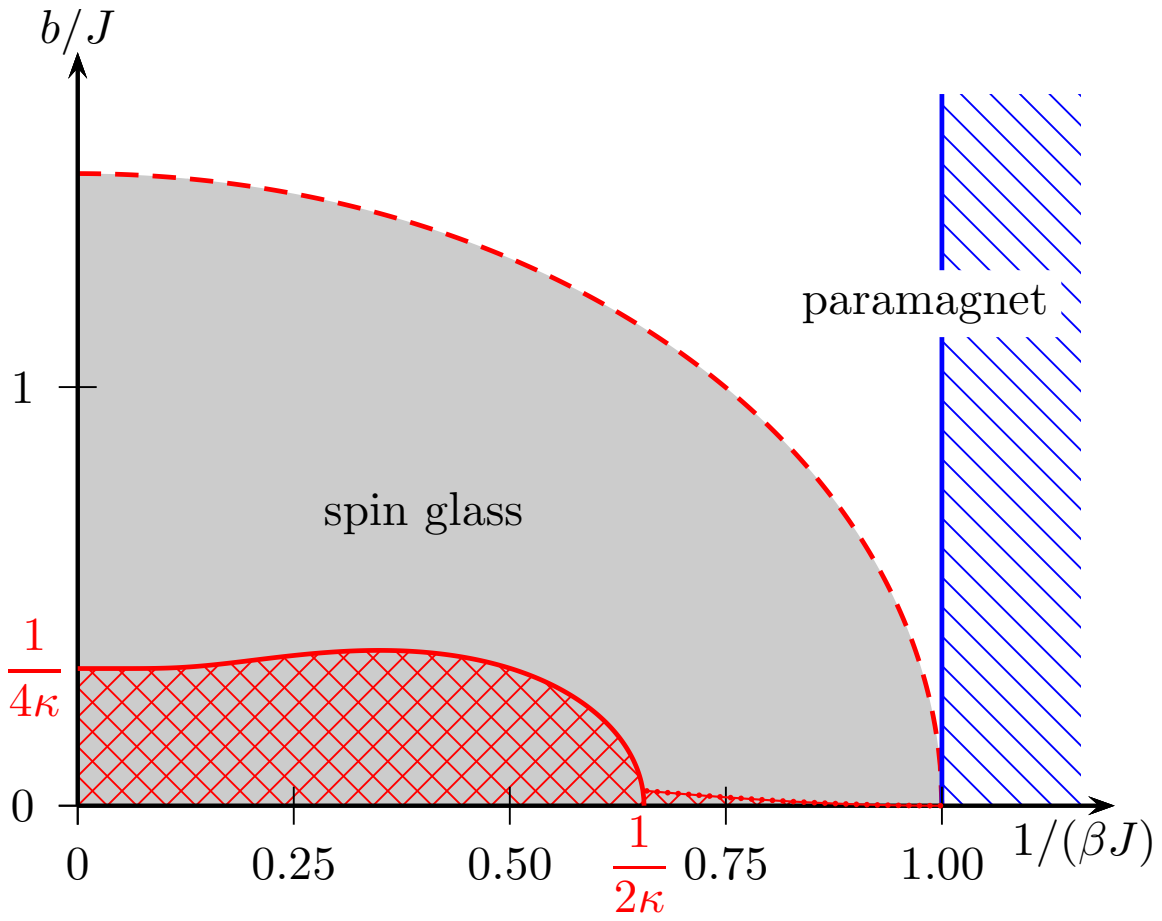

Figure 5.1: In the temperature-field plane the (red) cross-shaded regime indicates where we prove the existence of spin-glass order in the QSK model. The (red) dashed line is a cartoon of the critical line between the spin-glass and the paramagnetic phases as obtained by approximate arguments and/or numerical methods [78, 96, 139, 189, 192, 193]. The (blue) line-shaded regime for $\beta J < 1$ indicates where the spin-glass order parameter is rigorously known to vanish (Corollary 5.13 [126]). [125, Figure 1]

Our analytic results and the numerical predictions on the glass phase [78,96,139,189,192,193] are shown in Figure 5.1. The rigorously established glass regime is significantly smaller than what physicists predict. For instance, for $\beta \to \infty$ our methods only confirm glass order up to $b \approx 0.328\, J$, but the numerics suggests that the critical field strength is found at $b \approx 1.51J$ or $b \approx 1.6J$ [78, 189, 192, 193]. The precise location and nature of the true quantum critical point remains an important problem, in particular in the context of adiabatic algorithms. However, at the moment it appears illusive to find an exact characterization of the separation line. Future work might focus on qualitative questions which are still open. For instance, it would be of interest to show that glass order indeed vanishes for $\beta J > 1$ and b large enough. One might also turn to the question of replica symmetry breaking by establishing that q_{EA} does not concentrate around one specific value in (a part of) the glass phase. This would probably allow to show

replica-symmetric breaking in presence of a longitudinal field. We remark that extending our results to p-spin models is however rather straightforward. One may prove the similar bound

$$\mathbb{E}\big[\langle R_N^p\rangle_{\beta J,\beta b}^{\otimes 2}\big] \geq (1+o(N))\Lambda\Big(p\beta b\,\mathbb{E}\big[\langle S_1^x\rangle_{\beta J,\beta b}\big]\Big) + \frac{2}{\beta J}\frac{1}{N}\mathbb{E}\big[\langle U\rangle_{\beta J,\beta b}\big] + o(N)$$

which similarly leads to a nonvanishing Edwards-Anderson parameter [125, Theorem 2]. More fundamentally, it would be of high relevance to analyze how decisive the replica overlap is in the context of quantum models. Classically, we have seen that (Theorem 5.1) the overlap distribution determines the pressure, which is reflected in the Parisi formula. Such conclusion might not hold true for quantum glasses, but the replica overlap could still help understanding certain aspects of the glass phase. A similarly deep question is if there exists a quantum analog of the ultrametricity observed in the classical models (see Theorem 5.8) and what role if any is played by the Ruelle cascades.

The rest of this section is devoted to the proof of Theorem 5.14. Here, we extend a key observation of Bray and Moore [42], and of Aizenman, Lebowitz, and Ruelle [6], to the present quantum case $b > 0$: the mean order parameter $\mathbb{E}[q_{\mathrm{EA}}]$ is related to the mean internal energy $\mathbb{E}\big[\langle U\rangle_{\beta J,\beta b}\big]$ of the SK Hamiltonian. In a first step, we use the spin-index symmetry to obtain

$$\mathbb{E}\big[\langle U\rangle_{\beta J,\beta b}\big] = \frac{1}{\sqrt{N}}\sum_{1\leq j<k\leq N}\mathbb{E}[g_{j,k}\langle S_j^z S_k^z\rangle_{\beta J,\beta b}] = \frac{\sqrt{N}(N-1)}{2}\mathbb{E}[g_{1,2}\langle S_1^z S_2^z\rangle_{\beta J,\beta b}].$$

Now, we invoke Gaussian integration by parts [152, Lemma 1.2],

$$\mathbb{E}[g_{1,2}\langle S_1^z S_2^z\rangle_{\beta J,\beta b}] = \mathbb{E}\big[\partial\langle S_1^z S_2^z\rangle_{\beta J,\beta b}\big/\partial g_{12}\big].$$

Computing this derivative, leads to the important identity

$$-\frac{2}{N-1}\mathbb{E}\big[\langle U\rangle_{\beta J,\beta b}\big] = \beta J\,\mathbb{E}\big[\langle S_1^z S_2^z|S_1^z S_2^z\rangle_{\beta J,\beta b} - \langle S_1^z S_2^z\rangle_{\beta J,\beta b}^2\big] \tag{5.29}$$

where we have introduced the Duhamel–Kubo–Bogolyubov scalar product or Duhamel correlator [69, 119]. $\langle A|A\rangle_\beta$ can be defined for any observable A, Hamiltonian H and inverse temperature $\beta \geq 0$ as

$$\langle A|A\rangle_\beta := \int_0^1 \mathrm{d}t\,\big\langle e^{t\beta H}A^* e^{-t\beta H}A\big\rangle_\beta.$$

The Duhamel scalar product appears naturally as derivative of the exponential matrix in the noncommutative setting. If $A = A^*$, one has the a priori bounds

$$0 \leq \langle A\rangle_\beta^2 \leq \langle A|A\rangle_\beta \leq \langle A^2\rangle_\beta,$$

where the first inequality is trivial, for the second inequality one can use the representation $\langle A|A\rangle_\beta = \frac{\partial^2}{\partial s\partial t}\mathrm{Tr}\,e^{H+(s+t)A}$ and invoke convexity and the last inequality is essentially a convexity estimate, too [167, Theorem IV.7.2]. We are of course interested in the case where $A = S_1^z S_2^z$ and $H = H_N$ is the QSK Hamiltonian. Then, $\langle S_1^z S_2^z|S_1^z S_2^z\rangle_{\beta J,\beta b} \leq 1$. In the classical commutative case ($b = 0$), we in fact have the equality $\langle S_1^z S_2^z|S_1^z S_2^z\rangle_{\beta J,b=0} = 1$, which significantly simplifies the analysis of (5.29).

For nonvanishing magnetic fields $b > 0$, the main challenge is to find a lower bound on the Duhamel scalar product $\langle S_1^z S_2^z | S_1^z S_2^z \rangle_{\beta J, \beta b}$, which improves on $\langle S_1^z S_2^z \rangle_{\beta J, \beta b}^2$. Fortunately, the by now classical Falk-Bruch inequality is sharp enough:

Proposition 5.15 ([73],Theorem IV.7.5)
Let H be an Hamiltonian on a finite dimensional Hilbert space, A a self-adjoint bounded operator and Λ as in (5.26)*. Then, we have*

$$\langle A|A\rangle_\beta \geq \langle A^2\rangle_\beta \, \Lambda\Big(\frac{1}{4\langle A^2\rangle_\beta} \big\langle \big[A, [\beta H, A]\big] \big\rangle_\beta \Big). \tag{5.30}$$

The expression in the argument of Λ in (5.30) equals the scalar product $\big\langle [\beta H, A] \big| [\beta H, A] \big\rangle_\beta$ and is hence positive for a general self-adjoint observable A. In the present case, $A = S_1^z S_2^z$ commutes with the SK potential U, so the double commutator is independent of J and one may compute

$$\begin{aligned} \big[S_1^z S_2^z, [\beta H, A]\big] &= \beta b [S_1^z S_2^z, [S_1^x + S_2^x, S_1^z S_2^z]] = \beta b \left([S_1^z S_2^z, [-2iS_1^y S_2^z - 2iS_1^z S_2^y]] \right) \\ &= 4\beta b (S_1^x + S_2^x). \end{aligned}$$

Using again the spin symmetry, we arrive at

$$\mathbb{E}\big[\langle S_1^z S_2^z | S_1^z S_2^z \rangle_{\beta J, \beta b}\big] \geq \mathbb{E}\left[\Lambda\Big(2\beta b \, \langle S_1^x \rangle_{\beta J, \beta b} \Big) \right] \geq \Lambda\Big(2\beta b \, \mathbb{E}\big[\langle S_1^x \rangle_{\beta J, \beta b}\big] \Big),$$

where we used Jensen's inequality for the convex function Λ.

Bibliography

[1] D. A. Abanin, E. Altman, I. Bloch, M. Serbyn. Colloquium: Many-body localization, thermalization, and entanglement. Rev. Mod. Phys. 91, 021001 (2019).

[2] J. Adame, S. Warzel. Exponential vanishing of the ground-state gap of the QREM via adiabatic quantum computing. J. Math. Phys. 56: 113301 (2015).

[3] A. Adhikari, C. Brennecke. Free energy of the Quantum Sherrington-Kirkpatrick spin-glass model with transverse field. J. Math. Phys. 61: 083302 (2020).

[4] A. Adhikari, C. Brennecke, P. von Soosten, H.-T. Yau. Dynamical approach to the TAP equations for the Sherrington-Kirkpatrick model. J. Stat. Phys. 183: 35 (2021).

[5] U. Agrawal, A. Zabalo, K. Chen, J. H. Wilson, A. C. Potter, J. Pixley, S. Gopalakrishnan, R. Vasseur. Entanglement and Charge-Sharpening Transitions in U(1) Symmetric Monitored Quantum Circuits. Phys. Rev. X 12, 041002 (2022).

[6] M. Aizenman, J. L. Lebowitz, D. Ruelle. Some Rigorous Results on the Sherrington-Kirkpatrick Spin Glass Model. Commun. Math. Phys. 112: 3-20 (1987).

[7] M. Aizenman, M. Shamis, S. Warzel. Resonances and partial delocalization on the complete graph. Ann. Henri Poincare 16: 1969-2003 (2015).

[8] M. Aizenman, R. Sims, S. L. Starr. Extended variational principle for the Sherrington-Kirkpatrick spin-glass model. Phys. Rev. B, 68:214403 (2003).

[9] M. Aizenman, S. Warzel. Random Operators: Disorder Effects on Quantum Spectra and Dynamics. AMS 2015.

[10] T. Albash and D. A. Lidar. Adiabatic quantum computation. Rev. Mod. Phys. 90, 015002, 64 pp. (2018).

[11] A. Altland, M. Buchhold, S. Diehl, T. Micklitz. Dynamics of measured many-body quantum chaotic systems. Phys. Rev. Research 4, L022066 (2022).

[12] P. W. Anderson. Absence of Diffusion in Certain Random Lattices. Phys. Rev. 109 (5): 1492–1505 (1958).

[13] C. Appert-Rolland, B. Derrida, V. Lecomte, F. van Wijland. Universal cumulants of the current in diffusive systems on a ring. Phys. Rev. E, 78(2):021122 (2008).

[14] L. P. Arguin, N. Kistler, Microcanonical Analysis of the random energy model in a random magnetic field. J. Stat. Phys. 157: 1–16 (2014).

[15] L. P. Arguin, R. Persechino, The Free Energy of the GREM with random magnetic field. In: Gayrard V., Arguin LP., Kistler N., Kourkova I. (eds.), *Statistical Mechanics of Classical and Disordered Systems*. StaMeClaDys 2018. Springer Proceedings in Mathematics & Statistics, vol 293, 37-61, Springer, 2019.

[16] A. Auffinger, W.-K. Chen. The Parisi formula has a unique minimzer. Comm. Math. Phys. 335: 1429-1444 (2015).

[17] A. Auffinger, W.-K. Chen. Parisi formula for the ground state energy in the mixed p-spin model. Ann. Probab., 45: 4617-4631 (2017).

[18] A. Auffinger, W.-K. Chen, Q. Zeng. The SK Model is Infinite Replica Symmetry Breaking at Zero Temperature. Commun. Pure Appl. Math. 73, 921-943 (2020).

[19] L. Avena, O. Gün, M. Hesse. The parabolic Anderson model on the hypercube. Stoch. Proc. Appl. 130, 3369-3393 (2020).

[20] E. Baake, M. Baake, and H. Wagner. Ising quantum chain is equivalent to a model of biological evolution. Phys. Rev. Lett., 78: 559–562 (1997). Erratum: Phys. Rev. Lett. 79: 1782 (1997)

[21] E. Baake, H. Wagner. Mutation–selection models solved exactly with methods of statistical mechanics. Genet. Res. 78: 93–117 (2001).

[22] C. L. Baldwin, C. R. Laumann. Quantum algorithm for energy matching in hard optimization problems. Phys. Rev. B 97, 224201 (2018).

[23] C. L. Baldwin, C. R. Laumann, A. Pal, A. Scardicchio. The many-body localized phase of the quantum random energy model. Phys. Rev. B 93: 024202 (2016).

[24] V. Bapst, L. Foini, F. Krzakala, G. Semerjian, F. Zamponi. The Quantum Adiabatic Algorithm Applied to Random Optimization Problems: The Quantum Spin Glass Perspective. Physics Reports 523: 127–205 (2013).

[25] G. Ben Arous, A. Bovier, V. Gayrard. Glauber dynamics of the random energy model. I. Metastable motion on the extreme states. Comm. Math. Phys., 235: 379–425 (2003).

[26] G. Ben Arous, A. Bovier, V. Gayrard. Glauber dynamics of the random energy model. II. Aging below the critical temperature. Comm. Math. Phys., 236: 1–54 (2003).

[27] F. A. Berezin. Convex operator functions. Math. USSR Sbornik 17, 269–277 (1972).

[28] R. Bhatia. Matrix Analysis. Springer, 1997.

[29] G. Biroli, D. Facoetti, M. Schiró, M. Tarzia, P. Vivo. Out-of-equilibrium phase diagram of the quantum random energy model. Phys. Rev. B 103: 014204 (2021).

[30] M. Biskup, W. König. Eigenvalue order statistics for random Schrödinger operators with doubly-exponential tails. Commun. Math. Phys. 341, 179–218 (2016).

[31] P. G. Bolhuis, D. Chandler, C. Dellago, P. L. Geissler. Transition path sampling: throwing ropes over rough mountain passes, in the dark. Annu. Rev. Phys. Chem. 53:291 (2002).

[32] B. Bollobás, J. Leed, S. Letzter. Eigenvalues of subgraphs of the cube. Eur. J. Comb. 70: 125–148 (2018).

[33] E. Bolthausen and N. Kistler, On a nonhierarchical version of the Generalized Random Energy Model. Ann. Appl. Prob. Vol. 16: 1-14 (2006).

[34] A. B. Bortz, M. H. Kalos, J. L. Lebowitz. New algorithm for Monte-Carlo simulation of Ising spin systems. J. Comp. Phys. 17(1):10–18 (1975).

[35] S. Boucheron, G. Lugosi, P. Massart. Concentration Inequalities. A Nonasymptotic Theory of Independence. Oxford University Press, 2013.

[36] A. Bovier. Statistical Mechanics of Disordered Systems. A Mathematical Perspective. Cambridge University Press, 2012.

[37] A. Bovier. Gaussian Processes on Trees. Cambridge University Press, 2017.

[38] A. Bovier, A. Klimovsky. Fluctuations of the partition function in the generalized random energy model with external field. J. Math. Phys., 49(12):125202, 27 (2008).

[39] A. Bovier, I. Kurkova. Derrida's generalised random energy models. I. Models with finitely many hierarchies. Ann. Inst. H. Poincaré Probab. Statist., 40:439–480 (2004).

[40] A. Bovier, I. Kurkova. Derrida's generalized random energy models. II. Models with continuous hierarchies. Ann. Inst. H. Poincaré Probab. Statist., 40:481–495 (2004).

[41] A. Bovier, I. Kurkova, M. Löwe. Fluctuations of the free energy in the REM and the p-spin SK models. Ann. Probab., 30: 605–651 (2002).

[42] A.J. Bray, M.A. Moore. Replica theory of quantum spin glasses. J. Phys. C, Solid State Phys. 13: L655 (1980).

[43] C. Brennecke, H.-T. Yau. The replica symmetric formula for the SK model revisited. J. Math. Phys. 63, 073302 (2022).

[44] A. Burin. Localization and chaos in a quantum spin glass model in random longitudinal fields: Mapping to the localization problem in a Bethe lattice with a correlated disorder. Ann. Phys. 529: 1600292 (2017).

[45] A. Callison, M. Festenstein, J. Chen, L. Nita, V. Kendon, N. Chancellor. Energetic perspective on rapid quenches in quantum annealing. PRX Quantum **2**, 010338, 21 pp. (2021).

[46] D. Capocaccia, M. Cassandro, P. Picco. On the existence of thermodynamics for the generalized random energy model. J. Stat. Phys. 46:493–505 (1987).

[47] E. A. Carlen. Trace Inequalities and Quantum Entropy: An introductory course. Lecture notes (2009).

[48] P. Carmona, Y. Hu. Universality in Sherrington-Kirkpatrick's spin glass model. Ann. Inst. H. Poincaré Probab. Statist. 42, no. 2, 215-222 (2006).

[49] J. Černý, T. Wassmer. Aging of the metropolis dynamics on the random energy model. Probab. Theory Related Fields 167: 1–51 (2015).

[50] D. Chandler. Introduction to Modern Statistical Mechanics. Oxford University Press, 1987.

[51] W.-K. Chen. On the Almeida-Thouless transition line in the SK model with centered Gaussian external field Electron. Commun. Probab. Vol. 26, No. 65, 1–9 (2021).

[52] P. Contucci, C. Giardina. Perspectives on Spin Glases. Cambridge University Press, New York, 2013.

[53] N. Crawford. Thermodynamics and universality for mean field quantum spin glasses. Commun. Math. Phys. 274: 821–839 (2007).

[54] A. Crisanti and T. Rizzo. Analysis of the ∞-replica symmetry breaking solution of the Sherrington–Kirkpatrick model. Phys. Rev. E 65, 046137, 9 pp. (2002).

[55] A. Crisanti, H. J. Sommers. The spherical *p*-spin interaction spin glass model: the statics. Z. Phys. B. condensed Matter, 83, 341-354 (1992).

[56] D.M. Cvetković, M. Doob. H. Sachs. Spectra of graphs: Theory and applications. 3rd ed. Johann Ambrosius Barth, Heidelberg, 1995.

[57] J. R. L. de Almeida, D. J. Thouless. Stability of the Sherrington-Kirkpatrick solution of a spin glass model, J. Phys. A: Math. Gen. 11: 983–990 (1978).

[58] L. de Haan, A. Ferreira. Extreme Value Theory. An Introduction. Springer 2006.

[59] A. Dembo, A. Montanari, S. Sen. Extremal cuts of sparse random graphs. The Annals of Probability 45 , no. 2, 1190–1217 (2017).

[60] A. Dembo, O. Zeitouni. Large Deviations Techniques and Applications, Springer 2010.

[61] B. Derrida. Random energy model: limit of a family of disordered models. Phys. Rev. Lett. 45: 79-82 (1980).

[62] B. Derrida. Random energy model: an exactly solvable model of disordered systems. Phys. Rev. B 24: 2613-2326 (1981).

[63] B. Derrida. A generalization of the random energy model that includes correlations between the energies. J. Phys. Lett. 46: 401–407 (1985).

[64] B. Derrida, E. Gardner. Solution of the generalized random energy model. J. Phys. C 19: 2253–2274 (1986).

[65] B. Derrida, E. Gardner. Magnetic properties and function q(x) of the generalised random energy model. J. Phys. C 19 5783–5798 (1986).

[66] V Dobrosavljevic, D Thirumalai. 1/p expansion for a p-spin interaction spin-glass model in a transverse field. J. Phys. A: Math. Gen. 23: L767 (1990).

[67] P. Donnelly, G. Grimmett. On the asymptotic distribution of large prime factors. J. London Math. Soc. (2) 47, no. 3, 395–404 (1993).

[68] A. Dutta, G. Aeppli, B. K. Chakrabarti, U. Divakaran, T. F. Rosenbaum, D. Sen. Quantum Phase Transitions in Transverse Field Spin Models – From Statistical Physics to Quantum Information. Cambridge University Press, Delhi, 2015.

[69] F. J. Dyson, E. H. Lieb, B. Simon. Phase transitions in quantum spin systems with isotropic and nonisotropic interactions. J. Stat. Phys. 18, 335–383 (1978).

[70] S.F. Edwards, P.W. Anderson. Theory of Spin Glasses. Journal of Physics F: Metal Physics, 5, 965 (1975).

[71] M. Eigen, P. Schuster. The Hypercycle: a principle of natural self-organisation. Naturwissenschaften 64: 541-565 (1977).

[72] L. Erdős, D. Schröder. Phase Transition in the Density of States of Quantum Spin Glasses. D. Math Phys Anal Geom 17: 9164 (2014).

[73] H. Falk, L. W. Bruch. Susceptibility and fluctuation. Phys. Rev. 180, 442–444 (1969).

[74] M. Fang, O. Zeitouni. Branching random walks in time inhomogeneous environments. Electron. J. Probab. 17 1 - 18 (2012).

[75] L. Faoro, M. V. Feigelman and L. Ioffe. Non-ergodic extended phase of the quantum random energy model. Annals of Physics 409: 167916 (2019).

[76] E. Farhi, J. Goldstone, S. Gutmann, and D Nagaj. How to make the quantum adiabatic algorithm fail. International Journal of Quantum Information 6, 503-516 (2008).

[77] E. Farhi, J. Goldstone, S. Gutmann, L. Zhou. The Quantum Approximate Optimization Algorithm and the Sherrington-Kirkpatrick Model at Infinite Size. Quantum 6, 759 (2022).

[78] Y.V. Fedorov, E.F. Shender. Quantum spin glasses in the Ising model with a transverse field. JETP Lett. 43: 681 (1986).

[79] M. E. Fisher. Bounds for the derivatives of the free energy and the pressure of a hard-core system near close packing. J. Chem. Phys. 42, 3852–3856 (1965).

[80] K. H. Fischer, J. A. Hertz. Spin Glasses. Cambridge University Press, Cambridge, 1991.

[81] D. S. Fisher, D. A. Huse. Equilibrium behavior of the spin-glass ordered phase. Phys. Rev. B. 38(1), 386-411 (1988).

[82] P. J. Forrester. The Golden-Thompson inequality: Historical aspects and random matrix applications. Journal of Mathematical Physics 55, 023503 (2014).

[83] S. Friedli, Y. Velenik. Statistical Mechanics of Lattice Systems. A Concrete Mathematical Introduction. Cambridge University Press, 2018.

[84] J. Friedman, J. P. Tillich. Generalized Alon-Boppana theorems and error-correcting codes. Siam J. Descrete Math. 19: 700–718 (2005).

[85] A. Galves, S. Martinez, P. Picco. Fluctuations in Derrida's random energy and generalized random energy models. J Stat Phys 54: 515–529 (1989).

[86] E. Gardner. Spin glasses with p-spin interactions. Nucl. Phys. B 257, 747–765 (1985).

[87] J. P. Garrahan. Aspects of non-equilibrium in classical and quantum systems: Slow relaxation and glasses, dynamical large deviations, quantum non-ergodicity, and open quantum dynamics. Physica A, 504:130–154 (2018).

[88] J. P. Garrahan, C. Manai, S. Warzel. Trajectory phase transitions in non-interacting systems: all-to-all dynamics and the random energy model. Phil. Trans. R. Soc. A. 381: 20210415 (2022).

[89] V. Gayrard. Aging in Metropolis dynamics of the REM: a proof. Probab. Theory Relat. Fields 174, 501-551 (2019).

[90] J. P. Garrahan, R. L. Jack, V. Lecomte, E. Pitard, K. van Duijvendijk, F. van Wijland. Dynamical First-Order Phase Transition in Kinetically Constrained Models of Glasses. Phys. Rev. Lett. 98(19):195702 (2007).

[91] V. Gayrard, L. Hartung. Dynamic phase diagram of the REM. In: V. Gayrard, L.P. Arguin, N. Kistler, I. Kourkova (eds) Statistical Mechanics of Classical and Disordered Systems. StaMeClaDys 2018. Springer Proceedings in Mathematics & Statistics, vol 293. Springer, Cham 2019.

[92] A. Georges, O. Parcollet, S.Sachdev. Mean Field Theory of a Quantum Heisenberg Spin Glass. Phys. Rev. Lett. 85, 840 (2000).

[93] A. Georges, O. Parcollet, S. Sachdev. Quantum fluctuations of a nearly critical Heisenberg spin glass. Physical Review B 63, 134406 (2001).

[94] S. Ghirlanda, F. Guerra. General properties of overlap distribution in disordered spin systems. Towards Parisi ultrametricity. J. Phys. A 31, no. 46, 9149-9155 (1998).

[95] Y. Y. Goldschmidt. Solvable model of the quantum spin glass in a transverse field. Phys. Rev. B 41: 4858 (1990).

[96] Y. Goldschmidt, P.-Y. Lai. Ising spin glass in a transverse field: Replica-symmetry-breaking solution. Phys. Rev. Lett. 64, 2467–2470 (1990).

[97] F. Guerra, F. L. Toninelli. The thermodynamic limit in mean field spin glass models. Commun. Math. Phys. 230: 71–79 (2002).

[98] F. Guerra. Sum rules for the free energy in the mean field spin glass model. Fields Institute Communications 30, 161 (2001).

[99] F. Guerra. Broken replica symmetry bounds in the mean field spin glass model. Comm. Math. Phys. 23: 1–12 (2003).

[100] F. Guerra, F. L. Toninelli. The Thermodynamic Limit in Mean Field Spin Glass Models. Comm. Math. Phys. 230: 71–79 (2002).

[101] F. Guerra, F. L. Toninelli. The Infinite Volume Limit in Generalized Mean Field Disordered Models. Markov Process. Related Fields 9, 195-207 (2003).

[102] D. Hebb. The Organisation of Behavior: a Neurophysiological Theory. Wiley, New York, 1949.

[103] L. O. Hedges, R. L. Jack, J. P. Garrahan, D. Chandler. Dynamic order-disorder in atomistic models of structural glass formers. Science, 323(5919):1309 (2009).

[104] J. Hermisson, O. Redner, H. Wagner. E. Baake. Mutation-selection balance: ancestry, load, and maximum principle. Theor. Popul. Biol. 62: 9–46 (2002).

[105] J.J. Hopfield. Neural networks and physical systems with emergent collective computational abilities. Proc. Nat. Acad. Sci. USA, 79, no. 8, 2554-2558 (1982).

[106] D. A. Huse, J. Miller. Zero-temperature critical behavior of the infinite-range quantum Ising spin glass. Phys. Rev. Lett. 70: 3147-3150 (1993).

[107] R. L. Jack. Ergodicity and large deviations in physical systems with stochastic dynamics. Eur. Phys. J. B, 93(4):74, (2020).

[108] R. L. Jack, I. R. Thompson, P. Sollich. Hyperuniformity and Phase Separation in Biased Ensembles of Trajectories for Diffusive Systems. Phys. Rev. Lett. 114(6):060601 (2015).

[109] S. Jansen, M.-B. Ruskai, R. Seiler. Bounds for the adiabatic approximation with applications to quantum computation. J. Math. Phys. 48, 102111 (2007).

[110] T. Jörg, F. Krzakala, J. Kurchan, A.C. Maggs. Simple glass models and their quantum annealing. Phys. Rev Lett. 101: 147204 (2008).

[111] T. Jörg, F. Krzakala, G. Semerjian, F. Zamponi. First-Order Transitions and the Performance of Quantum Algorithms in Random Optimization Problems. Phys. Rev. Lett. 104: 207206 (2010).

[112] O. Kallenberg. Foundations of modern probability. 3rd edition. Springer Nature, 2021.

[113] T. Kato. Perturbation theory of linear operators. 2nd ed., Springer 1995.

[114] M. Keller, D. Lenz, R. K. Wojciechowski. Graphs and Discrete Dirichlet Spaces. Grundlehren der mathematischen Wissenschaften Volume 358. Springer, 2021.

[115] J. F. C. Kingman. A simple model for the balance between selection and mutation. J. Appl. Probab. 15: 1–12 (1978).

[116] J. F. C. Kingman, S. J. Taylor, A. G. Hawkes, A. M. Walker, D. R. Cox, A. F. M. Smith, B. M. Hill, P. J. Burville, T. Leonard. Random discrete distribution. J. Roy. Statist. Soc. Ser. B 37, 1–22 (1975).

[117] S. Knysh. Zero-temperature quantum annealing bottlenecks in the spin-glass phase. Nat. Commun. 7, 12370, 9 pp. (2016).

[118] V. E. Kravtsov, I. M. Khaymovich, E. Cuevas, M. Amini. A random matrix model with localization and ergodic transitions. New J. Phys. 17:122002, 2015.

[119] R. Kubo, M. Toda, N. Hashitsume. Statistical Physics II – Nonequilibrium Statistical Mechanics. Springer, Berlin, 1998, 2nd edition, 3rd corrected printing.

[120] G. Last, M. Penrose. Lectures on the Poisson Process. Cambridge University Press, 2017.

[121] C. R. Laumann, A. Pal, A. Scardicchio. Many-body mobility edge in a mean-field quantum spin glass. Phys. Rev. Lett. 113: 200405 (2014).

[122] M.R. Leadbetter, G. Lindgren, H. Rootzén. Extremes and related properties of random sequences and processes. Springer Series in Statistics. Springer-Verlag, New York, 1983.

[123] V. Lecomte, C. Appert-Rolland, F. van Wijland. Thermodynamic formalism for systems with markov dynamics. J. Stat. Phys. 127(1):51 (2007).

[124] D. A. Levin, Y. Peres, E. L. Wilmer, J. Propp, D. B. Wilson. Markov Chains and Mixing Times. 2nd ed. AMS, 2017.

[125] H. Leschke, C. Manai, R. Ruder, S. Warzel. Existence of replica-symmetry breaking in quantum glasses. Phys. Rev. Lett. 127: 207204 (2021).

[126] H. Leschke, S. Rothlauf, R. Ruder, W. Spitzer. The free energy of a quantum Sherrington-Kirkpatrick spin-glass model for weak disorder. J. Stat. Phys. 182: 55 (2021).

[127] Y. Li, X. Chen, M. P. A. Fisher. Quantum zeno effect and the many-body entanglement transition. Phys. Rev. B 98:205136 (2018).

[128] C. Manai and S. Warzel. Phase diagram of the quantum random energy model. J. Stat. Phys. 180: 654–664 (2020).

[129] C. Manai and S. Warzel. The quantum random energy model as a limit of p-spin interactions. Rev. Math. Phys. 33: 2060013 (2020).

[130] C. Manai, S. Warzel. Generalized random energy models in a transversal magnetic field: free energy and phase diagrams. Probab. Math. Phys. 3: 215–245 (2022).

[131] C. Manai, S. Warzel. The de Almeida-Thouless Line in Hierarchical Quantum Spin Glasses. J. Stat. Phys. 186:14 (2022).

[132] C. Manai, S. Warzel. Spectral Analysis of the Quantum Random Energy Model. Commun. Math. Phys. (2023). Extended version: https://arxiv.org/abs/2202.00334.

[133] B. Maurey. Some Deviation Inequalities. Geometric and functional analysis 1.2 : 188-197 (1991).

[134] M. Merolle, J. P. Garrahan, D. Chandler. Space-time thermodynamics of the glass transition. Proc. Natl. Acad. Sci. USA 102(31):10837 (2005).

[135] M. Mézard, G. Parisi, M. A. Virasoro. Spin Glass Theory and Beyond. World Scientific, Singapore (1987).

[136] M. Mezard, A. Montanari. Information, Physics, and Computation. Oxford University Press, Oxford, 2009.

[137] A. Montanari. Optimization of the Sherrington–Kirkpatrick Hamiltonian. SIAM J. Comput. **0** (0), FOCS19-1–FOCS19-38 (2021).

[138] S. Mukherjee, B. K. Chakrabarti. On the question of ergodicity in quantum spin glass phase and its role in quantum annealing. J. Phys. Soc. Jpn. 88, 061004, 10 pp. (2019).

[139] S. Mukherjee, A. Rajak, B. K. Chakrabarti. Possible ergodic-nonergodic regions in the quantum Sherrington–Kirkpatrick spin glass model and quantum annealing. Phys. Rev. E 97, 022146, 6 pp. (2018).

[140] R. Nandkishore, D A. Huse. Many-Body Localization and Thermalization in Quantum Statistical Mechanics. Annu. Rev. Condens. Matter Phys. 6: 15-38 (2015).

[141] T. Nemoto, E. Fodor, M. E. Cates, R. L. Jack, J. Tailleur. Optimizing active work: Dynamical phase transitions, collective motion, and jamming. Phys. Rev. E 99:022605 (2019).

[142] C. M. Newman, D. L. Stein. Multiple states and thermodynamic limits in short-ranged spin glass models. Phys. Rev. B, 46 (2), 973 (1992).

[143] C. M. Newman, D. L. Stein. Non-mean-field behavior of realistic spin glasses. Phys. Rev. Lett. 87 (7), 77201 (1996).

[144] M. A. Nielsen, I. L. Chuang. Quantum Computation and Quantum Information. 10th Anniversary Edition. Cambridge University Press, New York, 2010.

[145] H. Nishimori. Statistical Physics of Spin Glasses and Information Processing – An Introduction. Clarendon, Oxford, 2001.

[146] P. T. Nyawo, H. Touchette. A minimal model of dynamical phase transition. EPL 116(5):50009 (2016).

[147] T. Obuchi, H. Nishimori, D. Sherrington. Phase diagram of the p-spin-interacting spin glass with ferromagnetic bias and a transverse field in the infinite-p limit. J. Phys. Soc. Jpn. 76: 054002 (2007).

[148] E. Olivieri, P. Picco. On the existence of thermodynamics for the random energy model. Comun. Math. Phys. 96: 125-144 (1984)

[149] R. I. Oliveira. Concentration of the adjacency matrix and of the Laplacian in random graphs with independent edges. Preprint, arXiv:0911.0600 (2010).

[150] M. Ostilli, C. Presilla. Exact ground state for a class of matrix Hamiltonian models: quantum phase transition and universality in the thermodynamic limit. J. Stat. Mech. P11012 (2006).

[151] D. Panchenko. The Parisi ultrametricity conjecture. Ann. of Math. 177, 383-393 (2013).

[152] D. Panchenko. The Sherrington-Kirkpatrick model. Springer, 2013.

[153] D. Panchenko, The Parisi formula for mixed p-spin models, Ann. Prob. Vol. 42: 946–958 (2014).

[154] D. Panchenko. Free energy in the mixed p-spin models with vector spins. Ann. Probab. 46, no. 2, 865-896 (2018).

[155] G. Parisi. The order parameter for spin glasses: a function on the interval 0-1. J. Phys. A: Math. Gen., 13: 1101–1112 (1980).

[156] G. Parisi. A sequence of approximated solutions to the S–K model for spin glasses. J. Phys. A: Math. Gen. 13, L115–L121 (1980).

[157] G. Pisier. Probabilistic methods in the geometry of Banach spaces. Lecture Notes in Mathematics 1206, 167-241 (1986).

[158] P. Ray, B. K. Chakrabarti, A. Chakrabarti. Sherrington–Kirkpatrick model in a transverse field: Absence of replica symmetry breaking due to quantum fluctuations. Phys. Rev. B 39, 11828–11832 (1989).

[159] M. Reed, B. Simon. Methods of modern mathematical physics. Volume 1: Functional Analysis. Academic Press, 2nd Edition, 1981.

[160] D. W. Robinson. Statistical mechanics of quantum spin systems. Commun. Math. Phys. 6: 151–160 (1967).

[161] G. Roepstorff. A stronger version of Bogoliubov's inequality and the Heisenberg model. Commun. Math. Phys. 53, 143–150 (1977).

[162] M. J. Rozenberg, A. Camjayi. Specific heat in the $SU(N)$ Heisenberg spin-glass model. J. Phys.: Condens. Matter 16 S723 (2004).

[163] D. Ruelle. Statistical Mechanics: Rigorous Results. Imperial College Press, London, 1969.

[164] D. Ruelle. A mathematical reformulation of Derrida's REM and GREM. Comm. Math. Phys. 108: 225–239 (1987).

[165] M. Shcherbina, B. Tirozzi, C. Tassi. Quantum Hopfield Model. Physics 2, 184–196 (2020)

[166] D. Sherrington, S. Kirkpatrick. Solvable Model of a Spin-Glass. Phys. Rev. Lett. 35, 26, 1792-1796 (1975).

[167] B. Simon. The statistical mechanics of lattice gases. Princeton Univ. Press 1993.

[168] B. Simon. Functional Integration and Quantum Physics. Second Edition. AMS Chelsea Publishing, 2005.

[169] B. Simon. Convexity: An analytic viewpoint. Cambridge University Press, 2011.

[170] B. Simon. A Comprehensive Course in Analysis, Part 4. Operator Theory. American Mathematical Soc., 2015.

[171] B. Skinner, J. Ruhman, A. Nahum. Measurement-induced phase transitions in the dynamics of entanglement. Phys. Rev. X 9:031009 (2019).

[172] V. N. Smelyanskiy, K. Kechedzhi, S. Boixo, S. V. Isakov, H. Neven, B. Altshuler. Nonergodic delocalized states for efficient population transfer within a narrow band of the energy landscape. Phys. Rev. X 10: 011017 (2020).

[173] V. N. Smelyanskiy, K. Kechedzhi, S. Boixo, H. Neven, B. Altshuler. Intermittency of dynamical phases in a quantum spin glass. Preprint, arXiv:1907.01609 (2019).

[174] T. Speck, A. Malins, C. P. Royall. First-order phase transition in a model glass former: Coupling of local structure and dynamics. Phys. Rev. Lett. 109:195703 (2012).

[175] S. Suzuki, J. Inoue, B. K. Chakrabarti. Quantum Ising Phases and Transitions in Transverse Ising Models. 2nd ed. Springer 2013.

[176] I. G. Szendro, M. F. Schenk, J. Franke, J. Krug, J. A. G. M. de Visser. Quantitative analyses of empirical fitness landscapes. J. Stat. Mech. Theory Exp. 2013:P01005 (2013).

[177] K. Takahashi. Quantum fluctuations in the transverse Ising spin glass model: A field theory of random quantum spin systems. Phys. Rev. B 76, 784422, 10 pp. (2007).

[178] M. Talagrand. Concentration of measure and isoperimetric inequalities in product spaces. Publ. Math. IHES 81:73–205 (1995).

[179] M. Talagrand. The Parisi formula. Ann. of Math. 163: 221–263 (2006).

[180] M. Talagrand. Free energy of the spherical mean field model. Probab. Theory Relat. Fields 134, 339-382 (2006).

[181] M. Talagrand. Mean field models for spin glasses (Vol I+II). Springer 2011.

[182] T. Tao. Topics in random matrix theory. AMS 2012.

[183] W. Thirring. Quantum Mathematical Physics. Atoms, Molecules and Large Systems. Second Edition. Springer, Berlin Heidelberg, 2002.

[184] G. De Tomasi, I. M. Khaymovich, F. Pollmann, S. Warzel. Rare thermal bubbles at the many-body localization transition from the Fock space point of view. Phys. Rev. B 104: 024202 (2021).

[185] F. L. Toninelli. About the Almeida-Thouless transition line in the Sherrington-Kirkpatrick mean-field spin glass model. Europhysics Letters, 60: 764–767 (2002).

[186] H. Touchette. The large deviation approach to statistical mechanics. Phys. Rep. 478(1-3):1 (2009).

[187] J. A. Tropp. An introduction to matrix concentration inequalities. Foundations and Trends in Machine Learning 8:1–230 (2015).

[188] K. Usadel, Spin glass transition in an Ising spin system with transverse field. Solid State Commun. 58: 629–630 (1986).

[189] K. D. Usadel, B. Schmitz. Quantum fluctuations in an Ising spin glass with transverse field. Solid State Commun. 64, 975–977 (1987).

[190] L. M. Vasiloiu, T. H. E. Oakes, F. Carollo, J. P. Garrahan. Trajectory phase transitions in noninteracting spin systems. Phys. Rev. E 101:042115 (2020).

[191] P. von Soosten, S. Warzel. Non-ergodic delocalization in the Rosenzweig-Porter model. Lett. Math. Phys. 109: 905-922 (2019).

[192] T. Yamamoto, H. Ishii. A perturbation expansion for the Sherrington–Kirkpatrick model with a transverse field. J. Phys. C 20, 6053–6060 (1987).

[193] A. P. Young. Stability of the quantum Sherrington-Kirkpatrick spin glass model. Phys. Rev. E 96: 032112 (2017).

Appendix A

Core Articles

A.1 Phase diagram of the quantum random energy model

Phase diagram of the quantum random energy model

Chokri Manai and Simone Warzel

The Quantum Random Energy Model (QREM) is probably the simplest quantum spin glass model as it consists of the uncorrelated REM potential in a transversal field. Nevertheless, the QREM is of huge relevance, not only as a treatable toy model for disordered quantum mean field systems, but also due to its applications in quantum computing and mathematical biology [21–23, 110, 175]. In Core Article I, we present the first rigorous analysis of the QREM. We focus on the specific pressure in the thermodynamic limit. This work has been the basis for the study of more involved models [130, 131]

Main Results

Our main theorem establishes Goldschmidt's prediction on the limit of the specific pressure in the QREM [95] as an almost sure convergence. As a consequence, we determine the complete phase diagram of the QREM. The phase diagram consists of a classical phase, where the QREM thermodynamics agrees with the REM thermodynamics, and a pure paramagnetic phase where the REM potential does not contribute to the specific pressure in the thermodynamic limit. We confirm a first order magnetic transition, a second order glass transitions for a weak magnetic field, and a quantum phase transition for the ground state. We give explicit expressions for all phase lines.
The proof relies on asymptotically matching lower and upper bounds. The lower bound is derived via Gibbs' variational principle. The upper bound is based on the rough geometry of the REM energy landscape and standard methods from matrix analysis, in particular the Golden-Thompson inequality. Moreover, we discuss the concentration properties of the pressure, which turns out to be self-averaging.

Individual Contribution

I am the principal of the author of this article. I was involved in all stages of the work and contributed to the draft. The topic was suggested by my advisor Simone Warzel. After several attempts to prove Goldschmidt's formula via a path-integral approach - which ultimately only lead to partial results - Simone Warzel had the insights that operator theoretic methods could be used instead. We then figured out the details together. I contributed significantly to the proofs of Lemma 1, Lemma 2 and Lemma 3.

Permission to include:

Chokri Manai and Simone Warzel.
Phase diagram of the quantum random energy model.
Journal of Statistical Physics 180: 654–664 (2020).
https://doi.org/10.1007/s10955-020-02492-5.

How to obtain permission to reuse Springer Nature content not available online on SpringerLink

Requests for permission to reuse content (e.g. figure or table, abstract, text excerpts) from Springer Nature publications currently not available online must be submitted in writing. Please be as detailed and specific as possible about what, where, how much, and why you wish to reuse the content.

Your contacts to obtain permission for the reuse of material from:

- books: bookpermissions@springernature.com
- journals: journalpermissions@springernature.com

Author reuse

Please check the Copyright Transfer Statement (CTS) or Licence to Publish (LTP) that you have signed with Springer Nature to find further information about the reuse of your content.

Authors have the right to reuse their article's Version of Record, in whole or in part, in their own thesis. Additionally, they may reproduce and make available their thesis, including Springer Nature content, as required by their awarding academic institution. Authors must properly cite the published article in their thesis according to current citation standards.
Material from: 'AUTHOR, TITLE, JOURNAL TITLE, published [YEAR], [publisher - as it appears on our copyright page]'

If you are any doubt about whether your intended re-use is covered, please contact journalpermissions@springernature.com for confirmation.

Self-Archiving

- Journal authors retain the right to self-archive the final accepted version of their manuscript. Please see our self-archiving policy for full details: https://www.springer.com/gp/open-access/authors-rights/self-archiving-policy/2124

- Book authors please refer to the information on this link: https://www.springer.com/gp/open-access/publication-policies/self-archiving-policy

Journal of Statistical Physics (2020) 180:654–664
https://doi.org/10.1007/s10955-020-02492-5

Phase Diagram of the Quantum Random Energy Model

Chokri Manai[1] · **Simone Warzel**[1]

Received: 25 September 2019 / Accepted: 14 January 2020 / Published online: 23 January 2020

Abstract
We prove Goldschmidt's formula (Goldschmidt in Phys Rev B 47:4858–4861, 1990) for the free energy of the quantum random energy model. In particular, we verify the location of the first order and the freezing transition in the phase diagram. The proof is based on a combination of variational methods on the one hand, and bounds on the size of percolation clusters of large-deviation configurations in combination with simple spectral bounds on the hypercube's adjacency matrix on the other hand.

Keywords Disordered systems · Quantum spin glass · Phase transition

Mathematics Subject Classification 82D30 · 82B44

1 Introduction

The quantum random energy model (QREM) draws its motivation from various directions. In mathematical biology, it has been put forward as a simple model for the expression of genotypes under mutation in a random fitness landscape [4,14]. More recently, it gained attention as a basic testing ground of quantum annealing algorithms for searches in unstructured energy landscapes (cf. [6,18] and references therein) as well as in the context of many-body localization [5,9,15,19,25]. Its original motivation stems from the quest of understanding quantum effects in mean-field spin glasses [10,13,17,22,26].

The classical backbone, the random energy model (REM) was put forward by Derrida [11,12] in the early 1980s as the limiting and solvable case of a class of mean-field spin glasses. The space of N-bit strings $\mathcal{Q}_N = \{-1, 1\}^N$ serves as the configuration space of the REM. The energy associated with $\sigma = (\sigma_1, \ldots, \sigma_N) \in \mathcal{Q}_N$ is a rescaled Gaussian random variable

Communicated by Ivan Corwin.

This work was supported by the DFG under EXC-2111 – 390814868.

Simone Warzel
warzel@ma.tum.de

[1] MCQST & Zentrum Mathematik, Technische Universität München, Munich, Germany

$$U(\sigma) := \sqrt{N}\, g(\sigma)$$

with $g(\sigma)$ forming an independent and identically distributed (i.i.d.) process with standard normal law. $\mathcal{Q}_N$ may be interpreted as the state space of a system of N spin-$\frac{1}{2}$ quantum objects recorded, e.g., in the z-basis. The corresponding Hilbert space is given by the Nfold tensor product $\otimes_{j=1}^{N} \mathbb{C}^2$ which is unitarily equivalent to $\ell^2(\mathcal{Q}_N)$. Effects of a transversal (e.g. in the negative x-direction) constant magnetic field of strength $\Gamma \geq 0$ on the spins are taken into account through the componentwise flip operators $F_j\sigma := (\sigma_1, \ldots, -\sigma_j, \ldots, \sigma_N)$, which are implemented on $\psi \in \ell^2(\mathcal{Q}_N)$ as

$$(T\psi)(\sigma) := -\sum_{j=1}^{N} \psi(F_j\sigma).$$

This operator coincides with the negative sum of x-components of the Pauli matrices. The energy of the QREM is then given by an Anderson-type random matrix

$$H := \Gamma\, T + U \tag{1}$$

where U acts as a multiplication operator on $\ell^2(\mathcal{Q}_N)$.

The process $U(\sigma)$ is the limiting case $p \to \infty$ of the Gaussian family of p-spin models characterized by its mean and covariance function,

$$\mathbb{E}\,[U(\sigma)] = 0, \qquad \mathbb{E}\left[U(\sigma)U(\sigma')\right] = N\left(N^{-1}\sum_{j=1}^{N}\sigma_j\sigma'_j\right)^p =: N\xi_p(\sigma,\sigma'). \tag{2}$$

The case $p = 2$ corresponds to the famous Sherrington–Kirkpatrick model. The simplifying feature of the limit $p \to \infty$ is the lack of correlations. The quantum p-spin generalisation of the QREM is then given by the random matrix (1) in which U is a multiplication operator by the correlated field.

1.1 Main Result

In this paper, we will be interested in thermodynamic properties of the QREM which are encoded in its partition function

$$Z(\beta, \Gamma) := 2^{-N}\,\mathrm{Tr}\, e^{-\beta H}$$

at inverse temperature $\beta \in [0, \infty)$, or, equivalently, its pressure

$$p_N(\beta, \Gamma) := N^{-1}\ \ln Z(\beta, \Gamma). \tag{3}$$

Up to a factor of $-\beta^{-1}$, the latter coincides with the specific free energy.

In the thermodynamic limit $N \to \infty$ the pressure of the REM converges almost surely [7,11,12],

$$\lim_{N\to\infty} p_N(\beta, 0) = p^{\mathrm{REM}}(\beta) = \begin{cases} \frac{1}{2}\beta^2 & \text{if } \beta \leq \beta_c, \\ \frac{1}{2}\beta_c^2 + (\beta - \beta_c)\beta_c & \text{if } \beta > \beta_c. \end{cases} \tag{4}$$

It exhibits a freezing transition into a low-temperature phase characterized by the vanishing of the specific entropy above

$$\beta_c := \sqrt{2\ln 2}.$$

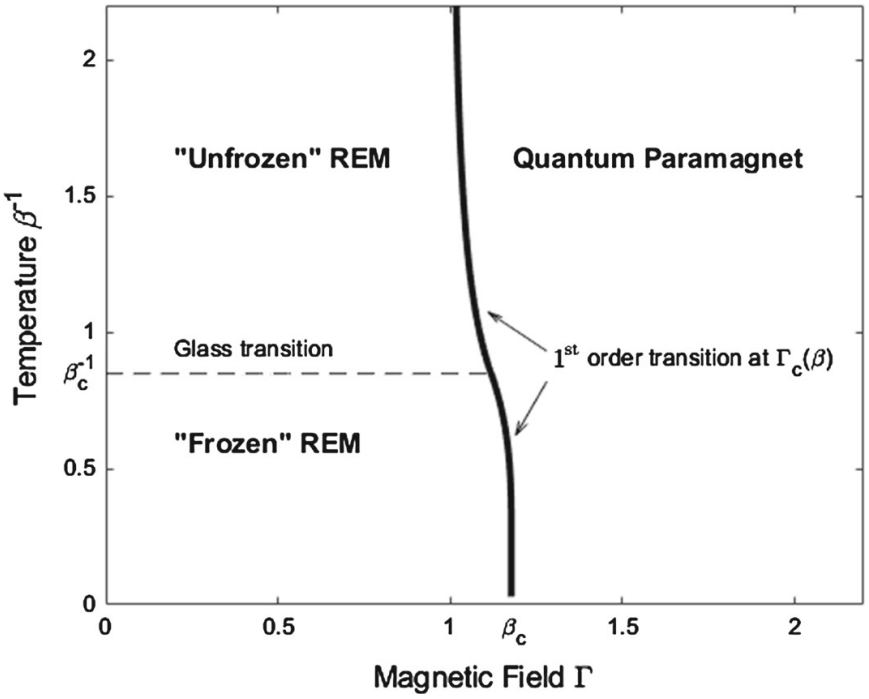

Fig. 1 Phase diagram of the QREM as a function of the transversal magnetic field Γ and the temperature β^{-1}. The first-order transition occurs at fixed β and $\Gamma_c(\beta)$. The freezing transition is found at temperature β_c^{-1}, which is unchanged in the presence of small magnetic field

Under the influence of the transversal field, the spin-glass phase of the REM disappears for large $\Gamma > 0$ and a first-order phase transition into a quantum paramagnetic phase characterised by

$$p^{\mathrm{PAR}}(\beta\Gamma) := \ln\cosh(\beta\Gamma)$$

is expected to occur. The precise location of this first-order transition and the shape of the phase diagram of the QREM has been predicted by Goldschmidt [17] in the 1990s on the basis of arguments using the replica trick and the so-called static approximation in the associated path integral. His calculations have been repeated and refined in various papers—all still based on the replica trick and further approximations [13,22] (see also [26] and references). As a main result of this paper, we give a rigorous proof of this result.

Theorem 1 *For any $\Gamma, \beta \geq 0$ almost surely:*

$$\lim_{N\to\infty} p_N(\beta, \Gamma) = \max\{p^{\mathrm{REM}}(\beta), p^{\mathrm{PAR}}(\beta\Gamma)\}.$$

As will become clear from the proof, which is found in Sect. 2 below, the special structure of the pressure as a maximum of competing extremal cases is mainly caused by the fact that the REM's energy landscape is steep and rough due to the lack of correlations. This renders the model solvable. Before diving into the details of the proof, let us add some comments (see also Fig. 1):

1. As in the classical case, the pressure $p_N(\beta, \Gamma)$ is self-averaging, i.e. in the thermodynamic limit it coincides with its probabilistic average, the so-called quenched pressure $\mathbb{E}[p_N(\beta, \Gamma)]$. For the QREM, this follows immediately from the Gaussian concentration inequality for Lipschitz functions. The Lipschitz constant of the pressure's variations with respect to the i.i.d. standard Gaussian variables $g(\sigma)$ is bounded by

$$\sum_{\sigma\in\mathcal{Q}_N}\left(\frac{\partial p_N(\beta,\Gamma)}{\partial g(\sigma)}\right)^2=\frac{\beta^2}{N\,2^{2N}Z(\beta,\Gamma)^2}\sum_{\sigma}\langle\sigma|e^{-\beta H}|\sigma\rangle^2\le\frac{\beta^2}{N}.$$

Here and in the following we use bracket notation for matrix elements. Consequently, we have the Gaussian tail estimate

$$\mathbb{P}\left(|p_N(\beta,\Gamma)-\mathbb{E}\left[p_N(\beta,\Gamma)\right]|>\frac{t\,\beta}{\sqrt{N}}\right)\le C\,\exp\left(-ct^2\right)\tag{5}$$

for all $t>0$ and all $N\in\mathbb{N}$ with some constants $c, C\in(0,\infty)$. In fact, self-averaging for more general quantum p-spin models has already been established in [10].

2. For fixed β a first-order phase transition is found at

$$\Gamma_c(\beta):=\beta^{-1}\,\mathrm{arcosh}\left(\exp\left(p^{\mathrm{REM}}(\beta)\right)\right).$$

In particular, $\Gamma_c(0)=1$ and $\Gamma_c(\beta_c)=\beta_c^{-1}\,\mathrm{arcosh}(2)$. In the low-temperature limit, $\lim_{\beta\to\infty}\Gamma_c(\beta)=\beta_c$, the first-order transition connects to the known location of the quantum phase transition of the ground state [18]. In this context, it is useful to recall that the REM's extreme energies are almost surely found at $\|U\|_\infty=\beta_c N+o(N)$, cf. [7, Ch. 9]. For $\Gamma<\beta_c$, the energetically separated ground state is sharply localized near the lowest-energy configuration of the REM. For $\Gamma>\beta_c$, the energetically separated ground state resembles the maximally delocalized state given by the ground state of T. Near $\Gamma=\beta_c$, the ground-state gap closes exponentially [1].

3. For $\Gamma>\Gamma_c(\beta)$, the magnetization in the x-direction is strictly positive,

$$\beta^{-1}\,\frac{\partial}{\partial\Gamma}\,p^{\mathrm{PAR}}(\beta\Gamma)=\tanh(\beta\Gamma)>0.$$

4. For all $\Gamma<\Gamma_c(\beta)$ the line of the freezing transition transition remains unchanged at $\beta=\beta_c$. In the frozen regime, the QREM has zero specific entropy.

1.2 Comments and Open Problems

We close the introduction with some further comments and open problems:

1. For the quantum p-spin model it is conjectured that the structure of the phase diagram in Fig. 1 only changes smoothly in $1/p$ at low temperatures (see e.g. [13]). Non-rigorous $1/p$ expansions in a replica analysis have been the basis of these assertions. (A tiny step towards a proof of the continuity of the pressure at $p=\infty$ has been undertaken recently on the basis of the methods presented here in [21].)
   Such expansion-based arguments have been extended in [22] to cover the case of ferromagnetic bias, in which the Gaussian spin-p couplings are tilted towards a ferromagnetic interaction. The paper [22] argues that the spin glass phase will also disappear in favour of a ferromagnetic phase for sufficiently large tilting.
2. As in the classical case, the quenched pressure $\mathbb{E}\left[p_N(\beta,\Gamma)\right]$ is generally smaller than the annealed pressure $N^{-1}\ln\mathbb{E}\left[Z(\beta,\Gamma)\right]$. However, in the high-temperature phase, $\beta<\beta_c$, asymptotic equality holds—even in the quantum case as is not hard to show by performing the annealed average in the path-integral representation. The fluctuation properties of the partition function are well studied in classical cases (see e.g. [3,8] and [7, Ch. 9–10] for further references). We leave it to a future work to extend these results to the quantum case.

3. For a large class of mean-field spin glasses, the pressure in the thermodynamic limit is known to be universal in that it does not depend on the details of the randomness (cf. [28] and references therein). Such universality results have been extended to the quantum case in [10].
4. Most recently, there has been some progress in understanding the free energy of the quantum Sherrington–Kirkpatrick model. The absence of a spin-glass phase for high temperatures was addressed in [20]. In particular, it is shown that in the high-temperature phase the quenched pressure asymptotically coincides with the annealed pressure thereby generalising some of the results in [3]. The paper [2] identified the thermodynamic limit of the quenched pressure with a certain limit of a variational principle involving classical vector-spin glasses.

2 Proof

The proof of Theorem 1 consists of a pair of asymptotically coinciding upper and lower bounds.

Proof of Theorem 1 The assertion is a consequence of Lemma 1 and Corollary 1 below. □

The following two subsections contain the details of the argument.

2.1 Lower Bound

Not surprisingly, our lower bound is more robust and will hold for more general p-spin models also. Let us first recall that if $U(\sigma)$ is a Gaussian random field of the form (2) with $p \in [1, \infty]$, then its pressure

$$p^{\mathrm{U}}(\beta) := \lim_{N\to\infty} N^{-1} \ln 2^{-N} \sum_{\sigma\in\mathcal{Q}_N} e^{-\beta U(\sigma)} \tag{6}$$

is known to converge almost surely to a non-random expression, which is in fact given by the famous Parisi formula [23,24,27,28]. In the special case $p = \infty$ this reduces to $p^{\mathrm{U}}(\beta) = p^{\mathrm{REM}}(\beta)$.

Lemma 1 *Consider the quantum p-spin model, i.e. $H = \Gamma T + U$ with U diagonal and Gaussian of the form (2) with $p \in [1, \infty]$. For any $\Gamma, \beta \geq 0$ and almost surely*

$$\liminf_{N\to\infty} p_N(\beta, \Gamma) \geq \max\{p^{\mathrm{U}}(\beta), p^{\mathrm{PAR}}(\beta\Gamma)\}. \tag{7}$$

Proof We use the Gibbs variational principle,

$$\ln \mathrm{Tr}\, e^{-\beta H} = -\inf_{\varrho} \left[\beta\, \mathrm{Tr}\, (H\varrho) + \mathrm{Tr}\, (\varrho \ln \varrho)\right] \tag{8}$$

in which the infimum is taken over all density matrices, $\varrho \geq 0$, $\mathrm{Tr}\, \varrho = 1$, on $\ell^2(\mathcal{Q}_N)$. There are two natural choices:

1. We may pick $\varrho = e^{-\beta U}/\mathrm{Tr}\, e^{-\beta U}$. In this case, the right-hand side is lower bounded by

$$\ln \mathrm{Tr}\, e^{-\beta U} - \beta\Gamma \mathrm{Tr}\, (T\varrho) = \ln \mathrm{Tr}\, e^{-\beta U}.$$

The last step follows from the fact that the diagonal matrix elements of T vanish. Consequently, we arrive at the bound,

$$p_N(\beta, \Gamma) \geq \frac{1}{N} \ln \left(\frac{1}{2^N} \sum_{\sigma \in \mathcal{Q}_N} e^{-\beta U(\sigma)} \right),$$

which together with the known convergence (6) yields the first part of the claim.

2. We may also pick $\varrho = e^{-\beta\Gamma T}/\mathrm{Tr}\, e^{-\beta\Gamma T}$. In this case, the right-hand side in (8) reduces to

$$\ln \mathrm{Tr}\, e^{-\beta\Gamma T} - \beta\, \mathrm{Tr}\, (U\varrho) = N \ln (2\cosh(\beta\Gamma)) - \frac{\beta}{2^N} \sum_{\sigma \in \mathcal{Q}_N} U(\sigma),$$

where we used $\langle \sigma | e^{-\beta\Gamma T} | \sigma \rangle = \cosh(\beta\Gamma)^N$ for the diagonal matrix element of the semigroup generated by $-T$. Consequently, we arrive at the bound,

$$p_N(\beta, \Gamma) \geq p^{\mathrm{PAR}}(\beta\Gamma) - \frac{\beta}{N2^N} \sum_{\sigma \in \mathcal{Q}_N} U(\sigma).$$

The last term converges to zero almost surely by the strong law of large numbers. More precisely, for any $\varepsilon > 0$, an exponential Chebychev bound yields

$$\begin{aligned} \mathbb{P}\left(\frac{1}{N2^N} \sum_{\sigma \in \mathcal{Q}_N} U(\sigma) > \varepsilon \right) &\leq e^{-N\varepsilon^2/2}\, \mathbb{E}\left[\exp\left(\frac{\varepsilon}{2^{N+1}} \sum_{\sigma \in \mathcal{Q}_N} U(\sigma) \right) \right] \\ &= e^{-N\varepsilon^2/2} \exp\left(\frac{\varepsilon^2}{2^{2(N+1)}} \sum_{\sigma,\sigma'} N\, \xi_p(\sigma, \sigma') \right) \\ &\leq e^{-N\varepsilon^2/4}. \end{aligned}$$

The same bound also applies to $-\sum_\sigma U(\sigma)$. Since the right-hand side is summable in N, a Borel–Cantelli argument ensures the claimed almost-sure convergence.

□

2.2 Upper Bound

Typical values of the REM $U(\sigma)$ fluctuate on order $\mathcal{O}(\sqrt{N})$. Our upper bound rests on the observation that configurations on which large negative deviations occur,

$$\mathcal{L}_\varepsilon := \left\{ \sigma \in \mathcal{Q}_N \,\middle|\, U(\sigma) \leq -\varepsilon N \right\}, \tag{9}$$

form gap-connected clusters whose maximal size remains bounded uniformly in N even for $\varepsilon > 0$ arbitrarily small. For the precise formulation of this result, it is useful to recall that the Hamming distance

$$d(\sigma, \sigma') := \sum_{j=1}^{N} 1\left[\sigma_j \neq \sigma'_j \right]$$

renders $\mathcal{Q}_N$ (through the nearest-neighbour relation) into a graph called the Hamming cube, in which each vertex has exactly N neighbours. For future purposes, we also introduce the Hamming ball of radius $r \in [0, N]$ centered at $\sigma \in \mathcal{Q}_N$,

$$B_r(\sigma) := \left\{\sigma' \in \mathcal{Q}_N \,\middle|\, d(\sigma,\sigma') \le r\right\}.$$

Its volume $|B_r|$ is known to be bounded by $\exp(N\gamma(r/N))$ for all $r < N/2$ in terms of the binary entropy, $\gamma(\xi) := -\xi\ln\xi - (1-\xi)\ln(1-\xi)$. Here, a simpler bound is sufficient:

$$|B_r| = \sum_{j=0}^{r}\binom{N}{j} \le \sum_{j=0}^{r}\frac{N^j}{j!} \le e\,N^r. \tag{10}$$

Definition 1 Let $\widetilde{\mathcal{Q}}_N$ be the supergraph of the Hamming cube $\mathcal{Q}_N$, which one obtains by adding the edges $\{\sigma,\sigma'\}$, where σ,σ' are two vertices with $d(\sigma,\sigma') = 2$. We call $\mathcal{C}_\varepsilon \subset \mathcal{L}_\varepsilon$ a gap-connected component, if $\mathcal{C}_\varepsilon$ is connected as a subset of $\widetilde{\mathcal{Q}}_N$. A gap-connected component $\mathcal{C}_\varepsilon$ is maximal if there is no other vertex $\sigma \in \mathcal{L}_\varepsilon\backslash\mathcal{C}_\varepsilon$ such that $\mathcal{C}_\varepsilon \cup \{\sigma\}$ forms a gap-connected component.

For each realisation of the randomness the large-deviation set then naturally decomposes into a finite (edge-)disjoint union of maximally gap-connected components,

$$\mathcal{L}_\varepsilon = \bigcup_\alpha \mathcal{C}_\varepsilon^{(\alpha)}.$$

On any gap-connected component $\mathcal{C}_\varepsilon$ for every vertex $\sigma \in \mathcal{C}_\varepsilon$ there is some $\sigma' \in \mathcal{C}_\varepsilon\backslash\{\sigma\}$ with $d(\sigma,\sigma') \in \{1,2\}$ – not necessarily $d(\sigma,\sigma') = 1$. By construction, we thus have for all $\alpha \neq \alpha'$:

$$d\left(\mathcal{C}_\varepsilon^{(\alpha)}, \mathcal{C}_\varepsilon^{(\alpha')}\right) = \min\left\{d(\sigma,\sigma') \,|\, \sigma \in \mathcal{C}_\varepsilon^{(\alpha)} \wedge \sigma' \in \mathcal{C}_\varepsilon^{(\alpha')}\right\} > 2. \tag{11}$$

The next lemma controls with good probability the size of each subset $\mathcal{C}_\varepsilon^{(\alpha)}$, which is just the number of its vertices and denoted by $|\mathcal{C}_\varepsilon^{(\alpha)}|$.

Lemma 2 *For all $\varepsilon > 0$ and $N \in \mathbb{N}$ there is some subset $\Omega_{\varepsilon,N}$ of realizations such that:*

1. *for some $c_\varepsilon > 0$, which is independent of N, and all N large enough:*

$$\mathbb{P}\left(\Omega_{\varepsilon,N}\right) \ge 1 - e^{-c_\varepsilon N},$$

2. *on $\Omega_{\varepsilon,N}$:* $\max_\alpha \left|\mathcal{C}_\varepsilon^{(\alpha)}\right| < K_\varepsilon := \left\lceil \frac{4\ln 2}{\varepsilon^2} \right\rceil$.

Proof We start by noting that the event

$$\Omega_{\varepsilon,N} := \bigcap_{\sigma_\in \mathcal{Q}_N} \left\{\left|B_{r_\varepsilon}(\sigma) \cap \mathcal{L}_\varepsilon\right| < K_\varepsilon\right\} \tag{12}$$

with $r_\varepsilon := 4K_\varepsilon$ implies the second assertion in the lemma. This follows from the fact that in the event $\Omega_{\varepsilon,N}$, in which there are at most $K_\varepsilon - 1$ large deviation sites in the ball of radius r_ε around any fixed $\sigma \in \mathcal{L}_\varepsilon$, the gap-connected component to which σ belongs, must be strictly contained in a ball of radius at most $2(K_\varepsilon - 1) < r_\varepsilon - 2$, i.e. it cannot gap-connect to other vertices outside the ball $B_{r_\varepsilon}(\sigma)$ and hence consists of at most K_ε vertices.

It therefore remains to estimate the probability of the event complementary to $\Omega_{\varepsilon,N}$. Using the union bound we obtain:

$$\begin{aligned}
\mathbb{P}\left(\bigcup_{\sigma\in\mathcal{Q}_N}\left\{\left|B_{r_\varepsilon}(\sigma)\cap\mathcal{L}_\varepsilon\right|\geq K_\varepsilon\right\}\right) &\leq \sum_{\sigma\in\mathcal{Q}_N}\mathbb{P}\left(\left|B_{r_\varepsilon}(\sigma)\cap\mathcal{L}_\varepsilon\right|\geq K_\varepsilon\right)\\
&\leq \sum_{\sigma\in\mathcal{Q}_N}\sum_{j=K_\varepsilon}^{|B_{r_\varepsilon}|}\mathbb{P}\left(\left|B_{r_\varepsilon}(\sigma)\cap\mathcal{L}_\varepsilon\right|=j\right)\\
&\leq 2^N\sum_{j=K_\varepsilon}^{|B_{r_\varepsilon}|}\binom{|B_{r_\varepsilon}|}{j}e^{-j\varepsilon^2N/2}\leq 2^N\sum_{k=K_\varepsilon}^{\infty}\frac{|B_{r_\varepsilon}|^j}{j!}e^{-j\varepsilon^2N/2}\\
&\leq 2^N\frac{|B_{r_\varepsilon}|^{K_\varepsilon}}{K_\varepsilon!}e^{-K_\varepsilon\varepsilon^2N/2}\exp\left(|B_{r_\varepsilon}|e^{-\varepsilon^2N/2}\right)\\
&\leq \frac{|B_{r_\varepsilon}|^{K_\varepsilon}}{K_\varepsilon!}e^{-K_\varepsilon\varepsilon^2N/4}\exp\left(|B_{r_\varepsilon}|e^{-\varepsilon^2N/2}\right). \qquad (13)
\end{aligned}$$

Here the third line relies on the fact that the number of subsets of a given size equals the binomial coefficient. Moreover, specifying the large-deviation sites in $B_{r_\varepsilon}(\sigma)$ allows one to compute the probability of the event using the independence of the random field $U(\sigma)$. To estimate this probability, we use the elementary estimate on the complementary error function,

$$\mathbb{P}(\sigma\in\mathcal{L}_\varepsilon)=\int_{-\infty}^{-\varepsilon\sqrt{N}}e^{-x^2/2}\frac{dx}{\sqrt{2\pi}}\leq e^{-\varepsilon^2N/2}, \qquad (14)$$

as well as the trivial bound on the probability of the complementary elementary event. The last inequality in the second line of (13) results from a simple bound on the binomial coefficient. The forth line is the standard estimate of the remainder of the exponential series. Finally, the last line follows by definition of K_ε. Since the volume of the ball $|B_{r_\varepsilon}|$ grows only polynomially in N by (10), the right-hand side of (13) is exponentially bounded for large enough N. This completes the proof. □

Our main idea behind an upper bound on the partition function $Z(\beta,\Gamma)$ is to decompose H into the multiplication operator U restricted to vertices in $\mathcal{L}_\varepsilon$ and the QREM H restricted to the complementary set $\mathcal{L}_\varepsilon^c$ plus a remainder term $A_{\mathcal{L}_\varepsilon}$. For this purpose, we write $\ell^2(\mathcal{Q}_N)=\ell^2(\mathcal{L}_\varepsilon)\oplus\ell^2(\mathcal{L}_\varepsilon^c)$ and set $U_{\mathcal{L}_\varepsilon}$ the multiplication operator by the REM values on $\ell^2(\mathcal{L}_\varepsilon)$. On the orthogonal complement $\ell^2(\mathcal{L}_\varepsilon^c)$, we define the natural restriction of (1). Note that $-T$ is the adjacency matrix on the Hamming cube. In the restriction $H_{\mathcal{L}_\varepsilon^c}$, we simply restrict the adjacency matrix to the subgraph associated with $\mathcal{L}_\varepsilon^c$. We then define $A_{\mathcal{L}_\varepsilon}$ through:

$$H=:U_{\mathcal{L}_\varepsilon}\oplus H_{\mathcal{L}_\varepsilon^c}-\Gamma A_{\mathcal{L}_\varepsilon}. \qquad (15)$$

Clearly, the matrix elements of the remainder term are related to all edges reaching $\mathcal{L}_\varepsilon$:

$$\langle\sigma|A_{\mathcal{L}_\varepsilon}|\sigma'\rangle=\begin{cases}1 & \text{if } \sigma\in\mathcal{L}_\varepsilon \text{ or } \sigma'\in\mathcal{L}_\varepsilon \text{ and } d(\sigma,\sigma')=1,\\ 0 & \text{else.}\end{cases} \qquad (16)$$

The following lemma contains an estimate on the operator norm of the remainder. In case the components in the decompositions are of small size, this estimate is not so wasteful.

Lemma 3 *Let $\mathcal{L}_\varepsilon=\bigcup_\alpha\mathcal{C}_\varepsilon^{(\alpha)}$ stand for a finite (edge-)disjoint union of maximally gap-connected components of the large deviation set (9). Then*

$$\left\|A_{\mathcal{L}_\varepsilon}\right\|\leq\sqrt{2N\max_\alpha\left|\mathcal{C}_\varepsilon^{(\alpha)}\right|}. \qquad (17)$$

Proof Since the components are edge-disjoint in the sense that (11) holds, we have

$$\left\| A_{\mathcal{L}_\varepsilon} \right\| = \max_\alpha \left\| A_{\mathcal{C}_\varepsilon^{(\alpha)}} \right\|,$$

where the operators in the right-hand side satisfy (16) with $\mathcal{L}_\varepsilon$ substituted by $\mathcal{C}_\varepsilon^{(\alpha)}$. Consequently, their operator norms are bounded by a Frobenius estimate

$$\left\| A_{\mathcal{C}_\varepsilon^{(\alpha)}} \right\| \leq \sqrt{\sum_{\sigma,\sigma'} \left| \langle \sigma | A_{\mathcal{C}_\varepsilon^{(\alpha)}} | \sigma' \rangle \right|^2}.$$

Since the double sum is restricted to $\sigma \in \mathcal{C}_\varepsilon^{(\alpha)}$ or $\sigma' \in \mathcal{C}_\varepsilon^{(\alpha)}$ and, in each of the two cases, the other sum has at most N terms, the assertion follows. □

The fact that the operator norm in the preceding lemma does not scale with N might sound remarkable at first sight. However, we remind the reader that even the full adjacency matrix $-T_{B_{N\rho}}$ restricted to a Hamming ball of radius $N\rho$ with $\rho \in (0, 1/2)$, is known [16] to be bounded by $\left\| T_{B_{N\rho}} \right\| \leq 2N\sqrt{\rho(1-\rho)} + o(N)$.

We are now ready to conclude our asymptotically sharp upper bound.

Corollary 1 *For any $\Gamma, \beta \geq 0$ almost surely:*

$$\limsup_{N\to\infty} p_N(\beta, \Gamma) \leq \max\left\{ p^{\mathrm{REM}}(\beta),\, p^{\mathrm{PAR}}(\beta\Gamma) \right\}.$$

Proof We pick $\varepsilon > 0$ arbitrarily small and start from the decomposition (15) of the Hamiltonian. The Golden–Thompson inequality yields

$$\begin{aligned} Z(\beta, \Gamma) &\leq 2^{-N} \operatorname{Tr} e^{-\beta U_{\mathcal{L}_\varepsilon} \oplus H_{\mathcal{L}_\varepsilon^c}}\, e^{-\beta\Gamma A_{\mathcal{L}_\varepsilon}} \\ &\leq 2^{-N}\, e^{\beta\Gamma \| A_{\mathcal{L}_\varepsilon} \|} \left(\operatorname{Tr}_{\ell^2(\mathcal{L}_\varepsilon)} e^{-\beta U_{\mathcal{L}_\varepsilon}} + \operatorname{Tr}_{\ell^2(\mathcal{L}_\varepsilon^c)} e^{-\beta H_{\mathcal{L}_\varepsilon^c}} \right). \end{aligned}$$

The first term in the bracket on the right-hand side is trivially estimated in terms of the partition function of the REM:

$$2^{-N} \operatorname{Tr}_{\ell^2(\mathcal{L}_\varepsilon)} e^{-\beta U_{\mathcal{L}_\varepsilon}} \leq Z(\beta, 0) = e^{N p_N(\beta, 0)}.$$

For the second term we use the fact that the adjacency matrix $-T_{\mathcal{L}_\varepsilon^c}$ has non-negative matrix elements and hence generates a positivity preserving semigroup on $\ell^2(\mathcal{L}_\varepsilon^c)$. Since the diagonal values of its perturbation are bounded from below by $-\varepsilon N$ by assumption on $\mathcal{L}_\varepsilon^c$, we conclude

$$\begin{aligned} 2^{-N} \operatorname{Tr}_{\ell^2(\mathcal{L}_\varepsilon^c)} e^{-\beta H_{\mathcal{L}_\varepsilon^c}} &\leq e^{\beta\varepsilon N} 2^{-N} \operatorname{Tr}_{\ell^2(\mathcal{L}_\varepsilon^c)} e^{-\beta\Gamma T_{\mathcal{L}_\varepsilon^c}} \\ &\leq e^{\beta\varepsilon N} 2^{-N} \operatorname{Tr} e^{-\beta\Gamma T} = \exp\left(N \left(\beta\varepsilon + p^{\mathrm{PAR}}(\beta\Gamma) \right) \right). \end{aligned}$$

Here, the last inequality follows from the monotonicity of $e^{-\beta\Gamma T_{\mathcal{L}_\varepsilon^c}}$ with respect to $\mathcal{L}_\varepsilon^c$, which is in turn a consequence of the non-negativity of the matrix elements of the adjacency matrix. To summarize, we thus obtain

$$p_N(\beta, \Gamma) \leq \max\left\{ p_N(\beta, 0),\, \beta\varepsilon + p^{\mathrm{PAR}}(\beta\Gamma) \right\} + \tfrac{1}{N} \left(\beta\Gamma \left\| A_{\mathcal{L}_\varepsilon} \right\| + \ln 2 \right). \tag{18}$$

According to Lemma 2 there is some $\Omega_{\varepsilon,N}$ whose complementary probability is exponentially small in N and on which Lemma 3 guarantees that for all N large enough:

$$p_N(\beta, \Gamma) \leq \max\left\{ p_N(\beta, 0),\, p^{\mathrm{PAR}}(\beta\Gamma) \right\} + 2\beta\varepsilon\,.$$

Since the probabilities of the complementary event are summable in N, a Borel–Cantelli argument together with the known almost sure convergence (4) of the REM thus finishes the proof. □

Acknowledgements Open Access funding provided by Projekt DEAL.

References

1. Adame, J., Warzel, S.: Exponential vanishing of the ground-state gap of the QREM via adiabatic quantum computing. J. Math. Phys. **56**, 113301 (2014). https://doi.org/10.1063/1.4934723
2. Adihikar, A., Brennecke, C.: Free energy of the quantum Sherrington-Kirkpatrick spin-glass model with transverse field (2019). Preprint arXiv:1912.13041
3. Aizenman, M., Lebowitz, J., Ruelle, D.: Some rigorous results on the Sherrington-Kirkpatrick spin glass model. Commun. Math. Phys. **116**, 527–527 (1988). https://doi.org/10.1007/BF01229207
4. Baake, E., Wagner, H.: Mutation-selection models solved exactly with methods of statistical mechanic. Genet. Res. **78**, 93–117 (2001). https://doi.org/10.1017/S0016672301005110
5. Baldwin, C., Laumann, C., Pal, A., Scardicchio, A.: The many-body localized phase of the quantum random energy model. Phys. Rev. B **93**, 024202 (2015). https://doi.org/10.1103/PhysRevB.93.024202
6. Bapst, V., Foini, L., Krzakala, F., Semerjian, G., Zamponi, F.: The quantum adiabatic algorithm applied to random optimization problems: the quantum spin glass perspective. Phys. Rep. **523**, 127 (2012). https://doi.org/10.1016/j.physrep.2012.10.002
7. Bovier, A.: Statistical Mechanics of Disordered Systems: A Mathematical Perspective. Cambridge Series in Statistical and Probabilistic Mathematics. Cambridge University Press, Cambridge (2006). https://doi.org/10.1017/CBO9780511616808
8. Bovier, A., Kurkova, I., Löwe, M.: Fluctuations of the free energy in the REM and the p-spin SK model. Ann. Probab. **30**, 605–651 (2002). https://doi.org/10.1214/aop/1023481004
9. Burin, A.: Localization and chaos in a spin glass model with random fields: mapping to the localization problem in a Bethe lattice with a correlated disorder. Annalen der Physik. https://doi.org/10.1002/andp.201600292
10. Crawford, N.: Thermodynamics and universality for mean field quantum spin glasses. Commun. Math. Phys. **274**, 821–839 (2007). https://doi.org/10.1007/s00220-007-0263-x
11. Derrida, B.: Random-energy model: limit of a family of disordered models. Phys. Rev. Lett. **45**, 79–82 (1980). https://doi.org/10.1103/PhysRevLett.45.79
12. Derrida, B.: Random-energy model: an exactly solvable model of disordered systems. Phys. Rev. B **24**, 2613–2626 (1981). https://doi.org/10.1103/PhysRevB.24.2613
13. Dobrosavljevic, V., Thirumalai, D.: 1/p expansion for a p-spin interaction spin-glass model in a transverse field. J. Phys. A **23**(15), L767–L774 (1990). https://doi.org/10.1088/0305-4470/23/15/013
14. Eigen, M., Schuster, P.: The hypercycle. a principle of natural self-organization. Part A: emergence of the hypercycle. Die Naturwissenschaften **64 11**, 541–65 (1977)
15. Faoro, L., Feigel'man, M.V., Ioffe, L.: Non-ergodic extended phase of the quantum random energy model. Ann. Phys. **409**, 167916 (2019). https://doi.org/10.1016/j.aop.2019.167916
16. Friedman, J., Tillich, J.P.: Generalized Alon-Boppana theorems and error-correcting codes. SIAM J. Discret. Math. **19**, 700–718 (2005). https://doi.org/10.1137/S0895480102408353
17. Goldschmidt, Y.Y.: Solvable model of the quantum spin glass in a transverse field. Phys. Rev. B **41**, 4858–4861 (1990). https://doi.org/10.1103/PhysRevB.41.4858
18. Jörg, T., Krzakala, F., Kurchan, J., Maggs, A.: Simple glass models and their quantum annealing. Phys. Rev. Lett. **101**, 147204 (2008). https://doi.org/10.1103/PhysRevLett.101.147204

19. Laumann, C., Pal, A., Scardicchio, A.: Many-body mobility edge in a mean-field quantum spin glass. Phys. Rev. Lett. **113**, 200405 (2014). https://doi.org/10.1103/PhysRevLett.113.200405
20. Leschke, H., Rothlauf, S., Ruder, R., Spitzer, W.: The free energy of a quantum sherrington-kirkpatrick spin-glass model for weak disorder (2019). Preprint arXiv:1912.06633
21. Manai, C., Warzel, S.: The quantum random energy model as a limit of p-spin interactions (2019). Preprint arXiv:1912.02041
22. Obuchi, T., Nishimori, H., Sherrington, D.: Phase diagram of the p-spin-interacting spin glass with ferromagnetic bias and a transverse field in the infinite- p limit. J. Phys. Soc. Jpn. **76**, 054002 (2006). https://doi.org/10.1143/JPSJ.76.054002
23. Panchenko, D.: The Parisi formula for mixed p-spin models. Ann. Probab. **42**, 946 (2011). https://doi.org/10.1214/12-AOP800
24. Parisi, G.: Order parameter for spin-glasses. Phys. Rev. Lett. **50**, 1946–1948 (1983). https://doi.org/10.1103/PhysRevLett.50.1946
25. Smelyanskiy, V.N., Kechedzhi, K., Boixo, S., Neven, H., Altshuler, B.: Intermittency of dynamical phases in a quantum spin glass (2019). Preprint arXiv:1907.01609
26. Suzuki, S., Inoue, J.i., Chakrabarti, B.K., Inoue, J.i., Chakrabarti, B.K.: Quantum Ising Phases and Transitions in Transverse Ising Models -, 2. aufl. edn. Springer, Berlin (2012)
27. Talagrand, M.: The Parisi formula. Ann. Math. **163**(1), 221–263 (2006)
28. Talagrand, M.: Mean Field Models for Spin Glasses (Volume I + II), vol. 2nd, Rev. and enlarged edn. Springer, Berlin (2011)

A.2 Generalized random energy models in a transversal magnetic field: free energy and phase diagrams

Generalized random energy models in a transversal magnetic field: free energy and phase diagrams

Chokri Manai and Simone Warzel

A few years after introducing the REM [61,62], Derrida considered a natural generalization of the random energy model, the so called GREM [63, 64]. The GREM potential consists of finitely many REM type random variables acting on sub-blocks of the total Hamming cube, which results in a correlated, yet hierarchical energy landscape. The built-in hierarchical structure simplifies the analysis of the GREM crucially in comparison to the SK-model with a hidden hierarchy. However, the GREM still comprises a rich mathematical structure which turned out to be very similar to the behavior of the order parameter in the more involved SK model [39,40,152,153]. Thus, it is natural to consider it is quantum counterpart, the QGREM, to shed some light on the nature of quantum spin glasses. Core Article II provides a complete picture of the phase diagram in the QGREM.

Main Results

In this publication we determine the almost sure limit of the pressure in the k-level QGREM, even with a random transversal field, based on an inductive technique which we dubbed peeling principle. Our results reveal an instructive physical picture of the QGREM, namely the hierarchical erasure of spin glass order. More precisely, the phase diagram shows multiple magnetic phase transitions as the magnetic field strength increases. Starting from a purely classical GREM phase, the determining blocks of the GREM undergo consecutively a transition from a fully classical order to a fully paramagnetic order. These findings were apparently not known before, even in the physics literature. We further extend our results on the QGREM in two ways. First, we consider the so called non-hierarchical GREM citeBK06 in a transversal field, where we also compute the limit of pressure. As in the classical case, a hierarchical structure emerges as Parisi-type formula for the pressure. On the other hand, we deal with the CREM, that is, the continuous limit of the GREM consisting of infinitely many levels. Using interpolation methods, we again determine the pressure in the thermodynamic limit. The corresponding phase diagrams are of independent interest as the multiple phase transition of the GREM merge to one or two second order transitions for appropriate choices of the model's parameter.

Individual Contribution

I am the principal author of this article. It was my idea to consider the QGREM after we had finished our first work on the QREM [128]. I developed the first proof idea on how to determine the pressure in the QGREM and QCREM. The final publication -the presentation of the results, the structure of the proof section and the derivation of various technical lemmas - is a result of a close collaboration with my advisor Simone Warzel.

Permission to include:

Chokri Manai and Simone Warzel
Generalized random energy models in a transversal magnetic field: free energy and phase diagrams.
Probability and Mathematical Physics 3: 215–245 (2022).
https://doi.org/10.2140/pmp.2022.3.215.

PAPER ID: 200715-Warzel
(e.g., 160223-Doe)

msp

Consent to Publish

Title of Contribution (hereafter, the "Work"): Generalized random energy models in a transversal magnetic field: Free energy and phase diagrams
(please also fill out the paper ID code in the upper right corner of this form)

Author(s) [redacted]

Name of Series: *Probability and Mathematical Physics.*

Publisher: Mathematical Sciences Publishers.

I Preamble

1 **Mathematical Sciences Publishers** (hereafter, the "Publisher"), a California nonprofit corporation and the publishers of *Probability and Mathematical Physics*, requires authors of articles in its publications to provide a written Consent to Publish. The signed Consent to Publish gives the Publisher the permission of the Author(s) to publish the Work.

2 The Publisher hereby requests that each Author complete and return this form promptly so that the Work may be readied for publication.

II Consent to Publish; Warranty

3 The Author hereby agrees that the Publisher has the right to publish the Work as described herein. The medium in which the Work will be published may change over time with advances in technology.

4 The Author hereby agrees that the Publisher has a worldwide, unlimited right:

(a) to publish and distribute the Work in any form and in all media now known or hereafter discovered;

(b) to translate the Work and exercise all rights in all media in the resulting translations;

(c) to transfer or sublicense all the rights granted herein in whole or in part to third parties; and

(d) to accept and retain payment for such publications, translations, sublicenses, or transfers.

5 The Author warrants that the Work has not been published before, in any form except as a preprint, that the Work is not being concurrently submitted to and is not under consideration by or under agreement with another publication, that all Authors are properly credited, that no rights in the Work have previously been assigned, and that the Author has the right to grant the assignments and permissions herein. The Author also warrants that the Work is an original work, does not libel anyone, infringe anyone's copyright, or otherwise violate any statutory or common law rights.

III Other Reproductions of the Work

6 The Work may be reproduced by any means for educational and scientific purposes by the Author(s) or by others without fee or permission, with the exception that reproduction by services that collect fees for delivery of documents may be licensed only by the Publisher. The Author may use part or all of this Work or its image in any future works of his/her/their own. In any reproduction, the original publication by the Publisher must be credited in the following manner: "First published in *Probability and Mathematical Physics* in [volume and number, or year], published by Mathematical Sciences Publishers," and the copyright notice in proper form must be placed on all copies. Any publication or other form of reproduction not meeting these requirements will be deemed to be unauthorized.

7 After ten years past the initial publication of the Work in *Probability and Mathematical Physics*, the Author(s) may license the reproduction or republication of the Work, including by services that collect fees, as long as the Publisher is notified in writing prior to such licensing.

IV Assignment of Copyright

8 The Author(s) hereby assigns to the Publisher all copyright rights in the Work, worldwide, in any form, and in all media now known or hereafter discovered, subject only to the limitations within this Consent to Publish.

9 In the event of receiving any request to reprint or translate all or part of the Work, the Publisher shall seek to inform the Author.

V Option to Retain Copyright

10 If the Author(s) wishes to retain the copyright in this Work, in the Author's name or the name of a third party (e.g., employer), the Author may strike out the contents of Section IV "Assignment of Copyright" above. If copyright is not to be assigned to the Publisher, please indicate the name of the copyright holder(s):

.....

11 If the copyright holder is someone other than the Author, the Author shall deliver all documents and take all other actions reasonably necessary to evidence, perfect, or defend the Publisher's rights under this Consent to Publish. All other provisions of this Consent to Publish shall remain in full force and effect.

VI Signature

12 This form must be signed by each Author or, in the case of a work made for hire, by the Author's employer or other copyright holder.

13 This Agreement shall be governed by California law, and will be binding on, and inure to the benefit of, the Author's heirs and personal representatives and the Publisher's successors and assigns.

Please note: If the Work was created by U.S. Government employees in the scope of their official duties, the Work cannot be copyrighted, and Section IV of this agreement is void and of no effect. The Consent to Publish must nonetheless be signed.

Date: [redacted]

Signature: [redacted]

Author Name: [redacted]

Address: [redacted]

Please email a scan of the signed form, or mail a signed hardcopy to:

pmp@consent.msp.org

Mathematical Sciences Publishers
798 Evans Hall #3840
c/o Department of Mathematics
University of California
Berkeley, CA 94720-3840
United States

PROBABILITY and MATHEMATICAL PHYSICS

GENERALIZED RANDOM ENERGY MODELS IN A TRANSVERSAL MAGNETIC FIELD: FREE ENERGY AND PHASE DIAGRAMS

CHOKRI MANAI AND SIMONE WARZEL

3:2
2022

msp

PROBABILITY and MATHEMATICAL PHYSICS

msp

Vol. 3, No. 2, 2022
https://doi.org/10.2140/pmp.2022.3.215

GENERALIZED RANDOM ENERGY MODELS IN A TRANSVERSAL MAGNETIC FIELD: FREE ENERGY AND PHASE DIAGRAMS

CHOKRI MANAI AND SIMONE WARZEL

We determine explicit variational expressions for the quantum free energy of mean-field spin glasses in a transversal magnetic field, whose glass interaction is given by a hierarchical Gaussian potential as in Derrida's generalized random energy model (GREM), its continuous version (CREM), or the nonhierarchical GREM. The corresponding phase diagrams, which generally include glass transitions as well as transitions to quantum paramagnetic and mixed quantum-classical phases, are discussed. In the glass phase, the free energy is generally determined by both the parameters of the classical model and the transversal field.

1. Introduction

Studying the fate of spin glass physics with respect to quantum effects induced by a transversal field has been a topic of continuing interest in the physics community. In the past 10 years this subject received an additional boost due to its relevance as a testing ground for quantum adiabatic algorithms and for many-body localized systems [1; 6; 13; 23]. Ever since exact solutions of the free energy of mean-field spin glasses became available, Parisi's famous replica calculations [29; 33] have been extended to approximations of the quantum free energy. Notwithstanding numerous works (see, e.g., [12; 20; 30; 21; 37; 41]), an ultimate consensus on various aspects of quantum spin glasses such as the quantum Sherrington–Kirkpatrick (SK) model seems to be lacking even from the physics point of view. From the point of view of disordered many-body systems the field offers toy models for exotic behavior of many-body wave functions on Fock space. A hint to the existence of partially nonergodic states is provided by the results of this work.

Although the theory classical mean-field spin glasses became an established branch of probability [8; 22; 31; 39; 40], efforts of mathematicians in the area of quantum glasses are so far rather limited. Crawford [15] laid the foundations for the quantum SK model. For this model, by generalizing classical arguments from [3], the absence of replica symmetry breaking in the high-temperature regime was proved in [25], and, more recently, the existence of spin-glass order at low temperatures and transversal field could also be established [24]. Adhikari and Brennecke [2] used a path-integral approach and Parisi's formula for vector-spin models to rewrite the free energy of the quantum SK model as a rather involved variational problem in terms of infinite-dimensional path overlaps.

MSC2020: 82B44, 82D30.
Keywords: quantum spin glass, phase transition, free energy.

The main aim of this work is to derive reasonably explicit variational expressions, which allow us to determine the structure of the phase diagram, for the quantum versions of three classic hierarchical and related mean-field spin glasses: (i) Derrida's generalized random energy model (GREM) [18], (ii) its continuous version (CREM), and (iii) the nonhierarchical GREM by Bolthausen and Kistler [7]. These models were invented so as to incorporate the effects of correlations of energy levels into the oversimplified random energy model (REM) [16; 17]. The GREM's and CREM's built-in ultra-metric structure constitutes the backbone of Parisi's solution of the SK mean-field spin glass — a fact which received its mathematical blessing through Talagrand's proof [38] and further analysis of the Gibbs measure [31].

Although the built-in ultra-metric structure and the prearrangement of types in the GREM or CREM are somewhat artificial as long as one does not clarify the role of ultrametricity in quantum glasses, it is nevertheless surprising that no physics prediction exists for the quantum version of these classic hierarchical mean-field spin glasses. All the more so since in 1990, Goldschmidt presented his formula for the free energy of the quantum REM [21], which was recently confirmed through a mathematical analysis [26]. This gap is closed with the present paper. We find formulae which express the principle that the types decide within the groups whether to collectively follow the transversal field or stay in their classical order. The free energy is then computed as a minimum over all group decompositions. We call this principle *hierarchical peeling*. It is based purely on a combination of a probabilistic-geometric decomposition of the spin-configuration space and operator-theoretic techniques, which are further developments of ideas in [26; 27]. In passing, we also generalize basic interpolation techniques to the quantum set-up. These main new technical tools are presented in Section 2.

We start the paper with a short introduction to classical hierarchical models. The quantum free energy is then presented in Section 1B. The introduction closes with a discussion of the nonhierarchical GREM and its quantum Parisi-type formula. The proofs of the novel quantum formulae are postponed to Section 3.

1A. ***Classical GREM and CREM.*** The GREM and CREM potential U is a centered Gaussian process on the Hamming cube $\mathcal{Q}_N := \{-1, 1\}^N$, whose covariance matrix is given by

$$\mathbb{E}[U(\boldsymbol{\sigma})U(\boldsymbol{\sigma}')] = N A(q(\boldsymbol{\sigma}, \boldsymbol{\sigma}')), \tag{1-1}$$

where $A := [0, 1] \to [0, 1]$ is a nondecreasing, right-continuous, and normalized function, i.e., $A(1) = 1$, which does not depend on N. Moreover, q denotes the normalized lexicographic overlap of spin configurations $\boldsymbol{\sigma}, \boldsymbol{\sigma}' \in \mathcal{Q}_N$, i.e.,

$$q(\boldsymbol{\sigma}, \boldsymbol{\sigma}') := \begin{cases} 1 & \text{if } \boldsymbol{\sigma} = \boldsymbol{\sigma}', \\ \frac{1}{N}(\min\{1 \le i \le N; \sigma_i \ne \sigma_i'\} - 1) & \text{else .} \end{cases} \tag{1-2}$$

The induced metric $d_A(\boldsymbol{\sigma}, \boldsymbol{\sigma}') = \mathbb{E}[|U(\boldsymbol{\sigma}) - U(\boldsymbol{\sigma}')|^2]^{1/2}$ on the Hamming cube is an ultrametric.

In the GREM one further assumes that the distribution function A is a step function with $n \in \mathbb{N}$ jumps of height a_k at the values $0 = x_0 < x_1 < x_2 < \cdots < x_n = 1$. The Gaussian potential U can then be expressed in terms of independent standard Gaussian variables. To this end, one decomposes $\boldsymbol{\sigma} \in \mathcal{Q}_N$

into n blocks ("types"), $\boldsymbol{\sigma} = (\boldsymbol{\sigma}_1, \ldots, \boldsymbol{\sigma}_n)$, each of which is represented by a spin vector on a reduced Hamming cube,

$$\boldsymbol{\sigma}_k \in \mathcal{Q}_N^{(k)} := \{-1, 1\}^{\lceil x_k N\rceil - \lceil x_{k-1} N\rceil}, \quad k \in \{1, \ldots, n\}. \tag{1-3}$$

Introducing independent standard Gaussian variables $X_{\boldsymbol{\sigma}_1}, X_{\boldsymbol{\sigma}_1\boldsymbol{\sigma}_2}, \ldots, X_{\boldsymbol{\sigma}_1\boldsymbol{\sigma}_2\cdots\boldsymbol{\sigma}_n}$ one then rewrites

$$U(\boldsymbol{\sigma}) = \sqrt{N}(\sqrt{a_1} X_{\boldsymbol{\sigma}_1} + \sqrt{a_2} X_{\boldsymbol{\sigma}_1\boldsymbol{\sigma}_2} + \cdots + \sqrt{a_n} X_{\boldsymbol{\sigma}_1\boldsymbol{\sigma}_2\cdots\boldsymbol{\sigma}_n}) \tag{1-4}$$

in the sense of distributional equality. The pressure or negative free energy

$$\Phi_N(\beta) := \frac{1}{N} \ln Z_N(\beta)$$

is given in terms of the partition function $Z_N(\beta) := \sum_{\boldsymbol{\sigma}\in\mathcal{Q}_N} e^{-\beta U(\boldsymbol{\sigma})}$, and converges for any distribution function A almost surely [14]. The limit depends on the concave hull $\bar{A}$ of A, i.e., the smallest concave function which is greater than or equal to A. In the GREM, the concave hull $\bar{A}$ is a piecewise linear function determined by the values $\{y_0, y_1, \ldots, y_m\} \subset \{x_0, x_1, \ldots, x_n\}$ where A and $\bar{A}$ agree. The increments of the concave hull $\bar{a}_l := A(y_l) - A(y_{l-1})$, the interval lengths $L_l := y_l - y_{l-1}$, and the slopes $\gamma_l := \bar{a}_l / L_l$ determine the limit of the pressure, which is given by [19; 14]

$$\lim_{N\to\infty} \Phi_N(\beta) = \Phi(\beta) = \sum_{l=1}^{m} \varphi^{(l)}(\beta) \tag{1-5}$$

with the partial pressures

$$\varphi^{(l)}(\beta) := \begin{cases} \frac{1}{2}\beta^2 \bar{a}_l + L_l \ln 2 & \text{if } \beta \le \sqrt{(2\ln 2)\gamma_l^{-1}} =: \beta_l, \\ \beta\sqrt{(2\ln 2)\bar{a}_l L_l} & \text{if } \beta > \sqrt{(2\ln 2)\gamma_l^{-1}}. \end{cases} \tag{1-6}$$

(For future reference, we note that this formula still holds if the weights (a_k) do not add up to 1.) The glass transition in the GREM occurs in steps with the components of the systems' spins corresponding to l freezing at β_l. Since $\beta_m > \cdots > \beta_2 > \beta_1$, the highest freezing temperature is found at $\beta_c = \beta_1$.

The CREM includes distribution functions A which are not step functions. Since they can be represented as a (uniform) limit of step functions, it is not surprising that the corresponding limit of the pressure $\Phi(\beta)$ turns into an integral. The increments $\bar{a}_l$ are replaced by the right derivative $\bar{a}(x)$ of $\bar{A}(x)$ which exists everywhere as a consequence of the convexity of $\bar{A}$. This allows one to give an explicit expression for the limiting pressure [11; 8]

$$\Phi(\beta) = \sqrt{2\ln 2}\,\beta \int_0^{x(\beta)} \sqrt{\bar{a}(x)}\,dx + \frac{\beta^2}{2}(1 - \bar{A}(x(\beta))) + (1 - x(\beta))\ln 2 \tag{1-7}$$

with the function

$$x(\beta) := \sup\{x \mid \bar{a}(x) > (2\ln 2)/\beta^2\}. \tag{1-8}$$

The glass transition in the CREM occurs at $\beta_c = \sqrt{(2\ln 2)/\lim_{x\downarrow 0} \bar{a}(x)}$.

1B. ***Quantum GREM and CREM and a Parisi formula.*** If a transversal magnetic field in the x-direction is turned on, the total Hamiltonian acting on the Hilbert space $\ell^2(\mathcal{Q}_N)$, which is unitarily equivalent to the tensor product $\otimes_{j=1}^N \mathbb{C}^2$, is

$$H_N = U - B, \tag{1-9}$$

where B is the sum of the x-Pauli matrices $\boldsymbol{s}_j$ with (possibly random) weights $b_j \in \mathbb{R}$,

$$(B\psi)(\boldsymbol{\sigma}) := \sum_{j=1}^N b_j\, (\boldsymbol{s}_j\psi)(\boldsymbol{\sigma}), \qquad (\boldsymbol{s}_j\psi)(\boldsymbol{\sigma}) := \psi(\sigma_1, \ldots, -\sigma_j, \ldots, \sigma_N), \tag{1-10}$$

and U acts as a random potential. Before further specifying U and B, we record a simple observation: the quantum partition function $\operatorname{Tr} e^{-\beta(U-B)}$ and the diagonal matrix-elements of $e^{-\beta(U-B)}$ in terms of the standard orthonormal z-basis, $\{|\boldsymbol{\sigma}\rangle \mid \boldsymbol{\sigma} \in \mathcal{Q}_N\}$ for which $\langle \boldsymbol{\sigma}|\psi\rangle = \psi(\boldsymbol{\sigma})$, only depend on the absolute values $(|b_j|)$. Here and in the following we use Dirac's bra-ket notation for matrix elements and scalar products.

Lemma 1.1. *Let U be an arbitrary potential on $\mathcal{Q}_N$ and B, B' two transversal field with weights b_j and b'_j which only differ by a sign, i.e., $|b_j| = |b'_j|$ for all j. Then, for all $\boldsymbol{\sigma} \in \mathcal{Q}_N$:*

$$\langle \boldsymbol{\sigma}|e^{-\beta(U-B)}|\boldsymbol{\sigma}\rangle = \langle \boldsymbol{\sigma}|e^{-\beta(U-B')}|\boldsymbol{\sigma}\rangle. \tag{1-11}$$

Proof. Expanding the exponential, we write $\langle \boldsymbol{\sigma}|e^{-\beta(U-B)}|\boldsymbol{\sigma}\rangle$ as a convergent series of terms of the form

$$\langle \boldsymbol{\sigma}|A_1 \cdots A_k|\boldsymbol{\sigma}\rangle \tag{1-12}$$

where each A_j is either $-U$ or some $b_j\boldsymbol{s}_j$. As $\boldsymbol{s}_j$ flips the sign of the j-th coordinate σ_j, the term (1-12) vanishes unless each operator $\boldsymbol{s}_j$ occurs n_j times, where n_j is an even number. We conclude that $\langle \boldsymbol{\sigma}|e^{-\beta(U-B)}|\boldsymbol{\sigma}\rangle$ only depends on the squares b_j^2 which proves (1-11). □

If all the weights $b_i \geq 0$ are nonnegative, the Trotter product formula shows that H_N generates a positive semigroup, i.e., for any $t \geq 0$ and $\boldsymbol{\sigma}, \boldsymbol{\sigma}' \in \mathcal{Q}_N$,

$$\langle \boldsymbol{\sigma}|e^{-tH_N}|\boldsymbol{\sigma}'\rangle \geq 0.$$

This is in general not true for an arbitrary transversal magnetic field B, but due to Lemma 1.1 we can assume without loss of generality that the weights (b_j) are indeed nonnegative if we are only interested in properties which can be derived from diagonal matrix elements such as the quantum partition function.

In the remaining part of this section, we restrict ourselves to the case where the weights (b_j) are independent copies of an absolutely integrable random variable $\mathfrak{b}$ and they shall be independent of the Gaussian potentials U. We are mainly interested in the thermodynamic properties of the hierarchical quantum spin glasses which are encoded in the quantum partition function

$$Z_N(\beta, \mathfrak{b}) := \operatorname{Tr}[e^{-\beta H_N}]$$

or, equivalently, in the pressure (or negative free energy)

$$\Phi_N(\beta, \mathfrak{b}) := \frac{1}{N} \ln Z_N(\beta, \mathfrak{b}).$$

In the special case that the weights $\mathfrak{b} = \Gamma$ are (almost surely) constant, we will sometimes write $B = \Gamma T$ and denote the pressure by $\Phi_N(\beta, \Gamma)$.

Our first main result concerns the free energy of the QGREM. We show that the free energy converges almost surely to a nonrandom limit, for which we derive an explicit expression in terms of the classical partial free energies (1-6) and the paramagnetic free energy. With the notation of Section 1A, we have the following:

Theorem 1.2. *For the GREM specified by U as in (1-4) in terms of its distribution function A, any $\beta \geq 0$, and an absolutely integrable random variable $\mathfrak{b}$, the quantum free energy converges almost surely*:

$$\lim_{N\to\infty} \Phi_N(\beta, \mathfrak{b}) = \Phi(\beta, \mathfrak{b}) := \max_{0\leq k\leq m} \left[\sum_{l=1}^{k} \varphi^{(l)}(\beta) + (1 - y_k)\mathbb{E}\left[\ln(2\cosh(\beta\mathfrak{b}))\right] \right]. \tag{1-13}$$

The maximum is taken over all points $\{y_0, y_1, \ldots, y_m\}$ supporting the convex hull $\bar{A}$ of A.

The proof of this theorem is found in Section 3A. We stress that as in the classical case the concave hull $\bar{A}$, rather than A, remains the determining function for the limit. The second term in (1-13) is the pressure of the random quantum paramagnet given by

$$\begin{aligned} p(\beta\mathfrak{b}) &:= \frac{1}{N}\mathbb{E}\left[\ln \operatorname{Tr}\left[e^{\beta B}\right]\right] = \frac{1}{N}\mathbb{E}\left[\ln \prod_{j=1}^{N} \operatorname{Tr}\left[e^{\beta b_j s_j}\right]\right] \\ &= \frac{1}{N}\sum_{j=1}^{N} \mathbb{E}\left[\ln(2\cosh(\beta b_j))\right] = \mathbb{E}\left[\ln(2\cosh(\beta\mathfrak{b}))\right]. \end{aligned} \tag{1-14}$$

If $\mathfrak{b} = \Gamma > 0$ is constant, the structure of the limit in (1-13) becomes more transparent if we introduce the critical field strengths

$$\Gamma_c^{(l)} := \frac{1}{\beta} \operatorname{arcosh}\left(\frac{1}{2}\exp\left(\frac{\varphi^{(l)}(\beta)}{L_l}\right)\right), \quad l \in \{1, \ldots, m\}.$$

In this situation, we may rephrase (1-13) as follows:

Corollary 1.3. *In the situation of Theorem 1.2 with $\mathfrak{b} = \Gamma > 0$,*

$$\Phi(\beta, \Gamma) = \sum_{l=1}^{m} \left(\varphi^{(l)}(\beta)\, \mathbb{1}_{\Gamma<\Gamma_c^{(l)}} + L_l \ln(2\cosh(\beta\Gamma))\mathbb{1}_{\Gamma\geq\Gamma_c^{(l)}}\right). \tag{1-15}$$

The proof is again found in Section 3A. The free energy coincides with the sum of m weighted and rescaled QREM terms; see [21; 27]. In particular, there are as many magnetic first-order transitions as second-order glass transitions. The glass transitions continue to occur at the (classical) critical inverse

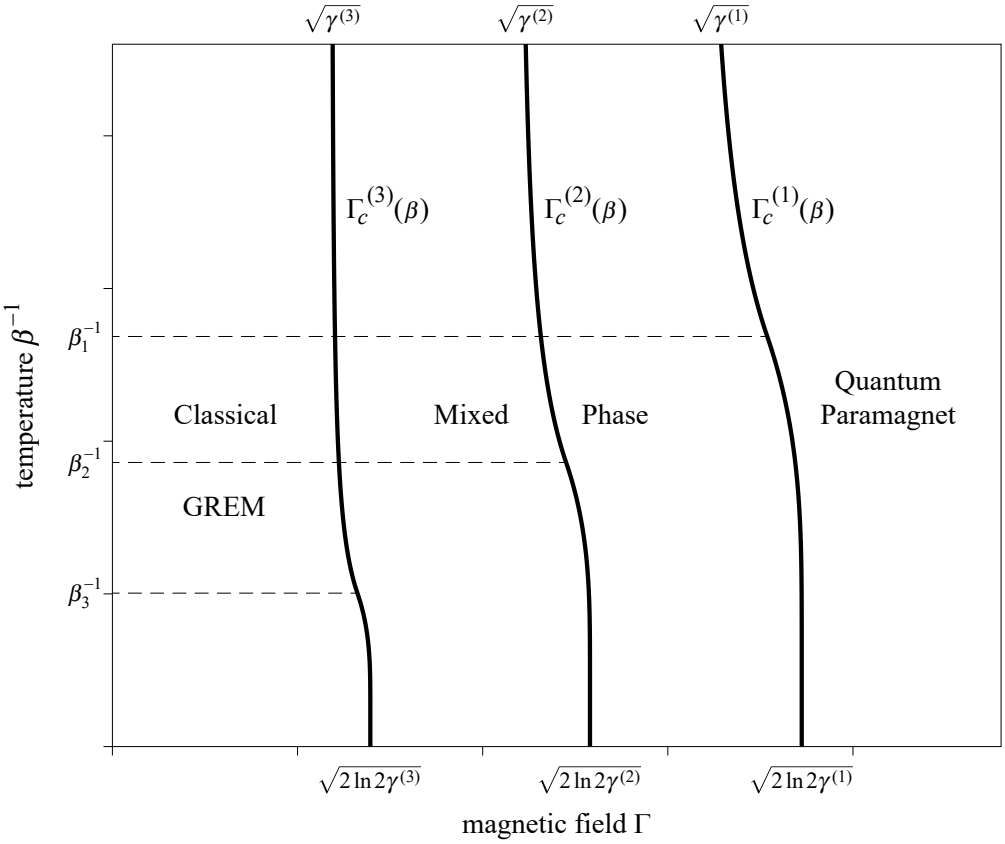

Figure 1. Phase diagram of the quantum GREM as a function of the transversal constant magnetic field Γ and the temperature β^{-1}. The figure shows an example with three second-order glass transitions (dotted lines) and three first-order magnetic transitions (bold lines). If $\Gamma < \Gamma_c^{(3)}(\beta_l)$, the free energy coincides with the classical one ($\Gamma = 0$), whereas, for $\Gamma > \Gamma_c^{(l)}(\beta_l)$, the system becomes a pure quantum paramagnet. In between mixed quantum-classical phases appear.

temperatures $\beta_l = \sqrt{(2\ln 2)\gamma_l^{-1}}$ as long as $\Gamma < \Gamma_c^{(l)}(\beta_l)$ and disappear for field strengths $\Gamma > \Gamma_c^{(l)}(\beta_l)$; see Figure 1. The specific magnetization in the x-direction

$$m_x(\beta, \Gamma) := \frac{1}{\beta}\frac{\partial}{\partial \Gamma}\Phi(\beta, \Gamma)$$

changes discontinuously at $\Gamma = \Gamma_c^{(l)}$. The physics described by (1-15) is that of the block or types of spins corresponding to l flipping into transversal order at $\Gamma = \Gamma_c^{(l)}$. At temperatures below β_l^{-1}, the transition is from spin-glass order to a quantum paramagnet in that block. At zero-temperature we find quantum phase transitions at $\Gamma = \lim_{\beta\to\infty} \Gamma_c^{(l)} = \sqrt{(2\ln 2)\gamma^{(l)}}$. It is an interesting question to determine the fate of Parisi's order parameter as well as the structure of the eigenvectors in the different low-temperature regimes. The picture suggested by our results on the free energy would point to functions which violate ergodicity partially in a mixed low-temperature phase in that they will be extended on a fraction of the Hamming cube only. The rigorous classical analysis of Parisi's order parameter for the GREM, which partially captures the geometric structure of the Gibbs measure, can be found in [10]. An extension of this analysis will be the subject of a future work.

Moving on to the more general CREM potentials, it is convenient to introduce truncated versions of the free energy in (1-7). For any $z \in [0, 1]$, we define

$$\Phi(\beta, z) := \sqrt{2\ln 2}\beta \int_0^{\min\{x(\beta),z\}} \sqrt{\bar{a}(x)}\, dx + \mathbb{1}_{z>x(\beta)}\left(\frac{\beta^2}{2}(\bar{A}(z) - \bar{A}(x(\beta))) + (z - x(\beta))\ln 2\right). \quad (1\text{-}16)$$

As in the quantum GREM, the free energy of the quantum CREM converges almost surely and the limit may be expressed as a variational formula involving $\Phi(\beta, z)$:

Theorem 1.4. *For the CREM specified by U as in (1-1) in terms of its distribution function A, let $\bar{A}$ be the concave hull of A, $\bar{a}$ the right-derivative of $\bar{A}$, $\Phi(\beta, z)$ as in (1-16) and $\mathfrak{b}$ an absolutely integrable random variable. Then, the quantum pressure $\Phi_N(\beta, \mathfrak{b})$ converges almost surely,*

$$\lim_{N\to\infty} \Phi_N(\beta, \mathfrak{b}) = \Phi(\beta, \mathfrak{b}) := \sup_{0\le z\le 1} [\Phi(\beta, z) + (1 - z)\mathbb{E}[\ln 2\cosh(\beta\mathfrak{b})]]. \quad (1\text{-}17)$$

The proof is found in Section 3A.

The free energy $\Phi_N(\beta, \mathfrak{b})$ does not only converge almost surely, but also in mean. This is a consequence of the usual Gaussian concentration of measure estimate, i.e., a special case of Proposition 2.9. If $\mathfrak{b}$ is even an L^r-random variable for some $r > 1$, the pressure even converges in r-th mean.

In order to determine the order of occurring magnetic phase transitions, we will replace the variational formula (1-17) in the case $\mathfrak{b} = \Gamma$ by a more explicit expression. To this end, we assume from now that the concave hull $\bar{A}$ is a continuously differentiable function different from the identity (in order to exclude the QREM situation). Since $\bar{a}(x(\beta)) = 2\ln 2/\beta^2$, $\Phi(\beta, z)$ is differentiable with respect to z with derivative

$$\frac{\partial\Phi(\beta, z)}{\partial z} = \sqrt{(2\ln 2)\bar{a}(z)}\ \beta\ \mathbb{1}_{z<x(\beta)} + \left(\ln 2 + \frac{\beta^2}{2}\bar{a}(z)\right)\mathbb{1}_{z\ge x(\beta)}.$$

We note that $\frac{\partial\Phi(\beta,\cdot)}{\partial z} : [0, 1] \to [s(\beta), t(\beta)]$ is a nondecreasing continuous function with values in the closed interval specified by its boundary values

$$s(\beta) := \frac{\partial\Phi(\beta, z)}{\partial z}\Big|_{z=1} \quad \text{and} \quad t(\beta) := \frac{\partial\Phi(\beta, z)}{\partial z}\Big|_{z=0}.$$

Corollary 1.5. *Let $g(\beta, \cdot) : [s(\beta), t(\beta)] \to [0, 1]$ be a (generalized) inverse of the derivative $\frac{\partial\Phi(\beta,z)}{\partial z}$ as a function of z. Then,*

$$\Phi(\beta, \Gamma) = \begin{cases} \Phi(\beta, 1), & p(\beta\Gamma) \le s(\beta), \\ \Phi(\beta, g_\beta(p(\beta\Gamma))) + (1 - g_\beta(p(\beta\Gamma)))p(\beta\Gamma), & s(\beta) < p(\beta\Gamma) < t(\beta), \\ p(\beta\Gamma), & t(\beta) \le p(\beta\Gamma), \end{cases} \quad (1\text{-}18)$$

with the paramagnetic pressure $p(\beta\Gamma) = \ln 2\cosh(\beta\Gamma)$.

Corollary 1.5 implies that there are either one or two magnetic phase transitions, depending on $s(\beta)$. If $s(\beta) = \ln 2$ or, equivalently, $\bar{a}(1) = 0$, we find a single magnetic phase transition at the critical magnetization

$$\Gamma_c^{(r)}(\beta) = \frac{1}{\beta}\operatorname{arcosh}\left(\frac{1}{2}e^{t(\beta)}\right).$$

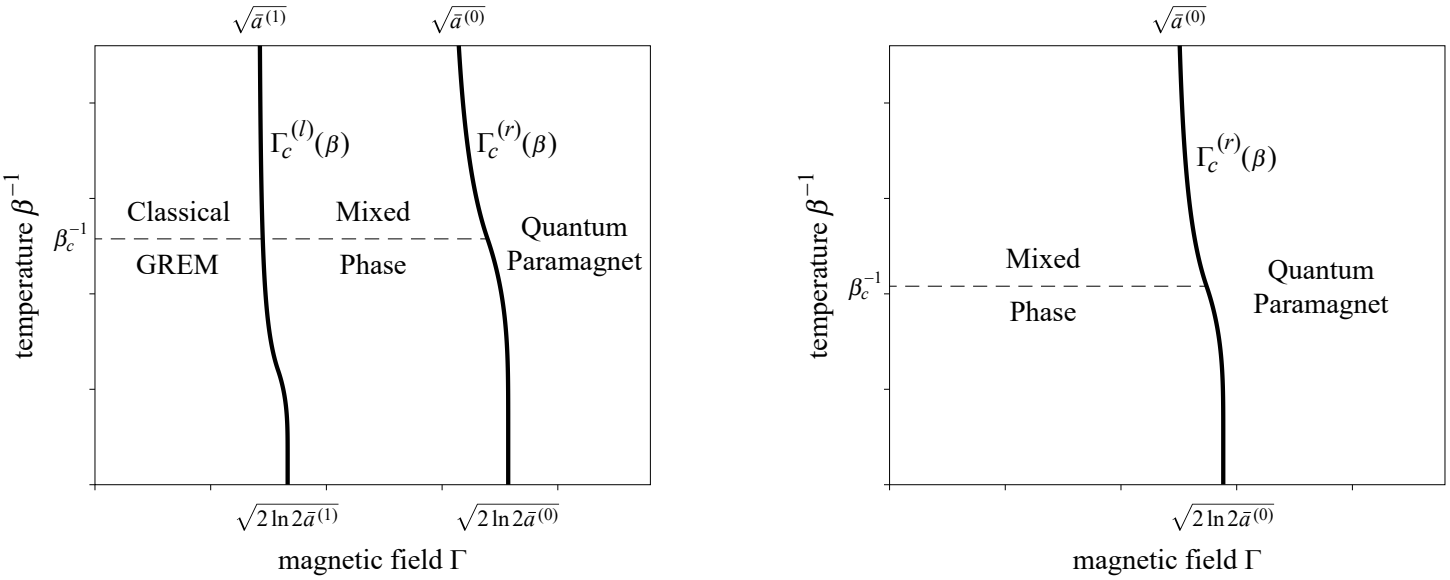

Figure 2. Both figures illustrate examples for the phase diagram of the quantum CREM as a function of the transversal magnetic field Γ and the temperature β^{-1}. The first plot contains two magnetic phase transitions (bold lines) into transversal magnetic order. The second plot shows the case of one magnetic phase transition. The dotted line corresponds to the glass transition at $\beta_c = \sqrt{(2\ln 2)/\bar{a}(0)}$. If $\bar{A}$ is continuously differentiable, the magnetic transitions are second order.

Otherwise, there is a second phase transition at

$$\Gamma_c^{(l)}(\beta) = \frac{1}{\beta}\operatorname{arcosh}\Big(\frac{1}{2}e^{s(\beta)}\Big).$$

An explicit computation using (1-18) shows that the specific magnetization in the transversal direction

$$m_x(\beta,\Gamma) = \frac{1}{\beta}\frac{\partial}{\partial\Gamma}\Phi(\beta,\Gamma) = \begin{cases} 0, & p(\beta\Gamma) \le s(\beta), \\ (1 - g_\beta(p(\beta\Gamma)))\tanh(\beta\Gamma), & s(\beta) < p(\beta\Gamma) < t(\beta), \\ \tanh(\beta\Gamma), & t(\beta) \le p(\beta\Gamma) \end{cases}$$

is continuous. This transversal magnetic order does not vanish over the line $\Gamma_c^{(r)}(\beta)$ but rather only at $\Gamma_c^{(l)}(\beta)$ (which is absent in the case $\bar{a}(1) = 0$). If the derivative of $\bar{a}(x)$ exists at $x = 0$ or $x = 1$, the second derivative of $\Phi(\beta,\Gamma)$ has a jump at the respective critical magnetic fields and we have a second-order magnetic transition and not first order as in the quantum GREM; see Figure 2. In the classical model, the low-temperature glass phase is described by a random probability measure which captures the distribution of the spin overlaps [8; 11]. As with the GREM, it is an interesting question, which will be postponed to a future work, to study the influence of the transversal field on these quantities as well as on the nature of the eigenstates.

1C. ***Quantum Parisi formula for the nonhierarchical GREM.*** The nonhierarchical GREM was introduced in [7] to illustrate Parisi's ultrametricity conjecture in an explicitly solvable model. We study the nonhierarchical GREM with a transverse field, since this is a basic test of whether our results in Section 2

are only strictly valid for hierarchical models or if one might hope that they still hold true to a certain extent for more complicated models. Indeed, we are again able to explicitly determine the free energy.

As in the GREM we write $\boldsymbol{\sigma} = \boldsymbol{\sigma}_1 \cdots \boldsymbol{\sigma}_n$ with $\boldsymbol{\sigma}_k \in \mathcal{Q}_N^{(k)}$ and $L_k = x_k - x_{k-1}$ are the corresponding interval lengths. We denote by $\mathcal{P}$ the power set of $\{1, \ldots, n\}$. To each subset $J = \{j_1, \ldots, j_m\} \in \mathcal{P}$ we assign the spin vector

$$\boldsymbol{\sigma}_J = \boldsymbol{\sigma}_{j_1} \cdots \boldsymbol{\sigma}_{j_m}$$

and a nonnegative number $a_J \geq 0$ with $a_\varnothing := 0$. We further assume that the numbers a_J add up to 1, $\sum_{J \in \mathcal{P}} a_J = 1$. For each $J \in \mathcal{P}$ we denote by $X^J_{\boldsymbol{\sigma}_J}$ independent standard Gaussian variables, which are also independent from each other for different superscripts $J_1 \neq J_2$. The total Gaussian process U of the nonhierarchical GREM on $\mathcal{Q}_N$ is then given by

$$U(\boldsymbol{\sigma}) := \sqrt{N} \sum_{J \in \mathcal{P}} \sqrt{a}_J X^J_{\boldsymbol{\sigma}_J}.$$

The GREM is the special case where $a_J \neq 0$ only if $J = \{1, \ldots, k\}$ for $k \in \{1, \ldots, n\}$.

In contrast to the GREM the induced metric $\mathbb{E}[|U(\boldsymbol{\sigma}) - U(\boldsymbol{\sigma}')|^2]^{1/2}$ does in general not satisfy ultrametricity. The hierarchical structure only emerges in the limit. For the formulation of the limiting free energy, we recall from [7] that a chain $S = \{A_0, A_1, A_2, \ldots, A_n\} \subset \mathcal{P}$ consists of nested sets A_i, i.e.,

$$\varnothing = A_0 \subset A_1 \subset A_2 \subset \cdots \subset A_n,$$

with cardinality $|A_i| = i$. To each chain $S = \{A_1, A_2, \ldots, A_n\}$ we assign a hierarchical GREM with weights

$$a_k^S := \sum_{D \subset A_k,\, D \not\subset A_{k-1}} a_D,$$

which satisfy $\sum_{k=1}^n a_k^S = 1$ for any chain S by construction, and endpoints

$$y_k^S := \sum_{j \in A_k} L_j.$$

The corresponding hierarchical GREM's pressure converges and we denote the limit by $\Phi(\beta, S)$. In [7], Bolthausen and Kistler showed that the limit of the pressure in the nonhierarchical GREM converges to a minimum of such GREMs,

$$\lim_{N \to \infty} \frac{1}{N} \ln \operatorname{Tr} e^{-\beta V} = \min_{S \in \mathcal{C}} \Phi(\beta, S), \tag{1-19}$$

where the minimum is taken over the set $\mathcal{C}$ of all chains.

After these preparations, we are able to consider the nonhierarchical GREM with a transverse magnetic field whose weights are independent copies of some random variable $\mathfrak{b}$. We define the pressure as before,

$$\Phi_N(\beta, \mathfrak{b}) := \frac{1}{N} \ln \operatorname{Tr} e^{-\beta(U - B)}.$$

The general theory developed in Section 2 also applies to the nonhierarchical GREM and yields:

Theorem 1.6. *Let $\beta \geq 0$ and $\mathfrak{b}$ an absolutely integrable random variable. Then, the pressure $\Phi_N(\beta, \mathfrak{b})$ converges almost surely and the limit is given by*

$$\Phi(\beta, \mathfrak{b}) := \lim_{N\to\infty} \Phi_N(\beta, \mathfrak{b}) = \max_{D\in\mathcal{P}} \min_{S\in\mathcal{C}^D} \left[\Phi_D(\beta, S) + \sum_{k\in D^c} L_k \, \mathbb{E}\left[\ln 2\cosh(\beta\mathfrak{b})\right] \right]. \tag{1-20}$$

Here, $\mathcal{C}^D$ denotes the set of chains which end at D, i.e., $S = \{A_0, A_1, \ldots, A_m\} \in \mathcal{C}^D$ if and only if

$$\varnothing = A_0 \subset A_1 \subset \cdots \subset A_m = D$$

and $|A_i| = i$ for any $1 \leq i \leq m$. Moreover, $\Phi_D(\beta, S)$ is the pressure of the corresponding GREM on the reduced hypercube associated to D.

The proof of this theorem is found in Section 3B.

The max-min structure of the limit in (1-20) seems to be quite universal as it also appears in the Parisi's formula for vector spin glasses [32]. This formula was used in [2] to obtain an expression for the limit in the quantum SK-model. However, there the maximum is essentially taken over the infinite-dimensional path overlap, which makes it hard to analyze. One might hope to find a less involved parametrization of the overlap distribution which is easier to access.

In fact, (1-20) can be further simplified, since the limit does only depend on a single chain.

Corollary 1.7. *There exists a chain $S \in \mathcal{C}$ such that for any $\beta \geq 0$ and any absolutely integrable variable $\mathfrak{b}$,*

$$\Phi(\beta, \mathfrak{b}) = \Phi(\beta, \mathfrak{b}, S). \tag{1-21}$$

Here $\Phi(\beta, \mathfrak{b}, S)$ denotes the pressure of quantum GREM assigned to S; see (1-13).

Corollary 1.7, whose proof is also found in Section 3B, shows that the nonhierarchical GREM in a transversal field is at least on a thermodynamical level equivalent to an ordinary quantum GREM.

2. Hierarchical peeling

In this section, we present the general principle, which we dubbed hierarchical peeling, from which the main results presented in the previous section will follow. We first describe the core of this idea in the binary setup.

2A. ***Peeling principle.*** We start by describing the general setting. Picking a parameter $0 < x \leq 1$, we will decompose the hypercube $\mathcal{Q}_N$ into two reduced hypercubes of spin arrays of length $\lceil xN \rceil$ and $N - \lceil xN \rceil$. Accordingly, we write

$$\boldsymbol{\sigma} = (\boldsymbol{\sigma}_1, \boldsymbol{\sigma}_2) \in \mathcal{Q}_N, \quad \text{where } \boldsymbol{\sigma}_1 \in \mathcal{Q}_N^{(1)} := \mathcal{Q}_{\lceil xN \rceil} \text{ and } \boldsymbol{\sigma}_2 \in \mathcal{Q}_N^{(2)} := \mathcal{Q}_{N-\lceil xN \rceil}.$$

We consider Hamiltonians $H = U - B$, where U is a random potential on $\mathcal{Q}_N$ and B is a random transversal field, which satisfy several assumptions. We start with U:

Assumption 2.1 (assumptions on U). The random potential U on $\mathcal{Q}_N$ takes the form

$$U(\boldsymbol{\sigma}) = V_N(\boldsymbol{\sigma}) + X_{\boldsymbol{\sigma}_1} \tag{2-1}$$

with some random potential V_N which is independent of the random process $X_{\boldsymbol{\sigma}_1}$. The random variables $X_{\boldsymbol{\sigma}_1}$ with $\boldsymbol{\sigma}_1 \in \mathcal{Q}_N^{(1)}$ are absolutely integrable, centered, and satisfy:

(1) $X_{\boldsymbol{\sigma}_1}$ are independent and identically distributed for each fixed $N \in \mathbb{N}$.

(2) The pushforward measures μ_N of the negative parts $X_{\boldsymbol{\sigma}_1}^-/N$ satisfy a large deviation principle (LDP) with a lower semicontinuous rate function $I : \mathbb{R} \to [0, \infty]$, i.e., for any Borel set $\mathcal{A} \subset \mathbb{R}$,

$$-\inf_{x \in \mathrm{int}(\mathcal{A})} I(x) \leq \liminf_{N\to\infty} \frac{1}{N} \ln \mu_N(\mathcal{A}) \leq \limsup_{N\to\infty} \frac{1}{N} \ln \mu_N(\mathcal{A}) \leq -\inf_{x \in \mathrm{clos}(\mathcal{A})} I(x). \tag{2-2}$$

Moreover, we assume

$$\inf_{x \in (-\infty, -\varepsilon]} I(x) > 0 \tag{2-3}$$

for any $\varepsilon > 0$.

(3) For any random weights $w_{\boldsymbol{\sigma}_1}$ which are independent from $X_{\boldsymbol{\sigma}_1}$ and further fulfill almost surely

$$w_{\boldsymbol{\sigma}_1} \geq 0, \quad \sum_{\boldsymbol{\sigma}_1 \in \mathcal{Q}_N^{(1)}} w_{\boldsymbol{\sigma}_1} = 1,$$

a generalized strong law holds true almost surely,

$$\lim_{N\to\infty} \frac{1}{N} \sum_{\boldsymbol{\sigma}_1 \in \mathcal{Q}_N^{(1)}} w_{\boldsymbol{\sigma}_1} X_{\boldsymbol{\sigma}_1} = 0. \tag{2-4}$$

As will be discussed in the next subsection, we are mostly interested in hierarchical V_N as in the GREM or CREM, but our results also apply to the more general situation. An important example where V_N is not of CREM type is the case of a nonvanishing longitudinal magnetic field. The addition of a pure longitudinal field to a classical hierarchical glass technically remains in the realm of probability theory and has been studied in [4; 5; 9]. As is further discussed in [28], which deals with the application of the peeling principle for a study of the combined effects of transversal and longitudinal fields, the two choices of field direction not only differ in the mathematics involved, but also cause different physical behavior.

The LDP (2-2) with (2-3) ensure that probabilities of the type $\mathbb{P}(X_{\boldsymbol{\sigma}_1} < -\varepsilon N)$ decay exponentially in N for any $\varepsilon > 0$. The assumption (2-4) is a technical condition needed for our proof of Theorem 2.3. The following examples of random variables $X_{\boldsymbol{\sigma}_1}$ meet Assumption 2.1, which can be seen by the sufficient criterion Lemma A.1 that we present in the Appendix:

(1) $X_{\boldsymbol{\sigma}_1} = \sqrt{Na}\, Y_{\boldsymbol{\sigma}_1}$ with independent standard Gaussian $Y_{\boldsymbol{\sigma}_1}$ and some $a > 0$. The rate function of the negative part is $I(x) = \frac{a}{2} x^2 \mathbb{1}_{x<0}$.

(2) Another example is $X_{\boldsymbol{\sigma}_1} = -N Y_{\boldsymbol{\sigma}_1}$, where $Y_{\boldsymbol{\sigma}_1}$ are independent and follow an exponential distribution with parameter N. The rate function of the negative part is $I(x) = |x| \mathbb{1}_{x<0}$.

(3) More generally, let $Y \leq 0$ be a random variable with a decay of the form $\exp(-Ct^\alpha)$ for some $\alpha, C > 0$, i.e.,

$$-\lim_{t\to\infty} t^{-\alpha} \ln \mathbb{P}(Y < t) = C.$$

Then, we define $X_{\sigma_1} = N^{1-1/\alpha} Y_{\sigma_1}$, where Y_{σ_1} are independent copies of Y. The corresponding rate function is given by $I(x) = C|x|^\alpha \mathbb{1}_{x<0}$.

We consider a not necessarily constant transversal magnetic field $B = \sum_{j=1}^N b_j s_j$ as in (1-10) with random variables (b_j) which do not need to be independent from each other. The transversal field B splits into two parts $B^{1,x}$ and $B^{2,x}$, which act exclusively on the respective part of the array,

$$B^{1,x} := \sum_{i=1}^{\lceil xN \rceil} b_i s_i, \quad B^{2,x} := \sum_{i=\lceil xN \rceil + 1}^{N} b_i s_i.$$

If $x = 1$, we simply set $B^{2,1} = 0$. Subsequently, we assume the following on the transversal field B:

Assumption 2.2 (assumptions on B). The random weights (b_j) are independent of the potential U and satisfy almost surely

$$\limsup_{N\to\infty} N^{-1} \sqrt{\sum_{j=1}^N |b_j|^2} = 0. \tag{2-5}$$

Let us discuss some sufficient conditions on (b_j) which ensure the validity of Assumption 2.2:

(1) Assumption 2.2 obviously covers the constant field case $b_j = \Gamma \geq 0$.

(2) If the weights are almost surely dominated by $\sqrt{N}$, that is,

$$\limsup_{N\to\infty} N^{-\frac{1}{2}} \max_{1\leq j\leq N} |b_j| = 0, \tag{2-6}$$

then (2-5) holds true.

(3) In view of the framework in Section 1, we are mostly interested in weights (b_j) forming independent copies of an absolute integrable random variable $\mathfrak{b}$. Then, (2-5) is satisfied and this result is presented as Lemma A.2 in the Appendix. If we additionally assume that $\mathbb{E}[|\mathfrak{b}|^r]$ is finite for some $r > 1$, Assumption 2.2 is easily verified. Namely if $r \in (1, 2]$, then

$$N^{-1} \sqrt{\sum_{i=1}^N |b_i|^2} \leq N^{-(1-1/r)} \left(N^{-1} \sum_{i=1}^N |b_i|^r \right)^{1/r}.$$

The term in the bracket converges almost surely to a constant by the strong law of large numbers. So (2-5) is fulfilled.

If Assumptions 2.1 and 2.2 hold true, our main results state that the pressure

$$\Phi_N(\beta) := \frac{1}{N} \ln \mathrm{Tr}\,[e^{-\beta(U-B)}]$$

asymptotically agrees with the maximum of the pressures of partially quantum or classical type

$$\Phi_N^{(\mathrm{qm})}(\beta) := \frac{1}{N} \ln \mathrm{Tr}\,[e^{-\beta(V_N-B)}] \quad \text{and} \quad \Phi_N^{(\mathrm{cl})}(\beta) := \frac{1}{N} \ln \mathrm{Tr}\,[e^{-\beta(U-B^{2,x})}]$$

even if $\Phi_N^{(\mathrm{qm})}(\beta)$ and $\Phi_N^{(\mathrm{cl})}(\beta)$ do not converge:

Theorem 2.3. *Under Assumptions 2.1 and 2.2, for any $x \in (0, 1]$ we have the almost sure convergence*

$$\limsup_{N\to\infty} |\Phi_N(\beta) - \max\{\Phi_N^{(\mathrm{qm})}(\beta), \Phi_N^{(\mathrm{cl})}(\beta)\}| = 0. \tag{2-7}$$

Roughly speaking, the Gaussian variables $(X_{\boldsymbol{\sigma}_1})$ and the partial magnetic term $B^{1,x}$ only contribute separately from each other to the free energy. This result may be regarded as a generalization of the limit theorem for the QREM in [27]. If the almost-sure limits

$$\Phi^{(\mathrm{qm})}(\beta) := \lim_{N\to\infty} \Phi_N^{(\mathrm{qm})}(\beta) \quad \text{and} \quad \Phi^{(\mathrm{cl})}(\beta) := \lim_{N\to\infty} \Phi_N^{(\mathrm{cl})}(\beta)$$

exist for any $\beta \geq 0$, we immediately obtain

$$\lim_{N\to\infty} \Phi_N(\beta) = \max\{\Phi^{(\mathrm{qm})}(\beta), \Phi^{(\mathrm{cl})}(\beta)\}. \tag{2-8}$$

For a proof of Theorem 2.3 the methods in [27] are robust enough to be extended. We briefly recall some notation and results necessary for doing so. For $\varepsilon > 0$ we denote the large deviation set of $X_{\boldsymbol{\sigma}_1}$ by

$$\mathcal{L}_\varepsilon := \{\boldsymbol{\sigma}_1 \in \mathcal{Q}_N^{(1)} \mid X_{\boldsymbol{\sigma}_1} \leq -\varepsilon N\}. \tag{2-9}$$

The operator $B^{1,x}_{\mathcal{L}_\varepsilon^c}$ is the Dirichlet restriction of $B^{1,x}$ to the complement $\mathcal{L}_\varepsilon^c$, that is, $B^{1,x}_{\mathcal{L}_\varepsilon^c} = P_{\mathcal{L}_\varepsilon^c} B^{1,x} P_{\mathcal{L}_\varepsilon^c}$ with the natural orthogonal projection $P_{\mathcal{L}_\varepsilon^c}$ induced by the complement of the set $\mathcal{L}_\varepsilon$ on the first component $\mathcal{H}^1 := \ell^2(\mathcal{Q}_N^{(1)})$ of the tensor-product Hilbert space $\ell^2(\mathcal{Q}_N) = \mathcal{H}^1 \otimes \mathcal{H}^2$ with $\mathcal{H}^2 := \ell^2(\mathcal{Q}_N^{(2)})$. We further introduce

$$A_{\mathcal{L}_\varepsilon} := A^1_{\mathcal{L}_\varepsilon} \otimes \mathbb{1}_{\mathcal{H}^2} := B^{1,x} - B^{1,x}_{\mathcal{L}_\varepsilon^c},$$

where $A^1_{\mathcal{L}_\varepsilon}$ only acts on $\mathcal{H}^1$ and $A_{\mathcal{L}_\varepsilon}$ is its trivial extension to the full Hilbert space. More precisely, the matrix elements of $A^1_{\mathcal{L}_\varepsilon}$ are given by

$$\langle \boldsymbol{\sigma}_1 | A^1_{\mathcal{L}_\varepsilon} | \boldsymbol{\sigma}_1' \rangle = \mathbb{1}_{[\{\boldsymbol{\sigma}_1, \boldsymbol{\sigma}_1'\} \cap \mathcal{L}_\varepsilon \neq \varnothing]} \sum_{j=1}^{\lceil xN \rceil} b_j \, \delta_{\boldsymbol{s}_j \boldsymbol{\sigma}_1, \boldsymbol{\sigma}_1'}, \tag{2-10}$$

where in a slight abuse of notation we extend the operators $\boldsymbol{s}_j$ to configurations by setting $s_j\boldsymbol{\sigma} := (\sigma_1, \sigma_2, \ldots, -\sigma_j, \ldots, \sigma_N)$. Moreover, $\delta_{\cdot,\cdot}$ denotes Kronecker's delta, so that the sum in the right side of (2-10) reduces to one term only.

We will need the following generalization of Lemma 2 and Lemma 3 in [27]:

Proposition 2.4. *Under Assumptions 2.1 and 2.2, for any $\varepsilon > 0$ and $x \in (0, 1]$ the operator norm of $A_{\mathcal{L}_\varepsilon}$ satisfies almost surely*:

$$\limsup_{N\to\infty} N^{-1} \| A_{\mathcal{L}_\varepsilon} \| = 0. \tag{2-11}$$

The proof of Proposition 2.4 is based on an estimate for the maximal size of the so-called gap-connected components of $\mathcal{L}_\varepsilon$, which are defined as follows:

Definition 2.5. Let $\widetilde{\mathcal{Q}}_N^{(1)}$ be the supergraph of the Hamming cube $\mathcal{Q}_N^{(1)}$, which one obtains by adding all edges $\{\boldsymbol{\sigma}_1, \boldsymbol{\sigma}_1'\}$, where $\boldsymbol{\sigma}_1, \boldsymbol{\sigma}_1'$ are any two vertices at distance $d(\boldsymbol{\sigma}_1, \boldsymbol{\sigma}_1') = 2$. We call $\mathcal{C}_\varepsilon \subset \mathcal{L}_\varepsilon$ a

gap-connected component if $\mathcal{C}_\varepsilon$ is connected as a subset of $\widetilde{\mathcal{Q}}_N^{(1)}$. A gap-connected component $\mathcal{C}_\varepsilon$ is *maximal* if there is no other vertex $\boldsymbol{\sigma}_1 \in \mathcal{L}_\varepsilon \backslash \mathcal{C}_\varepsilon$ such that $\mathcal{C}_\varepsilon \cup \{\boldsymbol{\sigma}_1\}$ forms a gap-connected component. We denote by $(\mathcal{C}_\varepsilon^\alpha)_\alpha$ the collection of *maximal gap-connected components* of $\mathcal{L}_\varepsilon$.

We claim that the maximum of the cardinality, $\max_\alpha |\mathcal{C}_\varepsilon^\alpha|$, is almost surely of order one:

Lemma 2.6. *Under Assumption 2.1, for any $\varepsilon > 0$ and $x \in (0, 1]$ there is $K > 0$ such that*

$$\limsup_{N\to\infty} \max_\alpha |\mathcal{C}_\varepsilon^\alpha| \le K \tag{2-12}$$

holds almost surely.

Proof. We follow the lines of the proof of Lemma 2 in [27]. We fix $K \in \mathbb{N}$ and introduce the event

$$\Omega_{\varepsilon,K,N} := \bigcap_{\boldsymbol{\sigma}_1 \in \mathcal{Q}_N^{(1)}} \{|B_{4K}(\boldsymbol{\sigma}_1) \cap \mathcal{L}_\varepsilon| < K\}.$$

We note that for $\omega \in \Omega_{\varepsilon,K,N}$ we always have $\max_\alpha |C_\varepsilon^\alpha| < K$, as any gap-connected component with K vertices is contained in some ball $B_{4K}(\boldsymbol{\sigma}_1) \subset \mathcal{Q}_N^{(1)}$ of radius $4K$, which is centered at some $\boldsymbol{\sigma}_1$. We estimate the probability of the complement $\Omega_{\varepsilon,K,N}^c$ using the union bound:

$$\mathbb{P}(\Omega_{\varepsilon,K,N}^c) \le \sum_{\boldsymbol{\sigma}_1 \in \mathcal{Q}_N^{(1)}} \mathbb{P}(|B_{4K}(\boldsymbol{\sigma}_1) \cap \mathcal{L}_\varepsilon| \ge K) \le 2^{\lceil xN \rceil} \binom{|B_{4K}|}{K} \mathbb{P}(X_{\boldsymbol{\sigma}_1} < -\varepsilon N)^K.$$

The second inequality follows from independence of the random variables $X_{\boldsymbol{\sigma}_1}$ and an estimate on the number of subsets of a given size in terms of the binomial coefficients. The rate function I of $X_{\boldsymbol{\sigma}_1}/N$ satisfies $\inf_{-\infty<z\le-\varepsilon} I(z) = \delta_\varepsilon > 0$, from which we conclude

$$\mathbb{P}(\Omega_{\varepsilon,K,N}^c) \le 2^{\lceil xN \rceil} \frac{|B_{4K}|^K}{K!} e^{-KN(\delta_\varepsilon + o(1))}.$$

Since $|B_{4K}| \le eN^{4K}$, we may choose $K = K(\varepsilon)$ large enough such that this probability decays exponentially fast. A Borel–Cantelli argument then yields the almost-sure bound

$$\limsup_{N\to\infty} \max_\alpha |C_\varepsilon^\alpha| \le K. \qquad \square$$

Proposition 2.4 is now a simple consequence of Assumption 2.2 and Lemma 2.6:

Proof of Proposition 2.4. The operator $A_{\mathcal{L}_\varepsilon}$ exhibits a natural decomposition as the direct sum

$$A_{\mathcal{L}_\varepsilon} = \bigoplus_\alpha A^1_{\mathcal{C}_\varepsilon^\alpha} \otimes \mathbb{1}_{\mathcal{H}^2},$$

where $A^1_{\mathcal{C}_\varepsilon^\alpha}$ denotes the restriction of $A^1_{\mathcal{L}_\varepsilon}$ to the subspace of vertices with nonempty intersection with the maximal gap-connected component $\mathcal{C}_\varepsilon^\alpha$. Estimating the operator norm on every block in terms of the

Frobenius norm using (2-10), we conclude

$$\|A^1_{\mathcal{C}^\alpha_\varepsilon}\|^2 \le \max_\alpha \sum_{\boldsymbol{\sigma}_1,\boldsymbol{\sigma}'_1} |\langle \boldsymbol{\sigma}_1|A^1_{\mathcal{C}^\alpha_\varepsilon}|\boldsymbol{\sigma}'_1\rangle|^2 \le \max_\alpha \sum_{\substack{\boldsymbol{\sigma}_1,\boldsymbol{\sigma}'_1\in\mathcal{Q}_N^{(1)}:\\ \{\boldsymbol{\sigma}_1,\boldsymbol{\sigma}'_1\}\cap\mathcal{C}^\alpha_\varepsilon\neq\varnothing}} \Bigg|\sum_{j=1}^{\lceil xN\rceil} b_j\,\delta_{s_j\boldsymbol{\sigma}_1,\boldsymbol{\sigma}'_1}\Bigg|^2 \le 2\max_\alpha |C^\alpha_\varepsilon| \sum_{j=1}^{N}|b_j|^2,$$

which together with Assumption 2.2 and Lemma 2.6 completes the proof. □

We finally spell out the proof of Theorem 2.3:

Proof of Theorem 2.3. We separately establish an asymptotically sharp lower and upper bound.

Lower bound: The lower bound rests on a twofold application of Gibbs' variational principle [34; 35]. First, let $\rho^{(\mathrm{qm})}_\beta$ be the Gibbs state of $H^{(\mathrm{qm})} = V_N - B$. An application of the Gibbs variational principle with $\rho = \rho^{(\mathrm{qm})}_\beta$ and $H = H^{(\mathrm{qm})} + X_{\boldsymbol{\sigma}_1}$ yields

$$\Phi_N(\beta) = N^{-1}\sup_\rho[-\beta\,\mathrm{Tr}\,(H\rho) - \mathrm{Tr}\,(\rho\ln\rho)] \ge \Phi^{(\mathrm{qm})}_N(\beta) - \beta N^{-1}\sum_{\boldsymbol{\sigma}_1} X_{\boldsymbol{\sigma}_1} w_{\boldsymbol{\sigma}_1}.$$

The weights $w_{\boldsymbol{\sigma}_1} := \sum_{\boldsymbol{\sigma}_2}\langle\boldsymbol{\sigma}_1\boldsymbol{\sigma}_2|\rho^{(\mathrm{qm})}_\beta|\boldsymbol{\sigma}_1\boldsymbol{\sigma}_2\rangle$ are nonnegative, add up to 1, and are independent of $X_{\boldsymbol{\sigma}_1}$. By Assumption 2.1 we conclude that almost surely

$$\liminf_{N\to\infty}(\Phi_N(\beta) - \Phi^{(\mathrm{qm})}_N(\beta)) \ge 0.$$

Next, the eigenstates $|\psi\rangle \in \ell^2(\mathcal{Q}_N)$ of $H^{(\mathrm{cl})} = U - B^{2,x}$ take the form of tensor products $|\psi\rangle = |\boldsymbol{\sigma}_1\rangle\otimes|\phi\rangle$ with a certain $|\phi\rangle \in \mathcal{H}^2$. As the matrix elements $\langle\psi|B^{1,x}|\psi\rangle$ vanish for these eigenstates, the Gibbs state $\rho^{(\mathrm{cl})}_\beta := e^{-\beta H^{(\mathrm{cl})}}/\mathrm{Tr}\,e^{-\beta H^{(\mathrm{cl})}}$ satisfies

$$\mathrm{Tr}\,B^{1,x}\rho^{(\mathrm{cl})}_\beta = 0. \tag{2-13}$$

The Gibbs variational principle with $\rho = \rho^{(\mathrm{cl})}_\beta$ and $H = H^{(\mathrm{cl})} - B^{1,x}$ then yields

$$\Phi_N(\beta) \ge \Phi^{(\mathrm{cl})}_N(\beta). \tag{2-14}$$

Combining both lower bounds, we obtain almost surely

$$\liminf_{N\to\infty}(\Phi_N(\beta) - \max\{\Phi^{(\mathrm{qm})}_N(\beta), \Phi^{(\mathrm{cl})}_N(\beta)\}) \ge 0.$$

Upper bound: Let $\varepsilon > 0$ be arbitrary and consider the direct-sum decomposition of the Hilbert space $\ell^2(\mathcal{Q}_N) = (\ell^2(\mathcal{L}_\varepsilon)\otimes\mathcal{H}^2)\oplus(\ell^2(\mathcal{L}^c_\varepsilon)\otimes\mathcal{H}^2)$. The only term in H connecting the two subspaces is $A_{\mathcal{L}_\varepsilon}$. The Golden–Thompson inequality (see [35, Corollary I.4.13]) together with the positivity of e^H for $H = H^*$ and trivial norm estimates thus yield

$$\begin{aligned}\mathrm{Tr}\,e^{-\beta(U-B)} &\le \mathrm{Tr}\,e^{-\beta A_{\mathcal{L}_\varepsilon}}e^{-\beta(U-B^{1,x}_{\mathcal{L}^c_\varepsilon}-B^{2,x})} \le e^{\beta\|A_{\mathcal{L}_\varepsilon}\|}\mathrm{Tr}\,e^{-\beta(U-B^{1,x}_{\mathcal{L}^c_\varepsilon}-B^{2,x})}\\ &\le e^{\beta\|A_{\mathcal{L}_\varepsilon}\|}\big(\mathrm{Tr}_{|\ell^2(\mathcal{L}_\varepsilon)\otimes\mathcal{H}^2}e^{-\beta(U-B^{2,x})} + e^{\beta\varepsilon N}\mathrm{Tr}_{|\ell^2(\mathcal{L}^c_\varepsilon)\otimes\mathcal{H}^2}e^{-\beta(V_N-B^{1,x}_{\mathcal{L}^c_\varepsilon}-B^{2,x})}\big).\end{aligned}$$

In the last term we additionally used the fact that $X_{\boldsymbol{\sigma}_1} \geq -\varepsilon N$ for all $\boldsymbol{\sigma}_1 \in \mathcal{L}_\varepsilon^c$. The first term is bounded by

$$\operatorname{Tr}_{|\ell^2(\mathcal{L}_\varepsilon)\otimes\mathcal{H}^2} e^{-\beta(U-B^{2,x})} \leq \operatorname{Tr} e^{-\beta(U-B^{2,x})}.$$

The second term is estimated using the nonnegativity of the diagonal matrix elements of the semigroups generated by B and the Golden–Thompson inequality again:

$$\operatorname{Tr}_{|\ell^2(\mathcal{L}_\varepsilon)\otimes\mathcal{H}^2} e^{-\beta(V_N - B^{1,x}_{\mathcal{L}_\varepsilon^c} - B^{2,x})} \leq \operatorname{Tr} e^{-\beta(V_N - B^{1,x}_{\mathcal{L}_\varepsilon^c} - B^{2,x})} \leq e^{\beta\|A_{\mathcal{L}_\varepsilon}\|} \operatorname{Tr} e^{-\beta(V_N - B)}$$

Since $\varepsilon > 0$ was arbitrary and $\|A_{\mathcal{L}_\varepsilon}\| = o(N)$ by Proposition 2.4, we conclude the almost-sure inequality

$$\limsup_{N\to\infty} \big(\Phi_N(\beta) - \max\{\Phi_N^{(\mathrm{qm})}(\beta), \Phi_N^{(\mathrm{cl})}(\beta)\}\big) \leq 0. \qquad \square$$

2B. ***Application to QGREM and QCREM.*** Since we are free in the choice of V_N in Theorem 2.3, we obtain the following corollary for GREM type potentials:

Corollary 2.7. *Let $X = \sqrt{a_1}X_{\boldsymbol{\sigma}_1} + \sqrt{a_2}X_{\boldsymbol{\sigma}_1\boldsymbol{\sigma}_2} + \cdots + \sqrt{a_n}X_{\boldsymbol{\sigma}_1\boldsymbol{\sigma}_2\cdots\boldsymbol{\sigma}_n}$ be a Gaussian vector as in (1-4). Then, we have the almost sure convergence*

$$\limsup_{N\to\infty} \Big| \frac{1}{N} \ln \operatorname{Tr} e^{-\beta(\sqrt{N}X - B)} - \max_{0\leq k\leq n} \frac{1}{N} \ln \operatorname{Tr} e^{-\beta(\sqrt{N}(\sqrt{a_1}X_{\boldsymbol{\sigma}_1}\cdots + \sqrt{a_k}X_{\boldsymbol{\sigma}_1\boldsymbol{\sigma}_2\cdots\boldsymbol{\sigma}_k}) - B^{2,x_k})} \Big| = 0. \tag{2-15}$$

Proof. We apply Theorem 2.3 iteratively backwards. We start with peeling off $\sqrt{a_n}X_{\boldsymbol{\sigma}_1\boldsymbol{\sigma}_2\cdots\boldsymbol{\sigma}_n}$ (which takes the role of $X_{\boldsymbol{\sigma}_1}$ in Theorem 2.3) setting $V_N = V_N^{(n)} := \sqrt{Na_1}X_{\boldsymbol{\sigma}_1} + \sqrt{Na_2}X_{\boldsymbol{\sigma}_1\boldsymbol{\sigma}_2} + \cdots + \sqrt{Na_{n-1}}X_{\boldsymbol{\sigma}_1\boldsymbol{\sigma}_2\cdots\boldsymbol{\sigma}_{n-1}}$. The peeling principle (2-7) yields

$$\limsup_{N\to\infty} \frac{1}{N} \big| \ln \operatorname{Tr} e^{-\beta(\sqrt{N}X - B)} - \max\{\ln \operatorname{Tr} e^{-\beta(\sqrt{Na_n}X_{\boldsymbol{\sigma}_1\boldsymbol{\sigma}_2\cdots\boldsymbol{\sigma}_n} + V_N^{(n)})}, \ln \operatorname{Tr} e^{-\beta(V_N^{(n)} - B)}\} \big| = 0.$$

As a next step, we write $V_N^{(n)} =: V_N^{(n-1)} + \sqrt{Na_{n-1}}X_{\boldsymbol{\sigma}_1\boldsymbol{\sigma}_2\cdots\boldsymbol{\sigma}_{n-1}}$ and again apply Theorem 2.3 to the second expression in the maximum. Thus,

$$\limsup_{N\to\infty} \frac{1}{N} \big| \ln \operatorname{Tr} e^{-\beta(V_N^{(n)} - B)} - \max\{\ln \operatorname{Tr} e^{-\beta(V_N^{(n)} - B^{2,x_{n-1}})}, \ln \operatorname{Tr} e^{-\beta(V_N^{(n-1)} - B)}\} \big| = 0.$$

Proceeding like this, we arrive after n steps at (2-15). $\square$

Theorem 1.2 and Corollary 2.7 look alike. However, in Theorem 1.2 we further evaluate the trace and claim that the maximum in (2-15) is attained at some endpoint y_l of the concave hull $\bar{A}$. We postpone this remaining part of the proof of Theorem 1.2 to Section 3A.

Now, instead, we will extend Corollary 2.7 to CREM type potentials. To this end, we introduce a useful shorthand notation. If X is a centered Gaussian vector with hierarchical distribution function A, we define for $0 \leq z \leq 1$ the centered Gaussian vector $X^{(z)}$ with hierarchical distribution function given by

$$A^{(z)}(x) := \begin{cases} A(x) & \text{if } x \leq z, \\ A(z) & \text{else.} \end{cases}$$

We are now ready to formulate the following theorem:

Theorem 2.8. *Let X be a centered Gaussian vector of CREM-type with distribution function A. Then, we have almost sure convergence*

$$\limsup_{N\to\infty}\left|\frac{1}{N}\ln\operatorname{Tr}e^{-\beta(\sqrt{N}X+V_N-B)}-\sup_{0\le z\le 1}\frac{1}{N}\ln\operatorname{Tr}e^{-\beta(\sqrt{N}X^{(z)}+V_N-B^{2,z})}\right|=0. \tag{2-16}$$

Our proof of Theorem 2.8 relies on an interpolation argument. We first adapt the classical arguments to our quantum setting with a transversal magnetic field. We fix some inverse temperature β and random field B. Let X, Y be two independent centered Gaussian processes on $\mathcal{Q}_N$, which are independent of V_N as well. For $t\in[0,1]$ we set the interpolated pressure Ψ,

$$\Psi(t)=\frac{1}{N}\ln\big[\operatorname{Tr}e^{-\beta(\sqrt{tN}X+\sqrt{(1-t)N}Y+V_N-B}\big],$$

where by Lemma 1.1 we may assume without loss of generality that $b_j\ge 0$ for all j. By standard Gaussian interpolation (see, e.g., [39, Lemma 1.3.1]), we obtain

$$\mathbb{E}_{X,Y}[\Psi(1)-\Psi(0)]=\frac{1}{2}\sum_{\boldsymbol{\sigma},\boldsymbol{\sigma}'}\int_0^1(\mathbb{E}[Y(\boldsymbol{\sigma})Y(\boldsymbol{\sigma}')]-\mathbb{E}[X(\boldsymbol{\sigma})X(\boldsymbol{\sigma}')])\mathbb{E}_{X,Y}\left[\frac{\partial^2\Psi(t)}{\partial X_{\boldsymbol{\sigma}}\partial X_{\boldsymbol{\sigma}'}}+\frac{\partial^2\Psi(t)}{\partial Y_{\boldsymbol{\sigma}}\partial Y_{\boldsymbol{\sigma}'}}\right]dt,$$

where $\mathbb{E}_{X,Y}$ denotes the expectation with respect to X and Y. In general, $\mathbb{E}_{X,Y}[\Psi(t)]$ is still a random variable due to the randomness of V_N and B. The second partial derivatives of $\Psi(t)$ differ from their classical expression but can still be computed using the Duhamel formula:

$$\frac{\partial^2\Psi(t)}{\partial X_{\boldsymbol{\sigma}}\partial X_{\boldsymbol{\sigma}'}}+\frac{\partial^2\Psi(t)}{\partial Y_{\boldsymbol{\sigma}}\partial Y_{\boldsymbol{\sigma}'}}=-\beta^2\frac{\langle\boldsymbol{\sigma}|e^{H_t}|\boldsymbol{\sigma}\rangle\langle\boldsymbol{\sigma}'|e^{H_t}|\boldsymbol{\sigma}'\rangle}{(\operatorname{Tr}e^{H_t})^2}+\beta^2\int_0^1\frac{\langle\boldsymbol{\sigma}|e^{sH_t}|\boldsymbol{\sigma}'\rangle\langle\boldsymbol{\sigma}'|e^{(1-s)H_t}|\boldsymbol{\sigma}\rangle}{\operatorname{Tr}e^{H_t}}\,ds$$

with the abbreviation $H_t:=-\beta(\sqrt{tN}X+\sqrt{(1-t)N}Y+V_N-B)$. Since we assumed without loss of generality that $b_j\ge 0$, the matrix elements $\langle\boldsymbol{\sigma}|e^{H_t}|\boldsymbol{\sigma}'\rangle$ are nonnegative for any $\boldsymbol{\sigma},\boldsymbol{\sigma}'$. Moreover, we know that

$$\sum_{\boldsymbol{\sigma},\boldsymbol{\sigma}'}\frac{\langle\boldsymbol{\sigma}|e^{H_t}|\boldsymbol{\sigma}\rangle\langle\boldsymbol{\sigma}'|e^{H_t}|\boldsymbol{\sigma}'\rangle}{(\operatorname{Tr}e^{H_t})^2}=1=\sum_{\boldsymbol{\sigma},\boldsymbol{\sigma}'}\int_0^1\frac{\langle\boldsymbol{\sigma}|e^{sH_t}|\boldsymbol{\sigma}'\rangle\langle\boldsymbol{\sigma}'|e^{(1-s)H_t}|\boldsymbol{\sigma}\rangle}{\operatorname{Tr}e^{H_t}}ds.$$

Consequently, we arrive at the bound

$$|\mathbb{E}_{X,Y}[\Psi(1)-\Psi(0)]|\le\beta^2\max_{\boldsymbol{\sigma},\boldsymbol{\sigma}'}|\mathbb{E}[X(\boldsymbol{\sigma})X(\boldsymbol{\sigma}')]-\mathbb{E}[Y(\boldsymbol{\sigma})Y(\boldsymbol{\sigma}')]|.$$

In case X and Y are of CREM-type with distribution functions A_X and A_Y, respectively, we thus conclude

$$|\mathbb{E}_{X,Y}[\Psi(1)-\Psi(0)]|\le\beta^2\|A_X-A_Y\|_\infty. \tag{2-17}$$

Analogously, we get

$$\frac{1}{N}\big|\mathbb{E}_{X,Y}\big[\ln\operatorname{Tr}e^{-\beta(\sqrt{N}X^{(z)}+V_N-B^{2,z})}-\ln\operatorname{Tr}e^{-\beta(\sqrt{N}Y^{(z)}+V_N-B^{2,z})}\big]\big|\le\beta^2\|A_X-A_Y\|_\infty \tag{2-18}$$

for any $z\in[0,1]$. The bounds (2-17) and (2-18) are our first main ingredients for the proof of Theorem 2.8. We observe, however, that an interpolation argument only controls the expectation value with respect to

the Gaussian variables. The following Gaussian concentration inequality is a convenient method to lift the convergence of expectation values to almost sure statements and vice versa.

Proposition 2.9. *Let X be a Gaussian vector of CREM-type, V_N a random potential, and B a random transversal field, all independent from each other. The corresponding pressure*

$$\Phi_N(\beta) = \frac{1}{N} \ln \operatorname{Tr} e^{-\beta(\sqrt{N}X + V_N - B)}$$

exhibits a Gaussian concentration estimate with respect to probability measure of X, i.e., for any $t > 0$ and $N \in \mathbb{N}$,

$$\mathbb{P}_X\left(|\Phi_N(\beta) - \mathbb{E}_X[\Phi_N(\beta)]| > \frac{t\beta}{\sqrt{N}} \right) \leq 2 \exp\left(-\frac{t^2}{4} \right). \tag{2-19}$$

The same bounds hold true for $\Phi_N^{(z)}(\beta) = \frac{1}{N} \ln \operatorname{Tr} e^{-\beta(\sqrt{N}X^{(z)} + V_N - B^{2,z})}$.

Proof. Since the lexicographic overlap (1-2) can only take values k/N with $k = 0, 1, \ldots, N$ for every fixed $N \in \mathbb{N}$, the CREM-type Gaussian vector X may be represented as a GREM-type distribution:

$$X(\boldsymbol{\sigma}) = \sqrt{a_1} X_{\boldsymbol{\sigma}_1} + \sqrt{a_2} X_{\boldsymbol{\sigma}_1 \boldsymbol{\sigma}_2} + \cdots + \sqrt{a_n} X_{\boldsymbol{\sigma}_1 \boldsymbol{\sigma}_2 \cdots \boldsymbol{\sigma}_n}$$

with independent standard Gaussian variables $X_{\boldsymbol{\sigma}_1}, \ldots, X_{\boldsymbol{\sigma}_1 \boldsymbol{\sigma}_2 \cdots \boldsymbol{\sigma}_n}$ and some $n = n(N)$. We calculate the free energy's variation with respect to the i.i.d Gaussian variables $X_{\boldsymbol{\sigma}_1, \ldots, \boldsymbol{\sigma}_k}$,

$$-\frac{\partial \Phi_N(\beta)}{\partial X_{\boldsymbol{\sigma}_1, \ldots, \boldsymbol{\sigma}_k}} = \frac{\beta \sqrt{a_k}}{\sqrt{N} \operatorname{Tr} e^{-\beta(X + V_N - B)}} \sum_{\hat{\boldsymbol{\sigma}}_k} \langle \boldsymbol{\sigma}_1 \cdots \boldsymbol{\sigma}_k \hat{\boldsymbol{\sigma}}_k | e^{-\beta(X + V_N - B)} | \boldsymbol{\sigma}_1 \cdots \boldsymbol{\sigma}_k \hat{\boldsymbol{\sigma}}_k \rangle.$$

Here, $\hat{\boldsymbol{\sigma}}_k$ is an abbreviation for the remaining entries of the element $\boldsymbol{\sigma} \in \mathcal{Q}_N$. Consequently, the square of the pressure's Lipschitz constant is bounded by

$$\sum_k \sum_{\boldsymbol{\sigma}_1 \cdots \boldsymbol{\sigma}_k} \left(\frac{\partial \Phi_N(\beta)}{\partial X_{\boldsymbol{\sigma}_1, \ldots, \boldsymbol{\sigma}_k}} \right)^2 \leq \frac{\beta^2}{N},$$

where we used that the weights a_k add up to 1. If we condition on V_N and B, the Gaussian concentration inequality for Lipschitz functions (see [39, Theorem 1.3.4]) yields

$$\mathbb{P}_X\left(|\Phi_N(\beta, B) - \mathbb{E}_X[\Phi_N(\beta)]| > \frac{t\,\beta}{\sqrt{N}} \right) \leq 2 \exp\left(-\frac{t^2}{4} \right).$$

A similar argument using the fact that the sum of the weights $a_k^{(z)}$ add up to at most 1, shows that we have the same concentration inequality for $\Phi_N^{(z)}(\beta)$. □

Let us remark that a Gaussian concentration estimate still holds true if the weights (a_k) do not add up to 1. Only the multiplicative constant in front of the exponential term changes. We move on to the proof of Theorem 2.8:

Proof of Theorem 2.8. We pick some $\varepsilon > 0$ and an independent Gaussian vector Y of GREM-type with distribution (step-)function $\tilde{A}$ such that

$$\|A - \tilde{A}\|_\infty \leq \varepsilon.$$

This is possible since A is an increasing, right-continuous function and therefore a uniform limit of increasing step functions. We denote by $0 = x_0 < x_1 < x_2 < \cdots x_n = 1$ the points supporting $\tilde{A}$.

We now exploit the estimates in (2-17), (2-18) and Proposition 2.9 in order to obtain the almost sure bounds

$$\limsup_{N\to\infty} \frac{1}{N} \left| \ln \operatorname{Tr} e^{-\beta(\sqrt{N}X+V_N-B)} - \ln \operatorname{Tr} e^{-\beta(\sqrt{N}Y+V_N-B)} \right| \le \beta^2 \varepsilon$$

and, since we also have $\|A^{(z)} - \tilde{A}^{(z)}\|_\infty \le \varepsilon$,

$$\limsup_{N\to\infty} \sup_{z\in[0,1]} \frac{1}{N} \left| \ln \operatorname{Tr} e^{-\beta(\sqrt{N}X^{(z)}+V_N-B^{2,z})} - \ln \operatorname{Tr} e^{-\beta(\sqrt{N}Y^{(z)}+V_N-B^{2,z})} \right| \le \beta^2 \varepsilon.$$

The expressions depending on Y do not necessarily converge. Nevertheless, we have almost surely

$$\begin{aligned} &\limsup_{N\to\infty} \frac{1}{N} \left| \ln \operatorname{Tr} e^{-\beta(\sqrt{N}Y+V_N-B)} - \sup_{0\le z\le 1} \ln \operatorname{Tr} e^{-\beta(\sqrt{N}Y^{(z)}+V_N-B^{2,z})} \right| \\ &\qquad = \limsup_{N\to\infty} \frac{1}{N} \left| \ln \operatorname{Tr} e^{-\beta(\sqrt{N}Y+V_N-B)} - \max_{k=0,1\ldots,n} \ln \operatorname{Tr} e^{-\beta(\sqrt{N}Y^{(x_k)}+V_N-B^{2,x_k})} \right| = 0. \end{aligned}$$

For the first equality we recall that for any $x_k \le z < x_{k+1}$ the processes agree, i.e., $Y^{(z)} = Y^{(x_k)}$. Consequently, the Gibbs' variational principle with $H = H' - (B^{2,x_k} - B^{2,z})$ and $H' = \sqrt{N}Y^{(x_k)} + V_N - B^{2,z}$ and an argument similar to (2-13)–(2-14) show that the maximum is attained at some x_k. The second equality follows from Corollary 2.7. Combining all these estimates, we arrive at

$$\limsup_{N\to\infty} \frac{1}{N} \left| \ln \operatorname{Tr} e^{-\beta(\sqrt{N}X+V_N-B)} - \sup_{0\le z\le 1} \ln \operatorname{Tr} e^{-\beta(\sqrt{N}X^{(z)}+V_N-B^{2,z})} \right| \le 2\beta^2 \varepsilon.$$

As $\varepsilon > 0$ is arbitrary, the proof of (2-16) is completed. □

3. Proofs of the main results

3A. ***The Quantum GREM and CREM.*** We first aim to prove Theorem 1.2, i.e.,

$$\lim_{N\to\infty} \frac{1}{N} \ln \operatorname{Tr} e^{-\beta(\sqrt{N}X-B)} = \max_{0\le l\le m} \left[\sum_{j=1}^{l} \varphi^{(j)}(\beta) + (1-y_l)\mathbb{E}\left[\ln 2\cosh(\beta \mathfrak{b})\right] \right]$$

for a GREM type variable X and transversal field B consisting of independent weights (b_j) with the same distribution as $\mathfrak{b}$. We recall that $x_1, \ldots, x_n$ denote the jump points of the function A, the points $y_1, \ldots, y_m$, over which the above maximum is taken, are the endpoints of the concave hull's $\bar{A}$ linear segments and $\varphi^{(j)}(\beta)$ are the partial free energies from (1-6). For the remainder of this subsection and since we are interested in the limit $N \to \infty$, we also assume without loss of generality that $x_k N \in \mathbb{N}$ for all $k \in \{0, \ldots, n\}$.

Our starting point is Corollary 2.7 which for any GREM-type vector X yields

$$\frac{1}{N}\ln \operatorname{Tr} e^{-\beta(\sqrt{N}X+B)} = \max_{0\le k\le n}\frac{1}{N}\ln \operatorname{Tr} e^{-\beta(\sqrt{N}X^{(x_k)}-B^{2,x_k})}+o(1)$$
$$= \max_{0\le k\le n}\left[\frac{1}{N}\ln \operatorname{Tr}_{|\mathcal{Q}_{x_kN}} e^{-\beta\sqrt{N}X^{(x_k)}}+\frac{1}{N}\sum_{i=\lceil x_kN\rceil}^{N}\ln 2\cosh(\beta b_i)\right]+o(1),$$

since

$$X^{(x_k)} = \sqrt{a_1}X_{\boldsymbol{\sigma}_1}+\sqrt{a_2}X_{\boldsymbol{\sigma}_1\boldsymbol{\sigma}_2}+\cdots+\sqrt{a_k}X_{\boldsymbol{\sigma}_1\boldsymbol{\sigma}_2\cdots\boldsymbol{\sigma}_k}$$

only acts nontrivially on the configurations $\boldsymbol{\sigma}_1\cdots\boldsymbol{\sigma}_k$ and B^{2,x_k} on $\boldsymbol{\sigma}_{k+1}\cdots\boldsymbol{\sigma}_n$ so that the total trace is simply the product of the partition functions of $X^{(x_k)}$ and B^{2,x_k} on the corresponding reduced Hilbert space; see (1-14). The limit $N\to\infty$ of the bracket on the right side exists for any $k\in\{0,\dots,n\}$. More precisely, the strong law of large numbers implies that the second term almost surely tends to $(1-x_k)\mathbb{E}[\ln 2\cosh(\beta\mathfrak{b})]$. Moreover, the first term converges since $X^{(x_k)}$ is still a GREM-type Gaussian vector on $\mathcal{Q}_{x_kN}$. The only difference is that the weights $a_1,\dots,a_k$ do not add up to 1. This minor obstacle can be easily done away with by rescaling the inverse temperature β. In particular, if x_k coincides with an endpoint y_l of the concave hull's segments,

$$\lim_{N\to\infty}\frac{1}{N}\ln \operatorname{Tr}_{|\mathcal{Q}_{x_kN}} e^{-\beta\sqrt{N}X^{(x_k)}} = \sum_{j=1}^{l}\varphi^{(j)}(\beta),$$

where the partial free energies $\varphi^{(j)}(\beta)$ remain unchanged, i.e., they are still given by (1-6). This follows from the observation that X and $X^{(y_l)}$ have the same concave hull up to the point y_l.

Since the limit $N\to\infty$ exists for each k, we may exchange the limit with the maximum. In order to prove Theorem 1.2, it therefore suffices to check that in

$$\lim_{N\to\infty}\frac{1}{N}\ln \operatorname{Tr} e^{-\beta(\sqrt{N}X+B)} = \max_{k=0,\dots,n}\left[\lim_{N\to\infty}\frac{1}{N}\ln \operatorname{Tr}_{|\mathcal{Q}_{x_kN}} e^{-\beta\sqrt{N}X^{(x_k)}}+(1-x_k)\mathbb{E}[\ln 2\cosh(\beta\mathfrak{b})]\right], \quad (3\text{-}1)$$

the maximum of the limit is always attained at some y_l. This is the content of the next lemma:

Lemma 3.1. *If X is a Gaussian vector of GREM type, we have*

$$\max_{k=0,\dots,n}\left[\lim_{N\to\infty}\frac{1}{N}\ln \operatorname{Tr}_{|\mathcal{Q}_{x_kN}} e^{-\beta\sqrt{N}X^{(x_k)}}+(1-x_k)\mathbb{E}[\ln 2\cosh(\beta\mathfrak{b})]\right]$$
$$= \max_{l=0,\dots,m}\left[\lim_{N\to\infty}\frac{1}{N}\ln \operatorname{Tr}_{|\mathcal{Q}_{y_lN}} e^{-\beta\sqrt{N}X^{(y_l)}}+(1-y_l)\mathbb{E}[\ln 2\cosh(\beta\mathfrak{b})]\right]. \quad (3\text{-}2)$$

Proof. If $\{x_0,\dots,x_n\}=\{y_0,\dots,y_m\}$, the statement is trivial. We thus consider one of the terms on the left side of (3-2) corresponding to x_k with $y_l<x_k<y_{l+1}$. We recall that the distribution function $A^{(x_k)}$ of $X^{(x_k)}$ is given by

$$A^{(x_k)} = \begin{cases} A(x) & \text{if } x\le x_k,\\ A(x_k) & \text{else,}\end{cases}$$

and introduce the Gaussian processes Y and Z of GREM type with the distribution functions

$$A_Y(x) := \begin{cases} A(x) & \text{if } x \le y_l, \\ A(y_l) & \text{if } y_l < x < x_k, \\ A(x_k) & \text{if } x \ge x_k, \end{cases} \qquad A_Z(x) := \begin{cases} A(x) & \text{if } x \le y_l, \\ A(y_l) & \text{if } y_l < x < x_k, \\ A(y_l) + \frac{x_k - y_l}{y_{l+1} - y_l}(A(y_{l+1}) - A(y_l)) & \text{if } x \ge x_k, \end{cases}$$

respectively. Slepian's lemma [8, Lemma 10.2.1] states that the less correlated a classical system is, the higher is the pressure, which yields the first inequality in

$$\lim_{N\to\infty} \frac{1}{N} \ln \operatorname{Tr}_{|\mathcal{Q}_{x_k N}} e^{-\beta\sqrt{N} X^{(x_k)}} \le \lim_{N\to\infty} \frac{1}{N} \ln \operatorname{Tr}_{|\mathcal{Q}_{x_k N}} e^{-\beta\sqrt{N} Y} \le \lim_{N\to\infty} \frac{1}{N} \ln \operatorname{Tr}_{|\mathcal{Q}_{x_k N}} e^{-\beta\sqrt{N} Z}. \tag{3-3}$$

For the second inequality, we recall that A is majorized by its concave hull $\bar{A}$ and agrees with $\bar{A}$ at y_l and y_{l+1}, i.e.,

$$A(x_k) \le A(y_l) + \frac{x_k - y_l}{y_{l+1} - y_l}(A(y_{l+1}) - A(y_l)).$$

Since the classical pressure is an increasing function of the jump heights, we arrive at the second bound in (3-3). As for (1-5), the classical free energy of Z is given in terms of the partial pressure (1-6) corresponding to the concave hull of A_Z, which agrees with $\bar{A}$ up to x_k,

$$\lim_{N\to\infty} \frac{1}{N} \ln \operatorname{Tr}_{|\mathcal{Q}_{x_k N}} e^{-\beta\sqrt{N} Z} = \sum_{j=1}^{l} \varphi^{(j)}(\beta) + \frac{x_k - y_l}{y_{l+1} - y_l} \varphi^{(l+1)}(\beta).$$

Plugging this into (3-3), we obtain

$$\begin{aligned} &\lim_{N\to\infty} \frac{1}{N} \ln \operatorname{Tr}_{|\mathcal{Q}_{x_k N}} e^{-\beta\sqrt{N} X^{(x_k)}} + (1 - x_k)\mathbb{E}\left[\ln 2\cosh(\beta\mathfrak{b})\right] \\ &\qquad \le \sum_{j=1}^{l} \varphi^{(j)}(\beta) + (1 - y_l)\mathbb{E}\left[\ln 2\cosh(\beta\mathfrak{b})\right] + \frac{x_k - y_l}{y_{l+1} - y_l}(\varphi^{(l+1)}(\beta) - (y_{l+1} - y_l)\mathbb{E}\left[\ln 2\cosh(\beta\mathfrak{b})\right]). \end{aligned}$$

Depending on the sign of the term in the last bracket we then arrive at

$$\lim_{N\to\infty} \frac{1}{N} \ln \operatorname{Tr}_{|\mathcal{Q}_{x_k N}} e^{-\beta\sqrt{N} X^{(x_k)}} + (1 - x_k)\mathbb{E}\left[\ln 2\cosh(\beta\mathfrak{b})\right] \le \sum_{j=1}^{l} \varphi^{(j)}(\beta) + (1 - y_l)\mathbb{E}\left[\ln 2\cosh(\beta\mathfrak{b})\right]$$

in case of a negative sign, or in case of a positive sign because of $x_k - y_l \le y_{l+1} - y_l$, at

$$\lim_{N\to\infty} \frac{1}{N} \ln \operatorname{Tr}_{|\mathcal{Q}_{x_k N}} e^{-\beta\sqrt{N} X^{(x_k)}} + (1 - x_k)\mathbb{E}\left[\ln 2\cosh(\beta\mathfrak{b})\right] \le \sum_{j=1}^{l+1} \varphi^{(j)}(\beta) + (1 - y_{l+1})\mathbb{E}\left[\ln 2\cosh(\beta\mathfrak{b})\right].$$

Consequently, the term corresponding to any x_k on the left side of (3-2) is bounded by one of the terms on its right side. □

The following observation is useful for the proof of Corollary 1.3:

Lemma 3.2. *Let $\varphi^{(j)}(\beta)$ be the partial pressures from (1-6) and $L_j := y_j - y_{j-1}$ the interval lengths. Then, the discrete concavity estimate*

$$\frac{\varphi^{(1)}(\beta)}{L_1} > \frac{\varphi^{(2)}(\beta)}{L_2} > \cdots > \frac{\varphi^{(m)}(\beta)}{L_m} \tag{3-4}$$

holds for any inverse temperature $\beta > 0$.

Proof. We call $\varphi^{(j)}(\beta)$ "frozen" if $\beta > \beta_j$, i.e., $\varphi^{(j)}(\beta)$ is given by the linear expression in (1-6). Otherwise we say $\varphi^{(j)}(\beta)$ is "unfrozen". By construction of the concave hull $\bar{A}$, we know that the slopes $\gamma_j = \bar{a}_j/L_j$ are strictly decreasing in j. The inequalities in (3-4), where two consecutive partial free energies are either both frozen or both unfrozen, are thus obvious. It remains to consider the case where $\varphi^{(j)}(\beta)$ is frozen, but $\varphi^{(j+1)}(\beta)$ is unfrozen. By (1-6) we then have

$$\frac{\varphi^{(j)}(\beta)}{L_j} = \beta\sqrt{(2\ln 2)\gamma_j} \quad \text{and} \quad \frac{\varphi^{(j+1)}(\beta)}{L_{j+1}} = \frac{\beta^2}{2}\gamma_{j+1} + \ln 2.$$

Moreover, as $\varphi^{(j)}(\beta)$ is frozen and $\varphi^{(j+1)}(\beta)$ is unfrozen, the inverse temperatures satisfy

$$\beta_j = \sqrt{(2\ln 2)\gamma_j^{-1}} < \beta \leq \sqrt{(2\ln 2)\gamma_{j+1}^{-1}} = \beta_{j+1}.$$

We thus conclude that

$$\frac{\varphi^{(j)}(\beta)}{L_j} = \frac{\beta}{\beta_j} 2\ln 2 > 2\ln 2 \geq \ln 2 + \frac{\beta^2}{\beta_{j+1}^2}\ln 2 = \ln 2 + \frac{\beta^2}{2}\gamma_{j+1} = \frac{\varphi^{(j+1)}(\beta)}{L_{j+1}}. \qquad \square$$

Remark. If f denotes the function on $[0, 1]$ which linearly interpolates between the restricted classical free energies $\lim_{N\to\infty} \frac{1}{N} \ln \mathrm{Tr}_{|\mathcal{Q}_{x_k N}} e^{-\beta\sqrt{N}X^{(x_k)}}$, then Lemmas 3.1 and 3.2 in particular show that F, the convex hull of the graph of f, is a polygon with the extreme points $(y_l, f(y_l))$. On the other hand, if this fact is assumed to be known, the assertion of Lemma 3.1 can be derived as follows. Consider the function $g(x, y) := (x, y + a(1 - x))$ with some $a > 0$. It is then easy to show that the set of extreme points of $g(F)$ coincides with $g(\mathrm{ext}(F))$. Since the maximum in (3-1) is attained at an extreme point of $g(K)$, the claim follows.

Proof of Theorem 1.2 and Corollary 1.3. Theorem 1.2 is an immediate consequence of (3-1) and Lemma 3.1.

It remains to show Corollary 1.3. To this end, let us introduce the energy differences

$$\Delta^{(j)}(\beta, \Gamma) := (y_j - y_{j-1}) \ln 2\cosh(\beta\Gamma) - \varphi^{(j)}(\beta).$$

In view of Lemma 3.2, we conclude:

(1) If $\Delta^{(j)}(\beta, \Gamma) < 0$ for some $j \geq 1$, then $\Delta^{(i)}(\beta, \Gamma) < 0$ for all $0 < i \leq j$.

(2) If $\Delta^{(j)}(\beta, \Gamma) \geq 0$ for some $j \geq 1$, then $\Delta^{(i)}(\beta, \Gamma) \geq 0$ for all $j \leq i \leq m$.

Consequently, the maximum in (1-13) is attained at m if all energy differences $\Delta^{(j)}$ are negative for $0 < j \leq m$ and, otherwise at the minimal integer $k < m$ such that $\Delta^{(k+1)} \geq 0$. We may thus rewrite the

pressure as

$$\Phi(\beta, \Gamma) = \sum_{l=1}^{m} \big(\varphi^{(l)}(\beta)\mathbb{1}_{\Delta^{(l)}\le 0} + L_l \ln 2 \cosh(\beta\Gamma)\mathbb{1}_{\Delta^{(l)}>0}\big).$$

We note that the condition $\Delta^{(l)} > 0$ is equivalent to $\Gamma > \Gamma_c^{(l)}(\beta)$. This concludes the proof of (1-15). □

Our next goal is to prove Theorem 1.4 and Corollary 1.5. It is convenient to use Theorem 1.2 and the interpolation estimate (2-17) rather than the general Theorem 2.8. To do so, we first establish some continuity properties of the functions

$$\Phi(\beta, A, z) := \sqrt{2\ln 2}\beta \int_0^{\min\{x(\beta),z\}} \sqrt{\bar a(x)}\, dx + \mathbb{1}_{z>x(\beta)}\Big(\frac{\beta^2}{2}(\bar A(z) - \bar A(x(\beta))) + \ln 2(z - x(\beta))\Big)$$

with respect to the distribution function A. Therefore, we emphasize here the dependence on A in notation.

Lemma 3.3. *Let A and $(A_n)_{n\in\mathbb{N}}$ be distribution functions on $[0, 1]$ such that A_n converges uniformly to A as $n \to \infty$. Then*:

(1) *The concave hulls $\bar A_n$ converge uniformly to $\bar A$ as $n \to \infty$, i.e.,*

$$\lim_{n\to\infty} \|\bar A - \bar A_n\|_\infty = 0.$$

(2) *The right derivatives $\bar a_n(x)$ converge to $\bar a(x)$ at any x where $\bar a$ is continuous.*

(3) *For any $\beta \ge 0$, the functions $\Phi(\beta, A_n, z)$ converge uniformly to $\Phi(\beta, A, z)$ as a function of z, i.e.,*

$$\lim_{n\to\infty} \|\Phi(\beta, A_n, \cdot) - \Phi(\beta, A, \cdot)\|_\infty = 0.$$

Proof. (1) The function $\bar A + \|\bar A - \bar A_n\|_\infty$ is a concave function which majorizes A_n; that is, $\bar A_n \le \bar A + \|\bar A - \bar A_n\|_\infty$. Similarly, one shows that $\bar A \le \bar A_n + \|\bar A - \bar A_n\|_\infty$. The first assertion is a direct consequence of these bounds.

(2) Since $\bar A_n$ is a sequence of concave functions converging uniformly to $\bar A$, the second claim follows from standard convex analysis (see, e.g., [36]).

(3) We first recall that $x(\beta, A) = \sup\{x \mid \bar a(x) > 2\ln 2/\beta^2\}$. Since $\bar a$ is a decreasing function, $\bar a$ is continuous except for an at most countable set. The second statement implies then that $x(\beta, A_n)$ converges to $x(\beta, A)$. Next, we rewrite

$$\Phi(\beta, A, z) = \int_0^z \varphi(\beta, A, x)\, dx$$

with the function

$$\varphi(\beta, A, x) := \beta\sqrt{(2\ln 2)\bar a(x)}\mathbb{1}_{x<x(\beta,A)} + \left(\frac{\beta^2}{2}\bar a(x) + \ln 2\right)\mathbb{1}_{x\ge x(\beta)}.$$

Therefore, it suffices to show

$$\lim_{n\to\infty} \int_0^1 |\varphi(\beta, A, x) - \varphi(\beta, A_n, x)|\, dx = 0.$$

Due to our previous considerations, we know that $\varphi(\beta, A_n, x)$ converges almost everywhere (with respect to the Lebesgue measure and x) to $\varphi(\beta, A_n, x)$. Moreover, the functions $\varphi(\beta, A_n, \cdot)$ are uniformly bounded at $[\delta, 1]$ for any $\delta > 0$, since $\varphi(\beta, A_n, x)$ is decreasing in x. By dominated convergence we then obtain

$$\lim_{n\to\infty} \int_\delta^1 |\varphi(\beta, A, x) - \varphi(\beta, A_n, x)|\, dx = 0$$

for any $\delta > 0$. On the other hand,

$$\int_0^\delta |\varphi(\beta, A, x) - \varphi(\beta, A_n, x)|\, dx \le \int_0^\delta \varphi(\beta, A, x) + \varphi(\beta, A_n, x)\, dx \le \frac{\beta^2}{2}(\bar{A}(\delta) + \bar{A}_n(\delta)) + 2\delta \ln 2.$$

Since $\bar{A}$ is continuous, $\bar{A}(0) = 0$ and the sequence $\bar{A}_n$ converges uniformly, the third assertion follows as $\delta \to 0$. □

We are now ready to show Theorem 1.4 and Corollary 1.5.

Proof of Theorem 1.4 and Corollary 1.5 . We pick a sequence of step functions A_n, which are also distribution functions and converge uniformly to the distribution function A. By Theorem 2.8, the expression for $\Phi(\beta, \mathfrak{b}, A_n)$ may be rewritten as

$$\Phi(\beta, \mathfrak{b}, A_n) = \sup_{0\le z\le 1} \big[\Phi(\beta, A_n, z) + (1-z)\mathbb{E}\,[\ln 2\cosh(\beta\mathfrak{b})]\big].$$

By the interpolation estimate (2-17), the left side converges to the corresponding limit of the quantum CREM's pressure $\Phi(\beta, \mathfrak{b}, A)$, whereas the right side converges to

$$\lim_{n\to\infty} \sup_{0\le z\le 1} \big[\Phi(\beta, A_n, z) + (1-z)\mathbb{E}\,[\ln 2\cosh(\beta\mathfrak{b})]\big] = \sup_{0\le z\le 1} \big[\Phi(\beta, A, z) + (1-z)\mathbb{E}\,[\ln 2\cosh(\beta\mathfrak{b})]\big]$$

by Lemma 3.3. This completes the proof of Theorem 1.4.

In the case where $\bar{A}$ is continuously differentiable and $\mathfrak{b} = \Gamma$, the convex function $[0, 1] \ni z \mapsto \Phi(\beta, A, z) + (1-z)\ln(2\cosh(\beta\Gamma))$ possesses a maximum in the interior of its domain if and only if there exists a solution $z \in (0, 1)$ of

$$\frac{\partial \Phi(\beta, A, z)}{\partial z} - \ln 2\cosh(\beta\Gamma) = 0.$$

Otherwise the maximum is attained at $z = 0$ or $z = 1$. A straightforward calculation then leads to the formula in Corollary 1.5. □

3B. ***The nonhierarchical GREM in a transversal field.*** We start with the proof of Theorem 1.6. In the following we will use the notation introduced in Section 1.3.

Proof of Theorem 1.6. Our strategy is to adapt the proof of Corollary 2.7. To be more precise, we introduce for any subset $J \in \mathcal{P}$ the restriction B^J of B to the subgraph spanned by the spins $\boldsymbol{\sigma}_J$,

$$B^J := \sum_{k\in J} B^{(k)}, \quad B^{(k)} := B^{1,x_k} - B^{1,x_{k-1}},$$

and set $B^{\varnothing} := 0$. For any two subsets $I, J \in \mathcal{P}$ and any potential V_N independent of $X^I_{\boldsymbol{\sigma}_I}$, we have

$$\limsup_{N\to\infty} \frac{1}{N} \left| \ln \operatorname{Tr} e^{-\beta(\sqrt{Na_I} X^I_{\boldsymbol{\sigma}_I} + V_N - B^J)} - \max\{\ln \operatorname{Tr} e^{-\beta(V_N - B^J)}, \ln \operatorname{Tr} e^{-\beta(\sqrt{Na_I} X^I_{\boldsymbol{\sigma}_I} + V_N - B^{J\setminus I}} \} \right| = 0. \quad (3\text{-}5)$$

We note that B^J can be represented as a transversal magnetic field whose weights corresponding to the complement J^c are set zero. Thus, (3-5) follows from Theorem 2.3 after possibly rearranging the spin components. Using (3-5) successively for each subset $J \in \mathcal{P}$ (where the remaining potential V_N might change from step to step), we finally arrive at

$$\limsup_{N\to\infty} \frac{1}{N} \left| \ln \operatorname{Tr} e^{-\beta(U-B)} - \max_{\mathcal{F}\subset\mathcal{P}, D\in\mathcal{P}, D^c\cap\mathcal{F}=\varnothing} \ln \operatorname{Tr} e^{-\beta\left(\sum_{F\in\mathcal{F}} \sqrt{a_F N} X^F_{\boldsymbol{\sigma}_F} - B^{D^c}\right)} \right| = 0$$

where $D^c \cap \mathcal{F} = \varnothing$ is understood elementwise, that is, $D^c \cap F = \varnothing$ for any $F \in \mathcal{F}$. We note that the convexity of the exponential and the variables $X^J_{\boldsymbol{\sigma}_J}$ being centered Gaussians, implies (e.g., by (3-5)) for any $D^c \cap \mathcal{F} = \varnothing$,

$$\liminf_{N\to\infty} \frac{1}{N} \left(\ln \operatorname{Tr} e^{-\beta\left(\sum_{F\in\mathcal{P}(D)} \sqrt{a_F N} X^F_{\boldsymbol{\sigma}_F} - B^{D^c}\right)} - \ln \operatorname{Tr} e^{-\beta\left(\sum_{F\in\mathcal{F}} \sqrt{a_F N} X^F_{\boldsymbol{\sigma}_F} - B^{D^c}\right)} \right) \geq 0,$$

where $\mathcal{P}(D)$ is the power set of D. On the other hand, the limit of the left term exists almost surely and is given by

$$\lim_{N\to\infty} \frac{1}{N} \ln \operatorname{Tr} e^{-\beta\left(\sum_{F\in\mathcal{P}(D)} \sqrt{a_F N} X^F_{\boldsymbol{\sigma}_F} - B^{D^c}\right)} = \min_{S\in\mathcal{C}^D} \Phi_D(\beta, S) + \sum_{k\in D^c} L_k \, \mathbb{E}\left[\ln 2\cosh(\beta\mathfrak{b})\right],$$

where we used the strong law of large numbers for the expression involving B^{D^c} and the known convergence [7] of the classical nonhierarchical GREM. We in fact need a slightly more generalized version of [7] which is also applicable to the reduced model on the subgraph generated by $\boldsymbol{\sigma}_{D^c}$. However, this can be proved in the exactly same manner as the result on the whole graph $\mathcal{Q}_N$. Combining our findings, we arrive at the claim (1-20). □

It remains to show Corollary 1.7. To this end, we need the corresponding result in the case $\mathfrak{b} = 0$ for the classical nonhierarchical GREM, which is a simple consequence of the derivation in [7] (see Remark 7 in that paper). For completeness, we spell out this classical result as Lemma A.3 in the Appendix.

Proof of Corollary 1.7. Let S_0 be the minimizing chain of the classical problem as spelled out in Lemma A.3. After relabelling the components of $\boldsymbol{\sigma}$, we may assume that

$$S_0 = \{\varnothing, \{1\}, \{1,2\}, \ldots, \{1,\ldots,n\}\}. \quad (3\text{-}6)$$

We will show that

$$\max_{D\in\mathcal{P}} \left[\min_{S\in\mathcal{C}^D} \Phi(\beta, S) + \sum_{k\in D^c} L_k \, \mathbb{E}\left[\ln 2\cosh(\beta\mathfrak{b})\right] \right] = \Phi(\beta, \mathfrak{b}, S_0)$$

by establishing two inequalities. First, abbreviating

$$D_k := \{1, \ldots, k\}$$

with $D_0 := \varnothing$, we have

$$\max_{D\in\mathcal{P}}\left[\min_{S\in\mathcal{C}^D}\Phi(\beta,S)+\sum_{k\in D^c}L_k\mathbb{E}\left[\ln 2\cosh(\beta\mathfrak{b})\right]\right]$$
$$\geq \max_{0\leq k\leq n}\left[\min_{S\in\mathcal{C}^{D_k}}\Phi(\beta,S)+\sum_{k\in D_k^c}L_k\,\mathbb{E}\left[\ln 2\cosh(\beta\mathfrak{b})\right]\right]$$
$$= \max_{0\leq k\leq n}\left[\Phi(\beta,S_0^{D_k})+\sum_{k\in D_k^c}L_k\,\mathbb{E}\left[\ln 2\cosh(\beta\mathfrak{b})\right]\right]=\Phi(\beta,\mathfrak{b},S_0).$$

Here S_0^D denotes the chain which coincides with S_0 but ends at D. The last line follows from Lemma A.3 as it implies that even in the constrained setting the cut versions of S_0 are indeed minimizing chains.

For the reverse inequality, let $I_1,\dots,I_m$ be the sets associated to the concave hull $\bar{A}_{S_0}$ and let $\varphi^{(l)}_{S_0}(\beta)$ be the partial pressure corresponding to the GREM assigned to the chain S_0; see (1-6). Moreover, for any $D\in\mathcal{P}$ we define the ordered-restriction chain S_0^D,

$$S_0^D := \{\{\varnothing\},\{j_1\},\{j_1,j_2\},\dots,\{j_1,\dots,j_{k_D}\}\},$$

where $j_1<j_2<\cdots j_{k_D}\in D$ and $\{j_1,\dots,j_{k_D}\}=D$. Then for any $D\in\mathcal{P}$,

$$\min_{S\in\mathcal{C}^D}\Phi(\beta,S)+\sum_{j\in D^c}L_j\,\mathbb{E}\left[\ln 2\cosh(\beta\mathfrak{b})\right]\leq\Phi(\beta,S_0^D)+\sum_{j\in D^c}L_j\,\mathbb{E}\left[\ln 2\cosh(\beta\mathfrak{b})\right]$$
$$=\sum_{l=1}^{m_D}\varphi^{(l)}_{S_0^D}(\beta)+\sum_{j\in D^c}L_j\mathbb{E}\left[\ln 2\cosh(\beta\mathfrak{b})\right]\leq\sum_{l=1}^{m}\frac{\sum_{k\in I_l\cap D}L_k}{\sum_{k\in I_l}L_k}\varphi^{(l)}_{S_0}(\beta)+\sum_{j\in D^c}L_j\mathbb{E}\left[\ln 2\cosh(\beta\mathfrak{b})\right].$$

The last inequality, follows from three observations. First, we recall that the weights $a_l^{S_0^D}$ assigned to the chain S_0^D are less than or equal to the weights $a_{j_l}^{S_0}$ of the chain (3-6). Secondly, we note that the increments $\Delta_l\bar{A}_{S_0^D}$ on the segments $D\cap I_l\neq\varnothing$ can be bounded,

$$\frac{\Delta_l\bar{A}_{S_0^D}}{\sum_{k\in I_l\cap D}L_k}\leq\frac{\Delta_l\bar{A}_{S_0}}{\sum_{k\in I_l}L_k},$$

since otherwise we may construct a chain S' violating Lemma A.3 using the first observation. Thirdly, an application of Slepian's lemma as in the proof of Lemma 3.1 extends the summation to m and yields the claimed inequality. We thus obtain

$$\sum_{l=1}^{m}\left[\frac{\sum_{k\in I_l\cap D}L_k}{\sum_{k\in I_l}L_k}\varphi^{(l)}_{S_0}(\beta)+\sum_{j\in D^c\cap I_l}L_j\mathbb{E}\left[\ln 2\cosh(\beta\mathfrak{b})\right]\right]$$
$$\leq\sum_{l=1}^{m}\sum_{k\in I_l}L_k\max\left\{\frac{\varphi^{(l)}_{S_0}(\beta)}{\sum_{k\in I_l}L_k},\mathbb{E}\left[\ln 2\cosh(\beta\mathfrak{b})\right]\right\}=\Phi(\beta,\mathfrak{b},S_0),$$

where the last equality is based on the concavity, Lemma 3.2 and the explicit expression (1-13) for the pressure of the quantum GREM. This completes the proof as D was chosen arbitrarily. □

Appendix: Supplementary results

Sufficient condition for Assumption 2.1. We want to present a quite general condition on the distribution of $X_{\boldsymbol{\sigma_1}}$ which implies the third point in Assumption 2.1:

Lemma A.1. *Let $X_{\boldsymbol{\sigma_1}}$ be independent and identically distributed centered random variables which satisfy an LDP with good rate function I, i.e., the sets $\{x \mid I(x) \le a\}$ are compact for any $a \ge 0$. Moreover, the rate function shall satisfy*

$$\inf_{|x|>\varepsilon} I(x) > 0$$

for any $\varepsilon > 0$. Then, $(X_{\boldsymbol{\sigma_1}})$ fulfills the conditions (1), (2) *and* (3) *in Assumption 2.1.*

Proof. The points (1) and (2) are clear and it remains to check (3). Let $w_{\boldsymbol{\sigma}_1}$ be random weights which are independent of $X_{\boldsymbol{\sigma}_1}$ and satisfy almost surely $w_{\boldsymbol{\sigma}_1} \ge 0$ and $\sum_{\boldsymbol{\sigma}} w_{\boldsymbol{\sigma}_1} = 1$. We introduce the sets

$$A_N := \{\boldsymbol{\sigma}_1 \in \mathcal{Q}_N^{(1)} \mid w_{\boldsymbol{\sigma}_1} \ge 1/N^2\}$$

and show separately

$$\lim_{N\to\infty} \frac{1}{N} \sum_{\boldsymbol{\sigma}_1 \in A_N} w_{\boldsymbol{\sigma}_1} X_{\boldsymbol{\sigma_1}} = 0 \tag{A-1}$$

and

$$\lim_{N\to\infty} \frac{1}{N} \sum_{\boldsymbol{\sigma} \in A_N^c} w_{\boldsymbol{\sigma}_1} X_{\boldsymbol{\sigma_1}} = 0. \tag{A-2}$$

Proof of (A-1). We apply the trivial bound

$$\left| \frac{1}{N} \sum_{\boldsymbol{\sigma}_1 \in A_N} w_{\boldsymbol{\sigma}_1} X_{\boldsymbol{\sigma_1}} \right| \le \frac{1}{N} \sup_{\boldsymbol{\sigma}_1 \in A_N} |X_{\boldsymbol{\sigma}_1}|,$$

and note that the cardinality of A_N is bounded by N^2. The independence of $w_{\boldsymbol{\sigma}_1}$ and $X_{\boldsymbol{\sigma_1}}$ then implies, for any $\delta > 0$,

$$\mathbb{P}\Big(\sup_{\boldsymbol{\sigma}_1 \in A_N} |X_{\boldsymbol{\sigma}_1}| \ge \delta N\Big) \le N^2\, \mathbb{P}(|X_{\boldsymbol{\sigma}_1}| \ge \delta N) \le N^2 e^{-(c_\delta + o(1))N} \qquad \text{with} \quad c_\delta = \inf_{|x|\ge\delta} I(x) > 0.$$

Therefore, the bound on the probability is summable in N for any $\delta > 0$ and a Borel–Cantelli argument finishes the proof of (A-1). □

Proof of (A-2). As I is a good rate function, we find a constant $C > 0$ such that

$$\inf_{|x|\ge C} I(x) \ge 2\ln 2,$$

and hence

$$\mathbb{P}\Big(\sup_{\boldsymbol{\sigma}_1 \in \mathcal{Q}_N^{(1)}} |X_{\boldsymbol{\sigma}_1}| \ge CN\Big) \le 2^N e^{-(2\ln 2 + o(1))N} = (2 + o(1))^{-N}.$$

By a Borel–Cantelli argument we may assume without loss of generality that $|X_{\boldsymbol{\sigma}_1}| \leq CN$ holds true for all sufficiently large N with probability one. Conditioning on $w_{\boldsymbol{\sigma}_1}$, the independence of $X_{\boldsymbol{\sigma}_1}$ and $\mathbb{E}[X_{\boldsymbol{\sigma}_1}] = 0$ implies

$$\mathbb{E}\left[\left(\frac{1}{N}\sum_{\boldsymbol{\sigma}_1 \in A_N^c} w_{\boldsymbol{\sigma}_1} X_{\boldsymbol{\sigma}_1}\right)^2\right] \leq \frac{1}{N^2}\mathbb{E}\left[\sum_{\boldsymbol{\sigma}_1 \in A_N^c} w_{\boldsymbol{\sigma}_1}^2 X_{\boldsymbol{\sigma}_1}^2\right] \leq C^2\,\mathbb{E}\left[\sum_{\boldsymbol{\sigma}_1 \in A_N^c} w_{\boldsymbol{\sigma}_1}^2\right] \leq \frac{C^2}{N^2}\,\mathbb{E}\left[\sum_{\boldsymbol{\sigma}_1 \in A_N^c} w_{\boldsymbol{\sigma}_1}\right] \leq \frac{C^2}{N^2}.$$

In the second and third inequalities, we use $|X_{\boldsymbol{\sigma}_1}| \leq CN$ and $w_{\boldsymbol{\sigma}_1} \leq N^{-2}$ for $\boldsymbol{\sigma}_1 \in A_N^c$. The Borel–Cantelli lemma again completes the proof. □

Assumption 2.2 for independent L^1 weights. The aim of this section is to verify that Assumption 2.2 is satisfied for independent copies (b_j) of an absolutely integrable variable $\mathfrak{b}$:

Lemma A.2. *If the weights b_i are independent copies of an absolutely integrable variable $\mathfrak{b}$, we almost surely have*

$$\limsup_{N\to\infty} N^{-1}\sqrt{\sum_{i=1}^{N} |b_i|^2} = 0. \tag{A-3}$$

Proof. Our proof relies on a thinning and truncation argument and is similar to the proof of the strong law of large numbers in the L^1-case.

Let us abbreviate the partial sums $S_N := \sum_{i=1}^{N} |b_i|^2$. We pick some $\varepsilon > 0$ and introduce the sequence $N_m := 2^m$. Suppose we have already shown the almost sure convergence

$$\lim_{m\to\infty} (N_m)^{-2} S_{N_m} = 0. \tag{A-4}$$

Since S_N is an increasing sequence we conclude that

$$\limsup_{N\to\infty} \frac{S_N}{N^2} \leq \limsup_{m\to\infty} \frac{S_{N_m}}{N_{m-1}^2} = 4 \limsup_{m\to\infty} \frac{S_{N_m}}{N_m^2} = 0.$$

So it suffices to show (A-4). To this end, let K_m be a nonnegative sequence which we will fix later and $S_{N_m}^{<}$, $S_{N_m}^{>}$ be the truncated sums given by

$$S_{N_m}^{<} := \sum_{i=1}^{N_m} |b_i|^2 \mathbb{1}_{|b_i|\leq K_m} \quad \text{and} \quad S_{N_m}^{>} := S_{N_m} - S_{N_m}^{>}.$$

For any $\varepsilon > 0$, a Markov-type estimate yields

$$\mathbb{P}(S_{N_m}^{<} > \varepsilon N_m^2) \leq \frac{\mathbb{E}[|\mathfrak{b}|^2 \mathbb{1}_{|\mathfrak{b}|\leq K_m}]}{\varepsilon N_m}.$$

We also have

$$\mathbb{P}(S_{N_m}^{>} \neq 0) \leq N_m\,\mathbb{P}(|\mathfrak{b}| > K_m).$$

The assertion follows by a Borel–Cantelli argument if we can choose K_m such that

$$\sum_{m=1}^{\infty} \frac{\mathbb{E}\,[|\mathfrak{b}|^2 \mathbb{1}_{|\mathfrak{b}|\le K_m}]}{N_m} + \sum_{m=1}^{\infty} N_m \mathbb{P}(|\mathfrak{b}| > K_m) < \infty.$$

We claim that this can be accomplished by setting $N_m = K_m$. To this end, we note that the second sum is finite as $\mathfrak{b}$ is absolutely integrable. Moreover,

$$\sum_{m=1}^{\infty} \frac{\mathbb{E}\,[|\mathfrak{b}|^2 \mathbb{1}_{|\mathfrak{b}|\le N_m}]}{N_m} \le 2 \sum_{m=1}^{\infty} N_m^2 \mathbb{P}(|\mathfrak{b}| \ge N_m) \sum_{k\ge m} N_m^{-1} \le 4 \sum_{m=1}^{\infty} N_m \mathbb{P}(|\mathfrak{b}| \ge N_m) < \infty,$$

where the first inequality is a consequence of the layer-cake representation and the last bound is again a consequence of $\mathfrak{b}$ being absolutely integrable. □

The pressure of the classical nonhierarchical GREM. The following lemma is contained in the analysis of [7]. We provide a proof for the convenience of the reader.

Lemma A.3. *Let X be a Gaussian vector of nonhierarchical GREM type. Then, there exists a chain S_0 such that for any chain S the pointwise estimate*

$$\bar{A}_S(x) \le \bar{A}_{S_0}(x) \tag{A-5}$$

holds true, where $\bar{A}_S$ and $\bar{A}_{S_0}$ are the concave hulls of the ordinary GREM vectors assigned to S and S_0, respectively. Moreover, we have, for any $\beta \ge 0$,

$$\Phi(\beta) = \min_{S\in\mathcal{C}} \Phi(\beta, S) = \Phi(\beta, S_0). \tag{A-6}$$

Proof. For any $\varnothing \ne J \subset \{1, \dots, n\}$ we define the corresponding slope γ_J;

$$\gamma_J := \frac{\tilde{a}_J}{L_J} := \frac{\sum_{I\subset J} a_I}{\sum_{k\in J} L_k}.$$

We now construct a (possibly incomplete) chain $J_1 \subset J_2 \subset \cdots J_m = \{1, \dots, n\}$ as follows. We first pick a subset J_1 with maximal slope γ_{J_1}. If $J_1 = \{1, \dots, n\}$, we are done. Otherwise we pick a subset J_2 such that

$$\gamma_{J_2} = \max_{I\subset\{1,\dots,n\}; I\not\subset J_1} a_I.$$

One easily checks that $\gamma_{J_2} \le \gamma_{J_1\cup J_2}$, so we may assume that $J_1 \subset J_2$. We stop if $J_2 = \{1, \dots, n\}$ and continue the procedure otherwise. After at most n steps we arrive at a (possibly incomplete) chain as claimed. We set S_0 to be a completion of $J_1, \dots, J_m$, that is, S_0 is a chain which contains $J_1, \dots, J_m$. Clearly, S_0 does not depend on β.

Both assertions follow now easily. We see that the concave hull $\bar{A}_{S_0}$ assigned to S_0 is the unique piecewise linear function satisfying $\bar{A}_{S_0}(L_{J_k}) = \tilde{a}_{J_k}$ for any k. By construction, $\bar{A}_{S_0}$ is pointwise maximal as we iteratively pick the subset J_k leading to the maximal mean slope. On the other hand, the bound $\bar{A}_{S_0} \ge \bar{A}_S$ for any chain S, by Slepian's lemma, yields $\Phi(\beta, S_0) \le \Phi(\beta, S)$ from which the second statement follows. □

Acknowledgments

This work was supported by the DFG under EXC-2111–390814868.

References

[1] J. Adame and S. Warzel, "Exponential vanishing of the ground-state gap of the quantum random energy model via adiabatic quantum computing", *J. Math. Phys.* **56**:11 (2015), art. id. 113301. MR Zbl

[2] A. Adhikari and C. Brennecke, "Free energy of the quantum Sherrington–Kirkpatrick spin-glass model with transverse field", *J. Math. Phys.* **61**:8 (2020), art. id. 083302. MR Zbl

[3] M. Aizenman, J. L. Lebowitz, and D. Ruelle, "Some rigorous results on the Sherrington–Kirkpatrick spin glass model", *Comm. Math. Phys.* **112**:1 (1987), 3–20. MR Zbl

[4] L.-P. Arguin and N. Kistler, "Microcanonical analysis of the random energy model in a random magnetic field", *J. Stat. Phys.* **157**:1 (2014), 1–16. MR Zbl

[5] L.-P. Arguin and R. Persechino, "The free energy of the GREM with random magnetic field", pp. 37–61 in *Statistical mechanics of classical and disordered systems*, edited by V. Gayrard et al., Springer Proc. Math. Stat. **293**, Springer, 2019. MR Zbl

[6] V. Bapst, L. Foini, F. Krzakala, G. Semerjian, and F. Zamponi, "The quantum adiabatic algorithm applied to random optimization problems: the quantum spin glass perspective", *Phys. Rep.* **523**:3 (2013), 127–205. MR

[7] E. Bolthausen and N. Kistler, "On a nonhierarchical version of the generalized random energy model", *Ann. Appl. Probab.* **16**:1 (2006), 1–14. MR Zbl

[8] A. Bovier, *Statistical mechanics of disordered systems: A mathematical perspective*, Cambridge Series in Statistical and Probabilistic Mathematics **18**, Cambridge University Press, 2006. MR Zbl

[9] A. Bovier and A. Klimovsky, "Fluctuations of the partition function in the generalized random energy model with external field", *J. Math. Phys.* **49**:12 (2008), art. id. 125202. MR Zbl

[10] A. Bovier and I. Kurkova, "Derrida's generalised random energy models, I: Models with finitely many hierarchies", *Ann. Inst. H. Poincaré Probab. Statist.* **40**:4 (2004), 439–480. MR Zbl

[11] A. Bovier and I. Kurkova, "Derrida's generalized random energy models, II: Models with continuous hierarchies", *Ann. Inst. H. Poincaré Probab. Statist.* **40**:4 (2004), 481–495. MR Zbl

[12] A. J. Bray and M. A. Moore, "Replica theory of quantum spin glasses", *Journal of Physics C*: *Solid State Physics* **13**:24 (1980), L655–L660.

[13] A. Burin, "Localization and chaos in a quantum spin glass model in random longitudinal fields: Mapping to the localization problem in a Bethe lattice with a correlated disorder", *Annalen der Physik* **529**:7 (2017), art. id. 1600292.

[14] D. Capocaccia, M. Cassandro, and P. Picco, "On the existence of thermodynamics for the generalized random energy model", *J. Statist. Phys.* **46**:3-4 (1987), 493–505. MR

[15] N. Crawford, "Thermodynamics and universality for mean field quantum spin glasses", *Comm. Math. Phys.* **274**:3 (2007), 821–839. MR Zbl

[16] B. Derrida, "Random-energy model: limit of a family of disordered models", *Phys. Rev. Lett.* **45**:2 (1980), 79–82. MR

[17] B. Derrida, "Random-energy model: an exactly solvable model of disordered systems", *Phys. Rev. B* (3) **24**:5 (1981), 2613–2626. MR Zbl

[18] B. Derrida, "A generalization of the random energy model which includes correlations between energies", *Journal de Physique Lettres* **46** (1985), 401–407.

[19] B. Derrida and E. Gardner, "Solution of the generalised random energy model", *Journal of Physics C*: *Solid State Physics* **19**:13 (may 1986), 2253–2274.

[20] Y. Fedorov and E. Shender, "Quantum spin glasses in the Ising model with a transverse field", *JETP Lett.* **43** (1986), 681–684.

[21] Y. Y. Goldschmidt, "Solvable model of the quantum spin glass in a transverse field", *Phys. Rev. B* **41** (Mar 1990), 4858–4861.

[22] F. Guerra and F. L. Toninelli, "The thermodynamic limit in mean field spin glass models", *Comm. Math. Phys.* **230**:1 (2002), 71–79. MR Zbl

[23] C. R. Laumann, A. Pal, and A. Scardicchio, "Many-body mobility edge in a mean-field quantum spin glass", *Phys. Rev. Lett.* **113** (Nov 2014), art. id. 200405.

[24] H. Leschke, C. Manai, R. Ruder, and S. Warzel, "Existence of replica-symmetry breaking in quantum glasses", *Phys. Rev. Lett.* **127**:20 (2021), art. id. 207204. MR

[25] H. Leschke, S. Rothlauf, R. Ruder, and W. Spitzer, "The free energy of a quantum Sherrington–Kirkpatrick spin-glass model for weak disorder", *J. Stat. Phys.* **182**:3 (2021), art. id. 55. MR Zbl

[26] C. Manai and S. Warzel, "Phase diagram of the quantum random energy model", *J. Stat. Phys.* **180**:1-6 (2020), 654–664. MR Zbl

[27] C. Manai and S. Warzel, "The quantum random energy model as a limit of p-spin interactions", *Rev. Math. Phys.* **33**:1 (2021), art. id. 2060013. MR Zbl

[28] C. Manai and S. Warzel, "The de Almeida–Thouless line in hierarchical quantum spin glasses", *J. Stat. Phys.* **186**:1 (2022), art. id. 14. MR

[29] M. Mézard, G. Parisi, and M. A. Virasoro, *Spin glass theory and beyond*, World Scientific Lecture Notes in Physics **9**, World Scientific Publishing Co., Teaneck, NJ, 1987. MR Zbl

[30] T. Obuchi, H. Nishimori, and D. Sherrington, "Phase diagram of the p-spin-interacting spin glass with ferromagnetic bias and a transverse field in the infinite-p limit", *Journal of the Physical Society of Japan* **76**:5 (2007), art. id. 054002.

[31] D. Panchenko, "The Sherrington–Kirkpatrick model: an overview", *J. Stat. Phys.* **149**:2 (2012), 362–383. MR Zbl

[32] D. Panchenko, "The Parisi formula for mixed p-spin models", *Ann. Probab.* **42**:3 (2014), 946–958. MR Zbl

[33] G. Parisi, "The order parameter for spin glasses: a function on the interval 0-1", *Journal of Physics A: Mathematical and General* **13**:3 (mar 1980), 1101–1112.

[34] D. W. Robinson, "Statistical mechanics of quantum spin systems", *Comm. Math. Phys.* **6** (1967), 151–160. MR Zbl

[35] B. Simon, *The statistical mechanics of lattice gases, Vol. I*, Princeton University Press, 1993. MR Zbl

[36] B. Simon, *Convexity: An analytic viewpoint*, Cambridge Tracts in Mathematics **187**, Cambridge University Press, 2011. MR Zbl

[37] S. Suzuki, J.-i. Inoue, and B. K. Chakrabarti, *Quantum Ising phases and transitions in transverse Ising models*, 2nd ed., Lecture Notes in Physics **862**, Springer, 2013. MR Zbl

[38] M. Talagrand, "The Parisi formula", *Ann. of Math.* (2) **163**:1 (2006), 221–263. MR

[39] M. Talagrand, *Mean field models for spin glasses, Volume I: Basic examples*, Ergeb. Math. Grenzgeb. **54**, Springer, 2011. MR

[40] M. Talagrand, *Mean field models for spin glasses*, *Volume II*: *Advanced replica-symmetry and low temperature*, Ergeb. Math. Grenzgeb. **55**, Springer, 2011. MR

[41] K. Usadel, "Spin glass transition in an Ising spin system with transverse field", *Solid State Communications* **58**:9 (1986), 629–630.

Received 15 Jul 2020. Accepted 27 Jun 2021.

CHOKRI MANAI: chokri.manai@tum.de
Zentrum Mathematik, Technische Universität München, Garching bei München, Germany

SIMONE WARZEL: warzel@ma.tum.de
Zentrum Mathematik, Technische Universität München, Garching bei München, Germany

PROBABILITY and MATHEMATICAL PHYSICS

msp.org/pmp

See inside back cover or msp.org/pmp for submission instructions.

Probability and Mathematical Physics (ISSN 2690-1005 electronic, 2690-0998 printed) at Mathematical Sciences Publishers, 798 Evans Hall #3840, c/o University of California, Berkeley, CA 94720-3840 is published continuously online. Periodical rate postage paid at Berkeley, CA 94704, and additional mailing offices.

PMP peer review and production are managed by EditFlow® from MSP.

PUBLISHED BY

mathematical sciences publishers

nonprofit scientific publishing

https://msp.org/

PROBABILITY and MATHEMATICAL PHYSICS

3:2 2022

A.3 The de Almeida-Thouless Line in Hierarchical Quantum Spin Glasses

The de Almeida-Thouless Line in Hierarchical Quantum Spin Glasses

Chokri Manai and Simone Warzel

It has been a longstanding problem to understand the influence of a longitudinal magnetic field on the spin glass order. Indeed, de Almeida and Thouless considered the stability of the SK model in a vertical field already in 1978 [57]. In this work, the authors predicted a curve, the so-called AT line, which separates the glass phase from the non-glass phase. So far, it has been only established that there exists spin glass order for temperatures below the AT line [185]. Despite numerous efforts and recent progress [4, 43, 51] the vanishing spin glass order has only been established in a subdomain above the AT line. Determining the exact quantum AT line in the QSK model appears elusive and, therefore, it is illuminating to consider models, where such an rigorous analytic treatment is feasible. Core Article III deals with the quantum AT line in the QGREM and QCREM.

Main Results

This article builds up on our work [130]. Indeed, we consider the QGREM and QCREM with an additional (random) longitudinal field. There are at least two choices on how to implement the magnetic field in z-direction: as a sum of weighted $h = \sum_i h_i \sigma_i^z$ operators or as hierarchical reorganization of the potential arising from h. Our main theorems determine the limit of the pressure in the QCREM and QGREM in both scenarios. In the first case, our main theorem is even with vanishing transversal field partially new and extends the prior work on the 2-level GREM [14, 15, 38]. We demonstrate that the corresponding AT line is unphysical as the spin glass enlarges if the magnetic fields becomes stronger. We thus argue that a hierarchical implementation of z-field, following the original construction of Derrida and Gardner [64], is physically more relevant. Indeed, here the spin glass phase shrinks with increasing field strengths. We also discuss the corresponding quantum AT line and compare it to the numerical predictions for the QSK [193].

Individual Contribution

I am the principal author of this article. It was my idea to implement an additional longitudinal field in the QGREM. I created a first draft of the paper which contained a sketch of the proof. Many discussions with Simone Warzel helped to clarify that a hierarchical longitudinal field yields physically more relevant results. It was Simone Warzel's idea to compare our findings with the expected quantum AT-line in the QSK. The final publication -the presentation of the results, the structure of the different section and the derivation of various technical lemmas - is a result of a close collaboration with my advisor Simone Warzel.

Permission to include:

Chokri Manai and Simone Warzel
The de Almeida-Thouless Line in Hierarchical Quantum Spin Glasses.
Journal of Statistical Physics 186: 14 (2022).
https://doi.org/10.1007/s10955-021-02860-9.

How to obtain permission to reuse Springer Nature content not available online on SpringerLink

Requests for permission to reuse content (e.g. figure or table, abstract, text excerpts) from Springer Nature publications currently not available online must be submitted in writing. Please be as detailed and specific as possible about what, where, how much, and why you wish to reuse the content.

Your contacts to obtain permission for the reuse of material from:

- books: bookpermissions@springernature.com
- journals: journalpermissions@springernature.com

Author reuse

Please check the Copyright Transfer Statement (CTS) or Licence to Publish (LTP) that you have signed with Springer Nature to find further information about the reuse of your content.

Authors have the right to reuse their article's Version of Record, in whole or in part, in their own thesis. Additionally, they may reproduce and make available their thesis, including Springer Nature content, as required by their awarding academic institution. Authors must properly cite the published article in their thesis according to current citation standards.
Material from: 'AUTHOR, TITLE, JOURNAL TITLE, published [YEAR], [publisher - as it appears on our copyright page]'

If you are any doubt about whether your intended re-use is covered, please contact journalpermissions@springernature.com for confirmation.

Self-Archiving

- Journal authors retain the right to self-archive the final accepted version of their manuscript. Please see our self-archiving policy for full details: https://www.springer.com/gp/open-access/authors-rights/self-archiving-policy/2124

- Book authors please refer to the information on this link: https://www.springer.com/gp/open-access/publication-policies/self-archiving-policy

Journal of Statistical Physics (2022) 186:14
https://doi.org/10.1007/s10955-021-02860-9

The de Almeida–Thouless Line in Hierarchical Quantum Spin Glasses

Chokri Manai[1] · **Simone Warzel**[1]

Received: 8 June 2021 / Accepted: 29 November 2021 / Published online: 17 December 2021

Abstract
We determine explicitly and discuss in detail the effects of the joint presence of a longitudinal and a transversal (random) magnetic field on the phases of the Random Energy Model and its hierarchical generalization, the GREM. Our results extent known results both in the classical case of vanishing transversal field and in the quantum case for vanishing longitudinal field. Following Derrida and Gardner, we argue that the longitudinal field has to be implemented hierarchically also in the Quantum GREM. We show that this ensures the shrinking of the spin glass phase in the presence of the magnetic fields as is also expected for the Quantum Sherrington–Kirkpatrick model.

Keywords Disordered systems · Quantum spin glass · Phase transition · Free energy

Mathematics Subject Classification 82D30 · 82B44

1 Introduction and Main Results

Mean-field spin glasses such as the Sherrington–Kirkpatrick (SK) model have long served as an inspiration to both physicists and mathematicians [23,25,30]. For these classical glasses, Parisi's replica ansatz for the free energy presents one of the rare gems of an exactly solvable case, whose solution covers extremely complex behavior—notably the occurrence of a frozen glass phase below a certain critical temperature T_c. Since spins are intrinsically quantum-mechanical objects, physicists have started early on to investigate the quantum effects caused by the inclusion of a transversal magnetic field. Unfortunately, unlike the inclusion of a longitudinal magnetic field in the SK-model, the transversal field seems to crash all attempts of an explicit Parisi solution. One either has to resort to approximations or numerical calculations for the full phase diagram [17,24,28,32–34] or bounds [18,19] or more qualitative results [1,9]

Communicated by Bernard Derrida.

This work was supported by the DFG under EXC-2111 – 390814868.

Simone Warzel
warzel@ma.tum.de

[1] MCQST & Zentrum Mathematik, Technische Universität München, Munich, Germany

for the Quantum SK-model. It is therefore rather remarkable that the associated hierarchical caricature, the generalized random energy model (GREM), still admits an explicit solution of Parisi type even in the presence of a transversal field [15,20,22]. The GREM was initially invented by Derrida [12,13] to qualitatively capture the behavior of the free energy of more complicated glasses. It was mathematically reformulated in [27] and its significance for Parisi's ansatz was later clarified in [3,16,29].

One central question for spin glasses in external magnetic fields is whether the fields destabilize the low-temperature glass phase or not. For the SK-model in a constant longitudinal field, de Almeida and Thouless [10] determined an equation for the critical temperature $T_c(h)$, which turns out to be decreasing in the field strength h and is known under the name de Almeida–Thouless (AT) line. Below $T_c(h)$ the replica symmetry has been proven to be broken [31]. Rigorous results above $T_c(h)$ are still incomplete (see e.g. [2] and refs. therein). Unlike for the SK-model, implementing the longitudinal field naively in GREM models causes the frozen phase to expand [4,5,7]. Derrida and Gardner [14] therefore suggested a hierarchical implementation of the longitudinal magnetic field, which then leads again to a destabilization of the frozen phase.

The present paper now investigates the question of the stability of the low-temperature phase in general GREM models under the joint presence of a longitudinal and transversal field. We will present explicit formulas for the free energy of such Q(uantum)GREMs for both cases: a naive implementation of the longitudinal magnetic field and a hierarchical implementation. We will discuss the stability of the glass phase and calculate associated critical exponents.

1.1 The Quantum GREM with a Random Longitudinal Field

The QGREM with a (random) external transversal and longitudinal magnetic field is a Hamiltonian on $\psi \in \ell^2(\mathcal{Q}_N)$ of the form

$$(H_N\psi)(\boldsymbol{\sigma}) = U(\boldsymbol{\sigma})\psi(\boldsymbol{\sigma}) - h(\boldsymbol{\sigma})\psi(\boldsymbol{\sigma}) - (B\psi)(\boldsymbol{\sigma}). \tag{1}$$

The first term represents the GREM energy landscape on the Hamming cube $\mathcal{Q}_N := \{-1, 1\}^N$ and is given by a centered Gaussian process $U(\boldsymbol{\sigma})$ with covariance function

$$\mathbb{E}\,[U(\boldsymbol{\sigma})U(\boldsymbol{\sigma}')] = NA(q_N(\boldsymbol{\sigma}, \boldsymbol{\sigma}')), \tag{2}$$

where $A\colon [0, 1] \to [0, 1]$ is a fixed non-decreasing, right-continuous, and normalized function, $A(1) = 1$, which does not depend on N. Moreover, q_N denotes the normalized lexicographic overlap of spin configurations $\boldsymbol{\sigma}, \boldsymbol{\sigma}' \in \mathcal{Q}_N$:

$$q_N(\boldsymbol{\sigma}, \boldsymbol{\sigma}') := \begin{cases} 1 & \text{if } \boldsymbol{\sigma} = \boldsymbol{\sigma}', \\ \frac{1}{N}\left(\min\{1 \le i \le N : \sigma_i \ne \sigma_i'\} - 1\right) & \text{else}. \end{cases} \tag{3}$$

GREM processes distinguish themselves through their choice of A, which may be a continuous distribution function. In the latter case, these processes are also called CREM, which is short for continuous REM. Other examples correspond to distribution functions A with a finite number n of atoms, which is referred to as an n-level GREM. The simplest case is one atom at $x = 1$, i.e. $A(x) = 0$ for $x < 1$ and $A(1) = 1$, which corresponds to the REM, i.e. the case of independent and identically distributed centered Gaussian variables $U(\boldsymbol{\sigma}), \boldsymbol{\sigma} \in \mathcal{Q}_N$, with variance N.

A straightforward implementation of a (random) longitudinal magnetic field is achieved through setting

$$h(\boldsymbol{\sigma}) = \sum_{j=1}^{N} h_j \sigma_j. \tag{4}$$

Interpreting the configuration basis $\boldsymbol{\sigma}$ as the z-components of N quantum spin-1/2, a (random) transversal field B in x-direction is given by the sum of the Pauli x-matrices $\boldsymbol{s}_j$ with weights $b_j \in \mathbb{R}$:

$$\begin{aligned} (B\psi)(\boldsymbol{\sigma}) &:= \sum_{j=1}^{N} b_j \left(\boldsymbol{s}_j \psi\right)(\boldsymbol{\sigma}), \qquad \left(\boldsymbol{s}_j \psi\right)(\boldsymbol{\sigma}) := \psi(F_j \boldsymbol{\sigma}), \\ F_j \boldsymbol{\sigma} &:= (\sigma_1, \ldots, -\sigma_j, \ldots, \sigma_N). \end{aligned} \tag{5}$$

We will assume throughout that the variables $(U(\boldsymbol{\sigma}))$, (h_j) and (b_j) are mutually independent and that the field variables h_j and b_j are independent copies of absolutely integrable random variables $\mathfrak{h}$ and $\mathfrak{b}$, respectively.

Occurring phase transitions, in particular the AT line, are encoded in the limit of the pressure (or the negative free energy times the inverse temperature β)

$$\Phi_N(\beta, \mathfrak{h}, \mathfrak{b}) := \frac{1}{N} \ln \operatorname{Tr} e^{-\beta H_N} \tag{6}$$

as the number of spins N goes to infinity. Our first main theorem is an explicit formula for this limit in terms of the concave hull $\bar{A}$ of A and the right derivative $\bar{a}$ of $\bar{A}$.

Theorem 1 *Let $U(\boldsymbol{\sigma})$ be a GREM with distribution function A and suppose that the longitudinal random field is implemented as in (4). For any $\beta \geq 0$ and any absolutely integrable random variables $\mathfrak{h}$, $\mathfrak{b}$, the pressure converges almost surely,*

$$\lim_{N\to\infty} \Phi_N(\beta, \mathfrak{h}, \mathfrak{b}) = \sup_{0\leq z\leq 1} \left(\int_0^z \varphi(\beta, \mathfrak{h}, x)\, dx + (1-z)\mathbb{E}\left[\ln 2\cosh(\beta\sqrt{\mathfrak{b}^2 + \mathfrak{h}^2})\right] \right). \tag{7}$$

The density $\varphi(\beta, \mathfrak{h}, x)$ is given by

$$\varphi(\beta, \mathfrak{h}, x) := \begin{cases} \ln 2 + \bar{a}(x)\frac{\beta^2}{2} + \mathbb{E}\left[\ln\cosh\beta\mathfrak{h}\right] & \text{if} \quad \beta \leq \beta_c(x), \\ \beta(\bar{a}(x)\beta_c(x) + \mathbb{E}\left[\mathfrak{h}\tanh\beta_c(x)\mathfrak{h}\right]) & \text{if} \quad \beta > \beta_c(x), \end{cases} \tag{8}$$

where $\beta_c(x) = \beta_c(x, \mathfrak{h})$ is the unique positive solution of the self-consistency equation

$$\frac{\bar{a}(x)}{2}\beta_c(x)^2 = \ln 2 + \mathbb{E}\left[\ln\cosh\beta_c(x)\mathfrak{h}\right] - \beta_c(x)\mathbb{E}\left[\mathfrak{h}\tanh\beta_c(x)\mathfrak{h}\right]. \tag{9}$$

Moreover, $\varphi(\beta, \mathfrak{h}, x)$ is a decreasing function of x and strictly increasing and convex in β, while $\beta_c(x)$ is increasing in x.

Theorem 1, whose proof will be spelled out in Sect. 3, is a generalization of Theorem 1.4 in [22], which addresses the case without a longitudinal field, $\mathfrak{h} = 0$. In the classical case without transversal magnetic field, $\mathfrak{b} = 0$, it generalizes the results of [7], which covers the case that $\mathfrak{h}$ is constant, and of [4,5], which treats the special case of a REM or two-level GREM in a random magnetic field.

1.2 Stability of the Glass Phase in the QGREM with Longitudinal Field

Glass behavior occurs if the inverse temperature $\beta \geq \beta_c(x)$ for at least one $x \in [0,1]$. From (8) and the monotonicity of $\varphi(\beta, \mathfrak{h}, x)$ and $\beta_c(x)$, it is evident that the location of the glass transition predicted by (7) coincides with $\beta_c(x=0)$ and, thus, is completely determined by $\varphi(\beta, \mathfrak{h}, 0)$ which agrees with a rescaled REM pressure [4]. In order to understand the qualitative behavior of the phase diagram and in particular the question of the stability of the glass phase in the QGREM with longitudinal field (4), it is thus convenient to restrict the discussion to the REM with constant fields, i.e., $\mathfrak{h} = h$ and $\mathfrak{b} = \Gamma$ for some positive constants $h, \Gamma \geq 0$. In fact, even quantitative properties such as the dependence of the critical temperature $T_c(h) = \beta_c(0,h)^{-1}$ on the longitudinal field h coincide for the general GREM with the REM except for some numerical factors which depend on $\bar{a}(0)$. We therefore state the application of Theorem 1 to the QREM as our next corollary.

Corollary 1 *Consider a REM process $U(\boldsymbol{\sigma})$ and constant longitudinal and transversal fields of strength $h, \Gamma \geq 0$. Then, almost surely*

$$\lim_{N\to\infty} \Phi_N(\beta, h, \Gamma) = \max\{\Phi^{\mathrm{REM}}(\beta, h), \ln 2\cosh(\beta\sqrt{h^2+\Gamma^2}).\}, \tag{10}$$

where, $\Phi^{\mathrm{REM}}(\beta, h)$ denotes the function

$$\Phi^{\mathrm{REM}}(\beta, h) = \begin{cases} \ln 2 + \frac{\beta^2}{2} + \ln\cosh\beta h & if \quad \beta \leq \beta_c(h) \\ \beta(\beta_c(h) + h\tanh(\beta_c(h)h)) & if \quad \beta > \beta_c(h) \end{cases} \tag{11}$$

and $\beta_c(h)$ is the unique positive solution of

$$\beta_c(h)^2 = 2r(\tanh(\beta_c(h)h)) \tag{12}$$

with the modified binary entropy $r\colon [-1,1] \to \mathbb{R}$,

$$r(x) := -\left(\frac{1-x}{2}\ln\frac{1-x}{2} + \frac{1+x}{2}\ln\frac{1+x}{2}\right). \tag{13}$$

The short proof of Corollary 1 can be found in Appendix A.

For fixed $h > 0$ the phase diagram, which is plotted in Fig. 1, resembles that of the QREM without longitudinal field [15,20]. The model undergoes a magnetic transition at

$$\Gamma_c(\beta, h) := \sqrt{\beta^{-2}\,\mathrm{arcosh}\left(\frac{1}{2}\exp(\Phi^{\mathrm{REM}}(\beta, h))\right)^2 - h^2}, \tag{14}$$

where the magnetization in x-direction jumps. At fixed $h > 0$, this line separates the quantum paramagnet characterized by a positive magnetization in x-direction, from the classical spin glass.

The unique positive solution $\beta_c(h) \in (0, \sqrt{2\ln 2})$ of the self-consistency equation (12) marks the inverse freezing temperature at longitudinal field $h > 0$. For fixed $h > 0$ this line separates the high-temperature regime of the classical paramagnet at $\Gamma < \Gamma_c(\beta, h)$ from the spin glass phase. In comparison to the case $h = 0$, the longitudinal field causes an extensive magnetization $M(\boldsymbol{\sigma}) := \sum_{i=1}^N \sigma_i$ in z-direction under the Gibbs average. The specific magnetization in z-direction is a self-averaging quantity which converges as $N \to \infty$ to

$$m_z(\beta, h) := \frac{1}{\beta}\frac{\partial\Phi}{\partial h}(\beta, h) = \begin{cases} \tanh(\min\{\beta, \beta_c(h)\}h), & \Gamma < \Gamma_c(\beta, h), \\ \frac{h}{\sqrt{h^2+\Gamma^2}}\tanh(\beta\sqrt{h^2+\Gamma^2}), & \Gamma > \Gamma_c(\beta, h). \end{cases}$$

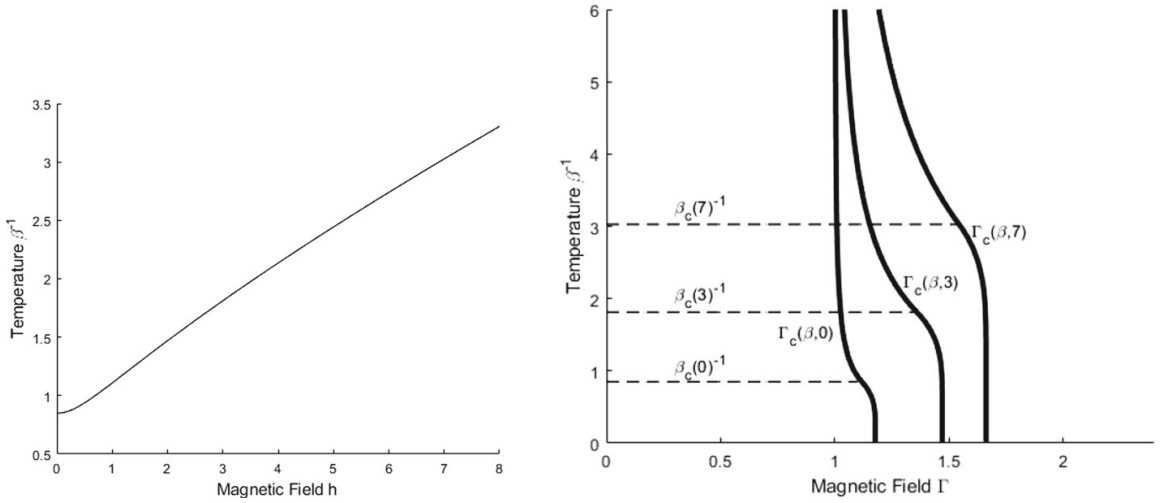

Fig. 1 The left figures illustrates the freezing temperature $T_c(h) = \beta_c^{-1}(h)$ as a function of the longitudinal field h. On the right is the $T - \Gamma$ phase diagram with the critical magnetic field $\Gamma_c(\beta, \Gamma)$ as well as the critical temperature evaluated at $h = 0, 3, 7$

The kink in its dependence on β for $\Gamma < \Gamma_c(\beta, h)$ reflects the second-order freezing transition at $\beta_c(h)$.

The following proposition summarizes some basic properties of the critical inverse temperature $\beta_c(h)$ and the critical transversal field $\Gamma_c(\beta, h)$ as functions of h.

Proposition 1 *The critical inverse temperature $\beta_c(h)$ and the critical magnetic field strength $\Gamma_c(\beta, h)$ have the following properties:*

1. *$\beta_c(h)$ is a strictly decreasing function. Moreover, $\beta_c(h) = \sqrt{2\ln 2}\,(1 - h^2/2) + \mathcal{O}(h^4)$ for small h and asymptotically $\lim_{h\to\infty} \frac{h\beta_c(h)}{\ln h} = 1$.*
2. *The high temperature limit $\Gamma_c(0, h) := \lim_{\beta\to 0} \Gamma_c(\beta, h) = 1$ does not depend on h, and the low temperature limit*

$$\lim_{\beta\to\infty} \Gamma_c(\beta, h) = \sqrt{(\beta_c(h) + \tanh(\beta_c(h)h)h)^2 - h^2}$$

   resembles the ground-state phase transition.
3. *For any $\beta > 0$ the critical field strength $\Gamma_c(\beta, \cdot)$ is a strictly increasing function. In addition, we asymptotically have $\lim_{h\to\infty} \frac{\Gamma(\beta,h)}{\sqrt{h\beta_c(h)}} = 1$.*

The proof of Proposition 1 is based on multiple elementary, but quite lengthy, computations, which we spelled out in Appendix A for the convenience of the reader.

Let us put these findings in a general context. In classical SK-type models, the freezing temperature $T_c(h) = \beta_c(h)^{-1}$ decreases as h becomes larger, i.e. the glass phase shrinks [10,31]. Numerical calculations support the conjecture that in the Quantum SK-model, the longitudinal and transversal field destabilize the glass phase as well (cf. [24,34] and [28]). In contrast, the REM and the QREM exhibit an expanding frozen phase for $h > 0$. This concerns not only the critical temperature $T_c(h)$ but also the critical transversal magnetic field strength $\Gamma_c(\beta, h)$, which also increases with h; see Fig. 1. In this sense the QREM, although the limit $p \to \infty$ of p-spin models (cf. [21]), features nonphysical characteristics in presence of a longitudinal field. As we will argue next, this is a consequence of the unrealistic lack of correlations.

1.3 The QGREM with a Hierarchical Longitudinal Field

That a longitudinal field stabilizes the frozen phase in the QREM and QGREM, can be regarded as a quite nonphysical behavior. We will bypass this problem by following Derrida and Gardner's approach to incorporate the magnetic field in z-direction as a hierarchical operator [14]. This choice can be physically justified: one should recall that the GREM was designed as a hierarchical approximation of the more involved SK-model, whose energy correlations are given by $\mathbb{E}\big[U(\boldsymbol{\sigma})U(\boldsymbol{\sigma}')\big] = Nr_N(\boldsymbol{\sigma},\boldsymbol{\sigma}')^2$ in terms of the spin overlap $r_N(\boldsymbol{\sigma},\boldsymbol{\sigma}') = N^{-1}\sum_{j=1}^{N}$. In fact, requiring that the entropy of likewise pair-correlated energies asymptotically coincides in the SK-model and the GREM, i.e.

$$\lim_{N\to\infty}\frac{1}{N}\ln\left(\frac{\big|\{\boldsymbol{\sigma} : r_N(\boldsymbol{\sigma},\boldsymbol{\sigma}^0)^2 > a\}\big|}{\big|\{\boldsymbol{\sigma} : A(q_N(\boldsymbol{\sigma},\boldsymbol{\sigma}^0)) > a\}\big|}\right) = 1$$

for all $a \in (0,1)$ and a fixed, but arbitrary, reference state $\boldsymbol{\sigma}^0$, determines the choice $A(x) = \gamma(x)^2$, where γ is the inverse function of

$$\gamma^{-1} : [0,1] \to [0,1], \quad \gamma^{-1}(a) := 1 - \frac{r(a)}{\ln 2} = \frac{1-x}{2\ln 2}\ln(1-x) + \frac{1+x}{2\ln 2}\ln(1+x) \tag{15}$$

with the binary entropy r from (13). This follows from the known asymptotics

$$\big|\{\boldsymbol{\sigma} : r_N(\boldsymbol{\sigma},\boldsymbol{\sigma}^0) > a/h\}\big| \simeq 2^N 2^{-N\gamma^{-1}(a/h)}$$

and $\big|\{\boldsymbol{\sigma} : q_N(\boldsymbol{\sigma},\boldsymbol{\sigma}^0) > a\}\big| \simeq 2^N 2^{-aN}$.

If we want to understand the SK-model with a longitudinal field, it is reasonable to consider the hierarchical reorganization of the magnetic field as well. We start by introducing the notion of a general hierarchical field on the Hamming cube $\mathcal{Q}_N$.

Definition 1 We call a function $h\colon \mathcal{Q}_N \to \mathbb{R}$ a hierarchical field with reference state $\boldsymbol{\sigma}^0 \in \mathcal{Q}_N$ if there exists a function $\eta\colon [0,1] \to \mathbb{R}$ such that

$$h(\boldsymbol{\sigma}) = N\eta(q_N(\boldsymbol{\sigma},\boldsymbol{\sigma}^0)), \tag{16}$$

where q is the lexicographic overlap (3). Furthermore, h is said to be a regular hierarchical field, if η is a regular function on $[0,1]$, i.e. η is a uniform limit of step functions.

Our second main result in this paper deals with general regular hierarchical fields. Nevertheless, let us in particular discuss the choice of $\boldsymbol{\sigma}^0$ and η that corresponds to a constant external magnetic field. To do so, we rewrite the original constant longitudinal magnetic field as follows

$$h\sum_{i=1}^{N}\sigma_i = hNr_N(\boldsymbol{\sigma},\boldsymbol{\sigma}^0), \tag{17}$$

where $\boldsymbol{\sigma}^0 = (+1,\ldots,+1)$ is the ferromagnetic state. In the hierarchical case one may also think of $\boldsymbol{\sigma}^0$ being the ferromagnetic state, but the free energy in fact does not depend on this reference state.

Determining the "correct" overlap function is a little more subtle. One might be tempted to pick $\eta(q) = hq$ which yields the analogous relation between the field and the respective

overlap as in (17). Similarly as discussed above, it is more reasonable though to demand that the entropy agrees, i.e. the number of (positive) energy states agree on an exponential scales

$$\lim_{N\to\infty} \frac{1}{N} \ln \left(\frac{\left|\{\boldsymbol{\sigma} : hr_N(\boldsymbol{\sigma}, \boldsymbol{\sigma}^0) > a\}\right|}{\left|\{\boldsymbol{\sigma} : v(q_N(\boldsymbol{\sigma}, \boldsymbol{\sigma}^0)) > a\}\right|} \right) = 1$$

for any $0 < a < h$. Comparing asymptotics leads to the choice

$$\eta(a) := h\gamma(a), \tag{18}$$

where again γ is the inverse function of (15). Let us record this as a definition:

Definition 2 We call $h(\boldsymbol{\sigma}) = N\eta(q_N(\boldsymbol{\sigma}, \boldsymbol{\sigma}^0))$ with reference state $\boldsymbol{\sigma}^0 = (+1, \ldots, +1)$ and overlap function η given by (18) the hierarchical magnetic field of strength h.

Our aim in the following is to determine the limit of the pressure $\Phi_N(\beta, \mathfrak{b}, h)$ of a Quantum GREM (1) where U is a GREM-type random process characterized by A in (2), h is a regular hierarchical field in the sense of Definition 1, and B is a random transversal field whose weights b_j are independent copies of an absolutely integrable variable $\mathfrak{b}$ (see (5)).

To formulate our main result, we need to introduce doubly-cut GREM processes $U^{(y,z)}$ for $0 \le y \le z \le 1$ on the reduced Hamming cube $\mathcal{Q}_{\lceil (z-y)N \rceil}$ with the (not normalized) distribution function $A^{(y,z)} : [0, z-y] \to [0, 1]$, $A^{(y,z)}(x) := A(x+y) - A(y)$. The corresponding concave hull and its right derivative are denoted by $\bar{A}^{(y,z)}$ and $\bar{a}^{(y,z)}$.
We further set $\varphi^{(y,z)} : \mathbb{R} \times [0, z-y] \to \mathbb{R}$,

$$\varphi^{(y,z)}(\beta, x) := \beta\sqrt{(2\ln 2)\, \bar{a}^{(y,z)}(x)}\, \mathbb{1}_{x < x^{(y,z)}(\beta)} + \left(\frac{\beta^2}{2} \bar{a}^{(y,z)}(x) + \ln 2 \right) \mathbb{1}_{x \ge x^{(y,z)}(\beta)}. \tag{19}$$

with

$$x^{(y,z)}(\beta) := \sup \left\{ x \mid \bar{a}^{(y,z)}(x) > 2\ln 2/\beta^2 \right\}. \tag{20}$$

With these preparations we recall from Theorem 1.4 and Theorem 2.8 in [22] that almost surely

$$\begin{aligned} \lim_{N\to\infty} \Phi_N(\beta, \mathfrak{b}, 0) &= \sup_{0\le z\le 1} \left[\int_0^z \varphi^{(0,1)}(\beta, x)\, dx + (1-z)\mathbb{E}\left[\ln 2\cosh(\beta\mathfrak{b})\right] \right] \\ &= \sup_{0\le z\le 1} \left[\int_0^z \varphi^{(0,z)}(\beta, x)\, dx + (1-z)\mathbb{E}\left[\ln 2\cosh(\beta\mathfrak{b})\right] \right]. \end{aligned} \tag{21}$$

In the presence of any regular hierarchical field h (not necessarily with η given by (18)), this result generalizes as follows.

Theorem 2 *Let $U(\boldsymbol{\sigma})$ be of GREM and B a random transversal field with independent weights (b_j) sharing the same distribution as $\mathfrak{b}$. Further, let $h(\boldsymbol{\sigma}) = N\eta(q(\boldsymbol{\sigma}, \boldsymbol{\sigma}^0))$ be a regular hierarchical field. Then, almost surely:*

$$\begin{aligned} \Phi(\beta, \mathfrak{b}, h) &:= \lim_{N\to\infty} \Phi_N(\beta, \mathfrak{b}, h) \\ &= \sup_{0\le y\le z\le 1} \left[\beta\eta(y) + \int_0^{z-y} \varphi^{(y,z)}(\beta, x)\, dx + (1-z)\mathbb{E}\left[\ln 2\cosh(\beta\mathfrak{b})\right] \right] \\ &= \sup_{0\le y\le z\le 1} \left[\beta\eta(y) + \int_0^{z-y} \varphi^{(y,1)}(\beta, x)\, dx + (1-z)\mathbb{E}\left[\ln 2\cosh(\beta\mathfrak{b})\right] \right]. \end{aligned} \tag{22}$$

That the two last equations in (22) agree, is a priori not clear, as the additional cut at $z < 1$ might change the concave hull $\bar{A}^{(y,z)}$ in the interval of interest. In other words, Theorem 2 in particular says that the maximizing z in (22) can only be a point, where $\bar{A}^{(y,1)} = A^{(y,1)}$ and consequently the z-cut has no effect on the concave hull.

Remarkably, the transversal field B and the hierarchical field h affect the glass phase quite differently. While the hierarchical field tends to shrink the glass region in its most correlated sector first (it acts through the choice of y from the 'left'), the transversal field begins by changing the unfrozen region and the less correlated sector (it acts through the choice of z from the 'right'). We will further discuss the consequences of our second main result, Theorem 2, in the next subsection and spell out its proof only in Sect. 2.

1.4 Instability of the Glass Phase in the QGREM with Longitudinal Hierarchical Field

If $A = \bar{A}$, i.e. A is a concave function, $\varphi^{(y,1)}$ is a just a translation of $\varphi^{(0,1)} =: \varphi$ such that

$$\Phi(\beta, \mathfrak{b}, h) = \sup_{0 \le y \le z \le 1} \left[\beta\eta(y) + \int_y^z \varphi(\beta, x)\, dx + (1-z)\mathbb{E}\left[\ln 2 \cosh(\beta\mathfrak{b})\right] \right], \tag{23}$$

with

$$\varphi(\beta, x) = \beta\sqrt{(2\ln 2)\,\bar{a}(x)}\,\mathbb{1}_{x<x(\beta)} + \left(\frac{\beta^2}{2}\bar{a}(x) + \ln 2\right)\mathbb{1}_{x\ge x(\beta)},$$
$$x(\beta) := \sup\left\{x \mid \bar{a}(x) > (2\ln 2)/\beta^2\right\}.$$

On the other hand, if A is not concave (which is always the case if A is a step function) the behavior of $\varphi^{(y,1)}$ is more subtle as one has to take into account that the slope of the concave hull's linear segments will change as y increases. In particular, (23) does not necessarily hold true. In contrast to a transversal field, a hierarchical field might lead to a change of the determining concave hull. As discussed in [14] this would happen for a hierarchical caricature of a p-spin glass with $p > 2$.

For an explicit prediction on the AT line we will now focus on the case that $A = \bar{A}$ is continuously differentiable with derivative $\bar{a}$. Then for any hierarchical field with an overlap function $\eta(\cdot) = hv(\cdot)$ with $h \ge 0$ and $v \ge 0$ an increasing function, the supremum in (23) is attained for fixed $\beta \ge 0$ at some $y(\beta, h)$ which is an increasing function of h. Since the critical temperature $T_c = \beta_c^{-1}$ only depends on $\bar{a}(y(\beta, h))$, it is thus a decreasing function of h and not increasing as in the QREM.

To be more specific, let us focus on the case of the hierarchical magnetic field $\eta = h\gamma$ of strength $h > 0$. We will proceed step by step, first discussing the limiting cases.

1.4.1 Vanishing Transversal Field $\mathfrak{b} = 0$

In this case, a straightforward differentiation shows that the supremum in (23) is attained at $z = 1$ and $y = y(\beta, h) \in (0, 1)$, which for fixed $\beta > 0$ and $h > 0$ is the unique solution of the equation

$$y = k\left(\frac{\varphi(\beta, y)}{\beta h}\right), \tag{24}$$

where $k : [0, \infty) \to (0, 1]$ is the inverse function of the derivative $\gamma' : (0, 1] \to [0, \infty)$ of γ. The uniqueness of the solution is most easily seen using the explicit form

$$k(x) = \begin{cases} 1, & x = 0, \\ \frac{1}{x} \tanh \frac{\ln 2}{x} - \frac{1}{\ln 2} \ln \cosh \frac{\ln 2}{x}, & x > 0, \end{cases}$$

from which we conclude the fact that k is continuous and monotone decreasing. More precisely, since $y \mapsto \varphi(\beta, y)$ is continuous and monotone decreasing as well with limiting values $\varphi(\beta, 0) \geq \varphi(\beta, 1) = \beta^2 \bar{a}(1)/2 + \ln 2 > 0$, the solution to (24) exists and is unique.

A low-temperature glass phase occurs in this case if and only if $y(\beta, h) < x(\beta)$. Clearly, this is only possible in case $x(\beta) > 0$, i.e. for temperatures below the critical temperature at $h = 0$, whose inverse is given by

$$\beta_c := \sqrt{\frac{2 \ln 2}{\bar{a}(0)}}.$$

Since $[\beta_c, \infty) \ni \beta \mapsto x(\beta)$ is monotone increasing and right-continuous and $\varphi(\beta, x(\beta)) = 2 \ln 2$, the inverse critical temperature at $h > 0$ is then well defined through the requirement

$$\beta_c(h) := \inf \{\beta : x(\beta) > k\,(2 \ln 2/(\beta h))\}\,. \tag{25}$$

The function $h \mapsto \beta_c(h)$ is referred to as the AT line. We record some elementary properties of the AT line and also of the solution of (24) for future purposes in the following proposition. Of particular interest is the critical exponent of the AT line $T_c(h) = \beta_c(h)^{-1}$ near $h = 0$. It is determined by the asymptotic behavior of $\bar{a}(x)$ near $x = 0$. To facilitate notation, we write $x(t) \propto y(t)$ $(t \to t_0)$ if and only if $\lim_{t \to t_0} \frac{x(t)}{y(t)} \in (0, \infty)$ exists. For the determination of the critical exponent, we add the following assumption, which may be satisfied or not.

Assumption 1 For $\alpha > 0$: $\quad \bar{a}(0) - \bar{a}(x) \propto x^\alpha \quad (x \downarrow 0)$.

E.g. in the SK-caricature case $A = \gamma^2$, we have $\bar{a}(0) = 2 \ln 2$, which yields the correct critical temperature $\beta_c = 1$ of the SK-model, and $\alpha = 1$. As is spelled out in (26), this leads to the critical exponent 2 of the AT-line for small transversal fields. This differs from the known asymptotics $T_c - T_c(h) \propto h^{2/3} \quad (h \downarrow 0)$ of the AT-line in the original SK-model as already noted in [14].

Proposition 2 *Suppose that $A = \bar{A}$ is continuously differentiable with derivative $\bar{a}$.*

1. *The inverse critical temperature $\beta_c(h)$ is monotone increasing in h. Its limiting values are $\lim_{h \downarrow 0} \beta_c(h) = \beta_c$ and*

$$\lim_{h \to \infty} \beta_c(h) = \begin{cases} \infty & \text{if } \bar{a}(1) = 0, \\ \frac{2 \ln 2}{\bar{a}(1)} & \text{if } \bar{a}(1) > 0. \end{cases}$$

In the situation of Assumption 1 the critical temperature satisfies:

$$T_c - T_c(h) \propto h^{2\alpha} \quad (h \downarrow 0). \tag{26}$$

2. *For any $\beta \in (0, \infty)$ and $h > 0$ the unique solution $y(\beta, h)$ of (24) enjoys the following properties:*

(a) *For fixed* $\beta \in (0,\infty)$ *the function* $(0,\infty) \ni h \mapsto y(\beta,h)$ *is continuous and increasing in* h *for any* $\beta > 0$ *with limiting values* $\lim_{h\downarrow 0} y(\beta,h) = 0$ *and* $\lim_{h\to\infty} y(\beta,h) = 1$. *Moreover,*

$$y(\beta,h) = \mathcal{O}(h^3) + h^2 \times \begin{cases} \frac{\beta^2}{2\ln 2}(1+\beta^2/\beta_c^2)^{-2}, & \beta < \beta_c \\ \frac{\beta_c^2}{8\ln 2}, & \beta > \beta_c \end{cases} \tag{27}$$

for small h.

(b) *The function* $(0,\infty) \ni h \mapsto \varphi(\beta, y(\beta,h))$ *is continuous and decreasing. Moreover, at any* $\beta > 0$ *its limiting values is* $\lim_{h\downarrow 0} \varphi(\beta, y(\beta,h)) = \varphi(\beta,0)$.

The proof of this proposition consists again of multiple lengthy, but elementary computations, which are sketched in Appendix B.

1.4.2 Vanishing Hierarchical Longitudinal Field $h = 0$

It was shown in Corollary 1.5 of [22] that in case $h = 0$ and a constant transversal field $\mathfrak{b} = \Gamma$ of strength $\Gamma > 0$ the supremum in (23) is attained at $y = 0$ and $z = z(\beta,\Gamma) \in [0,1]$ given by

$$z(\beta,\Gamma) := \begin{cases} 1 & p(\beta\Gamma) \le s(\beta) := \varphi(\beta,1) \\ g_\beta(p(\beta\Gamma)) & s(\beta) < p(\beta\Gamma) < t(\beta) := \varphi(\beta,0) \\ 0 & t(\beta) \ge p(\beta\Gamma). \end{cases} \tag{28}$$

Here $g(\beta,\cdot) : [s(\beta),t(\beta)] \to [0,1]$ is the generalized inverse of $\varphi(\beta,\cdot)$, which maximizes $z(\beta,\Gamma)$ and

$$p(\beta\Gamma) := \ln 2\cosh(\beta\Gamma),$$

is the pressure of a pure quantum paramagnet. As a consequence, the pressure $\Phi(\beta,\Gamma,0)$ has a magnetic transition at

$$\Gamma_c(\beta,0) := \frac{1}{\beta}\operatorname{arcosh}\left(\tfrac{1}{2}e^{t(\beta)}\right)$$

and possibly a second magnetic transition at $\Gamma_c^{(1)}(\beta) := \frac{1}{\beta}\operatorname{arcosh}\left(\frac{1}{2}e^{s(\beta)}\right)$ depending on whether $\bar{a}(1) > 0$ or equivalently $s(\beta) > \ln 2$ or not. In the regime $\Gamma < \Gamma_c(\beta,0)$ a glass transition occurs at fixed inverse temperature β_c.

In case of the SK-caricature for which $\bar{a}(1) = 0$, neither the value of the location of the quantum phase transition at zero temperature, $\lim_{\beta\to\infty}\Gamma_c(\beta,0) = \sqrt{(2\ln 2)\bar{a}(0)} = 2\ln 2 \approx 1.38\ldots$ agrees with the perturbative or numerical prediction of approximately 1.51 in [33,34], nor does the behavior of $\Gamma_c(T^{-1},0)$ near $T = 0$ agree with the T^2-scaling predicted in [17]. Presumably, this is a defect of the hierarchical implementation of the glass' correlations.

1.4.3 Constant Longitudinal and Transversal Field

To determine the pressure $\Phi(\beta,\Gamma,h)$ in the general case of a constant transversal and longitudinal field $\Gamma, h > 0$, we also need to discuss the behavior of the variational expression (23) at the diagonal $y = z$, which corresponds to the situation without a GREM. In this case, the supremum is attained at

$$\sigma(\beta,\Gamma,h) := k\left(\frac{p(\beta\Gamma)}{\beta h}\right). \tag{29}$$

Note that the condition $p(\beta\Gamma) < \varphi(\beta, y(\beta, h))$ ensures $y(\beta, h) < z(\beta, h)$ by the strict monotonicity of g_β. These findings then yield to the following explicit expression for the pressure in the general case.

Corollary 2 *Suppose that $A = \bar{A}$ is continuously differentiable. For the constant transversal field of strength $\Gamma > 0$ and the hierarchical magnetic field $h(\boldsymbol{\sigma}) = Nh\gamma(q(\boldsymbol{\sigma}, \boldsymbol{\sigma}^0))$ of strength $h > 0$ the pressure is almost surely*

$$\Phi(\beta, \Gamma, h) = \begin{cases} \beta h\gamma\left(y(\beta, h)\right) + \displaystyle\int_{y(\beta,h)}^{z(\beta,\Gamma)} \varphi(\beta, x)dx + (1 - z(\beta, \Gamma))\, p(\beta\Gamma), \\ \qquad\qquad\qquad\qquad\qquad\qquad p(\beta\Gamma) < \varphi(\beta, y(\beta, h)), \\ \beta h\gamma\left(\sigma(\beta, \Gamma, h)\right) + (1 - \sigma(\beta, \Gamma, h))\, p(\beta\Gamma), \\ \qquad\qquad\qquad\qquad\qquad\qquad p(\beta\Gamma) \geq \varphi(\beta, y(\beta, h)), \end{cases}$$

where $y(\beta, h)$, $z(\beta, \Gamma)$ and $\sigma(\beta, \Gamma, h)$ are specified in (24), (28) and (29) respectively.

Let us now discuss the physical significance of this formula. In case $h > 0$ the pressure in Corollary 2 changes its nature at $\varphi(\beta, z(\beta, \Gamma)) = p(\beta\Gamma) = \varphi(\beta, y(\beta, h))$, i.e. at

$$\Gamma_c(\beta, h) := \frac{1}{\beta} \operatorname{arcosh}\left(\tfrac{1}{2} e^{\varphi(\beta, y(\beta, h))}\right).$$

By strict monotonicity of p, the condition $\Gamma < \Gamma_c(\beta, h)$ is equivalent to $p(\beta\Gamma) < \varphi(\beta, y(\beta, h))$ and hence $y(\beta, h) \leq z(\beta, \Gamma)$.

The magnetization in the transversal direction

$$\begin{aligned} m_x(\beta, \Gamma, h) &:= \frac{1}{\beta} \frac{\partial}{\partial \Gamma} \Phi(\beta, \Gamma, h) \\ &= \begin{cases} (1 - z(\beta, \Gamma)) \tanh \beta\Gamma, & p(\beta\Gamma) < \varphi(\beta, y(\beta, h)), \\ (1 - \sigma(\beta, \Gamma, h)) \tanh \beta\Gamma, & p(\beta\Gamma) \geq \varphi(\beta, y(\beta, h)), \end{cases} \end{aligned}$$

changes continuously through the transition line $\Gamma = \Gamma_c(\beta, h)$. Only its second derivative is generally discontinuous. Note that the magnetization in x-direction neither attains its maximum value $\tanh(\beta\Gamma)$ of the pure quantum paramagnetic phase in the regime $\Gamma > \Gamma_c(\beta, h)$ nor does it vanish for $\Gamma < \Gamma_c(\beta, h)$. Similarly as in the case $h = 0$ covered in [22], the transversal magnetization vanishes only at $\Gamma_c^{(1)}(\beta)$, which is equal to zero in case $\bar{a}(1) = 0$. The critical magnetic field is continuous in h, and one recovers the limiting value $\lim_{h \downarrow 0} \Gamma_c(\beta, h) = \Gamma_c(\beta, 0)$ for any $\beta \in (0, \infty)$. A straightforward Taylor expansion and (27) imply that in the situation of Assumption 1:

$$\Gamma_c(\beta, 0) - \Gamma_c(\beta, h) \sim h^{2\alpha} \quad (h \downarrow 0). \tag{30}$$

In fact, this even holds in the zero temperature limit $\beta \to \infty$, i.e for the so called Quantum AT line which is plotted in Fig. 2.

A low-temperature glass phase occurs if and only if

$$y(\beta, h) < \min\{x(\beta), z(\beta, \Gamma)\}.$$

Clearly, this is only possible if two conditions are satisfied simultaneously:

1. $z(\beta, \Gamma) > y(\beta, h)$, i.e. for transversal fields $\Gamma < \Gamma_c(\beta, h)$. From the monotonicity of $h \mapsto \varphi(\beta, y(\beta, h))$, we conclude, $\Gamma_c(\beta, h) \leq \Gamma_c(\beta, 0)$ for any $\beta, h > 0$.

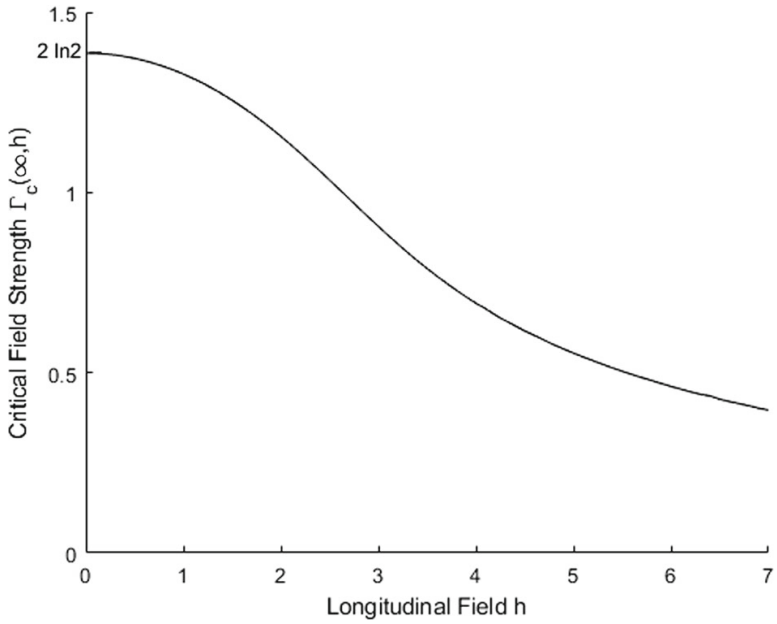

Fig. 2 Plot of the Quantum AT line, i.e. the dependence of the critical transversal field $\Gamma_c(\beta, h)$ on the longitudinal field h for zero temperature, $\beta = \infty$

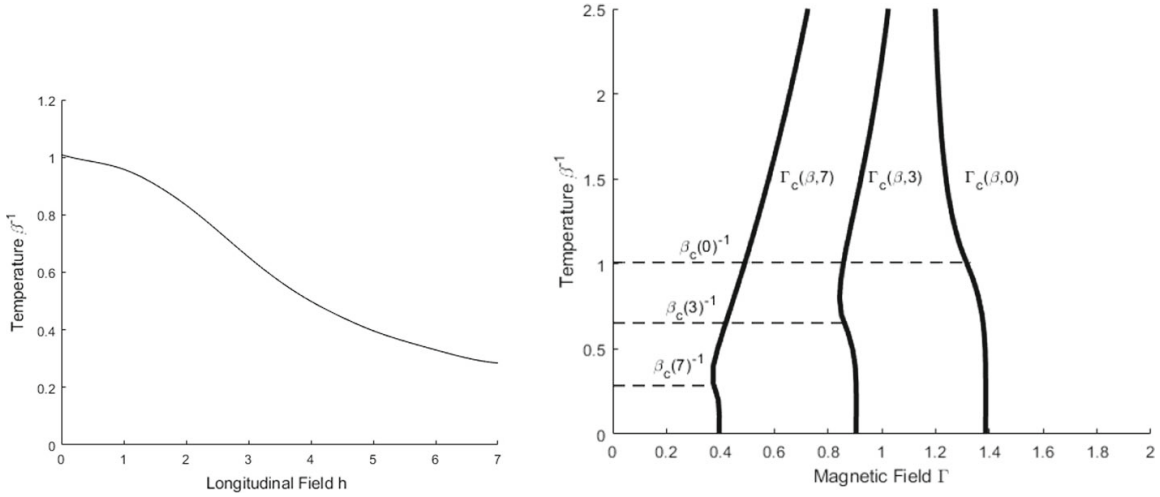

Fig. 3 On the left is a plot of the critical temperature $\beta_c(h)$ as a function of the longitudinal field. On the right figure is the $T - \Gamma$ phase diagram with the critical magnetic field $\Gamma_c(\beta, \Gamma)$ as well as the critical temperature $\beta_c(h)^{-1}$ evaluated at $h = 0, 3, 7$

2. $x(\beta) > y(\beta, h)$, i.e. for $\beta > \beta_c(h)$ given by (25), which we already identified as a monotone increasing function of h.

We thus conclude, that the presence of the transversal field $h > 0$ shrinks the spin glass' low-temperature phase. Qualitatively this behavior is in accordance with the numerical findings in case of the Quantum SK-model [34]. However, as already noted in [14] in the classical case $\Gamma = 0$, the critical exponents do not agree. Figure 3 plots the temperature-transversal field phase diagram for different values of h in case $A = \bar{A}$ and $\bar{a}(1) = 0$.

We finally close this section by pointing out that the expression for the pressure in case $p(\beta\Gamma) \geq \varphi(\beta, y(\beta, h))$ agrees with that of the hierarchical field h plus a constant transversal field Γ. It should be compared to the exact solution $p(\beta\sqrt{h^2 + \Gamma^2})$ without the hierarchical implementation of the longitudinal field and agrees qualitatively.

The magnetization in the longitudinal direction is given by

$$m_z(\beta, \Gamma, h) := \frac{1}{\beta}\frac{\partial}{\partial h}\Phi(\beta, \Gamma, h) = \begin{cases} \gamma\left(y(\beta, h)\right), & p(\beta\Gamma) < \varphi(\beta, y(\beta, h)), \\ \gamma\left(\sigma(\beta, \Gamma, h)\right)\right), & p(\beta\Gamma) \geq \varphi(\beta, y(\beta, h)), \end{cases}$$

and varies continuously through both the glass and the magnetic transitions.

2 Proof of Theorem 2

Let us first remark that the last equality in (22) already follows from results in [22]. Indeed, fix any $y \in [0, 1)$ and consider the Hamiltonian

$$H^{(y)} := U^{(y,1)} - B^{(2,y)}$$

on the reduced Hilbert space $\ell^2(\mathcal{Q}_{\lceil(1-y)N\rceil})$, where $U^{(y,1)}$ is the cut GREM corresponding to $A^{(y,1)}$ and $B^{(2,y)}$ denotes the cut transversal field acting only on spins in $\mathcal{Q}_{\lceil(1-y)N\rceil}$

$$B^{(2,y)} := \sum_{i=\lceil yN\rceil+1}^{N} b_i \boldsymbol{s}_i, \tag{31}$$

and we set $B^{(1,y)} := B - B^{(2,y)}$. Then, Theorem 2.8 in [22] implies

$$\lim_{N\to\infty}\frac{1}{N}\ln \mathrm{Tr}\, e^{-\beta H^{(y)}} = \sup_{y\leq z\leq 1}\left[\int_0^{z-y}\varphi^{(y,z)}(x)\,dx + (1-z)\mathbb{E}\left[\ln 2\cosh(\beta\mathfrak{b})\right]\right],$$

whereas an application of Theorem 1.4 in [22] yields

$$\lim_{N\to\infty}\frac{1}{N}\ln \mathrm{Tr}\, e^{-\beta H^{(y)}} = \sup_{y\leq z\leq 1}\left[\int_0^{z-y}\varphi^{(y,1)}(x)\,dx + (1-z)\mathbb{E}\left[\ln 2\cosh(\beta\mathfrak{b})\right]\right].$$

In both cases, the supremum is taken over $z \in [y, 1]$ at fixed y, which proves the second equality in (22). We now spell out the proof of the first equality in (22).

Proof of Theorem 2: We will proceed in three steps.

Step 1: Reduction to step functions

We claim that it is enough to show Theorem 2 for step functions η. This follows if we can prove that the left and right side of (22) are continuous with respect to η in the uniform norm. This is, however, trivial for the right side, and a simple operator norm bound implies for two hierarchical fields h, h' with overlap functions η, η',

$$\frac{1}{N}\left|\ln \mathrm{Tr}\, e^{-\beta(U-h-B)} - \ln \mathrm{Tr}\, e^{-\beta(U-h'-B)}\right| \leq \beta\|\eta - \eta'\|_\infty.$$

From now on, we will therefore only consider step functions η, i.e. we assume that there exist points $0 = q_0 < q_1 < \cdots q_m = 1$ and real numbers $\eta_1, \ldots, \eta_m$ such that $\eta(x) = \eta_k$ for $q_{k-1} \leq x < q_k$ and $\eta(1) = \eta_m$. The points q_k define blocks of spin vectors $\boldsymbol{\sigma}_k \in \mathcal{Q}_{\lceil q_k N\rceil - \lceil q_{k-1} N\rceil}$, and we will write $\boldsymbol{\sigma} = \boldsymbol{\sigma}_1\boldsymbol{\sigma}_2\cdots\boldsymbol{\sigma}_m$. Moreover, it is convenient to introduce for $k = 1, \ldots m$ the projections P_k and p_k:

$$P_k\boldsymbol{\sigma} = P_k\boldsymbol{\sigma}_1\boldsymbol{\sigma}_2\cdots\boldsymbol{\sigma}_m := \boldsymbol{\sigma}_1\cdots\boldsymbol{\sigma}_k, \qquad p_k\boldsymbol{\sigma} = p_k\boldsymbol{\sigma}_1\boldsymbol{\sigma}_2\cdots\boldsymbol{\sigma}_m := \boldsymbol{\sigma}_k.$$

Moreover, we set $P_0\boldsymbol{\sigma} = p_0\boldsymbol{\sigma} := 1$. Finally, we note that due to the fact that η only takes finitely many values, we may restrict the variational expression (22) to the maximum over points $y = q_k$:

$$\begin{aligned}&\sup_{0\le y\le z\le 1}\left[\beta\eta(y)+\int_0^{z-y}\varphi^{(y,1)}(x)\,dx+(1-z)\mathbb{E}\left[\ln 2\cosh(\beta\mathfrak{b})\right]\right]\\&=\max_{k=0,\dots,m-1}\sup_{q_k\le z\le 1}\left[\beta\eta_{k+1}+\int_0^{z-q_k}\varphi^{(y,1)}(x)\,dx+(1-z)\mathbb{E}\left[\ln 2\cosh(\beta\mathfrak{b})\right]\right].\end{aligned}$$

Step 2: Lower bound

Our lower bound on the pressure is based on Gibbs' variational principle [26]. We pick some $k \in \{1,\dots,m\}$ and consider on the subspace $\ell^2(\mathcal{Q}_{N-\lceil q_k N\rceil})$ the Hamiltonian:

$$H^{(k)} := U^{(k)} - B^{(2,q_k)}, \qquad U^{(k)}(\boldsymbol{\sigma}_{k+1}\cdots\boldsymbol{\sigma}_m) := U((P_k\boldsymbol{\sigma}^0)\boldsymbol{\sigma}_{k+1}\cdots\boldsymbol{\sigma}_m). \tag{32}$$

We denote by $\tilde{\rho}_{k,\beta}$ the corresponding Gibbs state at inverse temperature β. The density matrix $\tilde{\rho}_{k,\beta}$ has the extension $\rho_{k,\beta} := |P_k\boldsymbol{\sigma}^0\rangle\langle P_k\boldsymbol{\sigma}^0| \otimes \tilde{\rho}_{k,\beta}$ to the full space $\ell^2(\mathcal{Q}_N) = \ell^2(\mathcal{Q}_{\lceil q_k N\rceil}) \otimes \ell^2(\mathcal{Q}_{N-\lceil q_k N\rceil})$ and its matrix elements are given by

$$\langle\boldsymbol{\sigma}|\rho_{k,\beta}|\boldsymbol{\sigma}'\rangle := \begin{cases}\langle\boldsymbol{\sigma}_{k+1}\cdots\boldsymbol{\sigma}_m|\tilde{\rho}_{k,\beta}|\boldsymbol{\sigma}'_{k+1}\cdots\boldsymbol{\sigma}'_m\rangle & \text{if } P_k\boldsymbol{\sigma} = P_k\boldsymbol{\sigma}^0 = P_k\boldsymbol{\sigma}'\\ 0 & \text{else .}\end{cases}$$

By Gibbs' variational principle, we have

$$\begin{aligned}&\frac{1}{N}\ln\mathrm{Tr}\,e^{-\beta(U-h-B)}\\&\ge\frac{\beta}{N}\mathrm{Tr}\left[\rho_{k,\beta}(B^{(1,q_k)}+h+\hat{U}^{(k)}-U)\right]+\frac{1}{N}\ln\mathrm{Tr}_{|\ell^2(\mathcal{Q}_{N-\lceil q_k N\rceil})}e^{-\beta H^{(k)}},\end{aligned}$$

with the canonical extension $\hat{U}^{(k)}$ of $U^{(k)}$ to the Hilbert space $\ell^2(\mathcal{Q}_N)$, i.e.,

$$\hat{U}^{(k)}(\boldsymbol{\sigma}_1\cdots\boldsymbol{\sigma}_k\boldsymbol{\sigma}_{k+1}\cdots\boldsymbol{\sigma}_m) := U^{(k)}(\boldsymbol{\sigma}_{k+1}\cdots\boldsymbol{\sigma}_m).$$

Since the trial density matrix $\rho_{k,\beta}$ is diagonal with respect to $\boldsymbol{\sigma}_1\cdots\boldsymbol{\sigma}_k$ and fixes the first variables to $P_k\boldsymbol{\sigma}^0$, we have

$$\mathrm{Tr}\left[\rho_{k,\beta}B^{(1,q_k)}\right] = 0 = \mathrm{Tr}\left[\rho_{k,\beta}(U^{(k)}-U)\right].$$

Thus, it remains to show the almost sure identities

$$\lim_{N\to\infty}\frac{1}{N}\mathrm{Tr}\left[\rho_{k,\beta}h\right] = \eta_{k+1}, \tag{33}$$

and

$$\begin{aligned}&\lim_{N\to\infty}\frac{1}{N}\ln\mathrm{Tr}_{|\ell^2(\mathcal{Q}_{N-\lceil q_k N\rceil})}e^{-\beta H_k}\\&\qquad=\sup_{q_k\le z\le 1}\left[\int_0^{z-q_k}\varphi^{(y,1)}(x)\,dx+(1-z)\mathbb{E}\left[\ln 2\cosh(\beta\mathfrak{b})\right]\right].\end{aligned} \tag{34}$$

Step 2.1: Proof of (33): Using $h(\boldsymbol{\sigma}) = N\eta(q_N(\boldsymbol{\sigma}, \boldsymbol{\sigma}^0))$ we compute the trace in the z-basis:

$$\begin{aligned}\frac{1}{N}\mathrm{Tr}\,[\rho_{k,\beta}h] &= \sum_{l=0}^{m-1}\left(\eta_{l+1}\sum_{\boldsymbol{\sigma}:P_l\boldsymbol{\sigma}^0=P_l\boldsymbol{\sigma},\,P_{l+1}\boldsymbol{\sigma}^0\neq P_{l+1}\boldsymbol{\sigma}}\langle\boldsymbol{\sigma}|\rho_{k,\beta}|\boldsymbol{\sigma}\rangle\right)+\eta_m\langle\boldsymbol{\sigma}^0|\rho_{k,\beta}|\boldsymbol{\sigma}^0\rangle\\ &= \sum_{l=k}^{m-1}\left(\eta_{l+1}\sum_{\boldsymbol{\sigma}:P_l\boldsymbol{\sigma}^0=P_l\boldsymbol{\sigma},\,P_{l+1}\boldsymbol{\sigma}^0\neq P_{l+1}\boldsymbol{\sigma}}\langle\boldsymbol{\sigma}|\rho_{k,\beta}|\boldsymbol{\sigma}\rangle\right)+\eta_m\langle\boldsymbol{\sigma}^0|\rho_{k,\beta}|\boldsymbol{\sigma}^0\rangle,\end{aligned}$$

where the second equality is due to the construction of $\rho_{k,\beta}$. Since $\rho_{k,\beta}$ has unit trace,

$$1 = \sum_{\boldsymbol{\sigma}:P_k\boldsymbol{\sigma}^0=P_k\boldsymbol{\sigma}}\langle\boldsymbol{\sigma}|\rho_{k,\beta}|\boldsymbol{\sigma}\rangle, \tag{35}$$

and is non-negative, we may estimate both from above and below:

$$\left|\frac{1}{N}\mathrm{Tr}\,[\rho_{k,\beta}h]-\eta_{k+1}\right| \le \|\eta\|_\infty\sum_{\boldsymbol{\sigma}:P_{k+1}\boldsymbol{\sigma}^0=P_{k+1}\boldsymbol{\sigma}}\langle\boldsymbol{\sigma}|\rho_{k,\beta}|\boldsymbol{\sigma}\rangle.$$

We further deduce from the spin-flip covariance of $H^{(k)}$ that for any $\boldsymbol{\sigma}, \boldsymbol{\sigma}'$ with $P_k\boldsymbol{\sigma} = P_k\boldsymbol{\sigma}' = P_k\boldsymbol{\sigma}^0$:

$$\mathbb{E}\,[\langle\boldsymbol{\sigma}|\rho_{k,\beta}|\boldsymbol{\sigma}\rangle] = \mathbb{E}\,[\langle\boldsymbol{\sigma}'|\rho_{k,\beta}|\boldsymbol{\sigma}'\rangle].$$

Consequently, using the normalization (35) and counting the number of configurations, we have

$$\mathbb{E}\left[\sum_{\boldsymbol{\sigma}:P_{k+1}\boldsymbol{\sigma}^0=P_{k+1}\boldsymbol{\sigma}}\langle\boldsymbol{\sigma}|\rho_{k,\beta}|\boldsymbol{\sigma}\rangle\right] = \frac{2^{N(1-q_{k+1})}}{2^{N(1-q_k)}} = 2^{-N(q_{k+1}-q_k)}.$$

By a Borel-Cantelli argument, we thus arrive at the almost sure convergence

$$\lim_{N\to\infty}\left|\frac{1}{N}\mathrm{Tr}\,[\rho_{k,\beta}h]-\eta_{k+1}\right| = 0.$$

Step 2.2: Proof of (34): We may rewrite the restricted process (in distributional sense)

$$U((P_k\boldsymbol{\sigma}^0)\boldsymbol{\sigma}_{k+1}\cdots\boldsymbol{\sigma}_m) = U'(\boldsymbol{\sigma}_{k+1}\cdots\boldsymbol{\sigma}_m) + \sqrt{NA(q_k)}\,Y,$$

where $U'(\boldsymbol{\sigma}_{k+1}\cdots\boldsymbol{\sigma}_m)$ is a GREM process on $\mathcal{Q}_{N-\lceil q_kN\rceil}$ with (non-normalized) distribution function $A^{(q_k,1)}$ and Y is a standard Gaussian variable which is independent of U'. This distributional equality relies on the fact that centered Gaussian processes are uniquely determined by their covariance function. Of course, Y does not contribute to the limit of the pressure,

$$\lim_{N\to\infty}\frac{1}{N}\ln\mathrm{Tr}_{\,|\ell^2(\mathcal{Q}_{N-\lceil q_kN\rceil})}e^{-\beta H^{(k)}} = \lim_{N\to\infty}\frac{1}{N}\ln\mathrm{Tr}_{\,|\ell^2(\mathcal{Q}_{N-\lceil q_kN\rceil})}e^{-\beta(U'-B^{(2,q_k)})},$$

provided that the limit on the right side exists. This is warranted by Theorem 1.4 in [22], which almost surely yields

$$\begin{aligned}&\lim_{N\to\infty}\frac{1}{N}\ln\mathrm{Tr}_{\,|\ell^2(\mathcal{Q}_{N-\lceil q_kN\rceil})}e^{-\beta(U'-B^{(2,q_k)})}\\ &\qquad= \sup_{q_k\le z\le 1}\left[\int_0^{z-q_k}\varphi^{(y,1)}(x)\,dx + (1-z)\mathbb{E}\,[\ln 2\cosh(\beta\mathfrak{b})]\right].\end{aligned} \tag{36}$$

Step 3: Upper bound
The method is similar in spirit to the application of the peeling principle presented in [22]. However, we need to cut the transversal field B in a different manner which suits the hierarchical field h.
Step 3.1: Truncating the transversal field B
We define the partial fields

$$B_k := B^{(1,q_{k-1})} - B^{(1,q_k)} = \sum_{i=\lceil q_{k-1}N\rceil+1}^{\lceil q_k N\rceil} b_i \boldsymbol{s}_i$$

where we set $B^{(1,q_0)} = 0$. Hence B_k only acts on $\boldsymbol{\sigma}_k$. We also define the restriction B'_k of B_k to the complement of $(p_k\boldsymbol{\sigma}^0)$:

$$B_k - B'_k := \mathbb{1} \otimes \sum_{\lceil q_{k-1}N\rceil < j \le \lceil q_k N\rceil} b_j \left(|p_k(F_j\boldsymbol{\sigma}^0)\rangle\langle p_k\boldsymbol{\sigma}^0| + |p_k\boldsymbol{\sigma}^0\rangle\langle p_k(F_j\boldsymbol{\sigma}^0)| \right) \otimes \mathbb{1}.$$

Here, the first identity acts on $\boldsymbol{\sigma}_1 \cdots \boldsymbol{\sigma}_{k-1}$,the last identity on $\boldsymbol{\sigma}_{k+1} \cdots \boldsymbol{\sigma}_m$ and F_j denotes the jth flip operator (see (5)). We denote by B' the total truncated transversal field,

$$B' = \sum_{k=1}^{m} B'_k$$

By the triangle inequality and a Frobenius norm estimate we have

$$\|B - B'\| \le \sum_{k=1}^{m} \|B_k - B'_k\| \le m \sqrt{2 \sum_{i=1}^{N} |b_i|^2} = o(N).$$

Note that the L^1-property of the random variable $\mathfrak{b}$ and Lemma A.2 in [22] ensure that the right side is indeed of order $o(N)$.
Step 3.2: Finishing the proof: Using a trivial norm bound, we estimate

$$\begin{aligned}
&e^{-\beta\|B-B'\|}\,\mathrm{Tr}\, e^{-\beta(U-h-B)} \le \mathrm{Tr}\, e^{-\beta(U-h-B')} \\
&= \sum_{k=0}^{m-1} \left(e^{-\beta N\eta_{k+1}} \sum_{\boldsymbol{\sigma}: P_k\boldsymbol{\sigma}^0 = P_k\boldsymbol{\sigma},\, P_{k+1}\boldsymbol{\sigma}^0 \neq P_{k+1}\boldsymbol{\sigma}} \langle\boldsymbol{\sigma}|e^{-\beta(U-B')}|\boldsymbol{\sigma}\rangle \right) \\
&\quad + e^{-\beta N\eta_m} \langle\boldsymbol{\sigma}^0|e^{-\beta(U-B')}|\boldsymbol{\sigma}^0\rangle \\
&= \sum_{k=0}^{m-1} \left(e^{-\beta N\eta_{k+1}} \sum_{\boldsymbol{\sigma}: P_k\boldsymbol{\sigma}^0 = P_k\boldsymbol{\sigma},\, P_{k+1}\boldsymbol{\sigma}^0 \neq P_{k+1}\boldsymbol{\sigma}} \langle\boldsymbol{\sigma}_{k+1}\ldots\boldsymbol{\sigma_m}|e^{-\beta(U^{(k)}-B'^{(2,q_k)})}|\boldsymbol{\sigma}_{k+1}\ldots\boldsymbol{\sigma_m}\rangle \right) \\
&\quad + e^{-\beta N\eta_m} e^{-\beta U(\boldsymbol{\sigma}^0)}.
\end{aligned}$$

The first identity follows by an inclusion-exclusion type of summation over all spin configurations $\boldsymbol{\sigma} \in \mathcal{Q}_N$ together with the fact that the hierarchical field h commutes with B' (and clearly with U) and is constant on the respective spin configurations in the sum. The third line is a consequence of the fact that on the subspace generated by the elements $P_k\boldsymbol{\sigma}^0 = P_k\boldsymbol{\sigma}$, the magnetic field B' operates only on the remaining spins $\boldsymbol{\sigma}_{k+1} \cdots \boldsymbol{\sigma}_m$ and evaluates the potential at $U^{(k)}$, see (32). We now recall from Lemma 1 in [22] that the diagonal matrix elements $\langle\boldsymbol{\sigma}|e^{-\beta(U-B)}|\boldsymbol{\sigma}\rangle$ only depend on the square of the variables b_i, so that in the estimation of the trace we may always assume without loss of generality that $b_i \ge 0$ and hence B as well as

B' have positive matrix elements in the spin configuration basis, which for $b_i \geq 0$ dominate each other and in particular

$$\begin{aligned} 0 &\leq \langle \boldsymbol{\sigma}_{k+1} \dots \boldsymbol{\sigma}_{\boldsymbol{m}} | e^{-\beta(U^{(k)} - B'^{(2,q_k)})} | \boldsymbol{\sigma}_{k+1} \dots \boldsymbol{\sigma}_{\boldsymbol{m}} \rangle \\ &\leq \langle \boldsymbol{\sigma}_{k+1} \dots \boldsymbol{\sigma}_{\boldsymbol{m}} | e^{-\beta(U^{(k)} - B^{(2,q_k)})} | \boldsymbol{\sigma}_{k+1} \dots \boldsymbol{\sigma}_{\boldsymbol{m}} \rangle. \end{aligned}$$

This allows us to expand the summation over all matrix elements with $P_k \boldsymbol{\sigma}^0 = P_k \boldsymbol{\sigma}$, which leads to the upper bound

$$\begin{aligned} e^{-\beta \| B - B' \|} \operatorname{Tr} e^{-\beta(U-h-B)} \leq \sum_{k=0}^{m-1} e^{-\beta N \eta_{k+1}} \operatorname{Tr}_{|\ell^2(\mathcal{Q}_{N-\lceil q_k N \rceil})} e^{-\beta(U^{(k)} - B^{(2,q_k)})} \\ + e^{-\beta N \eta_m} e^{-\beta U(\boldsymbol{\sigma}^0)}. \end{aligned}$$

Together with (36) this finishes the proof of Theorem 2. □

3 Proof of Theorem 1

Based on the already established results and methods in [4,5,20,22], the proof of Theorem 1 is straightforward but quite lengthy. Before we move on to the details, we outline our proof strategy which consists of three main steps:

1. First, we need to generalize the results in [4,5] on the REM and two-level GREM with a random magnetic field to the general n-level GREM (see Theorem 3). Following [4, 5] closely, the argument is based on a large-deviation principle for the entropy which transforms the computation of the limit to a linear optimization problem with non-linear constraints.
2. Secondly, we extend the limit theorem for the classical GREM to the QGREM with a random longitudinal field (see Proposition 4). Using the peeling principle from [22], the proof is quite easy. The only subtle point is to ensure that the structure of the concave hull in the variational principle is preserved. Here we use an argument which is very similar to the proof of [22, Lemma 3.1].
3. Finally, we use an interpolation and continuity argument to the lift the n-level QGREM result to the more general QGREM setting. We refer to the interpolation and concentration estimates in [22] which are applicable here.

3.1 The GREM with a Random Magnetic Field

The main aim of this subsection to prove the following Theorem 3, which extends the discussion of the two-level GREM in [5] to the general n-level GREM. To this end, we will need to introduce some notation. Let $0 = x_0 < x_1 < x_2 < \cdots < x_n = 1$ be some points $a_1, \dots, a_n$ some nonnegative weights (we do not assume here that these weights add up to one). As in the proof of Theorem 2, we decompose the spin vector into blocks $\boldsymbol{\sigma} = \boldsymbol{\sigma}_1 \cdots \boldsymbol{\sigma}_n$ according to the partition formed by the points (x_k). The GREM process can be written as

$$U(\boldsymbol{\sigma}) = \sqrt{a_1 N} X_{\boldsymbol{\sigma}_1} + \sqrt{a_2 N} X_{\boldsymbol{\sigma}_1 \boldsymbol{\sigma}_2} + \cdots + \sqrt{a_n N} X_{\boldsymbol{\sigma}_1 \boldsymbol{\sigma}_2 \cdots \boldsymbol{\sigma}_n}, \tag{37}$$

where the appearing random variables $X_{\boldsymbol{\sigma}_1}, X_{\boldsymbol{\sigma}_1 \boldsymbol{\sigma}_2}, \dots, X_{\boldsymbol{\sigma}_1 \boldsymbol{\sigma}_2 \cdots \boldsymbol{\sigma}_n}$ are independent standard Gaussian variables. Note that $U(\boldsymbol{\sigma})$ coincides with the GREM process with (non-normalized) distribution function A,

$$A(x) = \sum_{k=1}^{n} a_k \mathbb{1}_{[x_k,1]}(x).$$

The limit depends on the concave hull $\bar{A}$ of A consisting of linear segments which are supported on a subset of points $0 = y_0 < y_1 < \cdots < y_m = 1$ where A and $\bar{A}$ agree. It is convenient to further introduce the following quantities: the increments of the concave hull $\bar{a}_l := A(y_l) - A(y_{l-1})$, the interval lengths $L_l := y_l - y_{l-1}$ and the slopes $\gamma_l := \bar{a}_l / L_l$.

As our main result in this section, we show that the limit of the classical pressure $\Phi_N(\beta, \mathfrak{h}) = \Phi_N(\beta, \mathfrak{h}, 0)$ can then be expressed in terms of the partial pressures

$$\varphi^{(l)}(\beta, \mathfrak{h}) := \begin{cases} \frac{\bar{a}_l}{2}\beta^2 + L_l \mathbb{E}\left[\ln 2\cosh \beta \mathfrak{h}\right] & if \quad \beta \le \beta_c^{(l)}, \\ \beta(\bar{a}_l \beta_c^{(l)} + L_l \mathbb{E}\left[\mathfrak{h} \tanh \beta_c^{(l)} \mathfrak{h}\right]) & if \quad \beta > \beta_c^{(l)} \end{cases} \tag{38}$$

where the critical temperatures $\beta_c^{(l)} = \beta_c^{(l)}(\mathfrak{h})$ are each the unique positive solution of the self-consistency equation

$$\frac{\gamma_l}{2}\beta_c^{(l)^2} = \ln 2 + \mathbb{E}\left[\ln\cosh \beta_c^{(l)} \mathfrak{h}\right] - \beta_c^{(l)} \mathbb{E}\left[\mathfrak{h} \tanh \beta_c^{(l)} \mathfrak{h}\right]. \tag{39}$$

The following generalizes results in [4,5], which in turn is build on [7,8].

Theorem 3 *Let $U(\boldsymbol{\sigma})$ be a GREM process as in (37), $\beta \ge 0$ and $\mathfrak{h}$ an absolutely integrable random variable. Then, almost surely*

$$\lim_{N\to\infty} \Phi_N(\beta, \mathfrak{h}) = \sum_{l=1}^{m} \varphi^{(l)}(\beta, \mathfrak{h}). \tag{40}$$

We stress that a random field does only change the partial pressures $\varphi^{(l)}$ but not the number of terms in the right side. In particular, the limit remains to be a function of the concave hull $\bar{A}$ and not A itself.

Our proof of Theorem 3 follows the large-deviation approach in [4,5]. We first need to understand the energy statistics of the random field. To this end, it is convenient to decompose the field $h(\boldsymbol{\sigma})$ into blocks

$$h_k(\boldsymbol{\sigma}_k) := \sum_{\lceil x_{k-1}N\rceil + 1 \le j \le \lceil x_k N\rceil} h_j \sigma_j.$$

We first study the occupation numbers

$$N(y_k) := \left|\{\boldsymbol{\sigma}_k | \quad h_k(\boldsymbol{\sigma}_k) \le -N y_k\}\right|.$$

With respect to the uniform distribution on spin configurations $\boldsymbol{\sigma}_k$, the random variables $h_k(\boldsymbol{\sigma}_k)/N_k$ with $N_k := (x_k - x_{k-1})N$ have a finite logarithmic-moment generating function given by

$$\begin{aligned} \Lambda_N(t) &:= \frac{1}{N_k} \ln\left(\frac{1}{2^{N_k}} \sum_{\boldsymbol{\sigma}_k} e^{t h_k(\boldsymbol{\sigma}_k)}\right) = N_k^{-1} \sum_{\lceil x_{k-1}N\rceil + 1 \le j \le \lceil x_k N\rceil} \ln\cosh(t h_j) \\ &=: \mathbb{E}\left[\ln\cosh(t\mathfrak{h})\right] + S_N(t), \end{aligned}$$

where $S_N(t)$ is a random variable. For any fixed $t \in \mathbb{R}$ by the strong law of large numbers the latter converges to zero as $N \to \infty$. In fact, we can find a set of full probability (with respect to the distribution of the iid variables (h_i)) such that the almost-sure convergence

$$\lim_{N\to\infty} \Lambda_N(t) = \mathbb{E}\left[\ln\cosh(t\mathfrak{h})\right]$$

holds true for all $t \in \mathbb{R}$ simultaneously. This follows from an 3ε-argument by considering a countable dense set first and extending this assertion by noticing that both sides are continuously differentiable in t (see the proof of Lemma 5 in [4]). The Gärtner Ellis theorem (cf. [11]) then ensures that

$$I(z) := \sup_{t\in\mathbb{R}} \{zt - \mathbb{E}\left[\ln \cosh t\mathfrak{h}\right]\} \tag{41}$$

is a rate function for $N_k^{-1} h_k(\boldsymbol{\sigma}_k)$ for any k. As a Legendre transform $I : \mathbb{R} \to \mathbb{R} \cup \{\infty\}$ is lower semicontinuous. It is straightforward to check that I is symmetric, $I(-z) = I(z)$, equal to $+\infty$ for $|z| > \mathbb{E}\left[|\mathfrak{h}|\right]$, continuously differentiable on $(-\mathbb{E}\left[|\mathfrak{h}|\right], \mathbb{E}\left[|\mathfrak{h}|\right])$, where it is bounded by $\ln 2$, and continuous and monotone on $[0, \mathbb{E}\left[|\mathfrak{h}|\right])$.

The Gärtner Ellis theorem also allows to determine the asymptotic behavior of occupation numbers $N(y_k)$, which we can rewrite as 2^{N_k} times the probability that

$$h_k/N_k \leq -y_k/(x_k - x_{k-1}) =: \xi_k(y_k) =: \xi_k.$$

More precisely, we almost surely have

$$\begin{aligned} \ln 2 - \inf_{z<-\xi_k} I(z) &\leq \liminf_{N\to\infty} \frac{1}{N_k} \ln N(y_k) \\ &\leq \limsup_{N\to\infty} \frac{1}{N_k} \ln N(y_k) \leq \ln 2 - \inf_{z\leq -\xi_k} I(z) = \ln 2 - I(\xi_k). \end{aligned} \tag{42}$$

By the aforementioned continuity of I, we thus obtain for $\xi_k \in (-\mathbb{E}\left[|\mathfrak{h}|\right], \mathbb{E}\left[|\mathfrak{h}|\right])$ the almost-sure convergence

$$\lim_{N\to\infty} \frac{1}{N_k} \ln N(y_k) = \ln 2 - I(\xi_k), \tag{43}$$

which describes the energy statistics of the magnetic field. As a next step, we analyze the energy statistics of the total Hamiltonian. We start by extending our definition of occupation numbers and introduce:

$$\begin{aligned} N(\boldsymbol{E}, \boldsymbol{y}) &:= N(E_1, \ldots, E_n, y_1, \ldots, y_n) \\ &:= |\{\boldsymbol{\sigma} \in \mathcal{Q}_N | \quad \sqrt{a_k} X_{\boldsymbol{\sigma}_1 \cdots \boldsymbol{\sigma}_k} \leq -\sqrt{N} E_k \\ &\qquad \text{and } h_k(\boldsymbol{\sigma}_k) \leq -N y_k \text{ for all } k = 1, \ldots, n\}|. \end{aligned} \tag{44}$$

Our next goal is to obtain the asmptotics for $N(\boldsymbol{E}, \boldsymbol{y})$. To this end, we introduce the entropy

$$S(\boldsymbol{E}, \boldsymbol{y}) := \ln 2 - \sum_{j=1}^{n} \left(\frac{E_j^2}{2a_j} + (x_j - x_{j-1}) I(\xi_j(y_j)) \right) \tag{45}$$

as well as the constraints

$$\begin{aligned} \mathcal{C} := \Big\{ (\boldsymbol{E}, \boldsymbol{y}) \in \mathbb{R}^n_{\geq 0} \times \mathbb{R}^n_{\geq 0} \;\Big|\; \sum_{j=1}^{k} \frac{E_j^2}{2a_j} + (x_j - x_{j-1}) I(\xi_j(y_j)) < x_k \ln 2 \\ \text{for all } k = 1, \ldots, n \Big\}. \end{aligned} \tag{46}$$

Note that $(\boldsymbol{E}, \boldsymbol{y}) \in \mathcal{C}$ guarantees that $I(\xi_k) < \infty$ for all k. By continuity of the involved functions on the domain, where they are finite, we conclude that $\mathcal{C}$ is an open set and $\xi_j(y_j) \in (-\mathbb{E}\left[|\mathfrak{h}|\right], \mathbb{E}\left[|\mathfrak{h}|\right])$ for any j in case $(\boldsymbol{E}, \boldsymbol{y}) \in \mathcal{C}$.

The following lemma on the asymptotics of $N(\boldsymbol{E}, \boldsymbol{y})$ is a natural generalization of Theorem 1.2 in [5]. We remark that $\frac{1}{N} \ln N(\boldsymbol{E}, \boldsymbol{y})$ is shown to converge almost surely, but not in expectation. As the event $\{N(\boldsymbol{E}, \boldsymbol{y}) = 0\}$ has a small, but nonvanishing, probability, we in fact have $\mathbb{E}[\ln N(\boldsymbol{E}, \boldsymbol{y})] = -\infty$.

Lemma 1 *Let X be an n-level GREM vector as in (37) and (h_i) independent copies of an absolutely integrable random variable $\mathfrak{h}$. Then, if $(\boldsymbol{E}, \boldsymbol{y}) \in \mathcal{C}$, we almost surely have*

$$\lim_{N\to\infty} \frac{1}{N} \ln N(\boldsymbol{E}, \boldsymbol{y}) = S(\boldsymbol{E}, \boldsymbol{y}). \tag{47}$$

On the other hand, if $(\boldsymbol{E}, \boldsymbol{y}) \notin \bar{\mathcal{C}}$, the topological closure of $\mathcal{C}$, almost surely and for all, but finitely many N:

$$N(\boldsymbol{E}, \boldsymbol{y}) = 0. \tag{48}$$

Proof Let us start with the case $(\boldsymbol{E}, \boldsymbol{y}) \notin \bar{\mathcal{C}}$. One then finds some $k \in \mathbb{N}$ and $\epsilon > 0$ such that

$$\sum_{j=1}^{k} \frac{E_j^2}{2a_j} + (x_j - x_{j-1}) I(y_j/(x_j - x_{j-1})) \geq x_k \ln 2 + \epsilon. \tag{49}$$

We condition on the weights (h_i) and compute the probability that a reduced spin vector $\boldsymbol{\sigma}_1 \cdots \boldsymbol{\sigma}_k$ meets the first k energy requirements

$$\begin{aligned} &\mathbb{P}(\sqrt{a_j} X_{\boldsymbol{\sigma}_1 \cdots \boldsymbol{\sigma}_j} \leq -\sqrt{N} E_j \text{ and } h_j(\boldsymbol{\sigma}_j) \leq -N y_j \text{ for all } j = 1, \ldots, k \,|(h_i)) \\ &= \prod_{j=1}^{k} \mathbb{P}(\sqrt{a_j} X_{\boldsymbol{\sigma}_1 \cdots \boldsymbol{\sigma}_j} \leq -\sqrt{N} E_j)\, \mathbb{P}(h_j(\boldsymbol{\sigma}_j) \leq -N y_j \,|(h_i)) \\ &\leq \prod_{j=1}^{k} e^{-N E_j^2/(2a_j)} 1[h_j(\boldsymbol{\sigma}_j) \leq -N y_j]. \end{aligned} \tag{50}$$

The first equality is due to the independence of the variables $X_{\boldsymbol{\sigma}_1 \cdots \boldsymbol{\sigma}_j}$ for different j. The bound on the first probability follows from the standard Gaussian estimate. This may be inserted into the following union bound

$$\begin{aligned} \mathbb{P}(N(\boldsymbol{E}, \boldsymbol{y}) \geq 1 | (h_i)) \leq \sum_{\boldsymbol{\sigma}_1 \cdots \boldsymbol{\sigma}_k} &\mathbb{P}\big(\sqrt{a_j N} X_{\boldsymbol{\sigma}_1 \cdots \boldsymbol{\sigma}_j} \leq -N E_j \\ &\text{and } h_j(\boldsymbol{\sigma}_j) \leq -N y_j \text{ for all } j = 1, \ldots, k \,|(h_i)) \\ &\leq \exp\Big(- N \sum_{j=1}^{k} \frac{E_j^2}{2a_j} \Big) \prod_{j=1}^{k} N(y_k), \end{aligned}$$

where the last inequality is the previous estimate.

We now distinguish two cases. If

$$\boldsymbol{y} \in \mathcal{G}_k := \{\boldsymbol{y} \in \mathbb{R}^n_{\geq 0} |\, I(\xi_j(y_j)) < \infty \text{ for all } j = 1, \ldots, k\},$$

we may further estimate the right side using (49) and the upper bound in (42) to conclude that for all, but finitely many N and almost surely with respect to the variables (h_i):

$$\mathbb{P}(N(\boldsymbol{E}, \boldsymbol{y}) \geq 1 | (h_i)) \leq e^{-N\epsilon/2}.$$

A Borel-Cantelli argument then shows that $N(\boldsymbol{E}, \boldsymbol{y})$ converges almost surely to zero.

In case $\boldsymbol{y} \notin \mathcal{G}_k$ there exist an integer $j \in \{1, \dots k\}$ such that $I(\xi_j(y_j)) = \infty$. Consequently, (42) implies the almost-sure convergence $\limsup_{N\to\infty} \frac{1}{N_j} \ln N(y_j) = -\infty$. Since $N(y_j) \in \mathbb{N}_0$, this implies that almost surely $N(y_j) = 0$ for all, but finitely many N. We conclude $\mathbb{P}(N(\boldsymbol{E}, \boldsymbol{y}) \geq 1 | (h_i)) = 0$ for all, but finitely many N and hence the claim (48) in this case.

It thus remains to show (47) for $(\boldsymbol{E}, \boldsymbol{y}) \in \mathcal{C}$. This proof will be based on Proposition 3. For its application, we introduce the following sequences of numbers

$$\begin{aligned} F_k(N) := & \frac{1}{N} \ln |\{\boldsymbol{\sigma}_1 \cdots \boldsymbol{\sigma}_k | \ \sqrt{a_i} X_{\boldsymbol{\sigma}_1 \cdots \boldsymbol{\sigma}_i} \leq -\sqrt{N} E_i \text{ and} \\ & h_j(\boldsymbol{\sigma}_j) \leq -N y_j \text{ for all } \ i = 1, \dots, k-1; \ \ j = 1, \dots, k\}| \\ G_k(N) := & \frac{1}{N} \ln |\{\boldsymbol{\sigma}_1 \cdots \boldsymbol{\sigma}_k | \ \sqrt{a_i} X_{\boldsymbol{\sigma}_1 \cdots \boldsymbol{\sigma}_i} \leq -\sqrt{N} E_i \text{ and} \\ & h_j(\boldsymbol{\sigma}_j) \leq -N y_j \text{ for all } i = 1, \dots, k; \ \ j = 1, \dots, k\}|, \\ G_0 := & \ 0. \end{aligned}$$

The definition of these sets are motivated by inclusion-exclusion. If we suppose that $G_k(N)$ converges as $N \to \infty$, the almost-sure convergence (43), for which we recall that $(\boldsymbol{E}, \boldsymbol{y}) \in \mathcal{C}$ implies $\max_j |\xi_j| < \mathbb{E}[|\mathfrak{h}|]$, yields

$$\lim_{N\to\infty} F_{k+1}(N) = (x_{k+1} - x_k) \ln 2 - (x_{k+1} - x_k) I(\xi_{k+1}) + \lim_{N\to\infty} G_k(N).$$

Moreover, Proposition 3 further implies

$$\lim_{N\to\infty} G_{k+1}(N) = -(2a_{k+1})^{-1} E_{k+1}^2 + \lim_{N\to\infty} F_{k+1}(N),$$

provided that the right side is positive. By definition of the constraint, this is always the case if $(\boldsymbol{E}, \boldsymbol{y}) \in \mathcal{C}$ such that

$$\begin{aligned} \lim_{N\to\infty} \frac{1}{N} \ln N(\boldsymbol{E}, \boldsymbol{y}) = \lim_{N\to\infty} G_n(N) &= \ln 2 - \sum_{j=1}^{n} \left(\frac{E_j^2}{2a_j} + (x_j - x_{j-1}) I\left(\xi_j(y_j)\right) \right) \\ &= S(\boldsymbol{E}, \boldsymbol{y}) \end{aligned}$$

almost surely. □

The second part of the proof of Lemma 1 relied on the following claim, whose proof follows that of Proposition 6 in [4].

Proposition 3 *Let $(D_N)_{N\in\mathbb{N}}$ be a family of finite sets, $(X_s)_{s\in D_N}$ independent standard Gaussian variables and $(Y_s)_{s\in D_N}$ a random vector, which is independent of X and whose entries only take the values 0 and 1. Further, suppose that almost surely*

$$\lim_{N\to\infty} \frac{1}{N} \ln |\{s \in D_N | Y_s = 0\}| = q > 0.$$

Then the number of large deviations

$$N(E) := |\{s \in D_N | Y_s = 0 \text{ and } \sqrt{a} X_s \leq -E\sqrt{N}\}|,$$

with $a > 0$ almost sure obeys

$$\lim_{N\to\infty} \frac{1}{N} \ln N(E) = q - (2a)^{-1} E^2$$

provided that $q > (2a)^{-1} E^2$.

Proof We apply the second moment method to $N(E)$ and the conditional expectation conditioned on the event $Z:=\{s \in D_N | Y_s = 0\}$. A standard calculation similar to (50) using elementary bounds on the Gaussian distribution function shows that

$$\mathbb{E}[N(E)|Z] = Z \exp(-((2a)^{-1}E^2 + o(1))N).$$

By explicit computation we determine the second moment of $N(E)$ conditioned on Z:

$$\begin{aligned}
&\mathbb{E}[N(E)^2|Z] - \mathbb{E}[N(E)|Z]^2 \\
&= \sum_{s,s':Y_s=Y_{s'}=0} \mathbb{P}\left(\sqrt{a}X_s \le -E\sqrt{N} \text{ and } \sqrt{a}X_{s'} \le -E\sqrt{N}\right) \\
&\quad - \mathbb{P}\left(\sqrt{a}X_s \le -E\sqrt{N}\right)\mathbb{P}\left(\sqrt{a}X_{s'} \le -E\sqrt{N}\right) \\
&= \sum_{s:Y_s=0} \mathbb{P}\left(\sqrt{a}X_s \le -E\sqrt{N}\right) - \mathbb{P}\left(\sqrt{a}X_s \le -E\sqrt{N}\right)^2 \le \mathbb{E}[N(E)|Z].
\end{aligned}$$

Thus, the Chebyshev inequality implies for any $\epsilon > 0$:

$$\mathbb{P}(|N(E) - \mathbb{E}[N(E)|Z]| > \epsilon\, \mathbb{E}[N(E)|Z]|Z) \le \epsilon^{-2}\, \mathbb{E}[N(E)|Z]^{-1}.$$

We note that $\mathbb{E}[N(E)|Z]$ is almost surely exponentially large; in fact, by assumption $\ln Z = N(q + o(1))$ with $q > (2a)^{-1}E^2$. Thus, a Borel-Cantelli argument yields almost surely

$$\limsup_{N\to\infty} \left| \frac{1}{N} \ln \frac{N(E)}{\mathbb{E}[N(E)|Z]} \right| = 0,$$

which completes proof using the expression for $\mathbb{E}[N(E)|Z]$. □

Based on Lemma 1, we may now establish a variational expression for the limiting pressure of the n-level GREM in a random magnetic field.

Lemma 2 *For any $\beta \ge 0$ and any absolutely integrable random variable $\mathfrak{h}$ the pressure $\Phi_N(\beta, \mathfrak{h})$ converges almost surely and its limit is given by*

$$\lim_{N\to\infty} \Phi_N(\beta, \mathfrak{h}) = \sup_{(\boldsymbol{E},\boldsymbol{y})\in\mathcal{C}} \left(\beta(E_1 + \cdots + E_n + y_1 + \cdots + y_n) + S(\boldsymbol{E}, \boldsymbol{y})\right). \tag{51}$$

Proof By elementary estimates it follows that

$$\exp(N\Phi_N(\beta, \mathfrak{h})) \ge \exp(\beta N(E_1 + \cdots + E_n + y_1 + \cdots + y_n))N(\boldsymbol{E}, \boldsymbol{y})$$

for any $(\boldsymbol{E}, \boldsymbol{y})$, which in view of Lemma 1 implies almost surely

$$\liminf_{N\to\infty} \Phi_N(\beta, \mathfrak{h}) \ge \sup_{(\boldsymbol{E},\boldsymbol{y})\in\mathcal{C}} \beta(E_1 + \cdots + E_n + y_1 + \cdots + y_n) + S(\boldsymbol{E}, \boldsymbol{y}).$$

To obtain an asymptotic upper bound we use a discretization argument. We set $\alpha := \max_{i=1,\ldots,n} a_i$ and define the compact box

$$F := [-(\sqrt{2\alpha \ln 2} + 1), \sqrt{2\alpha \ln 2} + 1]^n \times [-\mathbb{E}[|\mathfrak{h}|] - 1, \mathbb{E}[|\mathfrak{h}|] + 1]^n.$$

One easily sees that almost surely no configuration $(\boldsymbol{E}, \boldsymbol{y})$ outside of F contributes to the limit (51) of the pressure. To simplify the notation, we assume in the following that this holds true for any N. Thus, it suffices to consider configurations in F on which we set the grid

$$\begin{aligned}
F_K := \Big\{ (\boldsymbol{E}, \boldsymbol{y}) \in F \;\Big|\; E_j = \frac{k_j}{K}(\sqrt{2\alpha \ln 2} + 1),\ y_j = \frac{l_j}{K}(\mathbb{E}[\mathfrak{h}] + 1), \\
k_j, l_j = -K, -K+1, \ldots, K, \quad j = 1, \ldots, n \Big\}
\end{aligned}$$

with $K \in \mathbb{N}$. We pick $\epsilon > 0$ arbitrary and choose $K = K_\epsilon$ such that $\max\{\mathbb{E}[\mathfrak{h}]+1, \sqrt{2\alpha \ln 2}+1\} < \epsilon K_\epsilon$. Then, the ϵ-neighborhoods of the grid points in F_K cover the box F and therefore

$$e^{N\Phi_N(\beta,\mathfrak{h})} \leq \sum_{(\boldsymbol{E},\boldsymbol{y})\in F_K} N(\boldsymbol{E},\boldsymbol{y})\, e^{\beta N(E_1+\cdots+E_n+y_1+\cdots+y_n+2n\epsilon)}.$$

Let us now observe three points. First, if E_j or y_j is negative for some j we may replace this value by 0 without changing the number $N(\boldsymbol{E},\boldsymbol{y})$ on an exponential scale. This is just a consequence of symmetry and the LDP satisfied by h_j and the Gaussian vectors X. Secondly, without loss of generality we may assume that there are no grid points on the boundary of $\mathcal{C}$. Moreover, if $(\boldsymbol{E},\boldsymbol{y}) \notin \bar{\mathcal{C}}$, the corresponding term gives no contribution to the limit of Φ_N by (48). Thirdly, the entropy factor corresponding to the summation over the grid points does not depend on N and is thus irrelevant after taking the limit. Summarizing these points, we conclude almost surely

$$\limsup_{N\to\infty} \Phi_N(\beta,\mathfrak{h}) \leq 2\beta n\epsilon + \sup_{(\boldsymbol{E},\boldsymbol{y})\in\mathcal{C}} \beta(E_1+\cdots+E_n+y_1+\cdots+y_n) + S(\boldsymbol{E},\boldsymbol{y}),$$

which completes the proof as $\epsilon > 0$ was chosen arbitrarily. □

It remains to solve the variational problem (51) which is the last part in the proof of Theorem 3. Note that one may replace the sup on $\mathcal{C}$ by a maximum on $\bar{\mathcal{C}}$ as the involved expressions possess continuous extensions to $\bar{\mathcal{C}}$.

Proof of Theorem 3 We proceed via induction on m, the number of linear segments of the concave hull $\bar{A}$. If $m = 1$, the variational problem consists of $2n$ independent optimization problems which can be easily solved. This leads to

$$E_j = \beta a_j \text{ and } y_j = (x_j - x_{j-1})\mathbb{E}[\mathfrak{h}\tanh(\beta\mathfrak{h})] \quad j = 1,\ldots,n.$$

To obtain the expression for y_j, it is helpful to note that the rate function I is the Legendre transform of $\mathbb{E}[\ln\cosh(\beta\mathfrak{h})]$. The maximum is attained when $\xi_j(y_j) = y_j/(x_j - x_{j-1})$ equals the derivative of $\mathbb{E}[\ln\cosh(\beta\mathfrak{h})]$ with respect to β. We see that if β is small enough, all constraints are fulfilled and the maximum is given by

$$\Phi(\beta,\mathfrak{h}) = \ln 2 + \frac{\beta^2}{2}\left(\sum_{j=1}^{n} a_j\right) + \mathbb{E}[\ln\cosh(\beta\mathfrak{h})].$$

Since in the unconstrained variational problem the optimal value E_j is unbounded as β increases, the above considerations will hold true up to some critical value β_c, where the first constraining inequality is not satisfied, i.e., the maximum is located at the boundary of $\mathcal{C}$. Due to the structure of the optimal $(\boldsymbol{E},\boldsymbol{y})$ in the unconstrained setting, this needs to be the inequality corresponding to the highest slope $(a_1+\cdots+a_k)/x_k$ which is attained at $k = n$ since $m = 1$. If we denote the optimal configuration of the unconstrained problem at β_c by $(\boldsymbol{E}^c,\boldsymbol{y}^c)$ we thus have

$$S(\boldsymbol{E}^c,\boldsymbol{y}^c) = 0.$$

From there, one obtains after some algebra the self-consistency equation for β_c:

$$\frac{\sum_j a_j}{2}\beta_c^2 = \ln 2 + \mathbb{E}[\ln\cosh\beta_c\mathfrak{h}] - \beta_c\mathbb{E}[\mathfrak{h}\tanh\beta_c\mathfrak{h}].$$

Furthermore,

$$\max_{(\boldsymbol{E},\boldsymbol{y})\in\bar{\mathcal{C}}} \beta_c(E_1+\cdots+E_n+y_1+\cdots+y_n)+S(\boldsymbol{E},\boldsymbol{y}) = \max_{(\boldsymbol{E},\boldsymbol{y})\in\bar{\mathcal{C}}} \beta_c(E_1+\cdots+E_n+y_1+\cdots+y_n),$$

which is clearly still a valid identity for $\beta > \beta_c$. We conclude that Φ becomes a linear function of β for $\beta > \beta_c$ and the slope agrees with the derivative of Φ at β_c, i.e.

$$\Phi(\beta,\mathfrak{h}) = \beta\left(\beta_c\sum_{j=1}^{n} a_j + \mathbb{E}\left[\mathfrak{h}\tanh\beta_c\mathfrak{h}\right]\right).$$

This is exactly the statement of Theorem 3 in the case $m = 1$.

Now, suppose that the assertions are true for some m, and we want to show that it is still the case for $m+1$. Let us write $\boldsymbol{E}_{<m}$, $\boldsymbol{E}_{>m}$, $\boldsymbol{y}_{<m}$ and $\boldsymbol{y}_{>m}$, where the vectors denote the energy configurations corresponding to the first m segments and the last segment, respectively. Similarly, we set $\mathcal{C}_m$ the set of the constraints related to the first m segments. If we only demand that the energy configuration $(\boldsymbol{E}_{<m},\boldsymbol{y}_{<m})$ satisfy the constraints $\mathcal{C}_m$, then using the induction hypothesis and the analysis of the case $m = 1$, we end up with the expression

$$\sum_{l=1}^{m}\varphi^{(l)}(\beta,\mathfrak{h}) + (1-y_m)\ln 2 + \frac{\beta^2}{2}\left(\sum_{j\in I_{m+1}} a_j\right) + (1-y_m)\mathbb{E}\left[\ln\cosh(\beta\mathfrak{h})\right]$$

for the limit of the pressure, where I_{m+1} denotes the last segment. This is indeed a solution if $\beta \le \beta_c^{(m)}$, since the remaining constraints are also verified by the m-level solution $(\boldsymbol{E}_{<m},\boldsymbol{y}_{<m})$ and the unconstrained solution $(\boldsymbol{E}_{>m},\boldsymbol{y}_{>m})$ due to the concave-hull structure. We note that for $\beta > \beta_c^{(m)}$, we only need to consider the n-th inequality (for the same reason as in the case $m = 1$) which then may be rewritten as

$$(y_{m+1}-y_m)\ln 2 > \sum_{j\in I_{m+1}} (2a_j)^{-1} + (x_j - x_{j-1})I(\xi_j(y_j)).$$

Thus, the situation is analogous to the case $m = 1$ and the same arguments lead to the expression for $\beta_c^{(m+1)}$ and the pressure Φ if $\beta > \beta_c^{(m+1)}$. □

3.2 From GREM to QGREM: Application of the Peeling Principle

We now consider the QGREM with a random magnetic field in z-direction as in Theorem 1.

Theorem 4 *Let $U(\boldsymbol{\sigma})$ be a GREM process as in (37), $\beta \ge 0$ and $\mathfrak{h}$, $\mathfrak{b}$ absolutely integrable random variables. Then, almost surely*

$$\lim_{N\to\infty}\Phi_N(\beta,\mathfrak{h},\mathfrak{b}) = \max_{0\le k\le m}\left(\sum_{l=1}^{k}\varphi^{(l)}(\beta,\mathfrak{h}) + (1-y_k)\mathbb{E}\left[\ln 2\cosh(\sqrt{\mathfrak{b}^2+\mathfrak{h}^2})\right]\right). \quad (52)$$

Here, the empty sum is interpreted to be zero.

Proof We recall the definition of the cut GREM $U^{(x_k)} := U^{(0,x_k)}$ which may be represented as

$$U^{(x_k)}(\boldsymbol{\sigma}_1\boldsymbol{\sigma}_2\cdots\boldsymbol{\sigma}_k) = \sqrt{a_1}X_{\boldsymbol{\sigma}_1} + \sqrt{a_2}X_{\boldsymbol{\sigma}_1\boldsymbol{\sigma}_2} + \cdots + \sqrt{a_n}X_{\boldsymbol{\sigma}_1\boldsymbol{\sigma}_2\cdots\boldsymbol{\sigma}_k}.$$

The peeling principle [22, Theorem 2.3] implies that for any $0 \leq k \leq m$ either the Gaussians $X_{\boldsymbol{\sigma}_1\boldsymbol{\sigma}_2\cdots\boldsymbol{\sigma}_k}$ or the partial magnetic field $B^{(1,x_k)}$ contribute to the specific pressure (for a detailed discussion see Sect. 2 in [22, Theorem 2.3]). An iterative application of the peeling principle yields

$$\limsup_{N\to\infty}\left|\Phi_N(\beta,\mathfrak{h},\mathfrak{b})-\max_{0\leq k\leq n}\frac{1}{N}\ln \mathrm{Tr}\, e^{-\beta(U^{(x_k)}-h(\boldsymbol{\sigma})-B^{(2,x_k)})}\right|=0,$$

see also the proof of [22, Corollary 2.7] for a more precise execution of this method. The cut-magnetic field $B^{(2,x_k)}$ was defined in (31). We naturally split the longitudinal field,

$$h(\boldsymbol{\sigma})=h^{(1,x_k)}(\boldsymbol{\sigma}_1\cdots\boldsymbol{\sigma}_k)+h^{(2,x_k)}(\boldsymbol{\sigma}_{k+1}\cdots\boldsymbol{\sigma}_n);\quad h^{(1,x_k)}(\boldsymbol{\sigma}_1\cdots\boldsymbol{\sigma}_k):=\sum_{i=1}^{\lceil x_k N\rceil}h_i\sigma_i$$

and apply Theorem 3 to the Hamiltonian $H^{(x_k)}:=U^{(x_k)}-h^{(1,x_k)}$. Together with the strong law of large numbers for $h^{(2,x_k)}(\boldsymbol{\sigma}_{k+1}\cdots\boldsymbol{\sigma}_n)+B^{(2,x_k)}$. Thus we arrive at

$$\lim_{N\to\infty}\Phi_N(\beta,\mathfrak{h},\mathfrak{b})=\max_{0\leq k\leq n}\left(\Phi^{(x_k)}(\beta,\mathfrak{h})+(1-x_k)\mathbb{E}\left[\ln 2\cosh(\sqrt{\mathfrak{b}^2+\mathfrak{h}^2})\right]\right),\tag{53}$$

where $\Phi^{(x_k)}(\beta,\mathfrak{h})$ denotes the limit of the pressure of the Hamiltonian $H^{(x_k)}$ restricted to the Hilbert space of subgraph $\mathcal{Q}_{\lceil x_k N\rceil}$ spanned by $\boldsymbol{\sigma}_1\cdots\boldsymbol{\sigma}_k$. (Note that for $H^{(x_k)}$ on the total graph $\mathcal{Q}_N$ the resulting pressure is $\Phi^{(x_k)}(\beta,\mathfrak{h})+(1-x_k)\ln 2$.)

If the cut point coincides with and endpoint of the concave hull. i.e. $x_k=y_j$ for some j, we have

$$\Phi^{(y_j)}(\beta,\mathfrak{h})=\sum_{l=1}^{j}\varphi^{(l)}(\beta,\mathfrak{h}).$$

Thus, it only remains to show that the maximum in (53) is attained at some y_l. We follow the comparison argument presented in the proof of [22, Lemma 3.1]. If $\{x_0,\ldots,x_n\}=\{y_0,\ldots,y_m\}$, the assertion is trivial. So, let $y_l<x_k<y_{l+1}$. We recall that distribution function $A^{(x_k)}$ associated with $U^{(x_k)}$ is given by

$$A^{(x_k)}=\begin{cases}A(x) & \text{if } x\leq x_k,\\ A(x_k) & \text{else.}\end{cases}.$$

We introduce the Gaussian processes Y and Z of GREM type with the distribution functions

$$A_Y(x):=\begin{cases}A(x) & \text{if } x\leq y_l,\\ A(y_l) & \text{if } y_l<x<x_k,\\ A(x_k) & \text{if } x\geq x_k,\end{cases}$$

$$A_Z(x):=\begin{cases}A(x) & \text{if } x\leq y_l,\\ A(y_l) & \text{if } y_l<x<x_k,\\ A(y_l)+\frac{x_k-y_l}{y_{l+1}-y_l}(A(y_{l+1})-A(y_l)), & \text{if } x\geq x_k.\end{cases}$$

which shall be independent of the weights (h_i) After conditioning on the random weights (h_i), Slepian's lemma (cf. [6]) and the independence of (h_i) and the GREM processes imply:

$$\lim_{N\to\infty}\frac{1}{N}\ln \mathrm{Tr}_{|\ell^2(\mathcal{Q}_{x_kN})}e^{-\beta(U^{(x_k)}-h^{(1,x_k)})} \le \lim_{N\to\infty}\frac{1}{N}\ln \mathrm{Tr}_{|\ell^2(\mathcal{Q}_{x_kN})}e^{-\beta(\sqrt{N}Y-h^{(1,x_k)})}$$
$$\le \lim_{N\to\infty}\frac{1}{N}\ln \mathrm{Tr}_{|\ell^2(\mathcal{Q}_{x_kN})}e^{-\beta(\sqrt{N}Z-h^{(1,x_k)})}. \quad (54)$$

For the second inequality, we recall that A is majorized by its concave hull $\bar{A}$ and agrees with $\bar{A}$ at y_l and y_{l+1}:

$$A(x_k) \le A(y_l) + \frac{x_k - y_l}{y_{l+1} - y_l}\left(A(y_{l+1}) - A(y_l)\right).$$

Since the pressure is an increasing function of the jump heights (cf. (38)), we hence arrive at the second bound in (54). The resulting pressure is computed easily in terms of the partial pressures (38) corresponding to A:

$$\lim_{N\to\infty}\frac{1}{N}\ln \mathrm{Tr}_{|\mathcal{Q}_{x_kN}}e^{-\beta(\sqrt{N}Z-h^{(1,x_k)})} = \sum_{j=1}^{l}\varphi^{(j)}(\beta,\mathfrak{h}) + \frac{x_k - y_l}{y_{l+1}-y_l}\varphi^{(j+1)}(\beta,\mathfrak{h}).$$

Using the abbreviation $p(\beta,\mathfrak{h},\mathfrak{b}) := \mathbb{E}\left[\ln 2\cosh(\beta\sqrt{\mathfrak{b}^2+\mathfrak{h}^2})\right]$ we thus conclude

$$\lim_{N\to\infty}\frac{1}{N}\ln \mathrm{Tr}_{|\ell^2(\mathcal{Q}_{x_kN})}e^{-\beta(U^{(x_k)}-h^{(1,x_k)})} + (1-x_k)p(\beta,\mathfrak{h},\mathfrak{b})$$
$$\le \sum_{j=1}^{l}\varphi^{(j)}(\beta,\mathfrak{h}) + (1-y_l)p(\beta,\mathfrak{h},\mathfrak{b})$$
$$+ \frac{x_k-y_l}{y_{l+1}-y_l}\left(\varphi^{(l+1)}(\beta,\mathfrak{h}) - (y_{l+1}-y_l)p(\beta,\mathfrak{h},\mathfrak{b})\right).$$

Depending on the sign of the term in the last bracket, we have

$$\lim_{N\to\infty}\frac{1}{N}\ln \mathrm{Tr}_{|\ell^2(\mathcal{Q}_{x_kN})}e^{-\beta(\sqrt{N}X^{(x_k)}-V^{(1,x_k)})} + (1-x_k)p(\beta,\mathfrak{h},\mathfrak{b})$$
$$\le \sum_{j=1}^{l}\varphi^{(j)}(\beta,\mathfrak{h}) + (1-y_l)p(\beta,\mathfrak{h},\mathfrak{b})$$

or the sum on the right side runs to $l+1$ and y_l is replaced by y_{l+1}.

Consequently, the maximal pressure is indeed attained at some y_l. □

3.3 Finishing the Proof: The Interpolation Argument

Finally, we will lift Theorem 4 to the case of a general QGREM. The idea is to show that the left and right side of (7) are continuous with respect to the distribution function A and the uniform norm. We start with the continuity of the right side, i.e., spelling out explicitly the A-dependence of quantities for the moment, we need to show that

$$\Phi(\beta,\mathfrak{h},\mathfrak{b},A) = \sup_{0\le z\le 1}\left(\int_0^z \varphi(\beta,\mathfrak{h},A,x)\,dx + (1-z)\mathbb{E}\left[\ln 2\cosh(\beta\sqrt{\mathfrak{b}^2+\mathfrak{h}^2})\right]\right),$$

is continuous in A. We recall that the density is given by

$$\varphi(\beta,\mathfrak{h},A,x) := \begin{cases} \ln 2 + \bar{a}(x)\frac{\beta^2}{2} + \mathbb{E}\left[\ln\cosh\beta\mathfrak{h}\right] & \text{if} \quad \beta \le \beta_c(A,x) \\ \beta(\bar{a}(x)\beta_c(A,x) + \mathbb{E}\left[\mathfrak{h}\tanh\beta_c(A,x)\mathfrak{h}\right]) & \text{if} \quad \beta > \beta_c(A,x) \end{cases}$$

where the critical temperature $\beta_c(A, x)$ is the unique positive solution of the self-consistency equation

$$\frac{\bar{a}(x)}{2}\beta_c(A,x)^2 = \ln 2 + \mathbb{E}\left[\ln\cosh\beta_c(A,x)\mathfrak{h}\right] - \beta_c(A,x)\mathbb{E}\left[\mathfrak{h}\tanh\beta_c(A,x)\mathfrak{h}\right].$$

Lemma 3 *Let $\beta \geq 0$ and $\mathfrak{b}, \mathfrak{h}$ be absolutely integrable random variables. Moreover, let $(A_n)_{n\in\mathbb{N}}$, A be distribution functions on $[0, 1]$ such that A_n converges uniformly to A. Then,*

$$\lim_{n\to\infty} \Phi(\beta, \mathfrak{h}, \mathfrak{b}, A_n) = \Phi(\beta, \mathfrak{h}, \mathfrak{b}, A). \tag{55}$$

Proof It suffices to show that

$$\lim_{n\to\infty} \int_0^1 |\varphi(\beta, \mathfrak{h}, A, x) - \varphi(\beta, \mathfrak{h}, A_n, x)|\, dx = 0.$$

We first prove that the integrand converges almost everywhere (with respect to the Lebesgue measure and x) to zero. One easily sees that the concave hulls $\bar{A}_n$ converge uniformly to $\bar{A}$ and the right derivatives $\bar{a}_n(x)$ converge to $\bar{a}(x)$ at any x, where $\bar{a}(x)$ is continuous (cf. the proof of Lemma 3.3 in [22]). Since $\bar{A}$ is concave, this ensures that $\bar{a}_n(x)$ converge almost everywhere to $\bar{a}(x)$. Next, we observe that $\beta_c(x, A)$ is a continuous function of $\bar{a}(x)$ by the implicit function theorem and, thus, $\beta_c(x, A_n)$ converges almost everywhere to $\beta_c(x, A)$. This implies that $\varphi(\beta, \mathfrak{h}, A_n, x)$ converges almost everywhere. Now we pick some $\delta > 0$ and note that the sequence $\varphi(\beta, \mathfrak{h}, A_n, x)$ is uniformly bounded due to the general bound

$$0 \leq \varphi(\beta, \mathfrak{h}, A_n, x) \leq \ln 2 + \bar{a}_n(x)\frac{\beta^2}{2} + \mathbb{E}\left[\ln\cosh\beta\mathfrak{h}\right]$$

and the monotonicity of the derivatives $\bar{a}_n(x)$. We conclude that for any $\delta > 0$,

$$\lim_{n\to\infty} \int_\delta^1 |\varphi(\beta, \mathfrak{h}, A, x) - \varphi(\beta, \mathfrak{h}, A_n, x)|\, dx = 0.$$

Using the above bound on $[0, \delta]$, we obtain

$$\int_0^\delta |\varphi(\beta, \mathfrak{h}, A, x) - \varphi(\beta, \mathfrak{h}, A_n, x)|\, dx \leq \delta(2\ln 2 + (\bar{A}_n(\delta) + \bar{A}(\delta))\frac{\beta^2}{2} + 2\mathbb{E}\left[\ln\cosh\beta\mathfrak{h}\right]),$$

which vanishes if we take the limit $n \to \infty$ and then $\delta \to 0$. □

We turn to the interpolation argument for the left side in (7). Let U, U' be two GREM processes with distribution functions A, A' and pressures $\Phi(\beta, \mathfrak{h}, \mathfrak{b}, A), \Phi(\beta, \mathfrak{h}, \mathfrak{b}, A')$. From [22, Equation (2.16)] we conclude

$$|\mathbb{E}\left[\Phi(\beta, \mathfrak{h}, \mathfrak{b}, A) - \Phi(\beta, \mathfrak{h}, \mathfrak{b}, A')\right]| \leq \beta^2 \|A - A'\|_\infty, \tag{56}$$

The Gaussian concentration inequality (cf. [22, Proposition 2.9]) guarantees the almost-sure convergence

$$\limsup_{N\to\infty} |\mathbb{E}\left[\Phi(\beta, \mathfrak{h}, \mathfrak{b}, A)\right] - \Phi(\beta, \mathfrak{h}, \mathfrak{b}, A)| = 0.$$

We are ready to finish the proof of Theorem 1:

Proof of Theorem 1 We fix $\beta \geq 0$ and absolutely integrable random variables $\mathfrak{b}, \mathfrak{h}$ and use the shorthand notations $\Phi(A) := \Phi(\beta, \mathfrak{h}, \mathfrak{b}, A)$. Let U be a GREM process with distribution function A. We pick some $\epsilon > 0$ and an finite-level GREM U' with distribution function A'

such that $\|A - A'\|_\infty \leq \epsilon$ and $|\Phi(A) = \Phi(A')| \leq \epsilon$. This is possible thanks to Lemma 3. We then obtain

$$\begin{aligned}
&\limsup_{N\to\infty} |\Phi_N(A) - \Phi(A)| \\
&\qquad \leq \limsup_{N\to\infty} |\Phi_N(A) - \Phi_N(A')| + |\Phi_N(A') - \Phi(A')| + |\Phi(A) - \Phi(A')| \\
&\qquad \leq (\beta^2 + 1)\epsilon.
\end{aligned}$$

The final line follows from our preparatory estimate (56) and Theorem 4, which coincides with Theorem 1 for an n-level GREM. Since $\epsilon > 0$ is arbitrary, this proves (7).

The remaining assertions now follow easily: $\varphi(\beta, \mathfrak{h}, x)$ is clearly an increasing function of $\bar{a}(X)$ which in turn is decreasing in x. Thus, $\varphi(\beta, \mathfrak{h}, x)$ is a decreasing function of x. Similarly, the critical inverse temperature $\beta_c(x)$ is increasing as it is a decreasing function of $\bar{a}(x)$. Finally, the fact that $\varphi(\beta, \mathfrak{h}, x)$ is increasing and convex in β directly follows from (8). □

Funding Open Access funding enabled and organized by Projekt DEAL.

Appendix A: Proof of Corollary 1 and Proposition 1

We start with the straightforward proof of Corollary 1:

Proof of Corollary 1 To apply Theorem 1, we note that in the case of the QREM we have $\varphi(\beta, h, x) = \Phi^{\mathrm{REM}}(\beta, h)$ for any x. So, we directly obtain (10). It remains to show that the self-consistency equation

$$\frac{1}{2}\beta_c^2 = \ln 2 + \ln\cosh \beta_c h - \beta_c h \tanh \beta_c h,$$

which get from Theorem 1 is equivalent to (12), i.e. $\beta_c(h)^2 = 2r(\tanh(\beta_c(h)h))$. This follows from the elementary computation

$$\begin{aligned}
r(\tanh(x)) &= \ln 2 - \frac{1}{2}\left((1 - \tanh(x))\ln(1 - \tanh(x)) + (1 + \tanh(x))\ln(1 + \tanh(x))\right) \\
&= \ln 2 + \ln\cosh x - \frac{1}{2}\left((1 - \tanh(x))\ln(\cosh x - \sinh x) + (1 + \tanh(x))\ln(\cosh x + \sinh x)\right) \\
&= \ln 2 + \ln\cosh x - x\tanh x
\end{aligned}$$

for any $x \in \mathbb{R}$. □

The proof of Proposition 1 is based on multiple elementary, but quite lengthy, computations.

Proof of Proposition 1 1. The defining equation (12) immediately implies that $\beta_c(h)$ is a strictly decreasing function. The Taylor expansions $r(y) = \ln 2 - y^2/2 + \mathcal{O}(y^4))$ and $\tanh(y) = y + \mathcal{O}(y^2)$ yield for small $h > 0$

$$\frac{1}{2}\beta_c(h)^2 = \ln 2 - \frac{(\beta_c(h)h)^2}{2} + \mathcal{O}(h^4),$$

which in turn leads to the Taylor expansion of $\beta_c(h)$ in the small field limit.
By inspection of (12) as $h \to \infty$, the critical inverse temperature $\beta_c(h)$ tends to zero, but we still have that $h\beta_c(h) \to \infty$. Moreover, we recall that $\tanh(y) = 1 - 2e^{-2y} + \mathcal{O}(e^{-4y})$ for large y and $r(1-x) = \frac{1}{2}x\ln(1/x) + \mathcal{O}(x)$ for small x. After some algebra, we arrive at the asymptotic equation $2\beta_c(h)he^{2\beta_c(h)h} = 8h^2 + \mathcal{O}(h)$. In particular,

$$\lim_{h\to\infty} \frac{2\beta_c(h)h}{W(8h^2)} = \lim_{h\to\infty} \frac{\beta_c(h)h}{\ln h} = 1,$$

where W denotes Lambert W-function.

2. We first consider the high temperature limit. For small $\beta > 0$ a Taylor expansion yields

$$\begin{aligned}\operatorname{arcosh}\left(\frac{1}{2}\exp(\Phi^{\mathrm{REM}}(\beta,h))\right) &= \operatorname{arcosh}\left(1 + \frac{1}{2}\beta^2(1+h^2) + \mathcal{O}(\beta^4)\right)\\ &= \sqrt{1+h^2}\beta + \mathcal{O}(\beta^2),\end{aligned}$$

from which we conclude $\Gamma_c(0,h) = 1$. As the term $\operatorname{arcosh}\left(\frac{1}{2}\exp(\Phi^{\mathrm{REM}}(\beta,h))\right)/\beta$ converges to the absolute value of the ground state energy as $\beta \to \infty$, we obtain the claim concerning the low temperature limit.

3. Let us fix some $\beta > 0$. We show that

$$g(h) = \operatorname{arcosh}\left(\frac{1}{2}\exp(\Phi^{\mathrm{REM}}(\beta,h))\right)^2 - \beta^2h^2$$

is strictly increasing which is equivalent to the monotonicity of $\Gamma_c(\beta,h)$. We compute the derivative for $h > 0$

$$\begin{aligned}g'(h) &= 2\operatorname{arcosh}\left(\frac{1}{2}\exp(\Phi^{\mathrm{REM}}(\beta,h))\right)\frac{\frac{1}{2}e^{\Phi^{\mathrm{REM}}(\beta,h)}}{\sqrt{\frac{1}{4}e^{2\Phi^{\mathrm{REM}}(\beta,h)}-1}}\frac{\partial\Phi^{\mathrm{REM}}(\beta,h)}{\partial h} - 2\beta^2h\\ &= 2\beta\left(\operatorname{arcosh}\left(\frac{1}{2}\exp(\Phi^{\mathrm{REM}}(\beta,h))\right)\frac{\tanh(\min\{\beta,\beta_c(h)\}h)}{\tanh(\operatorname{arcosh}(1/2\exp(\Phi^{\mathrm{REM}}(\beta,h))))} - \beta h\right)\end{aligned}$$

We first note that $y/\tanh(y)$ is an increasing function. In the case $\beta \le \beta_c(h)$ we further use that $1/2\exp(\Phi^{\mathrm{REM}}(\beta,h)) > \cosh(\beta h)$. Hence $g'(h) > 0$ is an easy consequence of these observations for $\beta \le \beta_c$. On the other hand, if $\beta > \beta_c$ we use the convexity of

$$\eta(y) := \frac{\operatorname{arcosh}(e^y)}{\tanh(\operatorname{arcosh}(e^y))},$$

from which we obtain

$$\frac{\operatorname{arcosh}(\frac{1}{2}\exp(\Phi^{\mathrm{REM}}(\beta,h))}{\tanh(\operatorname{arcosh}(1/2\exp(\Phi^{\mathrm{REM}}(\beta,h))))} > \frac{\beta h}{\tanh(\beta_c(h)h)}$$

as the left half side is a convex function of β and the inequality holds true for $\beta = \beta_c(h)$.

Finally, we want to show the asymptotic formula for $\Gamma_c(\beta, h)$. Since $\beta_c(h)$ tends to zero, we only need to consider the "frozen" expression for $\Phi^{\mathrm{REM}}(\beta, h)$. Neglecting terms of subleading order, we may write after some manipulations

$$\beta^{-2}\,\mathrm{arcosh}\left(\frac{1}{2}\exp(\Phi^{\mathrm{REM}}(\beta,h))\right)^2 - h^2 \simeq 2h^2(\tanh(\beta_c(h)h) - 1) + 2\beta_c h.$$

We recall that $1 - \tanh(\beta_c(h)h) \simeq 2e^{-2\beta_c(h)h} = \frac{4\beta_c h}{2\beta_c h e^{2\beta_c(h)h}} \simeq \frac{\beta_c}{2h}$, where the last equality follows from the proof of part 1. Combining these asymptotic formulas, we arrive at $\lim_{h\to\infty} \frac{\Gamma(\beta,h)}{\sqrt{h\beta_c(h)}} = 1$. □

Appendix B: Proof of Proposition 2 and Corollary 2

In this section, we sketch the computations which lead to the results in Proposition 2 and Corollary 2.

Proof of Proposition 2 1. Let us first recall that $\bar{a}(x)$ is a continuous decreasing function from which it follows that $x(\beta) = \sup\{x|\,\bar{a}(x) > (2\ln 2)/\beta^2\}$ is well defined for $\beta > \beta_c(0) = \sqrt{2\ln 2/\bar{a}(0)}$ and increasing in β. Since k is a decreasing function, we see that $\beta_c(h)$ defined in (25) is an increasing function.
To discuss the limiting value $h \to 0$, we observe that $\lim_{h\to 0} k(2\ln 2/(\beta_c(h)h)) = 0$. Since $\bar{a}$ is continuous, $\lim_{\beta\to\beta_c} x(\beta) = 0$ from which we conclude $\lim_{h\to 0}\beta_c(h) = \beta_c(0)$. Using Assumption 1 we see that

$$x(\beta) \propto (\beta - \beta_c)^{1/\alpha}.$$

A direct calculation shows $k(x) \propto x^{-2}$ for large x. We thus arrive at $\beta_c(h) - \beta_c(0) \propto h^{2\alpha}$, and $T_c - T_c(h) \propto h^{2\alpha}$.
For the limit $h \to \infty$, we first consider the case $\bar{a}(1) > 0$. Then, $x(\beta)$ approaches 1 as $\beta \to \beta_c(\infty) := \sqrt{2\ln 2/\bar{a}(1)}$ and

$$\lim_{h\to\infty} k(2\ln 2/(\beta_c(h)h)) = 0.$$

Consequently, $\lim_{h\to\infty}\beta_c(h) = \beta_c(\infty)$. Similarly, if $\bar{a}(1) = 0$, $x(\beta)$ approaches 1 as $\beta \to \infty$ and we have $\lim_{h\to\infty}\beta_c(h) = \infty$.

2.a The continuity of $y(\beta, h)$ follows from the fact that it is a solution of a continuous implicit equation. Moreover, as $\phi(\beta, y)$ is decreasing in y and k is a decreasing function,too, it follows from (24) that $y(\beta, h)$ is increasing in h. As in part 1., one easily sees that

$$\lim_{h\to 0} k(\varphi(\beta, y(\beta,h))/(\beta h)) = 0 \quad \text{and} \quad \lim_{h\to\infty} k(\varphi(\beta, y(\beta,h))/(\beta h)) = 1,$$

which in turn implies $\lim_{h\to 0} y(\beta, h) = 0$ and $\lim_{h\to\infty} y(\beta, h) = 1$.
For the Taylor expansion, we use the fact that

$$k(1/x) = \frac{\ln 2}{2}x^2 + \mathcal{O}(x^4).$$

Consequently, we have

$$y(\beta,h) = \frac{\ln 2}{2}\left(\frac{\beta h}{\varphi(\beta, y(\beta,h))}\right)^2 + \mathcal{O}(h^4) = \frac{\ln 2}{2}\left(\frac{\beta h}{\varphi(\beta,0)}\right)^2 + \mathcal{O}(h^4).$$

Recalling that

$$\varphi(\beta, 0) = \begin{cases} \frac{\beta^2}{\ln 2 \beta_c^2} + \ln 2 & \beta < \beta_c, \\ \frac{2 \ln 2 \beta}{\beta_c} & \beta \geq \beta_c, \end{cases}$$

we arrive at (27).

2.b Both assertions follow immediately from part 2a) and the fact that $\varphi(\beta, x)$ is continuous and decreasing in x. □

Finally, we present the proof of Corollary 2:

Proof of Corollary 2 The limit of the pressure is given by

$$\Phi(\beta, \mathfrak{b}, h) = \sup_{0 \leq y \leq z \leq 1} \left[\beta h \gamma(y) + \int_0^{z-y} \varphi^{(y,1)}(\beta, x)\, dx + (1 - z) p(\beta, \Gamma) \right].$$

It follows that if $y(\beta, h) < z(\beta, \Gamma)$, then $y(\beta, h)$ and $z(\beta, \Gamma)$ remain the maximizer for this more general problem. We see that this holds true if and only if $p(\beta\Gamma) < \varphi(\beta, y(\beta, h))$ and the pressure is then given by

$$\Phi(\beta, \Gamma, h) = \beta h \gamma\left(y(\beta, h)\right) + \int_{y(\beta,h)}^{z(\beta,\Gamma)} \varphi(\beta, x) dx + (1 - z(\beta, \Gamma))\, p(\beta\Gamma).$$

Otherwise we have $y(\beta, h) \geq z(\beta, \Gamma)$ and, consequently, the corresponding maximizer satisfy $y^\star = z^\star$, i.e.

$$\Phi(\beta, \Gamma, h) = \sup_{0 \leq y \leq 1} \left[\beta h \gamma(y) + (1 - y) p(\beta\Gamma) \right].$$

Differentiating with respect to y yields the maximizer

$$y^\star = \sigma(\beta, \Gamma, h) = k\left(\frac{p(\beta\Gamma)}{\beta h} \right)$$

since k was defined to be the inverse of γ'. This completes the proof. □

References

1. Adhikari, A., Brennecke, C.: Free energy of the quantum Sherrington–Kirkpatrick spin-glass model with transverse field. J. Math. Phys. **61**, 083302 (2020)
2. Adhikari, A., Brennecke, C., von Soosten, P., Yau, H.-T.: Dynamical approach to the TAP equations for the Sherrington–Kirkpatrick model. J. Stat. Phys. **183**, 35 (2021)
3. Aizenman, M., Sims, R., Starr, S.L.: Extended variational principle for the Sherrington–Kirkpatrick spin-glass model. Phys. Rev. B **68**, 214403 (2003)
4. Arguin, L.P., Kistler, N.: Microcanonical analysis of the random energy model in a random magnetic field. J. Stat. Phys. **157**, 1–16 (2014)
5. Arguin, L.P., Persechino, R.: The Free Energy of the GREM with random magnetic field. In: Gayrard, V., Arguin, L.P., Kistler, N., Kourkova, I. (eds.) Statistical Mechanics of Classical and Disordered Systems. StaMeClaDys 2018. Springer Proceedings in Mathematics & Statistics, vol. 293. pp. 37–61. Springer, Berlin (2019)
6. Bovier, A.: Statistical Mechanics of Disordered Systems. A Mathematical Perspective. Cambridge University Press, Cambridge (2012)
7. Bovier, A., Klimovsky, A.: Fluctuations of the partition function in the generalized random energy model with external field. J. Math. Phys. **49**, 125202, 27 (2008)
8. Bovier, A., Kurkova, I.: Derrida's generalised random energy models. I. Models with finitely many hierarchies. Ann. Inst. H. Poincaré Probab. Stat. **40**, 439–480 (2004)

9. Crawford, N.: Thermodynamics and universality for mean field quantum spin glasses. Commun. Math. Phys. **274**, 821–839 (2007)
10. de Almeida, J.R.L., Thouless, D.J.: Stability of the Sherrington–Kirkpatrick solution of a spin glass model. J. Phys. A Math. Gen. **11**, 983–990 (1978)
11. Dembo, A., Zeitouni, O.: Large Deviations Techniques and Applications. Springer, New York (2010)
12. Derrida, B.: A generalization of the random energy model that includes correlations between the energies. J. Phys. Lett. **46**, 401–407 (1985)
13. Derrida, B., Gardner, E.: Solution of the generalized random energy model. J. Phys. C **19**, 2253–2274 (1986)
14. Derrida, B., Gardner, E.: Magnetic properties and function q(x) of the generalised random energy model. J. Phys. C **19**, 5783–5798 (1986)
15. Goldschmidt, Y.Y.: Solvable model of the quantum spin glass in a transverse field. Phys. Rev. B **41**, 4858 (1990)
16. Guerra, F.: Broken replica symmetry bounds in the mean field spin glass model. Commun. Math. Phys. **23**, 1–12 (2003)
17. Huse, D.A., Miller, J.: Zero-temperature critical behavior of the infinite-range quantum Ising spin glass. Phys. Rev. Lett. **70**, 3147–3150 (1993)
18. Leschke, H., Rothlauf, S., Ruder, R., Spitzer, W.: The free energy of a quantum Sherrington–Kirkpatrick spin-glass model for weak disorder. J. Stat. Phys. **182**, 55 (2021)
19. Leschke, H., Manai, C., Ruder, R., Warzel, S.: Existence of replica-symmetry breaking in quantum glasses. Phys. Rev. Lett. **127**, 207204 (2021)
20. Manai, C., Warzel, S.: Phase diagram of the quantum random energy model. J. Stat Phys. **80**, 654–664 (2020)
21. Manai, C., Warzel, S.: The quantum random energy model as a limit of p-spin interactions. Rev. Math. Phys. **33**, 2060013 (2021)
22. Manai, C., Warzel, S.: Generalized random energy models in a transversal magnetic field: free energy and phase diagrams. Preprint. arXiv: 2007.03290 To appear in Probability and Mathematical Physics
23. Mezard, M., Parisi, G., Virasoro, M.: Spin Glass Theory and Beyond. World Scientific, Singapore (1986)
24. Obuchi, T., Nishimori, H., Sherrington, D.: Phase diagram of the p-spin-interacting spin glass with ferromagnetic bias and a transverse field in the infinite-p limit. J. Phys. Soc. Jpn. **76**, 054002 (2007)
25. Panchenko, D.: The Sherrington–Kirkpatrick model. Springer, New York (2013)
26. Robinson, D.W.: Statistical mechanics of quantum spin systems. Commun. Math. Phys. **6**, 151–160 (1967)
27. Ruelle, D.: A mathematical formulation of Derrida's REM and GREM. Commun. Math. Phys. **108**, 225–237 (1987)
28. Suzuki, S., Inoue, J., Chakrabarti, B.K.: Quantum Ising Phases and Transitions in Transverse Ising Models, 2nd edn. Springer, Berlin (2013)
29. Talagrand, M.: The Parisi formula. Ann. Math. **163**, 221–263 (2006)
30. Talagrand, M.: Mean Field Models for Spin Glasses, vols. I+II. Springer, Berlin (2011)
31. Toninelli, F.L.: About the Almeida-Thouless transition line in the Sherrington-Kirkpatrick mean-field spin glass model. Europhys. Lett. **60**, 764–767 (2002)
32. Usadel, K.D., Schmitz, B.: Quantum fluctuations in an Ising spin glass with transverse field. Solid State Commun. **64**, 975–977 (1987)
33. Yamamoto, T., Ishii, H.: A perturbation expansion for the Sherrington–Kirkpatrick model with a transverse field. J. Phys. C **20**, 6053–6061 (1987)
34. Young, A.P.: Stability of the quantum Sherrington–Kirkpatrick spin glass model. Phys. Rev. E **96**, 032112 (2017)

Appendix B

Further articles as principal author

B.1 Spectral Analysis of the Quantum Random Energy Model

Spectral Analysis of the Quantum Random Energy Model

Chokri Manai and Simone Warzel

While our Core Article I [128] proves Goldschmidt's formula for the pressure and discusses the phase diagram in the thermodynamic limit, the spectral properties of the QREM Hamiltonian for finite N are not considered in more detail. However, a precise picture of the eigenvalues and eigenfunctions are crucial for a better physical understanding. For instance, in the context of quantum annealing, finite size corrections and the spectral gap are of particular interest [110, 111]. It also worth mentioning that the predicted transition between an ergodic phase and many body localization requires a thorough description of the eigenfunctions for all energies [23]. Article IV provides a comprehensive study of the QREM's low energy characteristics.

Main Results

A main theme of this article is the dichotomy between localization in the glass phase and delocalization in the paramagnetic phase. Indeed, we show that in the glass phase all low energy states are concentrated on one single site, namely the classical configuration with low energy. The rapid decay of the eigenfunctions close to the extremum and the exponential decay at larger distances allows us to compute the $O(1)$ energy corrections and all l^p-norms of the ground state. Our proof consists of three main ingredients: estimates on the Green functions of T restricted to Hamming balls, probabilistic considerations on the geometry of the REM energy landscape and the fluctuations nearby a deep hole, and a solution to the rank-one perturbation of the operator T by one deep hole. In the paramagnetic phase, the low energy states are in contrast exponentially delocalized and resemble the eigenstates of the transversal field T. Also in this phase, we determine the energetic $O(1)$ corrections. Here, our method relies on the Feshbach-Schur-Krein decomposition and random matrix techniques. We then extend our ideas to study the spectrum far away from the ground state in order to compute the pressure in all phases up to order $o(1)$. In the glass phase we are also able to describe the fluctuations of the pressure.
I have included the arxiv version since the published version is less comprehensive.

Individual Contribution

I am the principal of the author of this article. This work originated from a draft by Simone Warzel, where she mainly considered the Green function and delocalization estimates, which were the basis for Section 3 and also partially Section 2. The starting point of our approach to the localization regime and the free energy were my personal notes with proof ideas. These ideas have eventually become part of Section 2, 4 and 5. We refined our first drafts to complete proofs in several discussions and we both contributed strongly to the presentation and structure of the final submission.

Permission to include:

Chokri Manai and Simone Warzel
Spectral Analysis of the Quantum Random Energy Model.
Commun. Math. Phys. (2023).
https://doi.org/10.1007/s00220-023-04743-4
Extended version: https://arxiv.org/abs/2202.00334.

How to obtain permission to reuse Springer Nature content not available online on SpringerLink

Requests for permission to reuse content (e.g. figure or table, abstract, text excerpts) from Springer Nature publications currently not available online must be submitted in writing. Please be as detailed and specific as possible about what, where, how much, and why you wish to reuse the content.

Your contacts to obtain permission for the reuse of material from:

- books: bookpermissions@springernature.com
- journals: journalpermissions@springernature.com

Author reuse

Please check the Copyright Transfer Statement (CTS) or Licence to Publish (LTP) that you have signed with Springer Nature to find further information about the reuse of your content.

Authors have the right to reuse their article's Version of Record, in whole or in part, in their own thesis. Additionally, they may reproduce and make available their thesis, including Springer Nature content, as required by their awarding academic institution. Authors must properly cite the published article in their thesis according to current citation standards.
Material from: 'AUTHOR, TITLE, JOURNAL TITLE, published [YEAR], [publisher - as it appears on our copyright page]'

If you are any doubt about whether your intended re-use is covered, please contact journalpermissions@springernature.com for confirmation.

Self-Archiving

- Journal authors retain the right to self-archive the final accepted version of their manuscript. Please see our self-archiving policy for full details: https://www.springer.com/gp/open-access/authors-rights/self-archiving-policy/2124

- Book authors please refer to the information on this link: https://www.springer.com/gp/open-access/publication-policies/self-archiving-policy

Spectral Analysis of the Quantum Random Energy Model

Chokri Manai and Simone Warzel

Abstract
The Quantum Random Energy Model (QREM) is a random matrix of Anderson-type which describes effects of a transversal magnetic field on Derrida's spin glass. The model exhibits a glass phase as well as a classical and a quantum paramagnetic phase. We analyze in detail the low-energy spectrum and establish a localization-delocalization transition for the corresponding eigenvectors of the QREM. Based on a combination of random matrix and operator techniques as well as insights in the random geometry, we derive next-to-leading order asymptotics for the ground-state energy and eigenvectors in all regimes of the parameter space. Based on this, we also deduce the next-to-leading order of the free energy, which turns out to be deterministic and on order one in the system size in all phases of the QREM. As a result, we determine the nature of the fluctuations of the free energy in the spin glass regime.

Contents

1. Introduction and main results

1.1. Quantum random energy model

In the theory of disordered systems the random energy model (REM) is a simple, yet ubiquitous toy model. It assigns to every N-bit or Ising string $\boldsymbol{\sigma} = (\sigma_1, \ldots, \sigma_N) \in \{-1, 1\}^N =: \mathcal{Q}_N$ a rescaled Gaussian random variable

$$U(\boldsymbol{\sigma}) := \sqrt{N}\, \omega(\boldsymbol{\sigma})$$

with $(\omega(\boldsymbol{\sigma}))$ forming 2^N canonically realized independent and identically distributed (i.i.d.) random variables with standard normal law $\mathbb{P}$. The Hamming cube $\mathcal{Q}_N$ is rendered a graph by declaring two bit strings connected by an edge if they differ by a single bit flip: introducing the flip operators $F_j\boldsymbol{\sigma} := (\sigma_1, \ldots, -\sigma_j, \ldots, \sigma_N)$ on components $j \in \{1, \ldots, N\}$, the edges of the Hamming cube are formed by all pairs of the form $(\boldsymbol{\sigma}, F_j\boldsymbol{\sigma})$. The graph's negative adjacency matrix

$$(T\psi)(\boldsymbol{\sigma}) := -\sum_{j=1}^{N} \psi(F_j\boldsymbol{\sigma})$$

is defined on $\psi \in \ell^2(\mathcal{Q}_N)$, the 2^N-dimensional Hilbert space of complex-valued functions on N-bit strings. Since every vertex in $\mathcal{Q}_N$ has a constant degree N, the negative graph Laplacian, $T + N\mathbb{1}$, just differs by N times the identity matrix. We study the quantum random energy model (QREM) which is the random matrix

$$H := \Gamma\, T + U, \tag{1.1}$$

where $\Gamma \geq 0$ is a parameter, and U is diagonal in the canonical configuration basis $(\delta_{\boldsymbol{\sigma}})$ of $\ell^2(\mathcal{Q}_N)$, i.e., $U\delta_{\boldsymbol{\sigma}} = U(\boldsymbol{\sigma})\delta_{\boldsymbol{\sigma}}$ and $\psi(\boldsymbol{\sigma}) = \langle \delta_{\boldsymbol{\sigma}} | \psi \rangle$. As usual in mathematical physics, we choose the scalar product $\langle \cdot | \cdot \rangle$ on $\ell^2(\mathcal{Q}_N)$ to be linear in its second component.

The QREM is a random matrix of Anderson type – albeit on a quite unconventional graph whose connectivity grows to infinity with the system size N, and with a scaling of the random potential U which enforces the operator norm of both, T and U, to be of the same order N (cf. (1.4) and (1.9)). It is thus natural to investigate the localization properties of its eigenfunctions. The interest in the QREM is however many-faceted. In mathematical biology, the model has received attention under the name REM House-of-Cards model [62] as an element of a simplistic probabilistic model of population genetics, in which $\mathcal{Q}_N$ is the space of gene types and U encodes their fitness [7, 8, 39, 41]. In this interpretation, the operator T implements mutations of the gene type, and one is interested in the long-time limit of the semigroup generated by H (cf. [6], in which the parameter regime $\Gamma = \kappa/N$ with fixed $\kappa > 0$ corresponding to the normalized Laplacian is considered).

The Anderson-perspective has also attracted attention in discussions of many-body or Fock-space localization, where the QREM occasionally serves as an analytically more approachable toy to test ideas about more realistic disordered spin systems [9, 14, 48, 63]. We will comment on some of the conjectures in the physics literature concerning the localization properties of the eigenfunctions after presenting our results on this topic.

In statistical mechanics, the QREM was introduced [38] as a simplified model to investigate the quantum effects caused by a transversal magnetic field on classical mean-field spin-glass models [21, 32, 60, 67, 73]. In this context, the Hilbert space $\ell^2(\mathcal{Q}_N)$ is unitarily identified with the tensor-product Hilbert space $\otimes_{j=1}^N \mathbb{C}^2$ of N spin-$\frac{1}{2}$ quantum objects. A corresponding unitary maps the canonical basis $(\delta_{\boldsymbol{\sigma}})$ to the tensor-product basis in which the Pauli-z-matrix is diagonal on each tensor component. For completeness, we recall the form of the Pauli matrices in this basis:

$$\sigma^x = \begin{pmatrix} 0 & 1 \\ 1 & 0 \end{pmatrix}, \quad \sigma^y = \begin{pmatrix} 0 & -i \\ i & 0 \end{pmatrix}, \quad \sigma^z = \begin{pmatrix} 1 & 0 \\ 0 & -1 \end{pmatrix}.$$

The Pauli matrices are naturally lifted to $\otimes_{j=1}^N \mathbb{C}^2$ by their action on the jth tensor component, $\sigma_j^x := \mathbb{1} \otimes \cdots \otimes \sigma^x \otimes \cdots \otimes \mathbb{1}$. Upon the above unitary equivalence, T corresponds to $-\sum_{j=1}^N \sigma_j^x$, i.e., a constant field in the negative x-direction exerted on all N spin-$\frac{1}{2}$ (cf. [53]). In this interpretation, the random potential U is the energy operator of the spin-$\frac{1}{2}$-objects, which interact disorderly only through their z-components. Derrida [27, 28] originally invented the classical REM U as a simplification to other mean-field spin glasses such as the Sherrington-Kirkpatrick model.

The phenomenon common to such classical spin glass models is a glass freezing transition into a low temperature phase which, due to lack of translation invariance, is described by an order parameter (due to Parisi) more complicated than a global magnetization [55, 58, 59, 69]. In the absence of external fields the latter typically vanishes. These thermodynamic properties are encoded in the (normalized) partition function

$$Z(\beta, \Gamma) := 2^{-N} \operatorname{Tr} e^{-\beta H}$$

at inverse temperature $\beta \in [0, \infty)$, or, equivalently, its pressure

$$\Phi_N(\beta, \Gamma) := \ln Z(\beta, \Gamma). \tag{1.2}$$

Up to a factor of $-\beta^{-1}$, the latter coincides with the free energy. In the thermodynamic limit $N \to \infty$, the specific pressure of the REM converges almost surely [17, 27, 28, 56],

$$N^{-1}\Phi_N(\beta, 0) \to p^{\mathrm{REM}}(\beta) = \begin{cases} \frac{1}{2}\beta^2 & \text{if } \beta \leq \beta_c, \\ \frac{1}{2}\beta_c^2 + (\beta - \beta_c)\beta_c & \text{if } \beta > \beta_c. \end{cases} \tag{1.3}$$

It exhibits a freezing transition into a low-temperature phase characterized by the vanishing of the specific entropy above

$$\beta_c := \sqrt{2 \ln 2}.$$

In the presence of the transversal field, the spin-glass phase of the REM disappears for large $\Gamma > 0$ and a first-order phase transition into a quantum paramagnetic phase described by

$$p^{\mathrm{PAR}}(\beta\Gamma) := \ln \cosh(\beta\Gamma)$$

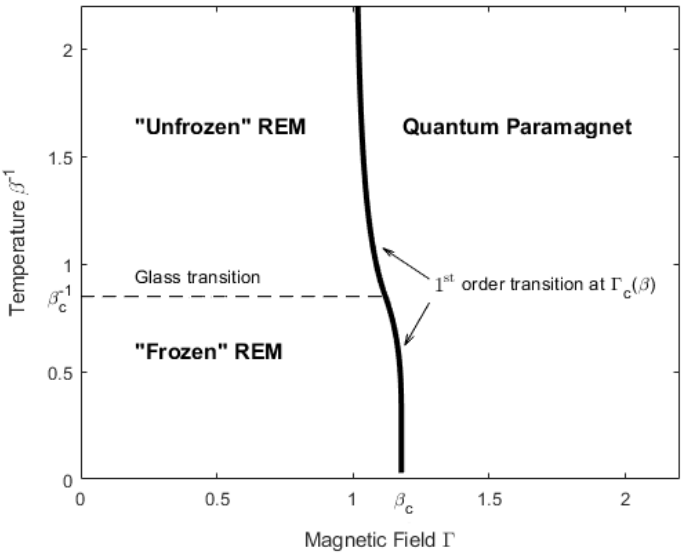

Figure 1: Phase diagram of the QREM as a function of the transversal magnetic field Γ and the temperature β^{-1} [38, 51]. The first-order transition occurs at fixed β and $\Gamma_c(\beta)$. The freezing transition is found at temperature β_c^{-1}, which is unchanged in the presence of a small magnetic field.

occurs at the critical magnetic field strength

$$\Gamma_c(\beta) := \beta^{-1} \operatorname{arcosh}\left(\exp\left(p^{\mathrm{REM}}(\beta)\right)\right).$$

In particular, $\Gamma_c(0) = 1$ and $\Gamma_c(\beta_c) = \beta_c^{-1} \operatorname{arcosh}(2)$. The precise location of this first-order transition and the shape of the phase diagram of the QREM, which we sketch in Figure 1, had been predicted by Goldschmidt [38] in the 1990s and was rigorously established in [51].

Proposition 1.1 ([51])**.** *For any $\Gamma, \beta \geq 0$ we have the almost sure convergence as $N \to \infty$:*

$$N^{-1}\Phi_N(\beta, \Gamma) \to \max\{p^{\mathrm{REM}}(\beta), p^{\mathrm{PAR}}(\beta\Gamma)\}.$$

1.2. Low energy states

Through the low-temperature limit $\beta \to \infty$, Proposition 1.1 contains also information on the ground state energy of the QREM,

$$N^{-1} \inf \operatorname{spec} H \to \begin{cases} -\beta_c & \text{if } \Gamma < \beta_c, \\ -\Gamma & \text{if } \Gamma > \beta_c. \end{cases}$$

The critical coupling for this quantum phase transition is at the endpoint $\lim_{\beta\to\infty} \Gamma_c(\beta) = \beta_c$ of the first order phase transition. As will be demonstrated below, this ground-state phase transition at $\Gamma = \beta_c$ is manifested by a change of the nature of the corresponding eigenvector from sharply localized to (almost) uniformly delocalized. To provide some heuristics, it is useful to compare the ground-state energy and eigenvectors of the two operators entering $H = \Gamma T + U$:

1. The spectrum of T consists of $N+1$ eigenvalues,

$$\operatorname{spec} T = \{2n - N \,|\, n \in \mathbb{N}_0,\ n \leq N\}, \tag{1.4}$$

with degeneracy given by the binomials $\binom{N}{n}$. The corresponding ℓ^2-normalized eigenvectors are the natural orthonormal basis for the Hadamard transformation, which diagonalizes T. They are indexed by subsets $A \subset \{1, \ldots, N\}$:

$$\Phi_A(\boldsymbol{\sigma}) := \frac{1}{\sqrt{2^N}} \prod_{j \in A} \sigma_j. \tag{1.5}$$

The eigenvalue to Φ_A is $2|A| - N$ with $|A|$ the cardinality of the set. In particular, the unique ground-state of ΓT is $\Phi_\emptyset$ with energy $-N\Gamma$. All eigenvectors Φ_A are maximally uniformly delocalized over the Hamming cube.

2. In contrast, all eigenvectors $\delta_{\boldsymbol{\sigma}}$ of U are maximally localized. The REM's minimum energy, $\min U$, is roughly at $-N\beta_c$. For $\eta > 0$ the event that $\|U\|_\infty := \max_{\boldsymbol{\sigma} \in \mathcal{Q}_N} |U(\boldsymbol{\sigma})| > (\beta_c + \eta)N$ has exponentially small probability, i.e,

$$\begin{aligned} \Omega^{\mathrm{REM}}_{N,\eta} &:= \{\|U\|_\infty \leq (\beta_c + \eta)N\}, \\ \mathbb{P}(\Omega^{\mathrm{REM}}_{N,\eta}) &\geq 1 - 2^{N+1} e^{-\frac{1}{2}(\eta+\beta_c)^2 N} = 1 - 2\, e^{-N(\eta\beta_c + \frac{\eta^2}{2})}, \end{aligned} \tag{1.6}$$

where the inequality follows from the union bound and a Markov-Chernoff estimate. A more precise description of the extremal value statistics of $\min U$ is [17, 44]

$$\mathbb{P}\left(\min U \geq s_N(x)\right) = \left(1 - 2^{-N} e^{-x + o(1)}\right)^{2^N} \tag{1.7}$$

for any x in terms of the function s_N given by

$$s_N(x) := -\beta_c N + \frac{\ln(N \ln 2) + \ln(4\pi)}{2\beta_c} - \frac{x}{\beta_c}. \tag{1.8}$$

By symmetry of the distribution, a similar expression applies to the maximum.

These limiting cases suggest the following heuristic, perturbative description of the ground-state of $H = \Gamma T + U$ in the regimes of small and large Γ. To our knowledge, it goes back to [46]:

1. For small Γ, second-order perturbation theory starting from the vector $\delta_{\boldsymbol{\sigma}_{\min}}$, which is localized at $\boldsymbol{\sigma}_{\min} := \arg\min U$, reads:

$$\inf \operatorname{spec} H \approx \min U + \Gamma\, \langle \delta_{\boldsymbol{\sigma}_{\min}} | T \delta_{\boldsymbol{\sigma}_{\min}} \rangle + \Gamma^2 \sum_{\boldsymbol{\sigma} \neq \boldsymbol{\sigma}_{\min}} \frac{|\langle \delta_{\boldsymbol{\sigma}} |\, T \delta_{\boldsymbol{\sigma}_{\min}} \rangle|^2}{U(\boldsymbol{\sigma}_{\min}) - U(\boldsymbol{\sigma})} \approx -N\beta_c - \frac{\Gamma^2}{\beta_c}. \tag{1.9}$$

The first-order term vanishes. The sum in the second-order term is restricted to the neighbors of the minimum, whose potential term typically is only of the order $\sqrt{N}$.

2. For large Γ, second-order perturbation theory starting from the ground state $\Phi_\emptyset$ of T reads:

$$\begin{aligned}\inf\operatorname{spec} H &\approx -N\Gamma + \langle\Phi_\emptyset|U\Phi_\emptyset\rangle - \sum_{A\neq\emptyset}\frac{|\langle\Phi_\emptyset|\ U\Phi_A\rangle|^2}{2|A|\ \Gamma}\\ &\approx -N\Gamma - \frac{\langle\Phi_\emptyset|\ U^2\Phi_\emptyset\rangle}{N\ \Gamma} \approx -N\Gamma - \frac{1}{\Gamma}. \end{aligned} \tag{1.10}$$

The next-to-leading term, $\langle\Phi_\emptyset|U\Phi_\emptyset\rangle = 2^{-N}\sum_{\boldsymbol{\sigma}\in\mathcal{Q}_N} U(\boldsymbol{\sigma})$, vanishes by the law of large numbers. In the order Γ^{-1}-term, one uses the approximation that most of the states of T are found near $|A| \approx N/2$. As will be explained in more detail in Section 3, one crucial point is that U is exponentially small when restricted to the eigenspace of T outside an interval around $|A| \approx N/2$. By a decomposition of unity one is therefore left with $\langle\Phi_\emptyset|\ U^2\Phi_\emptyset\rangle \approx N$, again by the law of large numbers.

Unlike in a finite-dimensional situation, higher orders in this naive perturbation theory turn out to be of lower order with N^{-1} the relevant parameter. One result of this paper is that these predictions can be confirmed: for $\Gamma < \beta_c$ the ground state is sharply localized near a lowest-energy configuration of the REM. In contrast, for $\Gamma > \beta_c$ the ground state resembles the maximally delocalized state given by the ground state of T. In both cases, the ground state is energetically separated and the ground-state gap only closes exponentially near $\Gamma = \beta_c$, see also [1]. In fact, we do not only restrict attention to the ground state but characterize a macroscopic window of the entire low-energy spectrum in the different parameter regimes.

Before delving into the details, let us emphasize that the localization-delocalization transition at extreme energies presented here relies on the delocalization properties of T on $\mathcal{Q}_N$, which fundamentally differ from the finite-dimensional situation. The eigenfunctions of T can only form localized states from linear combinations in the center of its spectrum. This is given a precise mathematical formulation in the form of novel estimates on the spectral shift and Green function of Dirichlet restrictions of T to Hamming balls in Section 2, and random matrix estimates on projections of multiplication operators in Section 3. A separation of the localized versus delocalized parts of the spectrum beyond the extremal energies, on which the subsequent results concerning the finite-size corrections of the free energy rest, is facilitated by a novel detailed description of the geometry of extremal fluctuations the REM in Section 5.

Aside from Theorem 1.10, our results pertain to fixed, but arbitrarily large N on the product probability space Ω_N corresponding to 2^N i.i.d. standard normal random variables whose product measure we denote by $\mathbb{P}$. We suppress its dependence on N. In this setting, the results apply to all realizations ω, aside from exceptional events whose probability will be estimated and goes (exponentially) to zero as $N \to \infty$. This strong concentration enables the use of Borel-Cantelli arguments in Theorem 1.10, which then apply to the product space $\prod_{N=1}^{\infty}\Omega_N$ (which is also the set-up in Proposition 1.1). To present our results and estimates in a precise, yet reader-friendly, manner, we will make use of an "indexed" version of Landau's O-notation.

Definition 1.2. *Let $\Theta = (\theta_1, \dots, \theta_k)$ be a tuple of parameters, $(a_N)_{N\in\mathbb{N}}$ a real and $(b_N)_{N\in\mathbb{N}}$ a positive sequence. We then write*

$$a_N = \mathcal{O}_\Theta(b_N) \quad \textit{if} \quad \limsup_{N\to\infty}\frac{|a_N|}{b_N} \leq C(\Theta), \tag{1.11}$$

for some positive constant $C(\Theta)$, which may depend on Θ. Analogously, we write

$$a_N = o_\Theta(b_N) \quad \text{if} \quad |a_N| \leq c_N(\Theta)|b_N|, \tag{1.12}$$

where $c_N(\Theta)$ denotes a sequence which tends to zero.

In particular, the appearing constant $C(\Theta)$ or, respectively sequence $c_N(\Theta)$, does not depend on any other parameters in question not included in Θ. That is, if a_N is a random sequence and the realization ω of the randomness is not included in the list Θ of parameters, the estimates are understood to hold uniformly on the event of interest.

1.2.1. Paramagnetic regime $\Gamma > \beta_c$

Our first main result shows that in the paramagnetic regime the addition of the REM shifts the eigenvalues (1.4) of T at energies below the minimum of U deterministically.

Theorem 1.3. *For $\Gamma > \beta_c$ and any $\tau \in (0,1)$ there are events $\Omega^{\mathrm{par}}_{N,\tau}$ with probability*

$$\mathbb{P}(\Omega^{\mathrm{par}}_{N,\tau}) \geq 1 - e^{-N/C}$$

and $C \in (0,\infty)$ a universal constant such that for all sufficiently large N and any $\eta > 0$ on $\Omega^{\mathrm{par}}_{N,\tau} \cap \Omega^{\mathrm{REM}}_{N,\eta}$ (cf. (1.6)) all eigenvalues of $H = \Gamma T + U$ below $-(\beta_c + 2\eta)N$ are found in the union of intervals of radius $\mathcal{O}_{\Gamma,\eta}(N^{\frac{\tau-1}{2}})$ centered at

$$(2n - N)\Gamma + \frac{N}{(2n-N)\Gamma} \tag{1.13}$$

with $n \in \{m \in \mathbb{N}_0 \,|(2m - N)\Gamma < -(\beta_c + 2\eta)N\}$. Moreover, the interval centered at (1.13) contains exactly $\binom{N}{n}$ eigenvalues of H .

For the ground-state in the regime $\Gamma > \beta_c$, Theorem 1.3 implies that with overwhelming probability

$$\inf \operatorname{spec} H = -\Gamma N - \frac{1}{\Gamma} + o_\Gamma(1). \tag{1.14}$$

The energy shift with respect to the ground state of ΓT is as predicted by naive second-order perturbation theory (1.10). Second-order perturbation theory for the eigenvalues corresponds to first-order perturbation theory for the eigenvectors: the eigenvectors are well approximated by their first order corrections. In particular, the ground state in the paramagnetic phase is close to the fully paramagnetic state $\Phi_\emptyset$. This is made more precise in our next main result, whose proof alongside that of Theorem 1.3 can be found in Section 3.

Theorem 1.4. *In the situation of Theorem 1.3 on the event $\Omega^{\mathrm{par}}_{N,\tau} \cap \Omega^{\mathrm{REM}}_{N,\eta}$ with $0 < \eta < (\Gamma - \beta_c)/4$ the ℓ^2-normalized ground state ψ of $H = \Gamma T + U$ satisfies:*

1. *The ℓ^2-distance of ψ and $\Phi_\emptyset$ is $\|\psi - \Phi_\emptyset\| = \mathcal{O}_\Gamma(N^{\frac{\tau-1}{2}})$.*
2. *The ground state ψ is exponentially delocalized in the maximum norm, i.e.*

$$\|\psi\|^2_\infty \leq 2^{-N} e^{N\gamma((\beta_c+\eta)/(2\Gamma)) + o_\Gamma(N)}, \tag{1.15}$$

where $\gamma\colon [0,1] \to \mathbb{R}$ denotes the binary entropy

$$\gamma(x) \coloneqq -x \ln x - (1-x)\ln(1-x). \tag{1.16}$$

The true ℓ^2-distance of the ground-state function to the fully delocalized state $\Phi_\emptyset$ is presumably of order $N^{-\frac{1}{2}}$ up to a logarithmic correction in N. The norm estimate (1.15) is not expected to be sharp: we conjecture a delocalization bound of the form $\|\psi\|_\infty^2 \leq 2^{-N+o(N)}$. Section 3, in which the proofs of Theorems 1.3 and 1.4 can be found, also contains (non-optimal) ℓ^∞-delocalization estimates for all eigenvalues strictly below the threshold $-\beta_c N$ in the paramagnetic regime. The optimal decay rates for excited states are not known. In Section 3.4 we record a method, which improves the estimate (1.15) if $\Gamma - \beta_c$ is small. A similar, but more elaborate, argument might result in better estimates for all field strengths $\Gamma > \beta_c$.

1.2.2. Spin glass regime $\Gamma < \beta_c$

In the spin glass phase the low-energy configurations of the REM, which occur on the extremal sites

$$\mathcal{L}_\varepsilon \coloneqq \{\boldsymbol{\sigma} |\, U(\boldsymbol{\sigma}) \leq -\varepsilon N\} \quad \text{with } \varepsilon \in (0, \beta_c), \tag{1.17}$$

are also shifted by a deterministic, order-one correction by the transverse field as predicted by second-order perturbation theory. To characterize localization properties of the corresponding eigenvectors in the canonical z-basis, i.e., the configuration basis $(\delta_{\boldsymbol{\sigma}})$ of $\ell^2(\mathcal{Q}_N)$, we let

$$B_R(\boldsymbol{\sigma}) \coloneqq \{\boldsymbol{\sigma}' |\, d(\boldsymbol{\sigma}, \boldsymbol{\sigma}') \leq R\}, \qquad S_R(\boldsymbol{\sigma}) \coloneqq \{\boldsymbol{\sigma}' |\, d(\boldsymbol{\sigma}, \boldsymbol{\sigma}') = R\}$$

stand for the Hamming ball and sphere of radius R, which are defined in terms of the Hamming distance

$$d(\boldsymbol{\sigma}, \boldsymbol{\sigma}') \coloneqq \frac{1}{2} \sum_{i=1}^N |\sigma_i - \sigma_i'|$$

of two configurations $\boldsymbol{\sigma}, \boldsymbol{\sigma}' \in \mathcal{Q}_N$.

Theorem 1.5. *For $\Gamma < \beta_c$ and $\delta > 0$ small enough there are events $\Omega^{\mathrm{loc}}_{N,\Gamma,\delta}$ with probability*

$$\mathbb{P}(\Omega^{\mathrm{loc}}_{N,\Gamma,\delta}) \geq 1 - e^{-cN}$$

for some $c = c(\Gamma, \delta)$ such that the following applies for sufficiently large N on $\Omega^{\mathrm{loc}}_{N,\Gamma,\delta}$:

1. *The eigenvalues E of $H = \Gamma T + U$ below $-(\beta_c - \delta)N$ and low-energy configurations $U(\boldsymbol{\sigma})$ are in a one-to-one correspondence such that*

$$E = U(\boldsymbol{\sigma}) + \frac{\Gamma^2 N}{U(\boldsymbol{\sigma})} + \mathcal{O}_{\Gamma,\delta}(N^{-1/4}). \tag{1.18}$$

   In particular, the estimate $\mathcal{O}_{\Gamma,\delta}(N^{-1/4})$ is independent of $\boldsymbol{\sigma} \in \mathcal{L}_{\beta_c - \delta}$.

2. *The ℓ^2-normalized eigenvector ψ corresponding to E and $\boldsymbol{\sigma}$ concentrates near this configuration in the sense that:*

   a) Close to extremum: *For any $K \in \mathbb{N}$ and for all $\boldsymbol{\sigma}' \in S_K(\boldsymbol{\sigma})$:*

$$|\psi(\boldsymbol{\sigma}')| = \mathcal{O}_{\Gamma,\delta,K}(N^{-K}), \quad \text{and} \quad \sum_{\boldsymbol{\sigma}' \notin B_K(\boldsymbol{\sigma})} |\psi(\boldsymbol{\sigma})|^2 = \mathcal{O}_{\Gamma,\delta,K}(N^{-(K+1)}).$$

b) Far from extremum: *For any* $0 < \alpha < 1$, *there is* $c_\alpha \in (0, \infty)$ *such that*

$$\sum_{\boldsymbol{\sigma}' \notin B_{\alpha N}(\boldsymbol{\sigma})} |\psi(\boldsymbol{\sigma}')|^2 \leq e^{-c_\alpha N}. \tag{1.19}$$

This theorem covers states in the extreme localization regime in which the eigenvectors are sharply localized – each in its own extremal site of the potential. In this regime, the estimates on the decay rate of the eigenvectors close to the extremum are optimal and far from the extremum they are optimal up to determining the decay rate c_α. Concrete, non-optimized values of the energy threshold $-N(\beta_c - \delta)$ as well as more precise values of the error terms can be found in the proof of Theorem 1.5 in Section 4. In essence, the localization analysis in Section 4 proves that resonances and tunneling among different large deviation sites does not play a role in this energy regime. An upper bound for our technique to fail is at $\delta = \beta_c/2$. The energy threshold at which eigenvectors are believed [9, 14] to occupy a positive fraction of $\mathcal{Q}_N$ is strictly larger than $-N\beta_c/2$ and for small fields yet smaller than $-N\Gamma$.

The precise low energy statistics of the REM U beyond the location of the minimum (1.7) is well known. Utilizing the rescaling (1.8) around its minimal value, the point process

$$\sum_{\boldsymbol{\sigma} \in \mathcal{Q}_N} \delta_{s_N^{-1}(U(\boldsymbol{\sigma}))} \to \mathrm{PPP}(e^{-x}\, dx) \tag{1.20}$$

converges weakly to the Poisson point process with intensity measure $e^{-x}\, dx$ on $\mathbb{R}$ (i.e, when integrating the random measure against a continuous compactly supported function, the resulting random variables converge weakly, see e.g. [17, Thm 9.2.2] or [44]). Theorem 1.5 implies a similar result for the low energy statistics in the QREM.

Corollary 1.6. *Let* $\Gamma < \beta_c$ *and let*

$$s_N(x; \Gamma) := -\beta_c N + \frac{\ln(N \ln 2) + \ln(4\pi)}{2\beta_c} - \frac{\Gamma^2}{\beta_c} - \frac{x}{\beta_c}. \tag{1.21}$$

Then the rescaled eigenvalue process $\operatorname{spec} H$ *of the QREM* $H = \Gamma T + U$ *converges weakly*

$$\sum_{E \in \operatorname{spec} H} \delta_{s_N^{-1}(E;\Gamma)} \to \mathrm{PPP}(e^{-x}\, dx). \tag{1.22}$$

In particular, the ground state energy converges weakly

$$\inf \operatorname{spec} H - \left(-\beta_c N + \frac{\ln(N \ln 2) + \ln(4\pi)}{2\beta_c} - \frac{\Gamma^2}{\beta_c} \right) \to -\frac{X}{\beta_c}, \tag{1.23}$$

where X *is a random variable distributed according to the law of the maximum of a Poisson point process* $\mathrm{PPP}(e^{-x}\, dx)$ *with intensity* $e^{-x}\, dx$ *on the real line.*

Proof. Corollary 1.6 is a straightforward consequence of Theorem 1.5 combined with (1.20). □

Theorem 1.5 in particular covers the ground-state of the QREM and thus extends the result [6, Lemma 2.1] on the leading asymptotics of the ground-state energy in the parameter regime $\Gamma = \kappa/N$ with $\kappa > 0$. The proof already contains more information on the ℓ^2-properties of the ground-state eigenvector, which we record next. More can be said in on its ℓ^1-localization properties. The latter is of interest in the context of the interpretation of the QREM in population genetics [7, 8, 39].

Theorem 1.7. *For $\Gamma < \beta_c$ there are events $\hat{\Omega}^{\mathrm{loc}}_{N,\Gamma}$ with probability*

$$\mathbb{P}(\hat{\Omega}^{\mathrm{loc}}_{N,\Gamma}) \geq 1 - e^{-cN}$$

for some $c = c(\Gamma)$ such that on $\hat{\Omega}^{\mathrm{loc}}_{N,\Gamma}$ for all N large enough there is $\delta > 0$ and $\boldsymbol{\sigma}_0 \in \mathcal{L}_{\beta_c - \delta}$ such that the positive ℓ^2-normalized ground state ψ of the QREM Hamiltonian is concentrated near $\boldsymbol{\sigma}_0$ in the sense that:

1. *the ℓ^2-distance of ψ and $\delta_{\boldsymbol{\sigma}_0}$ is $\|\psi - \delta_{\boldsymbol{\sigma}_0}\|^2 = \mathcal{O}_\Gamma\left(\frac{1}{N}\right)$, and its first order correction*

$$\xi \coloneqq \sqrt{1 - \frac{\Gamma^2}{\beta_c^2 N}}\delta_{\boldsymbol{\sigma}_0} + \frac{\Gamma}{\beta_c N}\sum_{\boldsymbol{\sigma} \in S_1} \delta_{\boldsymbol{\sigma}} \tag{1.24}$$

   has the same energy as ψ up to order one, and $\|\psi - \xi\|^2 = \mathcal{O}_\Gamma\left(\frac{1}{N^2}\right)$.

2. *the ℓ^1-norm of ψ converges to a bounded constant:*

$$\|\psi\|_1 = \sum_{\boldsymbol{\sigma}} \psi(\boldsymbol{\sigma}) = \frac{\beta_c}{\beta_c - \Gamma} + o_\Gamma(1), \tag{1.25}$$

   and, for any $1 < p < \infty$: $\quad \|\psi\|_p^p = \sum_{\boldsymbol{\sigma}} |\psi(\boldsymbol{\sigma})|^p = 1 + o_{\Gamma,p}(1).$

It is natural to assume that the configuration $\boldsymbol{\sigma}_0$ on which the ground-state is asymptotically localized and the classical minimal configuration $\boldsymbol{\sigma}_{\min} \coloneqq \arg\min U$ agree. While this is true with high probability, it does not hold almost surely. In the situation of Theorem 1.7 one may show that there are two constants $C \geq c > 0$ such that for N large enough:

$$\frac{c}{N} \leq \mathbb{P}(\boldsymbol{\sigma}_0 \neq \boldsymbol{\sigma}_{\min}) \leq \frac{C}{N}. \tag{1.26}$$

The reason for this is found in the following description of low-energy eigenvalues,

$$E_{\boldsymbol{\sigma}} = U(\boldsymbol{\sigma}) - \frac{\Gamma^2}{\beta_c} + \frac{\Gamma^2}{\beta_c^2 N} Z_{\boldsymbol{\sigma}} + \mathcal{O}_\Gamma(N^{-5/4}), \quad Z_{\boldsymbol{\sigma}} \coloneqq \frac{1}{N}\sum_{\sigma' \in S_1(\boldsymbol{\sigma})} U(\boldsymbol{\sigma}'),$$

which is proved in Lemma 4.3 below and which takes into account the next leading term in comparison to (1.18). The random variables $Z_{\boldsymbol{\sigma}}$ are standard normal distributed and independent of the large deviations $U(\boldsymbol{\sigma})$ with $\boldsymbol{\sigma} \in \mathcal{L}_{\beta_c - \delta}$ and $\delta > 0$ small enough. Since the extremal energies form a Poisson process with mean density of order one, the normal fluctuations in the energy-correction of order $\mathcal{O}(1/N)$ are able to cause the event (1.26). More generally, the method presented in this paper allows for a systematic control of subleading corrections in an expansion of the energy eigenvalues. As we will see, they are determined by potential fluctuations on increasing spheres around the extremal sites.

1.2.3. Critical case $\Gamma = \beta_c$

We complete the picture on the ground state by describing the situation in the critical case $\Gamma = \beta_c$, where the quantum phase transition occurs. Adapting techniques, one may also prove that typically one observes a paramagnetic behavior at criticality.

Proposition 1.8. *Let $\Gamma = \beta_c$. On an event of probability $1 - \mathcal{O}(N^{-1/2})$ the ground state is at $\inf \operatorname{spec} H = -\Gamma N - \Gamma^{-1} + \mathcal{O}(N^{-1/4})$ and the eigenvector ψ is paramagnetic in the sense that $\|\psi - \Phi_\emptyset\| = \mathcal{O}(N^{-1/4})$. On an event of probability $\mathcal{O}(N^{-1/2})$ the ground state is at $\inf \operatorname{spec} H = \min U - \Gamma + \mathcal{O}(N^{-1/4})$, and the eigenvector ψ is localized in the sense that $\|\psi - \delta_{\boldsymbol{\sigma}_0}\| = \mathcal{O}(N^{-1/4})$.*

The heuristics explanation for this is the following. For $\Gamma = \beta_c$ the ground state energy of ΓT is given by $-\beta_c N$, whereas the classical minimal energy is given by $\min U = -\beta_c N + C \ln(N) + \mathcal{O}(1)$ with $C > 0$. The logarithmic correction in this expression ensures that the paramagnetic behavior is dominant. This argument also suggests that the phase transition should be observed at the N-dependent field strength Γ_N, where the energy predictions of Theorem 1.3 and Theorem 1.5 agree,

$$-\Gamma_N N - \frac{1}{\Gamma_N} = \min U + \frac{\Gamma_N^2 N}{\min U}$$

which leads to

$$\Gamma_N = -\frac{\min U}{N} + \frac{1}{N}\left(\frac{N}{\min U} - \frac{\min U}{N}\right) + o(N^{-1}). \tag{1.27}$$

Indeed, in an $o(N^{-1})$ neighborhood of Γ_N one can observe a sign of critical behavior, the exponential vanishing gap of the Hamiltonian.

Proposition 1.9. *Let $\Delta_N(\Gamma) > 0$ denote the energy gap of the QREM Hamiltonian. Then, for some $c > 0$ and N large enough*

$$\min_{\Gamma \geq 0} \Delta_N(\Gamma) \leq e^{-cN} \tag{1.28}$$

except for a exponentially small event. The minimum is attained at some $\Gamma_N^\star$ satisfying (1.27).

The proof of both Proposition 1.8 and 1.9 are found in the appendix. It relies on a spectral analysis of H and is completely different from the derivation in [1].

1.3. Free energy and partition function

The spectral techniques presented here also allow to pin down the pressure Φ_N and its fluctuations up to order one in N in all three phases of the QREM: the spin-glass phase as well as the classical ('unfrozen REM') and quantum paramagnetic phase, cf. Figure 1.

Theorem 1.10. *1. If $\Gamma > \Gamma_c(\beta)$ the pressure $\Phi_N(\beta, \Gamma)$ is up to order one deterministic and one has the almost sure convergence*

$$\Phi_N(\beta, \Gamma) - (\ln \cosh(\beta\Gamma))N \to \frac{\beta}{\Gamma \tanh(\beta\Gamma)}. \tag{1.29}$$

2. If $\Gamma < \Gamma_c(\beta)$ and $\beta \leq \beta_c$, the pressure $\Phi_N(\beta, \Gamma)$ differs from the REM's pressure $\Phi_N(\beta, 0)$ by a deterministic β-independent shift of order one, i.e., one has the almost sure convergence

$$\Phi_N(\beta, \Gamma) - \Phi_N(\beta, 0) \to \Gamma^2. \tag{1.30}$$

3. *If* $\Gamma < \Gamma_c(\beta)$ *and* $\beta > \beta_c$*, the pressure* $\Phi_N(\beta, \Gamma)$ *differs from the REM's pressure by a deterministic* β*-dependent shift of order one, i.e., one has the almost sure convergence*

$$\Phi_N(\beta, \Gamma) - \Phi_N(\beta, 0) \to \frac{\Gamma^2 \beta}{\beta_c}. \tag{1.31}$$

The proof of the almost-sure convergence, for which the probability space is the product $\prod_{N=1}^{\infty} \Omega_N$ of independently redrawn variables for every single N, is based on a Borel-Cantelli argument and contained in Section 5.

At all values of $\beta > 0$, the fluctuations of the REM's pressure $\Phi_N(\beta, 0)$ below its deterministic leading term $Np^{\mathrm{REM}}(\beta)$ have been determined in [18] (see also [17, Thm. 9.2.1]). Their nature and scale changes from normal fluctuations on the scale $\exp\left(-\frac{N}{2}(\ln 2 - \beta^2)\right)$ for $\beta \leq \beta_c/2$ into a more interesting form of exponentially small fluctuations in the regime $\beta \in (\beta_c/2, \beta_c)$. In the spin glass phase $\beta > \beta_c$, the fluctuations are on order one [34] and asymptotically described by Ruelle's partition function of the REM [61]. More precisely, one has the weak convergence [18, Thm. 1.6]:

$$e^{-N[\beta\beta_c - \ln 2] + \frac{\beta}{2\beta_c}[\ln(N \ln 2) + \ln 4\pi]} Z_N(\beta, 0) \to \int_{-\infty}^{\infty} e^{x\beta/\beta_c} \, \mathrm{PPP}(e^{-x}\, dx). \tag{1.32}$$

As a consequence of Theorem 1.10, we thus obtain the analogous result for the QREM.

Corollary 1.11. *If* $\Gamma < \Gamma_c(\beta)$ *and* $\beta > \beta_c$*, we have the weak convergence:*

$$e^{-N[\beta\beta_c - \ln 2] + \frac{\beta}{2\beta_c}[\ln(N \ln 2) + \ln 4\pi] - \frac{\beta\Gamma^2}{\beta_c}} Z_N(\beta, \Gamma) \to \int_{-\infty}^{\infty} e^{x\beta/\beta_c} \, \mathrm{PPP}(e^{-x}\, dx).$$

Proof. By the continuity of the exponential function, this follows immediately from (1.31) and (1.32). □

The fluctuations of the QREM's partition function outside the spin glass phase are expected to be much smaller – for $\Gamma < \Gamma_c(\beta)$ and $\beta < \beta_c$ most likely on a similar scale as in the REM and for the paramagnetic regime presumably even smaller. The methods in this paper do not allow to determine fluctuations on an exponential scale.

1.4. Comments

We close this introduction by putting our main results into the broader context of related questions discussed in the physics and mathematics literature.

In the past years, the QREM has attained interest in the physics community as basic testing ground for quantum annealing algorithms [46, 47] and, somewhat related, physicist have started to investigate many-body localization in the QREM [9, 14, 22, 31, 48]. Based on numerical computations and non-rigorous methods such as the forward-scattering approximation and the replica trick, they predict a dynamical phase transition between ergodic and localized behavior in the parameter region $\Gamma < \Gamma_c(\beta), \beta < \beta_c$. This transition is expected to be reflected in a change in the spread of eigenfunctions at the correspond energies, which in the ergodic regime is neither uniform nor localized. It is an interesting mathematical challenge to investigate this. As this requires a good understanding of the eigenfunctions far away from the spectral edges, the methods presented in this paper are not yet sharp enough to tackle those problems.

In simplified models of Rosenzweig-Porter type such non-ergodic delocalization regimes have been predicted [42, 66] and confirmed by a rigorous analysis [72]. In an even more simplified model in which one replaces T by the orthogonal projection onto its ground-state $-|\Phi_\emptyset\rangle\langle\Phi_\emptyset|$ a fully detailed description of the localization-delocalization transition has been worked out in [4].

Focusing on the physics of spin glasses, the independence of the REM is an oversimplification. This was the main motivation for Derrida to introduce the Generalized Random Energy Model (GREM) [29, 30], in which the basic random variables are correlated, but still with a prescribed hierarchical structure. The free energy of the GREM has been studied extensively [19, 20, 23, 61]. On the quantum side, the specific free energy of the QGREM has been determined in [53]; and in [54] the effects of an additional longitudinal field have been considered. We expect that our methods can be adapted to the case of a finite-level QGREM to derive analogous results as in Theorems 1.3, 1.5 and 1.10. More precisely, we conjecture that the multiple phase transitions in the QGREM are reflected in the behavior of the ground state wavefunction, i.e., at the critical field strengths Γ_k the wavefunction undergoes a transition from being localized in the block $\boldsymbol{\sigma_k}$ to a delocalized states in the respective part of the spin components. The infinite-level case might require substantially new ideas, as standard interpolation techniques do not reveal order-one corrections. Our methods, however, are strong enough to cover non-Gaussian REM type models, i.e., i.i.d. a centered square integrable random process, whose distribution satisfies a large deviation principle (see also [53, Assumption 2.1]). Clearly, explicit expressions in analogous versions of Theorem 1.3, 1.5 and 1.10 will depend on the distribution of the process as already the parameter β_c is specific to Gaussians.

Among spin glass models with a transversal field, the Quantum Sherrington-Kirkpatrick (QSK) model, in which one substitutes in (1.1) for U the classical SK potential, is of particular interest [67]. In contrast to the classical SK model, which is solved by Parisi's celebrated formula, such an explicit expression for the free energy of the QSK is lacking, and its analysis remains a physical and mathematical challenge. So far, the universality of the limit of the free energy has been settled in [25], and in [2] the limit of the free energy was expressed as a limit of Parisi-type formulas for high-dimensional vector spin glass models. Unfortunately, despite the knowledge of a Parisi-type formula, the qualitative features of the phase transition in the QSK could only be analyzed by other means, adapting the methods of [3, 21]. In terms of the glass behavior, the analysis in [50] shows that the glass parameter vanishes uniformly in Γ for all $\beta \leq 1$. This is complemented by [49], where the existence of a glass phase has been established for $\beta > 1$ and weak magnetic fields Γ.

The localization-delocalization transition for the QREM differs drastically from related results on a finite-dimensional graph such as $\mathbb{Z}^d$ (see e.g. [5, 43] and references). Unlike on $\mathbb{Z}^d$, all low-energy eigenvectors on $\mathcal{Q}_N$ are delocalized in a regime of large Γ (a regime, which is also absent if one takes $\Gamma = \kappa/N$ as in [6]). The localized states appear only for small Γ. Although the norm of the adjacency matrix T is on the same scale N as the random potential U, which is not the case for the any of the variety of unbounded distributions studied on subsets of $\mathbb{Z}^d$, the localization of eigenvectors for extremal energies is even stronger on $\mathcal{Q}_N$. For the Gaussian distribution studied here, the mass of the eigenvectors sharply concentrates not only for a finite number of eigenvalues in one of the extremal sites of U, but rather for all eigenvalues below a threshold (cp. [37] with Theorem 1.5). In the finite-dimensional setting, the ground state and the first few excited states concentrate on a small, but growing subdomain of $\mathbb{Z}^d$ and, hence, a finite ℓ^1-norm for the ground state is specific to the QREM. This seemingly contradictory strong localization property compared to $\mathbb{Z}^d$ can be traced to the adjacencies matrix's T bad localization properties to balls, on which we elaborate in Section 2: the spectral shift due to localization on a ball of radius K is order of order N and not K^{-2} as on $\mathbb{Z}^d$. This together with the sparseness of the potential's extremal sites does

not allow for resonances (cf. Lemma 4.4). In this sense, our proof is in fact somewhat simpler (and hence also stronger) than existing proofs of localization in the extremal sites of a random potential on $\mathbb{Z}^d$. E.g. most recently and notably, in [15] the statistics of a finite number of eigenvalues above the ground state and the localization properties of their eigenvectors were studied for single-site distributions with doubly exponential tails (see also [43] for more references). While the degree of localization in the $\Gamma < \beta$ phase is significantly stronger than in the models studied in [15], we observe a similar exponential decay of the localized states for larger distances and in both cases the extremal statistics is governed by a Poisson process. In the study of the parabolic Anderson model, an interesting question is how the shape of the localized eigenstates and the speed of convergence depend on the underlying distribution of the random potential [43]. For the sake of concreteness, we only study the most prominent case of a Gaussian distribution. Although several quantities such as the constant β_c depend crucially on the Gaussian nature, we expect the qualitative aspects of the localization-delocalization transition to be persistent even with other unbounded distributions (e.g. those which meet [53, Ass 2.1]).

The operator T coincides up to a diagonal shift N with the Laplacian, i.e., the generator of a simple clock process on $\mathcal{Q}_N$. This correspondence gives rise to yet another link with the parabolic Anderson model on $\mathbb{Z}^d$. The dynamics of the Anderson model is a vast research topic and its study has revealed many interesting phenomena such as ageing. The spin glass nature is believed to be reflected in non-equilibrium properties and a slow relaxation to equilibrium. However, aging in spin glasses is typically not studied under an unbiased random walk, but rather under the Glauber dynamics for which the transition rates depend on the sites' energies. In the case of the REM, the related Glauber dynamics has drawn considerable interest as a well treatable case for metastability and aging [10, 11, 24, 35, 36]. Our spectral methods might provide some further insights into the dynamics of REM-type clock processes.

2. Adjacency matrix on Hamming balls

This section collects results on the spectral properties of the restriction of T to Hamming balls. We focus on the analysis of the Green's function, which by rank-one perturbation theory, is closely related to the ground state for potentials corresponding to a narrow deep hole - a situation typically encountered in potentials of REM type. Most of the spectral analysis in the literature related to T is motivated by the theory of error corrections (see e.g. [16, 26, 33] and references therein). The methods we use are rather different and neither rely on elaborate combinatorics nor a Hadamard transformation, which is applicable on a full Hamming cube only.

2.1. Norm estimates

In the following, we fix $\boldsymbol{\sigma}_0 \in \mathcal{Q}_N$ and $0 \le K \le N \in \mathbb{N}$. The restriction T_K of T to the Hamming ball $B_K(\boldsymbol{\sigma}_0)$ is defined through its matrix elements in the canonical orthonormal basis on $\ell^2(B_K(\boldsymbol{\sigma}_0))$, which is naturally embedded in $\ell^2(\mathcal{Q}_N)$:

$$\langle \delta_{\boldsymbol{\sigma}} | T_K \delta_{\boldsymbol{\sigma}'} \rangle = \begin{cases} \langle \delta_{\boldsymbol{\sigma}} | T \delta_{\boldsymbol{\sigma}'} \rangle & \text{if } \boldsymbol{\sigma}, \boldsymbol{\sigma}' \in B_K(\boldsymbol{\sigma}_0) \\ 0 & \text{otherwise.} \end{cases} \tag{2.1}$$

We start with two known results on T_K. The first part of the following lemma has been already proved in [33] in case $K = \varrho N$. The second part is just a special case of the spectral symmetry of any bipartite graph's adjacency matrix (cf. [26]).

Proposition 2.1 (cf. [33]). *For the restriction T_K to balls $B_K(\boldsymbol{\sigma}_0)$ of radius $K \leq N/2$:*

1. *The operator norm is bounded according to*

$$\|T_K\| \leq 2\sqrt{K(N-K+1)}, \tag{2.2}$$

and for any radius ϱN with $0 < \varrho < 1/2$:

$$E_N(\varrho) := \inf \operatorname{spec} T_{\varrho N} = -\|T_{\varrho N}\| = -2\sqrt{\varrho(1-\varrho)}N + o_\varrho(N). \tag{2.3}$$

2. *If φ is an eigenvector of T_K, then $\hat{\varphi}$ given by $\hat{\varphi}(\boldsymbol{\sigma}) := (-1)^{d(\boldsymbol{\sigma},\boldsymbol{\sigma}_0)}\varphi(\boldsymbol{\sigma})$ is also an eigenvector of T_K with $\langle\hat{\varphi}|T_K\hat{\varphi}\rangle = -\langle\varphi|T_K\varphi\rangle$. Consequently, the spectrum is symmetric,* $\operatorname{spec}(T_K) = -\operatorname{spec}(T_K)$.

Proof. 1. The operator $T_R - T_{R-1}$, when naturally defined on the full Hilbert space $\ell^2(\mathcal{Q}_N)$, describes the hopping between the Rth and $R-1$th Hamming sphere. Thus, $T_R - T_{R-1}$ and $T_{R-2} - T_{R-4}$ act on non overlapping parts of the configuration space. This allows us to write

$$T_K = \left(\bigoplus_{R\leq K,\ \mathrm{R\ even}} T_R - T_{R-1}\right) + \left(\bigoplus_{R\leq K,\ \mathrm{R\ odd}} T_R - T_{R-1}\right). \tag{2.4}$$

Consequently, it is enough to consider the operators $T_R - T_{R-1}$ on $\ell^2(\mathcal{Q}_N)$. As all matrix elements of $T_R - T_{R-1}$ are nonnegative, the Perron-Frobenius Theorem implies that its eigenvector ψ_R corresponding to the maximal eigenvalue, which coincides with $\|T_R - T_{R-1}\|$, is positive. Moreover, ψ_R is radial by symmetry and supported on $S_R(\boldsymbol{\sigma}) \cup S_{R+1}(\boldsymbol{\sigma})$, i.e., $\psi_R = s_{R+1}\sum_{\boldsymbol{\sigma}'\in S_{R+1}(\boldsymbol{\sigma})}\delta_{\boldsymbol{\sigma}'} + s_R\sum_{\boldsymbol{\sigma}'\in S_R(\boldsymbol{\sigma})}\delta_{\boldsymbol{\sigma}'}$. By an explicit calculation one thus has $(T_R - T_{R-1})^2\psi_R = R(N-R+1)\psi_R = \|T_R - T_{R-1}\|^2\psi_R$ and, hence using (2.4):

$$\begin{aligned}\|T_K\| &\leq \max_{R\leq K,\ \mathrm{R\ even}} \|T_R - T_{R-1}\| + \max_{R\leq K,\ \mathrm{R\ odd}} \|T_R - T_{R-1}\| \\ &\leq 2\max_{R\leq K} \|T_R - T_{R-1}\| = 2\sqrt{K(N-K+1)}.\end{aligned}$$

A complementing variational bound for a proof of (2.3) is in [33, Appendix C].
2. The second assertion follows from a direct computation. □

If K is of order one as a function of N, we have $\|T_K\| = \mathcal{O}_K(\sqrt{N})$. This drastic shift of the operator norm due to confinement should be compared to the finite-dimensional situation where this shift for a ball of radius K is propartional to K^{-2}.

In the remaining part of this section, we will analyze T_K and its Green function in the two extreme cases in relation to N: 1) fixed-size balls in Subsection 2.2, and 2) growing balls with radius $K = \varrho N$ with some $0 < \varrho < 1/2$ in Subsection 2.3.

2.2. Green function for balls of fixed size

The Green's function of the operator T_K on $\ell^2(B_K(\boldsymbol{\sigma}_0))$ is defined by

$$G_K(\boldsymbol{\sigma}, \boldsymbol{\sigma}_0; E) := \left\langle \delta_{\boldsymbol{\sigma}} \right| (-T_K - E)^{-1} \delta_{\boldsymbol{\sigma}_0} \left\rangle \right. . \tag{2.5}$$

Before we derive decay estimates in case $E \notin [-\|T_K\|, \|T_K\|]$, we recall some general facts:

1. By radial symmetry, $G_K(\boldsymbol{\sigma}, \boldsymbol{\sigma}_0; E)$ only depends on the distance $d(\boldsymbol{\sigma}, \boldsymbol{\sigma}_0)$.

2. All ℓ^2-normalized eigenvectors (φ_j) of T_K with eigenvalues (E_j) can chosen to be real, and we have

$$\begin{aligned} G_K(\boldsymbol{\sigma}, \boldsymbol{\sigma}_0; E) &= \sum_j \frac{\varphi_j(\boldsymbol{\sigma})\varphi_j(\boldsymbol{\sigma}_0)}{E_j - E} = \sum_j (-1)^{d(\boldsymbol{\sigma}, \boldsymbol{\sigma}_0)} \frac{\varphi_j(\boldsymbol{\sigma})\varphi_j(\boldsymbol{\sigma}_0)}{-E_j - E} \\ &= (-1)^{d(\boldsymbol{\sigma}, \boldsymbol{\sigma}_0)+1} G_K(\boldsymbol{\sigma}, \boldsymbol{\sigma}_0; -E), \end{aligned}$$

   where the second equality follows from the symmetry of the spectrum stated in Lemma 2.1. Thus, it is sufficient to derive decay estimates for $E < -\|T_K\|$.

3. The Green function at $E < -\|T_K\|$ is related to the ground-state φ of the rank-one perturbation

$$H^{(E)} \coloneqq T_K - \alpha^{(E)} |\delta_{\boldsymbol{\sigma}_0}\rangle\langle\delta_{\boldsymbol{\sigma}_0}| \tag{2.6}$$

   on $\ell^2(B_K(\boldsymbol{\sigma}_0))$. More precisely, by rank-one perturbation theory $\alpha^{(E)} := G_K(\boldsymbol{\sigma}_0, \boldsymbol{\sigma}_0; E)^{-1}$ is the unique value at which $H^{(E)}$ has a ground-state at $E < -\|T_K\|$, and

$$G_K(\boldsymbol{\sigma}, \boldsymbol{\sigma}_0; E) = \frac{1}{\alpha^{(E)}} \frac{\varphi(\boldsymbol{\sigma})}{\varphi(\boldsymbol{\sigma}_0)}, \tag{2.7}$$

   cf. [5, Theorem 5.3]. By the Perron-Frobenius theorem, φ and hence the Green function is strictly positive on $B_K(\boldsymbol{\sigma}_0)$. A decay estimate for $G_K(\cdot, \boldsymbol{\sigma}_0; E)$ translates to a bound on the ground state φ of $H^{(E)}$ and vice versa. Our proof of the localization results in Section 4 will make use of this relation.

In order to establish decay estimates, we employ the radial symmetry and write the Green function as a telescopic product

$$G_K(\boldsymbol{\sigma}, \boldsymbol{\sigma}_0; E) \;=\; \prod_{d=0}^{\operatorname{dist}(\boldsymbol{\sigma}, \boldsymbol{\sigma}_0)} \Gamma_K(d; E) \tag{2.8}$$

with factors $\Gamma_K(0; E) \coloneqq G_K(\boldsymbol{\sigma}_0, \boldsymbol{\sigma}_0; E)$ and

$$\Gamma_K(d; E) \coloneqq \frac{G_K(\boldsymbol{\sigma}, \boldsymbol{\sigma}_0; E)}{G_K(\boldsymbol{\sigma}', \boldsymbol{\sigma}_0; E)}, \quad \text{if } 1 \le d = \operatorname{dist}(\boldsymbol{\sigma}, \boldsymbol{\sigma}_0) = \operatorname{dist}(\boldsymbol{\sigma}', \boldsymbol{\sigma}_0) - 1.$$

The choice of $\boldsymbol{\sigma} \in S_d(\boldsymbol{\sigma}_0)$ and $\boldsymbol{\sigma}' \in S_{d-1}(\boldsymbol{\sigma}_0)$ in the last definition is irrelevant due to the radial symmetry.

The fundamental equation $(-T_K - E)G_K(\cdot, \boldsymbol{\sigma}_0; E) = \delta_{\cdot, \boldsymbol{\sigma}_0}$ yields for a configuration $\boldsymbol{\sigma}$ with $1 \le d = \operatorname{dist}(\boldsymbol{\sigma}, \boldsymbol{\sigma}_0) \le K$

$$\begin{aligned} 0 &= [(T_K - E)G_K(\cdot, \boldsymbol{\sigma}_0; E)](\boldsymbol{\sigma}) \\ &= -d \prod_{j=0}^{d-1} \Gamma_K(j; E) - E \prod_{j=0}^{d} \Gamma_K(j; E) - (N - d) \prod_{j=0}^{d+1} \Gamma_K(j; E) \\ &= \left(\frac{d}{\Gamma_K(d; E)} - E + (N - d)\Gamma_K(d + 1; E) \right) \prod_{j=0}^{d} \Gamma_K(j; E), \end{aligned}$$

where we use the convention $\Gamma_K(K+1;E) \coloneqq 0$. In the case $d=0$, we have $1 = (-N\Gamma_K(1;E) - E)\Gamma_K(0;E)$. That translates to the following recursive relation of Riccati type:

$$\Gamma_K(d;E) \;=\; \mathcal{M}_{d,E}(\,\Gamma_K(d+1;E)\,), \qquad 0 \le d \le K. \tag{2.9}$$

with the fractional linear transformation acting on $\mathbb{C}$:

$$\mathcal{M}_{d,E}(\Gamma) \;:=\; \frac{\max\{d,1\}}{-E-(N-d)\,\Gamma}. \tag{2.10}$$

We now analyze the behavior of solutions of the recursive relation in the various regimes of interest.

Proposition 2.2. *For any $K \in \mathbb{N}$ there is some $C_K < \infty$ such that for any $N > 2K$ and $E < -\|T_K\|$ we have*

$$G_K(\boldsymbol{\sigma},\boldsymbol{\sigma}_0;E) \le \frac{C_K}{|E+\|T_K\||}\binom{N}{d(\boldsymbol{\sigma},\boldsymbol{\sigma}_0)}^{-1/2}\left(\frac{\sqrt{N}}{|E|}\right)^{d(\boldsymbol{\sigma},\boldsymbol{\sigma}_0)}. \tag{2.11}$$

Proof. In case $E \le -2\sqrt{KN} \le -\|T_K\|$ (cf. Lemma 2.1), we use the recursive relations (2.9) with initial condition $\Gamma_K(K;E) = -\frac{K}{E}$ to prove that for $1 \le d \le K-1$:

$$\left(1 + \frac{(N-d)\Gamma_K(d+1;E)}{E}\right) \ge \frac{1}{2}.$$

This can be established directly in case $d = K-1$. For $1 \le d \le K-2$ we proceed by induction. Indeed, we have

$$\begin{aligned}\left(1 + \frac{(N-d)\Gamma_K(d+1;E)}{E}\right) &= 1 - \frac{\max\{d+1,1\}}{-E-(N-d-1)\Gamma_K(d+1;E)} \\ &\ge 1 - \frac{2\max\{d+1,1\}}{E^2} \ge \frac{1}{2},\end{aligned}$$

where we used the recursive relation (2.9), the induction hypothesis and the upper bound on E. This inductive argument also yields

$$\Gamma_K(d;E) \le \frac{2d}{|E|} \quad \text{for } E \le -2\sqrt{KN} \text{ and any } 1 \le d < K.$$

Utilising the abbreviation $d \coloneqq \operatorname{dist}(\boldsymbol{\sigma},\boldsymbol{\sigma}_0)$ and (2.8) together with the trivial bound $\Gamma_K(0;E) \le |E+\|T_K\||^{-1}$, this in turn implies:

$$G_K(\boldsymbol{\sigma},\boldsymbol{\sigma}_0;E) \le \frac{2^d d!}{|E|^d}\,\Gamma_K(0;E) \le \frac{2^K\sqrt{K!}}{|E+\|T_K\||}\binom{N}{d}^{-1/2}\left(\frac{\sqrt{N}}{|E|}\right)^d,$$

which agrees with the claim in case $E \le -2\sqrt{KN}$. In case $E \in (-2\sqrt{KN}, -\|T_K\|)$, we recall that

$$\sum_{\boldsymbol{\sigma}} G_K(\boldsymbol{\sigma},\boldsymbol{\sigma}_0;E)^2 \le \left\|(T_K-E)^{-2}\right\| \le \frac{1}{|E+\|T_K\||^2},$$

and the fact that $G_K(\cdot,\boldsymbol{\sigma}_0;E)$ is a radially symmetric function. Consequently,

$$G_K(\boldsymbol{\sigma},\boldsymbol{\sigma}_0;E) \le \frac{1}{|E+\|T_K\||}\binom{N}{d(\boldsymbol{\sigma},\boldsymbol{\sigma}_0)}^{-1/2},$$

and the claim follows with an appropriate choice for the constant C_K. □

2.3. Green function for growing balls

We now turn to the behavior of the Green's function on balls, which grow with N. This will require a more detailed analysis of the recursion relation (2.9). To see what to expect, we first derive an estimate on the Green's function of the full Hamming cube.

Lemma 2.3. *For any $N \in \mathbb{N}$, $E < -N = -\|T\|$ and $\boldsymbol{\sigma}, \boldsymbol{\sigma}_0 \in \mathcal{Q}_N$:*

$$G_N(\boldsymbol{\sigma}, \boldsymbol{\sigma}_0; E) \;\leq\; \frac{1}{|E+N|} \;\left(\frac{N}{|E|}\right)^d \;\binom{N}{d(\boldsymbol{\sigma}, \boldsymbol{\sigma}_0)}^{-1}. \tag{2.12}$$

Proof. The Neumann series formula readily implies the operator identity

$$\frac{1}{1-X} = \sum_{k=0}^{d-1} X^k + X^d \;\frac{1}{1-X} \tag{2.13}$$

for any operator with $\|X\| < 1$. Setting $d = d(\boldsymbol{\sigma}, \boldsymbol{\sigma}_0)$, we thus obtain

$$\big\langle \delta_{\boldsymbol{\sigma}} \big| (T-E)^{-1} \delta_{\boldsymbol{\sigma}_0} \big\rangle = \frac{-1}{E} \big\langle \delta_{\boldsymbol{\sigma}} \big| (1 - T/E)^{-1} \delta_{\boldsymbol{\sigma}_0} \big\rangle = \frac{1}{E^d} \left\langle \delta_{\boldsymbol{\sigma}} \Big| \frac{T^d}{T-E}\; \delta_{\boldsymbol{\sigma}_0} \right\rangle,$$

since terms in (2.13) corresponding to $k < d$ vanish. Radial symmetry of the Green function yields

$$\begin{aligned} \big\langle \delta_{\boldsymbol{\sigma}} \big| (T-E)^{-1} \delta_{\boldsymbol{\sigma}_0} \big\rangle &= \binom{N}{d}^{-1} \sum_{\boldsymbol{\sigma} \in S_d(\boldsymbol{\sigma}_0)} \big\langle \delta_{\boldsymbol{\sigma}} \big| (T-E)^{-1} \delta_{\boldsymbol{\sigma}_0} \big\rangle \\ &\leq \binom{N}{d}^{-1} \frac{\sqrt{2^N}}{E^d} \;\left\langle \Phi_\emptyset \big| T^d \frac{1}{T-E} \delta_{\boldsymbol{\sigma}_0} \right\rangle \;=\; \binom{N}{d}^{-1} \left(\frac{N}{|E|}\right)^d \;\frac{1}{|E|-N}\,, \end{aligned}$$

where $\Phi_\emptyset(\boldsymbol{\sigma}) = 2^{-N/2}$ denotes the lowest energy eigenfunction of T, and we applied the eigenfunction equation, $T\Phi_\emptyset \;=\; -N\Phi_\emptyset$, in the last step. □

A main difference between the small versus large ball behavior of the Green's function is in the factor $(\sqrt{N}/|E|)^d$ in (2.11) versus $(N/|E|)^d$ in (2.12). In the case of interest where $|E|$ is of order N, we arrive at a decay of the order $N^{-d/2}$ versus e^{-Cd}.

There are at least two strategies to derive upper bounds on the Green function $G_{\varrho N}(\boldsymbol{\sigma}, \boldsymbol{\sigma}_0; E)$ for $E < E_N(\varrho) = -2\sqrt{\varrho(1-\varrho)}N + o(N)$ and $0 < \varrho < 1/2$, cf. (2.3). The first strategy is to apply the arguments, which led to (2.12) and which yield

$$G_{\varrho N}(\boldsymbol{\sigma}, \boldsymbol{\sigma}_0; E) \leq \frac{1}{E_N(\varrho) - E} \;\left(\frac{E_N(\varrho)}{E}\right)^d \;\frac{\Psi_\varrho(\boldsymbol{\sigma}_0)}{\Psi_\varrho(\boldsymbol{\sigma})} \;\binom{N}{d}^{-1}, \tag{2.14}$$

with $\Psi_\varrho \in \ell^2(B_{\varrho N}(\boldsymbol{\sigma}_0))$ the ℓ^2-normalized, positive eigenfunction corresponding to $E_N(\varrho)$. It then remains to establish a bound on the ratio $\Psi_\varrho(\boldsymbol{\sigma}_0)/\Psi_\varrho(\boldsymbol{\sigma})$. We, however, will instead proceed by an analysis of the factors $\Gamma_{\rho N}$ defined in (2.8).

Proposition 2.4. *Let $0 < \varrho < 1/2$, and $\varepsilon > 0$. Then for $E \leq E_N(\varrho) - \varepsilon N$, all $\boldsymbol{\sigma} \in B_{\rho N}(\boldsymbol{\sigma}_0)$ and all N large enough:*

$$G_{\varrho N}(\boldsymbol{\sigma}, \boldsymbol{\sigma}_0; E) \;\leq\; \frac{1}{\varepsilon N} \binom{N}{d(\boldsymbol{\sigma}_0, \boldsymbol{\sigma})}^{-1/2} \; 2^{-\min\{d(\boldsymbol{\sigma}_0, \boldsymbol{\sigma}),\, \rho_0(\varrho) N\}} \tag{2.15}$$

where $0 < \varrho_0(\varrho) < \varrho$ is the unique solution of the equation $2\sqrt{\varrho(1-\varrho)} = 3\sqrt{\varrho_0(1-\varrho_0)}$. Moreover, for any fixed $K \in \mathbb{N}$ there is some $C_K < \infty$ such that for all N large enough:

1. *for all $\boldsymbol{\sigma} \in S_K(\boldsymbol{\sigma}_0)$:* $\displaystyle G_{\varrho N}(\boldsymbol{\sigma}, \boldsymbol{\sigma}_0; E) \;\leq \frac{1}{\varepsilon N} \frac{C_K}{\sqrt{N^K}} \binom{N}{d(\boldsymbol{\sigma}_0, \boldsymbol{\sigma})}^{-1/2}.$

2. $\displaystyle \sum_{\boldsymbol{\sigma} \notin B_K(\boldsymbol{\sigma}_0)} G_{\varrho N}(\boldsymbol{\sigma}, \boldsymbol{\sigma}_0; E)^2 \leq \frac{C_K}{\varepsilon^2 N^{K+2}}.$

Proof. It is convenient to separate the combinatorial factor $\binom{N}{d(\boldsymbol{\sigma}_0, \boldsymbol{\sigma})}^{-1/2}$ and study

$$\hat{G}_{\varrho N}(\boldsymbol{\sigma}, \boldsymbol{\sigma}_0; E) \coloneqq \binom{N}{d(\boldsymbol{\sigma}_0, \boldsymbol{\sigma})}^{1/2} G_{\varrho N}(\boldsymbol{\sigma}, \boldsymbol{\sigma}_0; E) = \prod_{d=0}^{d(\boldsymbol{\sigma}, \boldsymbol{\sigma}_0)} \hat{\Gamma}_{\varrho N}(d; E). \tag{2.16}$$

By direct inspection of (2.16) one obtains the relation $\hat{\Gamma}_{\varrho N}(d; E) \coloneqq \sqrt{\frac{N-d}{d}}\, \Gamma_{\varrho N}(d; E)$ for $d \geq 1$, which in turn implies the recursive relation

$$\hat{\Gamma}_{\varrho N}(d; E) = \frac{1}{\frac{|E|}{V(d)} - m(d) \hat{\Gamma}_{\varrho N}(d; E)} \qquad \text{for } 1 \leq d \leq \varrho N \tag{2.17}$$

$$\text{with} \quad V(d) \coloneqq \sqrt{d(N-d)}, \quad m(d) \coloneqq \sqrt{\frac{(d+1)(N-d)}{d(N-d+1)}}$$

$$\text{and} \quad \hat{\Gamma}_{\varrho N}(\varrho N + 1; E) = 0, \quad \hat{\Gamma}_{\varrho N}(0; E) = \Gamma_{\varrho N}(0; E) = G_{\varrho N}(\boldsymbol{\sigma}_0, \boldsymbol{\sigma}_0; E).$$

We will now analyze the solution of these recursive relations.

We first claim that for all N large enough:

$$\hat{\Gamma}_{\varrho N}(d; E) \leq 1 \text{ for all } d \in [\varrho_0 N, \varrho N]. \tag{2.18}$$

This is proven by induction on d starting from $d = \varrho N + 1$, where it trivially holds. For the induction step from $d+1$ to d, we recall that $E_N(\varrho) = -2\sqrt{\varrho(1-\varrho)} + o_\varrho(N)$ from (2.3). The monotonicity of $V(d)$ and $m(d)$ then implies that for all $\varrho_0 N \leq d \leq \varrho N$ and all N large enough:

$$\frac{|E|}{V(d)} \geq 2 + \frac{\varepsilon}{2\sqrt{\varrho(1-\varrho)}}, \quad m(d) \leq m(\varrho_0 N) = \sqrt{\frac{1 + 1/(\varrho_0 N)}{1 - 1/(\varrho N)}} = 1 + \mathcal{O}_\varrho(N^{-1}).$$

Inserting these estimates into the recursion relation (2.17), the claimed inequality (2.18) follows.

We now control the recursion relation in the regime $1 \leq d \leq \varrho_0 N$. To this end, note that the definition of ϱ_0 implies that for any $d \leq \rho N$ and N large enough: $|E|/V(d) \geq 3 + \varepsilon/(2\sqrt{\rho(1-\rho)})$. Using $\hat{\Gamma}_{\varrho N}(\varrho_0 N + 1; E) \leq 1$ one readily establishes $\hat{\Gamma}_{\varrho N}(d; E) \leq \frac{1}{2}$ inductively as long as $m(d) \leq 2$.

The monotonicity $m(d) \leq m(1) = \sqrt{2}\ (1 + \mathcal{O}(N^{-1}))$ implies that this is true for any $d \geq 1$ at sufficiently large N. The proof of the claimed exponential decay (2.15) is then completed using the trivial norm bound

$$\hat{\Gamma}_{\varrho N}(0; E) = G_{\varrho N}(\boldsymbol{\sigma}_0, \boldsymbol{\sigma}_0; E) \leq \left\|(T_{\varrho N} - E)^{-1}\right\| = \operatorname{dist}(E, \operatorname{spec}(T_{\varrho N}))^{-1} \leq \frac{1}{\varepsilon N}.$$

Let us finally consider the case of fixed integers K. Note that for any $K \geq 1$ we know by the above $\hat{\Gamma}_{\varrho N}(K+1; E) \leq 1/2$. The recursion relation (2.17) then yields for any $1 \leq d \leq K$

$$\hat{\Gamma}_{\varrho N}(d; E) \leq \frac{d_K}{\sqrt{N}}$$

with some constants $d_K = d_K(\rho)$. This completes the proof of the first item. For the second item we organize the summation into sums over spheres of radius greater or equal to $K+1$:

$$\begin{aligned}
&\sum_{\boldsymbol{\sigma} \notin B_K(\boldsymbol{\sigma}_0)} G_{\varrho N}(\boldsymbol{\sigma}, \boldsymbol{\sigma}_0; E)^2 \\
&\quad = \prod_{d=0}^{K} \hat{\Gamma}_{\varrho N}(d; E)^2 \left(\sum_{D=K+1}^{\varrho_o N} \prod_{d=K+1}^{D} \hat{\Gamma}_{\varrho N}(d; E)^2 + \sum_{D=\varrho_o N}^{\varrho N} \prod_{d=K+1}^{D} \hat{\Gamma}_{\varrho N}(d; E)^2 \right).
\end{aligned}$$

The product in the prefactor is estimated by $C_K/(\varepsilon^2 N^{K+2})$ using the first item. The second product is dominated by 4^{K-D} such that the summation over $D \geq K+1$ is bounded by a geometric series. The last product is bounded by $4^{K-\varrho_0 N}$ such that the sum is bounded trivially by this exponential factor times ϱN. This completes the proof. □

The decay established in Proposition 2.4 for fixed distance K to the center of the ball agrees in its dependence on N with the result of Proposition 2.2. Moreover, the rough decay estimate (2.15) is 'qualitatively correct' in the sense that we expect an estimate of the form

$$G_{\varrho N}(\boldsymbol{\sigma}, \boldsymbol{\sigma}_0; E) \ \leq \ \frac{1}{\varepsilon N} \binom{N}{d(\boldsymbol{\sigma}_0, \boldsymbol{\sigma})}^{-1/2} \ e^{-L(E, \varrho, d(\boldsymbol{\sigma}_0, \boldsymbol{\sigma}))N}$$

with some positive function $L(E, \varrho, d(\boldsymbol{\sigma}_0, \boldsymbol{\sigma}))$. However, it is clear from the proof of Proposition 2.4 that we did not attempt to derive a sharp bound for L as it requires a more elaborate analysis of the factors $\hat{\Gamma}_{\varrho N}(d; E)$.

3. Delocalization regime

3.1. Spectral concentration

The analysis of the low-energy spectrum in the paramagnetic phase is based on the Schur complement method [5, Theorem 5.10] for which we define the spectral projections for $\varepsilon \in (0, 1)$

$$Q_\varepsilon := \mathbb{1}_{(-\varepsilon N, \varepsilon N)}(T) \qquad P_\varepsilon := 1 - Q_\varepsilon, \tag{3.1}$$

which separate eigenstates of T with energies at the center of its spectrum from the edges. Here and in the following, $\mathbb{1}(\cdot)$ stands for the indicator function. A Chernoff bound shows that the dimension

of the range of P_ε is only an exponential fraction of the total dimension of Hilbert space:

$$\dim P_\varepsilon = \sum_{|k-\frac{N}{2}|>\frac{\varepsilon N}{2}} \binom{N}{k} \;\leq\; 2^{N+1}\, e^{-\varepsilon^2 N/2}\,. \tag{3.2}$$

The exact asymptotics of $\dim P_\varepsilon$ is in fact well-known, $\ln \dim P_\varepsilon = (\gamma(\frac{1-\varepsilon}{2}) + o(1))N$, in terms of the binary entropy γ defined in (1.16).

The following spectral concentration bound expresses the exponential smallness of the projection of symmetric random multiplication operators to the above subspace. It will be our main working horse in the paramagnetic phase.

Proposition 3.1. *Let $\varepsilon > 0$ and $W(\boldsymbol{\sigma})$, $\boldsymbol{\sigma} \in Q_N$, be independent and identically distributed random variables such that*

i. the mean is zero, $\mathbb{E}\left[W(\boldsymbol{\sigma})\right] = 0$,

ii. the variance of $W(\boldsymbol{\sigma})$ is bounded by one, i.e. $\mathbb{E}\left[W(\boldsymbol{\sigma})^2\right] \leq 1$, and

iii. W is bounded , i.e. $\|W\|_\infty \leq M_N$ with some $M_N < \infty$, and $M_N^2 N \dim P_\varepsilon / 2^N \leq 1$.

Then there are (universal) constants $c, C \in (0,\infty)$ such for any $\lambda > 0$:

$$\mathbb{P}\left(\|P_\varepsilon W P_\varepsilon\| - \mathbb{E}\left[\|P_\varepsilon W P_\varepsilon\|\right] > \lambda \sqrt{\frac{\dim P_\varepsilon}{2^N}} \right) \leq\; C e^{-c\lambda^2}. \tag{3.3}$$

Moreover, we have the following bound:

$$\mathbb{E}\left[\|P_\varepsilon W P_\varepsilon\|\right] \;\leq\; C\sqrt{N}\sqrt{\frac{\dim P_\varepsilon}{2^N}}\,. \tag{3.4}$$

Proof. The first statement follows from Talagrand's concentration inequality [68] (see also [70, Thm. 2.1.13]) by considering $F : \mathbb{R}^{Q_N} \to \mathbb{R}$ given by $F(W) := \|P_\varepsilon W P_\varepsilon\|$. We need to show that F is Lipschitz continuous and convex. Convexity, i.e., $F(\alpha W + (1-\alpha)W') \leq \alpha F(W) + (1-\alpha)F(W')$ for all $\alpha \in [0,1]$, is evident from the triangle inequality. To establish the Lipschitz continuity, let $W, W' \in \mathbb{R}^{Q_N}$ and $\psi \in P_\varepsilon \ell^2(Q_N)$ with $\|\psi\| = 1$ be such that $\|P_\varepsilon(W - W')P_\varepsilon\| = \langle \psi, (W-W')\psi\rangle$. Then one has

$$\begin{aligned}\left|F(W) - F(W')\right| &\leq \langle \psi, (W-W')\psi\rangle = \sum_{\boldsymbol{\sigma}} |\psi(\boldsymbol{\sigma})|^2 (W(\boldsymbol{\sigma}) - W'(\boldsymbol{\sigma})) \\ &\leq\; \|W - W'\|_2 \|\psi\|_4^2 \;\leq \|W-W'\|_2 \|\psi\|_\infty \leq \max_{\boldsymbol{\sigma}} \sqrt{\langle \delta_{\boldsymbol{\sigma}} | P_\varepsilon \delta_{\boldsymbol{\sigma}}\rangle}\; \|W - W'\|_2\,.\end{aligned}$$

The first estimate is the triangle inequality. The next two estimates are special cases of Hölder's inequality, in which we also use $\|\psi\| = 1$. The last estimate results from the Cauchy-Schwarz inequality applied to $\|\psi\|_\infty = \max_{\boldsymbol{\sigma}} |\langle P_\varepsilon \delta_{\boldsymbol{\sigma}} | \psi\rangle|$ and the fact that $\|P_\varepsilon \delta_{\boldsymbol{\sigma}}\| = \sqrt{|\langle P_\varepsilon \delta_{\boldsymbol{\sigma}} | \delta_{\boldsymbol{\sigma}}\rangle|}$. Since by symmetry for any $\boldsymbol{\sigma} \in \mathcal{Q}_N$:

$$\langle \delta_{\boldsymbol{\sigma}} | P_\varepsilon \delta_{\boldsymbol{\sigma}}\rangle = \frac{\dim P_\varepsilon}{2^N}\,, \tag{3.5}$$

we conclude that F is Lipschitz with constant $2^{-N/2}\sqrt{\dim P_\varepsilon}$. This finishes the proof of (3.3).

The second statement is derived from the matrix Bernstein inequality [57, 71]. For its application, we note that the matrix under consideration is a sum of independent random matrices,

$$P_\varepsilon W P_\varepsilon = \sum_{\boldsymbol{\sigma}} S(\boldsymbol{\sigma})\,, \qquad \text{with } S(\boldsymbol{\sigma}) := \tfrac{\dim P_\varepsilon}{2^N}\; W(\boldsymbol{\sigma})\; |\psi(\boldsymbol{\sigma})\rangle\langle\psi(\boldsymbol{\sigma})|,$$

where $|\psi(\boldsymbol{\sigma})\rangle\langle\psi(\boldsymbol{\sigma})|$ denotes the rank-one projection onto the vector $\psi(\boldsymbol{\sigma}) := \sqrt{\frac{2^N}{\dim P_\varepsilon}}\; P_\varepsilon \delta_{\boldsymbol{\sigma}}$, which in view of (3.5) is normalised. By assumption the matrices $S(\boldsymbol{\sigma})$ are centred, $\mathbb{E}\,[S(\boldsymbol{\sigma})] = 0$, and bounded

$$\|S(\boldsymbol{\sigma})\| \leq M_N \frac{\dim P_\varepsilon}{2^N} \leq \sqrt{\frac{\dim P_\varepsilon}{N\, 2^N}}.$$

The mean variance matrix of $P_\varepsilon W P_\varepsilon$ is

$$\sum_{\boldsymbol{\sigma}} \mathbb{E}\left[S(\boldsymbol{\sigma})^2\right] = \left(\frac{\dim P_\varepsilon}{2^N}\right)^2 \sum_{\boldsymbol{\sigma}} \mathbb{E}\left[W(\boldsymbol{\sigma})^2\right] |\psi(\boldsymbol{\sigma})\rangle\langle\psi(\boldsymbol{\sigma})| \leq \frac{\dim P_\varepsilon}{2^N}\; P_\varepsilon.$$

The last inequality follows from the assumption, $\mathbb{E}\left[W(\boldsymbol{\sigma})^2\right] \leq 1$, as well as the fact that $(\delta_{\boldsymbol{\sigma}})$ form an orthonormal basis. Consequently, [71, Thm. 6.6.1] together with the trivial bound, $\dim P_\varepsilon \leq 2^N$, on the dimension of the matrices implies

$$\mathbb{E}\left[\|P_\varepsilon W P_\varepsilon\|\right] \leq \left(\sqrt{2\ln 2^{N+1}} + \frac{\ln 2^{N+1}}{3\sqrt{N}}\right) \sqrt{\frac{\dim P_\varepsilon}{2^N}},$$

which completes the proof. □

Alternatively to Talagrand's concentration inequality, the concentration of measure part of the matrix Bernstein inequality [71, Thm. 6.6.1] would also have been sufficient for proving a slightly less sharp upper bound on the upper tail of the large-deviation probability (3.3).

As an application, we state the following straightforward corollary. Its assumptions are tailored to fit in particular the case of the REM.

Corollary 3.2. *Suppose that $W(\boldsymbol{\sigma})$, $\boldsymbol{\sigma} \in Q_N$ are i.i.d. random variables which are*

i. mean zero with variance $w_N := \mathbb{E}\left[W(\boldsymbol{\sigma})^2\right] \leq N$ and obey a moment bound $\mathbb{E}\left[W(\boldsymbol{\sigma})^8\right] \leq c\, N^4$ for some $c < \infty$.

ii. linearly bounded in the sense that there is some $c < \infty$ such that $\|W\|_\infty \;\leq\; c\, N$.

Then, there is some $C \in (0, \infty)$ such that for any $\tau \in (0, 1)$ there are events $\Omega_{N,\tau}$ with

$$\mathbb{P}(\Omega_{N,\tau}) \geq 1 - e^{-N/C} \tag{3.6}$$

such that for all sufficiently large N and at $\varepsilon = N^{\frac{\tau-1}{2}}$:

$$\|P_\varepsilon W P_\varepsilon\| \;\leq\; C\, N\, e^{-N^\tau/4}\,, \tag{3.7}$$

$$\left\|P_\varepsilon (W^2 - w_N) P_\varepsilon\right\| \;\leq\; C\, N^{\frac{3}{2}}\, e^{-N^\tau/4}\,, \tag{3.8}$$

$$\|P_\varepsilon W^p P_\varepsilon\| \;\leq\; C N^{\frac{p}{2}} \quad \textit{for all } p \in [1, 4]. \tag{3.9}$$

Proof. The proof of these inequalities follows by three applications of Proposition 3.1 with different W' always at the same $\lambda = \sqrt{N}$. We note that our choice $\varepsilon = N^{\frac{\tau-1}{2}}$ implies by (3.2) $\dim P_\varepsilon \leq 2^{N+1}e^{-N^\tau/2}$. This in turn yields for any polynomial M_N and N large enough $M_N^2 N \dim P_\varepsilon/2^N \leq 1$, which indeed checks one of the assumptions of Proposition 3.1. We then construct three events $\Omega_{N,\tau}^{(j)}$ with $j \in \{1,2,3\}$ each with probability $\mathbb{P}(\Omega_{N,\tau}^{(j)}) \geq 1 - 3^{-1}e^{-N/C}$ with some (universal) $C < \infty$ and all N large enough. Their intersection $\Omega_{N,\tau} := \Omega_{N,\tau}^{(1)} \cap \Omega_{N,\tau}^{(2)} \cap \Omega_{N,\tau}^{(3)}$ then defines the required events.

More specifically, for a proof of (3.7), we take $W'(\boldsymbol{\sigma}) = W(\boldsymbol{\sigma})/\sqrt{N}$. The event $\Omega_{N,\tau}^{(1)}$ on which (3.7) then satisfies the required probability estimate.
The proof of (3.8) follows again from Proposition 3.1 with $W'(\boldsymbol{\sigma}) = c^{-1/4}\,(W(\boldsymbol{\sigma})^2 - w_N)/N$ and the prefactor ensuring $\mathbb{E}\left[W'(\boldsymbol{\sigma})^2\right] \leq 1$. In this way, we construct $\Omega_{N,\tau}^{(2)}$.

By Jensen's inequality $\langle\psi, W^p\psi\rangle^{4/p} \leq \langle\psi, W^4\psi\rangle$ for any $p \in [1,4]$, it suffices to establish (3.9) for $p = 4$. We choose $W'(\boldsymbol{\sigma}) = c^{-1/2}\,(W(\boldsymbol{\sigma})^4 - \mathbb{E}\left[W(\boldsymbol{\sigma})^4\right])/N^2$ to define $\Omega_{N,\tau}^{(3)}$. □

3.2. Proof of Theorem 1.3

We now use the estimates of the preceding subsection in our Schur's complement analysis for the proofs of Theorem 1.3 and 1.4. These results will actually follow from a slightly more general theorem on operators $H = \Gamma T + W$ of QREM-type. As a preparation and motivation of the following lemma, we collect some basic facts about these operators. The kinetic part of the block component $Q_\varepsilon H Q_\varepsilon = \Gamma T Q_\varepsilon + Q_\varepsilon W Q_\varepsilon$ is estimated by

$$\|TQ_\varepsilon\| \;\leq\; \varepsilon N\,, \tag{3.10}$$

which implies

$$-\|W\|_\infty - \Gamma\varepsilon\, N \leq \inf\operatorname{spec} Q_\varepsilon H Q_\varepsilon\,. \tag{3.11}$$

For any $z \in \mathbb{C}$ with $\operatorname{Re} z < \|W\|_\infty - \Gamma\varepsilon\, N$, the operator $Q_\varepsilon H Q_\varepsilon - z$ is hence invertible on $Q_\varepsilon\ell^2(Q_N)$ with inverse denoted by $R_\varepsilon(z) := (Q_\varepsilon H Q_\varepsilon - zQ_\varepsilon)^{-1}$. The latter features in Schur's complement formula for the resolvent of H projected onto the subspace $P_\varepsilon\ell^2(Q_N)$:

$$P_\varepsilon(H-z)^{-1}P_\varepsilon = (P_\varepsilon(H-z)P_\varepsilon - P_\varepsilon W Q_\varepsilon R_\varepsilon(z) Q_\varepsilon W P_\varepsilon)^{-1}\,. \tag{3.12}$$

Our main observation is that Schur's complement is approximated by an operator proportional to the identity.

Lemma 3.3. *Consider the operator $H := \Gamma T + W$ on $\ell^2(\mathcal{Q}_N)$ with W satisfying the assumptions in Corollary 3.2 and let $\Omega_{N,\tau}$ with $\tau \in (0,1)$ be the events constructed there. Then on $\Omega_{N,\tau}$ and at $\varepsilon = N^{\frac{\tau-1}{2}}$ for all N large enough:*

$$\left\| P_\varepsilon W R_\varepsilon(z) W P_\varepsilon + P_\varepsilon \frac{w_N}{z} \right\| \;\leq\; \max\{1,\Gamma\}\frac{C}{d^2}\; N^{\frac{\tau-1}{2}}\,, \quad R_\varepsilon(z) := (Q_\varepsilon H Q_\varepsilon - zQ_\varepsilon)^{-1}, \tag{3.13}$$

for all $z \in \mathbb{C}$ such that $\min\{|z|\,,\, \operatorname{dist}(\operatorname{spec} Q_\varepsilon H Q_\varepsilon, z)\} \geq d\,N$ with $d \in (0,1]$.

Proof. We use the resolvent equation to write

$$\begin{aligned} P_\varepsilon\left(W R_\varepsilon(z) W + \frac{w_N}{z}\right) P_\varepsilon &= \frac{1}{z} P_\varepsilon\left(w_N - W Q_\varepsilon W + W R_\varepsilon(z) Q_\varepsilon H Q_\varepsilon W\right) P_\varepsilon \\ &= \frac{1}{z} P_\varepsilon (w_N - W Q_\varepsilon W) P_\varepsilon + \frac{1}{z} P_\varepsilon\left(W R_\varepsilon(z) Q_\varepsilon H Q_\varepsilon) W\right) P_\varepsilon, \end{aligned} \tag{3.14}$$

and estimate both terms in the second line separately. For the first expression we rewrite

$$P_\varepsilon(w_N - WQ_\varepsilon W)P_\varepsilon = \; P_\varepsilon(w_N - W^2)P_\varepsilon + P_\varepsilon W P_\varepsilon W P_\varepsilon \,. \tag{3.15}$$

According to (3.7) and (3.8), the norm of the two terms in the right side is negligible in comparison to $N^{\frac{\tau-1}{2}}$ for all N large enough. It hence remains to estimate the norm of the second term in the right side of (3.14). To do so, we split the terms as follows

$$\frac{1}{z}P_\varepsilon W R_\varepsilon(z) Q_\varepsilon H Q_\varepsilon W P_\varepsilon = \frac{1}{z}P_\varepsilon W R_\varepsilon(z) Q_\varepsilon \Gamma T Q_\varepsilon W P_\varepsilon + \frac{1}{z}P_\varepsilon W R_\varepsilon(z) Q_\varepsilon W Q_\varepsilon W P_\varepsilon$$

and use (3.10) together with $\|R_\varepsilon(z)\| \leq (dN)^{-1}$ (since $\operatorname{dist}(\operatorname{spec} Q_\varepsilon H Q_\varepsilon, z) \geq dN$) and $\|P_\varepsilon W\|^2 = \|P_\varepsilon W^2 P_\varepsilon\| \leq CN$ by (3.8). On $\Omega_{N,\tau}$ for all N large enough, we thus conclude:

$$|z|^{-1}\,\|P_\varepsilon W R_\varepsilon(z)\Gamma T Q_\varepsilon W P_\varepsilon\| \;\leq \frac{C}{d^2 N}\|TQ_\varepsilon\| \leq \frac{C}{d^2}\,N^{\frac{\tau-1}{2}}\,. \tag{3.16}$$

Similarly, we estimate

$$\begin{aligned} |z|^{-1}\,\|P_\varepsilon W R_\varepsilon(z) Q_\varepsilon W Q_\varepsilon W P_\varepsilon\| \;&\leq\; |z|^{-1}\,\|P_\varepsilon W\|\;\|R_\varepsilon(z)\|\;\|W Q_\varepsilon W P_\varepsilon\| \\ &\leq\; \frac{C}{d^2 N^{3/2}}\,\sqrt{\|P_\varepsilon W Q_\varepsilon W^2 Q_\varepsilon W P_\varepsilon\|}\,. \end{aligned} \tag{3.17}$$

In order to estimate the norm in the right side with the help of (3.9), we rewrite

$$P_\varepsilon W Q_\varepsilon W^2 Q_\varepsilon W P_\varepsilon = P_\varepsilon W^4 P_\varepsilon - P_\varepsilon W^3 P_\varepsilon W P_\varepsilon - P_\varepsilon W P_\varepsilon W^3 P_\varepsilon + P_\varepsilon W P_\varepsilon W^2 P_\varepsilon W P_\varepsilon\,. \tag{3.18}$$

On $\Omega_{N,\tau}$ the norm of this operator is bounded by $C\,N^2$ for all N large enough by (3.9). This concludes the proof. □

These preparations enable us to proof the following general result.

Theorem 3.4. *Consider the operator $H = \Gamma T + W$ on $\ell^2(\mathcal{Q}_N)$ with W satisfying the assumptions in Corollary 3.2 and let $\Omega_{N,\tau}$ with $\tau \in (0,1)$ arbitrary be the events constructed there. Then on $\Omega_{N,\tau}$ and for all N large enough the eigenvalues of H below $-\|W\|_\infty - \eta N$ with $\eta > 0$ are found in the union of intervals of radius $\mathcal{O}_{\Gamma,\eta}(N^{\frac{\tau-1}{2}})$ centered at*

$$(2n - N)\Gamma + \frac{w_N}{(2n-N)\Gamma} \tag{3.19}$$

with $n \in \{m \in \mathbb{N}_0\,|(2m-N)\Gamma < -\|W\|_\infty - \eta N\}$. Moreover, the ball centered at (3.19) contains exactly $\binom{N}{n}$ eigenvalues of H if $\Gamma > \eta + \|W\|_\infty/N$.

Proof. We write H using the block decomposition of $\ell^2(\mathcal{Q}_N)$ induced by P_ε and employ the Schur complement method. Since the Q_ε block is lower bounded according to (3.11), all eigenvalues E of H strictly below $-\|W\|_\infty - \Gamma\varepsilon N$ can be read from the equation

$$\begin{aligned} 0 \in \operatorname{spec}(T_\varepsilon(E)) \quad \text{with} \quad T_\varepsilon(E) &\coloneqq P_\varepsilon\Big(\Gamma T + \frac{N}{E}\Big) - E + Y_\varepsilon(E), \\ Y_\varepsilon(E) &\coloneqq\; P_\varepsilon W P_\varepsilon - \left(P_\varepsilon \frac{N}{E} + P_\varepsilon W R_\varepsilon(E) W P_\varepsilon\right). \end{aligned} \tag{3.20}$$

Lemma 3.3 combined with (3.11) and (3.7) implies that for any $\eta > 0$ at $\varepsilon = N^{(\tau-1)/2}$ and on the event $\Omega_{N,\tau}$ in Corollary 3.2

$$\sup_{E<-\|W\|_\infty-\eta N} \|Y_\varepsilon(E)\| \;\le\; C\max\{1,\Gamma\}\;\eta^{-2}\;N^{\frac{\tau-1}{2}}\,, \tag{3.21}$$

for all N large enough. As a consequence of standard perturbation theory [13, Corollary 3.2.6] and using the explicit values (1.4) of the spectrum of T, within this energy region the solution of (3.20) are found within the union of intervals of radius at most $C\max\{1,\Gamma\}\eta^{-2}N^{(\tau-1)/2}$ from the solutions to the equation

$$(2n-N)\Gamma + \frac{w_N}{z} - z = 0$$

with integers $2n < N(\Gamma - \|W\|_\infty - \eta)/\Gamma$. This leads to

$$z = \frac{2n-N}{2}\Gamma - \sqrt{\tfrac{1}{4}(2n-N)^2\Gamma^2 + w_N} = (2n-N)\Gamma + \frac{w_N}{(2n-N)\Gamma} + \mathcal{O}_\Gamma\left(N^{-1}\right),$$

which completes the proof of (3.19). The assertion concerning the range of the spectral projections on the small intervals around the above points follows from the monotonicity of $T_\varepsilon(E)$ and the fact that the eigenvalue $2n-N$ of T has multiplicity $\binom{N}{n}$. □

Theorem 1.3 now immediately follows.

Proof of Theorem 1.3. On $\Omega^{\mathrm{REM}}_{N,\eta/2}$ the REM's extremal values are bounded by $\|U\|_\infty \le N(\beta_c+\eta)$. Moreover, $\mathbb{E}\left[U(\boldsymbol{\sigma})^2\right] = N$ and $\mathbb{E}\left[U(\boldsymbol{\sigma})^8\right] = 105\;N^4$, so that U satisfies all requirements on W in Corollary 3.2. The claim is thus a straightforward consequence of Theorem 3.4 with $W = U$. □

3.3. Proof of Theorem 1.4

The proof of our second main result, Theorem 1.4, is based on delocalization properties of the eigenprojection of T, which will be derived using the semigroup properties of T. More generally, let $B \subset \mathcal{Q}_N$ be any subset of the Hamming cube and $T(B)$ the corresponding restriction, i.e, the operator with matrix elements $\langle\delta_{\boldsymbol{\sigma}}\,|\,T(B)\,\delta_{\boldsymbol{\sigma'}}\rangle \coloneqq -\mathbb{1}_{d(\boldsymbol{\sigma},\boldsymbol{\sigma'})=1}\mathbb{1}_B(\boldsymbol{\sigma})\mathbb{1}_B(\boldsymbol{\sigma'})$. For Hamming balls $B_K(\boldsymbol{\sigma}_0)$ the operator $T(B_K(\boldsymbol{\sigma}_0))$ was studied in Section 2 and abbreviated there by T_K. As all matrix elements are zero or negative, a stochastic representation is at hand: for any $\boldsymbol{\sigma},\boldsymbol{\sigma'} \in B$ and $\beta \ge 0$ there is a measure μ_B on the space of càdlàg-paths $\Omega(\boldsymbol{\sigma},\boldsymbol{\sigma'})$ on the hypercube with $\omega(0) = \boldsymbol{\sigma}$ and $\omega(1) = \boldsymbol{\sigma'}$ such that for any $V : B \to \mathbb{R}$ we have $\langle\delta_{\boldsymbol{\sigma}}\,|\,e^{-\beta(T(B)+V)}\delta_{\boldsymbol{\sigma'}}\rangle = \int_{\Omega(\boldsymbol{\sigma},\boldsymbol{\sigma'})} e^{-\beta\int_0^1 V(\omega(s))\,ds}\mu_B[d\omega]$. Such a representation can be derived via the Suzuki-Trotter-formula (see e.g. [50, Appendix B]). If $B = \mathcal{Q}_N$ the path measure is described in terms of independent Poisson jump processes, whereas for general B one has to take into account that the process is not allowed to leave the set B. Here, we do not use the stochastic representation but the related positivity of matrix elements for any $\beta \ge 0$:

$$0 \le \langle\delta_{\boldsymbol{\sigma}}\,|\,e^{-\beta(T(B)+V)}\delta_{\boldsymbol{\sigma'}}\rangle \le e^{-\min\beta V}\langle\delta_{\boldsymbol{\sigma}}\,|\,e^{-\beta T(B)}\delta_{\boldsymbol{\sigma'}}\rangle. \tag{3.22}$$

Since $-T(B)$ and $-T$ have nonnegative matrix elements and $\langle\delta_{\boldsymbol{\sigma}}\,|\,(-T(B))\,\delta_{\boldsymbol{\sigma'}}\rangle \le \langle\delta_{\boldsymbol{\sigma}}\,|\,(-T)\,\delta_{\boldsymbol{\sigma'}}\rangle$ for any $\boldsymbol{\sigma},\boldsymbol{\sigma'}$, we also conclude

$$\langle\delta_{\boldsymbol{\sigma}}\,|\,e^{-\beta T(B)}\delta_{\boldsymbol{\sigma'}}\rangle \le \langle\delta_{\boldsymbol{\sigma}}\,|\,e^{-\beta T}\delta_{\boldsymbol{\sigma'}}\rangle = (\cosh\beta)^N(\tanh\beta)^{d(\boldsymbol{\sigma},\boldsymbol{\sigma'})}, \tag{3.23}$$

where the last equality is by explicit calculation using the Hadamard transformation, i.e., the representation of T in terms of Pauli matrices.

Proposition 3.5. *Let $B \subset \mathcal{Q}_N$ and $V : B \to \mathbb{R}$ a potential with $V \geq -vN$ for some $0 \leq v < 1$. Then the eigenprojection $P_E := \mathbb{1}_{(-\infty,E)}(T(B)+V)$ onto eigenvalues $E \in [-N(1+v), -vN]$ satisfies:*

$$\max_{\boldsymbol{\sigma}} \langle \delta_{\boldsymbol{\sigma}} \,|\, P_E \, \delta_{\boldsymbol{\sigma}} \rangle \leq 2^{-N} \exp\left(N\gamma\left(\frac{1+\nu(E))}{2} \right) \right) \tag{3.24}$$

with the binary entropy γ from (1.16) *and $\nu(E) := \frac{E}{N} + v$. Moreover, for all normalised states $\psi \in \ell^2(B)$:*

$$\|P_E \psi\|_\infty^2 \ \leq 2^{-N} \exp\left(N\gamma\left(\frac{1+\nu(E))}{2} \right) \right). \tag{3.25}$$

Proof. The spectral theorem combined with an exponential Markov inequality implies for any $\beta \geq 0$:

$$\langle \delta_{\boldsymbol{\sigma}} \,|\, \mathbb{1}_{(-\infty,E)}(T(B)+V)\, \delta_{\boldsymbol{\sigma}} \rangle \leq e^{\beta E} \langle \delta_{\boldsymbol{\sigma}} \,|\, e^{-\beta(T(B)+V)}\, \delta_{\boldsymbol{\sigma}} \rangle \leq e^{\beta\nu(E)N} (\cosh\beta)^N.$$

The last inequality is a combination of (3.22) and (3.23). It remains to minimize the function $f(\beta) \coloneqq \beta\nu(E) + \ln\cosh\beta$ on $[0,\infty)$. The minimum is attained at $\beta^\star = \operatorname{artanh}(-\nu(E))$. To further simplify the result, we recall the elementary identities $\operatorname{artanh}(x) = \frac{1}{2}\ln\frac{1+x}{1-x}$ and $\cosh(\operatorname{artanh}(x)) = \frac{1}{\sqrt{1-x^2}}$ for $x \in (-1,1)$, which after some algebra lead to $f(\beta^\star) = -\ln 2 + \gamma((1+\nu(E))/2)$ and hence (3.24). The second assertion (3.25) is a direct consequence of (3.24). □

We are now ready to complete the proofs of the main results in the paramagnetic regime.

Proof of Theorem 1.4. We pick $\tau \in (0,1)$ and $0 < \eta < (\Gamma - \beta_c)/4$ arbitrary and restrict our attention to the event $\Omega_{N,\tau}^{\mathrm{per}} \cap \Omega_{N,\eta}^{\mathrm{REM}}$ on which the assertions of Corollary 3.2 for $W = U$ and Theorem 1.3 are valid.

For a proof of the first assertion, we apply Schur's complement formula to the ground state $\psi = \psi_1 + \psi_2$ of $H = \Gamma T + U$. We split ψ into $\psi_1 \in P_\varepsilon \ell^2(\mathcal{Q}_N)$ and $\psi_2 \in Q_\varepsilon \ell^2(\mathcal{Q}_N)$ such that:

$$\begin{aligned} (P_\varepsilon H P_\varepsilon - E - P_\varepsilon H R_\varepsilon(E) H P_\varepsilon)\, \psi_1 &= 0 \\ \psi_2 &= -R_\varepsilon(E) Q_\varepsilon H P_\varepsilon \psi_1, \end{aligned}$$

where $E = \inf\operatorname{spec} H = -\Gamma N - \frac{1}{\Gamma} + \mathcal{O}_\Gamma(N^{\frac{\tau-1}{2}})$ is the ground-state energy according to Theorem 1.3 since $\Gamma N - \|U\|_\infty > \frac{1}{2}(\Gamma - \beta_c)N > \eta N$ on $\Omega_{N,\eta}^{\mathrm{REM}}$ by the choice for η. Sticking to the notation (3.20), from the proof of Theorem 1.3 we conclude that the first equation can be rewritten in terms of

$$P_\varepsilon H P_\varepsilon - E - P_\varepsilon H R_\varepsilon(E) H P_\varepsilon = P_\varepsilon \Gamma T P_\varepsilon + (NE^{-1} - E) P_\varepsilon + Y_\varepsilon(E),$$

with $\|Y_\varepsilon(E)\| \leq \mathcal{O}_\Gamma(N^{\frac{\tau-1}{2}})$. Since T has an energy gap 2 above its unique ground state $\Phi_\emptyset$ (cf. (1.4)), we thus conclude

$$\|(\mathbb{1} - |\Phi_\emptyset\rangle\langle\Phi_\emptyset|)\psi_1\| \leq \mathcal{O}_\Gamma\left(N^{\frac{\tau-1}{2}}\right).$$

To further estimate the norm of $\psi_2 = -R_\varepsilon(E) Q_\varepsilon U \psi_1$, we recall that $\|R_\varepsilon(E)\| \leq \frac{C_\Gamma}{N}$ and $\|U\psi_1\|^2 \leq \|P_\varepsilon U^2 P_\varepsilon\| \leq \mathcal{O}(N)$ by Corollary 3.2. Hence, $\|\psi_2\|^2 \leq \mathcal{O}_\Gamma\left(\frac{1}{N}\right)$. We thus arrive at

$$\|\psi - \Phi_\emptyset\|^2 = \mathcal{O}_\Gamma\left(N^{\tau-1}\right). \tag{3.26}$$

For the second part, we recall the bound (1.7), and write $H = \Gamma(T + U/\Gamma)$. The claim now follows directly from Proposition 3.5. □

3.4. Improved delocalization estimates

The delocalization estimates on low-energy eigenfunctions established in Proposition 3.5 are not optimal. In particular, they become trivial in case the minimum of the potential v is close to one and E is close to $-N$. The latter corresponds to the critical case addressed in Proposition 1.8. In the following, we record an improved delocalization estimate, which involves the QREM with truncated potential on $\ell^2(\mathcal{Q}_N)$:

$$H_\delta \coloneqq \Gamma T + U_\delta, \qquad U_\delta \coloneqq U \mathbb{1}_{|U| \leq (\beta_c - \delta)N},$$

with truncation parameter $\delta > 0$, which will be allowed to be arbitrarily small. In that scenario we have the following non-optimal estimate:

Proposition 3.6. *There are $c, C > 0$ such that for any $\delta \in (0, \Gamma/25)$ there is some $\eta > 0$ and a sequence of events $\Omega_{N,\delta}$ with $\mathbb{P}(\Omega_{N,\delta}) \geq 1 - e^{-CN}$ on which for all N large enough at for all $\Gamma \geq \beta_c - \delta/4$:*

$$\max_{\boldsymbol{\sigma} \in \mathcal{Q}_N} \langle \delta_{\boldsymbol{\sigma}} \mid \mathbb{1}_{(-\infty, -(\Gamma - \eta)N)}(H_\delta)\, \delta_{\boldsymbol{\sigma}} \rangle \leq e^{-cN}, \tag{3.27}$$

Moreover, on $\Omega_{N,\delta}$ all eigenvalues of H_δ below $E < -(\Gamma - \delta/4)N \leq -(\beta_c - \delta/2)N$ are still described by (1.13) with an error $\mathcal{O}_{\Gamma,\delta}(N^{-\frac{1}{4}})$.

The proof of Proposition 3.6 is spelled at the end of this subsection.

As a preparation, we need the following probabilistic control on the frequency of large deviation sites in a ball of radius αN.

Lemma 3.7. *Let $\varepsilon, \alpha > 0$ be such that $\varepsilon^2 > 2\gamma(\alpha)$. Then there is $K = K(\varepsilon, \alpha) \in \mathbb{N}$ and $c = c(\varepsilon, \alpha) > 0$ such that the sequence of events*

$$\Omega_{N,\varepsilon,\alpha} \coloneqq \{\forall \boldsymbol{\sigma} \in \mathcal{Q}_N : \ |B_{\alpha N}(\boldsymbol{\sigma}_0) \cap \mathcal{L}_\varepsilon| < K\}$$

has a probability bounded by $\mathbb{P}(\Omega_{N,\varepsilon,\alpha}) \geq 1 - e^{-cN}$ for all sufficiently large N.

Proof. For any fixed $\boldsymbol{\sigma} \in \mathcal{Q}_N$ we estimate using the independence of the basic random variables and the standard Gaussian tail bound

$$\mathbb{P}(|B_{\alpha N}(\boldsymbol{\sigma}) \cap \mathcal{L}_\varepsilon| \geq K) \leq \binom{|B_{\alpha N}(\boldsymbol{\sigma})|}{K} e^{-K\varepsilon^2 N/2} \leq \exp\left(-\frac{KN}{2}\left(\varepsilon^2 - 2\gamma(\alpha) - o_\alpha(1)\right)\right).$$

The last estimate inserted the asymptotics $\ln |B_{\alpha N}| = N(\gamma(\alpha) + o_\alpha(1))$ of the size of a Hamming ball in terms of the binary entropy. The union bound implies $\mathbb{P}(\exists \boldsymbol{\sigma} \ : \ |B_{\alpha_0 N}(\boldsymbol{\sigma}) \cap \mathcal{L}_\varepsilon| \geq K) \leq 2^N \mathbb{P}(|B_{\alpha N}(\boldsymbol{\sigma}) \cap \mathcal{L}_\varepsilon| \geq K)$, which is exponentially small for all K large enough. □

Proposition 3.6 is based on a random-walk expansion for eigenvectors, which facilitates control of spherical means away from their maxima. Random walk techniques have been used in the theory of localization under the name 'locator' of 'Feenberg' expansions. We do not aim to extract optimal information from this technique, which would require much more work. Rather we highlight the usefulness dealing with the critical case. We will see another more refined use of spherical averaging techniques in Section 4.5.

As another preparation, we collect some basic properties of a simple random walk $(Z_k)_{k\in\mathbb{N}}$ on $\mathcal{Q}_N$, which starts at $Z_0 \coloneqq \boldsymbol{\sigma}_0 \in \mathcal{Q}_N$ and chooses in each unit time step one of the N neighboring vertices with equal probability $1/N$. Let

$$p_K(\boldsymbol{\sigma},\boldsymbol{\sigma}_0) \coloneqq \mathrm{Prob}(Z_K = \boldsymbol{\sigma} | Z_0 = \boldsymbol{\sigma}_0)$$

stand for the probability to arrive at $\boldsymbol{\sigma}$ after K steps. Moreover, for a subset $W \subset \mathcal{Q}_N$ let

$$M_K(W) \coloneqq \sum_{k=0}^{K} \mathbb{1}[Z_k \in W]$$

be the number of visits of the random walk in W up to time K. We will only need the following crude bounds, whose proofs we spell here for the reader's convenience. For further results on random walks on the Hamming cube, see e.g. [45] and references therein.

Lemma 3.8. *For all $\boldsymbol{\sigma},\boldsymbol{\sigma}_0 \in \mathcal{Q}_N$, all $\alpha \in (0, 3/16)$, and all N large enough:*

$$p_{\alpha N}(\boldsymbol{\sigma},\boldsymbol{\sigma}_0) \le \max\{e^{-\gamma(\alpha/8)N+o(N)}, e^{-\alpha N/8}\}. \tag{3.28}$$

For any finite subset $W \subset \mathcal{Q}_N$, all $t \in (0,\alpha]$ and all N large enough:

$$\mathrm{Prob}\left(M_{\alpha N}(W) \ge tN\right) \le \exp\left(-tN \ln\left(\frac{tN}{\alpha|W|e}\right)\right). \tag{3.29}$$

Proof. If $d = d(\boldsymbol{\sigma},\boldsymbol{\sigma}_0) \ge \alpha N/8$, we have by spherical symmetry and the asymptotics of the binomial coefficient

$$p_{\alpha N}(\boldsymbol{\sigma},\boldsymbol{\sigma}_0) = \binom{N}{d}^{-1} \sum_{\boldsymbol{\sigma}' \in S_d(\boldsymbol{\sigma}_0)} p_{\alpha N}(\boldsymbol{\sigma}',\boldsymbol{\sigma}_0) \le \binom{N}{d}^{-1} \le e^{-\gamma(\alpha/8)N+o(N)}.$$

To complete the proof (3.28), we discuss the case $d(\boldsymbol{\sigma},\boldsymbol{\sigma}_0) < \alpha N/8$. A simple random walk, which at step k is at distance $d = d(Z_k,\boldsymbol{\sigma}_0)) \in [1,\alpha N]$ to the starting point, has $N-d$ possibilities to move further away and only $d \le \alpha N$ to decrease the distance to $\boldsymbol{\sigma}_0$ by one. Hence, $\mathrm{Prob}(d(Z_{k+1},\boldsymbol{\sigma}_0) < d(Z_k,\boldsymbol{\sigma}_0)) \le \alpha$ for any $0 \le k \le \alpha N$. However, to end after αN steps at some $\boldsymbol{\sigma} \in B_{\alpha N/8}(\boldsymbol{\sigma}_0)$, the walk $(Z_k)_{k\in\mathbb{N}}$ has at least $\frac{3}{8}\alpha N$ steps, where it gets back closer to the center. Since the random variables $Y_k = \mathbb{1}[d(Z_{k+1},\boldsymbol{\sigma}_0) < d(Z_k,\boldsymbol{\sigma}_0)]$ are distributed as conditionally independent Bernoulli variables with success probability at most α, we thus arrive at

$$p_{\alpha N}(\boldsymbol{\sigma},\boldsymbol{\sigma}_0) \le \mathrm{Prob}\left(\sum_{k=1}^{\alpha N} Y_k \ge 3\alpha N/8\right) \le e^{-\alpha N/8},$$

by a standard Chernoff-bound for Bernoulli variables. This establishes (3.28).

For a proof of (3.29) we note that as $|W \cap S_1(\boldsymbol{\sigma})| \le |W|$ for any $\boldsymbol{\sigma} \in B_{\alpha N}(\boldsymbol{\sigma}_0)$

$$\mathrm{Prob}(Z_{k+1} \in W \,|\, Z_k = \boldsymbol{\sigma}) \le \frac{|W|}{N}.$$

The claim thus follows again by a standard Chernoff bound, since $M_{\alpha N}(W)$ is a sum of conditionally independent Bernoulli-type random variables with success probability smaller than $|W|/N$. □

Proof of Proposition 3.6. One easily sees that U_δ meets the requirements of Theorem 3.4 with variance $w_N = \mathbb{E}[U_\delta(\boldsymbol{\sigma})^2] = N(1 - \mathcal{O}(e^{-\frac{1}{2}(\beta_c-\delta)^2 N}))$. Consequently, for any $\tau \in (0,1)$ there is some sequence $\Omega_{N,\tau,\delta}$ with $\mathbb{P}(\Omega_{N,\tau,\delta}) \geq 1 - e^{-CN}$, and we arrive at the description of eigenvalues in (1.13) for all $E < -(\beta_c - \delta/2)N$. This also implies that for $\eta \in (0, \delta/2)$ and all N large enough:

$$\operatorname{Tr} \mathbb{1}_{(-\infty,-(\Gamma-\eta)N)}(H_\delta) \leq \operatorname{Tr} \mathbb{1}_{(-\infty,-(\Gamma-\eta)N)}(\Gamma T) = \sum_{n=0}^{N\eta/(2\Gamma)} \binom{N}{n} \leq e^{N\gamma(\eta/(2\Gamma))+o_\Gamma(N)}, \tag{3.30}$$

again by the known asymptotics of the binomial coefficients.

For a proof of the exponential delocalization estimate (3.27), we assume throughout the validity of $\Omega_{N,\tau,\delta}$ with some $\tau \in (0,1)$ and the event $\Omega_{N,\varepsilon,\alpha_0}$ of Lemma 3.7 with $\varepsilon \coloneqq \Gamma/100$ and some fixed $\alpha_0 > 0$ small enough such that $2\gamma(\alpha_0) < \varepsilon^2$. The intersection of these two events still has a probability, which is exponentially bounded from below independent of δ as required.

Let ψ be an ℓ^2-normalized eigenfunction of $\Gamma T + U_\delta$ with eigenvalue $E < -(\beta_c - \delta/2)N$ and suppose that $\boldsymbol{\sigma}_\psi \in \mathcal{Q}_N$ is a configuration, where ψ takes its maximum absolute value. To make the main idea transparent, we proceed in two steps.

Step 1: We first assume that $B_{\alpha_0 N}(\boldsymbol{\sigma}_\psi) \cap \mathcal{L}_\varepsilon = \emptyset$. The eigenvalue equation for ψ at any $\boldsymbol{\sigma} \in B_{\alpha_0 N}(\boldsymbol{\sigma}_\psi)$ together with the bound $U \geq -\varepsilon N$ implies

$$\begin{aligned} |\psi(\boldsymbol{\sigma})| &\leq \frac{\Gamma}{|E - U(\boldsymbol{\sigma})|} \sum_{\boldsymbol{\sigma}' \in S_1(\boldsymbol{\sigma})} |\psi(\boldsymbol{\sigma}')| \leq \frac{C_\Gamma(E,\varepsilon)}{N} \sum_{\boldsymbol{\sigma}' \in S_1(\boldsymbol{\sigma})} |\psi(\boldsymbol{\sigma}')|, \\ C_\Gamma(E,\varepsilon) &\coloneqq \frac{\Gamma}{|E|/N - \varepsilon} \end{aligned} \tag{3.31}$$

We start at $\boldsymbol{\sigma}_\psi$ and use this estimate iteratively αN times for some $\alpha < \alpha_0$ to arrive at

$$\begin{aligned} |\psi(\boldsymbol{\sigma}_\psi)| &\leq C_\Gamma(E,\varepsilon)^{\alpha N} \sum_{\boldsymbol{\sigma} \in B_{\alpha N}(\boldsymbol{\sigma}_\psi)} p_{\alpha N}(\boldsymbol{\sigma}, \boldsymbol{\sigma}_\psi) |\psi(\boldsymbol{\sigma})| \\ &\leq C_\Gamma(E,\varepsilon)^{\alpha N} \Big(\sum_{\boldsymbol{\sigma} \in B_{\alpha N}(\boldsymbol{\sigma}_\psi)} p_{\alpha N}(\boldsymbol{\sigma}, \boldsymbol{\sigma}_\psi)^2 \Big)^{1/2} \leq C_\Gamma(E,\varepsilon)^{\alpha N} \max_{\boldsymbol{\sigma} \in B_{\alpha N}(\boldsymbol{\sigma}_\psi)} p_{\alpha N}(\boldsymbol{\sigma}, \boldsymbol{\sigma}_\psi)^{1/2} \end{aligned} \tag{3.32}$$

where $p_{\alpha N}(\boldsymbol{\sigma}, \boldsymbol{\sigma}_\psi)$ is the probability of a simple random walk on $\mathcal{Q}_N$ starting at $\boldsymbol{\sigma}_\psi$ to arrive at $\boldsymbol{\sigma}$ after αN steps. Here we have the Cauchy-Schwarz inequality and the normalization of ψ as well as $p_{\alpha N}$. Since $|E| > (\Gamma - \delta/4)N \geq \Gamma N(1 - 1/100)$ we see that for N large enough: $C_\Gamma(E,\varepsilon) \leq \left(\frac{1}{1-1/50}\right)^{\alpha N} \leq e^{\alpha N/49}$. Together with the probability bound (3.28) our main estimate (3.32) yields

$$|\psi(\boldsymbol{\sigma}_\psi)|^2 \leq \max\{e^{(\frac{2\alpha}{49} - \gamma(\alpha/8) + o(1))\, N}, e^{-\frac{1}{12}\alpha N}\} =: e^{-c_\alpha N/2}. \tag{3.33}$$

Due to the bound (3.30) on the number of eigenvalues, which allows us to pick $\eta > 0$ arbitrarily small not to spoil any exponential decay of the eigenfunctions, the proof of the exponential bound (3.27) in case of Step 1 is completed if we choose $\alpha \in (0, \alpha_0)$ such that $\gamma(\alpha/8) > \frac{2\alpha}{49}$. This is always possible since γ has an infinite slope at zero.

Step 2: We now turn to general case, in which the intersection $W \coloneqq B_{\alpha_0 N}(\boldsymbol{\sigma}) \cap \mathcal{L}_\varepsilon$ is nonempty, but finite of size at most K. For $\boldsymbol{\sigma} \in W$ the spherical mean estimate (3.31) turns into

$$|\psi(\boldsymbol{\sigma})| \leq \frac{C_\Gamma(E, \beta_c - \delta)}{N} \sum_{\boldsymbol{\sigma}' \in S_1(\boldsymbol{\sigma})} |\psi(\boldsymbol{\sigma}')|$$

as we still have $U(\boldsymbol{\sigma}) \geq -(\beta_c - \delta)N$. For a random walk $(Z_k)_{k \in \mathbb{N}}$, which starts again at $Z_0 \coloneqq \boldsymbol{\sigma}_\psi$, let $M_{\alpha N}(W)$ stand for the number of visits of sites in W. We way modify our prior estimate by distinguishing between the random walks with a high visit number $M_{\alpha N}(W) > tN$ and low visit number $M_{\alpha N}(W) \leq tN$. Indeed, abbreviating by $p_{\alpha N}(\boldsymbol{\sigma}, \boldsymbol{\sigma}_\psi | M_{\alpha N}(W) < tN)$ the transition probability of the random walk to reach $\boldsymbol{\sigma}$ after αN steps and spending only less than tN steps in W, we have for any $t > 0$

$$\begin{aligned}
|\psi(\boldsymbol{\sigma}_\psi)| &\leq C_\Gamma(E, \varepsilon)^{(\alpha - t)N} C_\Gamma(E, \beta_c - \delta)^{tN} \sum_{\boldsymbol{\sigma} \in B_{\alpha N}(\boldsymbol{\sigma}_\psi)} p_{\alpha N}(\boldsymbol{\sigma}, \boldsymbol{\sigma}_\psi | M_{\alpha N}(W) < tN)\, |\psi(\boldsymbol{\sigma})| \\
&\quad + C_\Gamma(E, \beta_c - \delta)^{\alpha N} \sum_{\boldsymbol{\sigma} \in B_{\alpha N}(\boldsymbol{\sigma}_\psi)} p_{\alpha N}(\boldsymbol{\sigma}, \boldsymbol{\sigma}_\psi | M_{\alpha N}(W) \geq tN)\, |\psi(\boldsymbol{\sigma})| \\
&\leq C_\Gamma(E, \beta_c - \delta)^{tN} e^{-c_\alpha N/2} + C_\Gamma(E, \beta_c - \delta)^{\alpha N} \operatorname{Prob}(M_{\alpha N}(W) \geq tN),
\end{aligned}$$

where $c_\alpha > 0$ is the constant in (3.33). According to (3.29) the probability in the right side decays for any $t > 0$ faster than any exponential function. Thus, choosing $t = c_\alpha / (4 \ln C_\Gamma(E, \beta_c - \delta))$ yields $|\psi(\boldsymbol{\sigma}_\psi)|^2 \leq e^{-c_\alpha N/4}$ for N large enough and $c_\alpha > 0$ is a constant independent from δ and Γ. This completes the proof. □

4. Extreme localization regime

4.1. Deep-hole geometry

The proof of our main results in the spin-glass regime are based on the deep-hole geometry of the REM. They rest on the fact that the large extremal sites $\mathcal{L}_{\beta_c - \delta}$ of the REM, which were defined in (1.17), are well separated on $\mathcal{Q}_N$ at least if $\delta \in (0, \beta_c)$ is not too large.

Definition 4.1. *Let $\varepsilon, \delta > 0$ and $\alpha \in (0, \frac{1}{2})$. Then $U : \mathcal{Q}_N \to \mathbb{R}$ is said to satisfy:*

1. *a* local $(\varepsilon, \delta, \alpha)$-deep hole scenario on $B_{\alpha N}(\boldsymbol{\sigma})$ *with $\boldsymbol{\sigma} \in \mathcal{L}_{\beta_c - \delta}$ if:*
   a) $|U(\boldsymbol{\sigma}')| \leq \varepsilon N$ *for all $\boldsymbol{\sigma}' \in B_{\alpha N}(\boldsymbol{\sigma})$ with $\boldsymbol{\sigma}' \neq \boldsymbol{\sigma}$,*
   b) $u(\boldsymbol{\sigma}) \coloneqq \frac{1}{N^2} \sum_{\boldsymbol{\sigma}' \in S_1(\boldsymbol{\sigma})} |U(\boldsymbol{\sigma}')| \leq N^{-1/4}$.
2. *a* global $(\varepsilon, \delta, \alpha)$-deep hole scenario *if:*
   a) *U satisfies a local $(\varepsilon, \delta, \alpha)$-deep hole scenario on $B_{\alpha N}(\boldsymbol{\sigma})$ for all $\boldsymbol{\sigma} \in \mathcal{L}_{\beta_c - \delta}$,*
   b) *$B_{\alpha N}(\boldsymbol{\sigma}) \cap B_{\alpha N}(\boldsymbol{\sigma}') = \emptyset$ for all pairs $\boldsymbol{\sigma}, \boldsymbol{\sigma}' \in \mathcal{L}_{\beta_c - \delta}$ with $\boldsymbol{\sigma} \neq \boldsymbol{\sigma}'$.*

The probabilistic estimate for the occurrence of a global deep-hole scenario in the REM is the subject of the following lemma.

Lemma 4.2. *Let $\varepsilon, \delta > 0$ and $\alpha \in (0, 1/2)$ be such that*

$$2\gamma(3\alpha) + \delta(2\beta_c - \delta) < \varepsilon^2. \tag{4.1}$$

The event $\Omega_N(\varepsilon, \delta, \alpha) \coloneqq \{U$ satisfies a global $(\varepsilon, \delta, \alpha)$-deep hole scenario$\}$ occurs with probability exponentially close to one, i.e., there is some $c(\varepsilon, \delta, \alpha) > 0$ such that for all N sufficiently large:

$$\mathbb{P}\left(\Omega_N(\varepsilon, \delta, \alpha)\right) \geq 1 - e^{-c(\varepsilon,\delta,\alpha)N}. \tag{4.2}$$

Proof. We first bound the probability of the event

$$\widehat{\Omega}_N(\varepsilon, \delta, \alpha) \coloneqq \left\{\exists \boldsymbol{\sigma} \in \mathcal{L}_{\beta_c-\delta},\, \boldsymbol{\sigma}' \in B_{3\alpha N}(\boldsymbol{\sigma}) \backslash \{\boldsymbol{\sigma}\} \text{ s.t. } |U(\boldsymbol{\sigma}')| > \varepsilon N\right\}.$$

On its complement, all $\boldsymbol{\sigma} \in \mathcal{L}_{\beta_c-\delta}$ satisfy the first requirement in the local deep-hole definition on $B_{\alpha N}(\boldsymbol{\sigma}) \subset B_{3\alpha N}(\boldsymbol{\sigma})$, and the balls of radius αN around the large deviation sites are disjoint., i.e., the second requirement in the global deep-hole definition is also checked. By a union bound and independence, we conclude:

$$\begin{aligned}\mathbb{P}\left(\widehat{\Omega}_N(\varepsilon, \delta, \alpha)\right) &\leq \sum_{\boldsymbol{\sigma} \in \mathcal{Q}_N} \mathbb{P}(U(\boldsymbol{\sigma}) \leq -(\beta_c - \delta)N) \sum_{\boldsymbol{\sigma}' \in B_{3\alpha N}(\boldsymbol{\sigma}) \backslash \{\boldsymbol{\sigma}\}} \mathbb{P}(|U(\boldsymbol{\sigma}')| \geq \varepsilon N) \\ &\leq 2^{N+1} \left|B_{3\alpha N}\right| e^{-(\beta_c-\delta)^2 N/2} e^{-\varepsilon^2 N/2} \leq e^{\left(\gamma(3\alpha) + \beta_c\delta - \frac{\delta^2+\varepsilon^2}{2} + o(1)\right)N}.\end{aligned}$$

The second line is a result of the usual Gaussian-tail estimates and the fact that the volume of a Hamming ball of radius $\alpha N < N/2$ is asymptotically given in terms of the binary entropy, $\ln |B_{\alpha N}| = N(\gamma(\alpha) + o(1))$ as $N \to \infty$. Using assumption (4.1), we see that the above probability is exponentially small in N.

The proof is concluded by showing that the event

$$\Omega_N^u \coloneqq \left\{\max_{\boldsymbol{\sigma} \in \mathcal{Q}_N} u(\boldsymbol{\sigma}) \leq N^{-1/4}\right\} \tag{4.3}$$

occurs with a probability, which is exponentially close to one, i.e.

$$\mathbb{P}(\exists \boldsymbol{\sigma} \in \mathcal{Q}_N \text{ s.t. } u(\boldsymbol{\sigma}) > N^{-1/4}) \leq 2^{2N} e^{-N^{3/2}/2}. \tag{4.4}$$

For a proof of this bound, we rewrite the moment-generating function of $u(\boldsymbol{\sigma})$ for any $t > 0$ in terms of a standard normal variable g:

$$\mathbb{E}[e^{tu(\boldsymbol{\sigma})}] = \mathbb{E}[e^{tN^{-3/2}|g|}]^N \leq 2^N \mathbb{E}[e^{tN^{-3/2}g}]^N = 2^N e^{t^2/(2N^2)}.$$

By an exponential Chebychev-Markov estimate with $t = N^{7/4}$, this then yields $\mathbb{P}(u(\boldsymbol{\sigma}) > N^{-1/4}) \leq 2^N e^{-N^{3/2}/2}$, and hence the claim by a union bound using $|\mathcal{Q}_N| = 2^N$. □

4.2. Rank-one analysis

If U satisfies a local $(\varepsilon, \delta, \alpha)$-deep hole scenario on $B_{\alpha N}(\boldsymbol{\sigma})$ at some fixed $\boldsymbol{\sigma} \in \mathcal{L}_{\beta_c-\delta}$, it is natural to consider the Hamiltonian $H_{\alpha N}(\boldsymbol{\sigma}) = \Gamma T_{\alpha N} + U$ restricted to $\ell^2(B_{\alpha N}(\boldsymbol{\sigma}))$, i.e.

$$\langle \delta_{\boldsymbol{\tau}} | H_{\alpha N}(\boldsymbol{\sigma}) \delta_{\boldsymbol{\tau}'} \rangle = \langle \delta_{\boldsymbol{\tau}} | H \delta_{\boldsymbol{\tau}'} \rangle \; \mathbb{1}_{B_{\alpha N}(\boldsymbol{\sigma})}(\boldsymbol{\tau}) \mathbb{1}_{B_{\alpha N}(\boldsymbol{\sigma})}(\boldsymbol{\tau}'),$$

A spectral analysis of these self-adjoint matrices is facilitated by rank-one perturbation theory. Since $\delta_{\boldsymbol{\sigma}}$ is a cyclic vector for $H_{\alpha N}(\boldsymbol{\sigma})$, the spectrum can read from zeros of the meromorphic function given by

$$\begin{aligned}\langle\delta_{\boldsymbol{\sigma}}|\left(H_{\alpha N}(\boldsymbol{\sigma})-z\right)^{-1}\delta_{\boldsymbol{\sigma}}\rangle^{-1} &= U(\boldsymbol{\sigma})-\Sigma(\boldsymbol{\sigma},z),\\ \Sigma(\boldsymbol{\sigma},z) &\coloneqq -\langle\delta_{\boldsymbol{\sigma}}|\big(H'_{\alpha N}(\boldsymbol{\sigma})-z\big)^{-1}\delta_{\boldsymbol{\sigma}}\rangle^{-1},\end{aligned} \tag{4.5}$$

where $H'_{\alpha N}(\boldsymbol{\sigma})$ coincides with the matrix $H'_{\alpha N}(\boldsymbol{\sigma})$ when setting $U(\boldsymbol{\sigma})=0$. Moreover, an ℓ^2-normalized eigenvector φ_E corresponding to $E\in\operatorname{spec}H_{\alpha N}(\boldsymbol{\sigma})$ is given in terms of the free resolvent, i.e.,

$$\varphi_E(\boldsymbol{\tau})=-U(\boldsymbol{\sigma})\,\varphi_E(\boldsymbol{\sigma})\langle\delta_{\boldsymbol{\tau}}|\left(H'_{\alpha N}(\boldsymbol{\sigma})-E_{\boldsymbol{\sigma}}\right)^{-1}\delta_{\boldsymbol{\sigma}}\rangle, \tag{4.6}$$

for any $\boldsymbol{\tau}\in B_{\alpha N}(\boldsymbol{\sigma})$, cf. [5, Theorem 5.3]. The deep-hole scenario then entails the following information about the low-energy part of the spectrum.

Lemma 4.3. *Suppose U satisfies a local $(\varepsilon,\delta,\alpha)$-deep hole scenario on $B_{\alpha N}(\boldsymbol{\sigma})$ at some $\boldsymbol{\sigma}\in\mathcal{L}_{\beta_c-\delta}$ with*

$$2\Gamma\sqrt{\alpha(1-\alpha)}+\varepsilon<\beta_c-2\delta. \tag{4.7}$$

Then for all sufficiently large N, the spectrum $\operatorname{spec}_{E_\delta}H_{\alpha N}(\boldsymbol{\sigma})\coloneqq\operatorname{spec}H_{\alpha N}(\boldsymbol{\sigma})\cap(-\infty,E_\delta)$ below $E_\delta\coloneqq -N(\beta_c-\delta)$ consists only of one simple eigenvalue $E_{\boldsymbol{\sigma}}$ which satisfies

$$\begin{aligned}E_{\boldsymbol{\sigma}} &= U(\boldsymbol{\sigma})+\frac{\Gamma^2N}{E_{\boldsymbol{\sigma}}}+\frac{\Gamma^2}{E_{\boldsymbol{\sigma}}^2}\sum_{\boldsymbol{\sigma}'\in S_1(\boldsymbol{\sigma})}U(\boldsymbol{\sigma}')+\mathcal{O}_{\Gamma,\delta,\varepsilon}\left(N^{-5/4}\right)\\ &= U(\boldsymbol{\sigma})+\frac{\Gamma^2N}{U(\boldsymbol{\sigma})}+\mathcal{O}_{\Gamma,\delta}\left(N^{-1/4}\right).\end{aligned} \tag{4.8}$$

The ℓ^2-normalized eigenfunction $\psi_{\boldsymbol{\sigma}}$ corresponding to $E_{\boldsymbol{\sigma}}$ satisfies:

1. *for any $K\in\mathbb{N}$ and for all $\boldsymbol{\sigma}'\in S_K(\boldsymbol{\sigma})$*

$$|\psi(\boldsymbol{\sigma}')|=\mathcal{O}_{\Gamma,\delta,K}(N^{-K}),\quad \text{and}\quad \sum_{\boldsymbol{\sigma}'\notin B_K(\boldsymbol{\sigma})}|\psi(\boldsymbol{\sigma}')|^2=\mathcal{O}_{\Gamma,\delta,K}(N^{-(K+1)}). \tag{4.9}$$

2. *for any $\alpha'\in(0,\alpha]$ there are $C=C(\Gamma,\delta),c=c(\alpha,\alpha')\in(0,\infty)$, such that*

$$\sum_{\boldsymbol{\sigma}'\notin B_{\alpha' N}(\boldsymbol{\sigma})}|\psi_{\boldsymbol{\sigma}}(\boldsymbol{\sigma}')|^2\le CN\exp\left(-Nc\right). \tag{4.10}$$

Proof. The deep-hole scenario together with (2.3) and (4.7) implies that for all sufficiently large N:

$$H'_{\alpha N}(\boldsymbol{\sigma})\ge\Gamma T_{\alpha N}-\varepsilon N\ge-(\beta_c-2\delta)N>E_\delta. \tag{4.11}$$

By rank-one perturbation theory, there is exactly one zero of (4.5) and hence one simple eigenvalue $E_{\boldsymbol{\sigma}}$ of $H_{\alpha N}(\boldsymbol{\sigma})$ below $\inf\operatorname{spec}H'_{\alpha N}(\boldsymbol{\sigma})$. A Rayleigh-Ritz bound

$$E_{\boldsymbol{\sigma}}\le\langle\delta_{\boldsymbol{\sigma}}|H_{\alpha N}(\boldsymbol{\sigma})\delta_{\boldsymbol{\sigma}}\rangle=U(\boldsymbol{\sigma})\le E_\delta \tag{4.12}$$

provides a first, crude estimate on this eigenvalue. According to (4.6) the corresponding ℓ^2-normalized eigenvector $\psi_{\boldsymbol{\sigma}}$ satisfies for all $\boldsymbol{\sigma}' \in B_{\alpha N}(\boldsymbol{\sigma})$:

$$\begin{aligned}\psi_{\boldsymbol{\sigma}}(\boldsymbol{\sigma}') &= -U(\boldsymbol{\sigma})\,\psi_{\boldsymbol{\sigma}}(\boldsymbol{\sigma})\langle\delta_{\boldsymbol{\sigma}'}|\left(H'_{\alpha N}(\boldsymbol{\sigma})-E_{\boldsymbol{\sigma}}\right)^{-1}\delta_{\boldsymbol{\sigma}}\rangle\\ &\le -U(\boldsymbol{\sigma})\,\langle\delta_{\boldsymbol{\sigma}'}|\left(\Gamma T_{\alpha N}-(E_{\boldsymbol{\sigma}}+\varepsilon N)\right)^{-1}\delta_{\boldsymbol{\sigma}}\rangle\\ &\le -U(\boldsymbol{\sigma})\;\Gamma^{-1}\;\langle\delta_{\boldsymbol{\sigma}'}|\left(T_{\alpha N}-(U(\boldsymbol{\sigma})+\varepsilon N)\Gamma^{-1}\right)^{-1}\delta_{\boldsymbol{\sigma}}\rangle. \end{aligned}\tag{4.13}$$

As in (4.11), these inequalities are consequence of the deep-hole scenario, the crude bound (4.12) combined with the positivity of the semigroup, cf. (3.22). The assertions (4.9) and (4.10) concerning the decay rates of the eigenfunction are now a straightforward consequence of Proposition 2.4. For its application, we note that the assumption (4.7) ensure that $\operatorname{dist}(\Gamma^{-1}\operatorname{spec}T_{\alpha N}, U(\boldsymbol{\sigma})+\varepsilon N) \ge \Gamma^{-1}(E_\delta - U(\boldsymbol{\sigma})+\delta)N \ge \frac{\delta}{\Gamma}N$. The first inequality in Proposition 2.4 then yields

$$|\psi_{\boldsymbol{\sigma}}(\boldsymbol{\sigma}')| \le \frac{\beta_c-\delta}{\delta}\binom{N}{d(\boldsymbol{\sigma}_0,\boldsymbol{\sigma})}^{-1/2}\;2^{-\min\{d(\boldsymbol{\sigma},\boldsymbol{\sigma}'),\,\rho_0(\alpha)N\}},\tag{4.14}$$

where we also used that the function $U \mapsto \frac{-U}{x-U}$ is monotone increasing in U on $(-\infty, x)$. Hence, (4.10) follows after a summation over the spheres $S_d(\boldsymbol{\sigma})$ with $d \in (\alpha' N, \alpha N]$. The above binomial decay factor is thereby exactly compensated by the volume $|S_d(\boldsymbol{\sigma})| = \binom{N}{d}$. The claimed bounds (4.9) follow analogously from the respective bounds in Proposition 2.4.

For a proof of the asymptotics (4.8), we first consider the eigenvalue equation at any $\boldsymbol{\sigma}' \in S_1(\boldsymbol{\sigma})$:

$$\begin{aligned}E_{\boldsymbol{\sigma}}\psi_{\boldsymbol{\sigma}}(\boldsymbol{\sigma}') &= U(\boldsymbol{\sigma}')\psi_{\boldsymbol{\sigma}}(\boldsymbol{\sigma}') - \Gamma\psi_{\boldsymbol{\sigma}}(\boldsymbol{\sigma}) - \Gamma\sum_{\boldsymbol{\sigma}''\in S_1(\boldsymbol{\sigma}')\setminus\{\boldsymbol{\sigma}\}}\psi_{\boldsymbol{\sigma}}(\boldsymbol{\sigma}'')\\ &= U(\boldsymbol{\sigma}')\psi_{\boldsymbol{\sigma}}(\boldsymbol{\sigma}') - \Gamma\psi_{\boldsymbol{\sigma}}(\boldsymbol{\sigma}) + \mathcal{O}_{\Gamma,\delta}(N^{-1}).\end{aligned}\tag{4.15}$$

The uniform $\mathcal{O}_{\Gamma,\delta}(N^{-1})$ estimate is a direct consequence of (4.9). This equation can be rewritten as

$$\psi_{\boldsymbol{\sigma}}(\boldsymbol{\sigma}') = -\frac{\Gamma}{E_{\boldsymbol{\sigma}}-U(\boldsymbol{\sigma}')}\left(\psi_{\boldsymbol{\sigma}}(\boldsymbol{\sigma})+\mathcal{O}_{\Gamma,\delta}(N^{-1})\right),\tag{4.16}$$

which we insert into the eigenvalue equation at $\boldsymbol{\sigma}$:

$$\begin{aligned}E_{\boldsymbol{\sigma}}\psi_{\boldsymbol{\sigma}}(\boldsymbol{\sigma}) &= U(\boldsymbol{\sigma})\psi_{\boldsymbol{\sigma}}(\boldsymbol{\sigma}) - \Gamma\sum_{\boldsymbol{\sigma}'\in S_1(\boldsymbol{\sigma})}\psi_{\boldsymbol{\sigma}}(\boldsymbol{\sigma}')\\ &= U(\boldsymbol{\sigma})\psi_{\boldsymbol{\sigma}}(\boldsymbol{\sigma}) + \frac{\Gamma^2}{E_{\boldsymbol{\sigma}}}\left(\sum_{\boldsymbol{\sigma}'\in S_1(\boldsymbol{\sigma})}\frac{\psi_{\boldsymbol{\sigma}}(\boldsymbol{\sigma})+\mathcal{O}_{\Gamma,\delta}(N^{-1})}{1-U(\boldsymbol{\sigma}')/E_{\boldsymbol{\sigma}}}\right)\\ &= U(\boldsymbol{\sigma})\psi_{\boldsymbol{\sigma}}(\boldsymbol{\sigma}) + \frac{\Gamma^2}{E_{\boldsymbol{\sigma}}}\left(\sum_{\boldsymbol{\sigma}'\in S_1(\boldsymbol{\sigma})}\frac{\psi_{\boldsymbol{\sigma}}(\boldsymbol{\sigma})}{1-U(\boldsymbol{\sigma}')/E_{\boldsymbol{\sigma}}}\right)+\mathcal{O}_{\Gamma,\delta,\varepsilon}(N^{-5/4})\\ &= \left[U(\boldsymbol{\sigma})+\frac{\Gamma^2 N}{E_{\boldsymbol{\sigma}}}+\frac{\Gamma^2}{E_{\boldsymbol{\sigma}}}\left(\sum_{\boldsymbol{\sigma}'\in S_1(\boldsymbol{\sigma})}\frac{U(\boldsymbol{\sigma}')}{E_{\boldsymbol{\sigma}}}\right)\right]\psi_{\boldsymbol{\sigma}}(\boldsymbol{\sigma})+\mathcal{O}_{\Gamma,\delta,\varepsilon}(N^{-5/4}).\end{aligned}\tag{4.17}$$

The third equality follow from a second-order Taylor expansion with an error estimate using $|U(\boldsymbol{\sigma}')|^2 \leq \varepsilon N |U(\boldsymbol{\sigma}')|$ as well as the bound on $u(\boldsymbol{\sigma})$ in the deep-hole assumption in Definition 4.1. Since $\psi_{\boldsymbol{\sigma}}(\boldsymbol{\sigma}) = 1 + \mathcal{O}(N^{-1})$, the first identity in (4.8) follows. For a proof of the second identity, we again use the bound on $u(\boldsymbol{\sigma})$ as well as our crude estimate (4.12) to estimate the last term in the above square brackets by $\mathcal{O}_{\Gamma,\delta}(N^{-1/4})$. This concludes the proof. □

4.3. Spectral averaging

In order to control the probability of resonances between distinct extremal sites, we will use the spectral averaging technique from the theory of random operators [5, Chapter 4.1].

Lemma 4.4. *Let $\varepsilon, \delta > 0$ and $\alpha \in (0, 1/2)$ be such that (4.1) and (4.7) holds. Then there is some $c = c(\varepsilon, \delta, \alpha) > 0$ such that for all N sufficiently large and*

1. *for any real interval I:*

$$\mathbb{P}\left(\exists \boldsymbol{\sigma} \in \mathcal{L}_{\beta_c - \delta} \text{ s.t. } \operatorname{spec}_{E_\delta} H_{\alpha N}(\boldsymbol{\sigma}) \cap I \neq \emptyset\right) \leq 2|I| \, e^{\beta_c \delta N - \delta^2 N/2} + e^{-cN}. \tag{4.18}$$

2. *for any $r > 0$:*

$$\mathbb{P}\left(\exists \boldsymbol{\sigma}, \boldsymbol{\sigma}' \in \mathcal{L}_{\beta_c - \delta}, \boldsymbol{\sigma} \neq \boldsymbol{\sigma}' \text{ s.t. } \operatorname{dist}\left(\operatorname{spec}_{E_\delta} H_{\alpha N}(\boldsymbol{\sigma}), \operatorname{spec}_{E_\delta} H_{\alpha N}(\boldsymbol{\sigma}')\right) \leq r\right) \leq 4re^{(2\beta_c\delta - \delta^2)N} + e^{-cN}. \tag{4.19}$$

Proof. For a proof of the above estimates, we may thus restrict attention to events in $\Omega_N(\varepsilon, \delta, \alpha)$, cf. Lemma 4.2.

1. According to Lemma 4.3, under the deep-hole scenario $\operatorname{spec}_{E_\delta} H_{\alpha N}(\boldsymbol{\sigma}) \cap I \neq \emptyset$ if and only if $E_{\boldsymbol{\sigma}} = \inf \operatorname{spec} H_{\alpha N}(\boldsymbol{\sigma}) \in I$. Since $\psi_{\boldsymbol{\sigma}}(\boldsymbol{\sigma})^2 \geq 1/2$ by Lemma 4.3 for sufficiently large N and all $\boldsymbol{\sigma} \in \mathcal{L}_{\beta_c - \delta}$, the latter implies $\langle \delta_{\boldsymbol{\sigma}} | P_I \delta_{\boldsymbol{\sigma}} \rangle \geq 1/2$, where P_I denotes the spectral projection of $H_{\alpha N}(\boldsymbol{\sigma})$ onto I. A union bound hence enables to estimate the probability of the event in the left side of (4.18) and its intersection with $\Omega_N(\varepsilon, \delta, \alpha)$ by

$$\sum_{\boldsymbol{\sigma} \in \mathcal{Q}_N} \mathbb{P}\left(\boldsymbol{\sigma} \in \mathcal{L}_{\beta_c - \delta} \text{ and } \langle \delta_{\boldsymbol{\sigma}} | P_I \delta_{\boldsymbol{\sigma}} \rangle \geq 1/2\right) \leq 2 \, \mathbb{E}\left[\mathbb{1}[\boldsymbol{\sigma} \in \mathcal{L}_{\beta_c - \delta}] \, \langle \delta_{\boldsymbol{\sigma}} | P_I \delta_{\boldsymbol{\sigma}} \rangle\right].$$

The inequality is a Chebychev-Markov estimate. Conditioning on all random variables aside from $U(\boldsymbol{\sigma})$, the integration of $p_I(U(\boldsymbol{\sigma})) := \langle \delta_{\boldsymbol{\sigma}} | P_I \delta_{\boldsymbol{\sigma}} \rangle$ with respect to the random variable $U(\boldsymbol{\sigma})$ is bounded with the help of the spectral averaging lemma (also referred to as Wegner estimate, cf. [5, Thm. 4.1]). It yields

$$\int_{-\infty}^{-(\beta_c - \delta)N} p_I(u) \, e^{-\frac{u^2}{2N}} \frac{du}{\sqrt{2\pi N}} \leq e^{-(\beta_c - \delta)^2 N/2} |I|.$$

This completes the proof of the first assertion.

2. On $\Omega_N(\varepsilon, \delta, \alpha)$, we may assume that $B_{\alpha N}(\boldsymbol{\sigma}) \cap B_{\alpha N}(\boldsymbol{\sigma}') = \emptyset$ for all pairs $\boldsymbol{\sigma}, \boldsymbol{\sigma}' \in \mathcal{L}_{\beta_c - \delta}$. This ensures that the random variables $E_{\boldsymbol{\sigma}'} = \inf \operatorname{spec} H_{\alpha N}(\boldsymbol{\sigma}')$ and $U(\boldsymbol{\sigma}')$ are independent of all random

variables in $B_{\alpha N}(\boldsymbol{\sigma})$. Using the strategy as in 1., we thus bound the probability of the event in the left side of (4.19) and its intersection with $\Omega_N(\varepsilon, \delta, \alpha)$ by

$$\sum_{\boldsymbol{\sigma},\boldsymbol{\sigma}' \in \mathcal{Q}_N} \mathbb{E}\left[\mathbb{1}[\boldsymbol{\sigma}' \in \mathcal{L}_{\beta_c-\delta} \text{ and } B_{\alpha N}(\boldsymbol{\sigma}) \cap B_{\alpha N}(\boldsymbol{\sigma}') = \emptyset]\right.$$
$$\left. \times \mathbb{P}\left(\boldsymbol{\sigma} \in \mathcal{L}_{\beta_c-\delta} \text{ and } \langle \delta_{\boldsymbol{\sigma}} | P_{(E_{\boldsymbol{\sigma}'}-r, E_{\boldsymbol{\sigma}'}+r)} \delta_{\boldsymbol{\sigma}} \rangle \geq 1/2 \,|\, B_{\alpha N}(\boldsymbol{\sigma})^c\right)\right] \leq 2^{2N+2} e^{-(\beta_c-\delta)^2 N} r.$$

where $\mathbb{P}(\cdot | B_{\alpha N}(\boldsymbol{\sigma})^c)$ denotes the conditional expectation, conditioned on all random variables aside from those in $B_{\alpha N}(\boldsymbol{\sigma})$ and P_I is still the spectral projection of $H_{\alpha N}(\boldsymbol{\sigma})$ onto I. The last inequality resulted from an application of the bound from 1. to the conditional expectation. This completes the proof of the second assertion.

□

4.4. Proof of Theorem 1.5

The proof of Theorem 1.5 makes use of the deep-hole geometry of the REM. If U satisfies a global $(\varepsilon, \delta, \alpha)$-deep hole scenario, we study the auxiliary Hamiltonian

$$H' := \left(\bigoplus_{\boldsymbol{\sigma} \in \mathcal{L}_{\beta_c-\delta}} H_{\alpha N}(\boldsymbol{\sigma}) \right) \bigoplus H_r, \tag{4.20}$$

with operators $H_{\alpha N}(\boldsymbol{\sigma})$, whose action is restricted to the non-intersecting balls $B_{\alpha N}(\boldsymbol{\sigma})$ around extremal sites $\boldsymbol{\sigma} \in \mathcal{L}_{\beta_c-\delta}$. These operator have been introduced and studied in Subsection 4.2. The remainder H_r is that part of H which purely belongs to the complement of the union of balls,

$$\langle \delta_{\boldsymbol{\tau}} | H_r \delta_{\boldsymbol{\tau}'} \rangle = \langle \delta_{\boldsymbol{\tau}} | H \delta_{\boldsymbol{\tau}'} \rangle \left(1 - \sum_{\boldsymbol{\sigma} \in \mathcal{L}_{\beta_c-\delta}} \mathbb{1}_{B_{\alpha N}(\boldsymbol{\sigma})}(\boldsymbol{\tau}) \right) \left(1 - \sum_{\boldsymbol{\sigma} \in \mathcal{L}_{\beta_c-\delta}} \mathbb{1}_{B_{\alpha N}(\boldsymbol{\sigma})}(\boldsymbol{\tau}') \right).$$

The difference between the Hamiltonian of interest $H = \Gamma T + U$ and the auxiliary H' is

$$H - H' =: -\Gamma A =: -\Gamma \bigoplus_{\boldsymbol{\sigma} \in \mathcal{L}_{\beta_c-\delta}} A_{\boldsymbol{\sigma}}.$$

It describes the hopping between the balls and the complementary configuration space, i.e.,

$$\langle \delta_{\boldsymbol{\tau}} | A_{\boldsymbol{\sigma}} \delta_{\boldsymbol{\tau}'} \rangle = \mathbb{1}_{d(\boldsymbol{\tau},\boldsymbol{\tau}')=1} (\mathbb{1}_{d(\boldsymbol{\tau},\boldsymbol{\sigma})=\alpha N} \mathbb{1}_{d(\boldsymbol{\tau}',\boldsymbol{\sigma})=\alpha N+1} + \mathbb{1}_{d(\boldsymbol{\tau},\boldsymbol{\sigma})=\alpha N+1} \mathbb{1}_{d(\boldsymbol{\tau}',\boldsymbol{\sigma})=\alpha N}).$$

The norm of A can be bounded as follows

$$\|A\| = \max_{\boldsymbol{\sigma} \in \mathcal{L}_{\beta_c-\delta}} \|A_{\boldsymbol{\sigma}}\| \leq \|T_{\alpha N+1}\| = 2N\sqrt{\alpha(\alpha-1)} + o_\alpha(N), \tag{4.21}$$

where the last equality is (2.2). It is easy to see that $\|A\|$ is indeed of order N. However, for energies below $E_\delta = -N(\beta_c - \delta)$, the perturbation is of a much smaller magnitude. This is the basic idea in the proofs of our main results for the localization regime. As a preparation, we also need the following result, which is implicitly contained in [53].

Proposition 4.5 (cf. [53]). *For all $\Gamma, \delta > 0$ the truncated Hamiltonian $H \coloneqq \Gamma T + U \mathbb{1}_{U \geq -(\beta_c - \delta)N}$ acting on $\ell^2(\mathcal{Q}_N)$ is lower bounded by*

$$\inf \operatorname{spec} H \geq -N \max\{\Gamma, \beta_c - \delta\} + o_{\Gamma,\delta}(N)$$

except for an event of exponentially small probability.

Proof. The values of the truncated REM potential $U \mathbb{1}[U(\boldsymbol{\sigma}) \geq -(\beta_c - \delta)N]$ are still independently distributed and satisfy a large deviation principle. The peeling principle [53, Thm 2.3] then implies that the negative free energy of H at $\beta > 0$ is a maximum of the truncated REM and the pure paramagnet. The result on the ground-state energy thus follows in the limit $\beta \to \infty$. □

We remark that the methods in [53] can be used to replace the $o(N)$ estimate by $\mathcal{O}(\sqrt{N})$.

Proof of Theorem 1.5. We only study the joint event $\Omega_N(\Gamma, \delta, \alpha)$ on which i) the bound in Proposition 4.5 applies, and ii) U satisfies a global $(\varepsilon, \delta, \alpha)$-deep hole scenario with parameters

$$\varepsilon = \frac{\beta_c}{2} \quad \text{and} \quad \delta \in (0, \min\{\beta_c - \Gamma, \beta_c/8\}),$$

and $\alpha > 0$ small enough such that (4.1) and $2\Gamma\sqrt{\alpha(1-\alpha)} < \delta/8$, and hence in particular (4.7) is satisfied. Together with Lemma 4.2 this ensures that $\Omega_N(\Gamma, \delta, \alpha)$ occurs with a probability of at least $1 - e^{-cN}$ with at some $c \equiv c(\Gamma, \delta, \alpha) > 0$. Moreover:

1. From Lemma 4.3 we learn that for any $\boldsymbol{\sigma} \in \mathcal{L}_{\beta_c - \delta}$ the spectrum $\operatorname{spec} H_{\alpha N}(\boldsymbol{\sigma})$ below $E_\delta = -N(\beta_c - \delta)$ consists of just one eigenvalue $E_{\boldsymbol{\sigma}} = \inf \operatorname{spec} H_{\alpha N}(\boldsymbol{\sigma})$, which is given by (4.8) with an error term $\mathcal{O}_{\Gamma,\delta}\left(N^{-1/4}\right)$ uniformly for all $\boldsymbol{\sigma} \in \mathcal{L}_{\beta_c - \delta}$.

2. By the variational principle and the natural embedding of Hilbert spaces, the ground state energy of H_r is bounded from below by that of $\Gamma T + U \mathbb{1}_{U \geq -(\beta_c - \delta)N}$ on $\ell^2(\mathcal{Q}_N)$. The lower bound in Proposition 4.5 then shows that

$$\inf \operatorname{spec} H_r \geq -N \left(\beta_c - \delta + o_{\Gamma,\delta}(1)\right).$$

Hence, H_r does not contribute to the low-energy spectrum of H' below $E_{\delta/2} = -N(\beta_c - \delta/2)$ for all N large enough. Moreover, the spectral projection $P_\delta \coloneqq \mathbb{1}_{(-\infty, E_{\delta/2})}(H')$ can be written as

$$P_\delta = \sum_{\boldsymbol{\sigma} \in \mathcal{L}_{\beta_c - \delta},\, E_{\boldsymbol{\sigma}} < E_{\delta/2}} |\psi_{\boldsymbol{\sigma}}\rangle\langle\psi_{\boldsymbol{\sigma}}| \tag{4.22}$$

in terms of rank-one projections of the ℓ^2-normalized ground states $\psi_{\boldsymbol{\sigma}}$ of $H_{\alpha N}(\boldsymbol{\sigma})$. We thus conclude for some $C = C(\Gamma, \delta) < \infty$, and $c = c(\alpha) > 0$

$$\|AP_\delta\| = \max_{\boldsymbol{\sigma} \in \mathcal{L}_{\beta_c - \delta}} \|A_{\boldsymbol{\sigma}} \psi_{\boldsymbol{\sigma}}\| \leq \|A\| \max_{\boldsymbol{\sigma} \in \mathcal{L}_{\beta_c - \delta}} \Big(\sum_{\boldsymbol{\sigma}' \in S_{\alpha N}(\boldsymbol{\sigma})} \left|\psi_{\boldsymbol{\sigma}}\left(\boldsymbol{\sigma}'\right)\right|^2 \Big)^{1/2} \leq C\ N^2\ e^{-cN}, \tag{4.23}$$

where the inequalities follow from (4.21) and (4.10) together with the fact that $A_{\boldsymbol{\sigma}}$ only acts on the part of $\psi_{\boldsymbol{\sigma}}$ on $S_{\alpha N}(\boldsymbol{\sigma})$.

We then rewrite H using the block decomposition of $\ell^2(\mathcal{Q}_N)$ induced by P_δ and $Q_\delta \coloneqq 1 - P_\delta$ and again employ the Schur complement method. Since H' is diagonal in this decomposition and its Q_δ projection has a spectrum above the threshold energy $E_{\delta/2}$, it remains to investigate the blocks of the perturbation ΓA:

1. Since P_δ is supported entirely on the balls, the first diagonal term vanishes, i.e. $P_\delta A P_\delta = 0$. The operator norms of the off-diagonals $\|P_\delta A(1-P_\delta)\| \leq \|AP_\delta\|$ are exponentially small by (4.23).

2. The operator $Q_\delta A Q_\delta$ is bounded from below by $-\|A\|$ which is estimated in (4.21). We thus conclude that for all N large enough:

$$\begin{aligned} Q_\delta H' + Q_\delta A Q_\delta &\geq E_{\delta/2} - \|A\| \geq -N\left(\beta_c - \delta/2 + 2\Gamma\sqrt{\alpha(1-\alpha)} + o_{\Gamma,\alpha}(1)\right) \\ &\geq -N\left(\beta_c - \delta/4\right). \end{aligned}$$

   Consequently, the Schur complement matrix

$$S_\delta(E) := \left(Q_\delta H' + Q_\delta A Q_\delta - E\right)^{-1}$$

   is well defined on $Q_\delta \ell^2(\mathcal{Q}_N)$ and bounded, $\|S_\delta(E)\| \leq (E_{\delta/4} - E)^{-1}$ for any $E < E_{\delta/4}$.

The spectrum of H below $E_{\delta/4} = -N(\beta_c - \delta/4)$ is thus characterized using Schur's method, which yields:

1. $E < E_{\delta/4}$ is an eigenvalue of H if and only if $E \in \operatorname{spec}(P_\delta H' - P_\delta A S_\delta(E) A P_\delta)$.

2. The ℓ^2-normalized eigenvector ψ corresponding to E and H satisfies:

$$\begin{aligned} (P_\delta H' - E P_\delta)\psi &= P_\delta A S_\delta(E) A P_\delta \psi \\ Q_\delta \psi &= -S_\delta(E) A P_\delta \psi. \end{aligned} \tag{4.24}$$

We now proceed with the completion of the proof of the assertion on the spectrum and eigenvectors separately.

Spectrum: The spectrum of H below $E_{\delta/8}$ is determined through the above Schur complement method. Since for all $E \leq E_{\delta/8}$ at at some $C = C(\Gamma,\delta) < \infty$ and $c = c(\alpha) > 0$

$$\|P_\delta A S_\delta(E) A P_\delta\| \leq \|S_\delta(E)\| \, \|AP_\delta\|^2 \leq C \, N^3 \, e^{-2cN}, \tag{4.25}$$

the eigenvalues below $E_{\delta/8}$ thus coincide with the eigenvalues of $P_\delta H'$ below this energy up to an error, which is exponentially small in N [13, Corollary 3.2.6]. Since the eigenvalues of $P_\delta H'$ are given by (4.8), the assertion in Theorem 1.5 follows.

Eigenvectors: We concentrate our attention on energies below $E_s = -N(\beta_c - s)$ with $s \in (0, \delta/8]$ small enough such that $2\beta_c s < c$ with the decay rate $c > 0$ from (4.25). This ensures that $e^{-\alpha c N} < e^{-2\beta_c s N} =: r(s)$ for all sufficiently large N. According to the spectral averaging Lemma 4.4, since $s \leq \delta/8$ and the condition (4.7) is monotone in δ, the event

$$\left\{\forall \boldsymbol{\sigma}, \boldsymbol{\sigma}' \in \mathcal{L}_{\beta_c - s}, \boldsymbol{\sigma} \neq \boldsymbol{\sigma}' : \quad \operatorname{dist}\left(\operatorname{spec}_{E_s} H_{\alpha N}(\boldsymbol{\sigma}), \operatorname{spec}_{E_s} H_{\alpha N}(\boldsymbol{\sigma}')\right) > r(s)\right\} \tag{4.26}$$

has probability of at least $1 - 4e^{-s^2 N} - e^{-cN}$ for some $c > 0$. We may therefore assume its occurrence.

Perturbation theory based on the above Schur complement analysis and (4.25) (combined with the characterization of eigenvalues established in Theorem 1.5) then guarantees that the eigenvector

ψ of H corresponding to the eigenvalue $E = U(\boldsymbol{\sigma}) + \Gamma^2 N/U(\boldsymbol{\sigma}) + \mathcal{O}(N^{-1/4})$, which is uniquely characterized by $\boldsymbol{\sigma} \in \mathcal{L}_{\beta_c - s}$, is norm-close to the ground-state eigenvector $\psi_{\boldsymbol{\sigma}}$ of $H_{\alpha N}(\boldsymbol{\sigma})$, i.e.,

$$\begin{aligned} \|\psi - \psi_{\boldsymbol{\sigma}}\| &\leq \|P_\delta \psi - \psi_{\boldsymbol{\sigma}}\| + \|Q_\delta \psi\| \\ &\leq \frac{\|P_\delta A S_\delta(E) A P_\delta\|}{r(s)} + \|S_\delta(E)\| \, \|A P_\delta\| \leq C \, e^{-cN}. \end{aligned} \tag{4.27}$$

Here the inequalities combine (4.24)–(4.26). The rest of the claim on the ℓ^2-estimates of the eigenvectors then follows from the respective properties of $\psi_{\boldsymbol{\sigma}}$ established in Lemma 4.3. The event $\Omega^{\mathrm{loc}}_{N,\Gamma,\delta}$ is then defined by specifying a value for $\alpha_0 = \alpha_0(\Gamma, \delta)$ and intersecting $\Omega_N(\Gamma, \delta, \alpha_0)$ with (4.26).

□

4.5. Proof of Theorem 1.7

All assertions concerning the ℓ^2-properties of the ground-state can easily be collected from the proof of Theorem 1.5.

Proof of Theorem 1.7 – ℓ^2-properties. According to Theorem 1.5 for all events aside from one of exponentially small probability, there is some $\boldsymbol{\sigma}_0 \in \mathcal{Q}_N$ such that the ground state eigenvector is approximated by $\|\psi - \delta_{\boldsymbol{\sigma}_0}\|^2_{\ell^2} = \mathcal{O}_\Gamma\left(\frac{1}{N}\right)$. The estimate $\mathcal{O}_\Gamma\left(\frac{1}{N}\right)$ does not depend on δ anymore as we may fix δ, if we only consider the ground state. This will be always assumed in the following. Moreover, the ground-state energy is $E = U(\boldsymbol{\sigma}_0) + \frac{\Gamma^2 N}{U(\boldsymbol{\sigma}_0)} + \mathcal{O}_\Gamma\left(N^{-1/4}\right)$, where $U(\boldsymbol{\sigma}_0)$ is one of the REM's extremal energies for which we may assume that

$$|U(\boldsymbol{\sigma}_0) + \beta_c N| \leq \mathcal{O}(\sqrt{N}), \quad \text{and hence} \quad |E + \beta_c N| \leq \mathcal{O}(\sqrt{N}) \tag{4.28}$$

at the expense of excluding another event of exponentially small probability stemming from deviations to the known extremal statistics of the REM, cf. (1.7).

It thus remains to establish the assertion on the first order perturbation $\xi \in \ell^2(\mathcal{Q}_N)$. That $\langle \xi | H \xi \rangle$ agrees with the ground state energy up to order $o_\Gamma(1)$ is a result of a simple calculation and a comparison with the above formula for E. It remains to prove $\|\psi - \xi\|^2 = \mathcal{O}_\Gamma(N^{-2})$. To this end, we revisit the proof of Theorem 1.5. From the validity of the global $(\beta_c/2, \delta, \alpha)$-deep hole scenario specified there and in view of (4.9), it suffices to show

$$\left| \psi(\boldsymbol{\sigma_0}) - \sqrt{1 - \frac{\Gamma^2}{\beta_c^2 N}} \right|^2 = \mathcal{O}_\Gamma(N^{-2}) \quad \text{and} \quad \sum_{\boldsymbol{\sigma} \in S_1(\boldsymbol{\sigma}_0)} \left| \psi(\boldsymbol{\sigma}) - \frac{\Gamma}{\beta_c N} \right|^2 = \mathcal{O}_\Gamma(N^{-2}). \tag{4.29}$$

For a proof of these assertions, we use the eigenvalue equation (4.16) on $S_1(\boldsymbol{\sigma}_0)$ together with $\psi(\boldsymbol{\sigma}_0) = 1 + \mathcal{O}_\Gamma(N^{-1})$. If we pick $\boldsymbol{\sigma} \in S_1(\boldsymbol{\sigma}_0)$, this yields

$$\begin{aligned} \psi(\boldsymbol{\sigma}) - \frac{\Gamma}{\beta_c N} &= -\frac{\Gamma}{E - U(\boldsymbol{\sigma})} \left(1 + \mathcal{O}_\Gamma(N^{-1})\right) - \frac{\Gamma}{\beta_c N} \\ &= \frac{\Gamma U(\boldsymbol{\sigma})}{\beta_c N (E - U(\boldsymbol{\sigma}))} + \mathcal{O}_\Gamma(N^{-3/2}). \end{aligned}$$

Here the last step also relied on the estimate $|U(\boldsymbol{\sigma})| \leq \varepsilon N$ valid in the $(\varepsilon, \delta, \alpha)$-deep hole scenario, as well as (4.28). With a suitable constant $C = C(\Gamma) < \infty$, we then have

$$\sum_{\boldsymbol{\sigma} \in S_1(\boldsymbol{\sigma}_0)} \left| \psi(\boldsymbol{\sigma}) - \frac{\Gamma}{\beta_c N} \right|^2 \leq \frac{C}{N^4} \sum_{\boldsymbol{\sigma} \in S_1(\boldsymbol{\sigma}_0)} U(\boldsymbol{\sigma})^2 + \mathcal{O}_\Gamma(N^{-2})$$

An exponential Chebychev-Markov estimate leads to $\mathbb{P}(N^{-2} \sum_{\boldsymbol{\sigma} \in S_1(\boldsymbol{\sigma}_0)} (U(\boldsymbol{\sigma})^2 - N)) \geq 1) \leq e^{-cN}$ for some $c > 0$. Thus, except for an event of exponentially small probability the second claim in (4.29) holds. Since ψ is ℓ^2-normalized, this leads to

$$\psi(\boldsymbol{\sigma_0})^2 = 1 - \sum_{\boldsymbol{\sigma} \in S_1(\boldsymbol{\sigma}_0)} \psi(\boldsymbol{\sigma})^2 + \mathcal{O}_\Gamma(N^{-2}) = 1 - \frac{\Gamma^2}{\beta_c^2 N} + \mathcal{O}_\Gamma(N^{-2}),$$

which readily implies the first claim in (4.29). □

For a proof of the ℓ^1-estimate on the ground state eigenfunction, we need to sharpen estimates on the large-deviation geometry of the REM. To this end we define for $\varepsilon, \delta > 0$ the following tripartition of the Hamming cube:

$$\begin{aligned} A_1(\varepsilon) &\coloneqq \{\boldsymbol{\sigma} \in \mathcal{Q}_N \,|\, |U(\boldsymbol{\sigma})| \leq \varepsilon N\} \\ A_2(\varepsilon, \delta) &\coloneqq \{\boldsymbol{\sigma} \in \mathcal{Q}_N \,|\, \varepsilon N < |U(\boldsymbol{\sigma})| \leq (\beta_c - \delta) N\} \\ A_3(\delta) &\coloneqq \{\boldsymbol{\sigma} \in \mathcal{Q}_N \,|\, |U(\boldsymbol{\sigma})| > (\beta_c - \delta) N\}. \end{aligned}$$

A modification of ideas used in the proof of Lemma 4.2 and [52, Lemma 2] yields:

Lemma 4.6. *For any $\varepsilon > 0$ there exist $K = K(\varepsilon) \in \mathbb{N}$ and a family of events $\Omega_{\varepsilon,N}$ such that for N large enough*

(i) For any $\boldsymbol{\sigma} \in A_2(\varepsilon, \delta) \cup A_3(\delta)$: $\quad |B_4(\boldsymbol{\sigma}) \cap (A_2(\varepsilon, \delta) \cup A_3(\delta))| \leq K \quad$ *on $\Omega_{\varepsilon,N}$.*

(ii) $\mathbb{P}(\Omega_{\varepsilon,N}) \geq 1 - 2^{-N}$.

Proof. Let $\Omega_{\varepsilon,N,K}$ be the event, where the assertion (i) holds true with constant K. It remains to show that the complement satisfies $\mathbb{P}(\Omega^c_{\varepsilon,N,K}) \leq 2^{-N}$ for an appropriate choice for K and N large enough. To this end we estimate

$$\begin{aligned} &\mathbb{P}(\Omega^c_{\varepsilon,N,K}) = \mathbb{P}(\exists\, \boldsymbol{\sigma} \in A_2(\varepsilon, \delta) \cup A_3(\delta) \text{ s.t. } |B_4(\boldsymbol{\sigma}) \cap (A_2(\varepsilon, \delta) \cup A_3(\delta))| \geq K) \\ &\leq \sum_{\boldsymbol{\sigma}_0 \in \mathcal{Q}_N} \mathbb{P}(|U(\boldsymbol{\sigma}_0)| \geq \varepsilon N)\, \mathbb{P}(\exists\, K-1 \text{ different } \boldsymbol{\sigma}_1, \dots \boldsymbol{\sigma}_{K-1} \in B_4(\boldsymbol{\sigma}_0) \backslash \{\boldsymbol{\sigma}_0\} \text{ s.t.} \\ &\qquad\qquad |U(\boldsymbol{\sigma}_j)| \geq \varepsilon N \text{ for } j = 1, \dots, K-1) \cdot \\ &\leq \binom{N^4}{K-1} 2^N\, \mathbb{P}(|U(\boldsymbol{\sigma}_0)| \geq \varepsilon N)^K \leq N^{4K} 2^N e^{-KN\varepsilon^2/2}, \end{aligned}$$

Here the second line is a consequence of the union bound and the third line follows from the independence and a simple counting argument. Choosing $K > 4 \ln 2/\varepsilon^2$, we see that $\mathbb{P}(\Omega^c_{\varepsilon,N,K}) < 2^{-N}$ for N large enough.

□

As a final preparation, we also need the following elementary observation on the size of large deviation sites.

Lemma 4.7. *For any $\delta \in (0, \beta_c)$ and all N:*

$$\mathbb{P}\left(|A_3(\delta)| \geq 2e^{\beta_c \delta N}\right) \leq e^{-N\delta^2/2}.$$

Proof. The cardinality $|A_3(\delta)|$ is a sum of 2^N independent Bernoulli variables with success probability $p = \mathbb{P}(|U(\boldsymbol{\sigma})| > (\beta_c - \delta)N) \leq 2e^{-\frac{1}{2}(\beta_c-\delta)^2 N}$ such that $\mathbb{E}[|A_3((\delta))|] = 2^N p$. The claim thus follows from a standard Markov estimate. □

We are finally ready to finish the proof of our main result in the localization regime.

Proof of Theorem 1.7 – ℓ^p-properties. We first observe that the claims on the ℓ^p-norms immediately follow from the ℓ^1-norm asymptotics (1.25). To see this, recall that $\psi(\boldsymbol{\sigma}_0) = 1 + o_\Gamma(1)$ for some $\boldsymbol{\sigma}_0 \in \mathcal{Q}_N$, and that $\psi(\boldsymbol{\sigma}) \leq c\, N^{-1}$ for all $\boldsymbol{\sigma} \neq \boldsymbol{\sigma}_0$. Hence for any $1 < p < \infty$:

$$1 + o_\Gamma(1) \leq \|\psi\|_{\ell^p}^p \leq 1 + \frac{c^{p-1}}{N^{p-1}} \sum_{\boldsymbol{\sigma} \neq \boldsymbol{\sigma}_0} \psi(\boldsymbol{\sigma}) \leq 1 + \frac{c^{p-1}}{N^{p-1}} \|\psi\|_{\ell^1} = 1 + o_{\Gamma,p}(1).$$

It therefore remains to establish (1.25).

Recalling that the ground state wavefunction ψ is positive, we can write $\|\psi\|_{\ell^1} = \sum_{\boldsymbol{\sigma}} \psi(\boldsymbol{\sigma})$. The eigenvalue equation for ψ leads to

$$\begin{aligned} E \sum_{\boldsymbol{\sigma}} \psi(\boldsymbol{\sigma}) &= +\Gamma \sum_{\boldsymbol{\sigma}} (T\psi)(\boldsymbol{\sigma}) + \sum_{\boldsymbol{\sigma}} (U\psi)(\boldsymbol{\sigma}) = -\Gamma N \sum_{\boldsymbol{\sigma}} \psi(\boldsymbol{\sigma}) - \sum_{\boldsymbol{\sigma}} U(\boldsymbol{\sigma})\psi(\boldsymbol{\sigma}) \\ &= -\Gamma N \sum_{\boldsymbol{\sigma}} \psi(\boldsymbol{\sigma}) + U(\boldsymbol{\sigma}_0)\psi(\boldsymbol{\sigma}_0) + \sum_{\boldsymbol{\sigma} \neq \boldsymbol{\sigma}_0} U(\boldsymbol{\sigma})\psi(\boldsymbol{\sigma}). \end{aligned} \tag{4.30}$$

The second equality follows from the fact that each $\boldsymbol{\sigma}$ has N neighbors. The main idea is now to show that the remainder term $\sum_{\boldsymbol{\sigma} \neq \boldsymbol{\sigma}_0} U(\boldsymbol{\sigma})\psi(\boldsymbol{\sigma})$ can be controlled by the other two terms on the right side. Here, we use the tripartition $A_1(\varepsilon), A_2(\varepsilon, \delta), A_3(\delta)$ of the configuration space and bound the contribution of each A_i separately.

In the following, we fix $\delta, \alpha > 0$ small enough, such that the REM satisfies a global $(\beta_c/2, \delta, \alpha)$-deep hole scenario with a probability which is exponentially close to one. Moreover, we pick $\varepsilon > 0$ arbitrary and fix $K = K(\varepsilon) \in \mathbb{N}$ the assertions of Lemma 4.6 hold on a joint event on which the global $(\beta_c/2, \delta_0, \alpha_0)$-deep hole scenario applies as well. This event still has a probability of at least $1 - e^{-c(\delta,\alpha)N}$ with some $c(\delta, \alpha) > 0$, which is independent of ε.

Contribution of $A_1(\varepsilon)$: In this case we use the trivial estimate, $\left|\sum_{\boldsymbol{\sigma} \in A_1} U(\boldsymbol{\sigma})\psi(\boldsymbol{\sigma})\right| \leq \varepsilon N \|\psi\|_{\ell^1}$.

Contribution of $A_3(\delta)$: We only consider $\delta \leq \delta_0$, such that configurations $\boldsymbol{\sigma} \in A_3(\delta) \setminus \{\boldsymbol{\sigma}_0\}$ lie outside the ball $B_{\alpha_0 N}(\boldsymbol{\sigma}_0)$. In particular, there is some $c > 0$ such that for all N large enough and all $\boldsymbol{\sigma} \in A_3(\delta) \setminus \{\boldsymbol{\sigma}_0\}$ the ground state is uniformly bounded, $|\psi(\boldsymbol{\sigma})| \leq e^{-cN}$. We now pick $\delta \coloneqq \min\{\delta_0, c/(4\beta_c)\}$ and shrink the considered event such that $|A_3(\delta)| \leq 2\ e^{Nc/4}$. According to

Lemma 4.7 this event still has a probability greater than $1 - e^{-c(\delta,\alpha)N}$ with some $c(\delta,\alpha) > 0$. On this event, we conclude for all N large enough

$$\sum_{\boldsymbol{\sigma}\in A_3(\delta)\setminus\{\boldsymbol{\sigma}_0\}} |U(\boldsymbol{\sigma})|\psi(\boldsymbol{\sigma}) \leq e^{-Nc/2}.$$

Contribution of $A_2(\varepsilon,\delta)$: We first consider the configurations in $A_2(\varepsilon,\delta)$ close to the center $\boldsymbol{\sigma}_0$, which we estimate for N large by

$$\sum_{\boldsymbol{\sigma}\in A_2(\varepsilon,\delta)\cap B_4(\boldsymbol{\sigma}_0)} |U(\boldsymbol{\sigma})|\psi(\boldsymbol{\sigma}) \leq |A_2(\varepsilon,\delta)\cap B_4(\boldsymbol{\sigma}_0)| \max_{\boldsymbol{\sigma}\in B_4(\boldsymbol{\sigma}_0)\setminus\{\boldsymbol{\sigma}_0\}} |U(\boldsymbol{\sigma})|\psi(\boldsymbol{\sigma}) \leq C\,K$$

with some $C = C(\Gamma)$. We use $|U(\boldsymbol{\sigma})| \leq \beta_c N/2$ due to the validity of the global $(\beta_c/2,\delta,\alpha)$-deep hole scenario as well as the pointwise bound $\psi(\boldsymbol{\sigma}) \leq CN^{-1}$ for all $\boldsymbol{\sigma} \in B_4(\boldsymbol{\sigma}_0)$ with $\boldsymbol{\sigma} \neq \boldsymbol{\sigma}_0$.

It remains to consider $\boldsymbol{\sigma} \in A_2(\varepsilon,\delta) \setminus B_4(\boldsymbol{\sigma}_0)$. The eigenvalue equation reads

$$|E - U(\boldsymbol{\sigma})|\psi(\boldsymbol{\sigma}) = \Gamma \sum_{\boldsymbol{\sigma}'\in S_1(\boldsymbol{\sigma})} \psi(\boldsymbol{\sigma}').$$

Since $E \leq (\beta_c - \delta/2)N$ for N large enough, we obtain for $\boldsymbol{\sigma} \in A_2(\varepsilon,\delta)$ the bound

$$\psi(\boldsymbol{\sigma}) \leq \frac{2\Gamma}{\delta N} \sum_{\boldsymbol{\sigma}'\in S_1(\boldsymbol{\sigma})} \psi(\boldsymbol{\sigma}').$$

The essence of the following argument is that the value of any $\psi(\boldsymbol{\sigma})$ is comparable to the mean on the corresponding $S_1(\boldsymbol{\sigma})$ sphere and, thus, ψ cannot take especially large values on $A_2(\varepsilon,\delta)$. To make this intuition precise, we separate the $A_3(\delta)$ configurations, which we possibly encounter in the spherical mean and repeat the procedure for the remaining $\boldsymbol{\sigma}' \in S_1(\boldsymbol{\sigma})$. This leads to

$$\begin{aligned}\psi(\boldsymbol{\sigma}) &\leq \frac{2\Gamma}{\delta N} \sum_{\boldsymbol{\sigma}'\in S_1(\boldsymbol{\sigma})\cap A_3(\delta)} \psi(\boldsymbol{\sigma}') + \frac{4\Gamma^2}{\delta^2 N^2} \sum_{\boldsymbol{\sigma}'\in S_1(\boldsymbol{\sigma})\setminus A_3(\delta)} \sum_{\boldsymbol{\sigma}''\in S_1(\boldsymbol{\sigma}')} \psi(\boldsymbol{\sigma}'') \\ &\leq \frac{2\Gamma}{\delta N} \sum_{\boldsymbol{\sigma}'\in S_1(\boldsymbol{\sigma})\cap A_3(\delta)} \psi(\boldsymbol{\sigma}') + \frac{4\Gamma^2}{\delta^2 N}\psi(\boldsymbol{\sigma}) + \frac{8\Gamma^2}{\delta^2 N^2} \sum_{\boldsymbol{\sigma}'\in S_2(\boldsymbol{\sigma})} \psi(\boldsymbol{\sigma}'),\end{aligned}$$

which for N large enough implies

$$\psi(\boldsymbol{\sigma}) \leq \frac{4\Gamma}{\delta N} \sum_{\boldsymbol{\sigma}'\in S_1(\boldsymbol{\sigma})\cap A_3(\delta)} \psi(\boldsymbol{\sigma}') + \frac{16\Gamma^2}{\delta^2 N^2} \sum_{\boldsymbol{\sigma}'\in S_2(\boldsymbol{\sigma})} \psi(\boldsymbol{\sigma}').$$

We now further shrink the considered event to ensure that $\|U\|_\infty \leq 2\beta_c N$ holds true. This happens for all but an event of exponentially probability, cf. (1.6). Thus, for N large enough

$$\begin{aligned}\left|\sum_{\boldsymbol{\sigma}\in A_2\setminus B_4(\boldsymbol{\sigma}_0)} U(\boldsymbol{\sigma})\psi(\boldsymbol{\sigma})\right| &\leq 2\beta_c N \sum_{\boldsymbol{\sigma}\in A_2\setminus B_4(\boldsymbol{\sigma}_0)} \psi(\boldsymbol{\sigma}) \\ &\leq \sum_{\boldsymbol{\sigma}\in A_2\setminus B_4(\boldsymbol{\sigma}_0)} \Big(\frac{8\beta_c\Gamma}{\delta} \sum_{\boldsymbol{\sigma}'\in S_1(\boldsymbol{\sigma})\cap A_3(\delta)} \psi(\boldsymbol{\sigma}') + \frac{16\beta_c\Gamma^2}{\delta^2 N} \sum_{\boldsymbol{\sigma}'\in S_2(\boldsymbol{\sigma})} \psi(\boldsymbol{\sigma}')\Big) \\ &\leq \frac{8\beta_c K\Gamma}{\delta} \sum_{\boldsymbol{\sigma}\in A_3(\delta)\setminus\{\boldsymbol{\sigma}_0\}} \psi(\boldsymbol{\sigma}) + \frac{16\beta_c\Gamma^2 K}{\delta^2 N}\|\psi\|_{\ell^1} \leq e^{-Nc/4} + \frac{16\beta_c\Gamma^2 K}{\delta^2 N}\|\psi\|_{\ell^1}.\end{aligned}$$

In the third line we used the observation that each configuration $\boldsymbol{\sigma} \in \mathcal{Q}_N$ appears in the summation at most K times due to Lemma 4.6. The last step is a consequence of our exponential bound on $\psi(\boldsymbol{\sigma})$ on the $A_3(\delta)$-configurations.

Combining the partial results on each A_J, we arrive with some $C = C(\Gamma)$ at the bound

$$|\sum_{\boldsymbol{\sigma}\neq\boldsymbol{\sigma}_0} U(\boldsymbol{\sigma})\psi(\boldsymbol{\sigma})| \leq (2\varepsilon + \mathcal{O}_{K,\Gamma}(N^{-1}))N\|\psi\|_{\ell^1} + 4CK$$

which is valid on with probability of at least $1 - e^{-cN}$ with some $c > 0$ which in independent of ε. Since $\varepsilon > 0$ was arbitrary, the claimed convergence now follows from (4.30). □

5. Free energy asympotics

For our proof of Theorem 1.10 we exploit that the partition function is determined by the eigenvalues close to the thermal averages

$$\langle U\rangle_\beta^{\mathrm{cl}} \coloneqq \frac{\operatorname{Tr} U e^{-\beta U}}{\operatorname{Tr} e^{-\beta U}} \quad \text{or} \quad \langle T\rangle_\beta^{\mathrm{pm}} \coloneqq \frac{\operatorname{Tr} T e^{-\beta T}}{\operatorname{Tr} e^{-\beta T}}, \tag{5.1}$$

depending on the phase. To determine their behavior we consider the local region around $\boldsymbol{\sigma} \in \mathcal{L}_\varepsilon$, where $\varepsilon > 0$ has to be allowed to be arbitrarily small. In this case, we cannot guarantee anymore that all balls $B_R(\boldsymbol{\sigma})$ are disjoint. However, we will show that this is still true for isolated extremal sites $\boldsymbol{\sigma} \in \mathcal{L}_\varepsilon$, which are in the majority. Then, we establish the order-one corrections of Theorem 1.5 for those isolated large deviations. Based on these results, we prove Theorem 1.10 via a suitable approximation argument using auxiliary operators on cut domains of the configuration space.

5.1. Basic large deviations

We first record some standard facts in the statistical mechanics of the pure REM and pure paramagnet.

Proposition 5.1. *1. For any $\beta \geq 0$ we have $\langle T\rangle_\beta^{pm} = -N\tanh\beta$. Moreover, for any $\beta \geq 0, \delta > 0$ there exists some $c = c(\beta,\delta) > 0$ such that*

$$\frac{\operatorname{Tr} \mathbb{1}_{[-N(\tanh\beta+\delta),-N(\tanh\beta-\delta)]}(T)e^{-\beta T}}{\operatorname{Tr} e^{-\beta T}} \geq 1 - e^{-cN}. \tag{5.2}$$

2. For $\beta < \beta_c$ we have almost surely $\langle U\rangle_\beta^{cl} = -(\beta + o(1))N$. Moreover, for $\beta < \beta_c$ and $\delta > 0$ there exists some $c = c(\beta,\delta) > 0$ such that

$$\frac{\operatorname{Tr} \mathbb{1}_{[-N(\beta+\delta),-N(\beta-\delta)]}(U)e^{-\beta U}}{\operatorname{Tr} e^{-\beta U}} \geq 1 - e^{-cN} \tag{5.3}$$

except for an exponentially small event.

3. For $\beta > \beta_c$ we have almost surely $\langle U\rangle_\beta^{cl} = -(\beta_c + o(1))N$. Moreover, for $\beta > \beta_c$ and $\delta > 0$ there exists some $c = c(\delta) > 0$ such that

$$\frac{\operatorname{Tr} \mathbb{1}_{(-\infty,-N(\beta_c-\delta)]}(U)e^{-\beta U}}{\operatorname{Tr} e^{-\beta U}} \geq 1 - e^{-cN}. \tag{5.4}$$

The proof for the expressions of the thermal averages $\langle T\rangle_\beta^{\mathrm{pm}}, \langle U\rangle_\beta^{\mathrm{cl}}$ is by differentiating the explicit formulas for the pressure with respect to β. The results on the concentration of the Gibbs measure are then of Cramér type and follow from the usual convexity estimates of the (explicit) free energy.

5.2. Spectral analysis on clusters

In the proofs of Theorem 1.5 and 1.7 we derived the order-one correction of the energy levels $U(\boldsymbol{\sigma})$ caused by extremal sites $\boldsymbol{\sigma} \in \mathcal{L}_\varepsilon$ with $\varepsilon \approx \beta_c$ from a local analysis on non-overlapping balls $B_R(\boldsymbol{\sigma})$ of some radius R. For the proof of Theorem 1.10 however, we need good control on all eigenvalues with energy below $-\varepsilon N$ with $\varepsilon > 0$ arbitrary and, thus, the large deviation set $\mathcal{L}_\varepsilon$ has to be considered for any $\varepsilon > 0$. The balls $B_R(\boldsymbol{\sigma})$ then have a nonempty intersection and the aim of this subsection is to deal with this modified situation. Let us introduce some definitions and notation.

Definition 5.2. *Let $\varepsilon > 0$ and $k \in \mathbb{N}_0$. We denote $\boldsymbol{\sigma} \overset{k}{\sim} \boldsymbol{\sigma}' \iff d(\boldsymbol{\sigma}, \boldsymbol{\sigma}') \leq 2k + 2$. We call a set $G \subset \mathcal{L}_\varepsilon$ (k,ε)-*connected *(with respect to $\overset{k}{\sim}$) if for any $\boldsymbol{\sigma}, \boldsymbol{\sigma}' \in G$ there exists a sequence $\boldsymbol{\sigma} = \boldsymbol{\sigma}^{(0)}, \boldsymbol{\sigma}^{(1)}, \cdots, \boldsymbol{\sigma}^{(m)} = \boldsymbol{\sigma}'$ such that $\boldsymbol{\sigma}^{(i)} \in G$ and $\boldsymbol{\sigma}^{(i)} \overset{k}{\sim} \boldsymbol{\sigma}^{(i+1)}$ for all $0 \leq i \leq m-1$. If $G \subset \mathcal{L}_\varepsilon$ is (k,ε)-connected and for any (k,ε)-connected G' with $G \subset G' \subset \mathcal{L}_\varepsilon$ it follows $G = G'$, we call G a* (k,ε)-component. *We denote the family of (k,ε)-components of $\mathcal{L}_\varepsilon$ by $\mathcal{G}_{k,\varepsilon}$.*

We call $\boldsymbol{\sigma} \in \mathcal{Q}_N$ (k,ε)-isolated *if $G = \{\boldsymbol{\sigma}\} \in \mathcal{G}_{k,\varepsilon}$ and $I_{k,\varepsilon}$ denotes the collection of (k,ε)-isolated configurations.*

The case $k = 0$ coincides with the notion of 'gap-connected' used in [51, 52, 53].

The extremal set $\mathcal{L}_\varepsilon$ naturally decomposes in its components, i.e., $\mathcal{L}_\varepsilon = \cup_{G \in \mathcal{G}_{k,\varepsilon}} G$. We define for each (k,ε)-component G the corresponding cluster

$$C_k(G) \coloneqq \bigcup_{\boldsymbol{\sigma} \in G} B_k(\boldsymbol{\sigma}).$$

By construction $d(C_k(G), C_k(G')) \geq 2$ for different k-components $G \neq G'$.

We start with a combinatorial lemma which shows that the size of (k,ε)-components remains bounded and that most (k,ε)-components are isolated.

Lemma 5.3. *Let $\varepsilon > 0$ and $k \in \mathbb{N}_0$ be fixed, but arbitrary.*

1. *There exists an $M = M(k,\varepsilon) \in \mathbb{N}$ such that*

$$\Omega_{N,M}(\varepsilon, k) \coloneqq \left\{ \max_{G \in \mathcal{G}_{k,\varepsilon}} |G| \leq M \right\}. \tag{5.5}$$

   occurs with probability $\mathbb{P}(\Omega_{N,M}(k,\varepsilon)) \geq 1 - e^{-cN}$ for some $c > 0$.

2. *Let $\varepsilon < a < b$ and $b < \beta_c$. Then for all events, but one of exponentially small probability:*

$$\frac{|\mathcal{L}_{a,b} \cap I_{k,\varepsilon}^c|}{|\mathcal{L}_{a,b}|} \leq e^{-\varepsilon^2 N/4}, \tag{5.6}$$

   where $\mathcal{L}_{a,b} \coloneqq \mathcal{L}_a \cap \mathcal{L}_b^c$ and $(\cdot)^c$ indicates the complement of that set.

3. *Let $a = \beta_c - \delta$ and suppose that $\delta(2\beta_c - \delta) < \varepsilon^2$. Then, besides of an exponentially small event*

$$\mathcal{L}_a \cap I_{k,\varepsilon}^c = \emptyset. \tag{5.7}$$

Proof. For a proof of the first assertion, we estimate for any $M \in \mathbb{N}$ using a union bound

$$\begin{aligned}\mathbb{P}(\max_{G\in\mathcal{G}_{k,\varepsilon}} |G| \geq M) &\leq \mathbb{P}(\exists \boldsymbol{\sigma} \in \mathcal{Q}_N \text{ s.t. } |B_{(2k+2)M}(\boldsymbol{\sigma}) \cap \mathcal{L}_\varepsilon| \geq M) \\ &\leq 2^N \binom{|B_{(2k+2)M}|}{M} e^{-\frac{1}{2}\varepsilon^2 MN}.\end{aligned}$$

The first inequality follows from the definition of k-connectedness: any k-connected set with size M is contained in some ball $B_{(2k+2)M}(\boldsymbol{\sigma})$ and if $\max_{G\in\mathcal{G}_{k,\varepsilon}} |G| \geq M$ there exists a k-connected set with size M (e.g. as a subset of the component with maximal size). The second line follows from the union bound, the independence of the random variables U and the standard Gaussian tail estimate. As the binomial coefficient is a polynomial in N the claim follows for $M > 2\ln 2/\varepsilon^2$.

For a proof of the second assertion, we rewrite $|\mathcal{L}_{a,b}| = \sum_{\boldsymbol{\sigma}} Z_{\boldsymbol{\sigma}}$, where $Z_{\boldsymbol{\sigma}}$ are iid Bernoulli variables with success probability

$$p_N \coloneqq \mathbb{P}(\boldsymbol{\sigma} \in \mathcal{L}_{a,b}) \geq \frac{\sqrt{N}(b-a)}{\sqrt{2\pi}}\, e^{-Nb^2/2}. \tag{5.8}$$

Since $b < \beta_c$, the average size $\mathbb{E}[|\mathcal{L}_{a,b}|] = 2^N p_N$ is exponentially large and, by a Markov estimate, the same applies to all events aside from one of super-exponentially small probability, i.e., $\mathbb{P}(|\mathcal{L}_{a,b}| \leq 2^{N-1}p_N) \leq e^{-e^{CN}}$ for some $C > 0$. Similarly, the conditional probability $\mathbb{P}_{\boldsymbol{\sigma}} \coloneqq \mathbb{P}(\cdot|\{\boldsymbol{\sigma}\}^c)$ of the configuration to not be (ε, k)-isolated equals the probability to find on $B^o_{2k+2} \coloneqq B_{2k+2}(\boldsymbol{\sigma})\backslash\{\boldsymbol{\sigma}\}$ another large deviation in $\mathcal{L}_\varepsilon$ and hence $\mathbb{P}_{\boldsymbol{\sigma}}(\exists\, \boldsymbol{\sigma}' \in I^c_{k,\varepsilon} \cap B^o_{2k+2}) \leq |B_{2k+2}|e^{-N\varepsilon^2/2} \leq N^{2k+2}e^{-N\varepsilon^2/2}$ by the union bound and the Gaussian-tail estimate. This allows us to estimate

$$\mathbb{E}\left[|\mathcal{L}_{a,b} \cap I^c_{k,\varepsilon}|\right] = \sum_{\boldsymbol{\sigma}\in\mathcal{Q}_N} \mathbb{E}\left[\mathbb{1}[\boldsymbol{\sigma} \in \mathcal{L}_{a,b}]\, \mathbb{P}_{\boldsymbol{\sigma}}(\boldsymbol{\sigma} \in I^c_{k,\varepsilon})\right] \leq 2^N p_N\, N^{2k+2} e^{-N\varepsilon^2/2} \tag{5.9}$$

with p_N from (5.8). Excluding the event on which $|\mathcal{L}_{a,b}| \leq 2^{N-1}p_N$, we thus arrive at

$$\begin{aligned}\mathbb{P}\left(|\mathcal{L}_{a,b} \cap I^c_{k,\varepsilon}| \geq e^{-\varepsilon^2 N/4}|\mathcal{L}_{a,b}|\right) &\leq \mathbb{P}\left(|\mathcal{L}_{a,b} \cap I^c_{k,\varepsilon}| \geq e^{-\varepsilon^2 N/4}2^{N-1}p_N\right) + e^{-e^{CN}} \\ &\leq \frac{e^{\varepsilon^2 N/4}}{2^{N-1}p_N}\mathbb{E}\left[|\mathcal{L}_{a,b} \cap I^c_{k,\varepsilon}|\right] + e^{-e^{CN}}\end{aligned}$$

by a Chebychev-Markov estimate. Inserting the bound (5.9) completes the proof.

For the last assertion, we note that by Lemma 4.2 the condition on δ implies that for $\alpha > 0$ small enough a global $(\varepsilon, \delta, \alpha)$-deep hole scenario occurs with probability exponentially close to one. □

The next lemma establishes the spectral properties of the restriction $H_{C_k(G)}$ of the QREM Hamiltonian to the Hilbert space $\ell^2(C_k(G))$ of a cluster corresponding to $G \in \mathcal{G}_{k,\varepsilon}$. For its formulation, we define for $\delta > 0$ the spectral projections

$$P_\delta(G) \coloneqq \mathbb{1}_{(-\infty,-\delta N)}(H_{C_k(G)}), \quad Q_\delta(G) \coloneqq \mathbb{1} - P_\delta(G).$$

Recall the events Ω^u_N defined in (4.3) and $\Omega_{N,M}(k,\varepsilon)$ defined in (5.5).

Lemma 5.4. *Let $\varepsilon > 0$ and $k \geq 2$. On the event $\Omega^u_N \cap \Omega_{N,M}(\varepsilon, k)$ the following assertions are valid for all N large enough:*

1. $\max_{G\in\mathcal{G}_{k,\varepsilon}} \|H_{C_k(G)} - U_{C_k(G)}\| = \mathcal{O}_{\Gamma,k,M}(\sqrt{N})$.

2. *If ψ is an ℓ^2-normalized eigenfunction of $H_{C_k(G)}$ with $\langle \psi, H_{C_k(G)}\psi\rangle \leq -\frac{3}{2}\varepsilon N$, we have*

$$|\psi(\boldsymbol{\sigma})| = \mathcal{O}_{\Gamma,k,M,\varepsilon}(N^{-\operatorname{dist}(G,\boldsymbol{\sigma})}), \tag{5.10}$$

and

$$\|\mathbb{1}_{C_k(G)\setminus G}\psi\|^2 = \mathcal{O}_{\Gamma,k,M,\varepsilon}(N^{-1}), \qquad \|\mathbb{1}_{\partial C_k(G)}\psi\|^2 = \mathcal{O}_{\Gamma,k,M,\varepsilon}(N^{-k}), \tag{5.11}$$

where $\mathbb{1}_{\partial C_k(G)}$ is the natural projection onto the boundary of $C_k(G)$. In particular, all estimates are independent of ψ and G.

3. $\sup_{G\in\mathcal{G}_{k,\varepsilon}} \sup_{\boldsymbol{\sigma}\in\mathcal{L}_{2\varepsilon}\cap G} \langle \delta_{\boldsymbol{\sigma}} | Q_{3\varepsilon/2}(G)\delta_{\boldsymbol{\sigma}}\rangle = \mathcal{O}_{\Gamma,k,M,\varepsilon}(N^{-1})$.

4. *If $G = \{\boldsymbol{\sigma_0}\}$ is (k,ε)-isolated and $U(\boldsymbol{\sigma}_0) \leq -2\varepsilon N$, then the ground state energy of $H_{C_k(G)}$ is given by*

$$E_{\boldsymbol{\sigma_0}} \coloneqq \inf\operatorname{spec} H_{C_k(G)} = U(\boldsymbol{\sigma}_0) + \frac{\Gamma^2 N}{U(\boldsymbol{\sigma}_0)} + \mathcal{O}_{\Gamma,k,\varepsilon}(N^{-1/4}). \tag{5.12}$$

Proof. 1. We write $H_{C_k(G)} = U_{C_k(G)} + \Gamma T_{C_k(G)}$ and recall that $C_k(G)$ is a union of at most M Hamming balls $B_k(\boldsymbol{\sigma})$ with $\boldsymbol{\sigma} \in G$. Thus, by the triangle inequality and Proposition 2.1 we obtain $\|T_{C_k(G)}\| \leq Mc_k\sqrt{N}$, and hence the claim.

2. We introduce the modified spheres $S_r(G)$ for $0 \leq r \leq k$,

$$S_r(G) \coloneqq C_r(G) \setminus C_{r-1}(G) = \{\boldsymbol{\sigma} \in C_k(G) \,|\, \operatorname{dist}(\boldsymbol{\sigma}, G) = r\}$$

and for the eigenvector ψ the maximal values on the spheres, $s_r \coloneqq \max_{\boldsymbol{\sigma}\in S_r(G)} |\psi(\boldsymbol{\sigma})|$. We use the convention $S_0(G) = G$ and note that $S_k(G) = \partial C_k(G)$. Moreover, we observe that for any $\boldsymbol{\sigma} \in S_r(G)$ and $1 \leq r \leq k$:

$$\begin{aligned} |S_1(\boldsymbol{\sigma}) \cap S_r(G)| \leq M, \qquad r \leq |S_1(\boldsymbol{\sigma}) \cap S_{r-1}(G)| \leq rM, \\ N - (r+1)M \leq |S_1(\boldsymbol{\sigma}) \cap S_{r+1}(G)| \leq N - r. \end{aligned}$$

We now use the eigenvalue equation

$$-E\psi(\boldsymbol{\sigma}) = \Gamma \sum_{\boldsymbol{\sigma}'\in S_1(\boldsymbol{\sigma})} \psi(\boldsymbol{\sigma}') - U(\boldsymbol{\sigma})\psi(\boldsymbol{\sigma}),$$

to derive the claimed decay estimate. Inserting the above geometric bounds into the eigenvalue equation, we obtain for all $1 \leq r \leq k$ with the convention $s_{k+1} = 0$:

$$-Es_r \leq \Gamma r M s_{r-1} + \Gamma(N-r)s_{r+1} + (\varepsilon N + \Gamma M)s_r. \tag{5.13}$$

We claim that for all $1 \leq r \leq k$ and N large enough

$$s_r \leq \frac{2M\Gamma k}{|E| - \varepsilon N - \Gamma M} s_{r-1}.$$

This is immediate from (5.13) in case $r = k$ (even without the factor 2). In case $1 \leq r < k$, the bound is proven recursively. If the inequality holds for $r+1$, then (5.13) implies

$$|E|s_r \leq \Gamma r M s_{r-1} + \left(\frac{2N\Gamma^2 k}{|E| - \varepsilon N - \Gamma M} + \varepsilon N + \Gamma M\right) s_r,$$

and hence the claimed inequality for all N large enough. Since $s_0 \leq 1$, this establishes (5.10) by iteration.

The first claim in (5.11) follows from (5.10) using $|G| \leq M$. Indeed, for some $C = C(\Gamma, k, M, \varepsilon)$

$$\sum_{\boldsymbol{\sigma} \neq \boldsymbol{\sigma}_0} |\psi(\boldsymbol{\sigma})|^2 \leq C \sum_{r=1}^{K} N^{-2r} \, |\{\boldsymbol{\sigma} \mid \operatorname{dist}(\boldsymbol{\sigma}, G) = r\}| \leq CM \sum_{r=1}^{K} N^{-r} = \frac{CM}{N-1}.$$

Since $|\partial C_k(G)| \leq MN^k$ the second inequality in (5.11) follows similarly.

3. We will repeatedly make use of a coupling principle which follows from 1., namely the fact that the eigenvalues of $H_{C_k(G)}$ and $U_{C_k(G)}$ agree up to a uniform error of order $\mathcal{O}_{\Gamma,k,M}(N^{1/2})$. Since $|\mathcal{L}_\varepsilon \cap G| \leq |G| \leq M$, this implies that $\dim P_{3\varepsilon/2}(G) \leq M$ for any component $G \in \mathcal{G}_{k,\varepsilon}$ if N is chosen large enough. By the pigeon-hole principle, for any component G we find some $a = a(G) \in [3\varepsilon/2, 2\varepsilon]$ such that

$$P_{a-\varepsilon/(2M)}(G) - P_{a+\varepsilon/(2M)}(G) = \mathbb{1}_{(-(a+\varepsilon/(2M))N, -(a-\varepsilon/(2M))N}(H_{C_k(G)}) = 0. \tag{5.14}$$

Since $Q_{3\varepsilon/2}(G) \leq Q_a(G)$, it is enough to prove the assertion with $Q_{3\varepsilon/2}(G)$ replaced by $Q_a(G)$.

To this end, we fix a component $G \in \mathcal{G}_{k,\varepsilon}$ and observe that the coupling principle and (5.14) yield

$$|\mathcal{L}_a \cap G| = \dim P_a(G) =: m_a \tag{5.15}$$

with a natural number $m_a \leq M$. We denote by $\psi_1, \dots \psi_{m_a}$ the normalized low energy eigenfunctions of $H_{C_k(G)}$ corresponding to $P_a(G)$, which form an orthonormal basis for this subspace. The first inequality in (5.11) bounds the contribution of each eigenfunction to $C_k(G) \setminus G$. Moreover, the eigenvalue equation readily implies for $\boldsymbol{\sigma} \in G \setminus \mathcal{L}_a$:

$$|\psi_j(\boldsymbol{\sigma}))| \leq \frac{\Gamma}{|E_j - U(\boldsymbol{\sigma})|} \sum_{\boldsymbol{\sigma}' \in S_1(\boldsymbol{\sigma})} |\psi_j(\boldsymbol{\sigma}'))| \leq \frac{2M\Gamma}{\varepsilon N} \sum_{\boldsymbol{\sigma}' \in S_1(\boldsymbol{\sigma})} |\psi_j(\boldsymbol{\sigma}'))| \leq \frac{2M\Gamma}{\varepsilon \sqrt{N}},$$

with $E_j = \langle \psi_j, H_{C_k(G)} \psi_j \rangle \leq -aN$ the eigenvalue corresponding to ψ_j. The second inequality follows from (5.14) and the last step is a consequence of the Cauchy-Schwarz inequality and $\|\psi_j\| = 1$. As $|G \setminus \mathcal{L}_a| \leq M$, we also conclude that

$$\sum_{\boldsymbol{\sigma} \in C_k(G) \setminus \mathcal{L}_a} |\psi_j(\boldsymbol{\sigma})|^2 \leq \frac{C}{N}$$

with a uniform $C = C(\Gamma, k, M, \varepsilon) < \infty$. We thus learn that $\sup_j \|\mathbb{1}_{\mathcal{L}_a \cap G} \ \psi_j - \psi_j\|^2 \leq C/N$. Lemma 5.5 below shows that (with $P = \mathbb{1}_{\mathcal{L}_a \cap G}$ and $F = P_a(G)$)

$$\sup_{\boldsymbol{\sigma} \in \mathcal{L}_a \cap G} \langle \delta_{\boldsymbol{\sigma}} | Q_a(G) \delta_{\boldsymbol{\sigma}} \rangle \leq \|Q_a(G) \mathbb{1}_{\mathcal{L}_a \cap G}\| \leq 4(\sqrt{m_a} + m_a)^2 \frac{C}{N} \leq 16 M^2 \frac{C}{N}.$$

Since $a \leq 2\varepsilon$, this proves the claim.

4. By the Rayleigh-Ritz variational principle, we have $E_{\boldsymbol{\sigma}_0} \leq -2\varepsilon N$, and hence the results of 2. apply to the corresponding ground state wavefunction $\psi \in \ell^2(C_k(G))$. By (5.11) this ensures $\psi(\boldsymbol{\sigma}_0) = 1 + O_{\Gamma,k,\varepsilon}(N^{-1/2})$. Following the steps in analysis (4.15)–(4.17) of the eigenfunction equation, in which we use (5.10) and the assumed bound on u, we thus conclude that (4.8) remains valid. This concludes the proof of (5.12).

□

In the proof of Lemma 5.4 we used the following result on finite-rank projections:

Lemma 5.5. *Suppose $\mathcal{H}$ is a finite-dimensional Hilbert space, P an orthogonal projection of rank m and $f_1, f_2, \dots f_m$ a sequence of m orthonormal vectors in $\mathcal{H}$, which span the projection F. If for some $c < \infty$*

$$\max_{j=1,\dots,m} \|Pf_j - f_j\| \leq c, \tag{5.16}$$

then $\|P - F\| \leq (m + 2\sqrt{m})c$.

Proof. We employ the triangle inequality $\|P - F\| \leq \|PF - F\| + \|PF - PFP\| + \|P - PFP\|$ and bound the three terms on the right-hand side individually. For the first term we invoke that $PF - F$ vanishes on the orthogonal complement $\operatorname{Im} F^\perp$ and, thus, a Frobenius norm estimate yields

$$\|PF - F\| \leq \sqrt{\sum_{j=1}^{m} \|(P - F)f_j\|^2} = \sqrt{\sum_{j=1}^{m} \|Pf_j - f_j\|^2} \leq \sqrt{m}c.$$

Our bound on the second term, relies on the norm estimate for the first term, $\|PF - PFP\| = \|P(F - FP)\| \leq \|F - FP\| = \|PF - F\| \leq \sqrt{m}c$, where we used that $\|P\| = 1$ for the first bound and applied the elementary identity $\|A\| = \|A^*\|$. For the last term, we employ the operator inequality $0 \leq PFP \leq P$ and the fact that the operator norm is bounded by the trace norm $\|\cdot\|_1$:

$$\|P - PFP\| \leq \|P - PFP\|_1 = \operatorname{Tr} P - \operatorname{Tr} PFP = \sum_{j=1}^{m} \langle \psi_j, (1 - P)\psi_j \rangle \leq mc.$$

This completes the proof. □

5.3. Proof of Theorem 1.10

Before we dive into the details of the proof, we fix some notation. For $k \in \mathbb{N}$ and $\varepsilon > 0$, we will use the restricted Hamiltonian corresponding to the collection of all clusters $C_k(G)$,

$$H^{(c)} \coloneqq \bigoplus_{G \in \mathcal{G}_{k,\varepsilon}} H_{C_k(G)}$$

acting on the complete Hilbert space $\ell^2(\mathcal{Q}_N)$. We further denote by

$$P_\varepsilon^{(c)} \coloneqq \mathbb{1}_{(-\infty, -3N\varepsilon/2)}(H^{(c)}) = \bigoplus_{G \in \mathcal{G}_{k,\varepsilon}} P_{3\varepsilon/2}(G), \quad Q_\varepsilon^{(c)} \coloneqq \mathbb{1} - P_\varepsilon^{(c)}$$

the spectral projections of $H^{(c)}$. The factor $3/2$ is motivated by the third assertion of Lemma 5.4. The subspace corresponding to $P_\delta^{(c)}$ represents the "localized" part of the QREM and $Q_\delta^{(c)}$ corresponds to the "delocalized" part. Corresponding to this block decomposition, we set the diagonal parts of H as well as their partition functions:

$$H^{(1)} \coloneqq P_\varepsilon^{(c)} H P_\varepsilon^{(c)}, \quad H^{(2)} \coloneqq Q_\varepsilon^{(c)} H Q_\varepsilon^{(c)}, \tag{5.17}$$

$$Z_N^{(j)}(\beta, \Gamma) \coloneqq 2^{-N} \operatorname{Tr}_j e^{-\beta H^{(j)}}, \quad j = 1, 2. \tag{5.18}$$

Here the traces $\operatorname{Tr}_j(\cdot)$ run over the natural subspaces $P_\varepsilon^{(c)}\ell^2(\mathcal{Q}_N)$ in case $j=1$, or $Q_\varepsilon^{(c)}\ell^2(\mathcal{Q}_N)$ in case $j=2$, on which $H^{(j)}$ acts non-trivially.

The key observation is now that $P_\varepsilon^{(c)}$ commutes with the restriction of H to the clusters $H^{(c)}$. If we denote by A the adjacency matrix between the inner and outer boundaries of the clusters $C_k(G)$, we see

$$P_\varepsilon^{(c)} H Q_\varepsilon^{(c)} = \Gamma P_\varepsilon^{(c)} A Q_\varepsilon^{(c)}. \tag{5.19}$$

We recall that $d(C_k(G), C_k(G')) \geq 2$ for two different components $G \neq G' \in \mathcal{G}_{k,\varepsilon}$, which implies that the adjacency matrix A is a direct sum of operators $A_{C_k(G)}$ corresponding to each cluster $C_k(G)$. This in turn yields

$$\|A\| \leq M c_k \sqrt{N} \tag{5.20}$$

by Proposition 2.1on the event on which the assertions in Lemma 5.3 apply. We further observe that A only acts nontrivially on the boundaries $\partial C_k(G)$. Exploiting the decay estimate (5.11) from Lemma 5.4, we arrive at

$$\|P_\varepsilon^{(c)} H Q_\varepsilon^{(c)}\| = \mathcal{O}_{\Gamma,k,M,\varepsilon}(N^{-(k-1)/2}).$$

We conclude that for any $k \geq 2$:

$$Z_N(\beta,\Gamma) = e^{o_{\Gamma,k,M,\varepsilon}(1)}(Z_N^{(1)} + Z_N^{(2)}). \tag{5.21}$$

The proof of Theorem 1.10 now reduces to an analysis of $Z_N^{(1)}$ and $Z_N^{(2)}$.

Proof of Theorem 1.10. Since our claims in case $\beta = 0$ and $\Gamma = 0$ are trivial, we fix $\beta, \Gamma > 0$ away from the phase transition, and pick

$$0 < \varepsilon < \frac{1}{8}\min\{\beta, \beta_c, \Gamma\tanh\beta\Gamma, \min\{1,\beta^{-1}\}\ln\cosh\beta\Gamma\}.$$

In the following, we will only work on the event $\Omega_{N,\beta_c}^{\mathrm{REM}} \cap \Omega_N^u \cap \Omega_{N,M}(\varepsilon,k)$, where the conditions of Lemma 5.3 are valid at $k \geq 2$ and some M. According to Lemma 5.4 and (4.4) as well as (1.7), this event can be chosen to have a probability of at least $1 - e^{-cN}$.

We now proceed in four steps. We first analyze the localized part $Z_N^{(1)}$. As a second and third step we derive an upper and lower bound for $Z_N^{(2)}$. The last part then collects these estimates.

Step 1 – Analysis of $Z_N^{(1)}$: Let us first remark that $H^{(1)} = P_\varepsilon^{(c)} H P_\varepsilon^{(c)} = P_\varepsilon^{(c)} H^{(c)} P_\varepsilon^{(c)}$ and hence $H^{(1)} P_\varepsilon^{(c)} = H^{(c)} P_\varepsilon^{(c)}$. It thus remains to consider the low energy spectrum of $H^{(c)}$. We abbreviate

$$u \coloneqq u(\beta) \coloneqq \lim_{N\to\infty} \langle U\rangle_\beta^{\mathrm{cl}}/N = \begin{cases} -\beta, & \beta \leq \beta_c, \\ -\beta_c, & \beta > \beta_c, \end{cases}$$

by Proposition 5.1. Since $8\varepsilon < -u$, the dominant energy levels of U are not effected by the projection $P_\varepsilon^{(c)}$. We now split $Z_N^{(1)}$ into the contribution arising from energy levels within $J_\delta \coloneqq [(u-\delta)N, (u+\delta)N]$ with $0 < \delta < \min\{-u/2 - 3\varepsilon/4, \varepsilon^2/(16\beta)\}$ arbitrarily small, and a remainder:

$$Z_N^{(1)}(\beta,\Gamma) = 2^{-N}\left(\operatorname{Tr} e^{-\beta H^{(1)}} \mathbb{1}_{J_\delta}(H^{(1)}) + \operatorname{Tr} e^{-\beta H^{(1)}} \mathbb{1}_{(-\infty,-3\varepsilon N/2)\setminus J_\delta}(H^{(1)})\right).$$

The second term is estimated using Lemma 5.4 and subsequently Proposition 5.1, which yields some $c = c(\beta, \delta) > 0$ such that for all sufficiently large N:

$$\operatorname{Tr} e^{-\beta H^{(1)}} \mathbb{1}_{\mathbb{R}\setminus J_\delta}(H^{(1)}) \leq \; e^{\beta \mathcal{O}_{\Gamma,k,M}(\sqrt{N})} \operatorname{Tr} e^{-\beta U} \mathbb{1}_{\mathbb{R}\setminus J_{\delta/2}}(U) \leq e^{-cN}\, 2^N Z_N(\beta, 0). \tag{5.22}$$

The remaining term is decomposed further into the contribution of isolated and non-isolated clusters:

$$\begin{aligned}\operatorname{Tr} e^{-\beta H^{(1)}} \mathbb{1}_{J_\delta}(H^{(1)}) = &\sum_{G\in\mathcal{I}_{k,\varepsilon}} \operatorname{Tr} e^{-\beta H_{C_k(G)}} \mathbb{1}_{J_\delta}(H_{C_k(G)}) \\ &+ \sum_{G\in\mathcal{G}_{k,\varepsilon}\setminus I^c_{k,\varepsilon}} \operatorname{Tr} e^{-\beta H_{C_k(G)}} \mathbb{1}_{J_\delta}(H_{C_k(G)}).\end{aligned} \tag{5.23}$$

Since $\sup_{G\in\mathcal{G}_{k,\varepsilon}} \|H_{C_k(G)} - U_{C_k(G)}\| \leq \mathcal{O}_{\Gamma,k,M}(\sqrt{N})$ by Lemma 5.4, we bound the second term for all sufficiently large N as follows:

$$\begin{aligned}\sum_{G\in\mathcal{G}_{k,\varepsilon}\setminus I^c_{k,\varepsilon}} \operatorname{Tr} e^{-\beta H_{C_k(G)}} \mathbb{1}_{J_\delta}(H_{C_k(G)}) &\leq e^{-\beta N(u-\delta)} \sum_{G\in\mathcal{G}_{k,\varepsilon}\setminus I^c_{k,\varepsilon}} \operatorname{Tr} \mathbb{1}_{J_{2\delta}}(U_{C_k(G)}) \\ &\leq e^{-N\varepsilon^2/4} e^{3\beta N\delta} \sum_{G\in\mathcal{G}_{k,\varepsilon}} \operatorname{Tr} e^{-\beta U_{C_k(G)}} \mathbb{1}_{J_{2\delta}}(U_{C_k(G)}) \leq e^{-cN}\, 2^N Z_N(\beta, 0).\end{aligned} \tag{5.24}$$

At the expense of throwing out another event of exponentially small probability, we consult Lemma 5.3 and assume in case $u > -\beta_c$ the validity of (5.6) with $a = -u - 2\delta$ and $b = -u + 2\delta$ and in case $u = -\beta_c$ the validity of (5.7) with $a = -u - 2\delta$. This guarantees that non-isolated clusters are exponentially rare. The last inequality is a consequence of the choice of δ and of the fact our definition of the partition function Z_N includes a normilisation by 2^{-N}.

The first term on the right side of (5.23) can be expressed using the energy correction formula (5.12) for isolated extremal sites. At the expense of excluding or including small subintervals at the boundary of J_δ, which are negligible in comparison to the main term by Proposition 5.1, this first term is of the form

$$\sum_{\boldsymbol{\sigma}\in I_{k,\varepsilon}\cap\mathcal{L}_{u-\delta,u+\delta}} e^{-\beta(U(\boldsymbol{\sigma})+\frac{\Gamma^2 N}{U(\boldsymbol{\sigma})}+o(1))} = S - R,$$

where, similarly to (5.24), the remainder is again bounded using (5.6):

$$R \coloneqq \sum_{\boldsymbol{\sigma}\in I^c_{k,\varepsilon}\cap\mathcal{L}_{u-\delta,u+\delta}} e^{-\beta(U(\boldsymbol{\sigma})+\frac{\Gamma^2 N}{U(\boldsymbol{\sigma})}+o(1))} \leq e^{-cN}\, 2^N Z_N(\beta, 0).$$

The main term is

$$S \coloneqq \sum_{\boldsymbol{\sigma}\in\mathcal{Q}_N} e^{-\beta U(\boldsymbol{\sigma})+\frac{\Gamma^2 N}{U(\boldsymbol{\sigma})}+o(1))} \mathbb{1}[U(\boldsymbol{\sigma}) \in J_\delta].$$

By definition of J_δ and since the REM's partition function concentrates around u by Proposition 5.1, S equals $2^N Z(\beta, 0)$ plus an error which is bounded by $e^{-cN} 2^N Z(\beta, 0)$.

In summary, in this first step we have shown that for any $\delta > 0$ small and N large enough:

$$e^{-\frac{\beta\Gamma^2}{u-\delta}+o(1)} Z_N(\beta, 0) \leq Z_N^{(1)}(\beta, \Gamma) \leq e^{-\frac{\beta\Gamma^2}{u+\delta}+o(1)} Z_N(\beta, 0). \tag{5.25}$$

Step 2 – Upper bound on $Z_N^{(2)}$: We write $U_\varepsilon^< := U\mathbb{1}_{U\geq -2\varepsilon N}$ and $U_\varepsilon^> := U\mathbb{1}_{U>-2\varepsilon N}$ as well as $U_\varepsilon := U\mathbb{1}_{|U|\leq 2\varepsilon N}$, and estimate using the Jensen-Peierls inequality [12]:

$$\begin{aligned} 2^N Z_N^{(2)}(\beta,\Gamma) &= \operatorname{Tr}{}_2 e^{-\beta Q_\varepsilon^{(c)}[\Gamma T + U_\varepsilon^< + Q_\varepsilon^{(c)} U_\varepsilon^> Q_\varepsilon^{(c)}]Q_\varepsilon^{(c)}} \\ &\leq \operatorname{Tr} Q_\varepsilon^{(c)}\ e^{-\beta[\Gamma T + U_\varepsilon^< + Q_\varepsilon^{(c)} U_\varepsilon^> Q_\varepsilon^{(c)}]} \leq \operatorname{Tr} e^{-\beta[\Gamma T + U_\varepsilon + Q_\varepsilon^{(c)} U_\varepsilon^> Q_\varepsilon^{(c)}]}. \end{aligned}$$

The last inequality follows from a trivial extension of the trace and the monotonicity of eigenvalues in the potential, $U_\varepsilon^< \geq U_\varepsilon$. From Lemma 5.4 we learn that $\max_{\boldsymbol{\sigma}\in\mathcal{L}_{2\varepsilon}} \|Q_\varepsilon^{(c)}\delta_{\boldsymbol{\sigma}}\|^2 \leq CN^{-1}$. Moreover, if $\boldsymbol{\sigma} \in C_k(G)$ for some component G, the projection $Q_\varepsilon^{(c)}\delta_{\boldsymbol{\sigma}}$ has only support on $C_k(G)$. As any cluster $C_k(G)$ has at most M configurations $\boldsymbol{\sigma} \in \mathcal{L}_{2\varepsilon}$, these observations result in the norm estimate

$$\|Q_\varepsilon^{(c)} U_\varepsilon^> Q_\varepsilon^{(c)}\| \leq CM\|U\|_\infty N^{-1}.$$

Since on the event considered we also have $\|U\|_\infty \leq 2\beta_c$ and the operator $Q_\varepsilon^{(c)} U_\varepsilon^> Q_\varepsilon^{(c)}$ only acts non trivially on the clusters $C_k(G)$, we thus conclude that for some $D \in (0,\infty)$:

$$Q_\varepsilon^{(c)} U_\varepsilon^> Q_\varepsilon^{(c)} \geq V := -D\mathbb{1}_C = -D\sum_{G\in\mathcal{G}_{k,\varepsilon}} \mathbb{1}_{C_k(G)}, \quad \mathcal{C} := \bigcup_{G\in\mathcal{G}_{k,\varepsilon}} C_k(G)$$

To summarize, we have thus shown that $Z_N^{(2)}(\beta,\Gamma) \leq 2^{-N}\operatorname{Tr} e^{-\beta[\Gamma T + U_\varepsilon + V]}$.

From here, there are at least two possible ways to continue the proof. One could show that the potential $U_\varepsilon + V$ meets the requirements of Theorem 3.4. Then, one needs to control V, which is a little bit technical. Instead, we will employ a convexity argument. To this end, we introduce for $\lambda \in \mathbb{R}$ the family of pressures and corresponding Hamiltonians on $\ell^2(\mathcal{Q}_N)$:

$$\Phi_N(\beta,\Gamma,\lambda) := \ln 2^{-N}\operatorname{Tr} e^{-\beta H(\lambda)}, \qquad H(\lambda) := \Gamma T + U_\varepsilon + \lambda V \tag{5.26}$$

The pressure $\Phi_N(\beta,\Gamma,\lambda)$ is convex [65] in λ, and $\lambda = 1$ is the case of interest.

Let us first discuss the case $\lambda = 0$ in which case Theorem 3.4 is applicable with $W = U_\varepsilon$. Since $\|U_\varepsilon\|_\infty \leq 2\varepsilon N$ and $\mathbb{E}\left[U_\varepsilon(\boldsymbol{\sigma})^2\right] \leq N(1-e^{-2\varepsilon^2 N}) \leq N$, Theorem 3.4 guarantees that all eigenvalues of $\Gamma T + U_\varepsilon$ below $E < -4\varepsilon N$, counted with multiplicity, are shifted with respect to the eigenvalues E of ΓT to $E + \frac{N}{E} + o(1)$. Since $\langle \Gamma T\rangle_\beta^{\mathrm{pm}} = -N\Gamma\tanh\beta\Gamma \leq -8\varepsilon N$, Proposition 5.1 allows to spectrally focus the partition function onto an interval around $\langle \Gamma T\rangle_\beta^{\mathrm{pm}}$ of arbitrarily small size $0 < \delta < \Gamma\tanh\beta\Gamma - 4\varepsilon$. A similar argument as in Step 1, then yields for all sufficiently large N:

$$\Phi_N(\beta,\Gamma,0) \leq N\ln\cosh\beta\Gamma + \frac{\beta}{\Gamma\tanh\beta\Gamma - \delta} + o(1).$$

Next, we consider general parameters λ. Recall that $\mathbb{1}_{\mathcal{C}}$ stands for the orthogonal projection onto the subspace of the union of all clusters, and that $\mathbb{1}_{\mathcal{C}^c}$ is the orthogonal complement. In terms of the operator A introduced in (5.19), the norm estimate (5.20) yields: $\|H(\lambda) - \mathbb{1}_{\mathcal{C}}H(\lambda)\mathbb{1}_{\mathcal{C}} - \mathbb{1}_{\mathcal{C}^c}H(\lambda)\mathbb{1}_{\mathcal{C}^c}\| \leq \|A\| \leq C\sqrt{N}$ and hence

$$\begin{aligned} \operatorname{Tr} e^{-\beta H(\lambda)} &\leq e^{C\sqrt{N}}\operatorname{Tr} e^{-\beta(\mathbb{1}_{\mathcal{C}}H(\lambda)\mathbb{1}_{\mathcal{C}} + \mathbb{1}_{\mathcal{C}^c}H(\lambda)\mathbb{1}_{\mathcal{C}^c})} \\ &= e^{C\sqrt{N}}\left[\operatorname{Tr}\mathbb{1}_{\mathcal{C}}e^{-\beta(\mathbb{1}_{\mathcal{C}}H(\lambda)\mathbb{1}_{\mathcal{C}})} + \operatorname{Tr}\mathbb{1}_{\mathcal{C}^c}e^{-\beta(\mathbb{1}_{\mathcal{C}^c}H(\lambda)\mathbb{1}_{\mathcal{C}^c})}\right] \end{aligned}$$

at some $C < \infty$, which is independent of N and λ. Each of the traces in the right side is now estimated separately:

$$2^{-N}\mathrm{Tr}\,\mathbb{1}_{\mathcal{C}}e^{-\beta(\mathbb{1}_{\mathcal{C}}H(\lambda)\mathbb{1}_{\mathcal{C}})} \leq e^{\beta\|\mathbb{1}_{\mathcal{C}}H(\lambda)\mathbb{1}_{\mathcal{C}}\|} \leq \exp\left(\beta\left(C\Gamma\sqrt{N}+2\varepsilon N+\lambda D\right)\right)$$

where we used the triangle inequality for the operator norm as well as (5.20) again. Since $H(\lambda)$ and $H(0)$ agree on $\mathbb{1}_{\mathcal{C}^c}\,\ell^2(\mathcal{Q}_N)$, we also have

$$\begin{aligned}2^{-N}\mathrm{Tr}\,\mathbb{1}_{\mathcal{C}^c}e^{-\beta\mathbb{1}_{\mathcal{C}^c}H(\lambda)\mathbb{1}_{\mathcal{C}^c}} &= 2^{-N}\mathrm{Tr}\,\mathbb{1}_{\mathcal{C}^c}e^{-\beta\mathbb{1}_{\mathcal{C}^c}H(0)\mathbb{1}_{\mathcal{C}^c}}\\ &\leq 2^{-N}\mathrm{Tr}\,\mathbb{1}_{\mathcal{C}^c}e^{-\beta H(0)} \leq e^{\Phi_N(\beta,\Gamma,0)}.\end{aligned}$$

The first inequality relied on the Jensen-Peierls estimate, which allows to pull down the projections [12]. Since $\Phi_N(\beta,\Gamma,0) > 4\beta\varepsilon N$, the correction to the pressure at $\lambda_0 \coloneqq \frac{\varepsilon N}{D}$, is still of order $\mathcal{O}(\sqrt{N})$:

$$\Phi_N(\beta,\Gamma,\lambda_0) \leq \Phi_N(\beta,\Gamma,0) + C\sqrt{N}.$$

We are now in the situation to exploit convexity:

$$\begin{aligned}\Phi_N(\beta,\Gamma,1) &\leq (1-\lambda_0^{-1})\;\Phi_N(\beta,\Gamma,0) + \lambda_0^{-1}\Phi_N(\beta,\Gamma,\lambda_0)\\ &\leq N\ln\cosh\beta\Gamma + \frac{\beta}{\Gamma\tanh\beta\Gamma-\delta} + o(1).\end{aligned}$$

Step 3 – Paramagnetic lower bound: To show that the upper bound of Step 2 is also an asymptotic lower bound, it is more convenient to work with the full partition function Z_N, which by (5.21) is a lower bound on $Z_N^{(2)}$ up to a multiplicative error of $e^{o(1)}$.

For an estimate on Z_N, we split the potential $U = U_\varepsilon + V_\varepsilon$, where $V_\varepsilon \coloneqq U\mathbb{1}[|U| > 2\varepsilon]$. The pressure $\Phi_N(\beta,\Gamma,0)$ of $H(0) = \Gamma T + U_\varepsilon$, which is defined in (5.26), was already analyzed in Step 2. Here, we now consider the following family of Hamiltonians $H(\lambda) = \Gamma T + U_\varepsilon + \lambda V_\varepsilon$, which differs from the one in Step 2. By a slight abuse of notation, we nevertheless denote the corresponding pressure again by $\Phi_N(\beta,\Gamma,\lambda) \coloneqq \ln\mathrm{Tr}\,2^{-N}\mathrm{Tr}\,e^{-\beta H(\lambda)}$. The convexity of the pressure in λ is again the basis for our argument.

Since on the event considered, we may assume $\|U\| \leq 2\beta_c N$, the potential $W = U_\varepsilon + \lambda V_\varepsilon$ meets the requirements of Theorem 3.4 with $\|W\|_\infty \leq N\max\{2\varepsilon, 2\lambda\beta_c\}$ and $\mathbb{E}\left[W(\boldsymbol{\sigma})^2\right] \leq N(1-e^{-2\varepsilon^2 N}) \leq N$. Thus if $\lambda < \varepsilon/\beta_c$ the eigenvalues of $H(\lambda)$ below $E < -4\varepsilon N$, counted with multiplicity, are shifted with respect to the eigenvalues E of ΓT to $E + \frac{N}{E} + o(1)$ and we have $\Phi_N(\beta,\Gamma,\lambda) = \Phi_N(\beta,\Gamma,0) + o(1)$. Fixing $\lambda_0 \coloneqq \frac{\varepsilon}{2\beta_c} < 1$, convexity implies:

$$\begin{aligned}\Phi_N(\beta,\Gamma,1) &\geq \Phi_N(\beta,\Gamma,0) + \frac{1}{\lambda_0}(\Phi_N(\beta,\Gamma,\lambda_0) - \Phi_N(\beta,\Gamma,0))\\ &= N\ln\cosh(\beta\Gamma) + \frac{\beta}{\Gamma\tanh\beta\Gamma+\delta} + o(1).\end{aligned}$$

The last step, which holds for all $\delta > 0$ sufficiently small, is the desired lower bound, again relied on an explicit estimate based on the concentration of the partition function of ΓT around energies near $-\Gamma\tanh\beta\Gamma$, cf. Proposition 5.1.

Step 4 – Completing the proof. Away from the first-order phase transition at $\Gamma = \Gamma_c(\beta)$ described in Proposition 1.1 and on the event on which Step 1-3 are valid, the partition function (5.21) is either dominated by the REM-term $Z_N^{(1)}$ in case $\Gamma < \Gamma_c(\beta)$, or by the paramagnetic term $Z_N^{(2)}$ in case $\Gamma > \Gamma_c(\beta)$.

More precisely, in case $\Gamma < \Gamma_c(\beta)$ and since the probability of the event, which is excluded in Step 1–3, is exponentially small in N and hence summable, we conclude for any $\varepsilon > 0$:

$$\sum_{N\geq 1} \mathbb{P}\left(\left|\Phi_N(\beta,\Gamma) - \Phi_N(\beta,0) + \frac{\beta\Gamma^2}{u(\beta)}\right| > \varepsilon\right) < \infty. \tag{5.27}$$

The claimed almost-sure convergence then follows by a Borel-Cantelli argument. The analogous argument establishes the claim in case $\Gamma > \Gamma_c(\beta)$. □

A. Proof of Proposition 1.8 and 1.9

In this section, we sketch the modifications necessary for covering the critical case. For any $\varepsilon > 0$ we introduce the symmetrized large-deviation set

$$\mathcal{S}_\varepsilon := \{\boldsymbol{\sigma} \in \mathcal{Q}_N \,|\, |U(\boldsymbol{\sigma})| \geq \varepsilon N\}.$$

For parameters $\varepsilon, \alpha, \delta > 0$, we use the notion of a *symmetrized global* $(\varepsilon, \alpha, \delta)$*-deep-hole scenario* if $\mathcal{L}_{\beta_c-\delta}$ is replaced by $\mathcal{S}_{\beta_c-\delta}$ in Definition 4.1. As is evident from the proof of Lemma 4.2, due to the symmetry of the Gaussian distribution, if $\varepsilon, \alpha, \delta > 0$ satisfy (4.1) then the event

$$\Omega_N^s(\varepsilon,\alpha,\delta) := \{U \text{ satisfies a symmetrized global } (\varepsilon,\alpha,\delta)\text{-deep-hole scenario}\}$$

still has a probability bounded by $1 - e^{-c(\varepsilon,\alpha,\delta)N}$ for all sufficiently large N. We will again pick $\varepsilon = \beta_c/2$ and the values of α, δ will be given (implicitly) as we go along the proof. Similarly as in the proof of Theorem 1.5, under this scenario, we work with the auxiliary Hamiltonian

$$H' = \left(\bigoplus_{\boldsymbol{\sigma}\in\mathcal{S}_{\beta_c-\delta}} H_{\alpha N}(\boldsymbol{\sigma})\right) \bigoplus H_r, \tag{A.1}$$

which is well-defined, since the balls $B_{\alpha N}(\boldsymbol{\sigma})$ are disjoint for two different configurations in $\mathcal{S}_{\beta_c-\delta}$. That we work with $\mathcal{S}_{\beta_c-\delta}$ instead of $\mathcal{L}_{\beta_c-\delta}$ is due to purely technical reasons: we want to ensure that the restriction of U to the complement of the balls $H_{\alpha N}(\boldsymbol{\sigma})$ is still a symmetric random variable so that we can apply Theorem 3.4.

The first main step in the proof of Proposition 1.8 and 1.9 is to show that for $\Gamma \simeq \beta_c$ there are $c, r > 0$ (which may still depend on α, δ) such that

$$\|(H - H')\mathbb{1}_{(-\infty,(\Gamma-r)N}(H')\| \leq e^{-cN}.$$

However, the paramagnetic part causes a challenge, since the less energy levels we cut out (i.e. choosing a smaller parameter $\delta > 0$), the low energy states of H_r become less delocalized. Indeed our bound from Proposition 3.5 becomes trivial for $\Gamma = \beta_c$ and $r \leq \delta$. To overcome this problem, we use the improved delocalization estimate from Proposition 3.6, which deals with $H_\delta = \Gamma T + U\mathbb{1}_{|U|\leq(\beta_c-\delta)N}$ on $\ell^2(\mathcal{Q}_N)$. We first show that for $\delta > 0$ small enough the low energy states of H_r and

H_δ agree up to an experientially small error. Here and in the following we always assume that the parameter $\delta > 0$ coincides in the definition of H_r and H_δ. Then, we show that the low eigenvalues of H and H' again coincide besides an exponential error. From there, we establish Proposition 1.8 and 1.9.

Step 1: Comparison of the low energy spaces of H_r and H_δ: We abbreviate

$$B_\cup \coloneqq \bigcup_{\boldsymbol{\sigma}\in\mathcal{S}_{\beta_c-\delta}} B_{\alpha N}(\boldsymbol{\sigma}), \qquad B_\cup^+ \coloneqq \bigcup_{\boldsymbol{\sigma}\in\mathcal{S}_{\beta_c-\delta}} B_{\alpha N+1}(\boldsymbol{\sigma}).$$

and recall that H_r is the restriction of H onto the complement of $B_\cup$. In the following, $\hat{H}_r$ stands for its canonical extension to $\ell^2(\mathcal{Q}_N)$. Then, the spectra of H_r and $\hat{H}_r$ agree outside zero. Proposiotion 3.6 guarantees the existence of some $\eta = \eta(\delta) > 0$ and some $c > 0$, which is independent of δ, such that for all N large enough:

1. the spectral projection $P_\delta(\eta) \coloneqq \mathbb{1}_{(-\infty,-(\Gamma-\eta)N)}(H_\delta)$ is finite-dimensional, and the eigenvalue below $-(\Gamma-\eta)N$ are $(2n-N)\Gamma + \frac{N}{(2n-N)\Gamma} + \mathcal{O}_\Gamma(N^{-1/4})$ with $2n \leq \eta N/\Gamma$.
2. $\max_{\boldsymbol{\sigma}\in\mathcal{Q}_N} \langle \delta_{\boldsymbol{\sigma}} \,|\, P_\delta(\eta)\, \delta_{\boldsymbol{\sigma}}\rangle \leq e^{-2cN}$.

Since $\hat{H}_r$ and H_δ only differ on $B_\cup^+$, the triangle inequality thus yields

$$\begin{aligned}\|(H_\delta - \hat{H}_r)P_\delta(\eta)\| &\leq \sum_{\boldsymbol{\sigma}\in B_\cup^+} \|(H_\delta - \hat{H}_r)\delta_{\boldsymbol{\sigma}}\|\, \|P_\delta(\eta)\delta_{\boldsymbol{\sigma}}\| \\ &\leq (\beta_c+\Gamma)N\ |B_\cup^+| \max_{\boldsymbol{\sigma}\in\mathcal{Q}_N} \sqrt{\langle \delta_{\boldsymbol{\sigma}} \,|\, P_\delta(\eta)\, \delta_{\boldsymbol{\sigma}}\rangle} \\ &\leq |\mathcal{S}_{\beta_c-\delta}|\ e^{N\gamma(\alpha)+o(N)} e^{-cN}.\end{aligned}$$

Consulting Lemma 4.7, since the set $A_3(\delta)$ agrees with $\mathcal{S}_{\beta_c-\delta}$, the cardinality is bounded $|\mathcal{S}_{\beta_c-\delta}| \leq 2e^{\beta_c\delta N}$ except for an exponentially small event. We now use that c is independent of δ. We thus find some (possibly) smaller parameters $\alpha, \delta > 0$ such that $\beta_c\delta + \gamma(\alpha) < c/2$. It then follows that for some $\eta = \eta(\delta) > 0$ and all N large enough:

$$\|(H_\delta - \hat{H}_r)P_\delta(\eta)\| \leq e^{-cN}.$$

In particular, the 'off-diagonal' blocks $P_\delta(\eta)\hat{H}_r Q_\delta(\eta)$ and $Q_\delta(\eta)\hat{H}_r P_\delta(\eta)$ with $Q_\delta(\eta) = 1 - P_\delta(\eta)$ are bounded in norm by e^{-cN}. The spectrum of $\hat{H}_r$ hence agrees up to the error e^{-cN} with those of the block matrices $P_\delta(\eta)H_\delta$ and $Q_\delta(\eta)\hat{H}_r Q_\delta(\eta)$. In order to see that the low-energy spectrum is entirely determined by the first block, we need to derive a lower bound on ground state energy of the second block. We will prove below that for sufficiently large N:

$$\inf \operatorname{spec} Q_\delta(\eta)\hat{H}_r Q_\delta(\eta) \geq -(\Gamma - \eta/2)N. \tag{A.2}$$

Perturbation theory based on the Feshbach-Schur method and the fact that the spectrum of H_δ is discrete with eigenvalue clusters which are separated from each other by gaps of at least 1, then yields that $\|\mathbb{1}_{(-\infty,-(\Gamma-\eta_0)N)}(\hat{H}_r) - P_\delta(\eta_0)\| \leq Ce^{-cN}$ for some $\eta_0 = \eta_0(\delta) > 0$ and all sufficiently large N, and hence

$$\max_{\boldsymbol{\sigma}\in(B_\cup)^c} \langle \delta_{\boldsymbol{\sigma}} \,|\, \mathbb{1}_{(-\infty,-(\Gamma-\eta_0)N)}(H_r), \delta_{\boldsymbol{\sigma}}\rangle \leq \max_{\boldsymbol{\sigma}\in\mathcal{Q}_N} \langle \delta_{\boldsymbol{\sigma}} \,|\, P_\delta(\eta_0)\, \delta_{\boldsymbol{\sigma}}\rangle + Ce^{-cN} \leq (1+C)\, e^{-cN}.$$

It thus remains to proof (A.2). We will employ a counting argument based on the min-max principle. It rests on the following observations. For any $E < 0$ the eigenvalues of $\hat{H}_r$ and H_r below E agree. The same applies to $\hat{H}_r$ and the energy form $q_r^\infty : \ell^2(\mathcal{Q}_N) \to \mathbb{R} \cup \infty$:

$$q_r^\infty(\psi) \coloneqq \begin{cases} \langle \psi,\, H_r \psi \rangle, & \text{if } \psi \in \ell^2((B_\cup)^c), \\ +\infty & \text{otherwise .} \end{cases}$$

Denoting by $\hat{H}_r^\infty$ the corresponding operator, which results in driving the potential values on $B_\cup$) to infinity (see e.g. [64]), we thus have $H_\delta \leq \hat{H}_r^\infty$ and hence $\operatorname{Tr} \mathbb{1}_{(-\infty,E)}(\hat{H}_r) = \operatorname{Tr} \mathbb{1}_{(-\infty,E)}(\hat{H}_r^\infty) \leq \operatorname{Tr} \mathbb{1}_{(-\infty,E)}(H_\delta)$. However, since we have shown above that $\hat{H}_r$ is e^{-cN}-norm close to $P_\delta(\eta) H_\delta + Q_\delta(\eta) \hat{H}_r Q_\delta(\eta)$ and all eigenvalues of $P_\delta(\eta) H_\delta$ below $-(\Gamma - \eta)N$ are already accounted for at this energy, we conclude the validity of (A.2) (even with $\eta/2$ replaced by $\eta - e^{-cN}$).

Step 2: Comparison of the low energy spectra of H and H': We want to show that the low energies of H and H' coincide up to an exponentially small error. We abbreviate $P'_\delta(\eta) \coloneqq \mathbb{1}_{(-\infty,-(\Gamma-\eta)N)}(H')$ and $Q'_\delta(\eta) = \mathbb{1} - P'_\delta(r)$. As in the first step, by the Feshbach-Schur method it suffices to show

$$\|(H' - H) P'_\delta(\eta)\| \leq e^{-cN}, \quad Q'_\delta(\eta) H Q'_\delta(\eta) \geq -(\Gamma - \eta/2) N Q'_\delta(\eta)$$

for some $\eta, c > 0$. To this end, let $\eta < \eta_0$ with η_0 from the first step. Due to the direct-sum structure of H' we have

$$\begin{aligned} \|(H' - H) P'_\delta(\eta)\| \leq{}& \|(H' - H) \mathbb{1}_{(B_\cup)^c} \mathbb{1}_{(-\infty,-(\Gamma-\eta)N)}(H_r)\| \\ &+ \Big\| (H' - H) \mathbb{1}_{B_\cup} \mathbb{1}_{(-\infty,-(\Gamma-\eta)N)} \Big(\Big(\bigoplus_{\boldsymbol{\sigma} \in \mathcal{L}_{\beta_c - \delta}} H_{\alpha N}(\boldsymbol{\sigma}) \Big) \Big) \Big\| \end{aligned}$$

Note that we have replaced $\mathcal{S}_{\beta_c - \delta}$ by $\mathcal{L}_{\beta_c - \delta}$ in the above direct sum, as only those balls contain low energy states. That the first summand is exponentially small for t small enough follows from the same argument we used to compare the low energy projections of H_r and H_δ in the first step. The second summand is exponentially small, too. We simply recall the exponential decay estimate of the localized wavefunctions from Theorem 1.5. Moreover, we have

$$\begin{aligned} Q'_\delta(\eta) H Q'_\delta(\eta) &\geq -(\Gamma - t) N Q'_\delta(\eta) + Q'_\delta(\eta)(H - H') Q'_\delta(\eta) \\ &\geq -(\Gamma - \eta + 2\sqrt{\alpha(1-\alpha)} + o(N)) Q'_\delta(\eta), \end{aligned}$$

where we used that $H - H'$ is the direct sum of the hopping operators on the boundaries $\partial B_{\alpha N}(\boldsymbol{\sigma})$ and then used the norm estimate from Lemma 2.1. If we choose α small enough, we arrive at $Q'_\delta(\eta) H Q'_\delta(\eta) \geq -(\Gamma - t/2) N Q'_\delta(\eta)$. We conclude that the energy levels $E < -(\Gamma - \eta/4)N$ of H and H' agree up to an at most exponentially small shift e^{-cN} for t small enough.

Step 3: Proof of Proposition 1.8: To conclude the proof of Proposition 1.8, it remains to evaluate for $\Gamma = \beta_c$ the probability $\mathbb{P}(E_{\boldsymbol{\sigma}_0} < \inf \operatorname{spec} H_r)$, where $E_{\boldsymbol{\sigma}_0}$ denotes the minimal ball energy. As we are only interested in the order of this probability, we simplify the calculations and write $x \simeq y$ if $x/y = \mathcal{O}(1)$. Then,

$$\begin{aligned} \mathbb{P}(E_{\boldsymbol{\sigma}_0} < \inf \operatorname{spec} H_r) &\simeq \mathbb{P}(\min U < -\beta_c N) \simeq \mathbb{P}(\min U < s_N(\ln(N)/2)) \\ &= 1 - (1 - 2^{-N} e^{-\ln(N)/2})^{2^N} \simeq 1 - e^{-1/\sqrt{N}} \simeq \frac{1}{\sqrt{N}}. \end{aligned}$$

For the first line we recall that $E_{\boldsymbol{\sigma}_0} = \min U + \mathcal{O}(1)$ and $\inf \operatorname{spec} H_r = -\Gamma N + \mathcal{O}(1)$. Moreover, we recall the definition of s_N from (1.8) and its connection to the extreme value process of U via (1.7). The remaining expressions can derived by elementary calculus. This is enough to conclude the assertions on the ground state energy.

It remains to show that aside from an exponentially small event, the ground state wave function is localized if $E_{\boldsymbol{\sigma}_0} < \inf \operatorname{spec} H_r$ and otherwise delocalized. To this end, we observe case $\inf \operatorname{spec} H_r$ and $E_{\boldsymbol{\sigma}_0}$ are independent random variables. Thus, the spectral averaging method from Lemma 4.4 shows that for any $c > 0$ there exists some $b(c) > 0$ such that

$$|\mathbb{P}(\min_{\boldsymbol{\sigma}} E_{\boldsymbol{\sigma}} - \inf \operatorname{spec} H_r)| \leq e^{-cN}) \leq e^{-b(c)N}$$

for N large enough. The Feshbach-Schur formula then yields that except for an exponentially small event the ground state function ψ of H satisfies $\|\psi - \psi_{\boldsymbol{\sigma}_0}\| \leq e^{-cN}$ if $E_{\boldsymbol{\sigma}_0} < \inf \operatorname{spec} H_r$, and otherwise $\|\psi - \psi_r\| \leq e^{-cN}$ with the ground state wave functions $\psi_{\boldsymbol{\sigma}_0}$ of $H_{\alpha N}(\boldsymbol{\sigma}_0)$ and ψ_r of H_r. From the previous steps, it follows that $\psi_{\boldsymbol{\sigma}_0}$ satisfies the assertions of Theorem 1.5 and that ψ_r is exponentially delocalized and satisfies the first assertion of Theorem 1.5.

Step 4: Proof of Proposition 1.9. Since

$$\begin{aligned}\min_{\boldsymbol{\sigma} \in \mathcal{L}_{\beta_c - \delta}} E_{\boldsymbol{\sigma}}(\Gamma = 0) &< \inf \operatorname{spec} H_r(\Gamma = 0),\\ \min_{\boldsymbol{\sigma} \in \mathcal{L}_{\beta_c - \delta}} E_{\boldsymbol{\sigma}}(\Gamma = 2\beta_c) &> \inf \operatorname{spec} H_r(\Gamma = 2\beta_c),\end{aligned}$$

by continuity of the eigenvalues of the involved matrices there exists some Γ_N such that

$$\min_{\boldsymbol{\sigma} \in \mathcal{L}_{\beta_c - \delta}} E_{\boldsymbol{\sigma}}(\Gamma_N) = \inf \operatorname{spec} H_r(\Gamma_N).$$

For this Γ_N the functions $\min_{\boldsymbol{\sigma} \in \mathcal{L}_{\beta_c - \delta}} E_{\boldsymbol{\sigma}}(\Gamma_N)$ and $\inf \operatorname{spec} H_r(\Gamma_N)$ in particular agree up to order one, i.e., (1.27) holds. Since H and H' agree at these low energies up to an exponentially small shift, we conclude that $\Delta_N(\Gamma_N)$ is exponentially small. The minimum is attained at a possibly different $\Gamma_N^\star$. However, since still $\min_{\boldsymbol{\sigma} \in \mathcal{L}_{\beta_c - \delta}} E_{\boldsymbol{\sigma}}(\Gamma_N^\star) - \inf \operatorname{spec} H_r(\Gamma_N^\star) = o(1)$, we have $\Gamma_N^\star - \Gamma_N = o(N^{-1})$ as claimed. □

Acknowledgments

This work was supported by the DFG under EXC-2111 – 390814868.

References

[1] J. Adame, S. Warzel. Exponential vanishing of the ground-state gap of the QREM via adiabatic quantum computing, J. Math. Phys. 56: 113301 (2015).

[2] A. Adhikari, C. Brennecke. Free energy of the Quantum Sherrington-Kirkpatrick spin-glass model with transverse field. J. Math. Phys. 61: 083302 (2020).

[3] M. Aizenman, J. L. Lebowitz, D. Ruelle. Some Rigorous Results on the Sherrington-Kirkpatrick Spin Glass Model. Commun. Math. Phys. 112: 3-20 (1987).

[4] M. Aizenman, M. Shamis, S. Warzel. Resonances and partial delocalization on the complete graph, Ann. Henri Poincare 16: 1969-2003 (2015).

[5] M. Aizenman, S. Warzel. Random Operators: Disorder Effects on Quantum Spectra and Dynamics, AMS 2015.
[6] L. Avena, O. Gün, M. Hesse. The parabolic Anderson model on the hypercube. Stoch. Proc. Appl. 130, 3369-3393 (2020).
[7] E. Baake, M. Baake, and H. Wagner. Ising quantum chain is equivalent to a model of biological evolution. Phys. Rev. Lett., 78: 559–562 (1997). Erratum: Phys. Rev. Lett. 79: 1782 (1997)
[8] E. Baake, H. Wagner. Mutation–selection models solved exactly with methods of statistical mechanics. Genet. Res. 78: 93–117 (2001).
[9] C. L. Baldwin, C. R. Laumann, A. Pal, A. Scardicchio. The many-body localized phase of the quantum random energy model, Phys. Rev. B 93: 024202 (2016).
[10] G. Ben Arous, A. Bovier, V. Gayrard. Glauber dynamics of the random energy model. I. Metastable motion on the extreme states. Comm. Math. Phys., 235: 379–425 (2003).
[11] G. Ben Arous, A. Bovier, V. Gayrard. Glauber dynamics of the random energy model. II. Aging below the critical temperature. Comm. Math. Phys., 236: 1–54 (2003).
[12] F. A. Berezin. Convex operator functions. Math. USSR Sbornik 17, 269–277 (1972). Mat. Sbornik 88, 268–276 (1972).
[13] R. Bhatia. Matrix Analysis. Springer, 1997.
[14] G. Biroli, D. Facoetti, M. Schiró, M. Tarzia, P. Vivo. Out-of-equilibrium phase diagram of the quantum random energy model. Phys. Rev. B 103: 014204 (2021).
[15] M. Biskup, W. König. Eigenvalue order statistics for random Schrödinger operators with doubly-exponential tails. Commun. Math. Phys. 341, 179–218 (2016).
[16] B. Bollobás, J. Leed, S. Letzter. Eigenvalues of subgraphs of the cube, Eur. J. Comb. 70: 125–148 (2018).
[17] A. Bovier. Statistical Mechanics of Disordered Systems. A Mathematical Perspective. Cambridge University Press, 2012.
[18] A. Bovier, I. Kurkova, M. Löwe. Fluctuations of the free energy in the REM and the p-spin SK models. Ann. Probab., 30: 605–651 (2002).
[19] A. Bovier, I. Kurkova. Derrida's generalised random energy models. I. Models with finitely many hierarchies. Ann. Inst. H. Poincaré Probab. Statist., 40:439–480 (2004).
[20] A. Bovier, I. Kurkova. Derrida's generalized random energy models. II. Models with continuous hierarchies. Ann. Inst. H. Poincaré Probab. Statist., 40:481–495 (2004).
[21] A.J. Bray, M.A. Moore. Replica theory of quantum spin glasses. J. Phys. C, Solid State Phys. 13: L655 (1980).
[22] A. Burin. Localization and chaos in a quantum spin glass model in random longitudinal fields: Mapping to the localization problem in a Bethe lattice with a correlated disorder. Ann. Phys. 529: 1600292 (2017).
[23] D. Capocaccia, M. Cassandro, P. Picco. On the existence of thermodynamics for the generalized random energy model. J. Stat. Phys. 46:493–505 (1987).
[24] J. C̃erný, T. Wassmer. Aging of the metropolis dynamics on the random energy model, Probab. Theory Related Fields 167: 1–51 (2015).
[25] N. Crawford. Thermodynamics and universality for mean field quantum spin glasses, Commun. Math. Phys. 274: 821–839 (2007).
[26] D.M. Cvetković, M. Doob. H. Sachs. Spectra of graphs: Theory and applications, 3rd ed., Johann Ambrosius Barth, Heidelberg, 1995.
[27] B. Derrida. Random energy model: limit of a family of disordered models, Phys. Rev. Lett. 45:

79-82 (1980).
[28] B. Derrida. Random energy model: an exactly solvable model of disordered systems, Phys. Rev. B 24: 2613-2326 (1981).
[29] B. Derrida. A generalization of the random energy model that includes correlations between the energies, J. Phys. Lett. 46: 401–407 (1985).
[30] B. Derrida, E. Gardner. Solution of the generalized random energy model, J. Phys. C 19: 2253–2274 (1986).
[31] L. Faoro, M. V. Feigelman and L. Ioffe. Non-ergodic extended phase of the quantum random energy model, Annals of Physics 409: 167916 (2019).
[32] Y.V. Fedorov, E.F. Shender. Quantum spin glasses in the Ising model with a transverse field. JETP Lett. 43: 681 (1986).
[33] J. Friedman, J. P. Tillich. Generalized Alon-Boppana theorems and error-correcting codes. Siam J. Descrete Math. 19: 700–718 (2005).
[34] A. Galves, S. Martinez, P. Picco. Fluctuations in Derrida's random energy and generalized random energy models. J Stat Phys 54: 515–529 (1989).
[35] V. Gayrard. Aging in Metropolis dynamics of the REM: a proof. Probab. Theory Relat. Fields 174: 501-551 (2019).
[36] V. Gayrard, L. Hartung. Dynamic phase diagram of the REM. In: V. Gayrard, L.P. Arguin, N. Kistler, I. Kourkova (eds) Statistical Mechanics of Classical and Disordered Systems. StaMeClaDys 2018. Springer Proceedings in Mathematics & Statistics, vol 293. Springer, Cham 2019.
[37] L. N. Grenkova, S. A. Molchanov, Yu. N. Sudarev. Structure of spectrum edge for multidimensional Anderson model. Theor. Math. Phys. 85: 1033–1039 (1990).
[38] Y. Y. Goldschmidt. Solvable model of the quantum spin glass in a transverse field. Phys. Rev. B 41: 4858 (1990).
[39] J. Hermisson, O. Redner, H. Wagner. E. Baake. Mutation-selection balance: ancestry, load, and maximum principle. Theor. Popul. Biol. 62: 9–46 (2002).
[40] O. Kallenberg. Foundations of modern probability, Springer-Verlag, New York 2002.
[41] J. F. C. Kingman. A simple model for the balance between selection and mutation. J. Appl. Probab. 15: 1–12 (1978).
[42] V. E. Kravtsov, I. M. Khaymovich, E. Cuevas, M. Amini. A random matrix model with localization and ergodic transitions. New J. Phys. 17:122002, 2015.
[43] W. König. The Parabolic Anderson Model. Birkhäuser, Switzerland, 2016.
[44] M.R. Leadbetter, G. Lindgren, H. Rootzén. Extremes and related properties of random sequences and processes. Springer Series in Statistics. Springer-Verlag, New York, 1983.
[45] D. A. Levin, Y. Peres, E. L. Wilmer, J. Propp, D. B. Wilson. Markov Chains and Mixing Times. 2nd ed. AMS 2017.
[46] T. Jörg, F. Krzakala, J. Kurchan, A.C. Maggs. Simple glass models and their quantum annealing. Phys. Rev Lett. 101: 147204 (2008).
[47] T. Jörg, F. Krzakala, G. Semerjian, F. Zamponi. First-order transitions and the performance of quantum algorithms in random optimization problems. Phys. Rev. Lett. 104: 207206 (2010).
[48] C. R. Laumann, A. Pal, A. Scardicchio. Many-body mobility edge in a mean-field quantum spin glass, Phys. Rev. Lett. 113: 200405 (2014).
[49] H. Leschke, C. Manai, R. Ruder, S. Warzel. Existence of replica-symmetry breaking in quantum glasses, Phys. Rev. Lett. 127: 207204 (2021).

[50] H. Leschke, S. Rothlauf, R. Ruder, W. Spitzer. The free energy of a quantum Sherrington-Kirkpatrick spin-glass model for weak disorder, J. Stat. Phys. 182: 55 (2021).
[51] C. Manai and S. Warzel. Phase diagram of the quantum random energy model, J. Stat. Phys. 180: 654–664 (2020).
[52] C. Manai and S. Warzel. The quantum random energy model as a limit of p-spin interactions, Rev. Math. Phys. 33: 2060013 (2020).
[53] C. Manai, S. Warzel. Generalized random energy models in a transversal magnetic field: free energy and phase diagrams, Probab. Math. Phys. 3: 215–245 (2022).
[54] C. Manai, S. Warzel. The de Almeida-Thouless Line in Hierarchical Quantum Spin Glasses, J. Stat. Phys. 186:14 (2022).
[55] M. Mézard, G. Parisi, M. A. Virasoro. Spin Glass Theory and Beyond. World Scientific, Singapore (1987).
[56] E. Olivieri, P. Picco. On the existence of thermodynamics for the random energy model. Comun. Math. Phys. 96: 125-144 (1984)
[57] R. I. Oliveira. Concentration of the adjacency matrix and of the Laplacian in random graphs with independent edges. Preprint http://arXiv.org/abs/0911.0600, Feb. 2010.
[58] D. Panchenko. The Sherrington-Kirkpatrick model. Springer, 2013.
[59] G. Parisi. The order parameter for spin glasses: a function on the interval 0-1, J. Phys. A: Math. Gen., 13: 1101–1112 (1980).
[60] P. Ray, B. K. Chakrabarti, A. Chakrabarti. Sherrington–Kirkpatrick model in a transverse field: Absence of replica symmetry breaking due to quantum fluctuations, Phys. Rev. B **39**, 11828–11832 (1989).
[61] D. Ruelle. A mathematical reformulation of Derrida's REM and GREM. Comm. Math. Phys. 108: 225–239 (1987).
[62] I. G. Szendro, M. F. Schenk, J. Franke, J. Krug, J. A. G. M. de Visser. Quantitative analyses of empirical fitness landscapes. J. Stat. Mech. Theory Exp. 2013:P01005 (2013).
[63] G. De Tomasi, I. M. Khaymovich, F. Pollmann, S. Warzel. Rare thermal bubbles at the many-body localization transition from the Fock space point of view, Phys. Rev. B 104: 024202 (2021).
[64] B. Simon, A Comprehensive Course in Analysis, Part 4. Operator Theory, American Mathematical Soc., 2015
[65] B. Simon. *The statistical mechanics of lattice gases*, Princeton Univ. Press 1993.
[66] V. N. Smelyanskiy, K. Kechedzhi, S. Boixo, S. V. Isakov, H. Neven, B. Altshuler. Nonergodic delocalized states for efficient population transfer within a narrow band of the energy landscape. Phys. Rev. X 10: 011017 (2020).
[67] S. Suzuki, J. Inoue, B. K. Chakrabarti. Quantum Ising phases and transitions in transverse Ising models, 2nd ed., Springer 2013.
[68] M. Talagrand. Concentration of measure and isoperimetric inequalities in product spaces, Publ. Math. IHES 81:73–205 (1995).
[69] M. Talagrand. Mean field models for spin glasses (Vol I+II), Springer 2011.
[70] T. Tao. Topics in random matrix theory, AMS 2012.
[71] J. A. Tropp. An introduction to matrix concentration inequalities, Foundations and Trends in Machine Learning 8:1–230 (2015).
[72] P. von Soosten, S. Warzel. Non-ergodic delocalization in the Rosenzweig-Porter model, Lett. Math. Phys. 109: 905-922 (2019).

[73] T. Yamamoto, H. Ishii. A perturbation expansion for the Sherrington–Kirkpatrick model with a transverse field, J. Phys. C **20**, 6053–6060 (1987).

Chokri Manai and Simone Warzel
MCQST and Department of Mathematics
Technische Universität München

B.2 The quantum random energy model as a limit of p-spin interactions

The quantum random energy model as a limit of p-spin interactions.

Chokri Manai and Simone Warzel

Derrida originally derived the random energy model by considering the $p \to \infty$ limit of $p - spin$ models, which formally leads to an uncorrelated Gaussian process, namely the REM. By classical Gaussian interpolation one can prove that indeed if we consider the limiting specific p-spin pressure Φ_p, then Φ_p converges indeed to the REM pressure as $p \to \infty$. To put it in other words, one can exchange the thermodynamic limit $N \to \infty$ and the $p \to \infty$-limit. Article V establishes a similar result for the QREM and the quantum p-spin models.

Main Results

In this work, we consider a coupled limit of p and N, where $p, N \to \infty$. We assume that $p(N)$ grows superlogarithmic, that is, $p(N)/\ln(N) \to \infty$ as $N \to \infty$. In this situation, we prove that the specific p-spin pressure $\Phi_{p(N),N}$ converges to the QREM pressure Φ_{QREM}. Our theorem is slightly weaker than the classical version sketched above, as we do not show that the $p \to \infty$ and $N \to \infty$ limit can be exchanged. Nevertheless, our result justifies to regard the QREM as the $p \to \infty$ limit of the quantum p-spin models. Our proof is based on the technique introduced in [128]. The main difficulty is to verify that the weak correlations in the $p(N)$-spin potential still do not cause percolation of the large deviations set. To do so, we analyze the energy landscape via geometric and probabilistic methods.

Individual Contribution

I am the principal of the author of this article. Shortly after finishing our first publication on the QREM, I noticed that our methods can be extended to weakly correlated potentials. In a discussion with Simone Warzel we quickly realized that my observation can be used to prove that the QREM is the limit of quantum p-spin models. We created together a first draft for our article and cooperated closely to finish this work. I was mainly responsible for the proof section whereas Simone Warzel focused on the introduction.

Permission to include:

Chokri Manai and Simone Warzel.
The quantum random energy model as a limit of p-spin interactions.
Reviews in Mathematical Physics 33: 2060013 (2020).
https://doi.org/10.1142/S0129055X20600132

RE: Permission to reuse article in my thesis

Rights <rights@wspc.com>

Mi 16.11.2022 02:33

An: Manai, Chokri <chokri.manai@tum.de>;

Dear Chokri Manai

Yes that's correct.

Kind regards
Tu Ning

From: Manai, Chokri <chokri.manai@tum.de>
Sent: 2022年11月15日 17:23
To: Rights <rights@wspc.com>
Subject: AW: Permission to reuse article in my thesis

You don't often get email from chokri.manai@tum.de. Learn why this is important

Dear Tu Ning,

thank you very much!

So, do I understand correctly, that I am allowed to include my own preprint but not the version as it was printed in the journal?

Best regards,

Chokri Manai

Von: Rights <rights@wspc.com>
Gesendet: Dienstag, 15. November 2022 01:52:49
An: Manai, Chokri
Betreff: RE: Permission to reuse article in my thesis

Dear Chokri Manai

Thanks for getting in touch.
We are pleased to grant you the permission, as long as your own version of the article been included in your dissertation and full credit been given to the original source.

Kind regards
Tu Ning

From: Manai, Chokri <chokri.manai@tum.de>
Sent: 2022年11月13日 21:12
To: Rights <rights@wspc.com>
Subject: AW: Permission to reuse article in my thesis

Dear ladies and gentlemen,

as I have not received a response so far, I would like to remind you of my request concerning

the reuse of my article in my thesis (see below).

Best regards,

Chokri Manai

Von: Manai, Chokri
Gesendet: Sonntag, 30. Oktober 2022 01:00:09
An: rights@wspc.com.sg
Betreff: Permission to reuse article in my thesis

Dear ladies and gentlemen,

I am about to graduate and would like to use the following article in my dissertation:

Chokri Manai and Simone Warzel

The quantum random energy model as a limit of p-spin interactions
Reviews in Mathematical PhysicsVol. 33, No. 01, 2060013 (2021)
https://doi.org/10.1142/S0129055X20600132

I kindly ask for the permission to reprint this article in my doctoral thesis.

Best regards,
Chokri Manai

The Quantum Random Energy Model as a Limit of p-Spin Interactions

Chokri Manai and Simone Warzel

Abstract
We consider the free energy of a mean-field quantum spin glass described by a p-spin interaction and a transversal magnetic field. Recent rigorous results for the case $p = \infty$, i.e. the quantum random energy model (QREM), are reviewed. We show that the free energy of the p-spin model converges in a joint thermodynamic and $p \to \infty$ limit to the free energy of the QREM.

1 Introduction

A prominent class of classical mean-field spin glass models are p-spin interactions defined on N Ising-type spins

$$\boldsymbol{\sigma} = (\sigma_1, \dots, \sigma_N) \in \{-1, 1\}^N =: \mathcal{Q}_N. \tag{1.1}$$

For fixed $p \in [1, \infty)$ the interaction energy of these spins is random and given by

$$U_p(\boldsymbol{\sigma}) = \frac{1}{N^{\frac{p-1}{2}}} \sum_{j_1,\dots,j_p=1}^{N} g_{j_1,\dots,j_p} \sigma_{j_1} \cdots \sigma_{j_p} \tag{1.2}$$

in terms of an array $g_{\boldsymbol{j}} := g_{j_1,\dots,j_p}$ of independent and identically distributed (i.i.d.), centered Gaussian random variable with variance one. The process $U_p(\boldsymbol{\sigma})$, $\boldsymbol{\sigma} \in \mathcal{Q}_N$ is then Gaussian as well and uniquely characterized by its mean and covariance function,

$$\mathbb{E}\left[U_p(\boldsymbol{\sigma})\right] = 0, \qquad \mathbb{E}\left[U_p(\boldsymbol{\sigma}) U_p(\boldsymbol{\sigma}')\right] = N \left(N^{-1} \sum_{j=1}^{N} \sigma_j \sigma_j' \right)^p =: N\, \xi(\boldsymbol{\sigma}, \boldsymbol{\sigma}')^p. \tag{1.3}$$

The special case $p = 2$ corresponds to the Sherrington-Kirkpatrick model, and in the limit $p \to \infty$ we obtain Derrida's random energy model (REM) [1]. In the latter case, the correlations vanish and the variables $U_\infty(\boldsymbol{\sigma})$ form an i.i.d. Gaussian process on the hypercube $\mathcal{Q}_N$.

There is a wealth of results both in the physics as well as mathematics literature concerning properties of the Gibbs measure of these classical mean-field spin glasses. Most celebrated is a closed form expression for the free energy derived by Parisi [2] and later proven by Talagrand and Panchenko [3, 4]. This formula reflects the fact that at low temperatures the Gibbs measure fractures into many inequivalent pure states. A key quantity in this area is the distribution of the overlap $\xi(\boldsymbol{\sigma}, \boldsymbol{\sigma}')$ of independent copies or replicas of spins $\boldsymbol{\sigma}, \boldsymbol{\sigma}'$. We refer the mathematically interested reader to the monographs [5, 6, 7] and references therein.

Despite its popularity in physics (cf. [8, 9] and refs. therein), much less is rigorously established if one incorporates quantum effects in the form of a transversal magnetic field. In the quantum case, one views the spins configurations (1.1) as the z-components of N spin-1/2 quantum spins and the energy (1.2) is lifted to the corresponding Hilbert space $\otimes_{j=1}^{N}\mathbb{C}^2 \equiv \ell^2(\mathcal{Q}_N)$ as a diagonal matrix U_p. The random Hamiltonian of the quantum p-spin model with transversal magnetic field of strength $\Gamma \geq 0$ is

$$H_p = U_p + \Gamma\, T, \tag{1.4}$$

where $(T\psi)(\boldsymbol{\sigma}) := -\sum_{j=1}^{N} \psi(\sigma_1, \ldots, -\sigma_j, \ldots, \sigma_N)$ coincides with the action of the negative sum of x-components of the Pauli matrices in the z-basis. In this paper, we are concerned with the corresponding quantum free energy or pressure at inverse temperature $\beta \in [0, \infty)$

$$\Phi_N^p(\beta, \Gamma) := \frac{1}{N} \ln Z_N^p(\beta, \Gamma) \tag{1.5}$$

which derives from the partition function $Z_N^p(\beta, \Gamma) = 2^{-N} \mathrm{Tr}\, e^{-\beta H_p}$. The case $p = \infty$ corresponds to the pressure of the quantum random energy model (QREM), and we will write $\Phi^{\mathrm{QREM}}(\beta, \Gamma) := \Phi^{\infty}(\beta, \Gamma)$.

2 Rigorous results on the free energy

A basic property of the free energy of spin glasses is its self-averaging, i.e. the fact that in the thermodynamic limit $N \to \infty$ this quantity agrees almost surely with its average. For p-spin interactions even more general than (1.2) self-averaging of the quantum free energy has been established in [10]. Since we restrict ourselves to the Gaussian case, this property follows immediately from the standard Gaussian concentration inequality. We therefore include the short argument for pedagogical reasons.

Proposition 2.1 ([10])**.** *There are some constants $c, C \in (0, \infty)$ such that for any $p \in [1, \infty]$ the Gaussian concentration estimate*

$$\mathbb{P}\left(\left| \Phi_N^p(\beta, \Gamma) - \mathbb{E}\left[\Phi_N^p(\beta, \Gamma) \right] \right| > \frac{t\,\beta}{\sqrt{N}} \right) \leq C \, \exp\left(-ct^2\right) \tag{2.1}$$

holds for all $t > 0$ and all $N \in \mathbb{N}$.

Proof. The pressure's variations with respect to the i.i.d. standard Gaussian variables $g_{\boldsymbol{j}}$ is

$$-\frac{\partial \Phi_N^p(\beta, \Gamma)}{\partial g_{\boldsymbol{j}}} = \frac{\beta}{N^{\frac{p+1}{2}}\, 2^N Z(\beta, \Gamma)} \sum_{\boldsymbol{\sigma}} \sigma_{j_1} \cdots \sigma_{j_p} \, \langle \boldsymbol{\sigma} | e^{-\beta H} | \boldsymbol{\sigma} \rangle.$$

Here and in the following we use Dirac's bracket notation for matrix elements. Consequently, the Lipschitz constant is bounded by

$$\sum_{\boldsymbol{j}} \left(\frac{\partial \Phi_N^p(\beta, \Gamma)}{\partial g_{\boldsymbol{j}}} \right)^2 \leq \frac{\beta^2}{N}.$$

The claim thus follows from the Gaussian concentration inequality for Lipschitz functions. □

In the classical case $\Gamma = 0$, the free energy of any p-spin interaction is given in terms of Parisi's formula [4]. One of its main features is a transition at small enough temperatures to a spin glass regime. At $p = \infty$ this formula takes a simple form:

$$\Phi^{\mathrm{REM}}(\beta) = \lim_{N\to\infty} \Phi_N^{\infty}(\beta, 0) = \begin{cases} \frac{1}{2}\beta^2 & \text{if } \beta \le \beta_c, \\ \frac{1}{2}\beta_c^2 + (\beta - \beta_c)\beta_c & \text{if } \beta > \beta_c. \end{cases} \tag{2.2}$$

The non-differentiability at

$$\beta_c := \sqrt{2\ln 2}$$

reflects a first-order freezing transition into a low-temperature phase characterized by the vanishing of the specific entropy.

Under the addition of a constant transversal field, this freezing transition vanishes for Γ large enough. A first-order phase transition into a quantum paramagnetic phase, characterized by

$$\Phi^{\mathrm{PAR}}(\beta\Gamma) := \ln\cosh(\beta\Gamma),$$

occurs at $\Gamma_c(\beta) := \beta^{-1}\operatorname{arcosh}\left(\exp\left(\Phi^{\mathrm{REM}}(\beta)\right)\right)$. At $\beta = \infty$ this connects to the known location $\Gamma_c(\infty) = \beta_c$ of the quantum phase transition of the ground state [11, 12].

The shape of the phase diagram of the QREM in Figure 1 including the precise location of the first-order transition, was predicted by Goldschmidt [13] in the 1990s. His arguments are based on the replica trick and the so-called static approximation in the path-integral representation of $\mathbb{E}\left[Z_N^p(\beta,\Gamma)^n\right]$. In a recent paper [14], we confirmed this prediction.

Theorem 2.2 ([14]). *For any $\Gamma, \beta \ge 0$ almost surely:*

$$\Phi^{QREM}(\beta,\Gamma) := \lim_{N\to\infty} \Phi_N^{QREM}(\beta,\Gamma) = \max\{\Phi^{REM}(\beta), \Phi^{PAR}(\beta\Gamma)\}.$$

In broad terms, the main features of the phase diagram in Figure 1 such as a low-temperature frozen phase which gives way to a paramagnetic phase at both high temperatures or strong magnetic field are expected to stay for general p; cf. [8, 13, 15, 16]. The new features for general p are the richer structure of the low-temperature phase due to higher-order replica symmetry breaking and the conjectured endpoint of the first-order transition line in a critical point at a finite temperature which scales with $\sqrt{p}$. No closed expression for the free energy is known in the quantum case. Crawford [10] showed that the almost-sure limit

$$\Phi^p(\beta,\Gamma) := \lim_{N\to\infty} \Phi_N^p(\beta,\Gamma), \tag{2.3}$$

exists for any $p \in [1,\infty]$. All claims concerning the structure of the phase diagram for quantum p-spin models are based on non-rigorous calculations using the replica trick and a $1/p$ expansion [13, 15, 16]. In fact, it is widely believed that $\Phi^p(\beta,\Gamma)$ is continuous in $1/p$ and hence tends to the explicit expression for the QREM,

$$\lim_{p\to\infty} \Phi^p(\beta,\Gamma) = \Phi^{\mathrm{QREM}}(\beta,\Gamma).$$

We do not quite proof this conjecture in this paper. However, as a main new result we have the following continuity of the free energy.

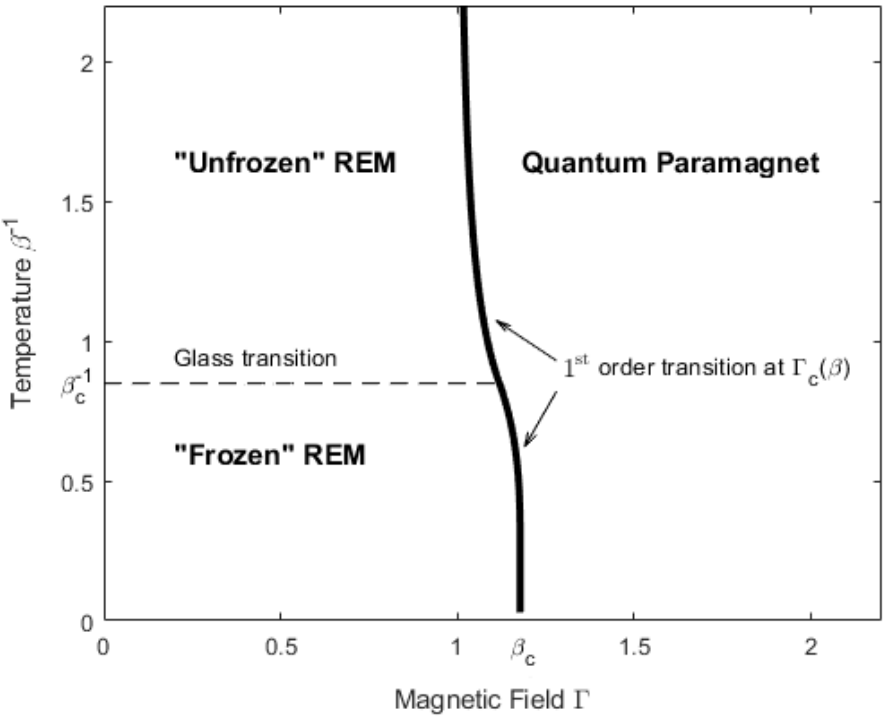

Figure 1: Phase diagram of the QREM as a function of the transversal magnetic field Γ and the temperature β^{-1}. The first-order transition occurs at fixed β and $\Gamma_c(\beta)$. The freezing transition is found at temperature $\beta_c^{-1} = (2\ln 2)^{-1/2}$, which is unchanged in the presence of a magnetic field of strength $\Gamma < \Gamma_c(\beta)$.

Theorem 2.3. *Let $p(N)$ be a nonnegative sequence which satisfies a superlogarithmic growth condition, i.e.*

$$\lim_{N\to\infty} \frac{p(N)}{\ln(N)} = \infty. \tag{2.4}$$

For any $\beta, \Gamma \geq 0$, we then have the almost sure convergence

$$\lim_{N\to\infty} \Phi_N^{p(N)}(\beta,\Gamma) = \Phi^{QREM}(\beta,\Gamma). \tag{2.5}$$

The proof of this statement heavily relies on the method of proof of Theorem 2.2 in [14]. It will be presented in Section 3 below.

Let us conclude with some remarks:

1. In the classical case $\Gamma = 0$, the quenched pressure $\mathbb{E}\left[\Phi_N^p(\beta,0)\right]$ is monotonically increasing in p and, in particular, we have $\mathbb{E}\left[\Phi_N^p(\beta,0)\right] \leq \mathbb{E}\left[\Phi_N^{\mathrm{REM}}(\beta)\right]$ for any $N \in \mathbb{N}$. This follows

with the help of Gaussian comparison [5, Lemma 10.2.1] from the following facts: i) $2\mathbb{N} \ni p \mapsto \mathbb{E}\left[U_p(\boldsymbol{\sigma})U_p(\boldsymbol{\sigma'})\right]$ is monotonically decreasing, and ii) $\frac{\partial^2 \Phi_N^p(\beta,0)}{\partial U_p(\boldsymbol{\sigma})\partial U_p(\boldsymbol{\sigma'})} < 0$ in case $\boldsymbol{\sigma} \neq \boldsymbol{\sigma'}$. Unfortunately, a similar monotonicity is not known in the quantum case.

2. Another intensively studied family of mean-field spin-glasses are the so-called spherical p-spin models, given by

$$\widehat{U}_p(\boldsymbol{\sigma}) = \sqrt{\frac{p!}{N^{p-1}}} \sum_{1 \leq j_1 < \cdots < j_p \leq N} g_{j_1,\ldots,j_p} \sigma_{j_1} \cdots \sigma_{j_p}. \tag{2.6}$$

In the classical case the spherical p-spin models give rise to the same pressure in the thermodynamic limit as the p-spin SK-models (1.2); however, the models have different scales of fluctuations [17].
Theorem 2.3 remains true (with minor changes in the proof) if one works instead with the spherical p-spin models. This follows from the observation that

$$\mathbb{E}\left[\widehat{U}_p(\boldsymbol{\sigma})\widehat{U}_p(\boldsymbol{\sigma'})\right] = N\left(\xi(\boldsymbol{\sigma},\boldsymbol{\sigma'})^p - \delta_N^p(\boldsymbol{\sigma},\boldsymbol{\sigma'})\right), \tag{2.7}$$

where $\delta_N^p(\boldsymbol{\sigma},\boldsymbol{\sigma'})$ is uniformly bounded,

$$|\delta_N^p(\boldsymbol{\sigma},\boldsymbol{\sigma'})| \leq \frac{1}{N^p} \sum_{\substack{1 \leq j_1 \leq \cdots \leq j_p \leq N \\ \exists 1 \leq k < l \leq p:\, j_k = j_l}} 1 \leq \frac{N^p - p!\binom{N}{p}}{N^p} \leq \min\left\{1, \frac{p(p-1)}{2N}\right\}. \tag{2.8}$$

3 Proof of Theorem 2.3

The proof is an adaptation of the strategy for the proof Theorem 2.2 in [14]. The lower bound in [14] was based on the Gibbs variational principle and established there already for general p-spin interactions. For convenience of the reader, we recall the corresponding lemma here.

Lemma 3.1 (=Lemma 2.1 in [14]). *For any $p \in [1,\infty]$, $N \in \mathbb{N}$ and $\Gamma, \beta \geq 0$:*

$$\Phi_N^p(\beta,\Gamma) \geq \max\left\{\Phi_N^p(\beta,0), p^{\mathrm{PAR}}(\beta\Gamma) - \frac{\beta}{N2^N} \sum_{\boldsymbol{\sigma} \in \mathcal{Q}_N} U_p(\boldsymbol{\sigma})\right\}. \tag{3.1}$$

The main new challenge is to cope with the correlations in U_p for $p < \infty$ in the upper bound of [14]. Since these correlations vanish in the limit $p \to \infty$, the large deviation sets

$$\mathcal{L}_\epsilon^p := \{\boldsymbol{\sigma} | U_p(\boldsymbol{\sigma}) < -\epsilon N\}, \tag{3.2}$$

with $\epsilon > 0$ are expected to consist of isolated small clusters. We write $\mathcal{L}_\epsilon^p = \bigcup_\alpha C_\epsilon^{\alpha,p}$ as a disjoint union of as its maximal edge-connected components $C_\epsilon^{\alpha,p}$, where we recall from [14]:

Definition 3.2. *An edge-connected component $\mathcal{C}_\varepsilon \subset \mathcal{L}_\varepsilon$ is a subset for which each pair $\sigma, \sigma' \in \mathcal{C}_\varepsilon$ is connected through a connected edge-path of adjacent edges. An edge-connected component $\mathcal{C}_\varepsilon$ is maximal if there is no other vertex $\sigma \in \mathcal{L}_\varepsilon \backslash \mathcal{C}_\varepsilon$ such that $\mathcal{C}_\varepsilon \cup \{\sigma\}$ forms an edge-connected component.*

In the situation of Theorem 2.3 we cannot expect that the size of the edge-connected components $C_\epsilon^{\alpha,p(N)}$ remains bounded as $N \to \infty$. However, we show that it is highly likely that all edge-connected components $C_\epsilon^{\alpha,p(N)}$ are contained in balls whose radius grows only sublinearly in N.

Proposition 3.3. *There exist a subset $\Omega_{\epsilon,N}$ of realisations and a constant $K \in \mathbb{N}$, which is independent of N, such that:*

1. *for some $c_\varepsilon > 0$, which is independent of N, and all N large enough:*

$$\mathbb{P}\left(\Omega_{\varepsilon,N}\right) \geq 1 - e^{-c_\varepsilon N},$$

2. *on $\Omega_{\varepsilon,N}$ any edge-connected component $C_\epsilon^{\alpha,p(N)}$ of $\mathcal{L}_\epsilon^{p(N)}$ is contained in a ball $B_{K\lceil \frac{N}{p(N)} \rceil}(\boldsymbol{\sigma})$ for some $\boldsymbol{\sigma} \in \mathcal{Q}_N$.*

Before turning to the proof of Proposition 3.3, we demonstrate how this result and the basic bounds in [14] imply the almost sure convergence (2.5) in Theorem 2.3.

Proof of Theorem 2.3. The lower bound in Lemma 3.1 yields

$$\begin{aligned} \liminf_{N\to\infty} \Phi_N^{p(N)}(\beta,\Gamma) &\geq \max\{\liminf_{N\to\infty} \Phi_N^{p(N)}(\beta,0), \Phi^{\mathrm{PAR}}(\beta\Gamma)\} \\ &= \max\{\ \Phi^{\mathrm{REM}}(\beta), \Phi^{\mathrm{PAR}}(\beta\Gamma)\} = \Phi^{\mathrm{QREM}}(\beta,\Gamma), \end{aligned} \tag{3.3}$$

Here the last equality follows from the continuity of the classical p-spin pressure, which is encoded in Parisi's formula [5, Thm. 11.3.7], and its monotonicity, stated as a remark after Theorem 2.3.

For the upper bound, we fix some $\epsilon > 0$ and we use the decomposition of the Hamiltonian

$$H_{p(N)} =: U_{\mathcal{L}_\epsilon^{p(N)}} \oplus H_{\mathcal{L}_\epsilon^{p(N),c}} - \Gamma A_{\mathcal{L}_\epsilon^{p(N)}} \tag{3.4}$$

where $U_{\mathcal{L}_\epsilon^{p(N)}}$ is the multiplication operator by the REM values on $\ell^2(\mathcal{L}_\epsilon^{p(N)})$ and $H_{\mathcal{L}_\epsilon^{p(N),c}}$ is the restriction of the Hamiltonian to the complementary subspace $\ell^2(\mathcal{L}_\epsilon^{p(N),c})$. The remainder term $A_{\mathcal{L}_\epsilon^{p(N)}}$ consists of the matrix elements of $-T$ reaching $\mathcal{L}_\epsilon^{p(N)}$, i.e.

$$\langle \boldsymbol{\sigma} | A_{\mathcal{L}_\varepsilon} | \boldsymbol{\sigma}' \rangle = \begin{cases} 1 & \text{if } \boldsymbol{\sigma} \in \mathcal{L}_\varepsilon \text{ or } \boldsymbol{\sigma}' \in \mathcal{L}_\varepsilon \text{ and } d(\boldsymbol{\sigma},\boldsymbol{\sigma}') = 1, \\ 0 & \text{else.} \end{cases} \tag{3.5}$$

As in the proof of [14, Corollary 2.5] one obtains from the Golden-Thompson inequality the upper bound

$$\Phi_N^{p(N)}(\beta,\Gamma) \leq \max\{\Phi_N^{p(N)}(\beta,0), \Phi^{\mathrm{PAR}}(\beta\Gamma) + \beta\epsilon\} + \frac{1}{N}\left(\beta\Gamma \| A_{\mathcal{L}_\epsilon^{p(N)}} \| + \ln 2\right). \tag{3.6}$$

The operator norm of the restriction of T to a Hamming ball B_r of radius r is known [18] to be bounded by $\|T_{B_r}\| \leq 2\sqrt{r(N-r+1)}$. Since the matrix elements of $-T$ are non-negative, the

restrictions of T satisfy a monotonicity property, i.e. if $A \subset B$, then $\|T_A\| \leq \|T_B\|$. Consequently, on the event $\Omega_{\epsilon,N}$ from Proposition 3.3 we have

$$\limsup_{N\to\infty} \frac{1}{N}\|A_{\mathcal{L}_\epsilon^{p(N)}}\| = \limsup_{N\to\infty} \max_\alpha \frac{1}{N}\|T_{\mathcal{C}_\epsilon^{\alpha,p(N)}}\| \leq \limsup_{N\to\infty} \frac{2\sqrt{K}}{\sqrt{N}}\sqrt{1+N/p(N)} = 0. \tag{3.7}$$

A Borel-Cantelli argument implies the almost sure bound

$$\limsup_{N\to\infty} \Phi_N^{p(N)}(\beta,\Gamma) \leq \Phi^{\mathrm{QREM}}(\beta,\Gamma) + \beta\epsilon, \tag{3.8}$$

for any $\epsilon > 0$ and the assertion of Theorem 2.3 follows. □

We prepare the proof of Proposition 3.3 with a bound on the probability that all components of a centered Gaussian vector are smaller than a certain constant:

Lemma 3.4. *Let $\boldsymbol{g} = (g_1, \ldots, g_L)$, $L \in \mathbb{N}$, a centered Gaussian random vector with*

$$C_L \coloneqq \max_{i=1,\ldots,L} \sum_{j=1}^{L} \mathbb{E}\left[g_i g_j\right]. \tag{3.9}$$

Then for any $\delta > 0$

$$\mathbb{P}\left(\max_j g_j < -\delta,\right) \leq \exp\left(-\frac{L\delta^2}{2C_L}\right). \tag{3.10}$$

Proof. The random variable $S_L \coloneqq \sum_{i=1}^{L} g_i$ is Gaussian, centered and with variance bounded by $\mathbb{E}(S_L^2) \leq LC_L$. A standard estimate for Gaussian variables implies

$$\mathbb{P}\left(\max_j g_j < -\delta\right) \leq \mathbb{P}(S_L < -L\delta) \leq \exp\left(-\frac{L^2\delta^2}{2\mathbb{E}(S_L^2)}\right) \leq \exp\left(-\frac{L\delta^2}{2C_L}\right). \tag{3.11}$$

□

We are now ready to spell out the proof of Proposition 3.3, which is based on a combinatorial argument.

Proof of Proposition 3.3. It turns out to be helpful for the purpose of this proof to introduce the notion of an edge-connected ray. We say that $\boldsymbol{\sigma_1}, \ldots, \boldsymbol{\sigma_L} \in \mathcal{Q}_N$ form an *edge-connected ray of length L* if the following properties are satisfied:

- $d(\boldsymbol{\sigma_i}, \boldsymbol{\sigma_{i+1}}) = 1$ or $d(\boldsymbol{\sigma_i}, \boldsymbol{\sigma_{i+1}}) = 2$ for any $i = 1, \ldots, L-1$,
- $d(\boldsymbol{\sigma_1}, \boldsymbol{\sigma_j}) = \sum_{i=1}^{j-1} d(\boldsymbol{\sigma_i}, \boldsymbol{\sigma_{i+1}})$ for any $j = 2, \ldots, L$,

where $d(\boldsymbol{\sigma}, \boldsymbol{\sigma'}) \coloneqq \frac{1}{2}\sum_{i=1}^{N} |\sigma_i - \sigma_i'|$ denotes the Hamming distance. Here, the first property ensures that $\boldsymbol{\sigma_1}, \dots, \boldsymbol{\sigma_L}$ form an edge-connected subset of $\mathcal{Q}_N$ and the second property forces the vertices to form a straight ray starting at $\boldsymbol{\sigma_1}$.
We now proceed in three steps. In the first step we give a bound for the probability that a certain edge-connected ray is a subset of $\mathcal{L}_\epsilon^p$. Then, we consider the probability that $\mathcal{L}_\epsilon^p$ contains an edge-connected ray of length L. Finally, we use the result from Step 2 to conclude the assertions of Proposition 3.3.

Step 1: Let $\boldsymbol{\sigma_1}, \dots, \boldsymbol{\sigma_L}$ be an edge-connected ray of length L. We are interested in the probability that $\{\boldsymbol{\sigma_1}, \dots, \boldsymbol{\sigma_L}\} \subset \mathcal{L}_\epsilon^p$. In view of Lemma 3.4, we calculate

$$\begin{aligned}\sum_{i=1}^{L} \mathbb{E}[U_p(\boldsymbol{\sigma_i}) U_p(\boldsymbol{\sigma_j})] &= N \sum_{i=1}^{L} \left(1 - \frac{2d(\boldsymbol{\sigma_i}, \boldsymbol{\sigma_j})}{N}\right)^p \leq 2N \sum_{k=0}^{L} \left(1 - \frac{2k}{N}\right)^p \\ &\leq 2N \sum_{k=0}^{L} e^{-2kp/N} \leq \frac{2N}{1 - e^{-2p/N}}. \end{aligned} \tag{3.12}$$

The first equality directly follows from (1.3) and the next inequality is based on the observation that for any vertex $\boldsymbol{\sigma_i}$ of an edge-connected ray and any number $0 \leq k \leq L$ there are at most two other vertices at distance k. Then, we have made use of the convexity of the exponential function and the geometric series formula.

We note that the function $h(x) \coloneqq \frac{x}{1-e^{-x}}$ is strictly positive and increasing on the interval $(0, 1]$. Therefore, we obtain the bound

$$\sum_{i=1}^{L} \mathbb{E}[U_p(\boldsymbol{\sigma_i}) U_p(\boldsymbol{\sigma_j})] \leq h(1) \frac{N^2}{p}, \tag{3.13}$$

and Lemma 3.4 implies

$$\mathbb{P}(\{\boldsymbol{\sigma_1}, \dots, \boldsymbol{\sigma_L}\} \subset \mathcal{L}_\epsilon^p) = \mathbb{P}(\max_{i=1,\dots,L} U_p(\boldsymbol{\sigma_i}) < -\epsilon N) \leq \exp\left(-\frac{Lp\epsilon^2}{2h(1)}\right). \tag{3.14}$$

Step 2: We denote by $D(L, N)$ the number of edge-connected rays of length L in $\mathcal{Q}_N$. We claim that

$$D(L, N) \leq 2^N N^{2L} \tag{3.15}$$

This can be seen as follows: we have 2^N choices for the first vertex $\boldsymbol{\sigma}_1$ and at most N^2 choices for any subsequent vertex. The bounds (3.14) and (3.15) together with the union bound then yield

$$\mathbb{P}(\{\exists\, \boldsymbol{\sigma_1}, \dots, \boldsymbol{\sigma_L} \in \mathcal{L}_\epsilon^p \text{ forming an edge-connected ray}\}) \leq 2^N N^{2L} \exp\left(-\frac{Lp\epsilon^2}{2h(1)}\right) \tag{3.16}$$

Step 3: We take some fixed $K \in \mathbb{N}$ and define $\Omega_{\epsilon,N}^K$ as the subset of realizations where the second assertion holds true. It remains to show the bound $\mathbb{P}((\Omega_{\epsilon,N}^K)^c) \leq e^{-c_\epsilon N}$ for a convenient

choice of K. For any $\omega \notin \Omega^K_{\epsilon,N}$, we find an edge-connected component $C^{p(N)}_\epsilon$ of $\mathcal{L}^{p(N)}_\epsilon$ such that $C^{p(N)}_\epsilon \not\subset B_{K\lceil \frac{N}{p(N)} \rceil}(\boldsymbol{\sigma})$ for any $\boldsymbol{\sigma} \in \mathcal{Q}_N$. In particular, for such an ω this implies the existence of an edge-connected ray $\boldsymbol{\sigma_1}, \dots, \boldsymbol{\sigma_L} \in \mathcal{L}^{p(N)}_\epsilon$ of length $L \coloneqq \lceil \frac{K}{2} \lceil \frac{N}{p(N)} \rceil \rceil$. Using (3.16), we arrive at

$$\begin{aligned} \mathbb{P}((\Omega^K_{\epsilon,N})^c) &\leq \mathbb{P}(\{\exists \boldsymbol{\sigma_1}, \dots, \boldsymbol{\sigma_L} \in \mathcal{L}^p_\epsilon \text{ forming an edge-connected ray}\}) \\ &\leq \exp\left(N \left(2 + \frac{K \ln N}{p(N)} - \frac{K\epsilon^2}{4h(1)} \right) + (K+1) \ln N \right), \end{aligned} \tag{3.17}$$

since $2L \leq K(N/p(N)+1)+1$. The first assertion of Proposition 3.3 follows for a suitable choice of K, since $p(N)$ satisfies the growth condition (2.4). □

Acknowledgements

This work was partially supported by the DFG under under EXC-2111 – 390814868.

References

[1] B. Derrida, Random energy model: an exactly solvable model of disordered systems, Phys. Rev. B 24: 2613-2326 (1981).
[2] G. Parisi, The order parameter for spin glasses: a function on the interval 0-1, J. Phys. A: Math. Gen., 13: 1101–1112 (1980).
[3] M. Talagrand, The Parisi formula. Ann. of Math. 163: 221–263 (2006).
[4] D. Panchenko, The Parisi formula for mixed p-spin models, Ann. Prob. Vol. 42: 946–958 (2014).
[5] A. Bovier. Statistical Mechanics of Disordered Systems. A Mathematical Perspective. Cambridge University Press, 2012.
[6] M. Talagrand, Mean Field Models for Spin Glasses (Vol I+II), Springer 2011.
[7] D. Panchenko, The Sherrington-Kirkpatrick Model. Springer 2013.
[8] S. Suzuki, J. Inoue, B. K. Chakrabarti, Quantum Ising Phases and Transitions in Transverse Ising Models, 2nd ed., Springer 2013.
[9] V. Bapst, L. Foini, F. Krzakala, G. Semerjian, F. Zamponi. The Quantum Adiabatic Algorithm Applied to Random Optimization Problems: The Quantum Spin Glass Perspective. Physics Reports 523: 127–205 (2013).
[10] N. Crawford, Thermodynamics and Universality for Mean Field Quantum Spin Glasses, Commun. Math. Phys. 274: 821–839 (2007).
[11] T. Jörg, F. Krzakala, J. Kurchan, A.C. Maggs. Simple Glass Models and Their Quantum Annealing. Phys. Rev Lett. 101: 147204 (2008).
[12] J. Adame, S. Warzel, Exponential vanishing of the ground-state gap of the QREM via adiabatic quantum computing, J. Math. Phys. 56: 113301 (2015).
[13] Y. Y. Goldschmidt, Solvable model of a quantum spin glass in a transverse field. Phys. Rev. B 41: 4858 (1990).
[14] C. Manai and S. Warzel, Phase diagram of the quantum random energy model, Preprint arXive: 1909.07180.

[15] V Dobrosavljevic, D Thirumalai, 1/p expansion for a p-spin interaction spin-glass model in a transverse field. J. Phys. A: Math. Gen. 23: L767 (1990).
[16] T. Obuchi, H. Nishimori, D. Sherrington. Phase Diagram of the p-Spin-Interacting Spin Glass with Ferromagnetic Bias and a Transverse Field in the Infinite-p Limit. J. Phys. Soc. Jpn. 76: 054002 (2007).
[17] A. Bovier, I. Kurkova and M. Lwe, Fluctuations of the free energy in the REM and the p-spin SK model. The Annals of Probability 30: 605-651 (2002).
[18] J. Friedman, J. P. Tillich, Generalized Alon-Boppana theorems and error-correcting codes. Siam J. Descrete Math. 19: 700–718 (2005).

Chokri Manai and Simone Warzel
MCQST & Zentrum Mathematik
Technische Universität München
Corresponding author: warzel@ma.tum.de

Appendix C

Articles as co-author

C.1 Existence of replica-symmetry breaking in quantum glasses

Existence of replica-symmetry breaking in quantum glasses

Hajo Leschke, Chokri Manai, Rainer Ruder and Simone Warzel

The Quantum Sherrington-Kirpatrick model (QSK) is probably among the most important quantum spin glass models. However, most physical predictions rely on numerical methods and non-rigorous analytic techniques such as the replica trick and the static approximation, which appears to be false in the QSK [126]. It is therefore all the more important to establish rigorous statements in order clarify the physics of the QSK. Article VI takes an important step in this direction since we prove the existence of a glass phase for low temperatures and a weak external field.

Main Results

Our main theorem shows the existence of a glass phase for all inverse temperatures $\beta > 1$ and magnetic fields $\Gamma < \Gamma_c(\beta)$. Here $\Gamma_c(\beta)$ is a positive function, which does not vanish in the $\beta \to \infty$ limit and, thus, we also find a glass phase at zero temperature. Together with the results in [126], where it has been shown that there is no glass order for $\beta < 1$, we in total have proven the existence of a glass transition. While the critical value $\beta = 1$ is sharp and agrees with the classical findings, the computed critical field strength $\Gamma_c(\beta)$ is strictly smaller than the expected phase line [78, 96, 139, 192, 193]. Our proof is based on a well-known approach to verify glass order in the classical SK model [6,42]. The main new challenge is to cope with the Duhamel correlators appearing in the non commutative setting. Fortunately, the Duhamel scalar product of interest is bounded from below, a fact which we prove by employing the Falk-Bruch inequality. Another difficulty one has to face is that one needs to find a lower bound on the internal energy. the simple bound using the ground state energy of the SK model is not sharp enough to prove the nonvanishing of the order parameter for all $\beta > 1$. We tackle this technical problem by invoking convexity estimates. These two technique yield a non-optimal critical field strength $\Gamma_c(\beta)$. As it is further shown in the article, our proof method easily generalizes to general p-spin models.

Individual Contribution

Hajo Leschke and Simone Warzel are the principal authors of this article. They realized how to extend the classical Bray-Moore to the QSK by applying the Falk-Bruch inequality. I contributed to the generalization of this idea to general p-spin models, and I was significantly involved in the convexity argument which guarantees the persistence of a glass phase for all inverse temperatures $\beta > 1$ and not only for large enough β as we had stated our results in our first submission. The draft was created in a joint collaboration.

Permission to include:

Hajo Leschke, Chokri Manai, Rainer Ruder and Simone Warzel.
Existence of replica-symmetry breaking in quantum glasses.
Physical Review Letters 127: 207204 (2021).
https://link.aps.org/doi/10.1103/PhysRevLett.127.207204

As the author of an APS-published article, may I use figures, tables, graphs, etc. in future publications?

Yes, as the author you have the right to use figures, tables, graphs, etc. in subsequent publications using files prepared and formatted by you or the APS-prepared versions. The appropriate bibliographic citation must be included.

As the author of an APS-published article, may I include my article or a portion of my article in my thesis or dissertation?

Yes, the author has the right to use the article or a portion of the article in a thesis or dissertation without requesting permission from APS, provided the bibliographic citation and the APS copyright credit line are given on the appropriate pages.

As the author of an APS-published article, may I give permission to a colleague or third party to republish all or part of the article in a print publication?

Yes, as the author you may grant permission to third parties to republish print versions of the article provided the APS-published version (e.g., the PDF from the online journal, or a copy of the article from the print journal) is not used for this purpose. The article may not be published in another journal, and the third party may not charge a fee. The appropriate bibliographic citation and notice of the APS copyright must be included.

As the author of an APS-published article, may I give permission to a colleague or third party to republish all or part of the APS-published version in an online journal, book, database compilation, etc.?

No, an author may not grant permission in this case. To request permission to republish APS-copyrighted material, please refer to the “Reuse & Permissions” link that can be found on each APS article page.

As the author of an APS-published article, may I provide a PDF of my paper to a colleague or third party?

The author is permitted to provide, for research purposes and as long as a fee is not charged, a PDF copy of his/her article using either the APS-prepared version or the author prepared version.

As a third party (not an author), may I republish an article or portion of an article published by APS?

Yes, APS will grant permission to republish articles or portions of articles (e.g., tables, graphs, excerpts) published by APS. Depending on the reuse and medium APS has the right to grant permission subject to APS terms and conditions and a fee may be assessed.

As a third party, may I use articles published by APS for lecture and classroom purposes?

Yes, you may use photocopied articles published by APS for lecture and classroom purposes without asking permission from APS as long as you remain an Authorized User of the APS online research per your institution’s site license. Also, there is no limitation on the use of APS articles using links to the material accessible through institutional subscriptions.

How do I request permission to republish APS-copyrighted material?

Editors' Suggestion

Existence of Replica-Symmetry Breaking in Quantum Glasses

Hajo Leschke
Institut für Theoretische Physik, Universität Erlangen–Nürnberg, 91058 Erlangen, Germany

Chokri Manai
Department of Mathematics and Munich Center for Quantum Science and Technology, TU München, 85747 Garching, Germany

Rainer Ruder
Institut für Theoretische Physik, Universität Erlangen–Nürnberg, 91058 Erlangen, Germany

Simone Warzel
Departments of Mathematics and Physics, Munich Center for Quantum Science and Technology, TU München, 85747 Garching, Germany

(Received 9 June 2021; revised 29 August 2021; accepted 11 October 2021; published 12 November 2021)

By controlling quantum fluctuations via the Falk–Bruch inequality we give the first rigorous argument for the existence of a spin-glass phase in the quantum Sherrington–Kirkpatrick model with a "transverse" magnetic field if the temperature and the field are sufficiently low. The argument also applies to the generalization of the model with multispin interactions, sometimes dubbed as the transverse p-spin model.

DOI: 10.1103/PhysRevLett.127.207204

Introduction.—Spin glasses constitute a particularly multifaceted topic in the statistical mechanics of disordered systems. Classical spin-glass models, such as the mean-field one by Sherrington and Kirkpatrick (SK) [1], were originally introduced to understand the unusual magnetic properties observed in some metal alloys with irregularly competing ferro- and antiferromagnetic interactions. Beyond their ongoing significance in condensed-matter physics [2], such models with their built-in frustration have evolved meanwhile into paradigms in optimization, information processing, and the theory of neural networks [3,4]. Their rich low-energy structure and complexity continues to generate deep scientific discoveries. For example, among the recent excitements in computation is a conditional proof (based on the widely believed assumption of ∞-replica-symmetry breaking) of the existence of a polynomial-time classical algorithm for finding an approximate bit string whose energy is with high probability ε close to the lowest SK energy [5]. Such an algorithm is not believed to exist for a search of the ground-state energy in p-spin generalizations of the SK model. Quantum mechanics promises to offer help in the form of quantum adiabatic annealing or quantum approximate optimization algorithms [6–12]. In this context, but also purely motivated by the fact that spin glasses are prototypes for the emergence of nonergodic behavior in disordered quantum systems [13–17], it is important to study quantum versions of classical spin-glass models. This can be done by taking the quantum nature of spins seriously and by adding a "transverse" magnetic field to the classical energy landscape, which induces quantum effects. Most prominent is the quantum Sherrington–Kirkpatrick model (QSKM) with $N \geq 2$ three-component vector spins of main quantum number $1/2$ (or qubits). Their z components interact with each other in a random fashion, while their x components interact individually with a constant magnetic field of strength $b \geq 0$ externally applied along the positive x direction. Up to a factor $1/2$, the jth spin operator may be represented by the triple

$$S_j^x = \begin{pmatrix} 0 & 1 \\ 1 & 0 \end{pmatrix}, \qquad S_j^y = \begin{pmatrix} 0 & -i \\ i & 0 \end{pmatrix}, \qquad S_j^z = \begin{pmatrix} 1 & 0 \\ 0 & -1 \end{pmatrix}$$

of Pauli matrices and is meant to act on the jth factor of the tensor-product Hilbert space $\mathcal{H}_N := \bigotimes_{j=1}^N \mathbb{C}^2$ and as the identity on the other factors. The Hamiltonian (or energy operator) of the QSKM is then defined on $\mathcal{H}_N$ by the sum

$$H_N := JU_N - b\sum_{j=1}^N S_j^x, \qquad J > 0, \qquad b \geq 0, \quad (1)$$

with its (dimensionless) classical zero-field SK part

$$U_N := -\frac{1}{\sqrt{N}} \sum_{1\leq j<k\leq N} g_{jk} S_j^z S_k^z. \quad (2)$$

Here the spin coupling is (only) pairwise and given by independent, identically distributed Gaussian random variables (g_{jk}) with mean $\mathbb{E}[g_{12}] = 0$ and variance $\mathbb{E}[g_{12}^2] = 1$, modeling frozen-in spatial disorder of the glass of strength $J > 0$.

As usual, the thermal average for reciprocal temperature $\beta \in]0,\infty[$ is given by the canonical Gibbs expectation $\langle\cdot\rangle := \mathrm{Tr}\, e^{-\beta H_N}(\cdot)/Z_N$ with the partition function $Z_N := \mathrm{Tr}\, e^{-\beta H_N}$ as the normalization factor. For $b = 0$ there is no *a priori* "globally" preferred spin orientation and no conventional magnetic order arises. Yet, one expects spin-glass order even for $b \geq 0$ in the sense that $\mathbb{E}[q_N] = \mathbb{E}[\langle S_1^z S_2^z\rangle^2] > 0$ in the limit of a "macroscopically" large number of spins ($N \to \infty$), provided that the temperature and the field are sufficiently low. Here we are using the model's spin-index symmetry under the (probabilistic) disorder expectation $\mathbb{E}[\cdot]$ and the [0, 1]-valued random variable

$$q_N := \frac{2}{N(N-1)} \sum_{1\leq j<k\leq N} \langle S_j^z S_k^z\rangle^2 \tag{3}$$

as the corresponding order parameter. It may be rewritten as

$$q_N = \frac{N}{N-1}\langle R_N^2\rangle^{\otimes} - \frac{1}{N-1}$$

in terms of $R_N := N^{-1}\sum_{j=1}^N S_j^z \otimes S_j^z$, the replica-overlap operator for the "duplicated model" with Hilbert space $\mathcal{H}_N \otimes \mathcal{H}_N$, Hamiltonian $H_N \otimes \mathbb{1} + \mathbb{1} \otimes H_N$, and associated Gibbs expectation $\langle\cdot\rangle^{\otimes}$. Strict positivity of $\mathbb{E}[q_N] = \mathbb{E}[\langle S_1^z S_2^z\rangle^2]$ is therefore equivalent to replica-symmetry breaking (as $N \to \infty$).

Main result.—The main result of this Letter is a proof of this replica-symmetry breaking at small enough temperature and field strength. This is facilitated by extending a key observation of Bray and Moore [18], generalized to certain non-Gaussian probability distributions of g_{12} by Aizenman, Lebowitz, and Ruelle [19], to the present quantum case $b > 0$: the mean order parameter $\mathbb{E}[q_N]$ is related to the mean $\mathbb{E}[\langle U_N\rangle]$ of the zero-field part of the Hamiltonian. Specifically, by the spin-index symmetry and a standard Gaussian integration by parts it is straightforward to obtain

$$\begin{aligned} -\frac{2}{N-1}\mathbb{E}[\langle U_N\rangle] &= \sqrt{N}\,\mathbb{E}[g_{12}\langle S_1^z S_2^z\rangle] \\ &= \sqrt{N}\,\mathbb{E}[\partial\langle S_1^z S_2^z\rangle/\partial g_{12}] \\ &= \beta J\,\mathbb{E}[\langle S_1^z S_2^z | S_1^z S_2^z\rangle - \langle S_1^z S_2^z\rangle^2] \\ &= \beta J\,\mathbb{E}[\langle A|A\rangle - \langle A\rangle^2] \end{aligned} \tag{4}$$

in terms of the observable $A := S_1^z S_2^z$ and its Duhamel–Kubo–Bogolyubov scalar product [20,21] with itself:

$$\langle A|A\rangle := \int_0^1 dt\, \langle e^{t\beta H_N} A^* e^{-t\beta H_N} A\rangle.$$

It satisfies the well-known *a priori* estimates $0 \leq \langle A\rangle^2 \leq \langle A|A\rangle \leq \langle A^2\rangle = 1$, where the inequalities hold for general (self-adjoint) $A = A^*$ and the equality is due to $A^2 = \mathbb{1}$ for the present A. In the classical commutative case, $b = 0$, the third inequality is also an equality and (4) turns into (4.3) of [18] and (4.1) of [19] (for Gaussian disorder).

For general $b \geq 0$ we need a lower bound on $\langle A|A\rangle$ better than $\langle A\rangle^2$ in order to obtain a nontrivial lower bound on $\mathbb{E}[\langle A\rangle^2]$ from (4). As our second main ingredient for the proof, we control the quantum fluctuations by the Falk–Bruch inequality [22] (see also [20,23]):

$$\langle A|A\rangle \geq \langle A^2\rangle\, \Phi\left(\frac{1}{4\langle A^2\rangle}\langle [A,[\beta H_N, A]]\rangle\right). \tag{5}$$

The function $\Phi : [0,\infty[\to]0,1]$ from the positive half-line to the left-open unit interval is defined implicitly by the relation $\Phi(r\tanh(r)) := r^{-1}\tanh(r)$. It is monotone decreasing and convex with $\Phi(0) = 1$. Moreover, it can be estimated from below according to $\Phi(t) \geq t^{-1}(1 - e^{-t}) \geq \max\{0, 1 - t/2\}$, see [20]. We also note that the Gibbs expectation of the double commutator in the argument of Φ in (5) equals the scalar product $\langle [\beta H_N, A] | [\beta H_N, A]\rangle$ and is hence positive for a general self-adjoint A. Since in the present case $A = S_1^z S_2^z$ commutes with U_N, the double commutator is independent of J and simply given by

$$[A,[\beta H_N, A]] = 4\beta b(S_1^x + S_2^x). \tag{6}$$

Combining (4)–(6) and using Jensen's inequality for the convex Φ together with spin-index symmetry, yields the basis for our main result:

Theorem 1.—The mean of the spin-glass order parameter (3) has a lower bound according to

$$\mathbb{E}[q_N] \geq \Phi(2\beta b\,\mathbb{E}[\langle S_1^x\rangle]) + \frac{2}{\beta J}\frac{1}{N-1}\mathbb{E}[\langle U_N\rangle]. \tag{7}$$

It is valid for any $\beta > 0$, $J > 0$, $b \geq 0$, and all $N \geq 2$.

For more explicit bounds we further estimate the right-hand side (rhs) of (7) starting with its first term. Adding to the Hamiltonian (1) the term $(b - b_1)S_1^x$ with $b_1 \geq 0$ and estimating the associated "local" susceptibility results in the differential inequality for the transverse magnetization

$$\frac{\partial}{\partial b_1}\langle S_1^x\rangle_{b_1} = \beta(\langle S_1^x | S_1^x\rangle_{b_1} - \langle S_1^x\rangle_{b_1}^2) \leq \beta(1 - \langle S_1^x\rangle_{b_1}^2).$$

Integrating by separation of variables and observing $\langle S_1^x\rangle_0 = 0$, we hence obtain $\langle S_1^x\rangle \leq \tanh(\beta b)$, which by the monotonicity of Φ results in the estimates

$$\Phi(2\beta b\,\mathbb{E}[\langle S_1^x\rangle]) \geq \Phi(2\beta b\tanh(\beta b)) \geq \Phi(2\beta b). \tag{8}$$

A simple bound on the second term in (7) results from the (nonrandom) ground-state energy $-\kappa J < 0$ of JU_N/N as $N \to \infty$ with the constant $\kappa \approx 0.763$ according to [24,25]. Combined with (8) this leads to the more explicit lower bound

$$\bar{q}(\beta J,\beta b) := \lim_{N\to\infty} \inf \mathbb{E}[q_N] \geq \Phi(2\beta b \tanh(\beta b)) - \frac{2\kappa}{\beta J} \quad (9)$$

on the lower limit of the sequence $(\mathbb{E}[q_N])_{N\geq 2}$ in the unit interval $[0, 1]$. For $b = 0$ the rhs of (9) is strictly positive for temperatures below $J/(2\kappa) \approx 0.655\ J$. This (not maximum) temperature regime for the existence of a spin-glass phase agrees with the one found in (4.14) of [19]. In this regime the spin-glass phase is seen to survive when turning on the transverse magnetic field, provided that $b/J > 0$ is so small that the rhs of (9) remains strictly positive. This condition is implied by the slightly stronger but simpler one $1 - e^{-2\beta b} > 4\kappa b/J$, yielding in the zero-temperature limit the same maximum field strength $J/(4\kappa) \approx 0.328\ J$ as from (9).

To establish the persistence of spin-glass order for sufficiently small b/J also for temperatures up to the zero-field critical (freezing) temperature J, we start from the observation that (5) and hence (7) are equalities for $b = 0$ and remain rather sharp for small $\beta b > 0$. Consequently, (7) should cover the whole regime $\beta b \ll 1 \leq \beta J$. To confirm this, we estimate the mean $\bar{u}(\beta J,\beta b) := \lim\inf_{N\to\infty}\mathbb{E}[\langle U_N\rangle]/N$ of the zero-field SK part (2) by the Fisher-type [26] inequality

$$\begin{aligned}&\bar{u}(\beta J,\beta b) + a^{-1}\ln(\cosh(\beta b)) \geq \bar{u}(\beta J + a, 0)\\ &= [\bar{q}(\beta J + a, 0) - 1](\beta J + a)/2 \end{aligned} \quad (10)$$

with an arbitrary $a > 0$. It results from the convexity of $\ln(Z_N(\beta J,\beta b))$ in βJ together with the Peierls–Bogolyubov and Golden–Thompson bounds $Z_N(\beta J, 0) \leq Z_N(\beta J,\beta b) \leq Z_N(\beta J, 0)(\cosh(\beta b))^N$ on the partition function. The equality in (10) is due to (7) for $b = 0$. Using (8) and (10) with $a = a_b := \sqrt{2\ln(\cosh(\beta b))}$ in (7) for $N \to \infty$ leads to

$$\begin{aligned}\bar{q}(\beta J,\beta b) &\geq \left(1 + \frac{a_b}{\beta J}\right)\bar{q}(\beta J + a_b, 0)\\ &\quad - \left(1 - \Phi(2\beta b\tanh(\beta b)) + \frac{2a_b}{\beta J}\right)\\ &\geq \bar{q}(\beta J + a_b, 0) - 3\beta b. \end{aligned} \quad (11)$$

The simplifying second inequality follows by observing $a_b \in [0,\beta b]$, estimating $\Phi(t)$ as above, and assuming $\beta J \geq 1$. Finally, we fix an arbitrary $\beta J > 1$ which is equivalent to $\bar{q}(\beta J, 0) > 0$ characterizing the spin-glass phase for $b = 0$, see [27]. The continuity of $\bar{u}(\beta J + a, 0)$ in a (by [30,31]) and hence of $\bar{q}(\beta J + a, 0)$ yields the continuity of the rhs of (11) in βb. Its strict positivity for $b = 0$ therefore extends to sufficiently small $\beta b \in]0, 1/3[$. In other words, the well-known spin-glass phase without a field persists with a low enough transverse field at any temperature below J.

Discussion.—Over the years various approximate and/or numerical studies like [32–37] have suggested for the QSKM a temperature-field phase diagram with a critical line between the spin-glass and the paramagnetic phases as sketched in Fig. 1, see also [38]. In particular, these studies have predicted a quantum phase transition at zero temperature and $b/J \approx 1.51$ or 1.6. The (red) cross-shaded regime in Fig. 1 illustrates where we prove the existence of spin-glass order by the lower bounds (9) and (11). Here, the tiny regime above the temperature $J/(2\kappa)$ is produced by inserting the asymptotic expansion of $\bar{q}(\beta J, 0)$ close to $\beta J = 1$ from [39] into the rhs of (11). Apart from that we have no prediction for the location of the true critical line. In particular, our zero-temperature "critical" field $J/(4\kappa)$ is very likely too small, as is the whole cross-shaded regime. The precise location and nature of the true quantum critical point remains an important problem, in particular in the context of adiabatic algorithms. Nevertheless, our rigorous result supports the conjecture that the ground state typically has localization properties with respect to the eigenbasis of U_N. It does not rule out, though, a weak form of restoration of ergodicity through quantum tunneling for those parameters put forward in [15,16,34,40]. To clarify this question it is necessary to consider the probabilistic distribution function of the order parameter and not just its mean, because the sequence $(q_N)_{N\geq 2}$ is not expected to be self-averaging in the spin-glass phase.

In this context, we recall that for $b = 0$ the mean free energy, $-\lim_{N\to\infty}\mathbb{E}[\ln(Z_N(\beta J, 0))]/(N\beta)$, and hence

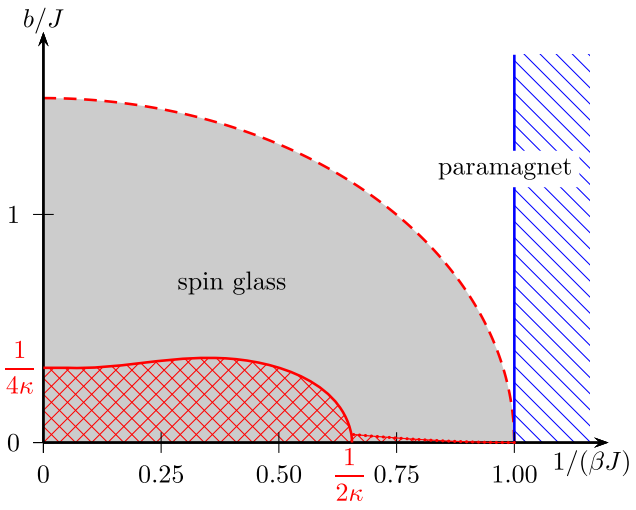

FIG. 1. In the temperature-field plane the (red) cross-shaded regime indicates where we prove the existence of spin-glass order in the QSKM by (9) and, respectively, by (11) combined with [39] (see text). The (red) dashed line is a cartoon of the critical line between the spin-glass and the paramagnetic phases as obtained by approximate arguments and/or numerical methods [32–37]. The (blue) line-shaded regime for $\beta J < 1$ indicates where the spin-glass order parameter is rigorously known to vanish [29].

also the rhs of (10), is exactly determined by Parisi's (zero-field) distribution function on [0, 1], which with increasing $\beta J > 1$ exhibits ∞-replica-symmetry breaking [24,25,30,31,41,42]. In contrast, no closed-form expressions are available for $b > 0$. Recently the QSKM free energy, which previously has been proved to exist and to be independent of the specific probability distribution of the coupling coefficient g_{12} as long as $\mathbb{E}[g_{12}] = 0$ and $\mathbb{E}[|g_{12}|^3] < \infty$ (see [43]), was shown to be given by a variational formula in terms of a Parisi-like functional for an infinite-component vector-spin model [44]. However, no conclusion could so far be drawn about emerging phases form this formula. In contrast, for the simpler case $\beta J < 1$ it is known [29] that the free energy coincides with its annealed version and that there is no spin-glass phase for any $b \geq 0$, see the (blue) line-shaded regime in Fig. 1. The combination of this result with the present one rigorously proves the existence of a phase transition in the QSKM related to replica-symmetry breaking. But Fig. 1 clearly calls for further rigorous work on this model.

For a family of quantum hierarchical models dubbed as QGREM, which for $b = 0$ were originally introduced by Derrida [45] as approximations to the more difficult SK model, explicit formulas for the free energy are available [46] also for $b > 0$. Unlike for their classical counterparts, the phase diagrams of these QGREMs seem to capture the QSKM only on a qualitative level though, since their critical lines reach up to $\beta J = 0$ separating a quantum paramagnetic phase from a classical one at high temperatures.

Extensions.—The above simple strategy for proving replica-symmetry breaking has straightforward extensions. From our proof it is evident that Theorem 1 remains true as it stands if one adds to (1) any term commuting with U_N that is possibly random but independent of U_N such as, for example, a Zeeman term corresponding to a magnetic field in z direction. Adapting the more-involved argument of [19], our bounds can also be extended from Gaussian to more general symmetric distributions of the coupling coefficients.

This strategy can also be applied to quantum spin-glass models with multispin interactions, for example to the "transverse p-spin model." This model generalizes the zero-field SK part (2) of (1) for each natural $p \geq 2$ to

$$U_N = -\sqrt{\frac{p!}{2N^{p-1}}} \sum_{1 \leq j_1 < \ldots < j_p \leq N} g_{j_1 j_2 \ldots j_p} S^z_{j_1} S^z_{j_2} \cdots S^z_{j_p},$$

where $(g_{j_1 j_2 \ldots j_p})$ are independent and identically distributed standard Gaussian random variables. For $p > 2$ this classical zero-field Hamiltonian exhibits at its freezing temperature finite and not ∞-replica-symmetry breaking [47]. Proceeding for the quantum model as in (4) and introducing $\alpha_p(N) \coloneqq N!/[(N-p)!N^p]$, which tends to one as $N \to \infty$, the mean zero-field energy

$$\mathbb{E}[\langle U_N \rangle] = -\alpha_p(N) \mathbb{E}[g_{12\ldots p} \langle S^z_1 S^z_2 \cdots S^z_p \rangle] \sqrt{\frac{N^{p+1}}{p!2}}$$

is now related to the mean of the pth power of the replica-overlap operator

$$\mathbb{E}[\langle R^p_N \rangle^{\otimes}] = \alpha_p(N) \mathbb{E}[\langle S^z_1 S^z_2 \cdots S^z_p \rangle^2] + o_p(N),$$

where $o_p(N)$ is a term which goes to zero as $N \to \infty$. Since the double commutator (6) for $A = S^z_1 S^z_2 \cdots S^z_p$ equals $4\beta b \sum_{j=1}^p S^x_j$, we thus obtain the following generalization of Theorem 1:

Theorem 2.—The mean of the pth power of the replica-overlap operator is lower bounded according to

$$\mathbb{E}[\langle R^p_N \rangle^{\otimes}] \geq \alpha_p(N) \Phi(p\beta b \mathbb{E}[\langle S^x_1 \rangle]) + \frac{2}{\beta J} \frac{1}{N} \mathbb{E}[\langle U_N \rangle] + o_p(N) \tag{12}$$

for any $\beta > 0$, $J > 0$, $b \geq 0$, and all $N \geq p$.

As before, we may further estimate the transverse magnetization, $\langle S^x_1 \rangle \leq \tanh(\beta b)$, and bound the second term in (12) by the ground-state energy of the zero-field p-spin model, which itself is asymptotically (as $N \to \infty$) lower bounded by $-J\sqrt{\ln(2)}$, the known value for $p \to \infty$, using Slepian's lemma (see [48]). This proves a spin-glass phase in a regime where the temperature and the field are low enough [49,50]. However, the larger we choose p, the smaller the regime becomes. In the limit $p \to \infty$ replica-symmetry breaking cannot be concluded by the above strategy.

This limit corresponds to the quantum random energy model (QREM). Its zero-field part U_N is given in its (canonical) eigenbasis by the eigenvalues $-g_{\boldsymbol{\sigma}}\sqrt{N/2}$ with standard Gaussian random variables $(g_{\boldsymbol{\sigma}})$, which are independent and identically distributed for distinct z configurations $\boldsymbol{\sigma} \in \{-1, 1\}^N$. In this case the phase diagram is known [51] for general β and $b \geq 0$, even at the rigorous level [52]. As Goldschmidt's calculations [51] suggest, in the spin-glass phase the whole distribution of the replica overlap $\langle R_N \rangle^{\otimes}$ of the QREM turns out to agree with its classical analog. In particular, for this phase one can prove [53] that $\lim_{N\to\infty} \mathbb{E}[\langle R_N \rangle^{\otimes}] = 1 - 2\sqrt{\ln(2)}/(\beta J)$.

Conclusion.—We have presented a simple argument that establishes replica-symmetry breaking in spin-glass models with a transverse field. It relies on a susceptibility bound from [22] combined with an extension of the classical relation between the mean spin-glass order parameter $\bar{q}$ and the mean of the zero-field part of the energy to the quantum case. For the prominent quantum SK model, we have discussed in detail two resulting strictly positive but not optimal lower bounds on $\bar{q}$. Nevertheless, our method has extensions beyond the quantum SK model.

We thank one of the referees for stimulating us to consider also temperatures between $J/(2\kappa)$ and J. C. M. and S. W. are supported by the DFG under Grant No. EXC-2111–390814868.

[1] D. Sherrington and S. Kirkpatrick, Solvable Model of a Spin-Glass, Phys. Rev. Lett. **35**, 1792 (1975).
[2] K. H. Fischer and J. A. Hertz, *Spin Glasses* (Cambridge University Press, Cambridge, England, 1991).
[3] M. Mézard and A. Montanari, *Information, Physics, and Computation* (Oxford University Press, Oxford, 2009).
[4] H. Nishimori, *Statistical Physics of Spin Glasses and Information Processing—An Introduction* (Clarendon, Oxford, 2001).
[5] A. Montanari, Optimization of the Sherrington–Kirkpatrick Hamiltonian, SIAM J. Comput. FOCS19-1 (2021).
[6] T. Albash and D. A. Lidar, Adiabatic quantum computation, Rev. Mod. Phys. **90**, 015002 (2018).
[7] C. L. Baldwin and C. R. Laumann, Quantum algorithm for energy matching in hard optimization problems, Phys. Rev. B **97**, 224201 (2018).
[8] V. Bapst, L. Foini, F. Krzakala, G. Semerjian, and F. Zamponi, The quantum adiabatic algorithm applied to random optimization problems: the quantum spin glass perspective, Phys. Rep. **523**, 127 (2013).
[9] A. Callison, M. Festenstein, J. Chen, L. Nita, V. Kendon, and N. Chancellor, Energetic perspective on rapid quenches in quantum annealing, PRX Quantum **2**, 010338 (2021).
[10] A. Dutta, G. Aeppli, B. K. Chakrabarti, U. Divakaran, T. F. Rosenbaum, and D. Sen, *Quantum Phase Transitions in Transverse Field Spin Models—From Statistical Physics to Quantum Information* (Cambridge University Press, Delhi, 2015).
[11] E. Farhi, J. Goldstone, S. Gutmann, and L. Zhou, The quantum approximate optimization algorithm and the Sherrington–Kirkpatrick model at infinite size, arXiv: 1910.08187.
[12] S. Knysh, Zero-temperature quantum annealing bottlenecks in the spin-glass phase, Nat. Commun. **7**, 12370 (2016).
[13] C. L. Baldwin, C. R. Laumann, A. Pal, and A. Scardicchio, Clustering of Nonergodic Eigenstates in Quantum Spin Glasses, Phys. Rev. Lett. **118**, 127201 (2017).
[14] C. R. Laumann, A. Pal, and A. Scardicchio, Many-Body Mobility Edge in a Mean-Field Quantum Spin Glass, Phys. Rev. Lett. **113**, 200405 (2014).
[15] S. Mukherjee and B. K. Chakrabarti, On the question of ergodicity in quantum spin glass phase and its role in quantum annealing, J. Phys. Soc. Jpn. **88**, 061004 (2019).
[16] P. Ray, B. K. Chakrabarti, and A. Chakrabarti, Sherrington–Kirkpatrick model in a transverse field: Absence of replica symmetry breaking due to quantum fluctuations, Phys. Rev. B **39**, 11828 (1989).
[17] V. N. Smelyanskiy, K. Kechedzhi, S. Boixo, S. V. Isakov, H. Neven, and B. Altshuler, Nonergodic Delocalized States for Efficient Population Transfer within a Narrow Band of the Energy Landscape, Phys. Rev. X **10**, 011017 (2020).
[18] A. J. Bray and M. A. Moore, Some observations on the mean-field theory of spin glasses, J. Phys. C **13**, 419 (1980).
[19] M. Aizenman, J. Lebowitz, and D. Ruelle, Some rigorous results on the Sherrington–Kirkpatrick spin glass model, Commun. Math. Phys. **112**, 3 (1987); **116**, 527 (1988).
[20] F. J. Dyson, E. H. Lieb, and B. Simon, Phase transitions in quantum spin systems with isotropic and nonisotropic interactions, J. Stat. Phys. **18**, 335 (1978).
[21] R. Kubo, M. Toda, and N. Hashitsume, *Statistical Physics II—Nonequilibrium Statistical Mechanics*, 2nd ed. (Springer, Berlin, 1998), 3rd corrected printing.
[22] H. Falk and L. W. Bruch, Susceptibility and fluctuation, Phys. Rev. **180**, 442 (1969).
[23] G. Roepstorff, A stronger version of Bogoliubov's inequality and the Heisenberg model, Commun. Math. Phys. **53**, 143 (1977).
[24] A. Crisanti and T. Rizzo, Analysis of the ∞-replica symmetry breaking solution of the Sherrington–Kirkpatrick model, Phys. Rev. E **65**, 046137 (2002).
[25] G. Parisi, A sequence of approximated solutions to the S–K model for spin glasses, J. Phys. A **13**, L115 (1980).
[26] M. E. Fisher, Bounds for the derivatives of the free energy and the pressure of a hard-core system near close packing, J. Chem. Phys. **42**, 3852 (1965).
[27] This well-known equivalence follows easily from the inequality $\int_0^{\beta J} dt\, t\bar{q}(t,0) \geq 2k(\beta^2 J^2/4)$ for any $\beta J > 0$. It is due to (7) and Guerra's observation [28] that the (replica-symmetric) SK approximation [1] provides a lower bound on $-\mathbb{E}[\ln(Z_N(\beta J, 0))]/(N\beta)$ for any $N \geq 2$. The differentiable function $\lambda \mapsto k(\lambda)$ is zero for $\lambda \leq 1/4$ and strictly positive and increasing for $\lambda > 1/4$, see [1,29].
[28] F. Guerra, Sum rules for the free energy in mean field spin glass models, Fields Inst. Commun. **30**, 161 (2001).
[29] H. Leschke, S. Rothlauf, R. Ruder, and W. Spitzer, The free energy of a quantum Sherrington–Kirkpatrick spin-glass model for weak disorder, J. Stat. Phys. **182**, 55 (2021).
[30] D. Panchenko, On differentiability of the Parisi formula, Electron. Commun. Probab. **13**, 241 (2008).
[31] M. Talagrand, Parisi measures, J. Funct. Anal. **231**, 269 (2006).
[32] Ya. V. Fedorov and E. F. Shender, Quantum spin glasses in the Ising model with a transverse field, Pis'ma Zh. Eksp. Teor. Fiz. **43**, 526 (1986) [JETP Lett. **43**, 681 (1986)].
[33] Y. Y. Goldschmidt and P.-Y. Lai, Ising Spin Glass in a Transverse Field: Replica-Symmetry-Breaking Solution, Phys. Rev. Lett. **64**, 2467 (1990).
[34] S. Mukherjee, A. Rajak, and B. K. Chakrabarti, Possible ergodic-nonergodic regions in the quantum Sherrington–Kirkpatrick spin glass model and quantum annealing, Phys. Rev. E **97**, 022146 (2018).
[35] K. D. Usadel and B. Schmitz, Quantum fluctuations in an Ising spin glass with transverse field, Solid State Commun. **64**, 975 (1987).
[36] T. Yamamoto and H. Ishii, A perturbation expansion for the Sherrington–Kirkpatrick model with a transverse field, J. Phys. C **20**, 6053 (1987).
[37] A. P. Young, Stability of the quantum Sherrington–Kirkpatrick spin glass model, Phys. Rev. E **96**, 032112 (2017).

[38] S. Suzuki, J.-i. Inoue, and B. K. Chakrabarti, *Quantum Ising Phases and Transitions in Transverse Ising Models*, 2nd ed. (Springer, Berlin, 2013).
[39] H.-J. Sommers, Parisi function $q(x)$ near T_c, J. Phys. Lett. **46**, L779 (1985).
[40] G. Büttner and K. D. Usadel, Replica-symmetry breaking for the Ising spin glass in a transverse field, Phys. Rev. B **42**, 6385 (1990).
[41] G. Parisi, The order parameter for spin glasses: A function on the interval 0–1, J. Phys. A **13**, 1101 (1980).
[42] M. Talagrand, The Parisi formula, Ann. Math. **163**, 221 (2006).
[43] N. Crawford, Thermodynamics and universality for mean field quantum spin glasses, Commun. Math. Phys. **274**, 821 (2007).
[44] A. Adhikari and C. Brennecke, Free energy of the quantum Sherrington–Kirkpatrick spin-glass model with transverse field, J. Math. Phys. (N.Y.) **61**, 083302 (2020).
[45] B. Derrida, A generalization of the random energy model which includes correlations between energies, J. Phys. Lett. **46**, L401 (1985).
[46] C. Manai and S. Warzel, Generalized random energy models in a transversal magnetic field: free energy and phase diagrams, arXiv:2007.03290 [Probab. Math. Phys. (to be published)].
[47] E. Gardner, Spin glasses with p-spin interactions, Nucl. Phys. **B257**, 747 (1985).
[48] A. Bovier, *Statistical Mechanics of Disordered Systems. A Mathematical Perspective* (Cambridge University Press, Cambridge, England, 2006).
[49] V. Dobrosavljevic and D. Thirumalai, $1/p$ expansion for a p-spin interaction spin-glass model in a transverse field, J. Phys. A **23**, L767 (1990).
[50] T. Obuchi, H. Nishimori, and D. Sherrington, Phase diagram of the p-spin-interacting spin glass with ferromagnetic bias and a transverse field in the infinite-p limit, J. Phys. Soc. Jpn. **76**, 054002 (2007).
[51] Y. Y. Goldschmidt, Solvable model of the quantum spin glass in a transverse field, Phys. Rev. B **41**, 4858 (1990).
[52] C. Manai and S. Warzel, Phase diagram of the quantum random energy model, J. Stat. Phys. **180**, 654 (2020).
[53] C. Manai and S. Warzel (to be published).

C.2 Trajectory phase transitions in non-interacting systems: all-to-all dynamics and the random energy model

Trajectory phase transitions in non-interacting systems: all-to-all dynamics and the random energy model

Juan P. Garrahan, Chokri Manai and Simone Warzel

Studying the free energy in the thermodynamic limit, unfolds the static equilibrium properties, in particular the phase transitions, of the considered model. However, the partition function does not encode dynamical information on the fluctuations of trajectory observables, such as the model's potential integrated along random walks on the Hamming cube. Instead, one needs to study the moment generating function of the trajectory observable or, equivalently, the corresponding large deviation functions [123]. The analysis of the trajectory dynamics reveals for example phase transitions in the dynamical activity of spin glasses [90, 103, 174]. In Article VII, we deal with the trajectory dynamics of the REM under a simple random walk on the complete graph.

Main Results

Our main results are twofold as we examine the statistics of the REM potential integrated along a trajectory via rigorous analytical methods and numerical computations. On the analytic side, we determine the large deviation function via a spectral analysis of the tilted generator of the Markov process. That enables us to provide a complete phase diagram for all times and coupling parameters. We observe three phases: an active phase dominated by the Markov generator and two inactive phases, one glassy phase governed by the extreme values of the REM and a second one resembling the paramagnetic phase of the REM. The tilted generator agrees up to a constant shift with a rank-one perturbation of the REM potential and has been studied before in [7]. In fact, our proof is based on the precise characterization of the eigenfunctions in [7]. The numerical computations make use of the Monte Carlo method which we use to realize typical rare trajectories. On one hand, the numerical results reflect our rigorous statements for the thermodynamic limit while. On the other hand, finite size corrections are present and have an impact on the observables probability distribution.

Individual Contribution

I am a coauthor of this article. Juan P. Garrahan, Simone Warzel and I have contributed significantly to this article. Juan P. Garrahan was the initiator of this work and introduced Simone Warzel and me to the topic of trajectories in disordered systems. He was mainly in charge of the numerical implementation. The interpretation of the numerical findings is a result of several joint meeting. Simone Warzel and I have focused on the analytic part, where we figured out the proof in a meeting together.

Permission to include:

Juan P. Garrahan, Chokri Manai and Simone Warzel.
Trajectory phase transitions in non-interacting systems: all-to-all dynamics and the random energy model.
Philosophical Transactions of the Royal Society A 381: 20210415 (2022).
https://doi.org/10.1098/rsta.2021.0415

Licence to Publish

Notice: you are the person first named under the heading 'Authors and Institutions' at stage 4 of the online process to 'Submit a Manuscript' (referred to as "**you**/**your**"). we are the Royal Society, a body incorporated by royal charter, with its place of business at 6-9 Carlton House Terrace, London SW1Y 5AG (referred to as "**we**/**us**/**our**").

You have indicated your intention to upload the article more fully detailed at stage 1 of the online submission process (the "**article**") to be considered for publication by us. In order to publish your article we need you to grant us a licence to publish*. This licence also sets out your rights regarding use of Preprints, Accepted Author Manuscripts and the Definitive Published Version of the article (as defined below). Please read the terms of this licence carefully before uploading the article.

Ticking the box next to the question "Confirm you accept the terms and conditions of the relevant Licence to Publish." at stage 6 of the online submission process will be taken as assurance that you have read, agree to grant and have the right to grant this licence.

Definitions

"**Preprints**" - the un-refereed version of the article;

"**Accepted Author Manuscript**" - your personal copy of the revised version of the article as accepted by us;

"**Definitive Published Version**" - the citable version of the article produced by us after peer review, copy editing and print and electronic production.

1. You grant to us for the full term of copyright in the article and any extensions thereto the exclusive right throughout the world to edit, adapt, translate, publish reproduce, distribute and display the article in printed, electronic or any other medium and format whether now known or yet to be developed; you agree to publish associated supplementary material under a CC-BY licence*; and

2. You represent to us that:

   a) the article is your original work, has not previously been published and is not currently under consideration for publication by any other entity;

   b) in the case of a multi-authored article, you have obtained written authorisation from all the co-authors of the article (if any) to grant this licence to us on their behalf as their agent, and you will supply a copy of the same to us if we so request;

   c) where any copyright material has been included in the article which has been sourced from third parties (e.g. illustrations, photographs, charts or maps), you have obtained all necessary written authorisations for the reproduction and distribution of these materials as

part of the article throughout the world, in all languages and in all media and formats whether now known or yet to be developed and you will supply a copy of the same to us if we so request;

d) if copyright in the article is owned by any third party, whether your employer or someone to whom you have assigned your rights, you have obtained written authorisation from such copyright owner to grant this licence to us on their behalf as their agent and will supply a copy of the same to us if we so request; and

e) the article does not contain anything which is obscene, defamatory, libellous, infringes any right of privacy or any intellectual property right (including without limitation rights in patents, copyright or trademarks) or any other rights of any person or entity, or is otherwise unlawful.

3. You assert your moral right to be identified as the Author or co-author of the article (as applicable). If your article is published, we will provide you with a PDF copy of the published article.

4. If you decide to make the Definitive Published Version of the article open access, this will be under this licence.

   You shall pay to us any relevant fee and we shall make the article so available from the later of the date of receipt of the relevant fee or the date of first publication of the article.

5. You retain copyright in the article. However, you authorise us to act on your behalf to defend your copyright in the article should anyone infringe it, and to retain half of any damages awarded after deducting our costs.

6. You retain the right to use the article in the following ways, provided that you acknowledge the Definitive Published Version of the article by placing the full bibliographic reference and URL of the relevant journal homepage close to the title of the article:

   a) In relation to the **Preprint**, **Accepted Author Manuscript** and **Definitive Published Version of the article**, you are free to: make copies for your own personal use; use the article for the internal teaching purposes of your own institution or company; and make and distribute copies (including through e-mail) of the article to research colleagues, for personal use by such colleagues on a non-commercial, non-systematic basis.

   b) In relation to the **Preprint** version only, you are free to post it on web sites, including electronic preprint servers.

   When the **Definitive Published Version** of the article is published the Author must acknowledge it by placing the full bibliographic reference and URL of the relevant journal homepage close to the title of the article.

   c) In relation to the **Accepted Author Manuscript** only, you are free to: post it on your personal or institutional web site and load it onto your institutional or subject repository once accepted for publication; use it in compilations of your work subsequent to publication of the Definitive Published Version of the article, expand the article into

book-length form, and/or otherwise re-use portions of the Accepted Author Manuscript of the article in other works. you are also free to present the article at a meeting or conference and to disseminate copies of such article to the delegates attending such meeting or conference and/or to use the Accepted Author Manuscript in a thesis or dissertation. A licence of CC-BY may be applied to the Accepted Author Manuscript, as required by some funders.

7. We are entitled to assign our rights under this licence to any third party without giving notice to you.

8. No change or modification of this licence will be valid unless confirmed in writing by us.

9. Failure or delay by us to exercise any right or remedy under this Agreement shall not be deemed to be a waiver of that right or remedy, or prevent us from exercising that or any other right or remedy on any occasion.

10. This licence is terminated in case the article is rejected for publication or the author withdraws the article for consideration for publication before publication has occurred.

US Government contracts

*For US government employees, works created within the scope of their employment are considered to be public domain (the article is not copyrightable in the US) and our publishing agreements do not require a transfer or license of rights for such works. For such works "you/your" is replaced with "United States government"

Where the author has notified us that this is the situation, the copyright line will indicate that the article constitutes a "work of the United States government" and a statement will be included in the article "US government may reproduce, without charge, all or portions of the contribution and may authorize others to do so, for official US government purposes only."

PHILOSOPHICAL TRANSACTIONS A

royalsocietypublishing.org/journal/rsta

Research

Cite this article: Garrahan JP, Manai C, Warzel S. 2022 Trajectory phase transitions in non-interacting systems: all-to-all dynamics and the random energy model. *Phil. Trans. R. Soc. A* **381**: 20210415.
https://doi.org/10.1098/rsta.2021.0415

Received: 15 May 2022
Accepted: 18 July 2022

One contribution of 12 to a theme issue 'Quantum annealing and computation: challenges and perspectives'.

Subject Areas:
mathematical physics, statistical physics

Keywords:
disordered systems, dynamical phase transition, glass transition, large deviations

Author for correspondence:
Simone Warzel
e-mail: simone.warzel@tum.de

Trajectory phase transitions in non-interacting systems: all-to-all dynamics and the random energy model

Juan P. Garrahan[1,2], Chokri Manai[3,5] and Simone Warzel[3,4,5]

[1]School of Physics and Astronomy, and [2]Centre for the Mathematics and Theoretical Physics of Quantum Non-Equilibrium Systems, University of Nottingham, Nottingham NG7 2RD, UK
[3]Department of Mathematics, and [4]Department of Physics, TU Munich, Germany
[5]MCQST, Munich, Germany

SW, 0000-0002-6250-4664

We study the fluctuations of time-additive random observables in the stochastic dynamics of a system of N non-interacting Ising spins. We mainly consider the case of all-to-all dynamics where transitions are possible between any two spin configurations with uniform rates. We show that the cumulant generating function of the time-integral of a normally distributed quenched random function of configurations, i.e. the energy function of the random energy model (REM), has a phase transition in the large N limit for trajectories of any time extent. We prove this by determining the exact limit of the scaled cumulant generating function. This is accomplished by connecting the dynamical problem to a spectral analysis of the all-to-all quantum REM. We also discuss finite N corrections as observed in numerical simulations.

This article is part of the theme issue 'Quantum annealing and computation: challenges and perspectives'.

1. Introduction

In statistical mechanics, we are used to studying static phase transitions from singularities in partition sums [1]: the value of a control parameter at which the

THE ROYAL SOCIETY PUBLISHING

free energy becomes non-analytic (in the infinite-size limit) indicates that the equilibrium ensemble of configurations undergoes a phase change. The standard equilibrium ensemble method can be generalized straightforwardly to stochastic dynamics by replacing configurations with trajectories, static observables with (time-extensive) functions of trajectories and the partition sum with the corresponding moment generating function of the trajectory observable [2,3]. The 'thermodynamics of trajectories' approach [4–6] allows to study dynamical or 'trajectory' phase transitions, that is, singular changes in the nature of dynamical fluctuations that often are not reflected in (thermo)static properties or occur at different parameters of the model. The singularities of the relevant large deviation (LD) functions [7] reveal phase transitions in, for example, the dynamical activity of glassy systems [8–10], in time-integrated currents in exclusion processes [11–13] and in (active) work in active matter [14].

An interesting question is what occurs in a system of many degrees of freedom whose dynamics is non-interacting when one considers the fluctuations of a (quenched) random trajectory-observable that couples them. Our main object of interest will be a system of N Ising spins which all flip independently from each other. For the case of non-random *local* observables and independent spins with single spin-flip dynamics recent results [15] show that in certain cases there is a phase transition in the LD function. While, naively, one might expect nothing interesting to occur due to the non-interacting nature of the dynamics, these results indicate that the optimal way to generate large fluctuations is by means of effectively highly correlated dynamics which is singularly different from the typical dynamics [16].

Here we start addressing the problem of *random and long-ranged* trajectory observables by considering the time integral of a function of configurations whose values are normally distributed with zero mean and variance N, that is, the energy function of the simplest mean-field spin glass: the random energy model (REM) [17,18]. For simplicity, we will consider dynamics which is all-to-all, that is, allowed configuration changes are those where any number of spins can flip simultaneously and independently. We also comment on the case of single-spin flips, which corresponds to the quantum random energy model (QREM).

The general problem we consider here has relevance in several areas. One is the minimization via trajectory sampling of (quasi-) random cost functions [19], which arises for example when training neural networks. A second one is in connection to measurement induced phase transitions in quantum systems [20,21], where the calculation of Renyi entropies reduces to computing the optimal dynamics of a random coupling function [22,23] in a system of classical replicas which evolve independently.

2. Unbiased dynamics

Any continuous-time Markov process with trajectories $\boldsymbol{\omega} : [0, \infty) \to \mathcal{Q}_N$ on the configuration space $\mathcal{Q}_N := \{-1, 1\}^N$ of N Ising spins is uniquely characterized in terms of the transition rates $w_{\boldsymbol{\sigma}\to\boldsymbol{\tau}}$ of spin configurations $\boldsymbol{\sigma} = (\sigma_1, \ldots, \sigma_N) \in \mathcal{Q}_N$ to any other configuration $\boldsymbol{\tau}$, and the associated escape rates $r_{\boldsymbol{\sigma}} := \sum_{\boldsymbol{\tau}\neq\boldsymbol{\sigma}} w_{\boldsymbol{\sigma}\to\boldsymbol{\tau}}$. The latter governs the law, $r_{\boldsymbol{\sigma}}\, \mathrm{e}^{-r_{\boldsymbol{\sigma}}\Delta t}$, of the sojourn time Δt until the next jump out of $\boldsymbol{\sigma}$. In the following, we choose $w_{\boldsymbol{\sigma}\to\boldsymbol{\tau}} := N2^{-N}$ independent of the configuration. Since the connectivity of this jump process is then described by the complete graph on 2^N vertices (i.e. spin configurations), this dynamics is called the completely connected or all-to-all stochastic dynamics on Ising configurations. Using Dirac's notation, in which $\{|\boldsymbol{\sigma}\rangle | \boldsymbol{\sigma} \in \mathcal{Q}_N\}$ stands for the canonical orthonormal basis in the Hilbert space $\ell^2(\mathcal{Q}_N) \equiv \otimes_{j=1}^N \mathbb{C}^2$, the generator of this Markov process is given by

$$W := \sum_{\substack{\boldsymbol{\sigma},\boldsymbol{\tau}\in\mathcal{Q}_N \\ \boldsymbol{\sigma}\neq\boldsymbol{\tau}}} w_{\boldsymbol{\sigma}\to\boldsymbol{\tau}} |\boldsymbol{\tau}\rangle\langle\boldsymbol{\sigma}| - \sum_{\boldsymbol{\sigma}\in\mathcal{Q}_N} r_{\boldsymbol{\sigma}} |\boldsymbol{\sigma}\rangle\langle\boldsymbol{\sigma}| = N\,(|-\rangle\langle -| - \mathbb{1})$$

in terms of the orthogonal projection $|-\rangle\langle -|$ onto the 'flat state' defined by $\langle\boldsymbol{\sigma}|-\rangle = 2^{-N/2}$. In its probabilistic interpretation, W is considered an operator on $\ell^1(\mathcal{Q}_N)$ and acts on probability

distributions $|p_t\rangle$, i.e. $p_t(\boldsymbol{\sigma}) \equiv \langle \boldsymbol{\sigma}|p_t\rangle \geq 0$ and $\sum_{\boldsymbol{\sigma}\in\mathcal{Q}_N} p_t(\boldsymbol{\sigma}) = 1$. The dynamics of any initial distribution is governed by the master equation

$$\partial_t |p_t\rangle = W|p_t\rangle.$$

The completely connected stochastic dynamics can be regarded as a further simplification of the dynamics of independent spin flips at infinite temperature. The latter is generated by $\widehat{W} := \sum_{j=1}^{N}(X_j - \mathbb{1})$, in terms of the Pauli-$X$ matrices, which flip the jth spin, i.e. $X_j|\boldsymbol{\sigma}\rangle = |\sigma_1, \ldots, -\sigma_j, \ldots, \sigma_N\rangle$. Both Markov processes are irreducible and share the equidistribution $p_{\mathrm{ss}}(\boldsymbol{\sigma}) := 2^{-N}$ as its unique invariant measure. One difference is their spectral gap, which governs the rate of approach to the equidistribution. While the spectral gap is N in the case of W, it is 2 in the case of $\widehat{W}$. In this paper, we focus on the completely connected dynamics W and only comment on the single spin-flip dynamics $\widehat{W}$.

The dynamics generated by W (and $\widehat{W}$) is 'infinite temperature' in the sense that transitions are completely independent of the initial and final states. The operator W is therefore bi-stochastic, $\langle -|W = 0, W|-\rangle = 0$, with the first equality indicating conservation of probability, and the second that the stationary state is also the flat state (the stationary probability vector being $2^{-N/2}|-\rangle$). Since the dynamics of all spins is independent, all correlation functions are unconnected.

3. Trajectory observable and random energy model

We study the statistics under the above defined all-to-all independent dynamics of a trajectory observable chosen to explore the energy landscape of the REM [17,18]. The REM, $U : \mathcal{Q}_N \to \mathbb{R}$, is a Gaussian random field (with randomness independent of the Markov process) in which the values $U(\boldsymbol{\sigma})$ are distributed independently for all $\boldsymbol{\sigma} \in \mathcal{Q}_N$ with identical normal law uniquely characterized by zero mean and covariance N. The units are chosen so that the REM's large deviations occur on order N which agrees with the norm of W. In this context, we recall [17,24] that the REM's minimum (and similarly for its maximum) satisfies the extremal value statistics:

$$\mathbb{P}(\min U \geq u_N(x)) = (1 - 2^{-N}\,\mathrm{e}^{-x+o(1)})^{2^N} \tag{3.1}$$

for any x with the scaling function $u_N(x) := -\beta_c N + ((\ln(N\ln 2) - \ln(4\pi))/2\beta_c) - (x/\beta_c)$, where $\beta_c = \sqrt{2\ln 2}$ and $\mathbb{P}$ denotes the joint law of the REM. In particular, the minimal energy of the REM is roughly at $-\beta_c N$.

The trajectory observable we consider is (up to a factor of t) the empirical average of the REM energy along a trajectory $\boldsymbol{\omega}$ of the Markov process

$$U_t[\boldsymbol{\omega}] := \int_0^t U(\boldsymbol{\omega}(s))\,\mathrm{d}s, \quad t > 0.$$

We will be interested in the probability distribution of this quantity under the law $\mathbb{P}_t$ on trajectories associated with W up to time t with the initial spin configurations equally distributed. The main result of this short note is a proof of a large deviation principle for this distribution in the limit of large system size N (for trajectories of any time extent t). This large deviation principle is described in terms of the moment generating function

$$Z(t,\lambda) := \int \mathrm{e}^{-\lambda U_t[\boldsymbol{\omega}]}\mathbb{P}_t(\mathrm{d}\boldsymbol{\omega}) = \sum_{\boldsymbol{\sigma},\boldsymbol{\tau}\in\mathcal{Q}_N} 2^{-N}\langle \boldsymbol{\sigma}|\mathrm{e}^{t(W-\lambda U)}|\boldsymbol{\tau}\rangle = \langle -|\mathrm{e}^{t(W-\lambda U)}|-\rangle. \tag{3.2}$$

Here the second equality is due to the Feynman–Kac formula for the Markov process under consideration (cf. [25,26]). Crucially, this formula connects the question concerning the (a)typical behaviour of U_t to properties of the tilted generator

$$W_\lambda := W - \lambda U,$$

which is a random matrix on $\ell^2(\mathcal{Q}_N)$. Note that by substituting W by $\widehat{W}$, this random matrix coincides, up to a constant shift and change of sign, with the Hamiltonian of the QREM—one of the simplest quantum spin glass models [27–30]. In our case, the operator $H_\lambda = -W_\lambda + N\mathbb{1}$

royalsocietypublishing.org/journal/rsta Phil. Trans. R. Soc. A 381: 20210415

instead corresponds to the Hamiltonian with an all-to-all kinetic energy studied in [31]. Owing to the symmetry of the REM's distribution the parameter λ can be taken non-negative without loss of generality, and the large deviation function also known as scaled cumulant generating function (SCGF) is then given by

$$\theta(t,\lambda) := \lim_{N\to\infty} \frac{1}{Nt} \ln Z(t,\lambda).$$

The SCGF plays the role of a free energy for trajectory ensembles.

It is important to emphasize that what we are considering here is very different from the study of classical thermal dynamics of the REM under Glauber or Metropolis schemes, as in e.g. [32–35]. In those cases, the dynamical Markov generator is interacting (as transitions depend on changes in U) and what is studied are the typical trajectories under that interacting dynamics. By contrast, we study rare trajectories under the non-interacting dynamics generated by W with large fluctuations of U_t.

4. Trajectory phase diagram

Our main result is the following:

Theorem 4.1. *For any $t > 0, \lambda \geq 0$ and almost all realizations of the REM:*

$$\theta(t,\lambda) = \max\{0, t^{-1} p_0(t\lambda) - 1\}, \tag{4.1}$$

with

$$p_0(\beta) := \lim_{N\to\infty} \frac{1}{N} \ln \frac{1}{2^N} \sum_{\boldsymbol{\sigma}} \mathrm{e}^{-\beta U(\boldsymbol{\sigma})} = \begin{cases} \frac{\beta^2}{2}, & \beta \leq \beta_c := \sqrt{2\ln 2} \\ \beta\beta_c - \ln 2, & \beta > \beta_c. \end{cases} \tag{4.2}$$

Before spelling out the short proof of theorem 4.1 in §7, let us put this result in some context and discuss some consequences. The quantity defined in (4.2) is the pressure corresponding to the REM's static (normalized) partition function at inverse temperature β. The critical value $\beta_c = \sqrt{2\ln 2}$ corresponds to the inverse of the REM's freezing temperature into a spin glass phase with one-step replica symmetry breaking (cf. [17]). The phase diagram resulting from theorem 4.1 is thus composed of three regimes depicted in figure 1*a*:

(i) An *Active* dynamical phase in which the Markov generator W dominates over the tilting, and which is characterized by $\theta(t,\lambda) = 0$ and the specific activity being unity (see below). It is separated from the remaining regimes by a first-order transition line. This regime persists for all $|\lambda| < \beta_c(2t)^{-1} + \beta_c^{-1}$ in case $t^{-1} < 2\beta_c^{-2}$ and $|\lambda| < \sqrt{2t^{-1}}$ in case $t^{-1} \geq 2\beta_c^{-2}$.
(ii) A regime of vanishing activity which occurs for $t^{-1} < 2|\lambda|\beta_c^{-1} - 2\beta_c^{-2}$ and which is dominated by the REM's extreme values where the system localizes. This regime is related to the spin-glass phase of the REM. We call this the *Inactive-1* dynamical phase.
(iii) The remaining parameter regime corresponds to a second inactive regime which we term *Inactive-2* dynamical phase. It occurs only if $t^{-1} > 2/\beta_c^2$ and is related to the classical paramagnetic phase of the REM.

In particular, in the long-time limit, $t \to \infty$, the value $\lambda = \beta_c^{-1}$ separates the Active and Inactive-1 phases, the latter dominating at large λ. Not surprisingly, this transition in the largest eigenvalue of the tilted generator $W_\lambda = W - \lambda U$ reflects the known location of its quantum-phase transition. As we will recall in §7, the eigenvector corresponding to the largest eigenvalue changes near $\lambda = \beta_c^{-1}$ from a delocalized state resembling $|-\rangle$ (indicating that trajectories visit all states equally giving rise to large activity) to a state localized at the REM's maximizing spin configuration (corresponding to trajectories that are inactive as they do not move away from this configuration).

The classification above of the trajectory phases in terms of their activity is obtained as follows. The dynamical activity is the total number of configuration changes in a trajectory. It can be calculated through the same tilting method used above for the time-integrated REM energy. Specifically, if we define the doubly tilted partition sum $Z(t,\lambda,s) := \langle -|\mathrm{e}^{tW_{\lambda,s}}|-\rangle$ with $W_{\lambda,s} =$

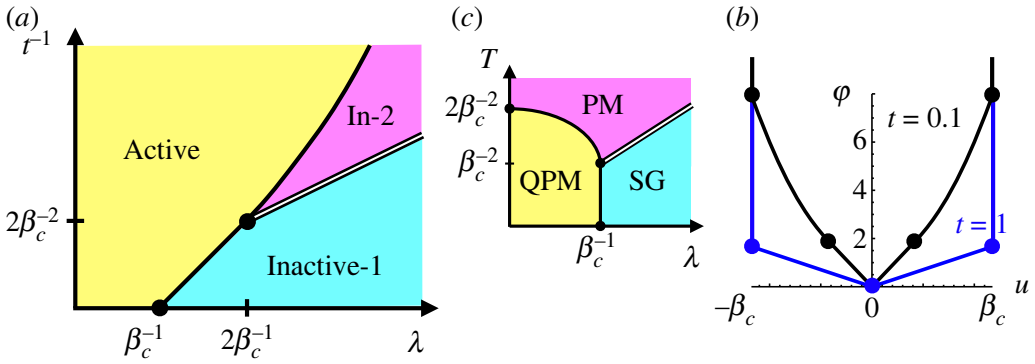

Figure 1. (*a*) Dynamical phase diagram in the limit of $N \to \infty$. The abscissa is the counting field λ conjugate to the time-integrated REM energy and the ordinate the inverse of the trajectory length t. The full lines indicate the first-order transitions between Active and Inactive-1 or Inactive-2 trajectory phases, while the double line indicates a one-step RSB transition between the Inactive-1 and Inactive-2 phases. (*b*) Large deviation function $\varphi(t,u)$ at two different values of t. For $t^{-1} = 1 < 2\beta_c^{-2}$ (blue lines) the rate function is one of coexistence between Active (which has $u = 0$) and Inactive-1 (which has $u = \pm\beta_c$, by symmetry). The linear portion of the rate function is the Maxwell construction indicative of phase coexistence (in time). For $t^{-1} = 10 > 2\beta_c^{-2}$, the rate function describes the coexistence between the three phases (black). The linear portion between 0 and $\sqrt{2t}$ is now the first-order coexistence between Active and Inactive-2. In Inactive-2 $|u|$ can take values with decreasing probability between $\sqrt{2t}$ and β_c. The rate function is infinite for any $|u|$ beyond β_c (indicative of zero probability for such trajectories). (*c*) Thermal phase diagram of the all-to-all QREM for comparison. (Online version in colour.)

$N\,\mathrm{e}^{-s}|-\rangle\langle -| - N(1-2^{-N}(1-\mathrm{e}^{-s}))\mathbb{1} - \lambda U$ (where the additional tilting by e^{-s} of the off-diagonal part of W allows to count jumps in trajectories), we get the activity from $-\partial_s \log Z(t,\lambda,s)|_{s=0}$. Using the results above, it is easy to see that the average activity per unit space and time is unity in the active phase and zero in the two inactive phases.

Via the Gärtner–Ellis theorem [36], the rate function of the large deviation principle obeyed by U_t is given by the Legendre–Fenchel transformation

$$\varphi(t,u) := \sup_{\lambda}(u\lambda - \theta(t,\lambda)) = \begin{cases} |u|\sqrt{\frac{2}{t}}, & |u| \le \min\left\{\sqrt{2t}, \beta_c\right\}, \\ 1 + \frac{u^2}{2t}, & \text{else}, \\ \infty, & |u| > \beta_c. \end{cases}$$

Note that, although in theorem 4.1 initially defined only for $\lambda \ge 0$, the function $\lambda \to \theta(t,\lambda)$ extends to all real values by symmetry. The rate function $u \to \varphi(t,u)$ is then symmetric as well. For times $t > \beta_c^2/2 = \ln 2$, the second case in the above equation is absent. As a corollary to theorem 4.1 and [36, Thm 2.3.6], we thus obtain the promised large deviation principle

$$\begin{aligned} -\inf_{u\in I^\circ} t\varphi(t,u) &\le \liminf_{N\to\infty} \frac{1}{N} \ln \mathbb{P}_t((Nt)^{-1}U_t \in I) \\ &\le \limsup_{N\to\infty} \frac{1}{N} \ln \mathbb{P}_t((Nt)^{-1}U_t \in I) = -\inf_{u\in\bar{I}} t\varphi(t,u) \end{aligned} \tag{4.3}$$

which holds for any Borel set $I \subset \mathbb{R}$ and any $t > 0$. The rate function is shown in figure 1*b* for two different times.

Clearly, under the *a priori* measure $\mathbb{P}_t$, which favours rapid changes of spin configurations at the rate $N(1-2^{-N})$, the typical value of the REM's empirical energy density $N^{-1}U_t[\boldsymbol{\omega}]$ along any trajectory $\boldsymbol{\omega}$ is close to zero. The fluctuations about this typical behaviour are described by (4.3): close to $u = 0$, these fluctuations are linearly suppressed with a rate proportionally to $N\sqrt{2t}$. Tilting the *a priori* measure, one encounters one or two phase transitions depending on whether $t > \ln 2$ or not. If $t < \ln 2$, one enters a regime $\sqrt{2t} < |u| < \beta_c$ with Gaussian fluctuations. Beyond this, i.e. at energy densities of the order of the REM's maximum or minimum (3.1), the energy

density effectively stops fluctuating. Trajectories freeze for long times in the REM's extremal values.

5. Thermal phase diagram and generalizations

The dynamical partition sum of the stochastic system we are considering is reminiscent of a quantum (thermal and static) partition sum for the all-to-all version of the QREM. While the calculation of both is analogous, there are some important differences, which we address next. Specifically, if we consider the tilted generator W_λ as (minus) a Hamiltonian, the (specific) free energy of the associated quantum problem at temperature T is

$$f(T,\lambda) := \lim_{N\to\infty} \frac{T}{N} \ln \frac{1}{2^N} \operatorname{Tr} \mathrm{e}^{(W-\lambda U)/T}. \tag{5.1}$$

As we will explain in §7, using results in [31] this quantity can easily be determined for a rather general Ising spin glass U in terms of its free energy.

Theorem 5.1. *Let $U : \mathcal{Q}_N \to \mathbb{R}$ be such that $\mathbb{P}(U(\boldsymbol{\sigma}) \in N\,\mathrm{d}v) = \varrho(v)\,\mathrm{d}v$ for all $\boldsymbol{\sigma} \in \mathcal{Q}_N$ with an N-independent distribution ϱ which has up to four finite moments with $\int v\varrho(v)\,\mathrm{d}v = 0$ and $\int v^2\varrho(v)\,\mathrm{d}v = 1$. If for almost all realizations the values $U(\boldsymbol{\sigma})/N$ as $N \to \infty$ fill a compact interval $[u_{\min}, u_{\max}]$ and the pressure $p_0(\beta) = \lim_{N\to\infty}(1/N)\ln(1/2^N)\sum_{\boldsymbol{\sigma}} \mathrm{e}^{-\beta U(\boldsymbol{\sigma})}$ exists, then the free energy at temperature T of the tilted generator W_λ is given by*

$$f(T,\lambda) = \max\left\{-T\ln 2, Tp_0\left(\frac{\lambda}{T}\right) - 1\right\}. \tag{5.2}$$

Restricting attention to the REM to which the theorem is applicable, we note that (5.2) and the explicit expression for p_0 in (4.2) implies that the all-to-all QREM exhibits three different phases depending on coupling and temperature: a delocalized quantum paramagnetic phase (QPM), a localized spin-glass phase (SG) and a classical paramagnetic phase (PM) (figure 1*c*). These three static quantum phases are similar to the dynamical ones of the stochastic problem of theorem 4.1. But it is worth pointing out that at $T > 0$ the (thermo)static phase transitions described by $f(T,\lambda)$ do not coincide with the dynamic phase transitions described by $\theta(t,\lambda)$. These differences arise because the boundary vectors in the dynamical partition sum involve information about eigenvectors of W_λ also versus the trace in the static quantum one depends on the eigenvalues only. For a comparison of the phase diagrams, see figure 1*a*,*c*.

In contrast to the all-to-all simplification studied in theorem 5.1, the free energy of transversal field models with U's having a correlation structure more complicated than the REM [27,29] or its generalized relatives [28,30] is not explicitly known. The most prominent example, to which theorem 5.1 also applies, is the all-to-all version of the Quantum Sherrington–Kirkpatrick (QSK) model. In contrast to its all-to-all simplification (5.2), the free energy and phase diagram of the QSK is predicted to consist of two phases only: a paramagnetic phase separated from a spin-glass phase at low temperatures and small transversal field (cf. [37,38] for numerical and [26,39] for recent analytical results). Clearly, the all-to-all version of the QSK will not exhibit an interesting entanglement structure predicted recently in [40].

In view of the general class of U's covered by theorem 5.1, one might wonder whether theorem 4.1 is generalizable to the class of U's covered above. In fact, from the proof in §7 it is easy to see that substituting in (4.1) the pressure of U, the right-hand side remains a lower bound on $\theta(t,\lambda)$, cf. (7.4). This lower bound is sharp only in case the eigenvectors corresponding to the bulk of eigenvalues remain localized (in the sense that $\lim_{N\to\infty} N^{-1}\ln\langle -|1_{(E-\delta_N,E+\delta N)}(H_\lambda)|-\rangle = -\ln 2$ for all sufficiently small $\delta > 0$ and $E/N \in [u_{\min}, u_{\max}]$). Motivated by results in [41], we conjecture this to hold for the SK model U. However, this will not hold in case correlations of U cause its values to cluster.

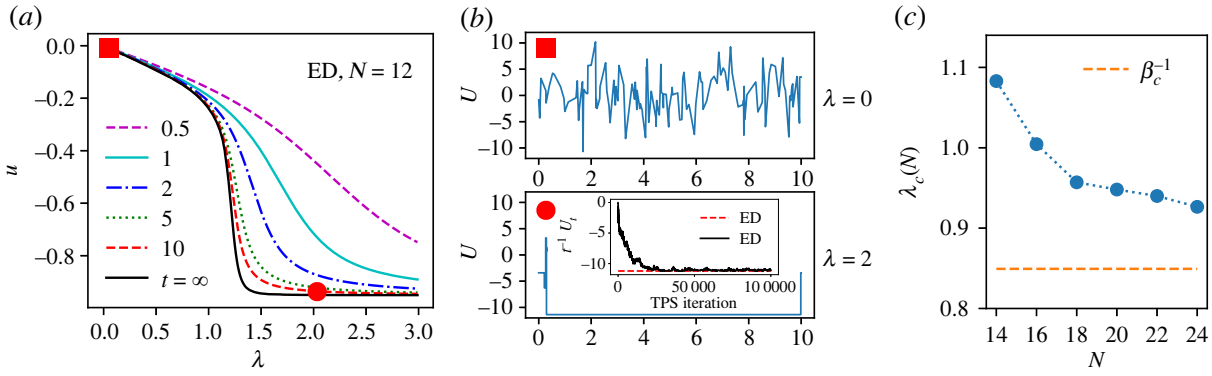

Figure 2. (*a*) Dynamical order parameter $-\partial_\lambda \theta(\lambda, t)$ for various times t, from exact diagonalization (ED) for one disorder realization with system size $N = 12$. (*b*) The top panel shows a typical trajectory of time extent $t = 10$, corresponding to unbiased dynamics, $\lambda = 0$ (generated from W via standard continuous-time Monte Carlo from a random initial configuration). The bottom panel shows a characteristic trajectory of the inactive phase, $\lambda = 2$. This was obtained via transition path sampling (TPS, see main text). The inset to the lower panel shows the convergence of the trajectory sampling (black): each iteration is a different trajectory and their time-integrated energy converges to the ED result (red dashed) with enough TPS iterations. (*c*) Transition point $\lambda_c(N)$ for $t = \infty$ as a function of system size, averaged over 20 disordered realizations. The dashed line is the large N value of λ_c. (Online version in colour.)

6. Numerical illustration of finite-size corrections

The exact results above are for the limit $N \to \infty$. At finite N there are of course finite-size corrections and sample-to-sample fluctuations between different realizations of the disorder U. Using numerics, we now illustrate some of these finite-size effects. (A comprehensive numerical study of both the all-to-all and single spin-flip problem will be presented in a future publication.)

When the system size is not too large the dynamical partition sum (3.2) can be computed numerically using exact diagonalization (ED). We illustrate results for one disorder realization in a system of size $N = 12$ of the dynamical order parameter:

$$u(\lambda, t) := \frac{1}{NtZ(t,\lambda)} \int U_t[\boldsymbol{\omega}]\, \mathrm{e}^{-\lambda U_t[\boldsymbol{\omega}]} \mathbb{P}_t(\mathrm{d}\boldsymbol{\omega}) = -\frac{\partial}{\partial \lambda} \theta_N(t, \lambda) \tag{6.1}$$

Figure 2*a* shows the following: (i) for finite size the phase transitions turn into crossovers, as expected; (ii) for all t there is a crossover from $u \approx 0$ at $\lambda = 0$ to a large negative u for large λ, eventually reaching the minimum of the potential (which changes from sample to sample); (iii) these crossovers are sharper the longer t, also expected due to the preference of the boundary states in (3.2) for the delocalized state.

In figure 2*b*, we show representative trajectories for two values of λ for $t = 10$. We plot the instantaneous energy as a function of time in the trajectory. The top panel shows a typical trajectory of the dynamics corresponding to $\lambda = 0$, cf. the red square in figure 2*a*. This trajectory generated by W is sampled using standard (continuous-time) Monte Carlo [42]. Since the unbiased dynamics connects all configurations with equal rates the trajectory jumps between the energy values: it corresponds to the phase which has high activity and is delocalized. The bottom panel shows a characteristic trajectory for $\lambda = 2$, cf. the red circle in figure 2*a*. This is a rare event (exponentially suppressed in N and t) of the dynamics, and as such cannot be easily sampled from running Monte Carlo with W (since W_λ is not a stochastic operator). We obtain such rare trajectories instead by performing importance sampling in trajectory space using transition path sampling (TPS) [43], essentially a Monte Carlo method in trajectory space that aims to 'equilibrate' to a reweighted trajectory distribution $Z(t,\lambda)^{-1}\, \mathrm{e}^{-\lambda U_t[\boldsymbol{\omega}]}$ (supplemented with bridge moves to improve acceptance; we will provide details of this method in a future publication). The inset to the lower panel shows the convergence of our TPS approach: it shows the evolution of the sampled trajectories with TPS iterations by showing their $U_t[\boldsymbol{\omega}]$ (per unit time). The $U_t[\boldsymbol{\omega}]$ in the

inset converges eventually to the value expected at $\lambda = 2$, showing that TPS converges to the tilted trajectory ensemble. The trajectory shown in the lower panel is the last trajectory from TPS. It is very different from the typical one in the upper panel: it has very low activity and is localized for most of the time in the minimum energy configuration, corresponding to the Inactive-1 dynamical phase. Note that while we only illustrate the numerics for the size $N = 12$, TPS can be used for larger system sizes in contrast to ED.

Figure 2*c* shows the location of the critical λ for $t = \infty$, averaged over 20 realizations of the disorder, for different systems sizes. The transition point is inferred from the maximum of the *dynamical susceptibility* $\partial_\lambda^2 \theta_N(\lambda)$, where $\theta_N(\lambda)$ is the largest eigenvalue of W_λ. This eigenvalue is calculated using (7.1), which allows to compute it for larger sizes than those accessible to ED. The figure suggests a convergence to the limiting value β_c^{-1} for large N, as expected from the analytics above.

7. Proof of the large deviation results

The Feynman–Kac formula (3.2) reduces the large deviation problem to a spectral analysis of the random matrix $W_\lambda = W - \lambda U$. Up to a constant shift and rescaling, the spectrum of W_λ for an REM U has been analysed in [31] both on the macro and microscopic scale of the eigenvalue process. The main technical tool for studying W_λ, which applies to U more generally than the REM, is rank-one perturbation theory. For non-degenerate values of U, the energy E is an eigenvalue of W_λ if and only if

$$1 = N\langle -|(E + N + \lambda U)^{-1}|-\rangle = \frac{1}{2^N} \sum_{\boldsymbol{\sigma}} \frac{N}{E + N + \lambda U(\boldsymbol{\sigma})}. \tag{7.1}$$

The corresponding eigenvectors ψ_E satisfy for all $\boldsymbol{\sigma}, \boldsymbol{\tau} \in \mathcal{Q}_N$:

$$\frac{\langle \boldsymbol{\sigma}|\psi_E\rangle}{\langle \boldsymbol{\tau}|\psi_E\rangle} = \frac{E + N + \lambda U(\boldsymbol{\tau})}{E + N + \lambda U(\boldsymbol{\sigma})}. \tag{7.2}$$

In the case of degeneracies of the values of U, the remaining eigenvalues remain unaffected by the rank-one perturbation. An immediate implication of this fact and (7.1) is the fact that all eigenvalues of W_λ aside from the largest one are interlaced with the energies of U and additionally shifted by $-N$ (cf. e.g. [44] and references therein for interlacing and finite-rank perturbation theory). In the case of the REM, all eigenvalues are in fact almost surely simple.

As we argue next, the largest solution of (7.1) is independent of the realization of U up to small fluctuations. More precisely, we study solutions with $E/N \geq \lambda u_{\max} - 1 + \varepsilon$ for arbitrary $\varepsilon > 0$ and all N (with $u_{\max} = \beta_c$ for the REM, cf. (3.1)). A strong law of large numbers implies that the right-hand side of (7.1) is then well approximated as $N \to \infty$ by the integral

$$\int_{-\infty}^{\infty} \frac{N}{E + N + \lambda\sqrt{N}v} \varrho(v)\, \mathrm{d}v = \frac{1}{1 + E/N} \left(1 + \frac{\lambda^2}{N(1 + E/N)} + \mathcal{O}(N^{-2})\right).$$

This explains the following results on the largest eigenvalue $E_0 := \max \sigma(W_\lambda)$, which are straightforward adaptations of results in [31]:

(i) In case $\lambda u_{\max} < 1$, on an event with probability close to one, the largest eigenvalue is at $E_0 := \max \sigma(W_\lambda) = \lambda^2 + \mathcal{O}(N^{-1})$ and the corresponding eigenvector satisfies $\langle \boldsymbol{\sigma}|\psi_{E_0}\rangle \propto (E_0 + N + \lambda U(\boldsymbol{\sigma}))^{-1}$. Since $2^{-N} \sum_{\boldsymbol{\sigma}} (E_0 + N + \lambda U(\boldsymbol{\sigma}))^{-2}$ is of order one up to small fluctuations by the law of large numbers, this vector is hence still delocalized (as in the case $\lambda = 0$).

(ii) In case $\lambda u_{\max} > 1$, the largest eigenvalue is at $E_0 = \max \sigma(W_\lambda) = (\lambda u_{\max} - 1)N + o(N)$. For the REM, one even has the fine asymptotics

$$E_0 = \max \sigma(W_\lambda) = (\lambda\beta_c - 1)N - N2^{-N} \left(1 - \frac{1}{\lambda\beta_c}\right)^{-1} + o(N2^{-N}) \tag{7.3}$$

and the corresponding eigenvector is mostly concentrated on the REM's minimizing configuration $\boldsymbol{\sigma}_0 : eqq \arg\min U$. This is specified through the ratios (7.2). Note that the error term in the above equation only holds with a probability up to $1 - \mathcal{O}(1/N)$ (cf. [31, App A]).

In particular, even in the case of degeneracies of U, the union of eigenvalues, $\sigma(W_\lambda)$, when divided by N, converges almost surely to the non-random set $\{0\} \cup [\lambda u_{\min} - 1, \lambda u_{\max} - 1]$. Together with the interlacing property, one then easily arrives at (5.2) for the free energy of W_λ.

The proof of theorem 4.1 requires slightly more detailed knowledge, since $\langle -|\mathrm{e}^{tW_\lambda}|-\rangle$ involves properties of the eigenvectors, too. The rough picture established in [31] through a more detailed analysis of the characteristic equation (7.1) is the following:

(i) Delocalization of one eigenstate near energy 0 is shown to persist up to $\lambda < \sqrt{2}$. From that value on, $\lambda > \sqrt{2}$, this eigenstates 'melts' into a narrow band of semi-delocalized states near energy 0.
(ii) The eigenvalue process, when rescaled to order one at some fixed energy outside $-N$ and 0, is given by a Poisson process. Correspondingly, outside those special energies the normalized eigenvectors are localized.

We will need the following result, which is contained in [31, Proof of Thm. 6.3].

Proposition 7.1. *For any $\delta > 0$ and any N there is some $a > 0$ and an event Ω_N whose complement is summable, $\sum_N \mathbb{P}(\Omega_N^c) < \infty$, such that in the event Ω_N any eigenvalue E of W_λ with $|E| > \delta N$ and $|E + N| > \delta N$ has a normalized eigenvector ψ_E, which satisfies $|\langle -|\psi_E\rangle|^2 \leq N^a\, 2^{-N}$. Moreover, for any such E, there is some $\boldsymbol{\sigma}_E \in \{-1, 1\}^N$ such that $|E + N - \lambda U(\boldsymbol{\sigma}_E)| \leq \delta N$.*

Proof of theorem 4.1. The proof proceeds by establishing asymptotically coinciding upper and lower bounds. For the lower bound, we use Jensen's inequality to conclude

$$\ln\langle -|\mathrm{e}^{tW_\lambda}|-\rangle \geq t\langle -|W_\lambda|-\rangle = \frac{t\lambda}{2^N}\sum_{\boldsymbol{\sigma}} U(\boldsymbol{\sigma}).$$

By the law of large numbers, this term converges to zero for almost all realizations of the REM. For another lower bound, which is sharper in case $t < p_0(t\lambda)$, we estimate

$$\begin{aligned}\langle -|\mathrm{e}^{tW_\lambda}|-\rangle = \frac{1}{2^N}\sum_{\boldsymbol{\sigma},\boldsymbol{\tau}}\langle \boldsymbol{\tau}|\mathrm{e}^{tW_\lambda}|\boldsymbol{\sigma}\rangle &\geq \frac{1}{2^N}\sum_{\boldsymbol{\sigma}}\langle \boldsymbol{\sigma}|\mathrm{e}^{tW_\lambda}|\boldsymbol{\sigma}\rangle \\ &\geq \frac{1}{2^N}\sum_{\boldsymbol{\sigma}}\exp\Big(tN(|\langle \boldsymbol{\sigma}|-\rangle|^2 - 1) - t\lambda U(\boldsymbol{\sigma})\Big), \end{aligned} \tag{7.4}$$

where the last step is again by Jensen's inequality. Using $|\langle \boldsymbol{\sigma}|-\rangle|^2 = 2^{-N}$ and (4.2), the combination of the above estimates yields (4.1) as a lower bound.

A complementing upper bound is based on proposition 7.1. Expanding in eigenfunctions and splitting the sum over all eigenvalues in three parts corresponding to energies E with $|E + N| \leq \delta N$, $|E| \leq \delta N$ and the rest, we write and estimate using proposition 7.1:

$$\langle -|\mathrm{e}^{tW_\lambda}|-\rangle = \sum_E \mathrm{e}^{tE}|\langle -|\psi_E\rangle|^2 \leq \mathrm{e}^{tN(\delta-1)} + \mathrm{e}^{tN\delta} + \frac{N^a}{2^N}\,\mathrm{e}^{tN(\delta-1)}\sum_{\boldsymbol{\sigma}}\mathrm{e}^{-t\lambda U(\boldsymbol{\sigma})}. \tag{7.5}$$

In the event Ω_N of proposition 7.1, we thus conclude

$$\limsup_{N\to\infty}\frac{1}{Nt}\ln\langle -|\mathrm{e}^{tW_\lambda}|-\rangle \leq \max\{0, t^{-1}p_0(t\lambda) - 1\} + \delta.$$

By a Borel–Cantelli argument, this establishes this almost-sure bound on the upper limit. Since $\delta > 0$ is arbitrary, this concludes the proof. ∎

8. Outlook: QREM

Let us conclude this note with some conjectures, partial results and comparison in case W is replaced by the spin-flip dynamics generated by $\widehat{W}$. In that case, the tilted generator $\widehat{H}_\lambda := \widehat{W} - \lambda U$ is the QREM. Its low-energy spectrum as well as the phase transitions in the free energy are well understood [29,45]. By the Feynman–Kac formula the dynamical phase transition is again described in terms of the asymptotic behaviour of $N^{-1} \ln\langle -|\mathrm{e}^{t\widehat{H}_\lambda}|-\rangle$.

The phase transition in the largest eigenvalue $\widehat{E}_0 := \max \sigma(\widehat{H}_\lambda)$ occurs on order N at the same location $\lambda = \beta_c^{-1}$ as for H_λ. However, the finite-volume corrections are different in the localization regime, i.e. for all realizations of the REM aside from a set of exponentially small probability (see [45] for details):

(i) if $\lambda > \beta_c^{-1}$ we have $\widehat{E}_0 = -\lambda \min U + (\lambda\beta_c)^{-1} + \mathcal{O}(N^{-1/4})$,
(ii) if $\lambda < \beta_c^{-1}$ we have $\widehat{E}_0 = \lambda^2 + \mathcal{O}(N^{-1/4})$.

Following the steps of the lower bound in the proof of theorem 4.1, it is easy to see that for almost all realizations of the REM one still has:

$$\liminf_{N\to\infty} \frac{1}{Nt} \ln\langle -|\mathrm{e}^{t\widehat{H}_\lambda}|-\rangle \geq \max\{0, t^{-1}p_0(t\lambda) - 1\}. \tag{8.1}$$

We conjecture that this bound is sharp. In fact, using the spectral decomposing as in (7.5) and decomposing the sum into positive and negative energies we may again estimate

$$\langle -|\mathrm{e}^{t\widehat{H}_\lambda}|-\rangle \leq \sum_{\substack{E\sigma(\widehat{H}_\lambda)\\ E>0}} \mathrm{e}^{tE}\, |\langle -|\psi_E\rangle|^2 + 1.$$

The first sum is estimated trivially by $\mathrm{e}^{t\widehat{E}_0}$. In case $\lambda < \beta_c^{-1}$ this yields the upper bound $\limsup_{N\to\infty}(1/Nt)\ln\langle -|\mathrm{e}^{t\widehat{H}_\lambda}|-\rangle \leq 0$, which coincides with the lower bound. In case $\lambda > \beta_c^{-1}$, we know from [45] that eigenvalues with energies $E > 0$ are in one-to-one correspondence with values $U(\boldsymbol{\sigma}_E) = E + \mathcal{O}(1)$. We conjecture that the local density of states at these energies satisfies $\lim_{N\to\infty} N^{-1} \ln\langle -|1_{(E-\delta_N, E+\delta N)}(\widehat{H}_\lambda)|-\rangle = -\ln 2$ for all sufficiently small $\delta > 0$. This would prove that (8.1) is indeed sharp.

Data accessibility. Research data are available from the Nottingham Research Data Management Repository at http://doi.org/10.17639/nott.7196 [46].

Authors' contributions. J.G.: conceptualization, data curation, formal analysis, funding acquisition, investigation, methodology, project administration, resources, software, visualization, writing—original draft, writing—review and editing; C.M.: formal analysis, investigation, validation, writing—original draft, writing—review and editing; S.W.: conceptualization, formal analysis, funding acquisition, investigation, methodology, project administration, supervision, validation, writing—original draft, writing—review and editing.

All authors gave final approval for publication and agreed to be held accountable for the work performed therein.

Conflict of interest declaration. We declare we have no competing interests.

Funding. J.P.G. acknowledges financial support from EPSRC grant no. EP/R04421X/1 and the Leverhulme Trust grant no. RPG-2018-181. Numerical simulations were performed using the Sulis Tier 2 HPC platform funded by EPSRC grant no. EP/T022108/1 and the HPC Midlands+ consortium. S.W. thanks the DFG for support under grant no. EXC-2111—390814868.

References

1. Chandler D. 1987 *Introduction to modern statistical mechanics*. Oxford, UK: Oxford University Press.
2. Lecomte V, Appert-Rolland C, van Wijland F. 2007 Thermodynamic formalism for systems with Markov dynamics. *J. Stat. Phys.* **127**, 51–106. (doi:10.1007/s10955-006-9254-0)
3. Ruelle D. 2004 *Thermodynamic formalism*. Cambridge, UK: Cambridge University Press.

4. Garrahan JP. 2018 Aspects of non-equilibrium in classical and quantum systems: slow relaxation and glasses, dynamical large deviations, quantum non-ergodicity, and open quantum dynamics. *Physica A* **504**, 130–154. (doi:10.1016/j.physa.2017.12.149)
5. Jack RL. 2020 Ergodicity and large deviations in physical systems with stochastic dynamics. *Eur. Phys. J. B* **93**, 74. (doi:10.1140/epjb/e2020-100605-3)
6. Merolle M, Garrahan JP, Chandler D. 2005 Space-time thermodynamics of the glass transition. *Proc. Natl Acad. Sci. USA* **102**, 10 837–10 840. (doi:10.1073/pnas.0504820102)
7. Touchette H. 2009 The large deviation approach to statistical mechanics. *Phys. Rep.* **478**, 1–69. (doi:10.1016/j.physrep.2009.05.002)
8. Garrahan JP, Jack RL, Lecomte V, Pitard E, van Duijvendijk K, van Wijland F. 2007 Dynamical first-order phase transition in kinetically constrained models of glasses. *Phys. Rev. Lett.* **98**, 195702. (doi:10.1103/PhysRevLett.98.195702)
9. Hedges LO, Jack RL, Garrahan JP, Chandler D. 2009 Dynamic order-disorder in atomistic models of structural glass formers. *Science* **323**, 1309–1313. (doi:10.1126/science.1166665)
10. Speck T, Malins A, Royall CP. 2012 First-order phase transition in a model glass former: coupling of local structure and dynamics. *Phys. Rev. Lett.* **109**, 195703. (doi:10.1103/PhysRevLett.109.195703)
11. Appert-Rolland C, Derrida B, Lecomte V, van Wijland F. 2008 Universal cumulants of the current in diffusive systems on a ring. *Phys. Rev. E* **78**, 021122. (doi:10.1103/PhysRevE.78.021122)
12. Derrida B. 2007 Non-equilibrium steady states: fluctuations and large deviations of the density and of the current. *J. Stat. Mech.* **2007**, P07023. (doi:10.1088/1742-5468/2007/07/P07023)
13. Jack RL, Thompson IR, Sollich P. 2015 Hyperuniformity and phase separation in biased ensembles of trajectories for diffusive systems. *Phys. Rev. Lett.* **114**, 060601. (doi:10.1103/PhysRevLett.114.060601)
14. Nemoto T, Fodor E, Cates ME, Jack RL, Tailleur J. 2019 Optimizing active work: dynamical phase transitions, collective motion, and jamming. *Phys. Rev. E* **99**, 022605. (doi:10.1103/PhysRevE.99.022605)
15. Vasiloiu LM, Oakes THE, Carollo F, Garrahan JP. 2020 Trajectory phase transitions in noninteracting spin systems. *Phys. Rev. E* **101**, 042115. (doi:10.1103/PhysRevE.101.042115)
16. Nyawo PT, Touchette H. 2016 A minimal model of dynamical phase transition. *EPL* **116**, 50009. (doi:10.1209/0295-5075/116/50009)
17. Bovier A. 2006 *Statistical mechanics of disordered systems: a mathematical perspective*. Cambridge Series in Statistical and Probabilistic Mathematics. Cambridge, UK: Cambridge University Press.
18. Derrida B. 1980 Random-energy model: limit of a family of disordered models. *Phys. Rev. Lett.* **45**, 79–82. (doi:10.1103/PhysRevLett.45.79)
19. Mair J, Rose D, Garrahan J. 2022 Training of neural network ensembles via trajectory sampling. Preprint. (https://arxiv.org/abs/2209.11116)
20. Li Y, Chen X, Fisher MPA. 2018 Quantum Zeno effect and the many-body entanglement transition. *Phys. Rev. B* **98**, 205136. (doi:10.1103/PhysRevB.98.205136)
21. Skinner B, Ruhman J, Nahum A. 2019 Measurement-induced phase transitions in the dynamics of entanglement. *Phys. Rev. X* **9**, 031009. (doi:10.1103/PhysRevX.9.031009)
22. Agrawal U, Zabalo A, Chen K, Wilson JH, Potter AC, Pixley J, Gopalakrishnan S, Vasseur R. 2021 Entanglement and charge-sharpening transitions in $U(1)$ symmetric monitored quantum circuits. Preprint. (https://arxiv.org/abs/2107.10279)
23. Altland A, Buchhold M, Diehl S, Micklitz T. 2021 Dynamics of measured many-body quantum chaotic systems. *Phys. Rev. Res.* **4**, L022066. (doi:10.1103/PhysRevResearch.4.L022066)
24. Leadbetter MR, Lindgren G, Rootzén H. 1983 *Extremes and related properties of random sequences and processes*. Berlin, Germany: Springer.
25. Keller M, Lenz D, Wojciechowski RK 2021 *Graphs and discrete dirichlet spaces*. **358**. Grundlehren der Mathematischen Wissenschaften, vol. Berlin, Germany: Springer.
26. Leschke H, Rothlauf S, Ruder R, Spitzer W. 2021 The free energy of a quantum Sherrington–Kirkpatrick spin-glass model for weak disorder. *J. Stat. Phys.* **182**, 55. (doi:10.1007/s10955-020-02689-8)
27. Goldschmidt YY. 1990 Solvable model of the quantum spin glass in a transverse field. *Phys. Rev. B* **41**, 4858–4861. (doi:10.1103/PhysRevB.41.4858)

28. Manai C, Warzel S. 2022 Generalized random energy models in a transversal magnetic field: free energy and phase diagrams. *Probab. Math. Phys.* **3**, 215–245. (doi:10.2140/pmp.2022.3.215)
29. Manai C, Warzel S. 2020 Phase diagram of the quantum random energy model. *J. Stat. Phys.* **180**, 654–664. (doi:10.1007/s10955-020-02492-5)
30. Manai C, Warzel S. 2021 The de Almeida–Thouless line in hierarchical quantum spin glasses. *J. Stat. Phys.* **186**, 14. (doi:10.1007/s10955-021-02860-9)
31. Aizenman M, Shamis M, Warzel S. 2015 Resonances and partial delocalization on the complete graph. *Ann. Henri Poincaré* **16**, 1969–2003. (doi:10.1007/s00023-014-0366-9)
32. Arous GB, Bovier A, Gayrard V. 2003 Glauber dynamics of the random energy model. *Commun. Math. Phys.* **236**, 1–54. (doi:10.1007/s00220-003-0799-3)
33. Arous GB, Bovier A, Gayrard V. 2003 Glauber dynamics of the random energy model. *Commun. Math. Phys.* **235**, 379–425. (doi:10.1007/s00220-003-0798-4)
34. Černý J, Wassmer T. 2017 Aging of the metropolis dynamics on the random energy model. *Probab. Theory Relat. Fields* **167**, 253–303. (doi:10.1007/s00440-015-0681-1)
35. Gayrard V, Hartung L. 2019 Dynamic phase diagram of the REM. In *Statistical mechanics of classical and disordered systems* (eds V Gayrard, L-P Arguin, N Kistler, I Kourkova). Berlin, Germany: Springer.
36. Dembo A, Zeitouni O. 1998 *Large deviations techniques and applications*. 2nd edn. Berlin, Germany: Springer.
37. Ray P, Chakrabarti BK, Chakrabarti A. 1989 Sherrington–Kirkpatrick model in a transverse field: absence of replica symmetry breaking due to quantum fluctuations. *Phys. Rev. B* **39**, 11 828–11 832. (doi:10.1103/PhysRevB.39.11828)
38. Young AP. 2017 Stability of the quantum Sherrington–Kirkpatrick spin glass model. *Phys. Rev. E* **96**, 032112. (doi:10.1103/PhysRevE.96.032112)
39. Leschke H, Manai C, Ruder R, Warzel S. 2021 Existence of replica-symmetry breaking in quantum glasses. *Phys. Rev. Lett.* **127**, 207204. (doi:10.1103/PhysRevLett.127.207204)
40. Schindler PM, Guaita T, Shi T, Demler E, Cirac JI. A variational Ansatz for the ground state of the quantum Sherrington-Kirkpatrick model. Preprint. (https://arxiv.org/abs/2204.02923)
41. Bovier A, Kurkova I. 2006 Local energy statistics in disordered systems: a proof of the local REM conjecture. *Commun. Math. Phys.* **263**, 513–533. (doi:10.1007/s00220-005-1516-1)
42. Bortz AB, Kalos MH, Lebowitz JL. 1975 New algorithm for Monte-Carlo simulation of Ising spin systems. *J. Comp. Phys.* **17**, 10–18. (doi:10.1016/0021-9991(75)90060-1)
43. Bolhuis PG, Chandler D, Dellago C, Geissler PL. 2002 Transition path sampling: throwing ropes over rough mountain passes, in the dark. *Annu. Rev. Phys. Chem.* **53**, 291–318. (doi:10.1146/annurev.physchem.53.082301.113146)
44. Aizenman M, Warzel S. 2015 *Random operators: disorder effects on quantum spectra and dynamics*, vol. 168. Graduate Studies in Mathematics. RI, USA: AMS.
45. Manai C, Warzel S. 2022 Spectral analysis of the quantum random energy model. Preprint. (https://arxiv.org/abs/2202.00334)
46. Garrahan JP, Manai C, Warzel S. 2022 Data from: Trajectory phase transitions in non-interacting systems: all-to-all dynamics and the random energy model. Nottingham Research Data Management Repository. (doi:10.17639/nott.7196)